RESEARCH REPORT

Analysis of the Hygrothermal Behavior of Residential High-Rise Building Components

CMHC ◆ SCHL
HOME TO CANADIANS

CMHC—HOME TO CANADIANS

Canada Mortgage and Housing Corporation (CMHC) has been Canada's national housing agency for more than 65 years.

Together with other housing stakeholders, we help ensure that the Canadian housing system remains one of the best in the world. We are committed to helping Canadians access a wide choice of quality, environmentally sustainable and affordable housing solutions that will continue to create vibrant and healthy communities and cities across the country.

For more information, visit our website at **www.cmhc.ca**

You can also reach us by phone at 1-800-668-2642 or by fax at 1-800-245-9274.

Outside Canada call 613-748-2003 or fax to 613-748-2016.

Canada Mortgage and Housing Corporation supports the Government of Canada policy on access to information for people with disabilities. If you wish to obtain this publication in alternative formats, call 1-800-668-2642.

NRC·CNRC

Client Report

A-3052.4

Analysis of the Hygrothermal Behavior of
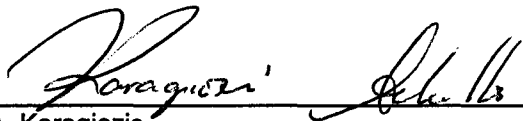Residential High-Rise Building Components

for

Canada Mortgage and Housing Corporation
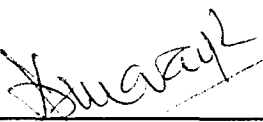700 Montreal Road
Ottawa, Ontario
K1A 0P7

25 August 1997

Analysis of the Hygrothermal Behavior of Residential High-Rise Building Components.

Author   _(signature)_

Dr. A. Karagiozis
Project Manager

Quality
Assurance   _(signature)_

Dr. M. K. Kumaran

Approved   _(signature)_

Dr. J. D. Quirt
Director, Building Envelope and Structure

Report No: A3052.4
Report Date: August 25, 1997
Contract No: A3052
Reference: Agreement for Joint Research Project, July 30, 1992
Program: Building Envelope and Structure

287 pages

Copy No.8 of 10 copies

ABSTRACT

Hygrothermal Performance of Residential High-Rise Buildings by Achilles Karagiozis of the National Research Council Canada.

A joint research project between the National Research Council Canada and the Canada Mortgage and Housing Corporation was conducted to determine the hygrothermal performance of various high-rise building envelope wall and roof assemblies. Basic understanding of the combined heat-air and moisture transport was developed by employing a state of the art hygrothermal model, LATENITE 1.1. A sensitivity analysis on the hygrothermal processes was first developed to determine the effects of accuracy of material properties, initial conditions, and boundary conditions. Three wall and roof systems were then examined in this study at seven different Canadian climatic locations. Two retrofitting strategies were employed for each wall system. The effect of the hygrothermal performance of the envelope on orientation, envelope height, wind-driven rain, retrofit placement, air leakage, and liquid transport was evaluated for high-rise envelopes. The hygrothermal performance of three basic wall and three roof systems were investigated for seven different climatic locations in Canada in an 1-D analysis. The wall systems considered were: a brick veneer steel stud back-up; a brick veneer and concrete block back-up and an exterior finish system Two retrofit strategies were performed on each wall system for each of the seven climatic locations. In addition four wall orientations were examined for all cases. A set of 2-D infiltration/exfiltration simulations of a brick veneer steel stud wall were performed with climatic data of Ottawa and some defects were included in the analysis.

A significant part of the study determined the sensitivity of various input parameters on the hygrothermal response of various high-rise wall systems. This study is unique in many regards; it is the first study of high-rise building envelopes systems that has quantitatively evaluated the long-term hygrothermal performance of the envelope which includes the effects of liquid transport, wind-driven rain and air movement. The hygrothermal performance for all wall and roof systems were evaluated employing the transient moisture capacity of each material layer (sorption-suction isotherms).

The conclusions presented show that by employing modeling, important understanding can be developed that assists in the development of design guidelines for moisture control. The results show a strong effect of climatic conditions/location on the moisture performance of the wall systems. Orientation, location and height of the building are all important design parameters that can influence the hygrothermal performance of the envelope system. For example, retrofitting using the same insulation placement strategy for the brick-veneer wall system, but for two different climatic locations (Vancouver and Resolute) produced positive and negative implications on the hygrothermal performance of the wall. The effects of infiltration/exfiltration of the wall systems considered showed that both wind-driven rain and convective vapor transport developed similar magnitudes of moisture accumulations during different times of the year. Including the effects of wind-driven rain liquid transport and convective vapor transport the hygrothermal response of the walls were found to be several times higher than those that only including the effects of vapor transport by diffusion. It was demonstrated that applied moisture engineering by modeling effectively allows one to assess various design and retrofit strategies and develop ranking of various envelope systems to climatic locations.

ACKNOWLEDGEMENTS

EXECUTIVE SUMMARY

The service life of a building envelope system depends in part on the integrated approach employed during conception. Even today, building envelope designs are not subject to a complete moisture engineering analysis, and as a consequence moisture is the leading cause of damage in high-rise residential buildings. Current building envelope design practices are far from state-of-the-art, and are still based on traditional know-how. Retrofitting activities of high-rise buildings are projected to increase steadily, however, our understanding of the combined heat-air and moisture behavior of building systems is not complete, this has in many instances lead to unacceptable rapid deterioration, high maintenance costs and occupant heath problems.

In this study, an advanced hygrothermal computer model, LATENITE 1.1 developed at National Research Council Canada NRCC, was used to simulate the long-term complex heat -air and moisture transport processes occurring in residential high-rise building envelope systems. The mechanisms included were: water vapor transport, liquid water transport, moisture storage, evaporation-condensation-freeze-thawing processes, solar radiation, rain penetration due to wind-driven rain and in some cases the air flow through the building envelope system. This study is a feasibility study on the application of modeling in moisture analysis. This field has evolved considerably during the last 4 years. For the majority of the project, the wall and roof systems were ideal systems (without the inclusions of unintentional defects).

The hygrothermal performance of three basic wall and three roof systems were investigated for seven different climatic locations in Canada in an 1-D analysis. The wall systems considered were: a brick veneer steel stud back-up; a brick veneer and concrete block back-up and an exterior finish system Two retrofit strategies were performed on each wall system for each of the seven climatic locations. In addition four wall orientations were examined for all cases. A set of 2-D infiltration/exfiltration simulations of a brick veneer steel stud wall were performed with climatic data of Ottawa and some defects were included in the analysis.

A significant part of the study determined the sensitivity of various input parameters on the hygrothermal response of various high-rise wall systems. This study is unique in many regards; it is the first study of high-rise building envelopes systems that has quantitatively evaluated the long-term hygrothermal performance of the envelope which includes the effects of liquid transport, wind-driven rain and air movement. The hygrothermal performance for all wall and roof systems were evaluated employing the transient moisture capacity of each material layer (sorption-suction isotherms).

The conclusions presented show that by employing modeling, important understanding can be developed that assists in the development of design guidelines for moisture control. The results show a strong effect of climatic conditions/location on the moisture performance of the wall systems. Orientation, location and height of the building are all important design parameters that can influence the hygrothermal performance of the envelope system.   For example, retrofitting using the same insulation placement strategy for the brick-veneer wall system, but for two different climatic locations (Vancouver and Resolute) produced positive and negative implications on the hygrothermal performance of the wall. The effects of infiltration/exfiltration of the wall systems considered showed that both wind-driven rain and convective vapor transport developed similar magnitudes of moisture accumulations during different times of the year. Including the effects of wind-driven rain liquid transport and convective vapor transport the hygrothermal response of the walls were found to be several times higher than those that only including the effects of vapor transport by diffusion. Today, vapor control diffusion has been the only element considered in building envelope designs in Canada.

SOMMAIRE

Performance hygrothermique des tours d'habitation par Achilles Karagiozis du Conseil national de recherches du Canada.

Le Conseil national de recherches du Canada et la Société canadienne d'hypothèques et de logement ont mené un projet de recherche conjoint dans le but de déterminer la performance hygrothermique de différents murs et toits constituant l'enveloppe de tours d'habitation. On en est arrivé à obtenir une compréhension fondamentale de la transmission combinée de la chaleur et de l'air ainsi que de l'humidité en ayant recours au modèle hygrothermique à la fine pointe de la technologie, le LATENITE 1.1. Une analyse de sensibilité des procédés hygrothermiques a d'abord été élaborée en vue de déterminer les effets de l'exactitude des propriétés des matériaux, des conditions d'origine et des conditions limites. Trois murs et toits ont ensuite été examinés dans le cadre de la présente étude dans sept zones climatiques canadiennes. Deux stratégies de rattrapage ont été utilisées pour chaque mur. L'effet de la performance hygrothermique de l'enveloppe sur l'orientation, la hauteur de l'enveloppe, la pluie poussée par le vent, la mise en place de mesures de rattrapage, l'étanchéité à l'air et le transport d'eau sous forme liquide ont été évalués à l'égard de l'enveloppe des bâtiments. La performance hygrothermique de trois murs et de trois toits a été étudiée pour six zones climatiques du Canada lors d'une analyse unidirectionnelle. Voici les murs pris en considération : un mur de fond à ossature d'acier revêtu d'un placage de brique; un mur de fond en blocs de béton revêtu d'un placage de brique et un système de finition extérieur. Deux stratégies de rattrapage ont été pratiquées sur chaque mur pour chacune des sept zones climatiques. De plus, quatre orientations murales ont été étudiées dans chacun des cas. Un jeu de simulations bidirectionnelles d'infiltration et d'exfiltration d'un mur à ossature d'acier avec placage de brique a été pratiqué en fonction des données climatiques d'Ottawa et certains défauts ont été inclus dans l'analyse.

Une proportion importante de l'étude était consacrée à l'effet de sensibilité de divers paramètres d'entrée sur la réaction hygrothermique de différents murs de tours d'habitation. Cette étude est particulière à bien des égards; c'est la première fois qu'une étude portant sur l'enveloppe de tours d'habitation évalue en termes quantitatifs la performance hygrothermique à long terme de l'enveloppe, en incluant les effets du transport de l'eau sous forme liquide, de la pluie poussée par le vent et du mouvement d'air. La performance hygrothermique de tous les murs et toits a été évaluée à l'aide de la capacité d'humidité transitoire de chaque couche de matériau (isothermes de sorption-succion).

Les conclusions présentées montrent que la modélisation permet de bien comprendre le phénomène de manière à favoriser l'élaboration de directives conceptuelles axées sur l'élimination de l'humidité. Les résultats indiquent l'énorme effet des conditions climatiques ou de l'endroit sur la performance à l'humidité des murs. L'orientation, l'endroit et la hauteur du bâtiment constituent tous des paramètres de conception importants qui risquent d'influer sur la performance hygrothermique de l'enveloppe. À titre d'exemple, procéder à des mesures de rattrapage en utilisant la même stratégie de mise en oeuvre de l'isolant thermique pour le mur revêtu de placage de brique, mais pour deux zones climatiques différentes (Vancouver et Resolute) a eu des répercussions positives et négatives sur la performance hygrothermique du mur. Les effets de l'infiltration/de l'exfiltration des murs considérés montrent que la pluie poussée par le vent et le

transport de vapeur d'eau par convection accumulent l'humidité avec des ampleurs semblables à différents moments de l'année. La réaction hygrothermique des murs qui incluaient les effets du transport de la pluie poussée par le vent et de la vapeur d'eau par convection, a été plusieurs fois plus élevée que dans ceux qui ne tenaient compte que des effets du transport de la vapeur d'eau par diffusion. Il a été démontré que le génie appliqué en matière d'humidité grâce à la modélisation efficace permet d'évaluer différentes stratégies de conception et de rattrapage et de coter différents systèmes d'enveloppe selon les zones climatiques.

RÉSUMÉ

La durée utile de l'enveloppe d'un bâtiment dépend en partie de la démarche intégrée adoptée lors de la conception. Même de nos jours, l'enveloppe des bâtiments n'est pas soumise à une analyse hygrométrique complète au stade conceptuel; c'est pourquoi l'humidité est la cause la plus importante de méfaits dans les tours d'habitation. Les techniques courantes en matière de conception de l'enveloppe des bâtiments sont loin d'être à la fine pointe de la technologie; au contraire, elles sont toujours fondées sur le savoir-faire traditionnel. Selon les projections, les activités de rattrapage à l'égard des tours d'habitation devraient accuser une augmentation constante, mais notre compréhension du comportement des ensembles de construction sous l'effet de la chaleur et de l'air ainsi que de l'humidité n'est pas parfaite, si bien que cette situation donne lieu, dans bien des cas, à une détérioration rapide inacceptable, à des frais d'entretien élevés et causé des ennuis de santé aux occupants.

Dans cette étude, un modèle informatique perfectionné de comportement hygrothermique, LATENITE 1.1, mis au point au Conseil national de recherches du Canada (CNRC), a servi à simuler le processus complexe du transport de chaleur et d'air et d'humidité à long terme auquel est soumise l'enveloppe des tours d'habitation. Les mécanismes étudiés portaient sur la transmission de vapeur d'eau; la transmission d'eau sous forme liquide; le stockage d'humidité; le processus d'évaporation, de condensation, de gel et de dégel; le rayonnement solaire; la pénétration de la pluie poussée par le vent; et, dans certains cas, le mouvement d'air à travers l'enveloppe du bâtiment. Cette recherche se veut une étude de faisabilité quant à l'application de la modélisation pour l'analyse hygrométrique. Cette sphère d'activité a connu une évolution remarquable au cours des quatre dernières années. Pour la majorité du projet, les murs et toits constituaient des systèmes idéaux (sans l'inclusion de défauts non intentionnels).

La performance hygrothermique de trois murs de base et de trois toits a été étudiée en fonction de sept zones climatiques canadiennes dans le cadre d'une analyse unidirectionnelle. Voici les murs pris en considération : un mur de fond à ossature d'acier revêtu d'un placage de brique; un mur de fond en blocs de béton revêtu d'un placage de brique et un système de finition extérieur. Deux stratégies de rattrapage ont été pratiquées sur chaque mur pour chacune des sept zones climatiques. De plus, quatre orientations murales ont été étudiées dans chacun des cas. Un jeu de simulations bidirectionnelles d'infiltration et d'exfiltration d'un mur à ossature d'acier avec placage de brique a été pratiqué en fonction des données climatiques d'Ottawa et certains défauts ont été inclus dans l'analyse.

Une proportion importante de l'étude était consacrée à l'effet de sensibilité de divers paramètres d'entrée sur la réaction hygrothermique de différents murs de tours d'habitation. Cette étude est particulière à bien des égards; c'est la première fois qu'une étude portant sur l'enveloppe de tours d'habitation évalue en termes quantitatifs la performance hygrothermique à long terme de l'enveloppe, en incluant les effets du transport de l'eau sous forme liquide, de la pluie poussée par le vent et du mouvement d'air. La performance hygrothermique de tous les murs et toits a été évaluée à l'aide de la capacité d'humidité transitoire de chaque couche de matériau (isothermes de sorption-succion).

Les conclusions présentées montrent que la modélisation permet de bien comprendre le phénomène de manière à favoriser l'élaboration de directives conceptuelles axées sur l'élimination de l'humidité. Les résultats indiquent l'énorme effet des conditions climatiques ou de l'endroit sur la performance à l'humidité des murs. L'orientation, l'endroit et la hauteur du bâtiment constituent tous des paramètres de conception importants qui risquent d'influer sur la performance hygrothermique de l'enveloppe. À titre d'exemple, procéder à des mesures de rattrapage en utilisant la même stratégie de mise en oeuvre de l'isolant thermique pour le mur revêtu de placage de brique, mais pour deux zones climatiques différentes (Vancouver et Resolute) a eu des répercussions positives et négatives sur la performance hygrothermique du mur. Les effets de l'infiltration/de l'exfiltration des murs considérés montrent que la pluie poussée par le vent et le transport de vapeur d'eau par convection accumulent l'humidité avec des ampleurs semblables à différents moments de l'année. La réaction hygrothermique des murs qui incluaient les effets du transport de la pluie poussée par le vent et de la vapeur d'eau par convection, a été de plusieurs fois plus élevée que dans ceux qui ne tenaient compte que des effets du transport de la vapeur d'eau par diffusion. De nos jours, la diffusion de vapeur d'eau constitue le seul élément pris en considération lors de la conception de l'enveloppe de bâtiments au Canada.

National Office Bureau national

700 Montreal Road 700 chemin de Montréal
Ottawa ON K1A 0P7 Ottawa ON K1A 0P7
Telephone: (613) 748-2000 Téléphone : (613) 748-2000

Puisqu'on prévoit une demande restreinte pour ce document de recherche, seul le résumé a été traduit.

La SCHL fera traduire le document si la demande le justifie.

Pour nous aider à déterminer si la demande justifie que ce rapport soit traduit en français, veuillez remplir la partie ci-dessous et la retourner à l'adresse suivante :

Centre canadien de documentation sur l'habitation
Société canadienne d'hypothèques et de logement
700, chemin Montréal, bureau C1-200
Ottawa (Ontario)
K1A 0P7

Titre du rapport: _____

_____

Je préférerais que ce rapport soit disponible en français.

NOM _____

ADRESSE_____
  rue   App.

_____
  ville   province   Code postal

No de téléphone (   ) _____

2.2 INFLUENCE OF MATERIAL PROPERTIES ON THE HYGROTHERMAL PERFORMANCE OF HIGH RISE WALLS 21

2.3 TASK A: RELATIVE INFLUENCE OF HEAT, AIR AND MOISTURE TRANSPORT PROPERTIES SUBJECTED TO ± 25% UNIFORM VARIATIONS IN PROPERTIES OF INDIVIDUAL MATERIALS 22

2.4 TASK B: EFFECT OF SIMPLIFYING MATERIAL PROPERTY TO DETERMINE INFLUENCE ON THE HYGROTHERMAL PERFORMANCE OF A WALL 23

2.5 TASK C: EVALUATION OF THE IMPACT OF VARIABLE MATERIAL PROPERTIES USING STOCHASTIC MODELING 25

3.0 HEAT-AIR-MOISTURE MODELING 30

3.1 MODEL APPLICABILITY 30

High-Rise Hygrothermal Modeling Requirements 30

Assessment of Model Applicability 31
TCCC-2D VTT/IRC Model (1992) 31
Moist Model 32
LATENITE Model 1.0 (1992) and LATENITE 1.2 (1994) 33
CMHC WALLFEM-3D v1.0 Model (1992-93) 33

LATENITE 1.0 GOVERNING EQUATIONS 36

4.0 BOUNDARY CONDITIONS 40
Introduction...40

4.1 WALL BOUNDARY CONDITIONS 42
Comparison of Weather Data 44

4.2 NUMERICAL 3-D SIMULATION OF WIND FLOW AND WIND DRIVEN RAIN 46
Introduction...46
Wind Driven Rain 48
Modeling Method 48
Rain Droplet Modeling 48
Building Structures and Computation Domain 50
Simulation Cases 51

List of Tables and Figures

TABLES IN APPENDIX A

FIGURES IN APPENDIX A

FIGURES IN APPENDIX C

NOMENCLATURE
List of Symbols

c_P	Effective heat capacity of material	$J / kg.K$
$D_{w_{.,}}$	Moisture diffusivity in x and y direction	m^2 / s
F	Flux vector in the x-direction	
G	Flux vector in the y-direction	
k_j	Thermal conductivity in j direction	W / mK
l	Latent heat	J / kg
P_v	Vapor pressure	Pa
$\dot{m}_m$	Total moisture flux	$kg / m^2 s$
$\dot{m}_{vap}$	Vapor moisture flux	$kg / m^2 s$
$\dot{m}_{liq}$	Liquid moisture flux	$kg / m^2 s$
q_T	Heat flux	W / m^2
t	Time	s
R	Jacobian matrix due to linearization	$\dfrac{\partial F}{\partial U}$
S	Jacobian matrix due to linearization	$\dfrac{\partial F}{\partial U}$
$\dot{S}$	Heat source	W / m^3
T	Temperature	°C
u	moisture content of material	kg / kg
U	Unknown vector	
V	Viscous vector in the x-direction	
v	Velocity component	m / s
W	Viscous vector in the y-direction	
x	Cartesian direction x	
y	Cartesian direction x	

Greek Symbols

ρ_o	Dry density of porous material	kg / m^3
ρ_{eff}	Effective density of material	kg / m^3
ρ_v	Vapor density	kg / m^3
δ_{Px}	Vapor permeability in x direction $kg / s.Pa.m$	
δ_{P_y}	Vapor permeability in y direction $kg / s.Pa.m$	
θ	Time-step parameter	
Δt	Time-step	s

PREFACE

This document reports on the results of a joint research project between CMHC and NRC concerning the "Analysis of the Hygrothermal Behaviour of High Rise Residential Building Components" (contract A3052). Following is a brief summary of events that altered and hopefully enhanced in several ways the scope and the objectives of this project. In July 1992, NRC was approached by CMHC, to develop a working relationship on common areas of strategic research concentrating on hygrothermal modelling of building envelope systems. NRC, recognised internationally for its expertise in the area of applied heat-air and moisture transport modelling, accepted to undertake jointly with CMHC a research project entitled "Analysis of the Hygrothermal Behaviour of High Rise Residential Building Components". Both CMHC and NRC recognised that such a modelling initiative was unique world-wide, especially since a model to handle such highly demanding conditions encountered by high-rise building envelopes was not yet available, although CMHC had invested resources in various heat and moisture model developments, and in particular, the more recent WALLFEM-3D hygrothermal model. WALLFEM-3D promised capabilities that would have made this particular model very powerful and suitable for high-rise simulations. NRC's involvement was to thoroughly apply this model to understand the complex interaction of heat, air and moisture transport on the energy and durability performance of various high-rise building envelope parts. The long-term outcome from this joint CMHC-NRC venture was to thoroughly benchmark and further develop WALLFEM into a unique building envelope design tool. This tool would be employed both by researchers and consultants to assess the design and retrofit strategies of new and existing buildings with respect to hygrothermal performance. Indeed, the concurrent involvement by CMHC (by Mr. Hamlin and Mr. Hill) and NRC (by Dr.'s Kumaran and Karagiozis) in the activities of International Energy Agency (IEA) Annex 24 allowed access to the most current information about hygrothermal performance on building envelopes, in addition to the collaboration with some of the most knowledgeable people world-wide in moisture. Involvement in IEA Annex 24 complimented the overall objectives of this work.

In October 1992, the first attempt to use WALLFEM-3D in the second IEA Annex 24 common exercise was only half successful. CMHC and NRC jointly participated in the IEA Annex common exercise. The results from this common exercise demonstrated that the WALLFEM-3D model was not capable of handling convective air flow transport of moisture. However, WALLFEM-3D did perform satisfactory with regards to vapor diffusion transport and good agreement with other moisture models was found for those conditions (this common exercise did not involve liquid moisture flow). Further studies carried out at CMHC (Mr. Hamlin and Mr. Gusdorf and NRC (Dr. Karagiozis) indicated additional inconsistencies with the model. Upon repeated requests by Mr. Hamlin to G.K. Yuill &

Associates to address these deficiencies resulted in a new theoretical approach. Dr. Kerestecioglu, the WALLFEM-3D model developer adopted a different set of governing potentials for moisture transport (Luikov type). The new revamped WALLFEM-3D was delivered mid-1993 and again several major limitations were found upon critically reviewing the model by Mr. Gusdorf, Mr. Hamlin, Dr. Karagiozis and Mr. Salonvaara. Having already spent a considerable amount of time on benchmarking WALLFEM-3D, it became clear that another model was needed to carry out this project.

A hygrothermal model to predict the long-term performance of high-rise envelope components did not exist according to the IEA Annex 24 report "Enquiry on HAMCat Codes" in 1993. This provided a major challenge toward the viability and the direction of this joint project by altering the initial scope of the project. At this critical stage of the project, NRC undertook a strategic initiative to further enhance the in-house hygrothermal model development. This task was deemed impossible to achieve within the time constraints of this project but nonetheless a model was delivered in February 1994. The NRC hygrothermal model entitled LATENITE, developed by Dr. Karagiozis, has been used in this project to understand the fundamentals involved in the energy and moisture transport of high-rise walls and roofs. Many simulations were developed to determine the hygrothermal performance of high-rise walls and roofs, ideally designed (without flaws). Some retrofit strategies on selected wall systems were also examined. Most of the work concentrated with one-dimensional sections but a few two dimensional cases with air flow were also investigated. This work carried out pioneering research in the area of moisture engineering modeling for high rise envelope systems. The work concentrated on investigating the influence of important parameters that affect the overall hygrothermal performance of building envelope systems, these being; material properties, wall design, and boundary conditions. Material properties were found to significantly influence the total building envelope system heat and moisture performance. Wall design and retrofit strategy layout dominated the hygrothermal performance of the system. The two most important boundary conditions that influenced the hygrothermal performance were infiltration/exfiltration (air leakage) characteristics and wind-driven rain. Emphasis was given mostly on wind-driven rain as this is suspected to be one of the most important cause for high-rise facade deterioration. The combined influence of infiltration/exfiltration mechanisms and stack effect as a function of height of the high-rise structure was also investigated in detail for one wall system.

During this period (1994-1995), NRC's LATENITE hygrothermal model had been theoretically as well as experimentally, benchmarked against several IEA Annex 24 common exercises and very good agreement was observed. This gave additional confidence that the simulation result, can be of strategic value as far as design and retrofit consequences are of concern.

This report is formatted in the following manner:

- Section 1 gives a general overview of Canadian high-rise residential buildings, the main objectives of the work and the type of wall and roof sections analyzed.

- Section 2 describes the necessary boundary condition information required to predict the hygrothermal performance of high-rise building envelope systems.

- Section 3 gives details about the three wall and three roof building envelope system studied in this work.

  Section 4 presents all relevant information about the results from the simulations and conclusion drawn from these results.

  APPENDIX
- Appendix A1 this appendix demonstrates the influence of hygrothermal material properties on the simulation results.

- Appendix B1 formulates the turbulent Navier Stokes equations for flow around high-rise buildings
- Appendix C tabulates the total moisture content and heat fluxes for the high-rise wall and roof structures examined in this report

1.   INTRODUCTION

High-rise buildings as defined by the Canadian National Building Code is a construction entity that does not fall under Part 9 of the Code. Usually, high-rise buildings are composed of four or more floors. Two general types of high-rise buildings exist: commercial and residential. This project deals with high-rise buildings of the residential type. Being residential high-rise buildings, they are more diverse in design layout, mechanical systems employed, in the choice of exterior facade types and in their specific site. The hygrothermal (combined heat-air and moisture transfer) performance of various building envelope systems are investigated in this report for residential high-rise buildings. The primary aim of this joint IRC-CMHC project was to understand the system performance of various high-rise wall and roof parts with respect to heat-air and moisture transport.   Another important aim was to predict the long-term performances of various retrofit strategies from which these wall systems benefited.

In this section relevant background information is presented on Canadian high-rise buildings, followed by an outline of the objectives of this project and the definition of the wall and roof types investigated.

1.1   Background

Strategic Importance of High-Rise Buildings

Residential high-rise buildings constitute a major portion of Canada's housing, particularly in urban areas. By all indications, it is a type of housing that will continue to represent a significant portion of the total housing projects in Canada.   Historically in Canada, residential high-rise constructions are almost exclusively a product of the post-war era, with approximately 98% of the building constructed after 1945. Most high-rise buildings, about 65%, have been built between 1961 and 1975 coinciding with the rental building boom.   The City of Toronto alone has an estimated 90,000 units (Hemson Consulting Ltd. 1992), accounting for approximately one-third of the city's housing stock. About 62,000 units , are private rental apartments. They make up 23% of the total housing stock. Other cities report lower figures. In Halifax for example, private rental apartment units make up 10.2% of the total housing stock (Chambers, 1993) or Edmonton, where the proportion is as low as 8.3% (S.P.B., 1991). In Ontario, estimates made by the Province and CMHC show 350,000 to 465,000 units derived from about 3,500 high-rise buildings, are currently occupied. These figures represent approximately 40 % of the Ontario rental stock (Green 1992). In summary, the residential high-rise buildings, and especially the private rental apartment units, make up a significant part of the total housing stock across the country.

Figure 1-1 shows the trend followed by private rental high-rise construction over the past several decades in the City of Toronto. The vast majority of these buildings are 20 years old or more, not particularly well built or maintained, resulting in a large number of durability problems associated with this type of building.

City of Toronto

Total Buildings = 464

Number of Buildings

250	
200	
150	
100	
50	
0	Pre 1920 1920-40 1940-50 1950-60 1960-70 1970-80 1980-90

Decade
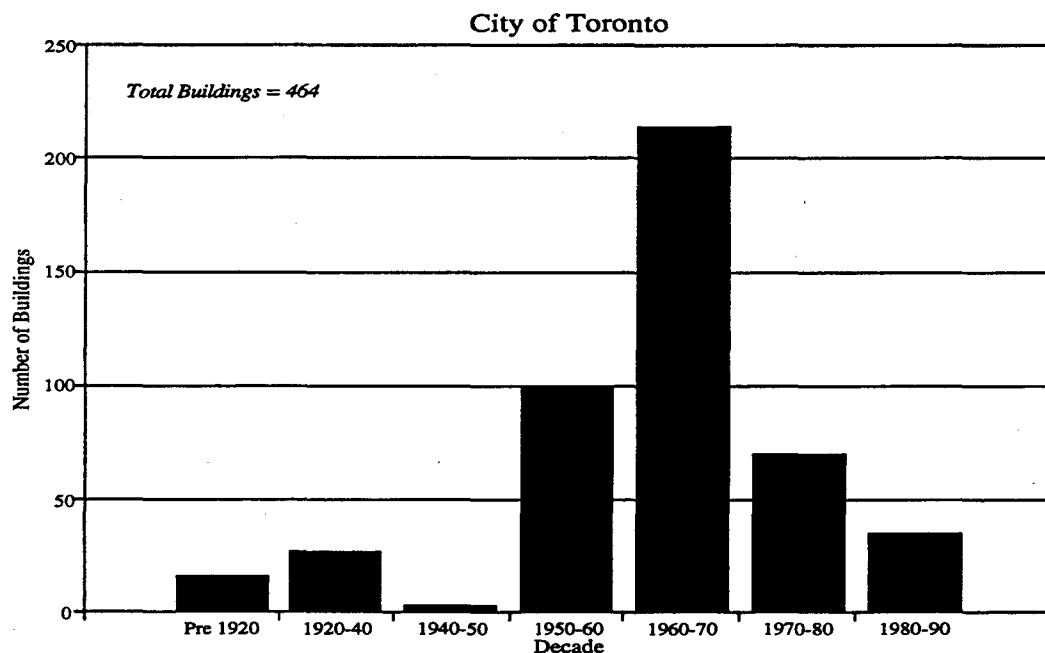
Figure 1-1: Private Rental High-rise Building Constructions

Figure 1-2, on the other hand, shows the trend in private rental high-rise unit construction in the City of Toronto over the same time period. Note the definite shift in quantities toward the more recent decades between Figure 1-1 and Figure 1-2. This shift demonstrates that although fewer buildings were built in the later decades, these were much larger than earlier structures. Problems with these buildings, therefore, would be even more expensive to repair.

City of Toronto

Total Units = 62056
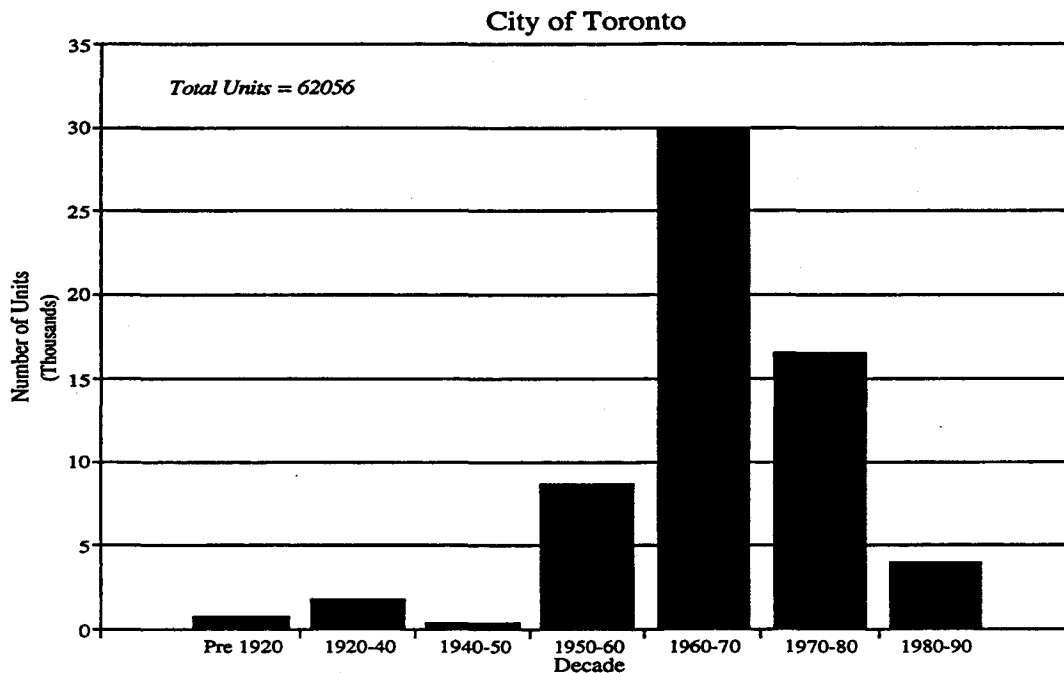
Figure 1-2: Private Rental High-rise unit Constructions

Hygrothermal Problems Experienced in High Rise Buildings

High-rise wall systems with load or non-load-bearing capabilities have been implemented with various degrees of success in the Canadian market. Some of these systems attempt to incorporate the open rain-screen principle i.e. a curtain wall, by using glass, stone, metal, or pre-cast concrete facades, masonry with an appropriately designed vent air space to provide the necessary capillary break and air pressure equalization to minimize rain penetration. Other non-load-bearing wall systems, such as the insulated masonry block walls, use a suitable facade, such as brick or metal siding or other durable material, as well as a vented air space for the same purposes as those used by curtain walls. Cast-in-place or pre-cast concrete spandrel and panels are a variation of the previous wall systems. Another variation is the load-and non-load-bearing light-steel framing walls including different types of veneer facings. Masonry walls have functioned reasonably well, but were massive, ranging from 0.3 to 1.8 m in thickness (BIA 1985) and were under constant compression due to the structural load thereby mininizing water entry and accumulation. Furthermore, older high-rise buildings were built with cornices (large overhangs at the top), and other architectural features which reduced the amount of direct wind-driven rain on the facades of the buildings. Newer high-rise buildings seldom include such features and as a consequence, walls are exposed to greater amounts of liquid water, giving rise to possible water penetration problems.

Detailed literature is available concerning design details and the performance of these types of high-rise walls in publication notes/papers/reports by Division of Building Research(DBR,NRCC), CMHC, Drysdale, Keller, and Hemson. However this does not imply that design flaws, premature deterioration and loss of service life have been eliminated. A considerable amount of work is still required to properly document and provide design guidelines for various building envelope parts at different locations in Canada. A recent survey conducted by CMHC (Drysdale 1991) showed that most of the high-rise buildings reviewed, though less than 2 years old, reported rain penetration problems. Older buildings display similar, but considerably advanced, freeze-thaw damage, corrosion, spalling due to lack of movement joints, more staining and damage due to in-wall condensation.

During the 1960s, when the construction of private rental high-rises reached its peak, the construction techniques and expert knowledge necessary to prevent building envelopes from moisture related problems were not available. As a result, many of these buildings now suffer serious surface/facade and concealed deterioration problems and therefore require major repairs.

Water can be present in high-rise building envelopes in three physical states: vapour, liquid, and ice. Under certain conditions, a wall holding a significant amount of water can be damaged. Freeze-thaw conditions may cause cracking, crazing, spalling and disintegration. Water can also cause dimensional changes to walls, corrosion of metal components, deterioration of insulation, damage of interior and exterior finishes, and efflorescence on exterior surfaces. Water penetration can also be linked to the growth of moulds in wall cavities and on interior surfaces.

Recently, the Ontario New Home Warranty Program (ONHWP, 1993) reported costs on claims relating to high-rise condominiums have increased drastically from $4.3 million in 1986 to $20 million in 1990. A total of 52 high-rise condominiums constructed in the late 1980's were studied and more than half had developed problems in the initial years of occupancy. Most of these were identified as moisture-related, caused by rain or snow penetration or by high interior moisture levels.

Public Works and Government Services Canada reported a case in Montreal in which the air/vapour barrier did not perform properly and had to be replaced (Cheung, 1993). The lack of air tightness allowed moisture-laden air to circulate throughout the building envelope, causing moisture-related deterioration. Due to the location of the barrier within the wall cavity, the repairs entailed the replacement of not only the air/vapour barrier but also the insulation and the facing brick. Another building, located in Toronto, experienced similar problems. In this case, the major contributing factors included brick veneer with poor freeze-thaw resistance, poorly installed flashing,

and inadequate detailing. This building was only 10 years old yet already suffered from extensive damage.

Typically, the maintenance and repair standards for the class of rental high-rise buildings are inferior when compared to condominium apartments or private dwellings (Green, 1992). This, combined with the advanced age of many of these apartment complexes, are the primary reasons for this type of building falling victim to moisture-related deterioration problems. To repair them can be very expensive. One such case involving a high-rise condominium complex in Nepean Ontario, resulted in a repair bill of $20,000 per condominium unit (this cost included electrical, mechanical and interior finish upgrades). In this instance the resident-owners were responsible for the cost of repair (Ottawa Citizen, 1992). In a private rental apartment complex, however, it becomes the owner's problem.

Maintenance and Repair

According to Hemson Consulting Ltd. (1992), the cost of preventive maintenance aimed at avoiding such major problems can be very expensive, particularly in poorly constructed buildings. As can be expected, the older the building, the more expensive the initial cost. [Table 1-1 gives estimated costs related to building conservation (cost to upgrade and subsequently maintain the building). Note that the initial costs vary significantly with building age, while the ongoing costs are much more consistent.]

These values represent the average costs for buildings in "good" and "poor" condition combined, not the average cost for buildings in "average" condition. Again, these costs would be directly applied to the building owner in private rental apartments, along with the problem of recovering the financial loss.

Maintenance and repairs can be minimized or even avoided through proper design of the building envelope. Expert knowledge in moisture control and strict guidelines are imperative for a properly designed building envelope. Achieving such a goal requires the determination of the best design method for a given location. Marrying experimental and modeling results of the long-term hygrothermal performance of high-rise residential buildings, it is possible to predict (a) the long-term performance with respect to durability and energy and (b) the expected problems associated with a specific wall configuration. This information allows the designer to examine possibilities for second line of defence strategies. Consequently, steps can be taken to alter the wall configuration to eliminate the problem.

Table 1-1: Conservation costs per unit.		
Typical Building	Start-up Costs ($)	Annual Ongoing Costs ($)
1950s	8600	510
1960s	7200	500
1970s	1400	390
1980s	-	495

Hemson Consulting Ltd, "City of Toronto High-Rise Apartment Conservation Study", Nov. 1992

1.2   Objectives

The main objective of this project was to examine the use of computer simulations (modeling) to predict the hygrothermal performance of selected high-rise wall and roof systems, then to apply a retrofit strategy to these walls and re-examine the influence of the retrofit with respect to hygrothermal performance. These can be summarized as:

1. Evaluation of hygrothermal performance of high-rise walls and roof assemblies via computer simulations,
2. Identify major likely influences on durability,
3. Assess the sensitivity of the model to various simplifications and assumptions

To fulfil the objectives of this project it was necessary to limit the scope to a few representative types of building structures. A preliminary investigation was conducted to determine some of the most common envelope construction designs found in Canadian residential high-rise structures. Through consultation with various researchers and building envelope consultants (Kumaran, Karagiozis, Poirier, from IRC.; Lawton, of Morrison Hershfield Ltd.; Jacques Rousseau and Tom Hamlin, of CMHC), and an extensive literature search, Table 1-2, it was found that there exists a multitude of wall and roof design variations and combinations in residential high-rises. However, further discussions revealed that for each part of the building there are a few limited number of basic designs.

For example, there are three primary wall configurations utilized in Canadian high-rises, each having several variations which will be described in detail later. Similarly, three primary roof construction methods exist for high-rise buildings.

Another objective of this project was to uncover specific problem areas related to the long term hygrothermal behaviour of high-rise building components, that should receive special attention during the design stage.

1.3 Construction Variations

Wall Systems

There are three primary (basic) wall systems studied in this report. These reflect common practice for many residential high-rise constructions in Canada. Two of these consist of a brick veneer supported by a backup wall. The third variety is known as EIFS or exterior insulated finish system. Though each has many variations, the project concentrates on one specific common variation of each type of wall.

Table 1-2: Typical high-rise apartment construction				
Decade	% Market Penetration Cladding	Roof Membrane	Suite Windows	Balcony
1951 - 1960	Brick - 100%	BUR - 100%	Single-glaze, Painted Steel Frame - 100%	None - 25% Guards: Metal Panels - 75% Glass Panels - 25%
1961 - 1970	Brick - 95% CIP - 5%	BUR - 100%	Single-glaze - 100% Painted Steel - 7% Unpainted Aluminum - 93%	None - 5% Guards: Metal - 75% Glass - 15% CIP - 10%
1971 - 1980	Brick - 60% Precast - 20% M/C CW - 10%	BUR - 33% IRMA - 67%	Single-glaze - 60% Double-glaze - 40% Prefinished Aluminum Frame - 100%	None - 50% Guards: Precast - 100%
1981 - 1990	Brick - 33% Precast - 21% CIP - 13% CIP + Precast - 14% CIP + Brick - 7% Concrete Block - 7%	IRMA - 100%	Double-glaze, Prefinished Aluminum Frame - 100%	None - 100%

Notes: BUR - Built-up Roof
    CIP - Cast-in-place Concrete
    IRMA - Inverted Roof Membrane Assembly
    M/C CW - Metal/Glass Curtain Wall

Source:Hemson Consulting Ltd. Nov. 1992, Report to the Toronto Housing Department on " City of Toronto High-Rise Apartment Conservation Study".

Brick Veneer/Steel Stud Wall

The first wall examined (see Figure 1-3) is composed of a brick veneer over a steel-stud backup wall. This is currently the most popular type of exterior wall arrangement for new buildings in Canada, primarily because of the ease of construction, lightweight, and less expensive. It has also the advantage of contributing little weight to the building structure, since the weight of the steel-stud wall system is particularly low compared to that of a concrete-block backup wall.
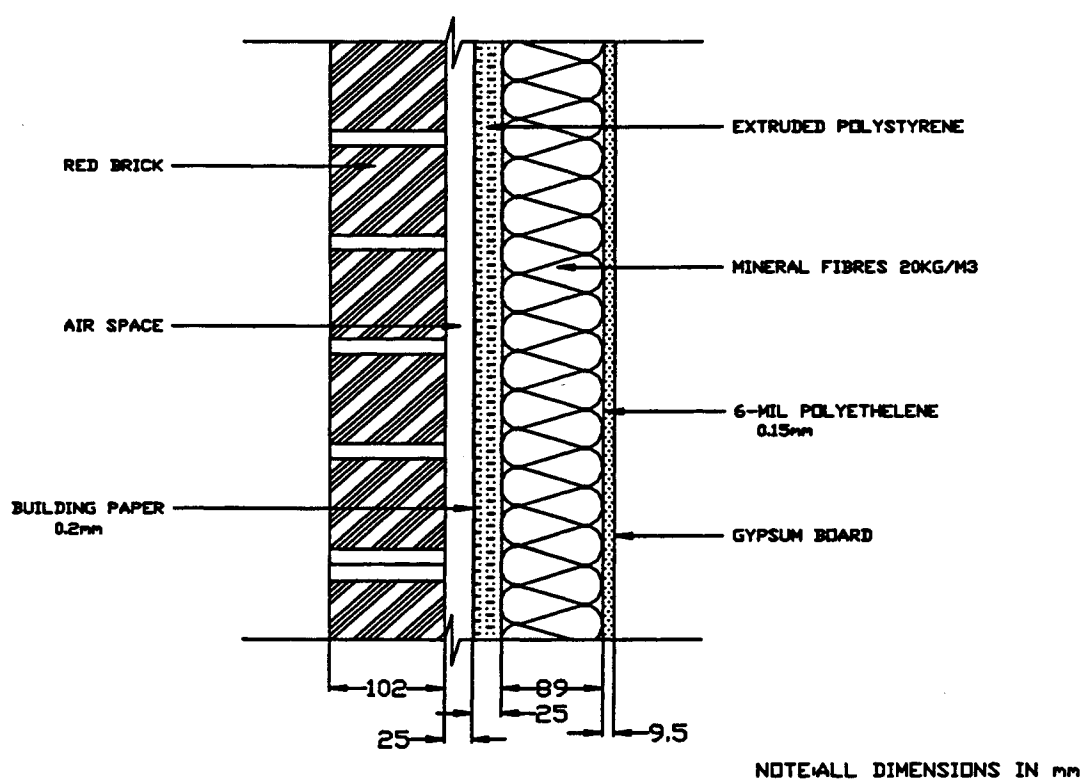
Figure 1-3: Brick veneer/steel stud wall composition

Note that this type of wall is commonly insulated with semi-rigid insulation applied to the outer edge of the studs as well as batt insulation fitted between the studs themselves. A vapour barrier is normally placed on the inside edge of the steel studs and then covered with gypsum board or other interior finish. The semi-rigid insulation is attached directly to the outer face of the steel studs and covered with a sheathing paper that is sometimes intended to act as an air barrier. Several types of insulation used for this purpose are manufactured with the sheathing paper

already attached. The air space is usually designed to be 25 mm wide, but this can also vary significantly. Keller (1989) reports typical wall sections of this sort from various parts of the country that have air spaces ranging from 18 to 55 mm. For the hygrothermal analysis, unvented cavity of a 25-mm air space was used.

Table 1-3 lists the various components of a typical brick veneer over steel-stud wall and also gives the thermal conductivities (k) and the vapour permeabilities (δ_p) associated with each.

Table 1-3: Material thermal and vapour properties for wall 1.			
Material	Thickness (mm)	Thermal Conductivity k (dry) (W/m °C)	Vapor Permeability δ_p (RH=40%) (kg/ m•Pa•s)
Brick Veneer	102	0.4	1.25E-11
Air Space	25	0.15	1.97E-11
Sheathing Paper	0.2	0.16	1.75E-13
Extruded Polystyrene	25	0.028	1.25E-12
Steel Stud System	92	nac.	nac.
Glass Fibre Batt Insulation	89	0.036	1.5-10
Polyethylene Vapour Barrier	0.15	0.17	1.5E-16
Gypsum Board	9.5	0.26	2.0E-11

Brick Veneer/Concrete Block Wall

The second wall considered consists of brick veneer with a backup non-load bearing wall (ie - the block was not parged in and reinforced) built with concrete block. Here, a semi-rigid insulation is placed outside the concrete block. The outer face of the block is coated with a combined air and vapor barrier. This product is usually torched on and becomes a continuous layer. This type of wall construction is detailed below in Figure 1-4. The thermal and vapor properties values of each component are tabulated in Table1-4..

Table 1-4: Material thermal and vapour properties for wall 2.			
Material	Thickness (mm)	Thermal Conductivity k (dry) (W/m °C)	Vapor Permeability δ_p (RH=40 %) (kg/ m Pa s)
Brick Veneer	102	0.4	1.25E-11
Air Space	25	0.15	1.97E-10
Semi-Rigid Glass Fibre Insulation	102	0.038	1.5E-10
Combined Air and Vapour Barrier	0.17	0.16	1.5E-16
Concrete Block with Hollow Core	70	2.7	1.60E-12
Air Space	60	0.15	1.97E-10
Concrete	70	2.7	1.60E-12
Gypsum Board	9.5	0.26	2.00E-11

RED BRICK

AIR SPACE

MINERAL FIBRES 20KG/M3

6-MIL POLYETHELENE
0.15mm

ANNEX CONCRETE

AIR SPACE

ANNEX CONCRETE

GYPSUM BOARD

|—102—| |—102—|—70—| |—70—|
25—| |—   60—| |—9.5
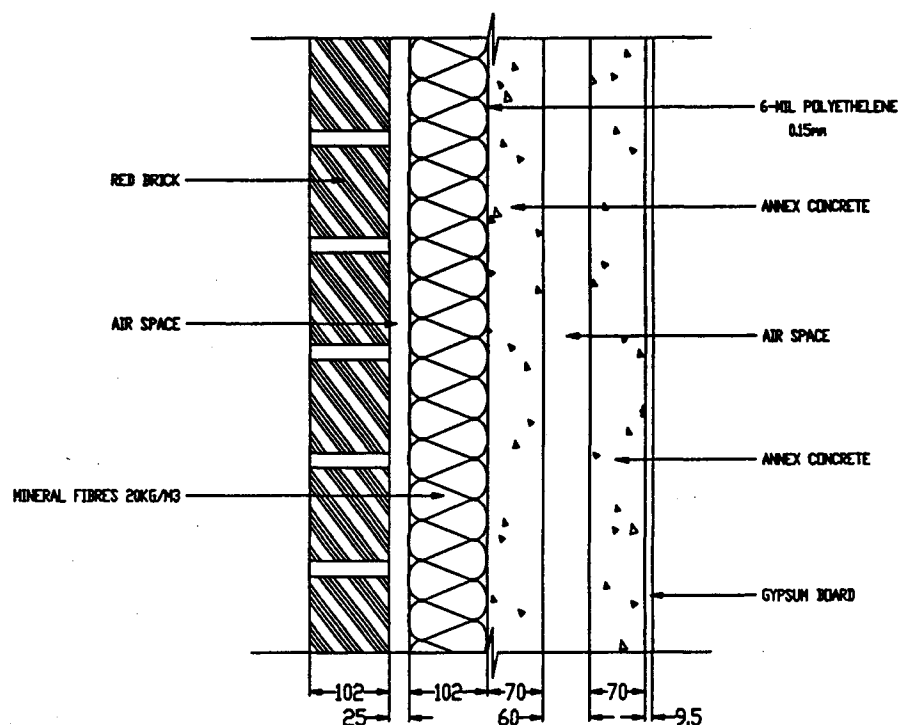
NOTE: ALL DIMENSIONS IN mm

Figure 1-4: Non Load Bearing Brick veneer/concrete block wall composition.

Exterior Insulated Finish System

The third wall system considered is an exterior insulated finish system (EIFS). Though the first two wall types are by far more commonly used in Canada, the EIFS is (1993) quickly gaining popularity, particularly on the West Coast. It has the advantage of allowing the area between the steel studs to be used for services without affecting the insulating capacity of the wall. According to Edgar (1992), other advantages include the placement of the insulation on the outside of the wall, which is more effective, and the versatility concerning finishes.

Again, there are several variations of the EIFS method of construction. The variant used is shown in Figure 1-5. An exterior grade gypsum board is fastened to the

STUCCO FINISH

EXTRUDED POLYSTYRENE

GYPSUM BOARD

AIR SPACE

GYPSUM BOARD

5
75
13
92
9.5

NOTE: ALL DIMENSIONS IN mm
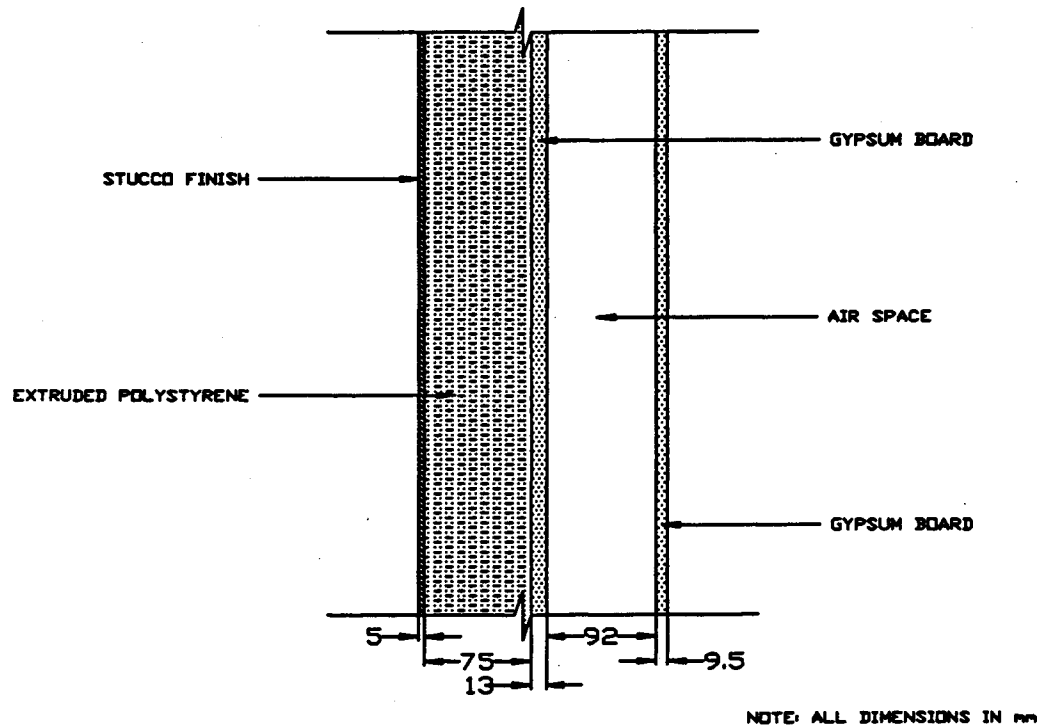
Figure 1-5: Site Applied EIFS wall composition

outer edge of the steel studs. The insulation is then applied to the outer face of this gypsum sheathing, normally by gluing or by mechanical fastening. The insulation is, in turn, protected by a primer, a polymer-based or polymer-modified base coat and then a finish that can be textured as desired, similar to a stucco finish. Many different colours, textures and shapes are available. These exterior finish layers also act as a vapour control layers. A reinforcing mesh is embedded in the base coat to provide increased support for the finish. Also, most new installations include an air barrier between the exterior sheathing and the insulation. Table 1-5 lists the respective thermal and vapour resistances for an EIFS system.

One of the major problem with EIFS construction involves the joints in the insulation, and at penetrations such as windows, mechanical and electrical services, and much care must be taken to ensure a proper seal.

Table 1-5: Material thermal and vapour resistances, wall 3.			
Material	Thickness (mm)	Thermal Conductivity k (dry) (W/m °C)	Vapor Permeability δ_p (RH=40 %) (kg/ m Pa s)
Textured Finish Base Coat Primer	5	0.15	8.0E-12
Reinforcing Mesh	N/A	nac.	nac.
Extruded Polystyrene Insulation	75	0.024	1.25E-12
Exterior Grade Gypsum Board	13	0.28	2.2E-11
Steel Stud System	92	nac.	nac.
Gypsum Board	9.5	0.26	2.0E-11

Roof Systems

Fortunately, here as with the walls, only three primary roof types are commonly used in Canada. These basic roof configurations are known as built-up roofs, single membrane roofs and inverted assembly roofs. The variations tend to be very minor, such as a differing number of plies of asphalt felt or a different thickness of insulation. The overall arrangement, however, remains very consistent. Specific details were taken from CRCA (1990).

Built-up Roof

The first type of roof construction considered was the built-up roof (see Figure 1-6). Note that the structural support for this roof, as with each of the other two roof configurations, is shown as a concrete slab. In some cases this structural support is actually a steel deck instead of a concrete slab. These roof designs depict a concrete slab since it is by far the most common support used in Canada for residential high-rise .
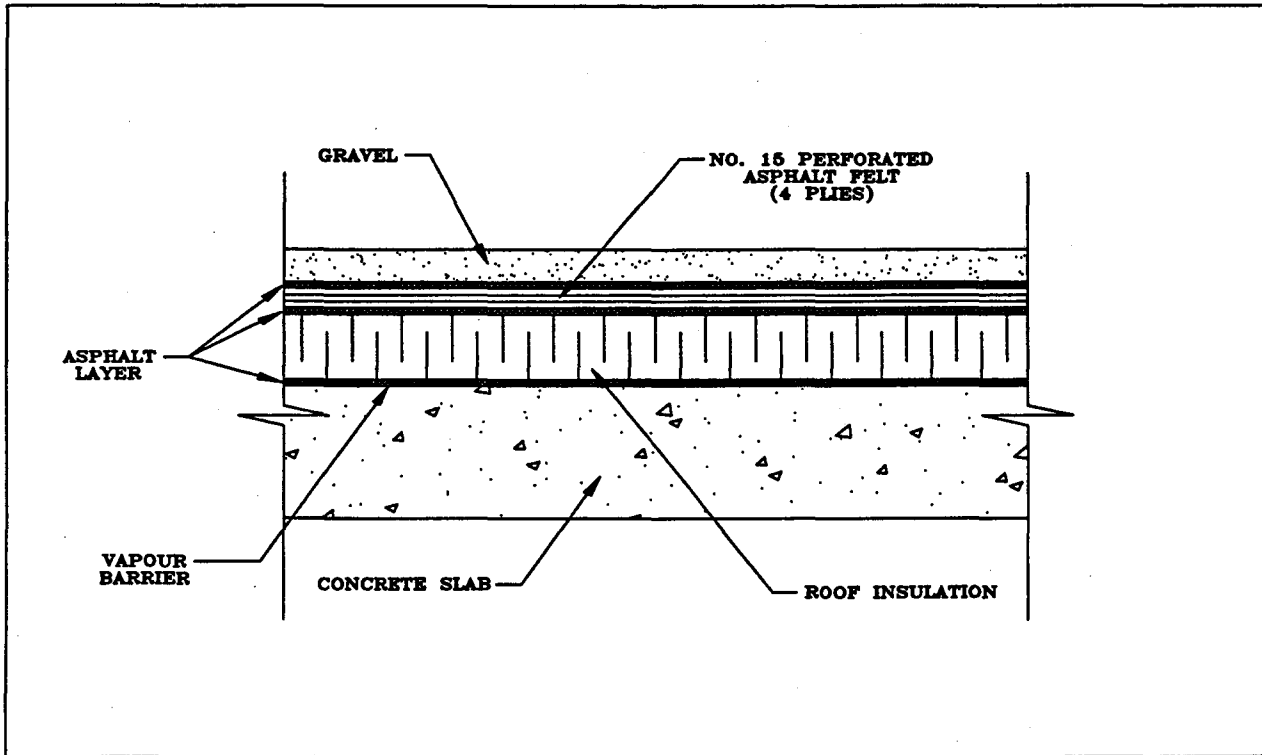
Figure 1-6: Built-up roof configuration

On top of the concrete slab lies a vapour barrier, which is normally a polyethylene sheet or a torched-on compound. Next, a layer of asphalt is mopped over the vapour barrier, sealing any joints or imperfections before the roof insulation is laid. Over the insulation, several layers of perforated asphalt felt are placed and embedded in hot asphalt. Normally, four plies are used, but this may vary from two to four. Finally, for protection and to hold everything in place, a ballast of gravel is spread over the top .

Single Membrane Roof

Another common roof configuration is shown in Figure 1-7. This is known as a single-membrane roof. It differs from the built-up roof, only in that the layers of perforated asphalt felt have been replaced with a single layer of impervious membrane. The membrane is embedded in hot asphalt to help maintain its integrity, especially at its joints.
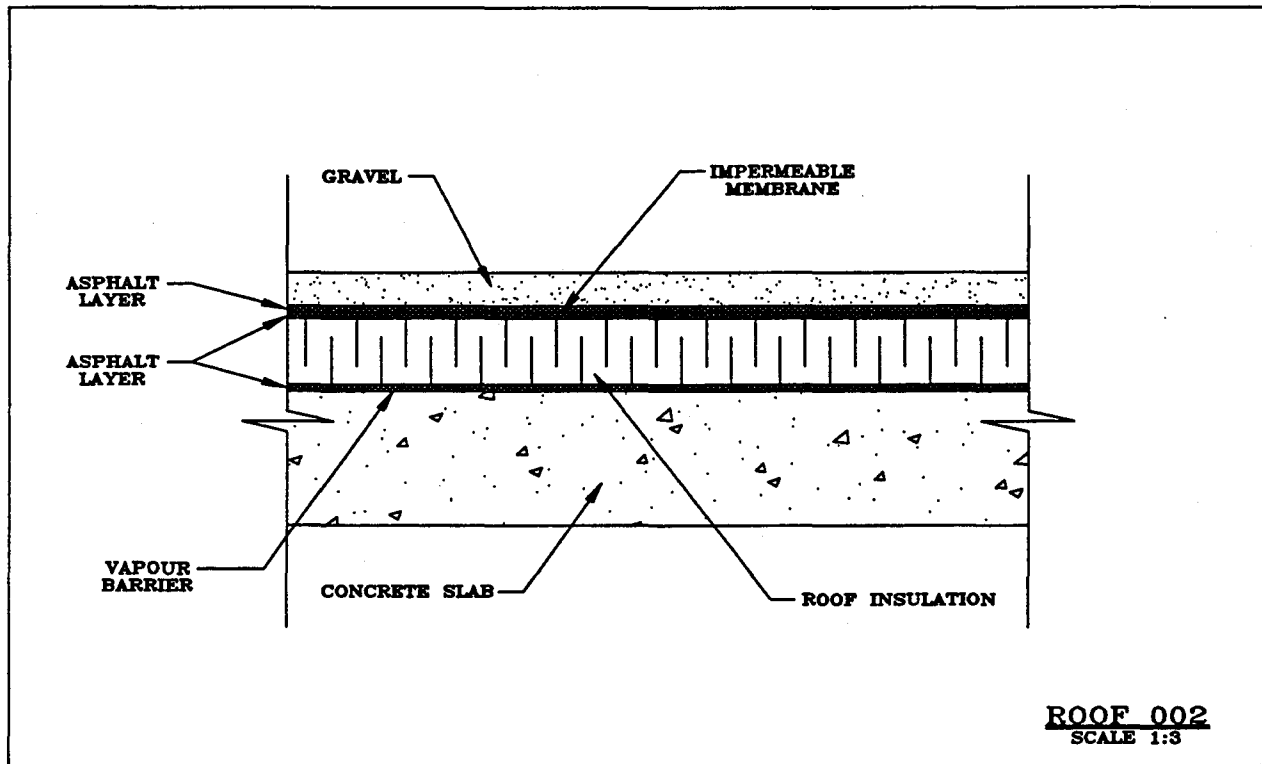
Figure 1-7: Single membrane roof configuration

Inverted Roof

The third type of roof is referred to as an inverted roof system. As Figure 1-8 shows, the configuration of this roof is very similar to the built-up roof except, as the name implies, it is constructed upside down, or inverted. An asphalt primer is applied to the concrete slab and then covered with a bituminous layer, usually asphalt. Next, perforated asphalt felt is applied with each layer embedded in a coating of hot asphalt. Once the perforated asphalt felt has been applied the insulation is place on top of the final coating of hot asphalt. This asphalt acts as an adhesive, holding the insulation in place. An impermeable membrane is embedded on the insulation to prevent moisture penetration.
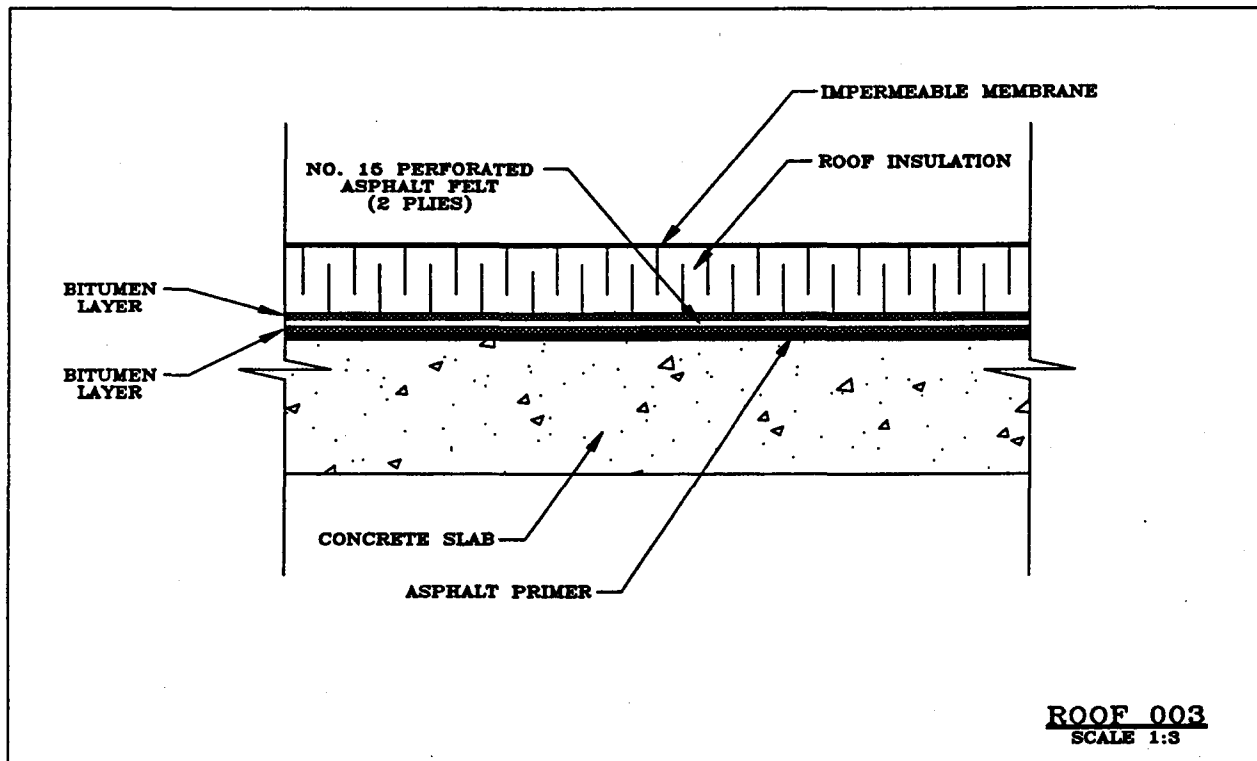
Figure 1-8: Inverted roof configuration

2.0 MODELLING HEAT, AIR AND MOISTURE TRANSPORT PROCESSES

Computer simulations of hygrothermal transport processes require knowledge of four important components:

a)   Mathematical formulation of the heat, air and moisture transport mechanisms that describe the phenomena. Enhanced models include more sophisticated and detailed physical descriptions (i.e. describing the porous media moisture transport more correctly). These transport processes are vapor diffusion, liquid diffusion or capillary flow, moisture convection, hydraulic seepage flows , electrokinetics and thermodiffusion.

b)   Accurate environmental components (exterior / interior boundary conditions as well as initial conditions).

c)   Definition of physical model/structure. What is to be modelled and what is required from the results?

d)   Material properties

Each of these components have a direct influence on the ability to accurately predict the hygrothermal performance of a building envelope component. Because designers and building practitioners are interested in understanding the long-term performance (durability) of building envelope structures, the role of computer simulation becomes critical. This approach allows one to understand how the total system performance behaves by analysis (modelling). Modelling requires, however, expertise in all of the above listed components. One can greatly appreciate the practicality and cost effectiveness of employing computer-based analytical models to predict the hygrothermal performances of building envelope structures.

2.1 MATERIAL PROPERTIES

During hygrothermal transport in construction materials, several distinct phenomena occur. The transport of heat, air and moisture is carried out in a porous system. Moisture is transported in two different phases, vapour and liquid. Material transport properties that influence the flow of moisture when subjected to concurrent and parallel transport potentials can be very complex. Vapour and

liquid flow can co-exist in both low and high relative humidity regimes. The functional form of these transport coefficients (water vapor permeability and liquid diffusivity) should be available for both

hygric regions. Phase change phenomena present during evaporation and condensation can also provide additional serious interactions and influences, especially since they occur during the separation of the moisture fluxes. The material properties employed in this project originate from the LATENITE Hygrothermal Database (Karagiozis et al). The LATENITE Database compiles properties measured/collected/reported at NRCC (Kumaran,) VTT (Kohonen) , International Energy Agency Annex 24 DATABASE (Kumaran), CMHC (Jacques Rousseau) and from NIST (Doug Burch). In the LATENITE hygrothermal model, for each material layer used in the simulations, the following properties are required:

- Thermal Conductivity $\dfrac{W}{m\,K}$

- Heat Capacity $\dfrac{J}{kg\,K}$

- Density $\dfrac{kg}{m^3}$

- Porosity ———

- Vapour Permeability $\dfrac{kg}{m\,s\,Pa}$

- Liquid Diffusivity $\dfrac{m^2}{s}$

- Sorption Isotherm $\dfrac{kg_{wet}}{kg_{dry}}$

- Air Permeability m^2

- Liquid Viscosity $\dfrac{N\,s}{m^2}$

The thermal conductivity and vapour permeability for most of the materials used in the simulations are both functions of the moisture content or relative humidity and temperature. The sorption isotherm is composed of two parts: one lying within the hygroscopic region, the other in the capillary suction region. In the suction region, the material properties are influenced only during phase change by temperature. Liquid diffusivity, and vapour permeabilities extend in both the hygroscopic and capillary regimes.

The transport coefficient employed in various hygrothermal models depend on the choice of driving potential. In LATENITE, moisture content and vapour pressure potentials are employed in the liquid and vapour regimes respectively. These driving potentials thus require liquid diffusivity and vapor permeability as transport coefficients. In the mathematical formulation of LATENITE, the vapour

permeability is constant and taken at a value corresponding to 40% relative humidity. However, at high relative humidity values close to 100%, a decay function is employed for vapor permeability, and liquid diffusivity to allow these properties to approach zero. In Figures 2-1 to 2-10 the moisture and thermal transport properties for vapor permeability, moisture diffusivity, volumetric heat capacity, sorption and suction isotherms, and thermal conductivities are plotted out as a function of relative humidity for a red brick and gypsum sample. These figures show the substantial effect of moisture on the transport properties. Very steep gradients occur with some of these material properties, which, in turn, make the governing equation highly non-linear. This alone makes the solution of the equations describing heat and moisture transport challenging to numerically solve. For example, the moisture diffusivity of red brick as shown in Figure 2-3 changes values of the order of 10^7 from a relative humidity value between 40% and 100%. This particular behaviour for liquid diffusivity is present in most capillary transport materials and less important in macroporous materials. However, in macroporous building materials, the sorption-suction isothermal becomes highly non-linear when approaching full saturation. Furthermore, the thermal conductivity also is strongly affected by the level of moisture present as can be seen in Figures 2-2 and 2-7. This may have a direct consequence on the thermal performance of a wall, contributing to higher heat loss.
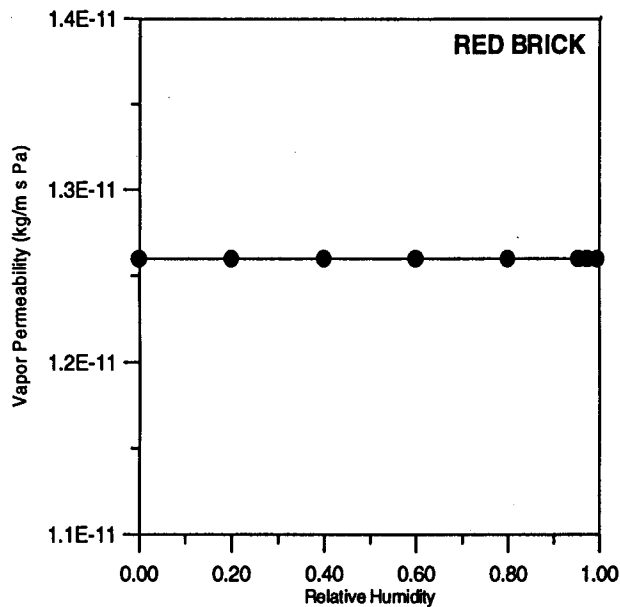
Figure 2-1: Vapor permeability as a function of relative humidity
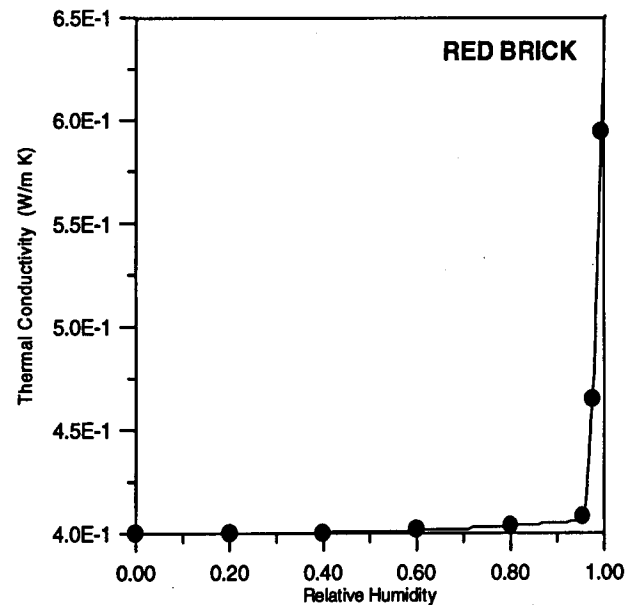
Figure 2-2: Thermal conductivity as a function of relative humidity
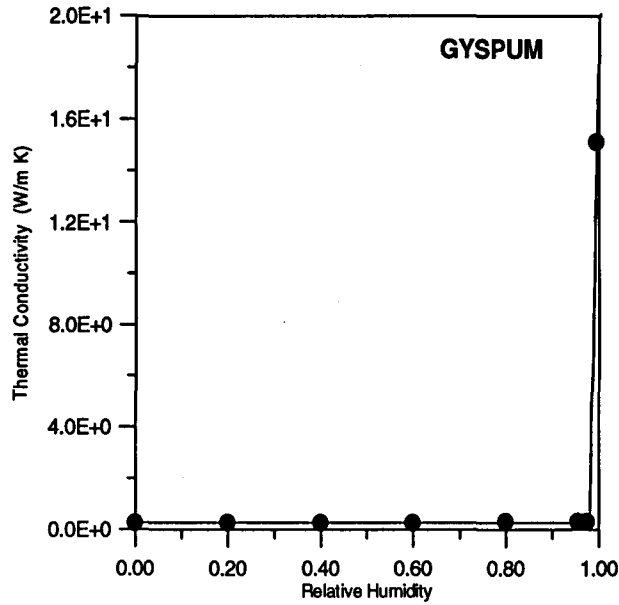
Figure 2-7: Thermal conductivity as a function of relative humidity

Figure 2-9: Volumetric heat capacity as a function of relative humidity

Figure 2-8: Moisture diffusivity as a function of relative humidity
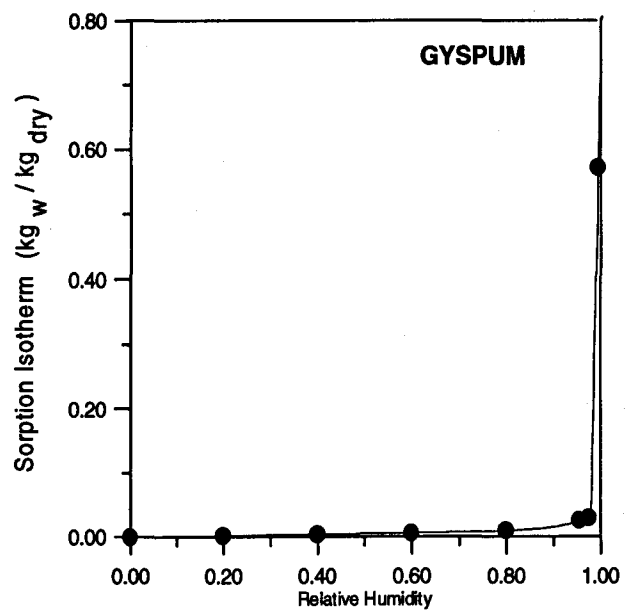
Figure 2-10: Sorption isotherm as a function of relative humidity
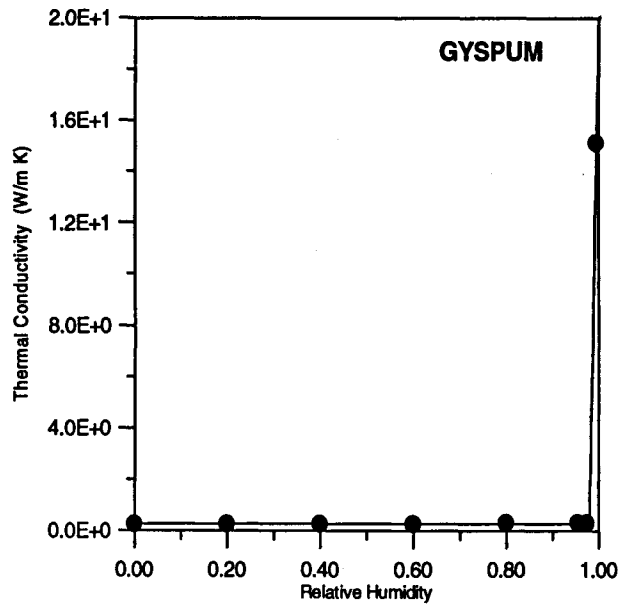
Figure 2-7: Thermal conductivity as a function of relative humidity

Figure 2-9: Volumetric heat capacity as a function of relative humidity

Figure 2-8: Moisture diffusivity as a function of relative humidity
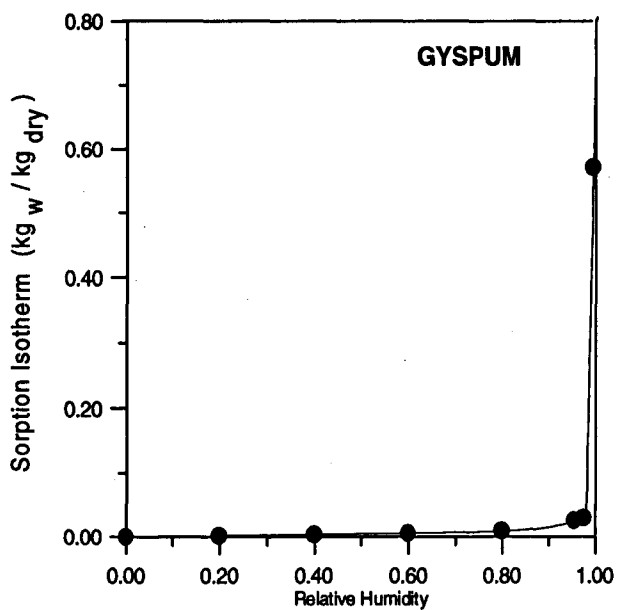
Figure 2-10: Sorption isotherm as a function of relative humidity

2.2   INFLUENCE OF MATERIAL PROPERTIES ON THE HYGROTHERMAL PERFORMANCE OF HIGH RISE WALLS

Building consultants, design engineers, and construction materials and system manufacturers have had limited or no modeling tools to assist them in the prediction of the hygrothermal performance. Even with the recent development of several hygrothermal models [a detailed analysis may be found in Hens and Janssens 1993], very few have included all important transport physics. Obstacles are primarily of computational/numerical nature and lack of availability of complete sets of material properties. Today, some of the most sophisticated models, such as TRATMO-2 (Salonvaara and Ojanen 1991), LATENITE (Karagiozis 1993), MATCH (Pederson 1990) and FSEC (1992), have demonstrated good agreement with both experimental and field data (KieBl 1993 and Hens 1991).

The predictive ability of hygrothermal simulations depend extensively on the accuracy and reliability of the material properties used. Such material properties are:

- dry and wet heat capacity
- dry and moist thermal conductivity
- sorption and desorption isotherms, the suction curves
- water vapor permeability
- moisture diffusivity,
- thermal moisture diffusivity and
- air permeability in both dry and wet stages.

Test methods are available to determine material properties although they are not standardized. For example, in a round-robin testing, some properties, such as liquid diffusivity, show disagreement of the order of 40% (Kumaran 1993). Traditionally this has discouraged researchers from enhancing the model capabilities by citing material properties discrepancies as a major contributor in the disagreement of model predictions and field tests.

It then becomes apparent that a systematic transient heat and moisture transport investigation is required to determine the sensitivity of the hygrothermal performance of a wall system to material properties. This step is important before effective guidelines can be deduced from any modeling analysis. This part of the work investigates the effect of the accuracy/variability of moisture transport properties of building materials on the modeling of hygrothermal performance high-rise wall systems. Due to the significant amount of modeling required in this project, any possible simplification of functional form of the material property transport coefficients would reduce the computational time for each run. This is important because more

linear matrix equation sets are assembled when employing simplified transport properties. In addition, fewer update iterations are required. To address the influence of material properties on the modeling of the hygrothermal performance of walls, three major tasks were implemented :

a) **TASK A** to determine the relative influence of hygrothermal transport properties subjected to ± 25% uniform variations.   The issue of how accurately material transport properties must be measured is investigated in this task.

b) **TASK B** to determine the effect of simplifying the functional form of the material properties and to determine how important it is to know all these properties in full detail or just the order of magnitude. Issues addressed in this task are: how extensive should these measurements be, are constant properties acceptable?, how many point values of vapor permeability and liquid diffusivity are needed, and how do these affect the accuracy of the simulation results.

c) **TASK C** to address the concern that among construction materials, no two are alike. Many materials exhibit considerable variation in properties within the same batch during manufacturing, and in most cases within the same material block, inhomogenieties can cause properties to differ near surfaces, cores and corners.   This task investigates the issue of the affect of variations in material properties on the heat, air and moisture transport in wall systems.

2.3   TASK A: Relative Influence of Heat, Air and Moisture Transport Properties Subjected to ± 25 % Uniform Variation in Properties of Individual Materials

In this study, three important hygrothermal material properties were significantly varied: the sorption isotherm, vapor permeability, and liquid diffusivity.   These transport properties were varied using the same full functional form properties. In addition, three walls that only differed to the extent of the material used on their exterior facade were used. Since this effort is aimed mainly at investigating the influence of experimental property measurement inaccuracies, a one-dimensional simulation was chosen.   In Appendix A1, the details for all the simulations performed for this task are presented.

TASK A   CONCLUSIONS

The hygrothermal behavior of the brick insulated cavity high-rise wall construction (explained in detail in APPENDIX A1) showed that the ±25% variation in the complete moisture transport

properties (water vapor permeability and liquid diffusivity), may have a minor effect dependent on the type of exterior facade used. In the cases examined in this report, material properties such as water vapor permeability and liquid diffusivity could have systematic variations of ±25% without any major hygrothermal effect.   However, the hygrothermal effect is comparatively greater for variations of the sorption curve of the facade. This means that the sorption isotherm must be accurately determined to model the hygrothermal performance of high-rise building envelope systems. The thermal performance (as the thermal conductivity was a function of moisture content) showed insensitivity to the seasons, in Ottawa. This insensitivity exists when one looks at monthly or even weekly averaged moisture or heat-flow conditions.

As a result from conducting TASK A, special care was taken within this high-rise project to more accurately define the sorption isotherms for all simulations.

2.4   TASK B: EFFECT OF SIMPLIFYING MATERIAL PROPERTY TO DETERMINE INFLUENCE ON THE HYGROTHERMAL PERFORMANCE OF A WALL

Hygrothermal analysis of building envelope components requires material property data such as thermal conductivity, vapor permeability, liquid moisture diffusivity and sorption curves to mention but a few. Many of these properties are hard to determine, they are nonlinear functions of temperature or moisture content. Furthermore test methods have not been standardized as it is not always certain what is actually being measured. For instance, vapor permeability or liquid moisture diffusivity measurements usually give the total moisture diffusivity instead of the individual vapor or liquid transport property. Sources for the errors in material properties are numerous: inhomogeneous material, measurement errors, and errors in the method for determining the material property. Some methods used to determine liquid moisture diffusivity (D_W), for example, rely on the assumption that liquid diffusivity is either constant or has a certain profile. Unless local moisture contents are measured during the water sorption experiment, which is commonly used to determine the moisture diffusivity, all of these methods may satisfy the mass increase per time function, but they fail to satisfy the moisture content distribution. Since the moisture transport properties are so hard to determine, certain questions arise: How important is it actually to know all these properties in full detail? Is it enough if we know the magnitude of, for example, liquid diffusivity? This work gives some answers to these questions. The hygrothermal behavior of a brick cavity wall has been analyzed using heat and moisture transfer properties with different levels of details or simplicity. In APPENDIX A1, the complete set of simulations are described in detail and extensive results are presented.

TASK B THERMAL BEHAVIOR RESULTS

The effect of material property simplification on the heat loss through the wall structure was minimal. The yearly heat loss varied between 38.35 and 38.9 kWh/m^2 (see Figure A1-13). The largest differences in heat flux can be seen at the beginning of the year when the wall is drying after wet initial conditions (see Figures A1-14 and A1-15). After the drying period, the moisture content in the wall are low, which allows the thermal conductivities of the bricks to remain almost constant throughout the year.

TASK B HYGRIC BEHAVIOR RESULTS

The simplification of moisture transport properties strongly influences the drying of the initial moisture from the wall (see Figures A1-16, A1-17 and A1-18). After the drying period, the moisture contents in the bricks remain low. Liquid-moisture diffusivity at low moisture contents is highest when constant properties are used (cases with designation key C) and lowest when exponential profile is used (cases with designation key E). The modeling results show that walls with constant properties dry faster, display more transient variations in moisture contents, and respond to the changes in boundary conditions faster than other walls.

The moisture content and relative-humidity distributions show major differences depending on the material properties used in the calculations (see Figures A1-19 to A1-41). The range of relative humidities at the inside surface of the external brick varied in the summer from 45%-RH (ECH) to approximately 95% (CFH). In winter, the same values existed but now in reverse order: 45% (CFH) and 95% (ECH). At time 225 hours from the beginning of the year, differences in local relative humidities can be 40%-rh.

These relative humidity differences between the full and the two simplified properties can be considered as unacceptable. It is evident here, that only the full functional form of the hygrothermal properties should be employed in modeling high-rise building envelope parts.

TASK B EFFECT OF TIME-AVERAGING

The total moisture content of the wall behaves similarly when using hourly, daily and weekly time-averaged weather data with the same material properties (Figures A1-22 to A1-25). The total moisture contents of hourly time-averaging results differ from those of daily and weekly averaging results during the initial drying period. Hourly weather data cases take longer than others to dry out. This phenomenon may be due to diurnal variations in temperatures and solar radiation.

The relative-humidity distributions show differences that depend on the time averaging used in the calculations (see Figures A1-26 to A1-41). The time-averaging has a smaller effect on the moisture contents and relative humidity distributions than simplification of material properties. At time 225 hours from the beginning of the year, differences in local relative humidities can be 10%-rh.

TASK B CONCLUSIONS

The simplification of material properties has significant effects on the simulation results of the hygrothermal behavior of a wall. The local relative humidities can differ by as much as 50%-rh in the simulated cases. The trend of moisture behavior also differs with material property functions. It seems that the type of liquid moisture diffusivity function had a great effect on the accumulation and dissipation of water in the wall as well as on its dissipation through drying. Time-averaging the boundary conditions affected the results less than the material properties. The maximum differences found in daily averaged local relative humidities were approximately 10%-rh.   From the results of TASK B it was determined that the full functional material property profiles, and hourly weather data were to be employed in high-rise project.

2.5 TASK C: EVALUATION OF THE IMPACT OF VARIABLE MATERIAL PROPERTIES USING STOCHASTIC MODELING

A 1-dimensional stochastic computer model was used to numerically analyze the effect of random porous material transport properties, under cold-climate conditions. The hourly hygrothermal performance of a brick-layered cavity wall, as examined in TASK B, was investigated using a randomly changing material structure. A first-order spatial stochastic random-walk method was implemented in the LATENITE model. Two independent tests were conducted:

• first, where the stochastic processes require that both the means and the variances of each investigated transport property vary simultaneously with every time step (Case 1); and

• second, only once at the start of each simulation (Case 2).

A Monte Carlo method (Welndell Fleming, 1988) was used to generate the uniform probability density functions of each investigated transport property by a controlled variation of ± 40%.

INTRODUCTION

To date, only a handful of hygrothermal models are available that integrate all important transport physics. Most of these models, are research tools requiring an enormous amount of data entry (Karagiozis 1993). The distribution of these models to building designers is impeded for two reasons: first, the long computational time required for simulation on conventional PC; and second, the sophistication of the input parameters, functional forms for the moisture transport properties, diffusivities and permeability, thermal properties, and such weather conditions as the ambient temperature, relative humidity, solar radiation, wind speed, wind direction and rain precipitation. Simplification of the entry of data is necessary so that building designers and architects can use hygrothermal models. **TASK A** investigated the influence of the accuracy/reliability of the inputted material properties on the predictive capability of the hygrothermal simulation results. Results showed that a uniform simultaneous variation of ± 25% in both vapor permeability and liquid diffusivity (full functional dependencies included) of all materials in the wall system produced no significant differences in temporal moisture accumulation.

TASK B evaluated the effect of simplification of the material properties by using three different functional forms ranging from the most complex to just constant properties throughout the analysis. An inherent assumption in TASK B was that homogeneous time invariant material properties were employed. In those simulations, material properties of each material in the brick-layered cavity wall were assumed deterministic.

However, in most construction materials, no two materials are completely alike. In addition, most materials have great variances in both pore size and pore distributions even within the same manufactured batch. Hence, to determine whether a potential for simplified modeling exists, a sophisticated stochastic/Monte-Carlo module was implemented in the **LATENITE** hygrothermal model.

Stochastic Monte Carlo Simulations

From a fundamental point of view of porous media heat and mass transfer mechanisms, porous material properties are strongly related to the packing pattern of the porous media as well as to the mechanical and thermal properties of each substance. Due to the random nature of the packed-bed system, there are no analytical or deterministic solutions to heat and mass transfer problems in porous media in a strict sense. But a probabilistic method, the Monte Carlo technique, can be used to generate the material properties that occur during moisture transport.

This technique can be used to randomize the partial differential equations that describe heat and mass transfer through the porous media. This randomization must be constrained to satisfy conservation principles at all times. Solving a large number of these equations for each time step allows the methods to be extended to what is referred in this paper as quasi-stochastic modeling. The implementation of this method for hygrothermal modeling allows a comprehensive parametric study to be conducted with minimal computational effort. In Appendix A1, a brief introduction is given for the implementation theory of the method.

Results

Details and information on the simulations carried out are presented in Appendix A1. The summary and conclusions are presented below:

Histograms

Figures A1-46 to A1-48 show the frequency distributions along the cumulative behavior for some of the runs of Case 1. Figures A1-46 and A1-47 demonstrate the randomness of each simulation. The y-label frequency is defined as the number of control volumes that have the same probability factor. The x-axis bins are arranged from values of 0.1 to 0.9, representing multiplication factors between 0.6 to 1.4, giving the -40 % and +40 % variation range for the material properties. These figures show the statistical distributions of the multiplication factor. Each of the 28 control volumes used had a randomly assigned multiplication factor and Figures A1-46 and A1-47 show the frequency of occurrence for those simulations. As, an example in Figure A1-46 there are 3 control volumes at bin 0.1, and this corresponds to the multiplication factor of 0.6. In Figure A1-48 all frequency histograms are summed up and the total frequency distribution is shown for Case 1. Here we can see that as the number of simulations enlarges, the probability density trend becomes the same (giving the same chance to each multiplication factor).

Hygrothermal Results

In Figures A1-49 to A1-55, results on hygrothermal behavior of the brick-layered cavity wall are presented. Figure A1-49 depicts the relative humidity difference by daily averaging both Case 1 and Case 2 results. Results are shown for the control volume node closest to the interior of the external brick layer (node 10). The results show the maximum and minimum values as well as the actual relative humidity difference distribution for one simulation. Results clearly demonstrate that differences of up to ±40 % in material properties can cause differences in the order of 10 % in the calculated daily relative humidities. The hourly differences can be considerably higher up to 15 %. It is important to note that while a random ±40 % factor was

used, the full functional form was followed. Figure A1-50 presents the maximum and minimum range results using Case1 and Case 2 stochastic approaches. It is evident that in Case 1 simulations, where the Monte Carlo simulations were carried out each time step, gave smaller differences with respect to the deterministic solution. Figure A1-51 shows the spatial relative humidity distribution after 225 days (mid August). Four curves are plotted out, one the deterministic solution, one from Case 1, and two from Case 2. The agreement observed between these different simulations, is indeed remarkable. *This signifies that during that instant of time ±40 % differences in material properties have no effect on the calculated hygrothermal performance of the wall.* Figure A1-52 shows a similar plot but after a time period of 63 days (March). Here the deterministic and Case 1 simulations are compared, and differences of up to 14 % in relative humidities are present. Figures A1-52,A1-54 and A1-55 show the differences in total moisture between the deterministic and stochastic maximum and minimum values for both Cases 1 and 2. Figure A1-52 shows the full year results, while Figure A1-54 only the drying period and Figure A1-55 the remaining period. It becomes clear that with the exception of the drying period, where the majority of the stochastic results indicate faster drying, differences are small between the deterministic and stochastic results.

Figure A1-56 shows the maximum and minimum heat fluxes of all the stochastic runs. Results show very small influences, these primarily being the effect of the variation of the thermal properties of the interior and exterior brick. Most of these differences are present only during the drying and wetting seasons. Figure A1-57 shows the percentage differences in the yearly heat losses for Case 1 (first ten) and Case 2 (last ten). Maximum differences between the individual simulations and the average, are approximately 7 %.

CONCLUSIONS

Irrespective of the two stochastic procedures (randomness in material properties), the results show minor influences of the total moisture temporal distribution and the heat flux distribution. Maximum differences in yearly averaged heat losses for both stochastic methods fall under 7 %. The thermal performance is influenced mostly by the random changes in thermal conductivities. The general conclusion is that the ± 40 % level of randomly varying material properties for this brick layered cavity wall did not produce major differences in the modeling of the hygrothermal performance of this building envelope system. This implies the accuracy of the properties around the functional forms for transport properties may not be critically important, as long as the correct functional form is employed. This means that variances of the properties of any given material should not be a major concern- nominal values can be used as long as they are within ±40 % of the actual.

Using the real (most complex) material property functions for material properties but randomly changing them by up to ±40 % produced local differences in relative humidities less than 15 %. Results further confirm PART B results that most of the differences exhibited arise from the effect of liquid diffusivities. Any differences in Case 1 and Case 2 simulations are attributed to differences in the probability density function employed in these cases. As the probability density function gives equal opportunity to each location, results deviate less from those determined by deterministic solutions. The simplification from real stochastic to point defined deterministic approaches can be carried out in this project, as long as the full functional form of the material properties are employed.

3.0 HEAT-AIR-MOISTURE MODELING

The prediction of the long term hygrothermal performance of residential building components is important in order to assess the durability, energy efficiency and the effects of rehabilitation of high rise structures. Currently, a rash of moisture related problems (concerning high-rise building) reported to IRC and CMHC, both directly and through various agencies, have resulted in damages that are very costly to repair. Most of the recommended repair and retrofit guidelines on high-rise structures have been based on relatively little scientific knowledge. The review of the literature and of the few recently documented high-rise moisture damages have suggested that the problem could be better understood by a systematic parametric investigation of the combined heat, air and moisture transfer in high-rise building envelope components using advanced computer simulation techniques. This requires the capability of predicting the envelope behavior subjected to thermal and moisture excitations. Sophisticated hygrothermal models can provide useful behavioral analysis of building components when all important transport physics and building envelope system details are included in the mathematical formulation. Only then can such models be employed in parametric studies to determine the relative importance of each critical parameter of the building envelope system. The following sections describe some of the important attributes required for hygrothermal models used in this project.

3.1 MODEL APPLICABILITY

The heat, air and moisture transport in high-rise residential buildings is a complex hygrothermal process since it is a 3-dimensional function that encompasses both hygrothermal spectrums, vapor and liquid moisture transport. After a review of high-rise construction, the following key features were found to be important components in modeling of high rise structures.

High-rise hygrothermal modeling requirements:

The key modeling features required to research the moisture transfer in high-rise residential buildings are:
- Transient heat, air and moisture transfer formulation
- 2-dimensional spatial formulation (as a minimum)
- Permitting variable material properties; e.g., as functions of moisture content and temperature

- Accounting for: -vapor transport
  -liquid transport
  -moisture capacity in the materials
  -condensation and evaporation processes
  -freezing and thawing processes
  -incident solar radiation and night sky radiation on exterior surfaces of
    the high rise
  -rain penetration on exterior surfaces of the building
  -air flow through the building envelope

As a result of IRC's ongoing involvement in the International Energy Agency (IEA) Annex XXIV on Heat-Air and Moisture Transport in New and Retrofitted Building Envelopes, IRC staff kept up to date on the international state-of-the-art hygrothermal models. Based on our review and understanding of existing models (till 1993), it was concluded that no single model had all of the features needed to fully address the moisture transport in high-rise residential buildings. Nevertheless, it was felt that adaptation of an existing model to address the key features was feasible.

Assessment of Model Applicability

A considerable amount of time has been spent on reviewing, selecting, testing and adapting appropriate models for this research. IRC and CMHC staff (Achilles Karagiozis, Tom Hamlin, Kumar Kumaran, and Mikael Salonvaara) have since identified several models other than those originally mentioned in the proposed work plan. According to the proposed plan by mid-1993 the following four numerical models (of which three ranked within the five most sophisticated hygrothermal models in the world, (Hens 1993)) were considered. The majority of the time spent on investigating the applicability of the hygrothermal simulation model was initially concentrated on the CMHC **WALLFEM** model. An overview of the current hygrothermal models investigated so far is given below.

TCCC2D VTT/IRC MODEL (1992)

The **TCCC2D** (*Transient Coupled Convection* and *Conduction* in 2-dimensions) was developed at VTT Finland. It is a hygrothermal model developed for light-weight constructions of multilayer building structures where macroporous building materials are present. **TCCC2D** solves the heat, air and moisture transport and conservation equations that represent vapor transport flow and incorporates condensation/evaporation and freezing/thawing processes. The transport equations are based on temperature, pressure

and water vapor pressure as driving potentials. It is a finite-difference model, where the moisture content is coupled with the vapor pressure and temperature through the sorption isotherms.

Limitations of the TCCC2D model are:
- the model can only be used for fixed rectangular structures,
- the formulation is based on the vapor transport equations (no liquid is modeled),
- the implementation of boundary conditions are very cumbersome,
- the implementation of internal interface resistances and moisture sources is difficult, and
- it is very costly to run a series of calculation as required by the high rise project.

MOIST MODEL

The **MOIST** model was developed at **NIST (USA)** by Burch and Thomas in 1992 and is a 1-dimensional heat and moisture transport model. Driving forces for moisture transport are the gradients in moisture content and temperature. While air through the insulation is claimed to be modeled, the approach used can produce serious errors. The material properties data base for moisture diffusivity at high moisture contents, i.e. in the capillary regime exhibit abrupt discontinuity. The **MOIST** model has been used in many wood frame constructions calculations. It can not be recommended for use in high-rise constructions.

Limitations of the MOIST model are:
- It is a 1-dimensional model and cannot be applied the high-rise constructions,
- The prescription of boundary conditions is not flexible,
- Air flow is not incorporated into the model,
- The models does not incorporate latent heat within insulation (too difficult to numerically handle, according to the authors of MOIST), and
- the model is not capable of including rain (liquid flow at the boundaries).

These two issues are both very important in the hygrothermal performance assessment of high-rise buildings.

LATENITE MODEL 1.0 (1992)

LATENITE is a recently developed IRC hygrothermal model for heat and moisture transport through macroporous and capillary-type materials. LATENITE 1.0 is based on the well known Luikov-type equations, which employs potentials for heat and moisture flows as temperature and moisture content respectively. For the solution of the full set of coupled equations, one can choose the finite element (Galerkin), Finite Difference or Finite Volume method. A numerical procedure is used for calculating the moisture flow through the interface of two materials, since the moisture content potential can be discontinuous. The geometrical limitations for the L-shaped geometry of a basement are also present in this model. The prescription of interface resistances (such as vapor retarders or paper sheathing cannot be directly incorporated into the model), and boundary conditions such as solar irradiance, moisture sources cannot be easily implemented. The mathematical formulation of version 1.0 was based on moisture content and temperature potentials requiring non-measurable material properties.

By 1995, the LATENITE 1.0 Model was upgraded to LATENITE 1.2 and was able to handle air flow and various interface resistances. Indeed the moisture transport potentials were also altered to vapor pressure and moisture content. Wind-driven rain was also included in the model. These upgrades overcame the previous limitations.

CMHC WALLFEM-3D Version 1.0 MODEL (1992-1993)

The **WALLFEM 1.0** model, a 3-D general purpose software package, is especially designed to simulate complex building science problems. The major feature is its ability to solve user-defined systems of governing equations. The use of finite elements allows the model to accommodate very complex structures and geometries, which is an important feature in the high-rise residential project. The moisture transport modules (of the first version of **WALLFEM**) uses the *Evaporation and Condensation theory*, which assumes:

- moisture travels due to water vapor density (partial water vapor pressure) gradients,
- local thermodynamic equilibrium exists,
- the total pressure is constant, and
- the solid matrix is rigid.

In a control volume (element), the net amount of water increase in the pores is equal to the amount of water vapor brought to the pore by diffusion minus the amount of liquid water accumulated. Additionally, the net amount of energy stored in the same control volume is equal to the amount of heat conducted plus the energy liberated during the phase conversion. Because a thermodynamic equilibrium prevails at all times, the amount of liquid

water at any given point can be calculated through the equilibrium sorption isotherm, given the temperature and water vapor density at that point. The **WALLFEM** model has been applied to the IEA Annex XXIV Second Common Exercise, and the heat and moisture results produced good agreement with other state of the art models.

A limitation of the **WALLFEM** model is the complexity of the input and processing modules. One the most severe limitations was that documentation for the model did not exist. In fact, the use of finite elements augments the complexities of the formulation of the supportive subroutines. The following were considered important limitations:

1. The material properties are unidirectional, i.e., thermal conductivity, vapor permeability, etc.
2. The model does not account for freezing/thawing processes occurring in cold climates.
3. The vapor diffusivities, while strong functions of moisture content, are represented as constants.
4. Air flow is not accounted for in the porous building materials.
5. Fluctuating pressure boundary condition prescriptions.
6. Only vapor transport is modeled.

In 1992-1993, it was apparent that the **WALLFEM** model was appropriate for this investigation because of the flexibility and adaptability to the multi-layered (2-D) structures of the high rise project. CMHC then worked to overcome limitations 1 to 5.

Preliminary Calculations and Adaptations of WALLFEM
The **WALLFEM** model was applied to the IEA Annex XXIV Second Common Exercise. The results agreed well with those of other models when only pure moisture diffusion took place. Additional software was developed at IRC and incorporated into the **WALLFEM** model to account for the solar incident flux and wind pressure boundary conditions. This module was used in the Second Common Exercise and good agreement was found for the solar flux incident cases. Further analysis of the **WALLFEM** computer code revealed that the only pure vapour transport is modeled, Darcy's equation for porous flow was incorrectly imbedded into the model, and the modules of **WALLDRY** were disconnected. These inconsistencies were not addressed or even indicated in the **WALLFEM** user's manual (1992).

From the experiences gained from the application of the original **WALLFEM** program to the IEA Annex XXIV Second Common Exercise, it became evident that the program is very

structured and can be used as the basis of more advanced theoretical models. When a second version of the **WALLFEM** model was commissioned by CMHC, a new set of driving potentials were chosen in an attempt to address some of the shortcomings of previous version such as liquid transport, porous flow equations and handling of pressure boundary conditions, identified by IRC. All these developments were required before high-rise modeling could commence. Because of development problems, however, the use of the **WALLFEM** model for these simulations could not be realized. Another model had to be used.

As a result of IRC's ongoing involvement in the International Energy Agency, (IEA) Annex XXIV on Heat-Air and Moisture Transport in New and Retrofitted Building Envelopes, IRC staff kept up to date on the international state-of-the-art hygrothermal models. Based on IRC's review and understanding of existing models, it was concluded that no single model had all of the features needed to fully address the moisture transport in high-rise residential buildings. The only alternative was the adaptation of the IRC model, **LATENITE 1.0**, to address the key features. The adaptation and further enhancement of **LATENITE** was accomplished and employed in this study. The model (1994- Feb. 1995) incorporated all features other than that for air flow. The air flow module was implemented at the end of November 1995.

Verification of the LATENITE Hygrothermal Model

The **LATENITE** model was applied to the IEA Annex XXIV First, Third, Fifth and Sixth Common Exercise. The model was also independently compared to building envelope application cases with models, such as **TCCC2D** (Ojanen 1992) and **TRATMO2** (Salonvaara 1991), both state of the art hygrothermal models from Finland. The agreement was to be found excellent both among these models and also when compared to experimental results from IEA Annex 24 Third Common Exercise (1993) and Fifth Common Exercise (1994). In **LATENITE,** the model decouples the vapor and liquid transport of the total moisture transport, and this alleviates the need of several ambiguous assumptions (fractional behavior between total and vapor transport) that are needed for the calculation of latent heat contributions. An additional feature is that a new interface was completed that allowed one to input parameters for the simulation, that are stored and thoroughly checked with extensive error handling capabilities, prior to each run. This reduced the chances of human error that plagues such complex input files. All these issues are important factors that needed to be addressed before the initiation of the intensive modeling of parts of a high-rise building envelope.

LATENITE 1.0 GOVERNING EQUATIONS

Several publications discussing the combined hygrothermal transport formulation of the LATENITE model are presented by Karagiozis 1993, Karagiozis et al 1994 and Salonvaara et al 1994. LATENITE 1.2 is currently the most state-of-the-art heat, air and moisture transport model and some main features are presented next.

MOISTURE BALANCE

The moisture balance is considered for two classes of materials: the macroporous and the capillary-type materials. Assuming that the dry density of the material remains unchanged during the moistening process, i.e., no excessive swelling or shrinkage phenomena occur) the moisture transport balance is given as,

$$\rho_o \frac{\partial u}{\partial t} = -\nabla \dot{m}_m \qquad (3\text{-}1)$$

where $u =$ the moisture content kg_w / kg_d

   $t =$ time in seconds

   $\dot{m}_m =$ the moisture flux $kg/m^2 s$

   $\rho_o =$ Dry density of the material

   $\nabla =$ rate of change spatial tensor

The equation for moisture flux can be written for macroporous materials and for capillary materials, using slightly different potentials. Nevertheless, they are similar and can be stated as Macroporous moisture flow:

$$\dot{m}_m = -\delta_P(u, T)\nabla P_v \qquad (3\text{-}2)$$

where $\delta_P =$ the vapor permeability in (kg/s Pa m), and

   $T =$ Temperature (°C)

   $p_v =$ the vapor pressure in the porous material

This type of moisture flux equation has been extensively used in literature and has the advantage of using a continuous potential field.

Capillary moisture flow

$$\dot{m}_m = \dot{m}_{vap} + \dot{m}_{liq} + \dot{m}_{air-flow} \qquad (3\text{-}3)$$

$$\dot{m}_m = -\rho_o \delta_P(u, T)\nabla P_v - \rho_o D_w(u, T)\nabla u - \rho_v v \qquad (3\text{-}4)$$

where D_w (m^2/s) is the moisture transport diffusivity for isothermal conditions. The first term in the RHS of Equation (3-4) of the capillary (liquid) moisture flux equation is due to

moisture gradients present in the porous material, whereas the second term is due to the vapor moisture flux generated by vapor gradients.

HEAT BALANCE

The heat transfer is as complex as the moisture transport and includes such components as conduction, convection, evaporation/condensation sources (due to moisture), and radiation heat transfer. The equation governing this scalar quantity is given as,

$$(\rho \cdot c_P)_{eff} \frac{DT}{Dt} = -\nabla q_T + \overset{\bullet}{S} \tag{3-5}$$

where ρ_{eff} = is defined as the effective density of the material (including both the

dry and   wet contribution in the material matrix)

c_P = the effective heat capacity of the material (may be composed of more

than one   state),

q_T = the conduction heat flux,

t = time (s),

$\overset{\bullet}{S}$ = the heat source due to the phase change phenomena occurring due to

moisture   transport.

The conduction heat flux q_T is defined as

$$q_T = -k_j \frac{\partial T}{\partial x_j} \tag{3-6}$$

where the index j designates the specific coordinate of interest; and k_j is the thermal conductivity.

The heat source $\overset{\bullet}{S}$ has 2-phase change components: one due to evaporation-condensation, the other due to the freezing -thawing process.

$$\overset{\bullet}{S} = -L_v \nabla \dot{m}_{vap} - L_{ice}\rho_o u \frac{\partial f_l}{\partial t} \tag{3-7}$$

where L_v = the latent heat of evaporation,

L_{ice} = the latent heat due to freezing,

ρ_o = the dry density of the material,

$f_i(T)$ = the liquid fraction having a value between 0 and 1.

This liquid fraction behavior is very material type dependent.

NUMERICAL METHOD

The system of equations are rewritten to take advantage of the conservative form. The conservative form allows multiple time differencing schemes to be easily implemented. The moisture and heat balance equations become,

$$\frac{\partial U}{\partial t} = \frac{\partial V(u,T)}{\partial x} + \frac{\partial W(u,T)}{\partial y} \tag{3-8}$$

where $U=$ the unknown vector

V and $W=$ the vectors containing the diffusion terms.

Vector U is defined as a function of the dependent variables u and T as

$$U = \begin{bmatrix} u \\ T \end{bmatrix} \tag{3-9}$$

Vectors V and W are defined as diffusive vectors. Using a 1-step time discretization relationship between the solutions at the old time n and the new time step $n+1$ leads to

$$U^{n+1} = U^n + \Delta t\left[\theta\left[\frac{\partial U}{\partial t}\right]^{n+1} + (1+\theta)\left(\frac{\partial U}{\partial t}\right)^n\right] \tag{3-10}$$

The conservative form of the equations can be discretized in time by using the 1-step time differencing schemes:

$$U^{n+1} - \theta\Delta t(\ \frac{\partial V(u,T)}{\partial x} + \frac{\partial W(u,T)}{\partial y}\ )^{n+1} =$$

$$U^n + (1-\theta)\Delta t(\ \frac{\partial V(u,T)}{\partial x} + \frac{\partial W(u,T)}{\partial y}\ )^n \tag{3-11}$$

With applying Newton-Raphson linearizations to the diffusive vectors V and W

$$V^{n+1} = V^n + R^n\left(U^{n+1} - U^n\right) \tag{3-12}$$

and

$$W^{n+1} = W^n + S^n\left(U^{n+1} - U^n\right) \tag{3-13}$$

where S and R are the Jacobian for the diffusive terms. They are defined by the expressions

$$R = \frac{\partial V}{\partial U_x} \tag{3-14}$$

$$S = \frac{\partial W}{\partial U_y} \tag{3-15}$$

On substituting the Newton-Ralphson linearizations into the general conservation equation after time differencing, the governing equations become

$$\left[I - \theta\Delta t\left(-\frac{\partial^2}{\partial x^2}R^n - \frac{\partial^2}{\partial y^2}S^n\right)\right]U^{n+1} = \left[I + \theta\Delta t\left(-\frac{\partial^2}{\partial x^2}R^n - \frac{\partial^2}{\partial y^2}S^n\right)\right]U^n - \Delta t\left(\frac{\partial V}{\partial x} + \frac{\partial W}{\partial y}\right)^n$$

$$\tag{3-16}$$

The Delta form, i.e., using Δ as the corresponding operator, is defined as

$$\Delta U^n = U^{n+1} - U^n \tag{3-17}$$

This delta form increases the accuracy of the formulation, since the solution will be a progression of ΔU instead of U. With rewriting the equation in the delta form it becomes

$$\left[I + \theta \Delta t \left(-\frac{\partial^2}{\partial x^2} R^n - \frac{\partial^2}{\partial y^2} S^n \right) \right] \Delta U^n = -\Delta t \left(\frac{\partial V}{\partial x} + \frac{\partial W}{\partial y} \right)^n \tag{18}$$

This system of partial differential equations can be factored into two tensorial products without loss of accuracy in time:

$$\left[I + \theta \Delta t \left(-\frac{\partial}{\partial x^2} R^n \right) \right] \otimes \left[I + \theta \Delta t \left(-\frac{\partial}{\partial y^2} S^n \right) \right] \Delta U^n = -\Delta t \left(\frac{\partial V}{\partial x} + \frac{\partial W}{\partial y} \right)^n \tag{3-19}$$

To solve this set of equations, an intermediate vector of unknowns ΔU^* is introduced, namely

$$\Delta U^* = \left[I + \theta \Delta t \left(-\frac{\partial}{\partial x^2} S^n \right) \right] \Delta U^n \tag{3-20}$$

The steps required to solve this set of equations are

$$\text{Step 1:} \quad \left[I + \theta \Delta t \left(-\frac{\partial}{\partial x^2} R^n \right) \right] \Delta U^* = -\Delta t \left(\frac{\partial V}{\partial x} + \frac{\partial W}{\partial y} \right)^n \tag{3-21}$$

$$\text{Step 2:} \quad \left[I + \theta \Delta t \left(-\frac{\partial}{\partial y^2} S^n \right) \right] \Delta U^{n+1} = \left(\Delta U^* \right) \tag{3-22}$$

This allows the original system of partial differential equations to be split into two linear systems of block tridiagonal structure, which can be solved efficiently by standard numerical methods. The final coupled equations can be transformed into algebraic block tridiagonal structures.

Summary

The transport processes of heat, air, and moisture transport in high-rise structure were identified. Hygrothermal model selection requirements were determined and the model selection and adaptation processes involved in this project were discussed. **LATENITE** was then chosen for the simulation of the hygrothermal behavior of high rise building structures. Vapor and liquid transport, with material properties of any functional form, phase changes due to evaporation/condensation as well as freezing and thawing mechanisms, internal vapor and heat resistances, and heat and moisture internal sources were included in **LATENITE**. Boundary conditions including the influence of wind driven rain, solar irradiation, ambient relative humidity and temperature, and wind air pressure differences were accounted for in **LATENITE**.

4.0   BOUNDARY CONDITIONS

Introduction

Within the scope of this work, it was required to determine the applicable boundary conditions for the proceeding high-rise simulations. High-rise buildings are exposed to more severe environmental conditions than the low-rise buildings, however, both have similar driving potentials for heat and moisture transport. As discussed in Section 3 on modeling, the **WALLFEM** model was initially proposed for simulating the hygrothermal performance of high rise structures. In this model, vapor and liquid moisture is transported by diffusion processes. Only recently has air-flow modeling (Karagiozis, 1995) been implemented in a building envelope hygrothermal model in the presence of vapor and liquid moisture flows. Therefore, most of the effort in this section concentrated on the development of boundary conditions that are representative during diffusion processes of moisture, and recently this information has been upgraded to include air-flow mechanisms. The effect of environmental conditions on the long-term performance of various wall and roof systems was investigated by using different cities within Canada. They were chosen to represent a wide variation of environmental climatic conditions and are:

- Ottawa
- Vancouver
- Winnipeg
- Fredericton
- Montreal
- Resolute Bay
- Toronto

The exterior and interior boundary conditions acting on typical residential buildings vary with time of day and time of year, making boundary conditions time-dependent (transient). The exterior variations are part of the seasonal effects associated with the geographical location of the building. The internal variations are greater due to the time of day and the particular events undertaken by the inhabitants of the building. Some of the internal moisture sources or sinks depend primarily on the behavior of the inhabitants with respect to preferred interior-climate comfort levels, the number of baths taken, type of cooking, and cleaning. This makes the definition of interior-climate classes complex and dependent on time, location and people's behavior. This study assumed constant conditions for the interior of the high-rise buildings: with the indoor

air temperature of 20°C and relative humidity of 40%. These values correspond to typical conditions in Canada's residential low rise buildings (Hamlin et al. 1994). On the exterior of the building, boundary conditions for diffusion processes that were prescribed for the building envelope wall or roof were:

- Exterior air temperature   (°C)
- Exterior relative humidity   (%)
- Solar radiation   (W/m2)
- Aborptivity of exterior surface   (-)
- Emissivity of exterior surface   (-)
- Convective heat transfer coefficients (W/m^2 °C)
- Mass transfer coefficients   (kg/m^2 Pa)
- Water resistant substances   (kg/m^2,s,Pa)
- Rain fall on exterior surface   (kg/m^2 hr)

with additional boundary conditions when using the airflow cases:

- Wind speed   (m/s)
- Wind Orientation   (degrees)
- Stack pressure   (Pa)
- Over or Under Pressurization   (Pa)

These boundary conditions were provided hourly, coinciding with the time-step employed in the   simulations.   Adoption of the 1-hour step was determined by examination of the effect of time-averaging as presented in the section on material properties. This, of course, requires information on an enormous number of boundary conditions that in some cases is not available. Especially in the case of rain fall on the exterior surface of the building, no such information was available. Yet, rain constitutes the most important source of moisture in high-rise walls with capillary-type facades. Today, even within the international research community, moisture-modeling that includes the effect of rain has not been implemented for two main reasons:

- the complexity in the mathematical and numerical procedures to handle rain flow at the exterior boundary surface, and
- the lack of information regarding the amount of rain striking the exterior surfaces of a building.

Since, both these challenges were overcome during the duration of this project, results were obtained that include the effects of rain. Work in wind-driven rain was carried out

by Building Performance and National Fire Laboratory at IRC to determine the influence of turbulent wind flow conditions on the amount of wind driven rain received on each surfaces of the high-rise building.

4.1   WALL BOUNDARY CONDITIONS

For each high-rise wall type, four different wall orientations were simulated because of the strong effects of solar radiation and wind-driven rain on hygrothermal performance. Simulations were performed for each wall using orientations facing north, south, east, and west. Additional details of the seven weather locations are shown in Figure 4-1.

Interior conditions were kept constant at a temperature 20°C and relative humidity 40% RH (P_v = 997 Pa) throughout the year, as explained previously. The heat and mass transfer coefficients for external and internal surfaces were constant during the simulations in order to obtain comparable results in the parametric study. These coefficients are presented in Table 4-1. Each 1-year weather file was repeated during the 3-year simulations, i.e., the second and third year had the same exterior boundary conditions as the first year. A three year period was selected to investigate if a net yearly accumulation in the wall structure was present. Furthermore for most of the simulations, the walls were located on the fifth floor of a 10-storey high-rise building. This reduced the severity of the amount of rain striking the wall section. This issue is discussed in detail in a subsection about wind-driven rain.

Comparison of Weather Data

The Best Meteorological Year (BMY) weather files (Schwarz et al. 1973) of seven chosen Canadian cities were used in the simulations. The BMY data files consist of a pick for a particular year that is based on a weighting of temperature (dry-bulb temperature), wind speed, cloud cover, and moisture ratio. The picks are based on the "best fit" of the year for a 10-year average. This pick yields five or six sets of contiguous months. From this set, the final chosen set had the widest possible temperature distribution. The Atmospheric Environment Services (Canadian Climate Centre) attempted to fill in as many gaps as possible in the 10-year weather file. In some cases, such as the precipitation indicator and precipitation amount, this was not possible. To determine the relevance of the weather data provided by the BMY weather files to other published or measured data, a few comparisons were made. Figure 4-2 shows BMY monthly average temperatures and vapor pressures for Ottawa and Vancouver. The yearly average temperatures and vapor pressures in Ottawa and

WEATHER
(input weather data files)

NO RAIN DATA

RESOLUTE
(resol.dat)

FREDERICTON
(fred.dat)

WINNIPEG
(winn.dat)

WITH RAIN DATA

TORONTO
(toro.dat)

MONTREAL
(mont.dat)

VANCOUVER
(vanc.dat)

OTTAWA
(ott.dat)
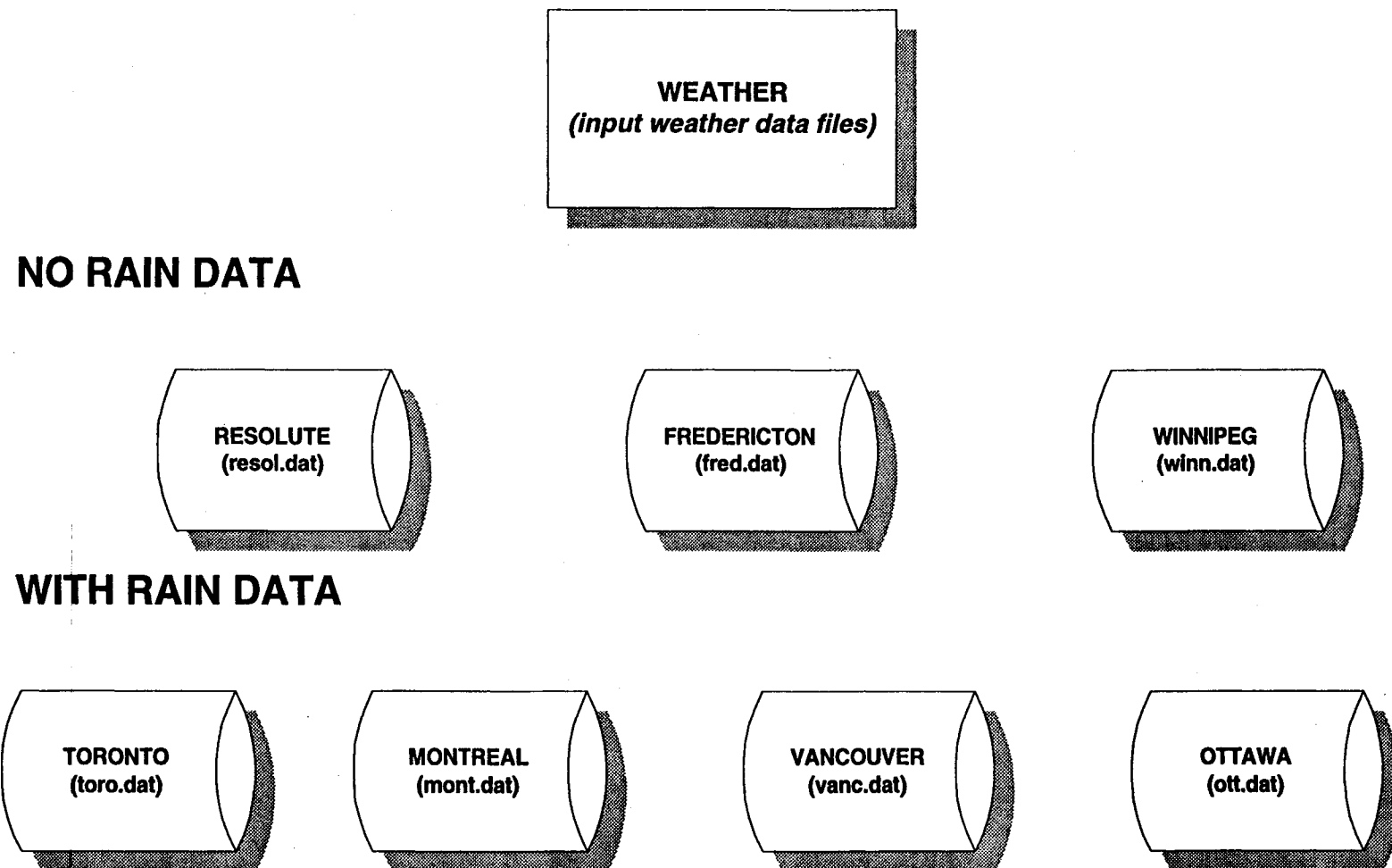
Figure 4-1: Weather data file structure

Vancouver are 5.6°C, 832 Pa and 9.1°C, 958 Pa, respectively. The total amount of driving rain, when temperatures are above freezing (T>0°C) on a vertical south facing wall (5th floor, center of the wall), was 79 mm and 209 mm in Ottawa and Vancouver, respectively. The total amount of precipitation was 570 in Ottawa and 1124 mm in Vancouver. The long-term (1950-1980) average yearly precipitation is 846 mm in Ottawa and 1329 mm in Vancouver (according to data provided by Environment Canada), i.e., the BMY weather files used in the simulations accounted for less precipitation than the average year for these locations. Figure 4-2 depicts weather data measured at an IRC weather station located next to NRC's Ottawa test huts. Comparing Figures 4-2 and 4-3, the BMY temperature data and the NRC measured temperature for the year of 1994 show remarkable agreement. This gives good confidence in the use of the BMY weather data files.
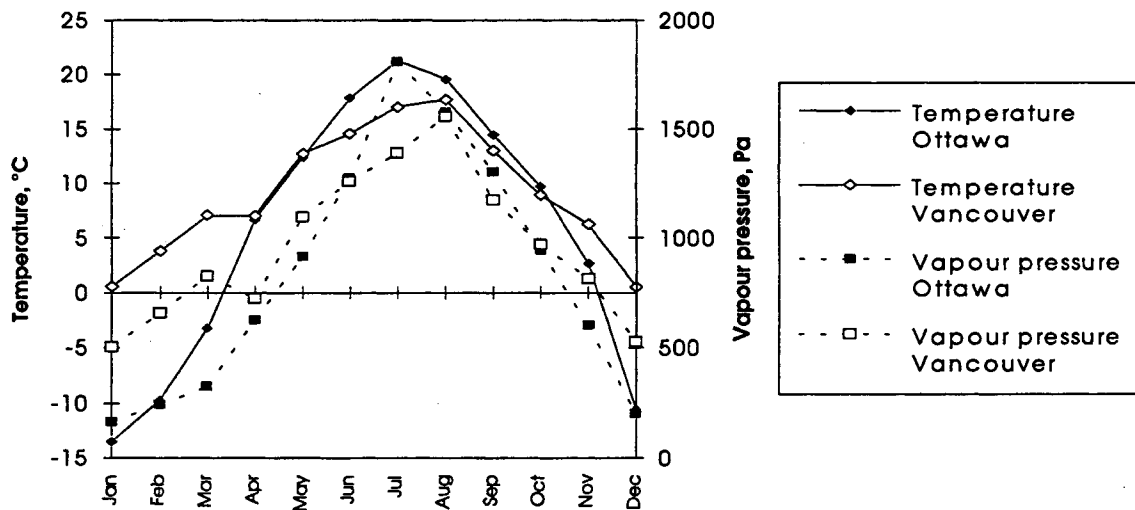
Figure 4-2:   The monthly average temperatures and vapor pressures in Ottawa and Vancouver BMY weather files
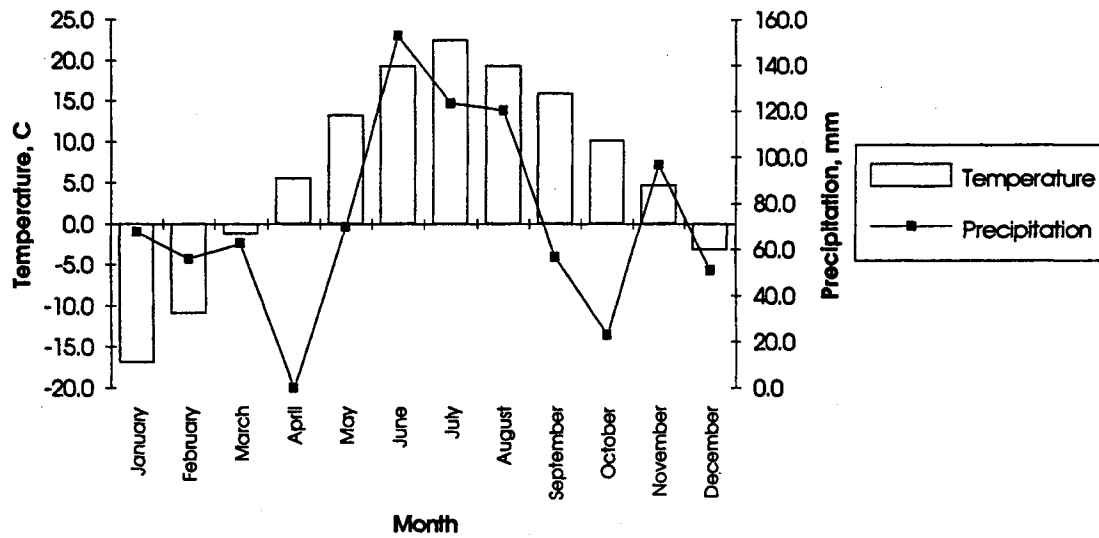
Figure 4-3: The monthly average temperatures and precipitation at IRC weather station in Ottawa during 1994

Table 4-1: Heat and moisture transfer coefficients for the external and internal surfaces.

Property	External surface	Internal surface
Heat transfer coefficients, W/ m^{2}K	20	8
Mass transfer coefficients, kg/m^2,s,Pa	$9.8 \cdot 10^{-8}$	$7.4 \cdot 10^{-8}$
Short wave absorptivity	0.8	-
Long wave emissivity	0.6	-

ROOF BOUNDARY CONDITIONS

For each high-rise roof, only one orientation was used. Simulations were performed on three different roof structures for only the horizontal orientation (flat-roof setup). The same seven locations used for the wall study were also used for the roof simulations. The heat and mass transfer coefficients for external and internal surfaces were, like those for the wall surfaces, kept constant during the simulations. These coefficients are also presented in Table 4-1.

4.2   NUMERICAL 3-D SIMULATION OF WIND FLOW AND WIND-DRIVEN RAIN

INTRODUCTION

The exterior surface (facade) is constantly interacting with the ambient temperature, solar radiation, wind pressure, relative humidity, and wind-driven rain. Wind-driven rain is defined here as rain droplets carried along by wind having a characteristic angle relative to the vertical. This part of the project presents results on wind-driven rain on a high-rise building envelope.

In a recent publication by Karagiozis and Salonvaara (1995), wind-driven rain was determined to be an important contributor to the total amount of moisture entering the structure. The instantaneous amount of moisture accumulation within the structure was found to increase tenfold or more, depending on the specific topographical location of the building. In situations where moisture accumulates at rather high levels, structural deterioration due to freeze-thaw cycles may occur. Wind-driven rain entering the facade of the structure accelerates the normal deterioration process and therefore reduces the service life of the building. Therefore, any short or long-term hygrothermal study on building envelopes requires the accurate prescription of wind-driven rain information as boundary condition inputs, especially when these studies lead to design guidelines. The effective run-off that can increase the amount of available water many times over can be determined by knowing the wind-driven rain intensity as a function of height and the water absorption characteristics of the exterior surface.

Rain droplets with a wide range of sizes are transported by wind that has a distinct 3-D behavior near buildings. The droplet trajectories are time-dependent due to the effect of turbulence. Furthermore, rain droplet size distributions vary randomly with respect to time and space. For these reasons, the amount of rain striking the exterior surfaces of a building is unique to that building as it depends on the local geometry of the building, topography around the building, wind speed, wind direction, rain intensity, and rain droplet distribution.

Knowledge available on wind-driven rain, albeit limited, has been predominately determined by field experiments (Lacy (1951), Schwarz and Frank (1973)). Recently however, investigations employing computational fluid dynamics methods (Choi (1991), and Wisse (1994)) have appeared. Lacy , a pioneer in the area of wind-driven rain, carried out extensive on-site measurements, and recently the British Code of Practice (BCP, (BSI 1992) presented an updated method for estimating driving rain. Robinson

and Baker (1995) from NRC also carried out an qualitative field investigation. Wisse critically evaluated the assumptions involved in the estimating method of the BCP, compared it to measurements by Schwarz and Franc , and found major disagreements. Wisse also predicted rain wetting patterns using a 2-D CFD approach. Hens and Mohamed (1994) experimentally measured driving rain striking a two storey school and compared it to driving-rain calculation methods and found that the simplified theory approach (modification of BCP) overestimated the amount of driving rain by 25%. Choi (1992) presented 2-D and 3-D CFD results for wind-driven rain conditions, and determined several rain intensity factors for stand alone buildings. In these studies, however a turbulent particle tracking method for modeling rain droplet trajectories was not used. Furthermore, the flow and rain droplets were not fully coupled. This uncoupling between air and rain droplets may become critical at very high rain intensities. Preliminary laboratory investigations with wind tunnel methods have been performed by Surry et al (1994). The authors showed higher wind-driven rain striking at the upper parts of the building model, thus confirming some of the previous field and computational results. High-rise buildings are exposed to harsher environmental conditions than those for low-rise buildings. The present study numerically examines wind-driven rain hitting the exterior surface of a stand-alone high-rise building. The influence of wind speed and rain intensity on the amount of rain striking the exterior surfaces of a high-rise building was investigated.

WIND-DRIVEN RAIN

Wind-driven rain, as just discussed, is strongly affected by the local wind around a building. Rain droplets, in the absence of wind, fall down vertically, under the influence of gravity. This would imply that the amount of rain hitting the walls of a building in the absence of wind is theoretically zero. Near the vicinity of a building, raindrop trajectories are affected not only by the unobstructed wind flow, but also strongly affected by the particular flow distribution surrounding the building. Some of the important governing factors for the wind-driven-rain problem, (Choi, 1991) are

(1) the upstream wind conditions, including the unobstructed wind velocity profile, turbulence intensity profile and turbulence eddy length scale, as well as, the ground surface roughness height.

(2) the local flow pattern around a building, which is related to the upstream wind conditions, the surface roughness of the building, the geometrical configuration of the building and the surrounding conditions of the building;

(3) rainfall intensity, and

(4) the size and distribution of the raindrops.

Each high-rise building has its own distinct wetting pattern during a rain storm. This implies that the present results on wind-driven rain depend on the local weather conditions and building geometry.

MODELING METHOD

WIND FLOW AROUND THE BUILDINGS

The prediction of wind-driven rain distribution on high-rise buildings requires the determination of the local 3-D time-averaged velocities, velocity fluctuations, and the time-averaged pressures. (The flow field around a bluff body, even for a simple cube, is very complicated. It includes a turbulent boundary layer, stagnation region, separation, reattachment, circulation, and von Karman's vortex streets.) The equations governing wind flow around buildings are the incompressible Navier-Stokes equations and the continuity equation. Closure to these equations is provided by various turbulence models, including the k-ε two equation model, the algebraic second-moment closure model (ASM) and the Large-Eddy Simulation. Specific details about these models can be found in Rodi (1981), Launder and Spalding (1974) , and Murakami (1992). The k-ε model is one of the most commonly used model in the field of wind-engineering, and it has been adopted for this study. The details and equations employed are described in detail in Appendix B1.

RAIN DROPLET MODELING

In this section, information is presented regarding the size distribution of rain droplets, followed by a discussion on the 3-D Lagrangian Turbulent Particle Tracking method employed.

The size distribution of raindrops

Calculation of the amount of rainfall impinging on the building facades requires knowledge on the size distribution of raindrops in a particular storm. Best carried out an extensive experimental study of rain droplet size distributions and their relationship with rainfall intensity. The results of his study can be summarized by the following simple correlation:

$$F(d) = 1 - \exp[-d/a]^n \qquad (4\text{-}1)$$

$$a = AI^P \qquad (4\text{-}2)$$

$$W = CI^r \qquad (4\text{-}3)$$

where

F = fraction of liquid water in the air comprised by drops with diameter less than d,

I = rate or intensity of rainfall

d = droplet diameter

W = amount of liquid water per unit volume of air

A, c, p, r and n = constants.

If d is measured in mm, I in mm/hr and W in mm³/m³, the mean value of A, c, p, r and n are 1.30, 67, 0.232, 0.846 and 2.25 respectively. Figure 4-4 shows the rain droplet distribution for different rain intensity rates.

Rain trajectories using the Lagrangian Particle Tracking Method

Many engineering problems, such as wind-driven rain, involve the study of mixtures containing a continuous phase which exhibits fluid properties and a dispersed phase which is discretely distributed in the fluid. With the dispersed phase, there is no continuum, the phase can be considered a set of individual discrete rain particles, and each particle interacts with the fluid and other particles discretely.
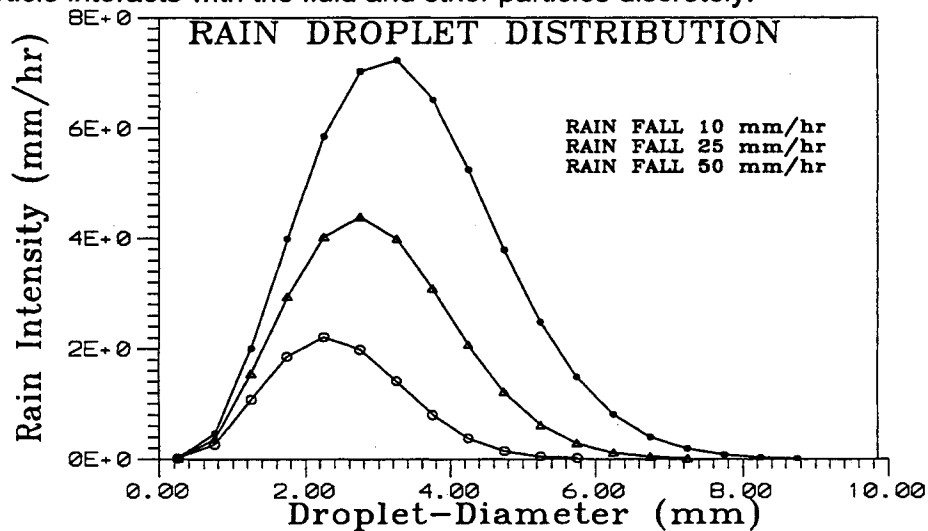
Figure 4-4 : Effect of rain droplet diameter distribution on rain intensity

A Lagrangian tracking model can be used to predict the behavior of the dispersed phase. The Lagrangian tracking method tracks several individual rain droplets through the flow field, and involves the integration of particle paths through the discretized domain. Individual rain droplets are tracked from their injection point until they escape the domain or some integration limit criterion is met. The rain droplets are assumed to have a spherical shape and their density much greater than the air fluid density. The governing equations are presented in APPENDIX B1.

BUILDING STRUCTURES AND COMPUTATIONAL DOMAIN

In this wind-driven rain analysis, high-rise buildings located in an area sparsely populated by low-rise buildings will be referred to as an the open-country case (see Figure 4-5a) and high-rise buildings close to other high-rise buildings will be referred to as city-centre case (See Figure 4-5b). The width of the high-rise building, defined as h, is used as the measuring unit for the geometry of the domain. The simulation domain, with a downstream length of 16.0h, an upstream length of 16.0h, a lateral width of 4h on each side, and a vertical height of 10 h was discretized. The computational domain was extended far before and after the building structure to accommodate far field effects. To avoid using a highly non-uniform spacing grid system, grid embedding close to the high-rise building was used. For the open-country case, a building model of 1 x 2 x 1 h was used with 81 x 31 x 31 control volumes in the grid embedding zone and 36 x 11 x 10 control volumes outside the embedding zone in the x, y and z directions respectively.

BOUNDARY CONDITIONS

Upstream boundary

Wind velocity turbulence intensity profiles for the upstream inlet were assigned values given by Baskaran (1992), suburban open-country conditions.

Upper faces of the computational domain

The upper faces of the computational domain are defined as a slip-wall with zero shear stresses.

Downstream boundary and side faces of the computational domain

These boundaries are set to be pressure-specified openings. Pressures outside the boundaries were assumed to be zero.

High-rise wall boundary

The building's walls and ground are assumed as rough surfaces. For the high-rise walls and ground, an equivalent sand-grain roughness height of 0.1m and 0.03 respectively are used in the simulations.

Rain droplet tracking

In this study, the rain droplets are divided into a number of groups according to their size. A maximum of 18 groups, depending on the rain intensity, with approximately 3000 droplets in each group, were injected from different planes of the domain. The droplet terminal velocities, and the mass flow rate for each group were defined prior to the simulations at the injection joints.

SIMULATION CASES

In this study, the water mass flow distributions, due to wind-driven rain water on the four walls of the high-rise building, were computed for three different wind speeds, three wind angles and three rain intensities. The chosen rain intensities are representative of the rain patterns found in most of the habitable areas of Canada.

Overview

Using the TASCflow3D (ASC 1993) Computational Fluid Dynamics model, the wind flow for two high rise buildings were investigated. These buildings differ because of their particular geographic location and are named throughout this report as either the open-country case or the city-centre case. For each of these two high-rise cases, three different wind speeds at gradient height were used: 5 m/s, 10 m/s, and 25 m/s. For each of these wind speeds three wind directions (angles), were examined, at 0 degrees, 30 degrees and 45 degrees. For each wind speed and wind direction (angles) three rain precipitation intensities were used. The rain intensities were representative of the rain patterns found in most of the habitable areas of Canada; they are 10 mm/h 25 mm/h and 50 mm/h. A total of 27 simulations were carried out for each case of the high-rise buildings, which amounted to 54 complete wind and wind-driven rain cases (see Table 4-2). The simulations were carried out simultaneously on two very fast workstations, a HP 735 with 40 Mflops (40 times faster than a 386 33Mz PC machine) and a Silicon Graphics with 18 Mflops of computing power. These simulations ran uninterrupted for over 7 months from October 1993. The effort in both user assistance and CPU time for rain droplet tracking is immense compared to just the wind-induced fluid flow predictions. Following are a few figures included to show the high-rise arrangements, the model grid sizes, the flow field characteristics, and some of the few post-processed wind-driven rain results. From these extensive calculations the exterior pressure and rain mass flow rates for each surface of the high-rise are deduced for use in the hygrothermal models.

WIND DRIVEN RAIN RESULTS

In Figures 4-6 and 4-7 wind velocity distributions are displayed around the high-rise building for the open country and city center cases. The velocity field at the center (X-Y) plane of the building is shown for a gradient height velocity of 5 m/s. The flow around the high-rise building clearly indicates that high velocity gradients surround the building. Furthermore, since rain droplets are dispersed in the continuous air phase, the local acceleration and deceleration create rapidly changing transport forces on each rain droplet. Figures 4-7a , 4-7b and 4-8a, 4-8b show a limited number of wind-driven rain trajectories at different rain droplet diameters (0.5 and 5.0 mm) for the open-

country and city-centre cases respectively. Trajectory results are shown for the same x-y plane as the one used for the velocity distributions. While the figures depict trajectories with fairly straight lines, in 3-D presentations, this is far from true. The influence of droplet diameter size on wetting behavior due to wind-driven rain is demonstrated to be very important.

Table 4-2: Simulation runs with different parameters

wind speed (m/s)		5 m/s			10 m/s			25 m/s	
wind angle degree) (West face at 0 degrees)	0	30	45	0	30	45	0	30	45
rain	10	10	10	10	10	10	10	10	10
intensity	25	25	25	25	25	25	25	25	25
(mm/hr)	50	50	50	50	50	50	50	50	50

These figures, at the gradient height velocity of 5 m/s, show that the velocity field has a greater influence on the droplet trajectories for small-diameter particles than for droplets much larger diameter (5.0 mm). For the 5.0 mm rain droplet, the trajectories become more parallel to each other. In Figure 4-9 the rain droplet trajectories are shown for all droplet sizes, for a wind speed of 25 m/s for the city-centre case. Here the additional influence of higher wind speeds is clearly demonstrated. Figure 4-10 shows the effect of wall orientation, (west-, east- and north- facing, on the amount of rain each wall receives, when using a rain intensity of 10 mm/h and a wind speed of 10 m/s for the open-country case. The south wall receives an amount of rain similar to that of the north wall. The ratio Iwall/Irain is defined here as the intensity of rain that strikes the wall over the normal rainfall intensity. A distinct vertical wetting pattern distribution from the bottom to the top of the building occurs. The west face, which is normal to the wind speed, receives more wind-driven rain, and the upper top area of the building receives the highest amount of rain for all faces. Irregularities in the trend, as we move from bottom of the building to the top are due to the randomness of the turbulent Lagrangian particle tracking method used. Figure 4-11 shows the rain intensity factors (Iwall/Irain) as a function of rain intensities of 10, 25 and 50 mm/hr for a west-facing wall. Results indicate that rain intensity has a minor effect on the wind-driven rain distribution as a function of height. Finally, Figure 4-12 illustrates the

significant effect of wind speed on the rain intensity factor Iwall/Irain, again on the west face of the building using a rain intensity of 25 mm/h. All results generated by the wind-driven rain work were imbedded into the LATENITE hygrothermal model.

4.3 CONCLUSIONS

Both interior and exterior boundary conditions were examined in this section for both the wall and roof structures. Transient boundary conditions for ambient temperature, relative humidity, solar irradiation, rain flux, and wind pressures varying hourly were used for the exterior surface of the building.

Wind-driven rain is an important consideration in the hygrothermal performance of a building envelope. To date, very little work is available that provides field or laboratory data for wind-driven rain that can be used with moisture transport models. This information is a definite requirement as a boundary condition by the more sophisticated hygrothermal models before one can predict the hygrothermal performance of a building envelope A CFD method for predicting the wetting patterns at high-rise structures during wind-driven rain is used in this work. For all cases, the amount of wind-driven rain striking the building increases from bottom to top. The results show distinct wetting patterns on the top of the building. The patterns are parabolic in shape when the wind orientation is normal to the exterior facade. The results show that the downstream side (east was the case considered) of the wall receives no rain except near the top due to the wind induced recirculation in that region. This investigation found that, at a 25-m/s wind speed, the upper top areas of the high-rise building received twice the horizontal rain intensities. The results show that the rainfall intensity does not significantly affect the wetting pattern of the building walls. Higher wind speeds, however, were found to increase significantly the amount of water received on the building facade. The higher the wind speed, the higher the amount of water received. Information generated by using this complex 3-D flow and turbulent particle tracking approach is essential for accurate hygrothermal modeling. The amount of rain hitting the exterior facades of a building must be incorporated into hygrothermal models, to account for liquid transport at the surfaces. The analysis of durability with respect to the hygrothermal performance can only start when models are equipped with methods for incorporating driving rain. Wind speed and direction also alter the infiltration or exfiltration patterns because of stack effect. These effects are accounted for in the model.
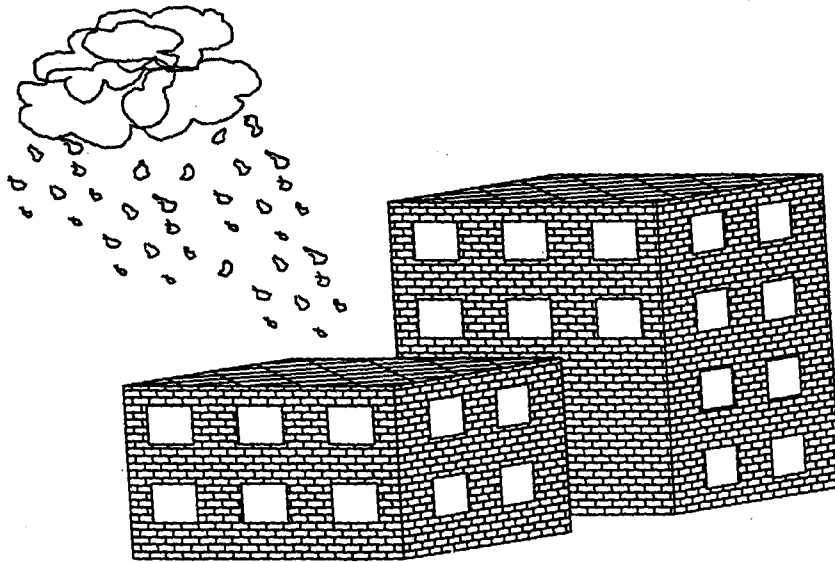
Figure 4-5a: Geometry for the city center high-rise building
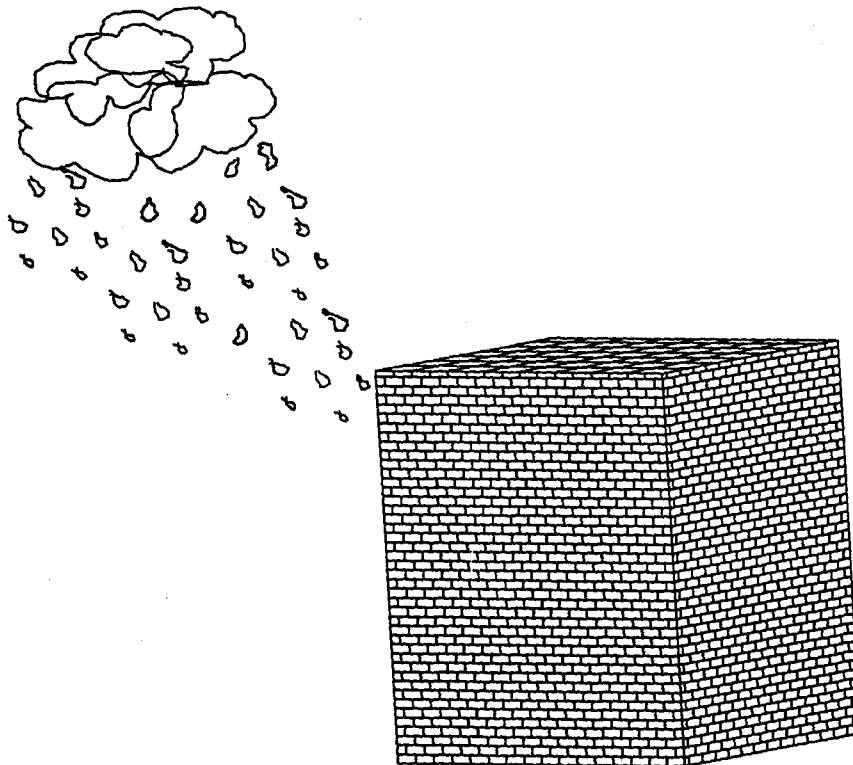
Figure 4-5b: Geometry for the open country high-rise building
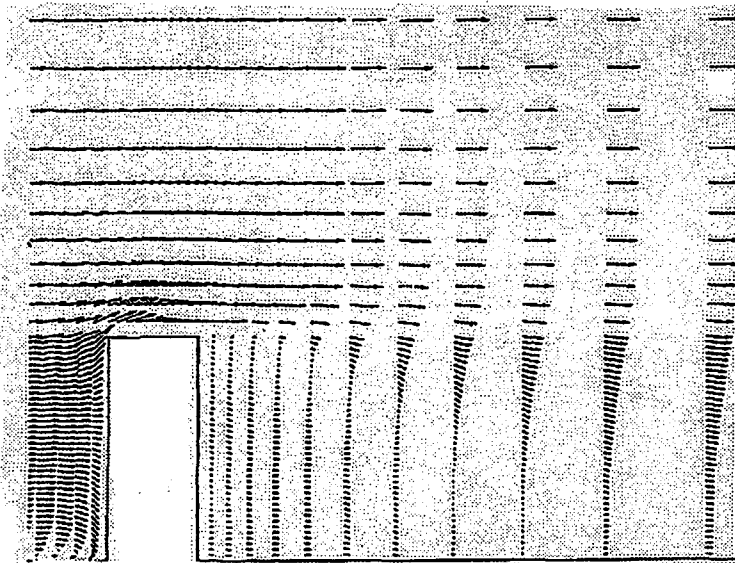
Figure 4-6a: Open country velocity distribution for the symmetric X-Y plane
using a gradient height velocity of 5 m/sec from west to east
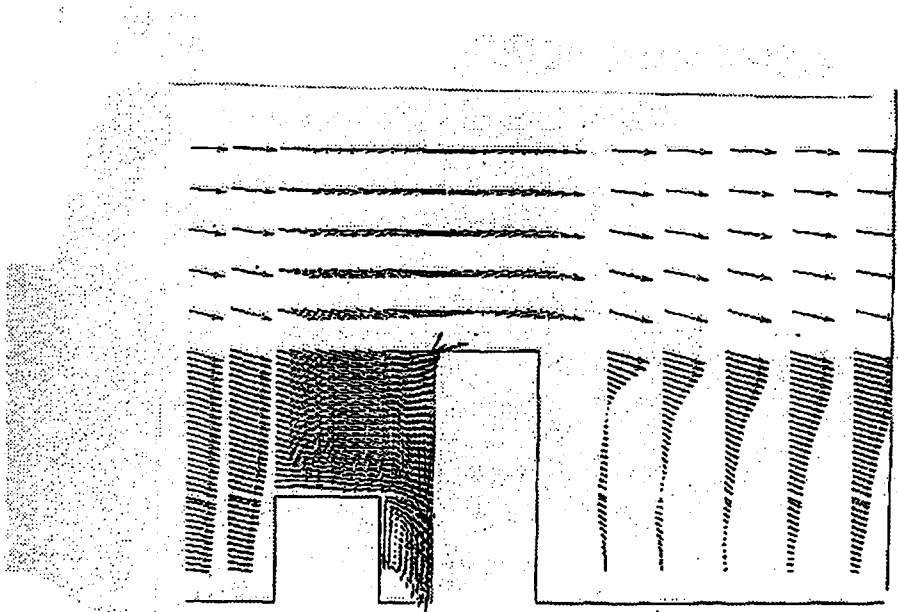
Figure 4-6b: City center velocity distribution for the symmetric X-Y plane using a gradient height
velocity of 5 m/sec from west to east.
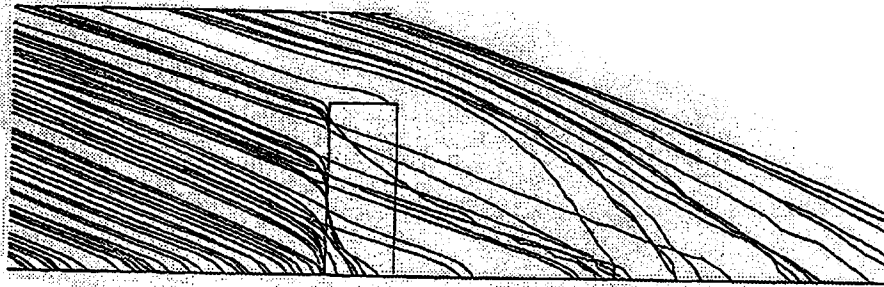
Figure 4-7a: Trajectories for 0.25 mm diameter rain droplets at 5 m/sec gradient height wind

speed (Open country case)
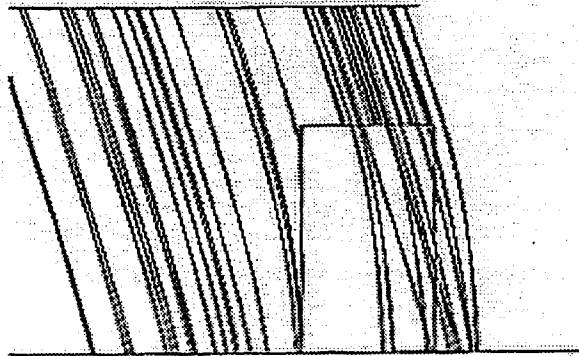
Figure 4-7b: Trajectories for 5 mm diameter rain droplets at 5 m/sec gradient height wind speed

(Open country case)
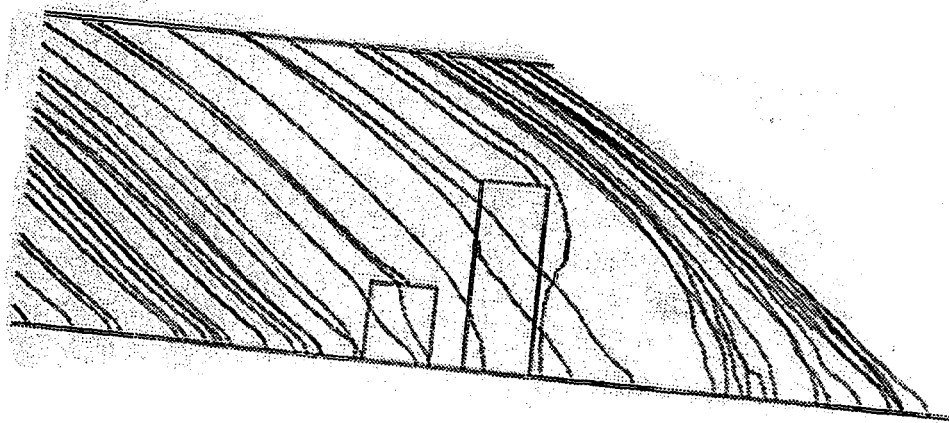
Figure 4-8a: Trajectories for 0.25 mm diameter rain droplets at 5 m/sec gradient height wind speed (City center case)
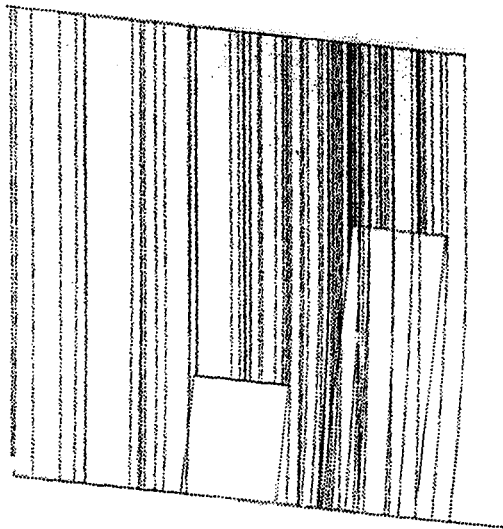
Figure 4-8b: Trajectories for 5 mm diameter rain droplets at 5 m/sec gradient height wind speed (City center case)
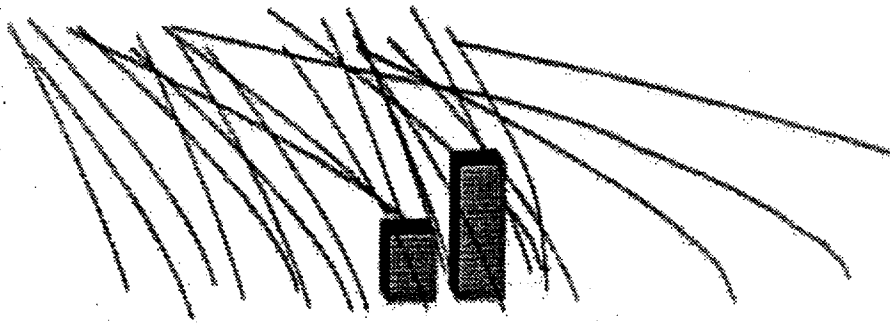
Figure 4-9:   3-D Trajectories for rain droplets using a wind velocity of 25 m/sec and a rain
intensity of 25 mm/hr
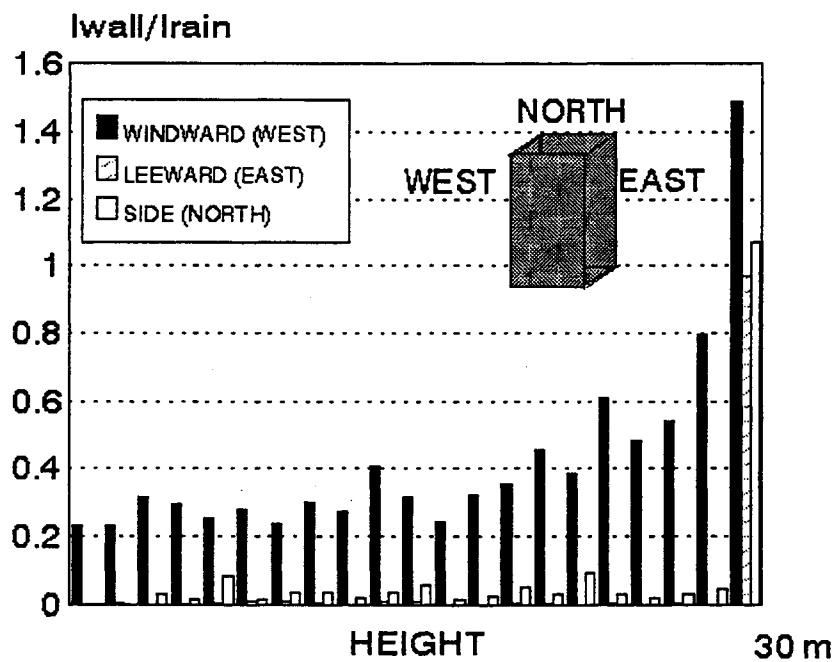
Figure 4-10: Wind-driven rain intensity factors for the West, East, and North
faces of the high-rise building, using U=10 m/s, and Irain=10 mm/hr.

Iwall/Irain
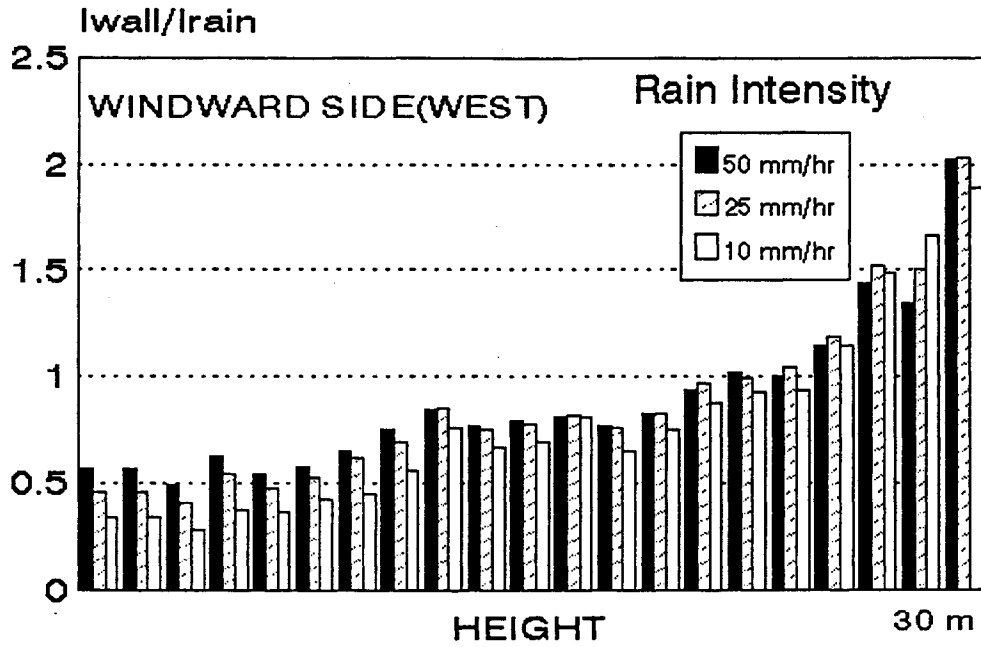
Figure 4-11: Wind-driven rain intensity factors for the West facing wall as a function of rain intensities, using U=25 m/sec.

Iwall/Irain
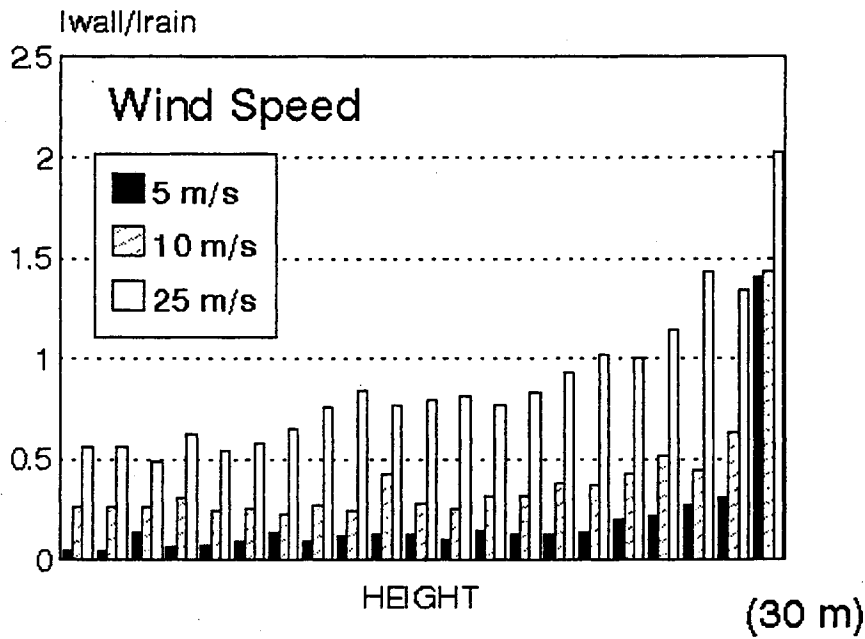
Figure 4-12: Wind-driven rain intensity factors for the West facing wall as a function of wind speed, using Irain=50 mm/hr

5.0 SIMULATION CASES

5.1 CONVENTIONS FOR WALL AND ROOF DEFINITION

In this section, information is presented about wall and roof structures used in this high-rise hygrothermal study. Two main sets of simulations were carried out, those with 1-dimensional cross-sections and those with 2-dimensional cross-sections.

1-D SIMULATIONS

For the 1-D simulations, initially three walls and roofs were considered (see Section 1). These simulations comprise most of the work of this research project. For convenience, these walls and roofs have been named WALLS, (base-case) 1, 2 and 3 and ROOFS, (base-case) 1, 2 and 3 respectively. Long-term (3 years) hygrothermal simulations were performed on these building envelope structures. The three walls were then retrofitted using common, but not necessarily correct, practices. In some cases these retrofits represent intentional theoretical examinations that are not necessary practical. Depending on whether the retrofit was carried out on the right side (interior of the building) or on the left side (exterior of the building), the retrofit strategy was named left or right case wall followed by the numbering 1, 2 and 3.

2-D SIMULATIONS

These results were carried out on the latest version of LATENITE 1.2 that included the effect of air flow. For these simulations only, one wall was chosen, that being WALL-1 (base case). Modifications were made to allow air leakage pathways for investigating the effects of exfiltration/infiltration.

1-D WALL PREPARATION CASE

In Phase IV, the three high rise wall structures (see Figures 5-1, 5-3 and 5-4) were numerically discretized in the computational domain. In these figures, the dimensions are shown for each layer. Each material layer was divided into several smaller control volumes, and the partial differential equations describing the transport of energy and moisture were algebraically solved. The number of control volumes were then increased until results exhibited grid-independence. This was required to produce numerically error-free results because of space discretization; it was carried out for each one of the wall and roof structures. The LATENITE 1.2 model, as described in the modeling section, was employed throughout Phase IV. The retrofit strategy for insulating the left side is shown in Figures 5-4, 5-5 and 5-6 for WALL1, WALL2 and WALL3 respectively. Similarly, Figures 5-7, 5-8 and 5-9 show the left-retrofit

application for WALL1, WALL2 and WALL3. For each high-rise wall, four different wall orientations were used because of the strong effects of orientation on solar radiation and wind-driven rain. Simulations were performed for each wall case using orientations facing, north, south, east, and west. Furthermore, seven Canadian weather locations were used in this high-rise project.

1-D ROOF PREPARATION

The three high-rise roof sections (see Figures 5-10, through 5-12) were employed to determine the hygrothermal performance as a function of weather conditions. These roof systems were numerically discretized in a computational grid. Each material layer was divided into several smaller control volumes and the partial differential equations describing the transport of energy and moisture were algebraically solved. Simulations were performed for these three roof structures for the horizontal orientation only (flat roof set-up). The same seven locations used in the wall study were also employed for the roof simulations.

2-D SIMULATION CASES

The wall structure used (see Figure 5-15) is similar to WALL1 (base case) with the exception that a 2-D analysis was applied with the addition of cracks. As depicted in Figure 5-15, two interior and one exterior openings were introduced to the wall structure. Air exfiltration or infiltration could occur by two main paths, one direct and the other indirect. The obvious paths from the inside to the outside or vice versa could occur from the bottom where a continuous crack exists, or from the inside through the insulation continuing through the air space. However, an additional path occurs at the interior surface of the structure, where air may infiltrate at one opening and exfiltrate from another. Natural convection in the porous insulation materials was also included. Stack effect with regards to the height of the building wall was also examined using this 2-D simulation. All the 2-D simulations used weather data for the City of Ottawa. The influence of a mechanical overpressurization of 10 Pa was also investigated.

SIMULATION LAYOUT

The major effort in this part of the study was setting-up, documenting, and executing each simulation. For each case, (base case, left-retrofit and right-retrofit), preliminary simulations were performed to determine grid size requirements, so that the results could be grid-independent. The criterion chosen for this part was that as soon as the control volumes displayed differences of less than 0.005 in relative humidity from a 50% reduction in volume of the control volume. This criterion is quite stringent. The number of simulations involved, particularly in the wall study, is enormous (3 walls x 3

insulation strategies x 4 orientations x 7cities). Key results from this part of the study were systematically processed soon after the simulations had been completed. This allowed some quality control over the full simulation process. Figures 5-13 and 5-14 show the hygrothermal simulation involved in the wall and roof along with the associated input and output file structures.

5.2   NUMERICAL TIME STEP CONSIDERATIONS

For all the wall and roof simulations, a 1-hour time step was chosen, as demonstrated in Section 2, so that reasonable hygrothermal results can be obtained. Most of the data available from Environment Canada, ASHRAE or other weather service organizations are also stored in 1-hour intervals.

5.3   INITIAL CONDITIONS

The results produced from this study are independent of initial conditions. Three year simulations were performed, but only the 3rd year results are presented in this report. In most cases, very little influence was observed from year 1 to year 2 in moisture and thermal behaviours. This was further decreased with the results produced from the year of simulations. An initial temperature of -5°C and 80% relative humidity was assigned for all roof and wall control volumes for both the 1-D and 2-D simulations.

RED BRICK

AIR SPACE

BUILDING PAPER
0.2mm

EXTRUDED POLYSTYRENE

MINERAL FIBRES 20KG/M3

6-MIL POLYETHELENE
0.15mm

GYPSUM BOARD

102   89   25

25   9.5

NOTE:ALL DIMENSIONS IN mm
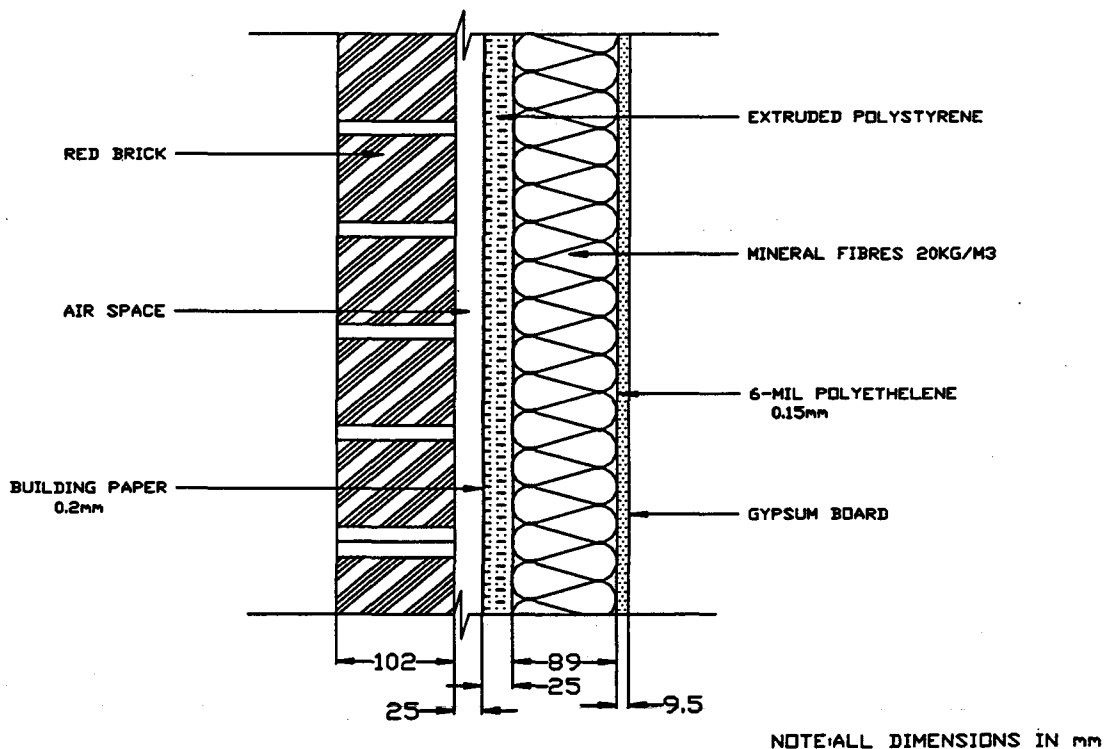
Figure 5-1: WALL1 (base case)

RED BRICK

AIR SPACE

MINERAL FIBRES 20KG/M3

6-MIL POLYETHELENE
0.15mm

ANNEX CONCRETE

AIR SPACE

ANNEX CONCRETE

GYPSUM BOARD

102   102   70   70
25   60   9.5

NOTE: ALL DIMENSIONS IN mm
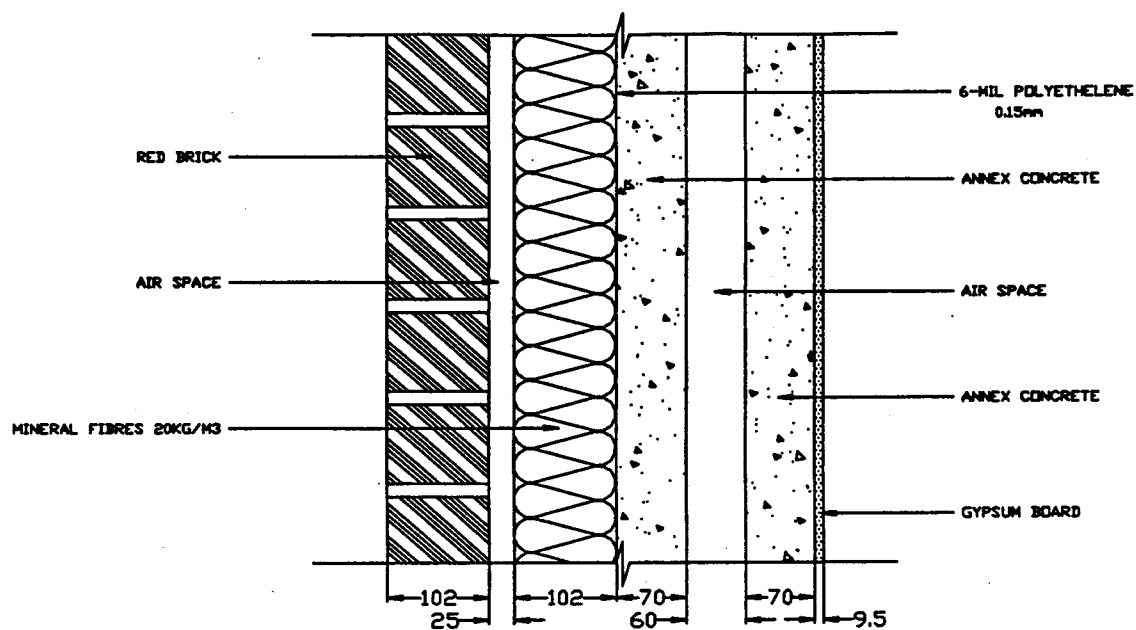
Figure 5-2:WALL2 (base case)

STUCCO FINISH

EXTRUDED POLYSTYRENE

GYPSUM BOARD

AIR SPACE

GYPSUM BOARD

5   75   92   9.5
     13

NOTE: ALL DIMENSIONS IN mm
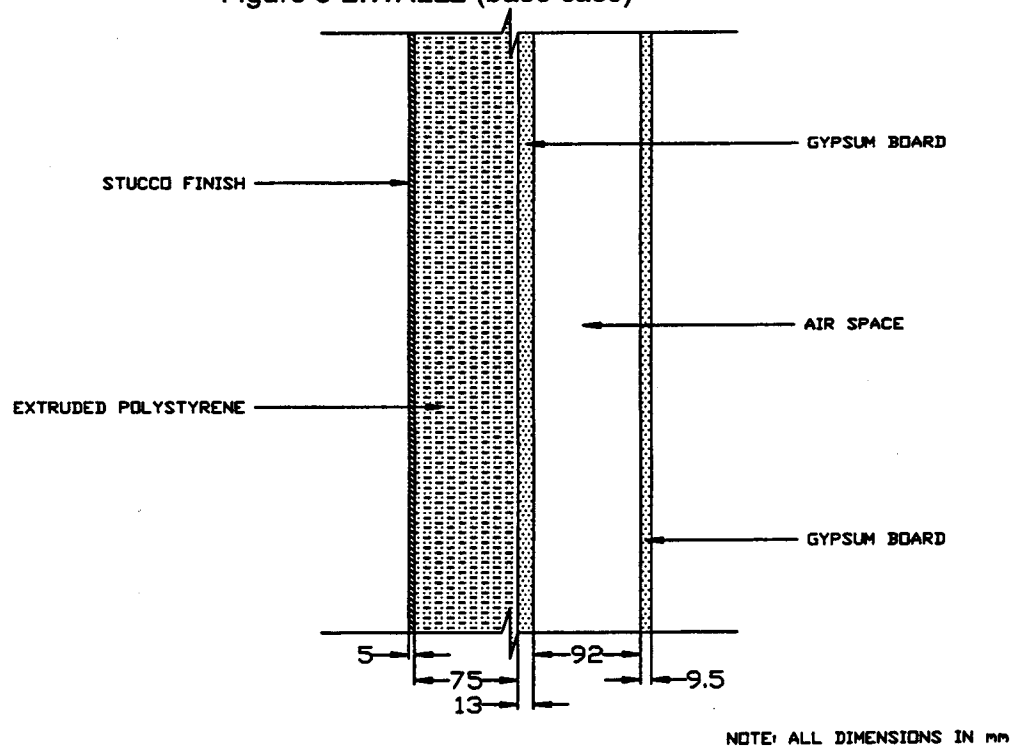
Figure 5-3: WALL3 (base case)

STUCCO FINISH

EXTRUDED POLYSTYRENE

RED BRICK

AIR SPACE

BUILDING PAPER
0.2mm

EXTRUDED POLYSTYRENE

MINERAL FIBRES 20KG/M3

6-MIL POLYETHELENE
0.15mm

GYPSUM BOARD

5
25
102
25
25
89
9.5

NOTE: ALL DIMENSIONS IN mm
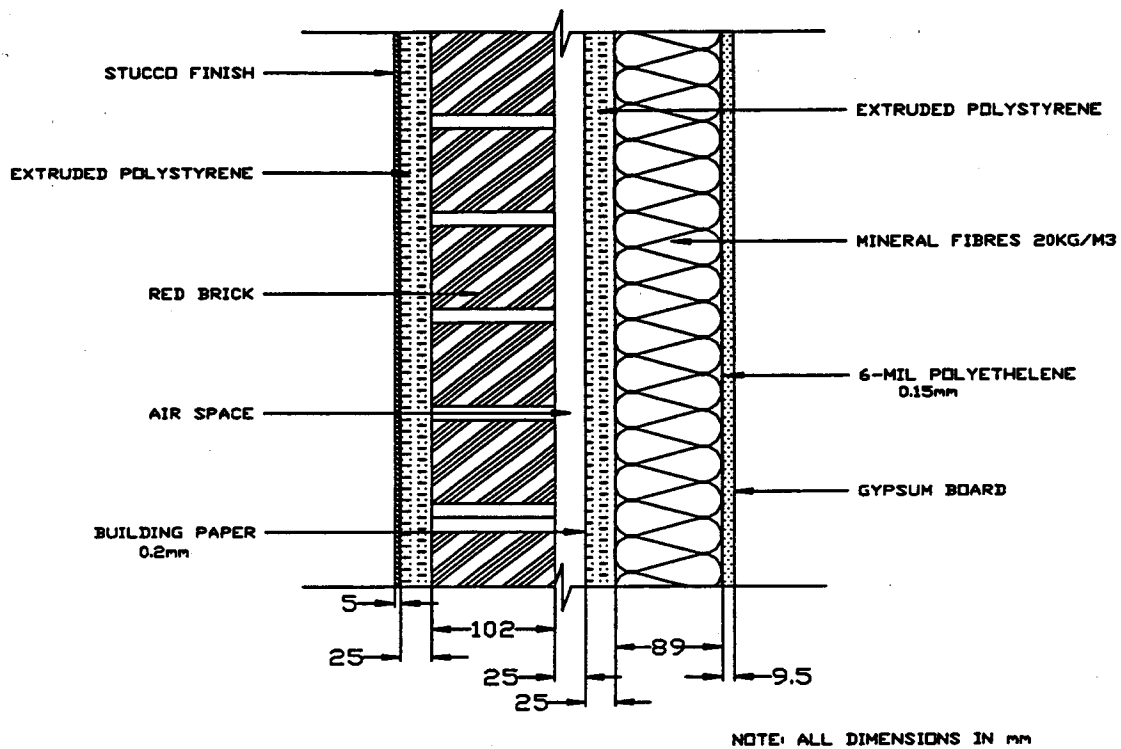
Figure 5-4: WALL1 (left-retrofit case)

STUCCO FINISH

EXTRUDED POLYSTYRENE

RED BRICK

AIR SPACE

MINERAL FIBRES 20KG/M3

6-MIL POLYETHELENE
0.15mm

ANNEX CONCRETE

AIR SPACE

ANNEX CONCRETE

GYPSUM BOARD

5
25
102
25
102
70
60
70
9.5

NOTE: ALL DIMENSIONS IN mm
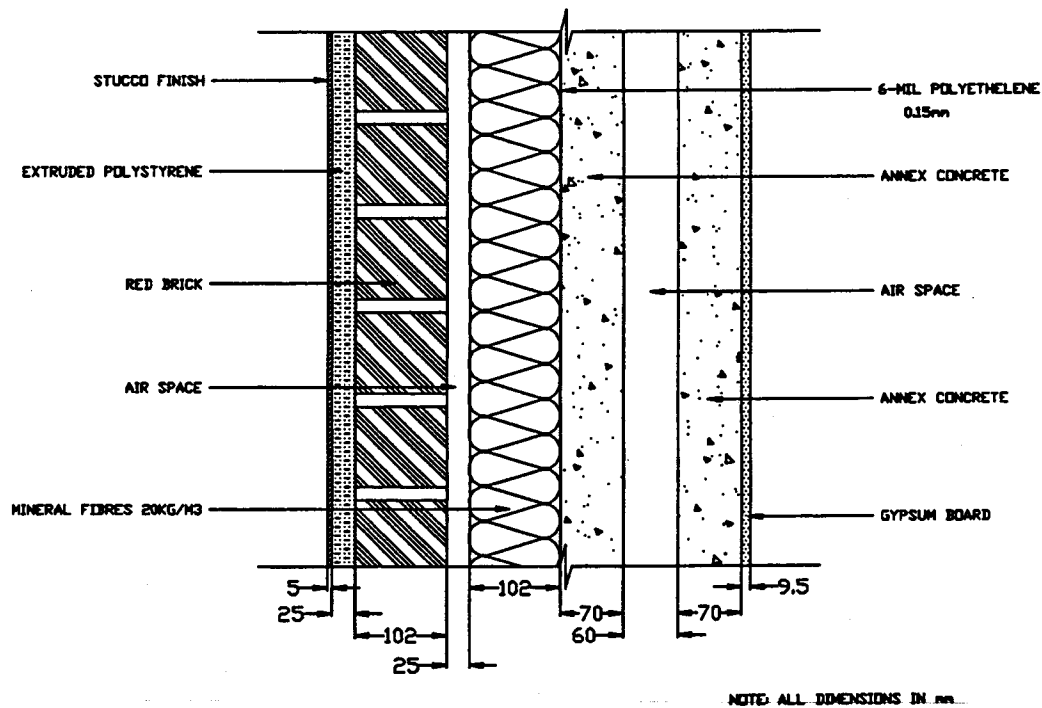
Figure 5-5: WALL2 (left-retrofit case)

STUCCO FINISH

EXTRUDED POLYSTYRENE

MINERAL FIBRES 20KG/M3

GYPSUM BOARD

AIR SPACE

GYPSUM BOARD

5

75   89   92

13

9.5

NOTE: ALL DIMENSIONS IN mm
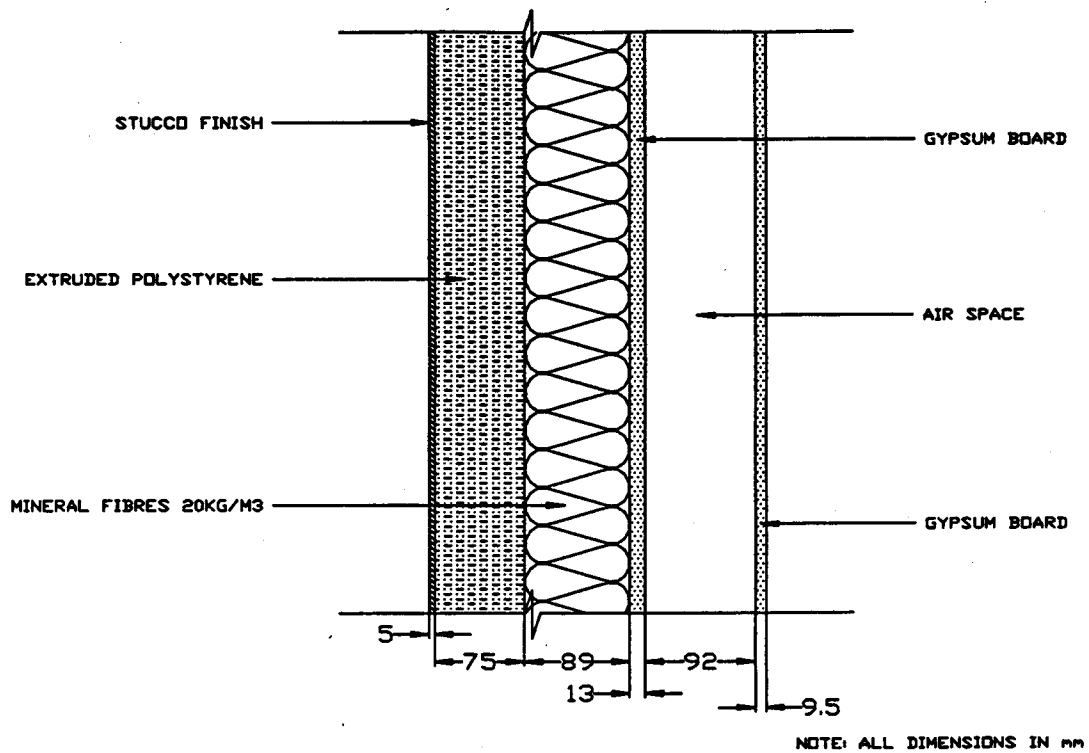
Figure 5-6: WALL3 (left-retrofit case)

RED BRICK

AIR

BUILDING PAPER
0.2mm

EXTRUDED POLYSTYRENE

GYPSUM BOARD

6-MIL POLYETHELENE
0.15mm

MINERAL FIBRES 20KG/M3

102   140
25   9.5
25

NOTE: ALL DIMENSIONS IN mm
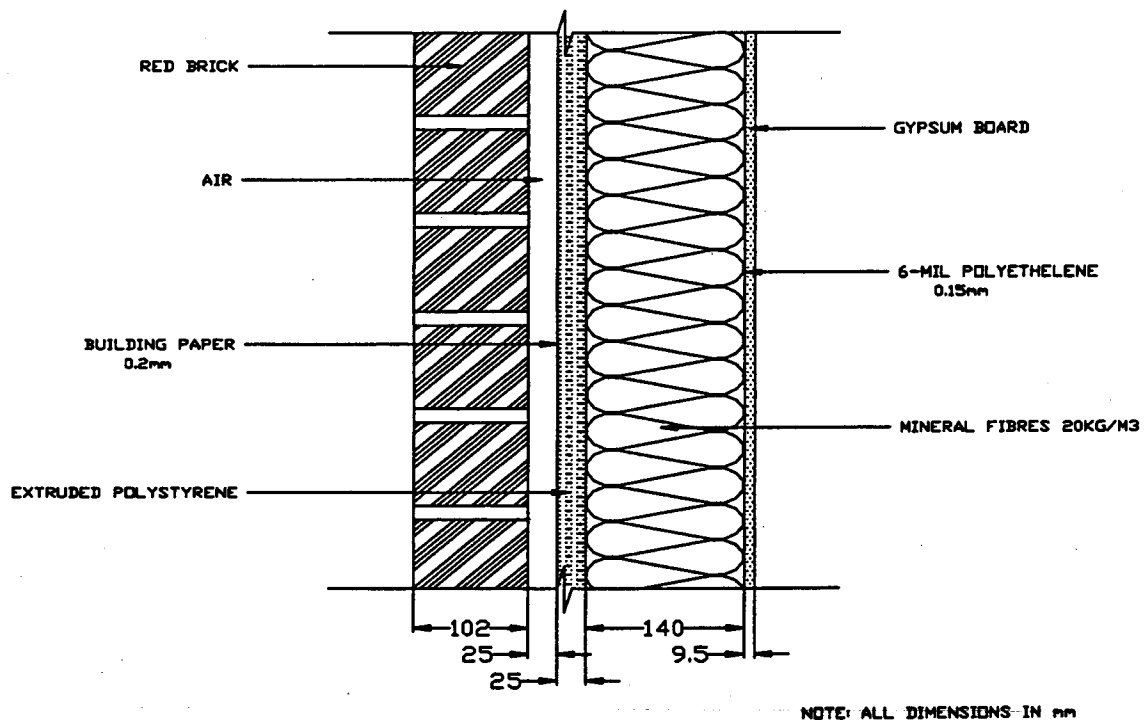
Figure 5-7: WALL1 (right-retrofit case)

RED BRICK

AIR

MINERAL FIBRES 20KG/M3

6-MIL POLYETHELENE SHEET
0.15mm

ANNEX CONCRETE

AIR SPACE

ANNEX CONCRETE

MINERAL FIBRES 20KG/M3

GYPSUM BOARD

102   140   89

25   70   70   9.5

60

NOTE: ALL DIMENSIONS IN mm
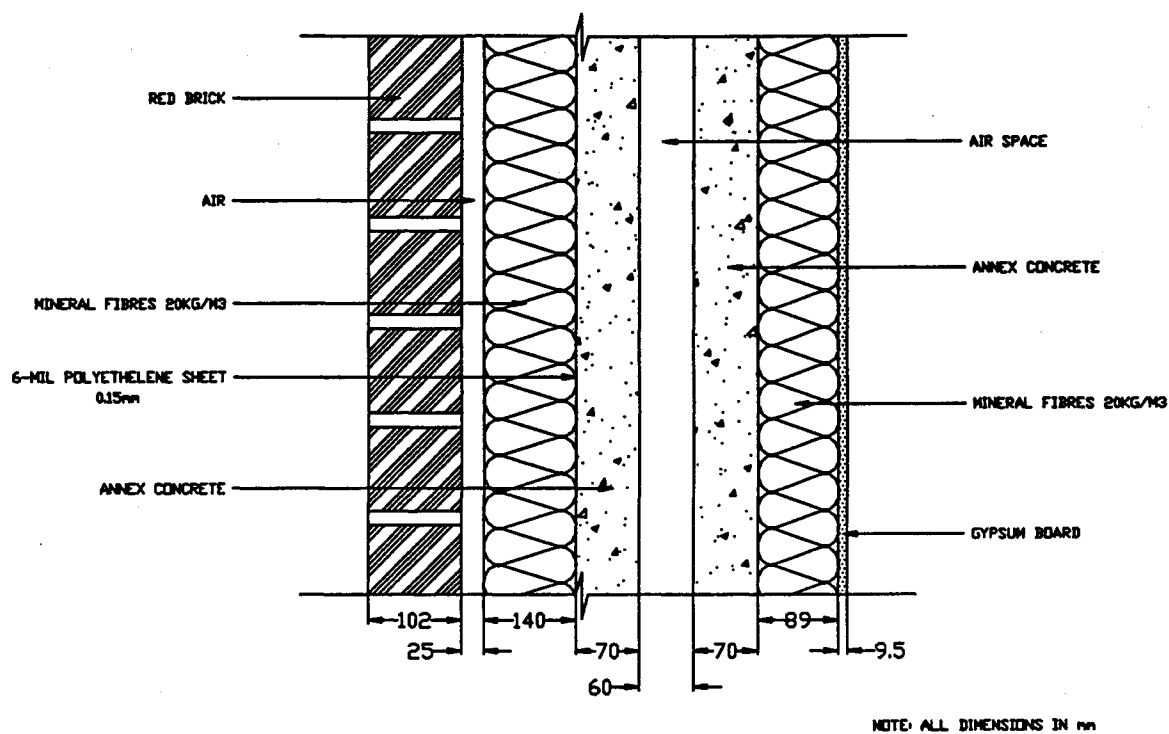
Figure 5-8: WALL2 (right-retrofit case)

STUCCO FINISH

EXTRUDED POLYSTYRENE

GYPSUM BOARD

CELLULOSE

GYPSUM BOARD

5   75   92   9.5

13

NOTE: ALL DIMENSIONS IN mm
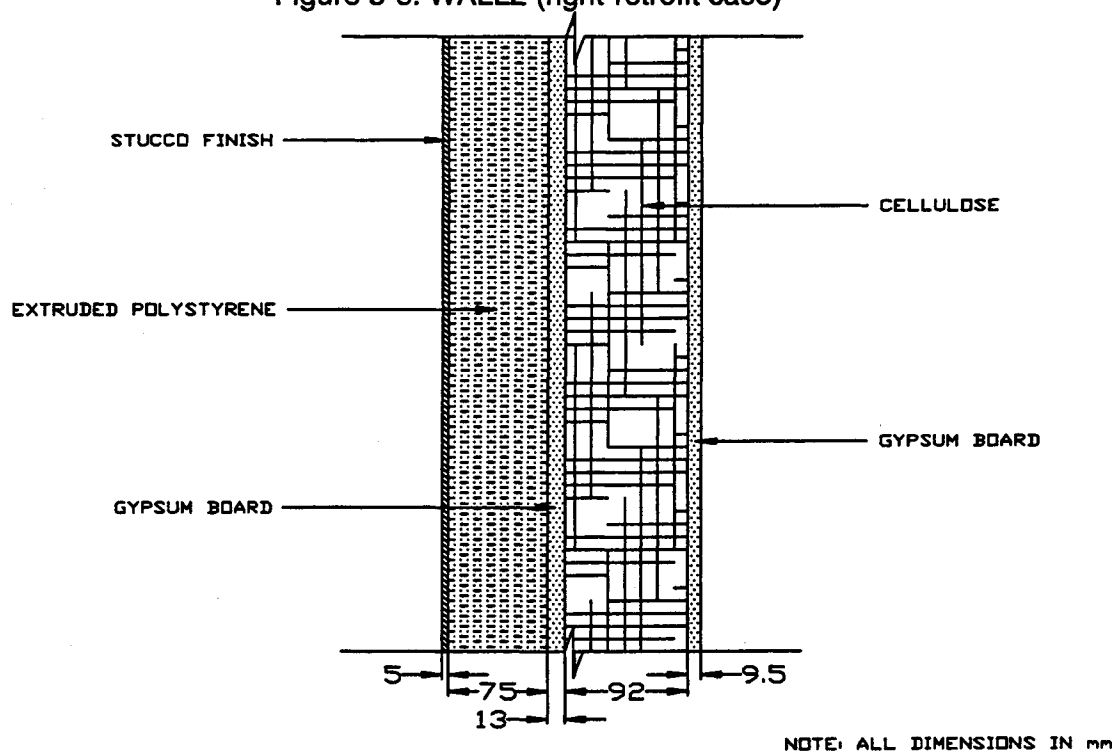
Figure 5-9: WALL3 (right-retrofit case)
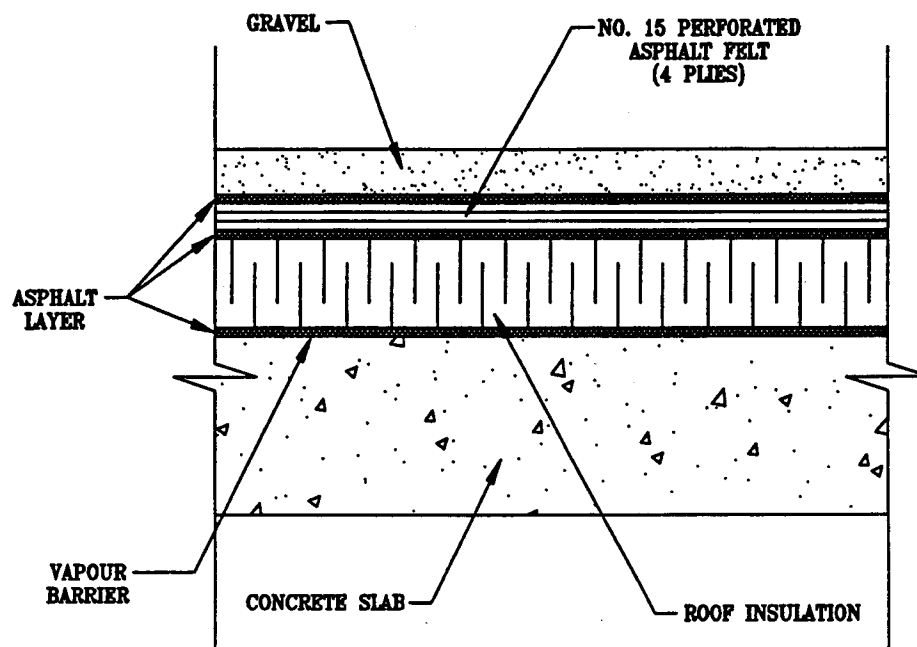
Figure 5-10: ROOF1 case

Figure 5-11: ROOF2 case

IMPERMEABLE MEMBRANE

NO. 15 PERFORATED
ASPHALT FELT
(2 PLIES)

ROOF INSULATION

BITUMEN
LAYER

BITUMEN
LAYER

CONCRETE SLAB

ASPHALT PRIMER
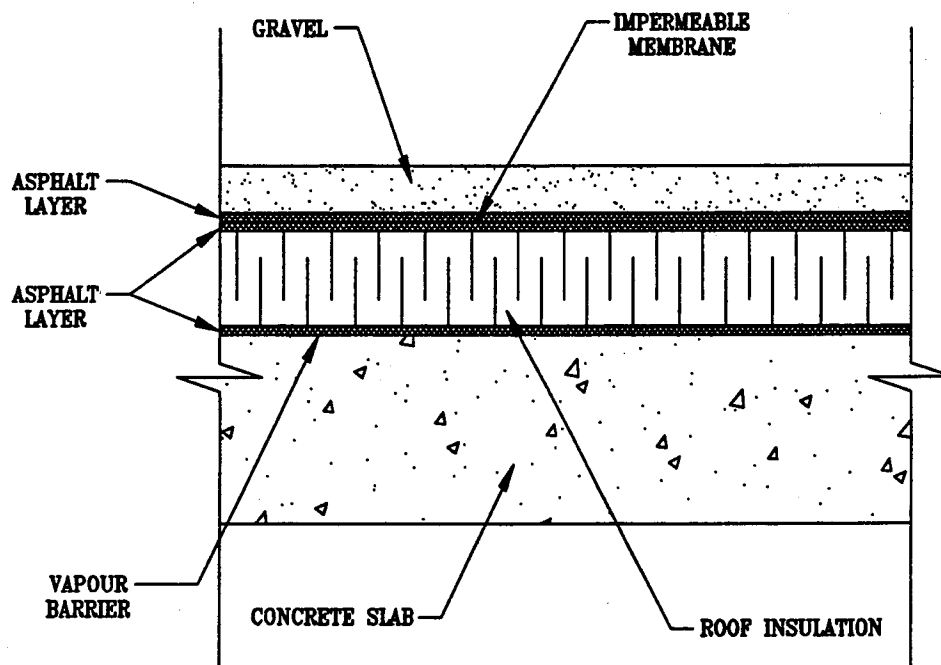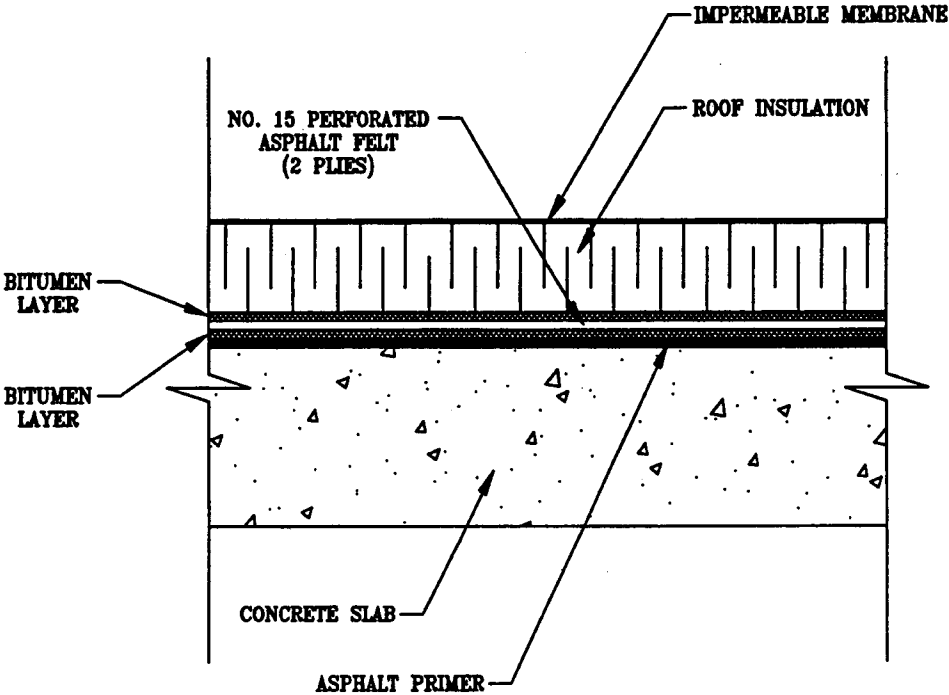
Figure 5-12: ROOF3 case
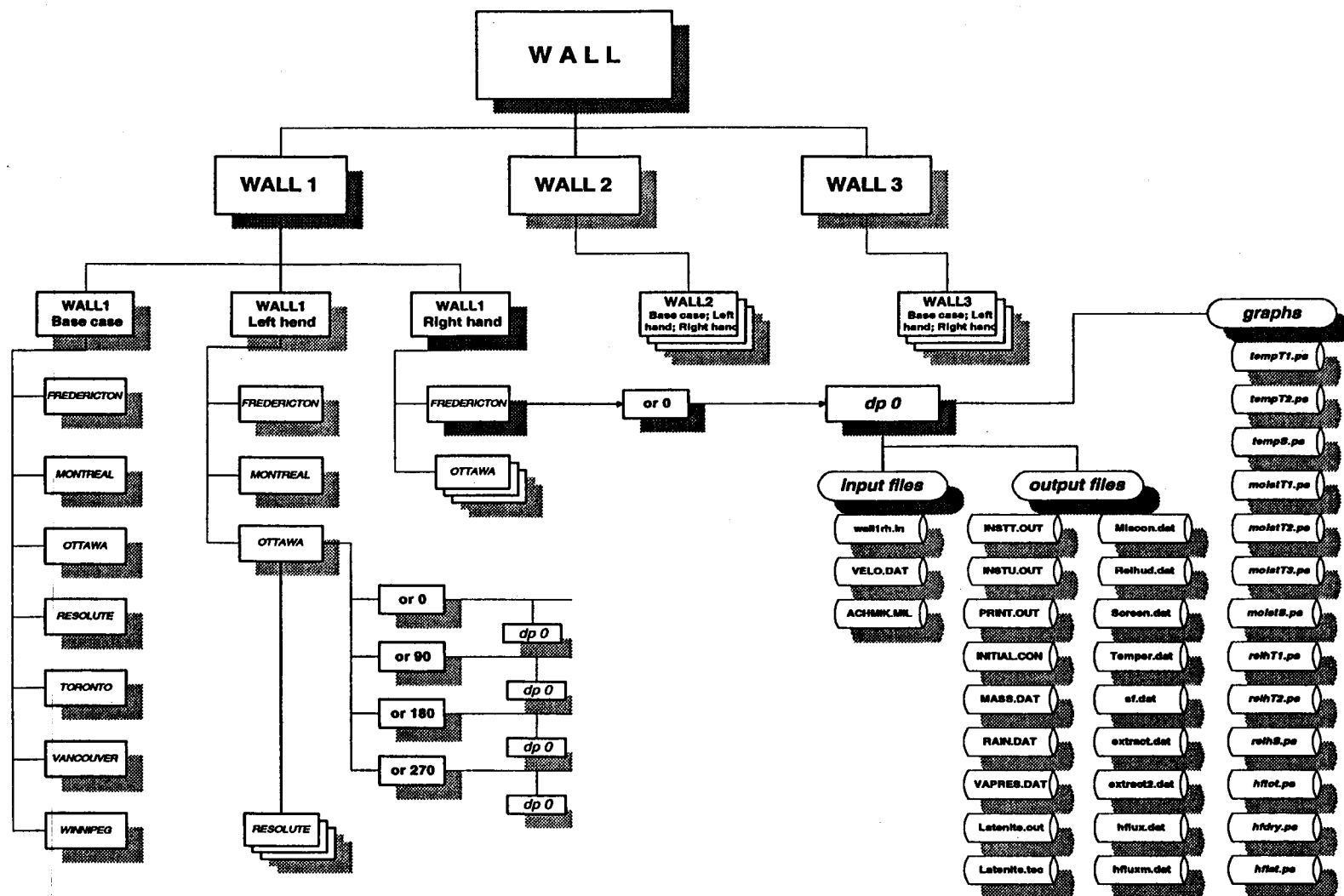
Figure 5-13: Wall simulation set up for 1-D simulations
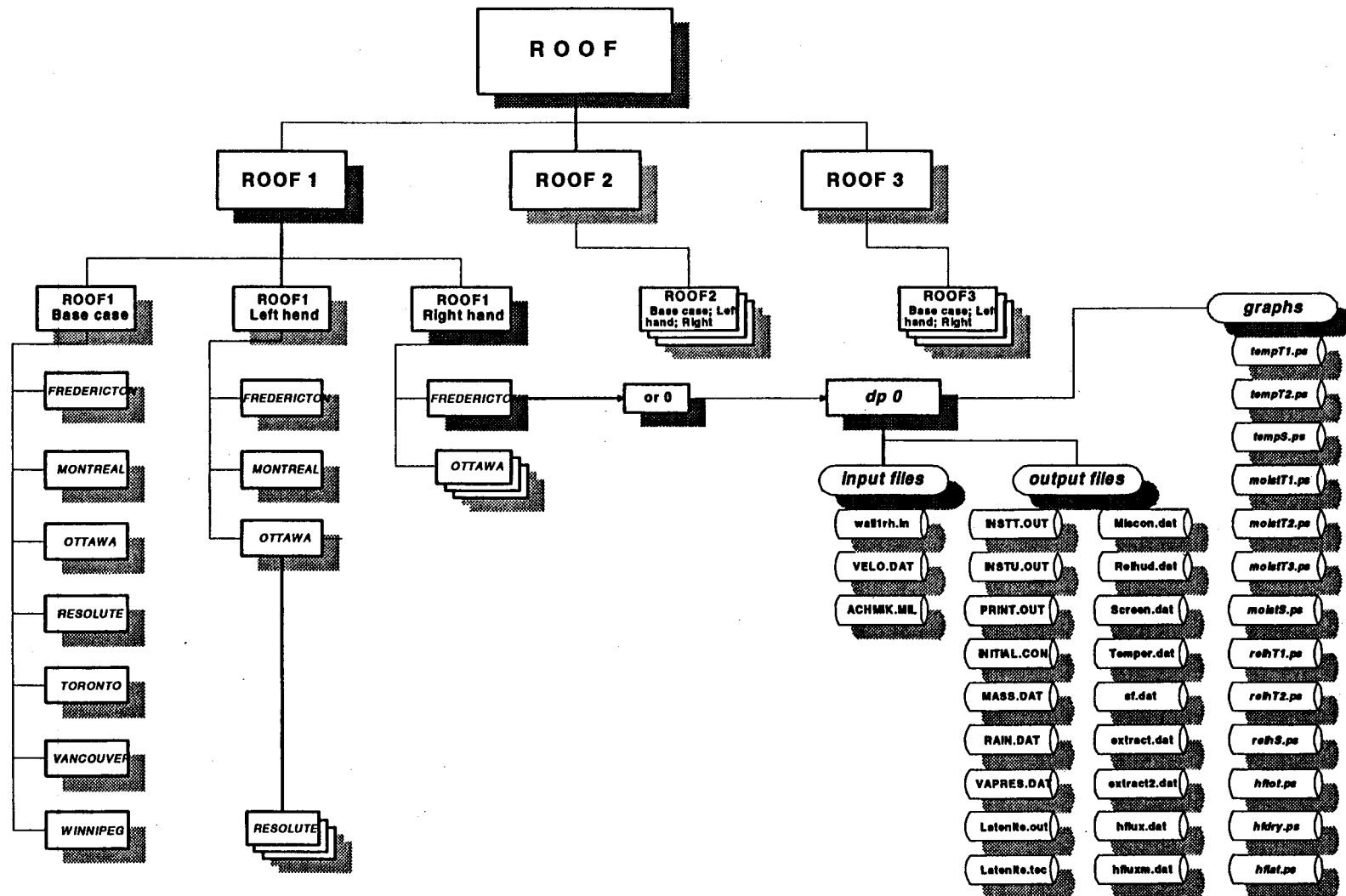
Figure 5-14: Roof set up for 1-D simulations
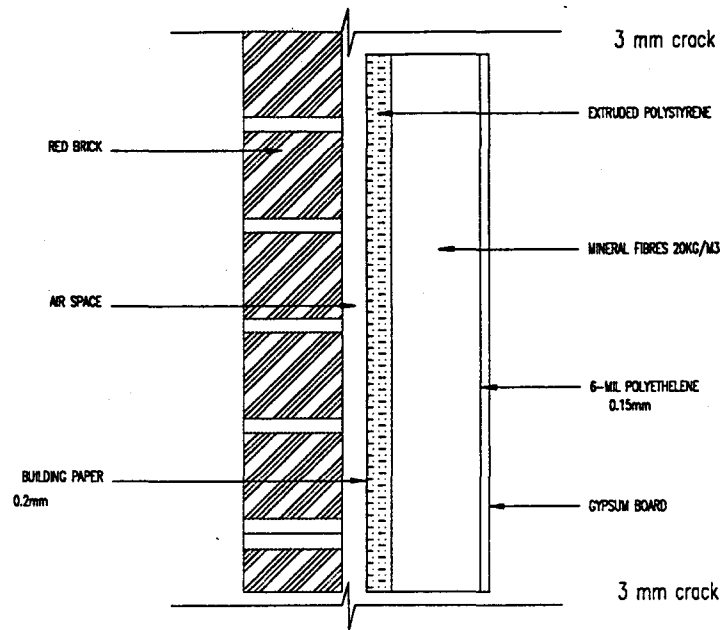
Figure 5-15: 2-D WALL1

6.0 HYGROTHERMAL RESULTS

6.1   INTRODUCTION

In this section, results are presented for all hygrothermal simulations for each of the three wall systems, along with the two retrofit strategies and the three roof sections. For each wall system, walls of buildings in seven cities have been used at four orientations (North-East-South-West). The same seven cities have been used for the roof systems, but only the horizontal orientation (flat roof) was investigated.

Due to the large number of simulations involved in this investigation, a systematic approach was developed for the presentation of the data. Most of the simulation results are 1-D. They are shown first, followed by the 2-D simulation results that include the effects of exfiltration and infiltration. For both parts (1-D and 2-D results) a few spatial distributions will be presented because of the shear amount of numerical data available. Most of the spatial data are lumped in terms of average-time quantities that allow better understanding of the overall hygrothermal performances. This approach allows the presentation whether the structure is accumulating moisture or drying at different periods of the year. The effects of orientation and weather can also be easily identified by showing the total average behavior of the wall systems in the form of total moisture content. Furthermore, some of the spatial (point-by-point) behaviors will be demonstrated by selecting a few representative cases.

In Tables 6.1 through 6.3, the wall thermal and vapor resistances are shown for the base case, left and right retrofit conditions for WALL1, WALL2 and WALL3 respectively. As a consequence of using layers with standard sizes, the moisture and thermal resistances are not identical for the walls being considered. This implies that the evaluation and critical review for the hygrothermal performances are carried out on a relative basis. The approach by using resistances for comparison is only valid for the thermal analysis part because vapor resistances do not solely dictate the moisture transport mechanism. In wet conditions, the liquid diffusivity dominates the moisture phenomena and the concept of vapor resistance is meaningless. The moisture performance of building envelope systems should be evaluated by examining both the vapor and liquid mechanisms. This issue is particularly important since the concept of vapor resistance is widely used by "moisture experts" as the only concept for comparing building envelope system moisture performances.

Table 6.1: Total thermal and moisture dry-resistances for WALL1

	Thermal Resistance (°K m²/ W)	Vapor Resistance (GPa s/kg)
Base Case	3.63	1.012
Left Retrofit	4.70	1.033
Right Retrofit	5.04	1.021

Table 6.2: Total thermal and moisture dry-resistances for WALL2

	Thermal Resistance (°K m²/ W)	Vapor Resistance (GPa s/kg)
Base Case	4.22	1.096
Left Retrofit	4.81	1.117
Right Retrofit	6.22	1.097

Table 6.3 Total Thermal and moisture dry-resistances for WALL3

	Thermal Resistance (°K m²/ W)	Vapor Resistance (GPa s/kg)
Base Case	3.84	0.074
Left Retrofit	6.31	0.082
Right Retrofit	5.47	0.083

Before presenting the core results of this investigation, the effect of wind-driven rain on the hygrothermal performance of high-rise walls will be first demonstrated, followed by an analysis of the weather data used for each city.

6.2   Effect of Wind-Driven Rain on Hygrothermal Performance

The effect of height is parametrically investigated by using both vapor and liquid diffusion transport mechanisms for moisture flow. The hygrothermal performance of a high-rise wall section depends on the height location (elevation from ground surface) for various reasons. The particular height above ground not only affects the amount of wind-driven rain striking the exterior surface of the building but also the magnitude of the convective heat and mass transfer coefficients. Wind-driven rain depends heavily

on the height of the wall section. This is due primarily to the 3-D airflow fields around the high-rise building, as discussed in detail in Section 3 dealing with the effect of boundary conditions. Work carried out by this author, as well as other researchers (Kunzel 1994), (Hens 1994), (Sanders 1995) has shown that wind-driven rain can be the single most important source of moisture. Since wind-driven rain is strongly influenced by height of the high-rise building, different parts of the wall with the same orientation have different long-term service-life and durability performances. For example, for a high-rise wall facing a moderate wind of 10 m/s at the highest floor (at an elevation of 30 m above ground) can receive on average 2 to 2.5 times the normal precipitation rate. Narrowing the region to simply a 1 m^2 area at the corners of the building both laboratory testing (CMHC 1995, U of Western) and field measurements (Kunzel 1994) have shown these corner areas received 10 to 40 times the normal precipitation rates. This makes the hygrothermal performance of a high-rise envelope a compilation of very localized performances.

To date (world-wide) almost all of the hygrothermal models and simulations performed on building envelope systems have been carried out by using only vapor transport mechanisms at both the boundaries and domain of the structure. More recently, a few models have the capability of including vapor and liquid transport within the domain, but only vapor transport at surfaces. In the NRC hygrothermal model LATENITE, both vapor and liquid transport are accounted for at all boundary surfaces and also within the domain. To demonstrate the severe limitation imposed when only vapor transport mechanisms are included, a set of simulations for a brick cavity wall with 90-mm exterior brick, 120-mm fiber-glass board, and 140- mm interior brick were performed. Vancouver weather data were used for two simulation cases: in the first simulation, only vapor-type boundary conditions were used; while the second case both vapor and liquid (rain) were used. Figure 6.1 shows the total moisture content as a function of time during the third year of the simulated period for the wall in Vancouver when driving rain is taken into account or ignored. The maximum moisture content in the wall system in the case where liquid transport at the surface is not being taken into account was 0.32 kg/wall-m^2, whereas walls where the effects of rain are being taken into account accumulated 12 kg/wall-m^2 . These results show quantitatively that rain penetration can outweigh the effects of vapor transport in building structures. Regarding thermal performance, the thermal conductivity of each of the cavity wall layers was a function of moisture content. The higher moisture contents in the exterior layer produced a decrease in the thermal resistance of the wall and therefore in an increase of heat loss. Furthermore, the water that was absorbed in liquid form by the exterior brick during rainy periods can eventually evaporate outward and the latent

heat involved in this process also further increases the heat loss. Moisture that comes into the wall in vapor phase and is absorbed by the structure does not affect the long-term average heat flux, unless yearly accumulation occurs. However, instantaneous heat fluxes may be influenced by the phase changes of vapor or liquid. The effect of driving rain on the additional yearly heat losses through the structure was computed to be 8% (including the free solar energy) for the wall facing South in Vancouver. This means an increase of 8% over the case in which wind-driven rain is not accounted for. This additional heat loss due to liquid transport at the exterior surface depends on weather location, wind-speed, wind direction, precipitation rates and construction type (i.e. cavity wall versus non cavity wall). For the location at Ottawa with approximately 79 mm of rain striking the south-facing exterior wall surface (Vancouver had 209 mm), the additional yearly heat loss increase was 2%.
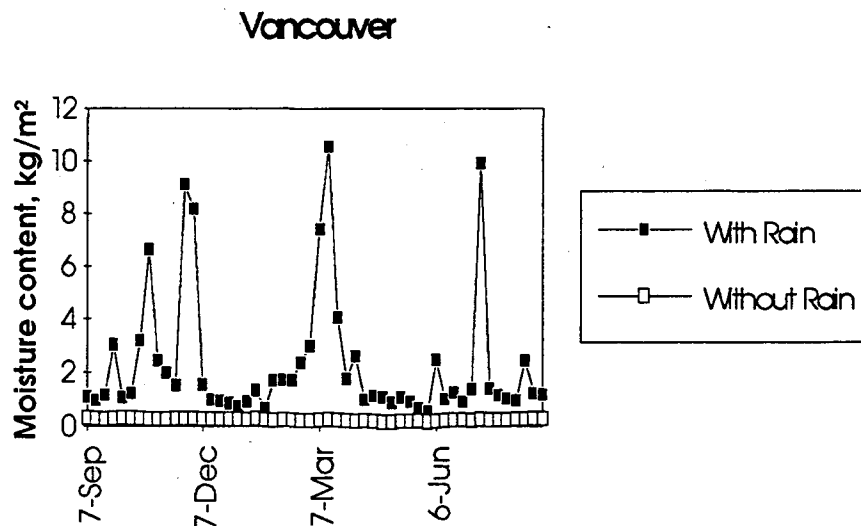
Figure 6.1:   Hygrothermal results with and without rain for a brick cavity wall.
(90 mm exterior brick, 120mm fiber-glass, 140mm interior brick)

6.3   Effect of Height

The effect of location, above the ground level (i.e. elevation), was investigated for three different heights. A 10-floor high-rise building using a wall system identical to WALL1, in the middle of the building width was studied. The wall sections modeled were located at the following heights:

a) bottom of the high-rise building (1st floor)

b) middle of the high-rise building (5th floor)

c) top of the building (10th floor)

The 1-D wall structure was composed of an exterior red brick, air space, building paper, polystyrene board, fiber-glass insulation, polyethylene, and a gypsum layer. A 3-year simulation period starting from the 1st of January using hourly BMY meteorological data was employed. Figures 6.2 to 6.6 show the transient instantaneous snap-shots of the spatial RH fields throughout the domain of the structure (exterior at thickness equal to 0 m). These figures show results only from the 3rd year, making them independent of initial conditions. It becomes evident that height had a significant effect on the RH fields within the walls throughout the year. Maximum RH difference due to the height of the walls of 20 to 30% were found. Different low- or high- suction brick material properties could further influence these distributions. Figure 6.7 shows the transient moisture accumulation in the fiber-glass insulation layer as a function of the height of the wall. Again the characteristic moisture accumulation in the insulation layer was observed: it varied with height. Figure 6.8 depicts the total moisture in the wall as a function of time during the 3rd year of simulation. It shows further the total performance of this wall system, since it depicts the moisture accumulation and not the RH fields. In the first quarter of the year (Jan.-Mar.), drying occurs and the wall section at the top of the building is wetter than the middle and bottom wall sections. In addition, drying rates vary with distance from the ground. For the remaining year, the differences between bottom- and middle- height cases are not so pronounced as for the top case, especially during the rainy periods. In October, for example, the bottom wall accumulated 5 kg/m^2; the middle wall, 9 kg/m^2; the top wall, 17 kg/m^2. The thermal performances deteriorated, because of the presence of moisture, by approximately 1.7% from the bottom to the middle and an additional 2% from the middle to the top. Because most of the moisture accumulation occurs in the exterior brick, this has a minimal effect on the thermal performance. When considering service-life and durability issues, however, it becomes evident that using the same wall/material system throughout the face of a building will result in different maintenance frequencies and priorities. Hygrothermal modeling investigations such as the one used here allows the characterization of a newly designed wall system and quantifies both the thermal and moisture performances as well as the interactions between them. The quantification of the hygrothermal performance of the building envelope can lead to better optimized constructions by understanding the thresholds and distributing these more uniformly by proper choice of material properties for each element (say as a function of height).
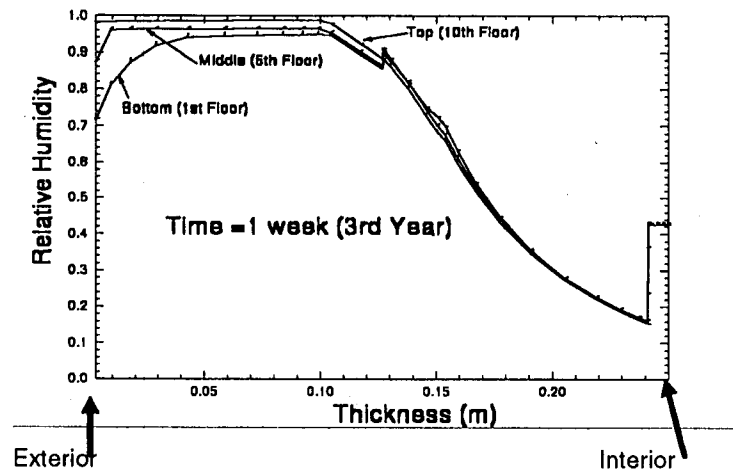
Figure 6.2: Spatial Relative Humidities for week 1 of year 3

Figure 6.4: Spatial Relative Humidities for week 15 of year 3

Figure 6.3: Spatial Relative Humidities for week 25 of year 3
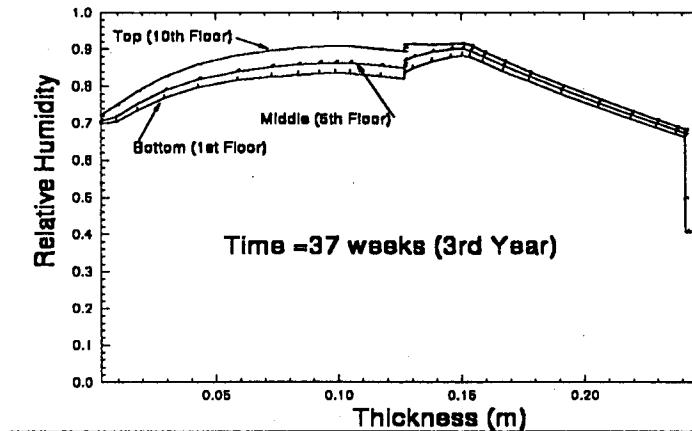
Figure 6.5: Spatial Relative Humidities for week 37 of year 3
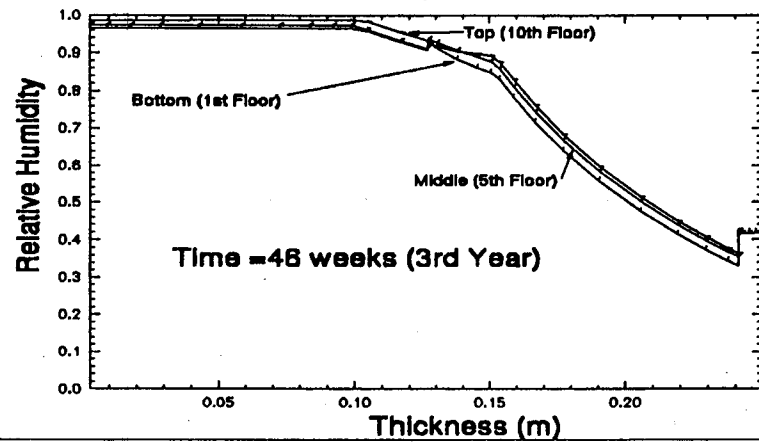
Figure 6.6: Spatial Relative Humidity's for Week 47 of year 3

Figure 6.8: Total Moisture in Wall as a Function of Time

Figure 6.7: Moisture Accumulation in Fiberglass Insulation

6.4   WEATHER AND RAIN ANALYSIS

The effect of climatic location on the hygrothermal performance of a building envelope system can be appreciable. As already shown, wind-driven rain is an extremely important environmental parameter that affects the performance of the wall system even at the same weather location. A weather analysis is performed to show the monthly behavior of rainfall and heating hours for each the cities used in the simulations. In Figure 6.9, the rainfall analysis is shown for four cities (Vancouver, Ottawa, Toronto, Montreal). The total maximum and wall incident rainfall are shown as a function of orientation (North, East, South and West). The total maximum represents the total possible rain that could strike the surface of a building assuming am 180-degree angle of acceptance. The incident rainfall is the actual amount that strikes the wall. By far the wettest conditions are those in Vancouver, followed by Ottawa, Toronto, and Montreal. These rainfall values were obtained by both weather data analysis (AES, BMY data) and the use of TASCflow 3-D CFD model. In Figure 6.10, the monthly heating hours are plotted out for Montreal, Toronto, Vancouver, Ottawa, Resolute, Winnipeg, and Fredericton. These results were also determined from the BMY hourly weather data files, the same files used in the simulations. In Table 6.4 the annual heating hours for each city are tabulated. From these it is evident that the coldest city is Resolute, followed by Winnipeg, Ottawa, Montreal, Fredericton, Toronto, and Vancouver.

6.5   Moisture Spatial Performance for WALL1

The results of the spatial RH distributions for WALL1 (base case, left- and right-retrofit) are shown for the City of Vancouver. The wall section was located in the middle face of the building at the 5th floor of a 10 storey high-rise building, facing east. This city was selected because of the high amount of rainfall. Rain usually gives an extreme condition on the exterior surface of a high-rise building, but not necessary a condensation plane. Results will be presented for various node points, see figure 6.11, as a function time for the three cases of WALL1. For the base and right-retrofit cases, the node number designation is the same (see Figure 6.11), while Figure 6.12 shows the node numbering for the left-retrofit case.
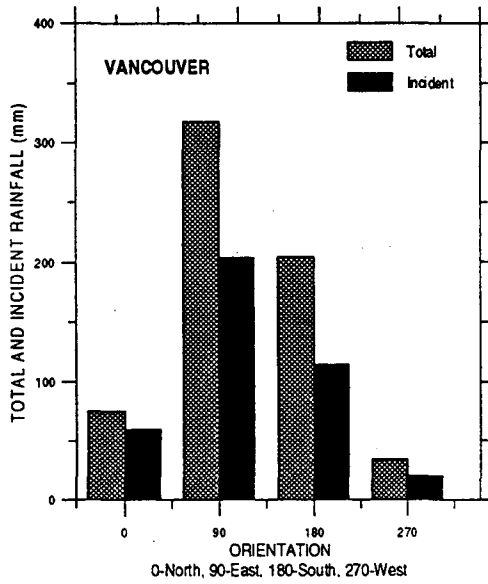
(a) Vancouver rainfall
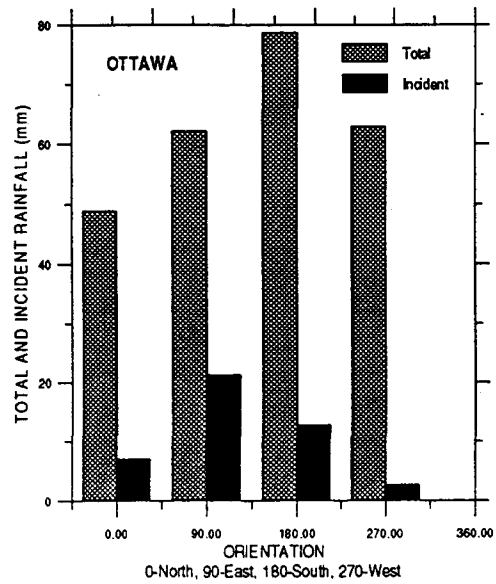
(b) Ottawa rainfall
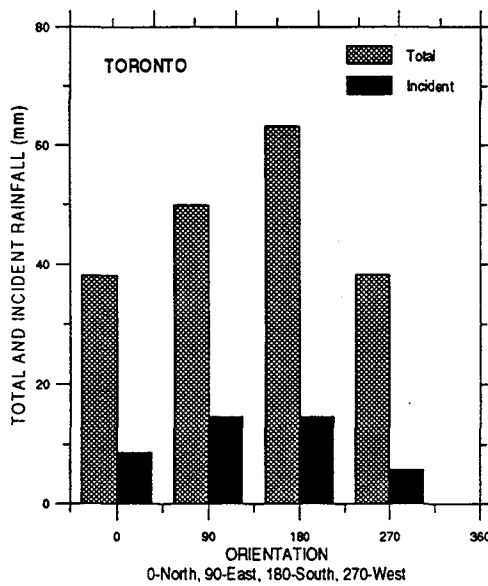
(c) Toronto rainfall
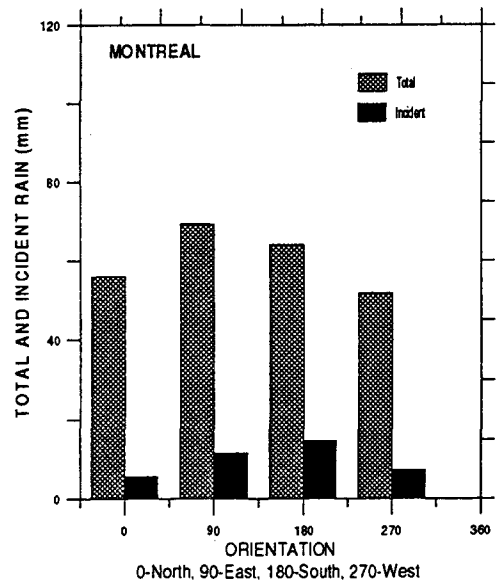
(d) Montreal rainfall

Figure 6.9 Rainfall at various cities in Canada
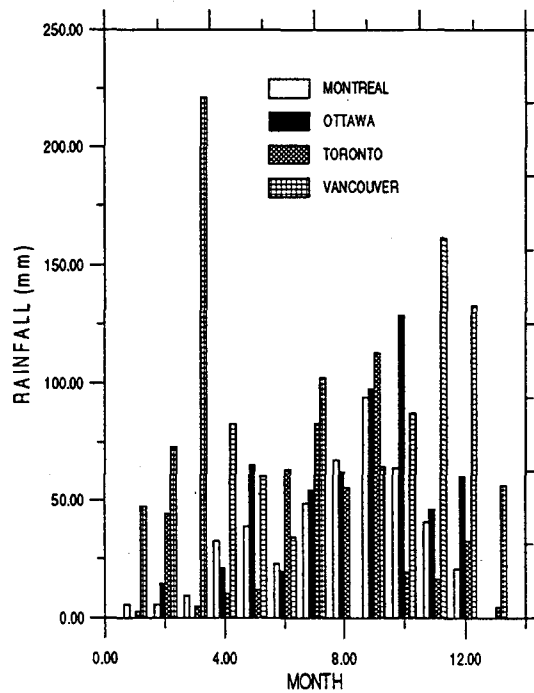
(e) Monthly rainfall

Figure 6.9: Rainfall at various cities in Canada
(Month defined as 4 weeks)
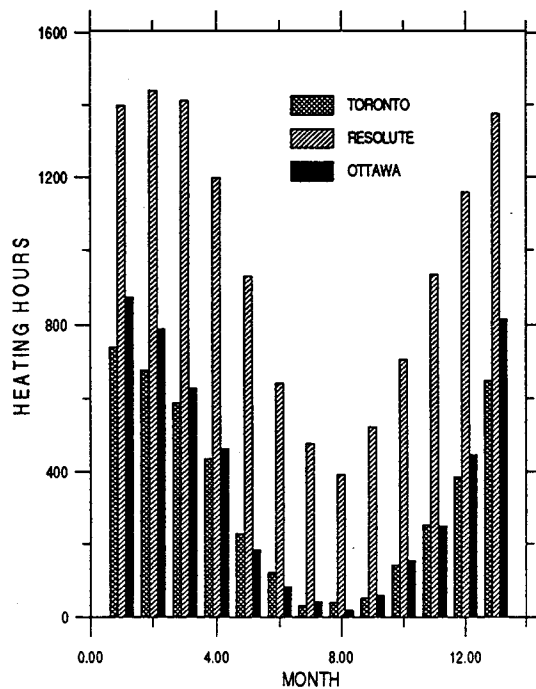
6.10 (a) Monthly heating hours
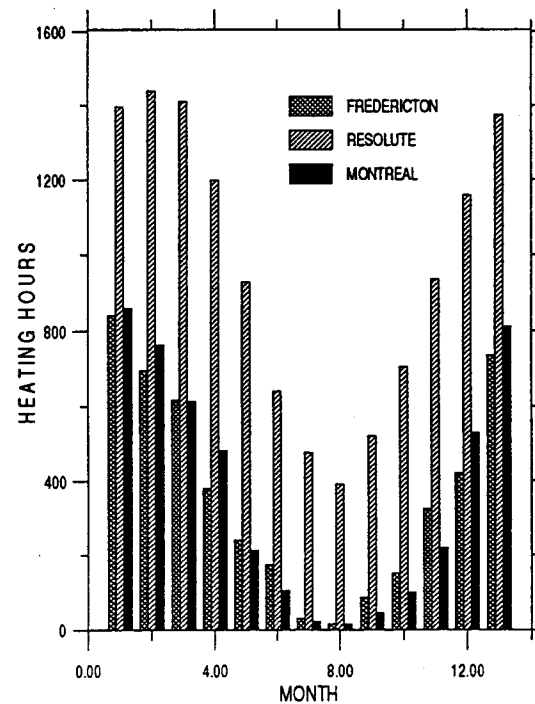
6.10 (c) Monthly heating hours
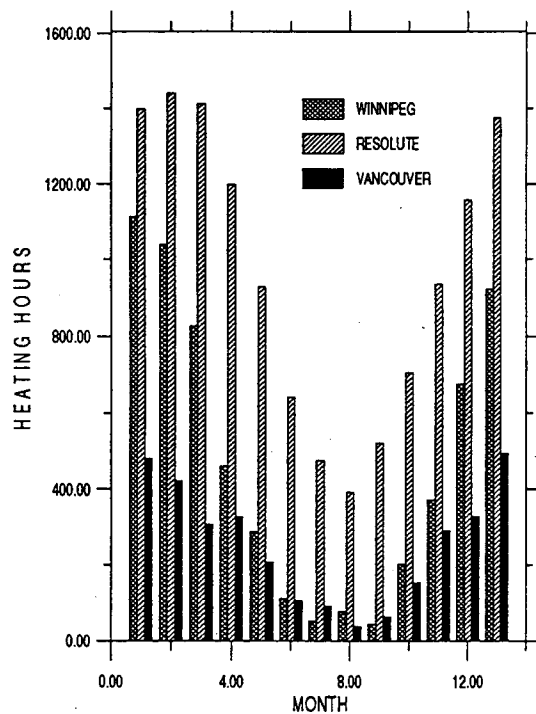
6.10 (b) Monthly heating hours

Figure 6.10 (a to c) Comparison of Monthly Heating Hours
(Month defined as 4 week period)

Table 6.4:
ANNUAL HEATING HOURS BY CITY (°C DAY)

City	Heating Hours
VANCOUVER	3310
WINNIPEG	6176
RESOLUTE	12578
TORONTO	4331
OTTAWA	4801
MONTREAL	4774
FREDERICTON	4708

Figure 6.11: Node grid Layout for WALL1 base case and right-retrofit case
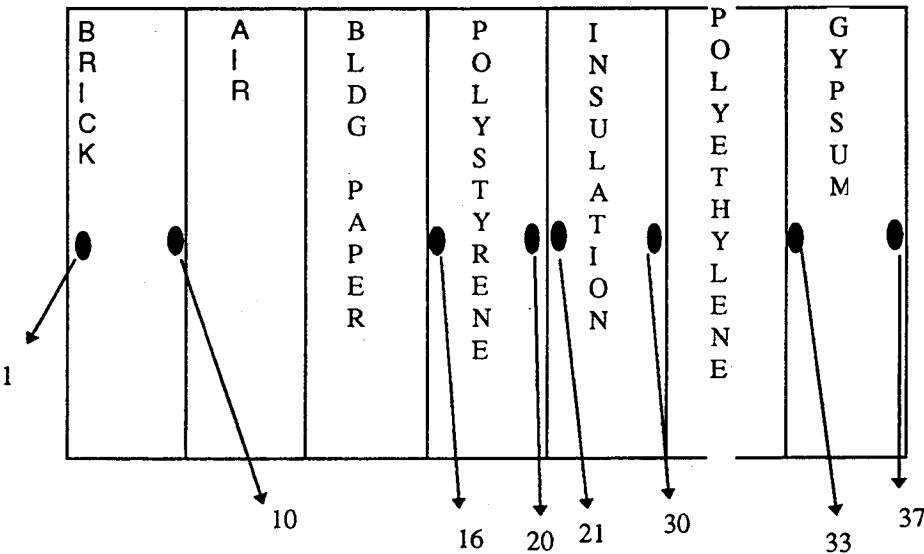
Figure 6.12: Node grid layout for WALL1 left-retrofit case
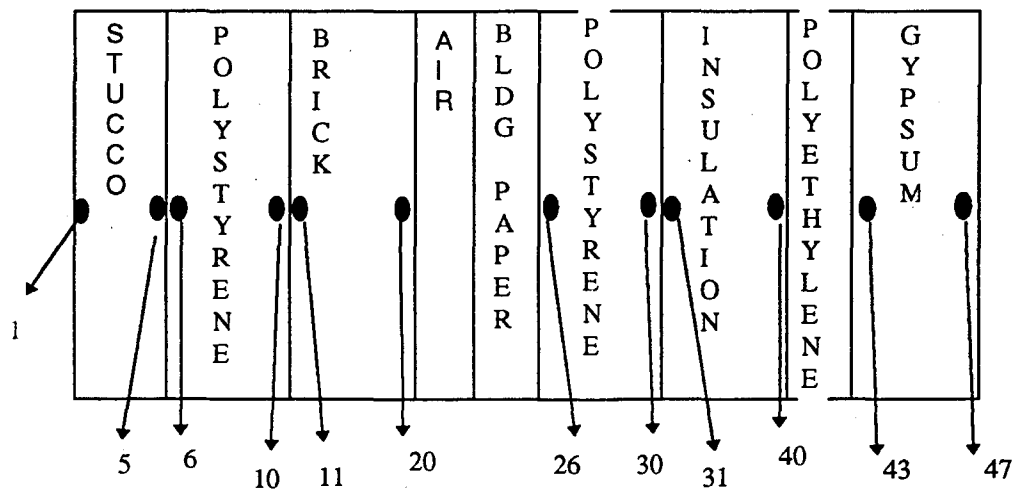
Figures 6.11 and 6.12 define the node points for which Figures 6.13 through 6.19 show the transient spatial RH fields.

BASE CASE

For the base case WALL1, the brick veneer maintained RH's above 95 % during the fall and winter periods and temporarily dried out during the summer periods with the exception of the wetting during rainy periods. Also, the exterior surface of the polystyrene layer had very high RHs following closely the behavior of the interior most brick node. In Figure 6.14, the exterior most nodal point for fiberglass accumulated moisture during the winter and fall period and this eventually dried out during the spring and summer period. A slightly lower amplitude, but opposite behavior, during this yearly cycle of moisture accumulation and drying was observed at the inner most node of the insulation layer. This behavior is due to the near-decoupling of the interior and exterior by the high vapor resistance of the vapor retarder. The reversed moisture cycle for this inner most insulation point is due to the effect of a temperature-gradient-driven moisture flow. The spatial relative humidity for the gypsum board was maintained at approximately 41%.

RIGHT RETROFIT

The same spatial RH behavior as the base case is observed for the right-retrofit WALL1 for the brick layer and exterior most polystyrene board node. A slight increase in RH was observed for the innermost node of the polystyrene board. A maximum 5% increase in RH was observed for the exterior most node of glass-fiber insulation. As the insulation layer for the right-retrofit case was thicker than the base case, the

temperature gradient across was also larger, thereby making it colder. This allowed the presence of high relative humidities at the colder side of the structure. The cyclic behavior was also repeated here but again without any net yearly accumulation. Indeed, within a few months, all the initial conditions had fully dissipated, allowing similar results for year 1, 2 and 3.

LEFT RETROFIT

The results for the left-retrofit WALL1 are shown in Figures 6.17 to 6.19. For this wall, while having a considerably greater volume of construction material, the amount of moisture accumulation was considerably less. The maximum relative humidities did not approach 100% but were in the low 90% range. The brick was kept dry and did not exceed 80% RH throughout the year. The insulation layer showed results similar to those of the base case wall- type behavior, but the maximum RH range in the high 70%.

GENERAL REMARKS

A condensation plane never occurred for the WALL1 base, left and right retrofit cases in Vancouver. For colder climatic conditions, such as Ottawa, Resolute, Winnipeg, Montreal, etc., the spatial relative humidities can be substantially different. In these 1D analysis of the hygrothermal performance, no air-leakage was considered. With the exterior facade component being brick, the unvented air space and expanded-polystyrene board has more pronounced fluctuations, since the thermal gradients for the colder weather locations are greater. The exterior most node of fiberglass insulation, when considering colder climatic conditions, have condensation periods that last approximately 18 weeks/ year for the base case and 22 weeks/year for the right retrofit case for the weather location of Ottawa. The right retrofit option for both Ottawa and Winnipeg prolonged the condensation period. This retrofit option did not develop any beneficial hygrothermal response for these colder climatic conditions. When WALL1 was retrofitted using the left side insulation strategy no condensation was present for the Ottawa. The same behavior was found for Winnipeg. While for both the base and right retrofit cases a condensation plane existed, no net yearly accumulation was present. For the Resolute climatic location, base, left and right retrofit cases show a net yearly accumulation. The left side retrofit, however reduced the amount of moisture accumulation by approximately half of that of the base case. The most critical location for this wall system is the outermost mineral fiber layer. WALL1 (base case) therefore must be redesigned for application in climatic conditions like those found in Resolute. The steel studs could corrode, and mold growth and rapid deterioration of assembly could lead to the degradation of the thermal and durability performance.
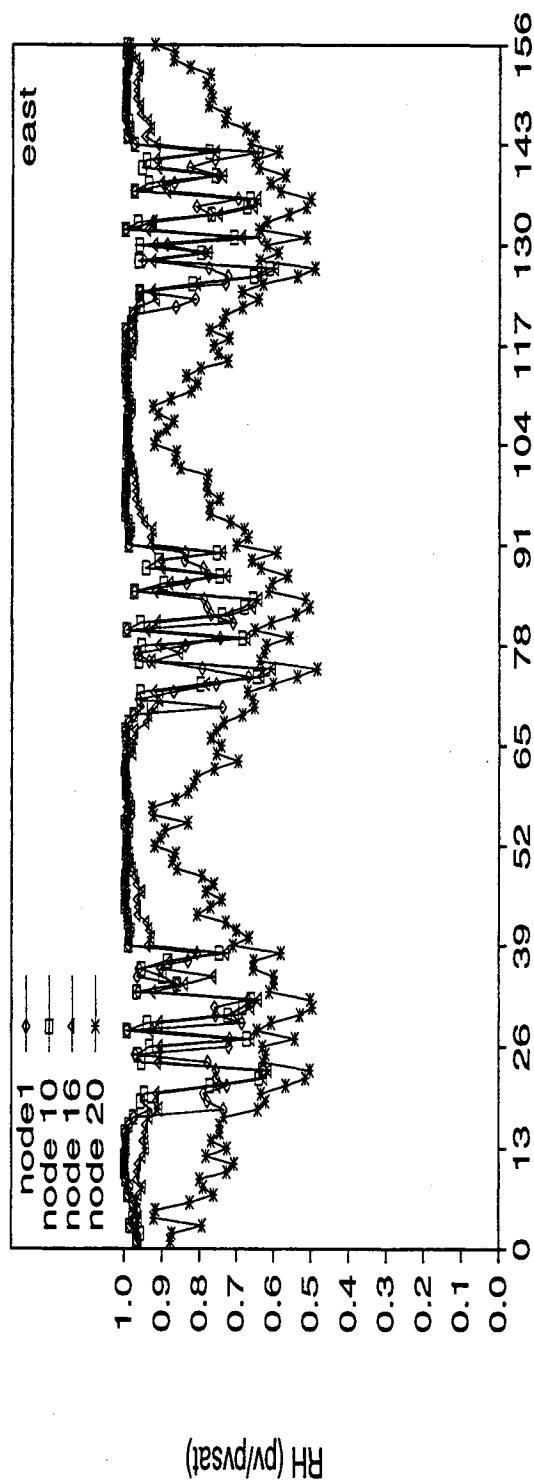
Figure 6.13 Vancouver RH versus
              Time in Weeks (WALL1
              Base Case)
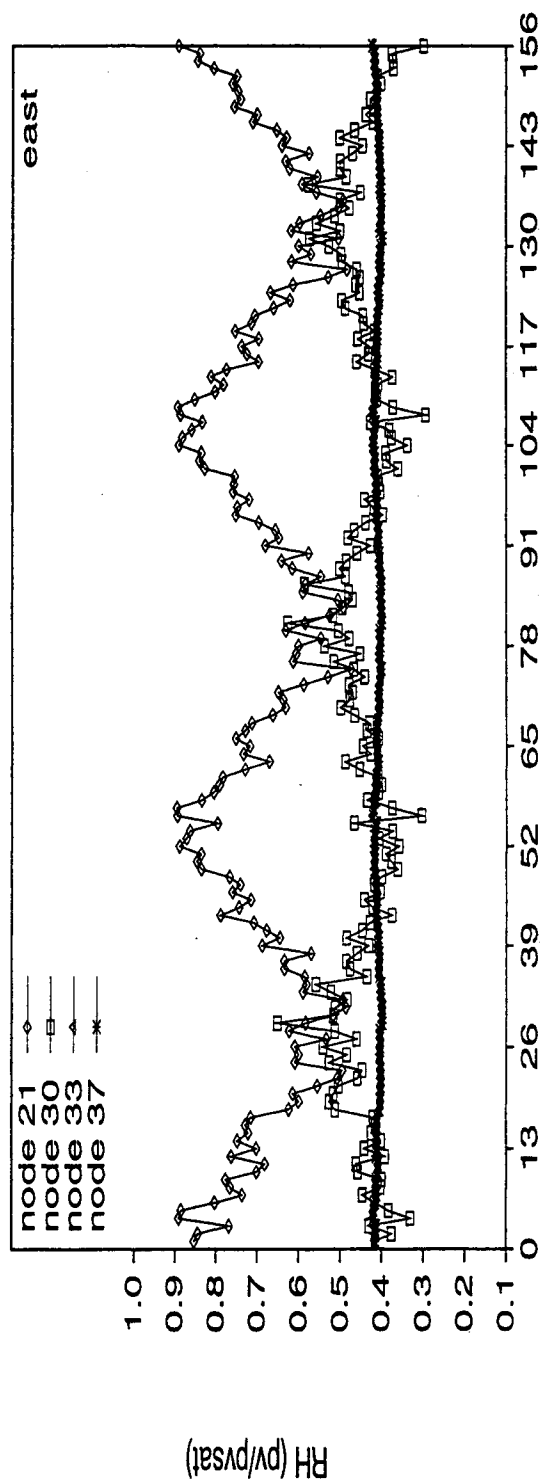
Figure 6.14 Vancouver RH versus
              Time in Weeks (WALL1
              Base Case)
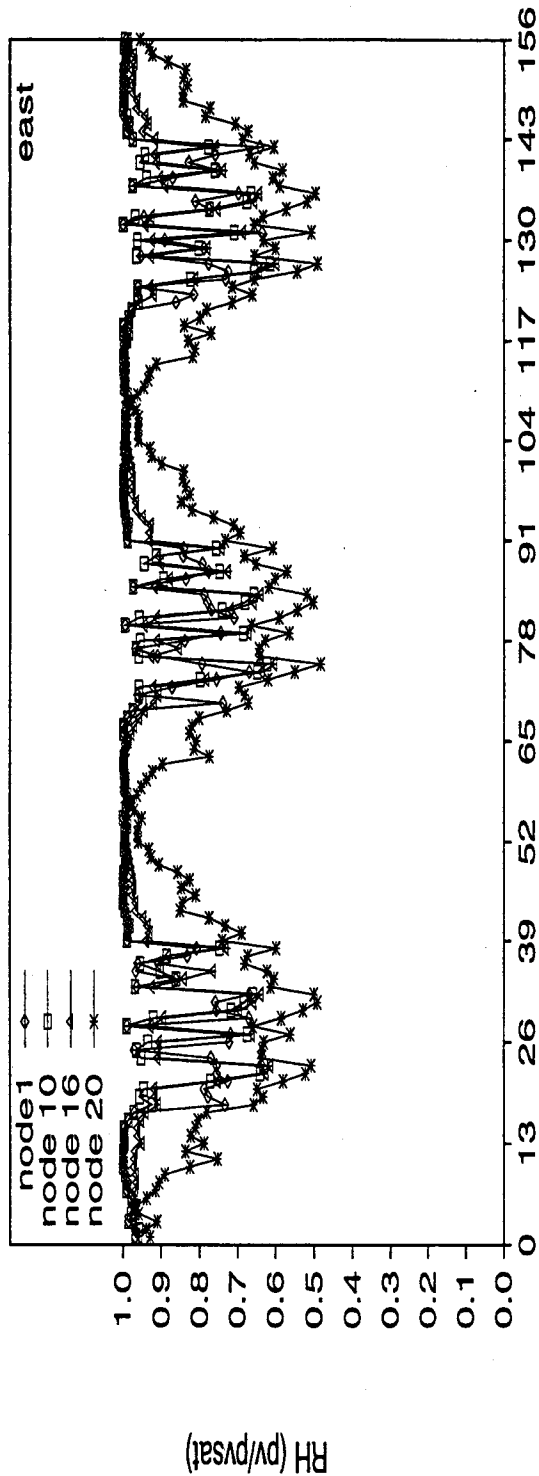
Figure 6.15   Vancouver RH versus
Time in Weeks (WALL1
Right Case)
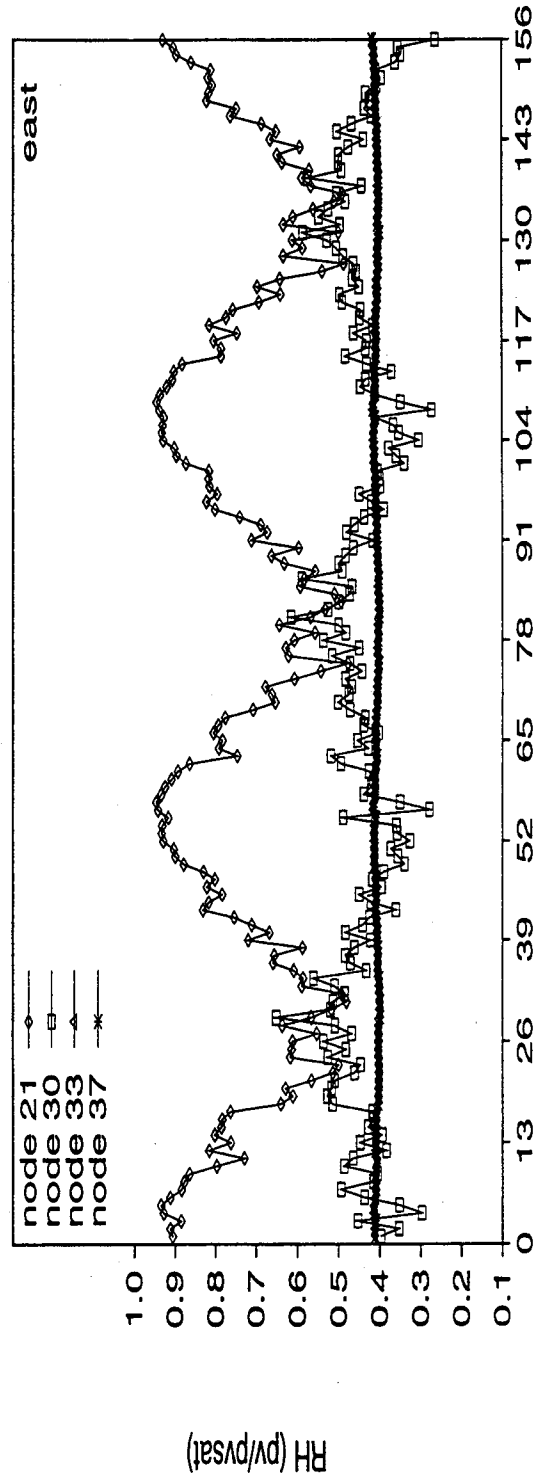
Figure 6.16 Vancouver RH versus
Time in Weeks (WALL1
Right Case)
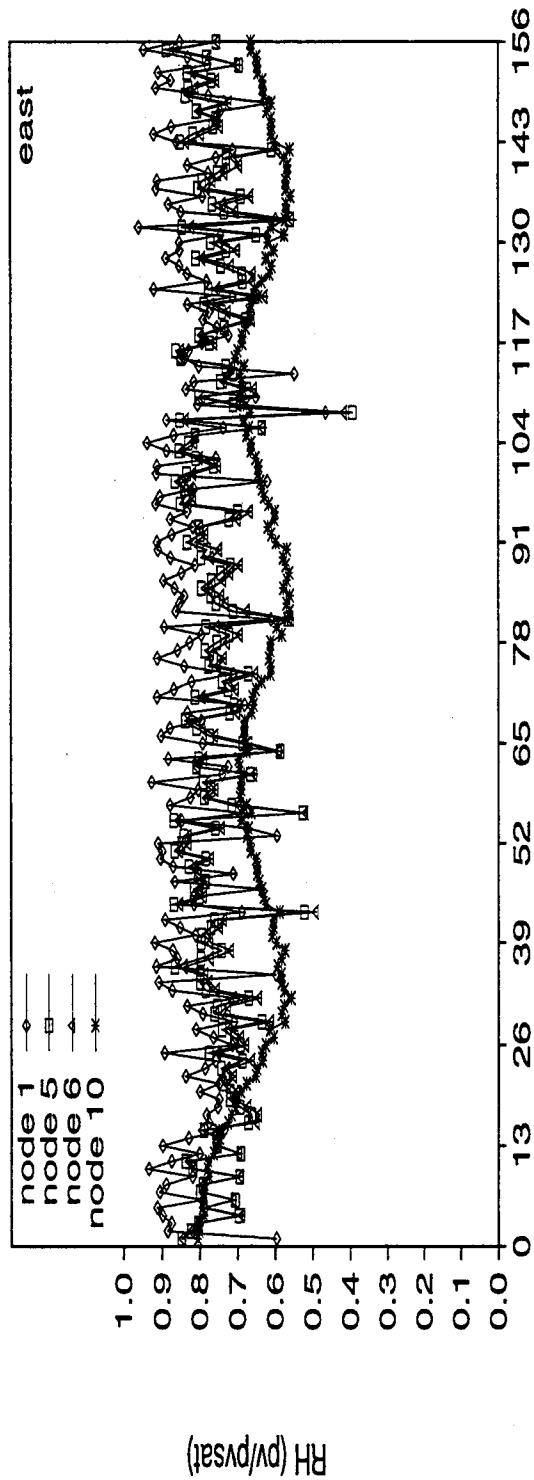
Figure 6.17 Vancouver RH versus Time in Weeks (WALL1 Left Case)
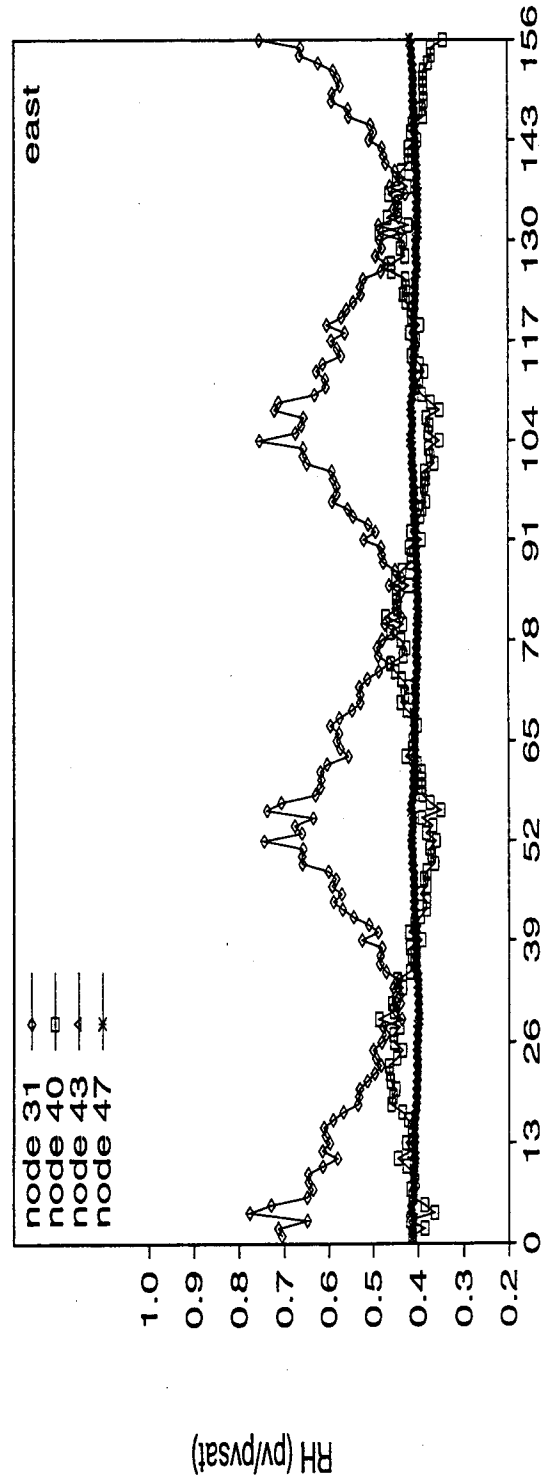
Figure 6.18 Vancouver RH versus Time in Weeks (WALL1 Left Case)
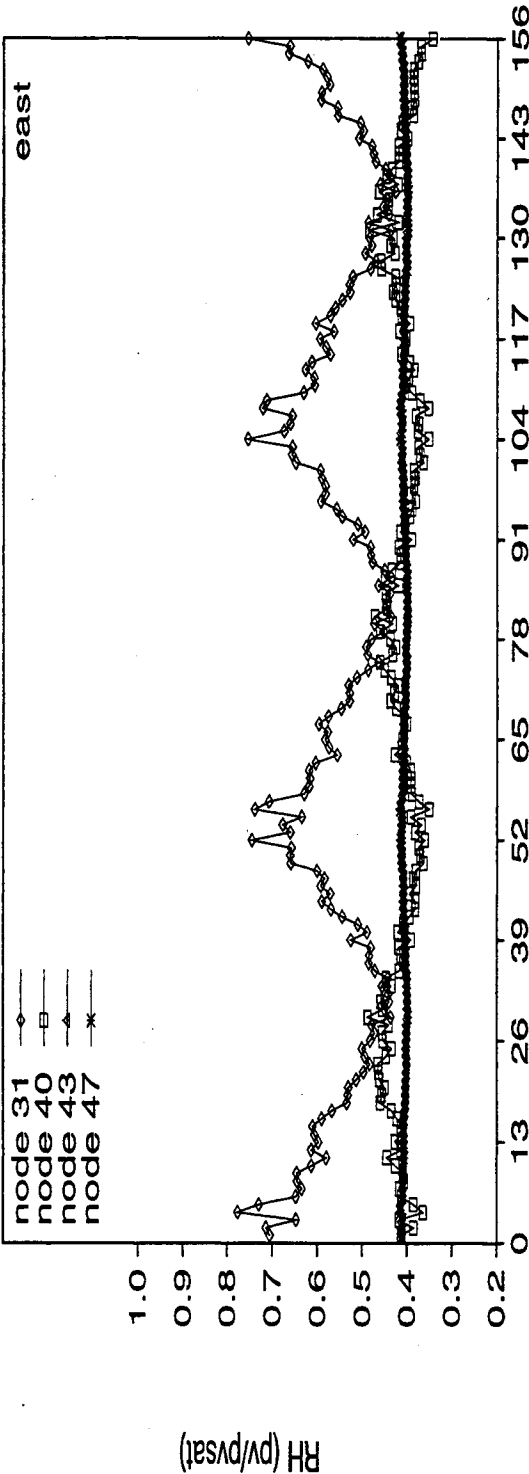
Figure 6.19 Vancouver RH versus
          Time in Weeks (WALL1
          Left Case)
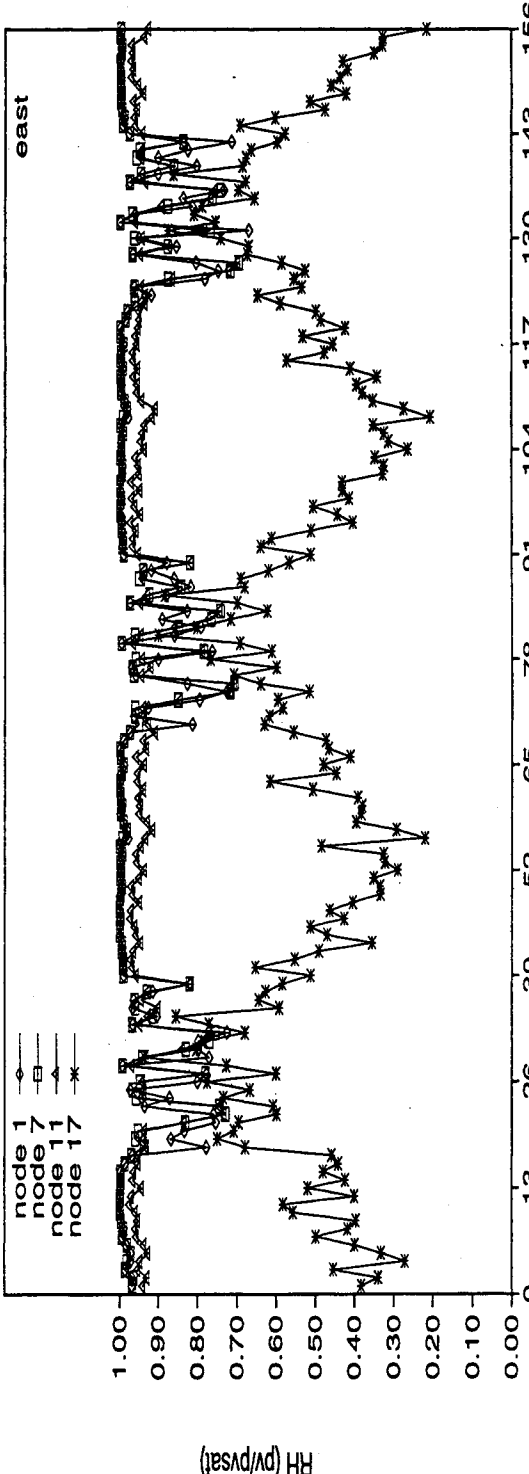
Figure 6.23 Vancouver RH versus
          Time in Weeks (WALL2
          Base Case)

However, with the exception of Resolute location, WALL1 left side retrofit performed better than WALL1 base and right retrofit with respect to moisture transport.

6.6   Moisture Spatial Performance for WALL2

Results of the spatial RH distributions for WALL2 (base case, left- and right-retrofit) are presented next, again for the city of Vancouver. Results will be presented like those for WALL1, for various node points as a function time for the three cases of WALL2. In Figures 6-20 to 6-23 show the three WALL2 systems with their respective node-numbering.

Figure 6.20: Node grid layout for WALL2 base case
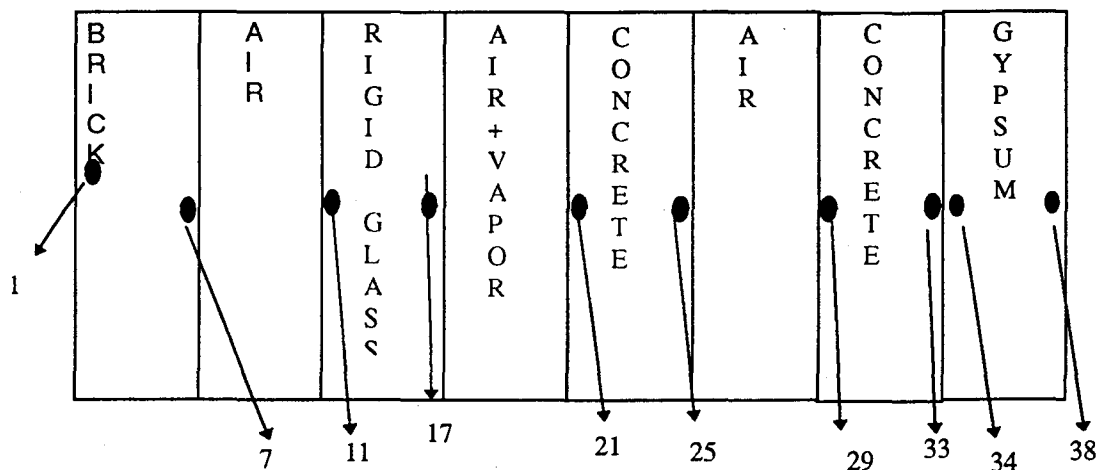
Figure 6.21: Node grid layout for WALL2 right-retrofit case
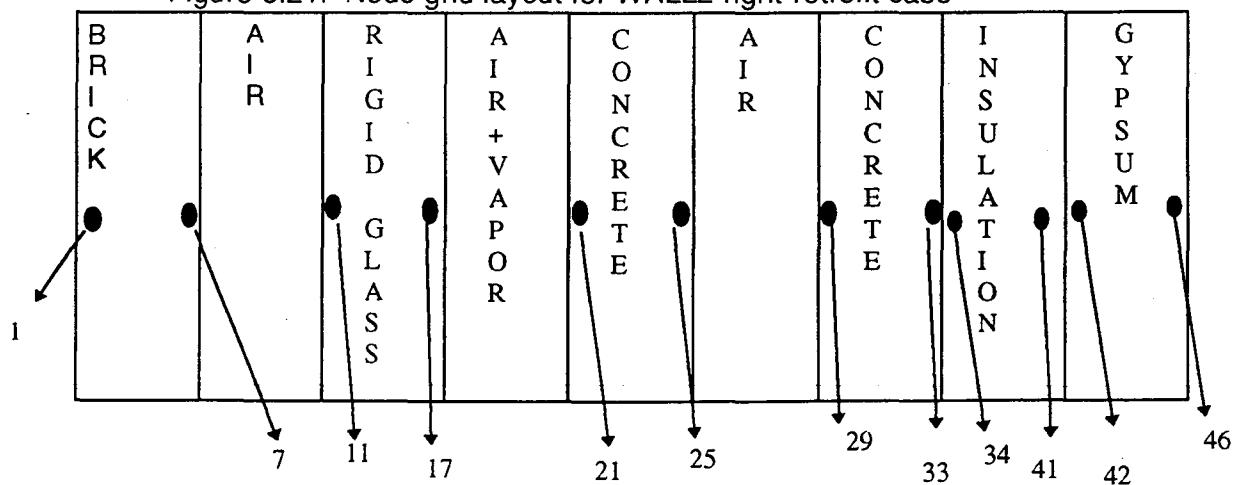
Figure 6.22: Node grid layout for WALL2 left-retrofit case

S T U C C O	P O L Y S T Y R E N E	B R I C K	A I R	R I G I D G L A S S	A I R + V A P O R	C O N C R E T E	A I R	C O N C R E T E	G Y P S U M

1   5   6   10   11   17   21   27   31   35   39   43   44   49
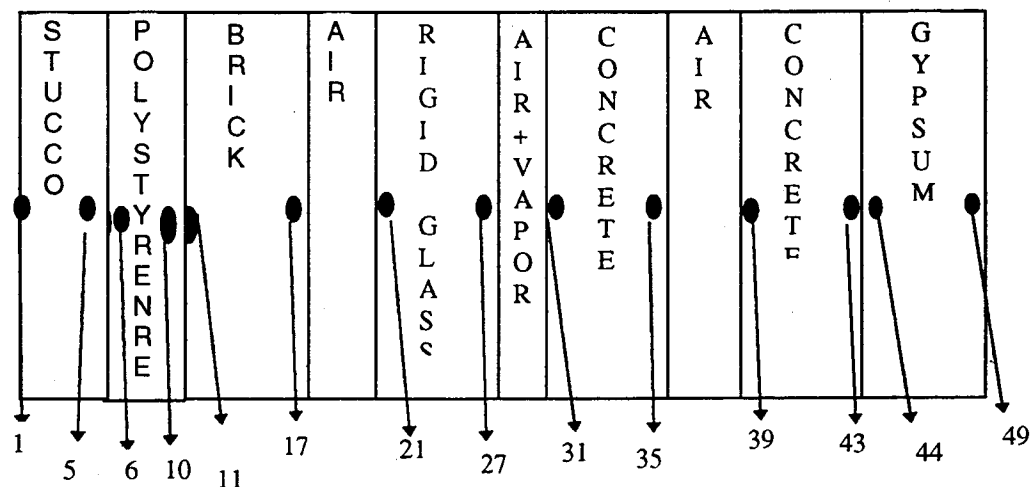
BASE CASE

Results for the base case are shown in Figures 6.23 and 6.24. For WALL2, the exterior brick veneer maintained fairly high relative humidities,   slightly above 95% during the fall and winter periods and dried out during the summer periods.   The exterior most node of the rigid glass-fiber followed the exterior brick closely; however, the interior most node (of the rigid glass) showed a behavior   that is dry (highest relative humidity of 85% during the year) with seasonal cycles that were opposite to the exterior brick. This occurred because of the air layer and vapor membrane adjacent to node 17.   This membrane acted as a vapor retarder and decoupled the interior and exterior environments. Since an interior polyethylene retarder was not used and the concrete block layer dried out from the imposed initial condition. Even after a period of 3 years, complete drying of the concrete block had not been achieved.   This is important since the moisture time constant for concrete is much slower than for fiber-glass insulation.

RIGHT RETROFIT

Figures 6.25 through 6.27 show the spatial RHs for WALL2 (right-retrofit) for the City of Vancouver. The same spatial RH behavior as the base case is observed for the right-retrofit WALL2 for the brick layer and exterior most fiber-glass rigid-board node.

LEFT RETROFIT

For results for the left-retrofit WALL2 see Figures 6.28 through 6.30. For this wall, while having a considerably greater volume of construction material, the amount of
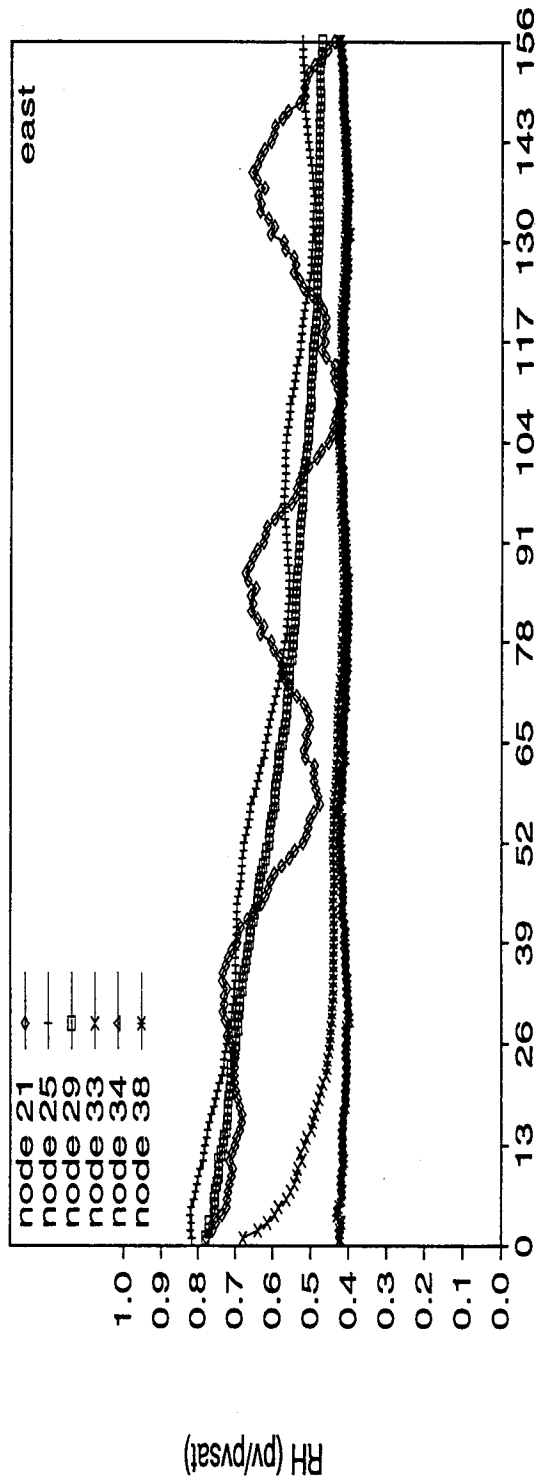
Figure 6.24 Vancouver RH versus
Time in Weeks (WALL2
Base Case)
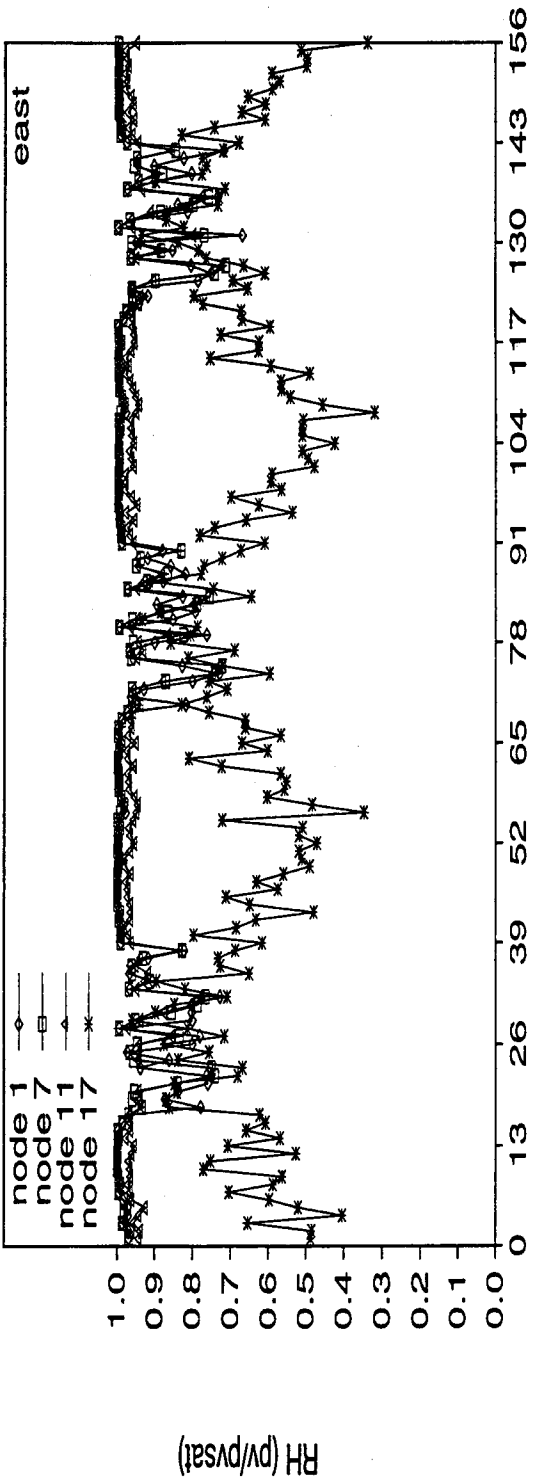
Figure 6.25 Vancouver RH versus
Time in Weeks (WALL2
Right Case)
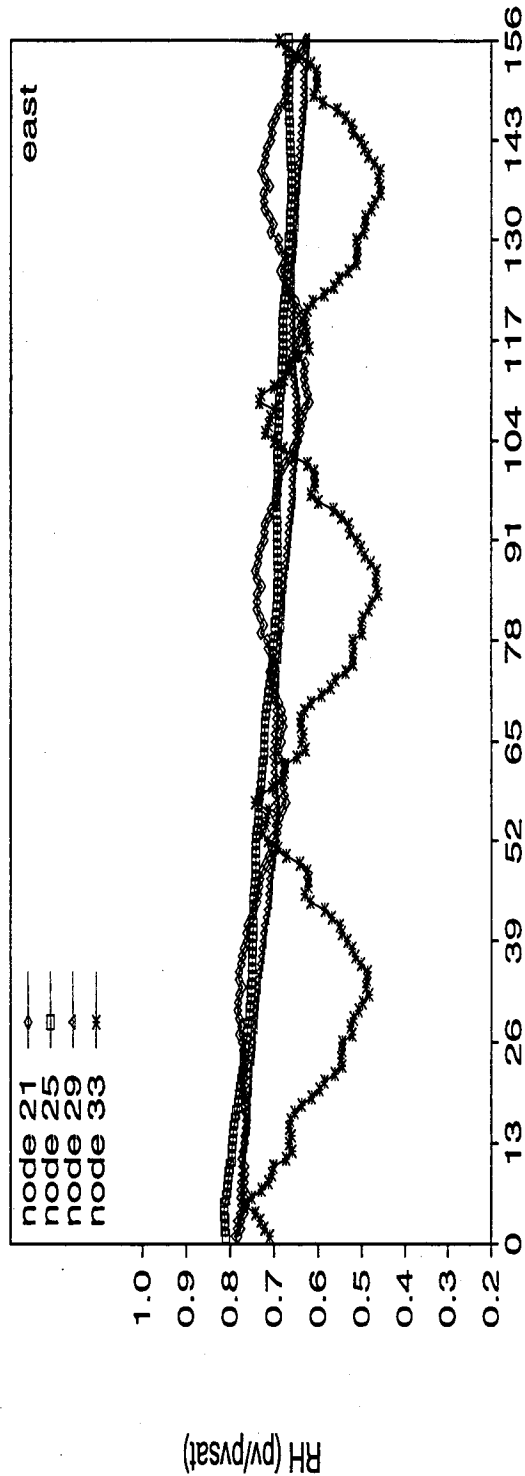
Figure 6.26 Vancouver RH versus
          Time in Weeks (WALL2
          Right Case)
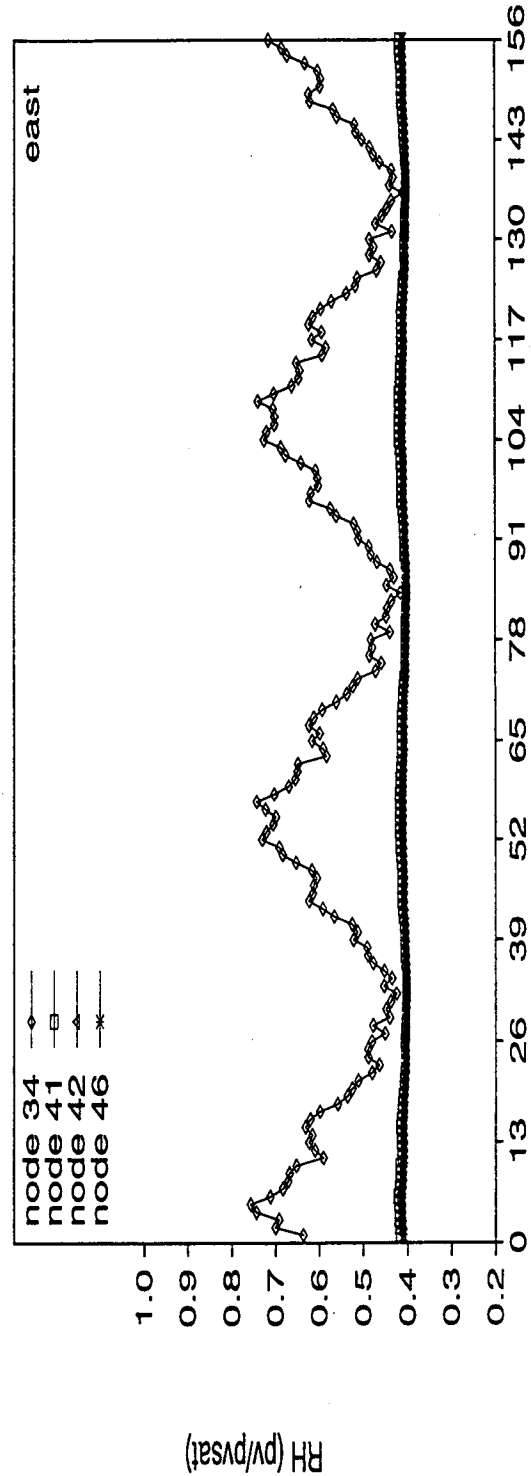
Figure 6.27 Vancouver RH versus
          Time in Weeks (WALL2
          Right Case)
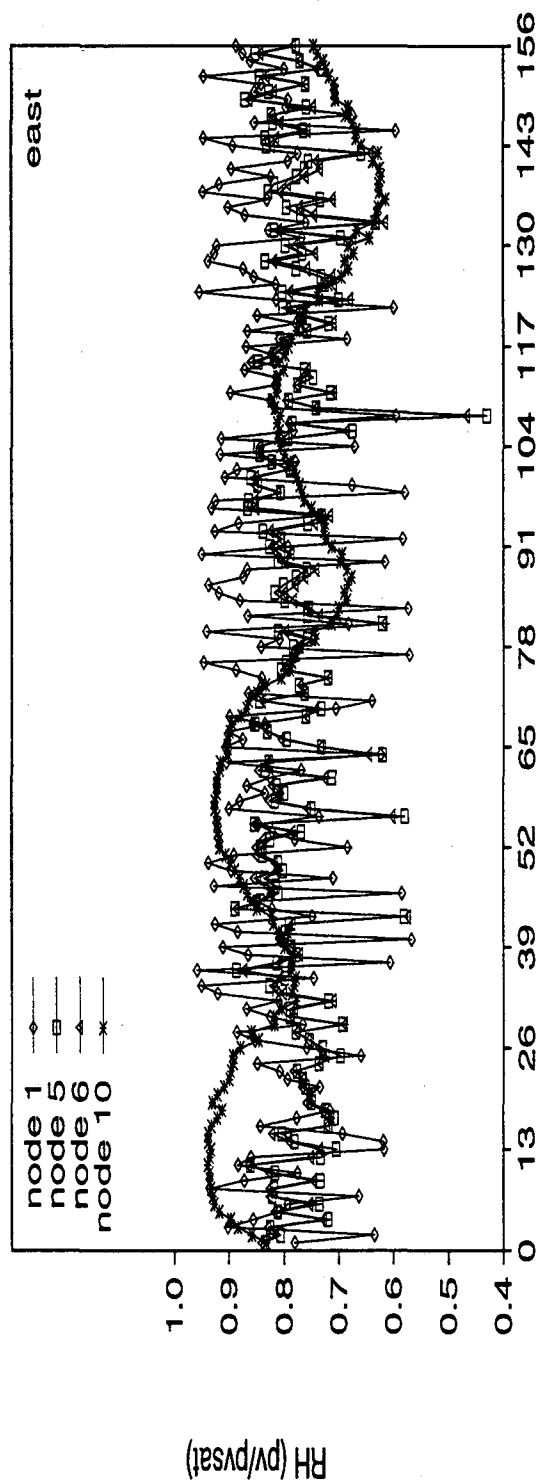
Figure 6.28 Vancouver RH versus
          Time in Weeks (WALL2
          Left Case)
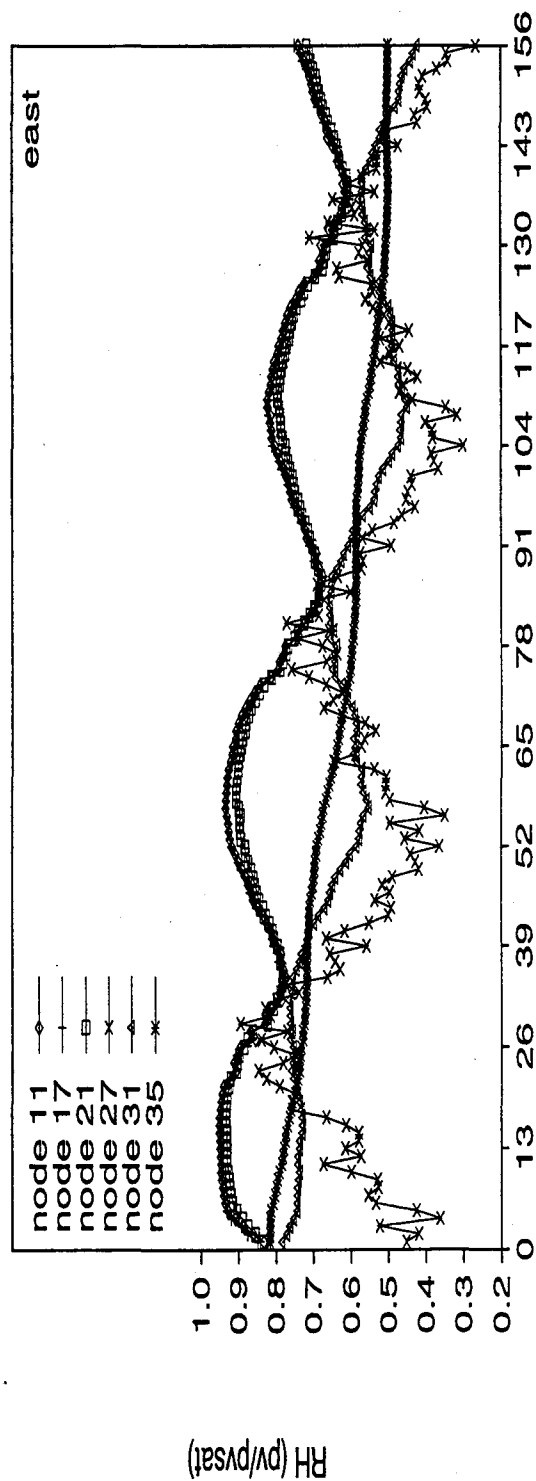
Figure 6.29 Vancouver RH versus
          Time in Weeks (WALL2
          Left Case)
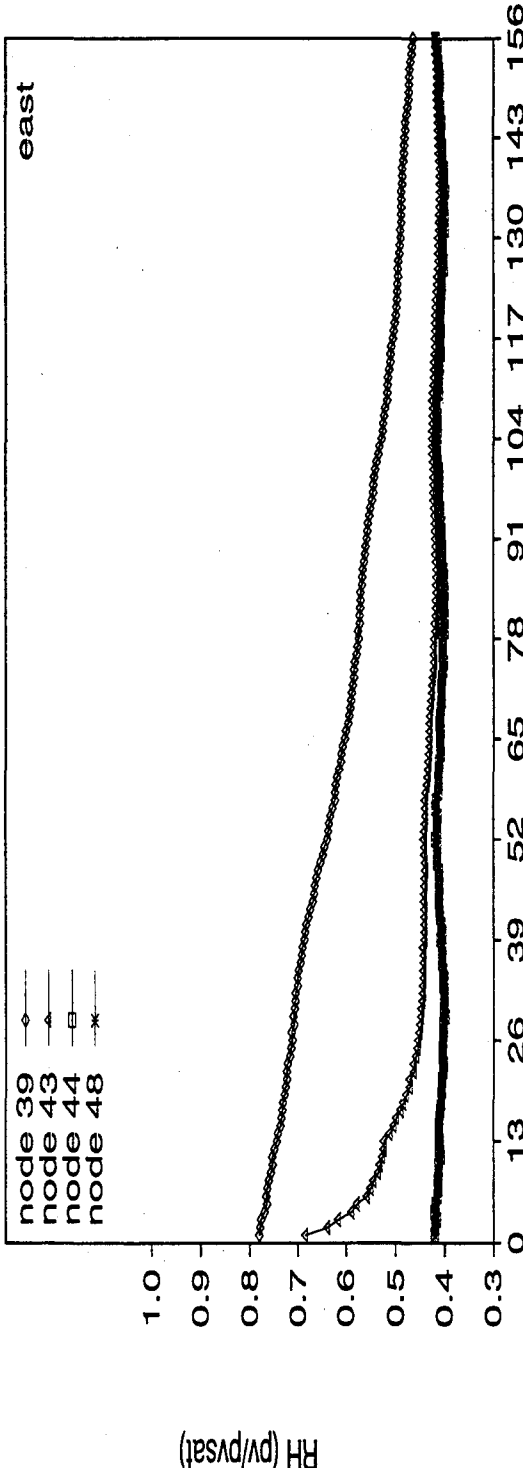
Figure 6.30 Vancouver RH versus
            Time in Weeks (WALL2
            Left Case)
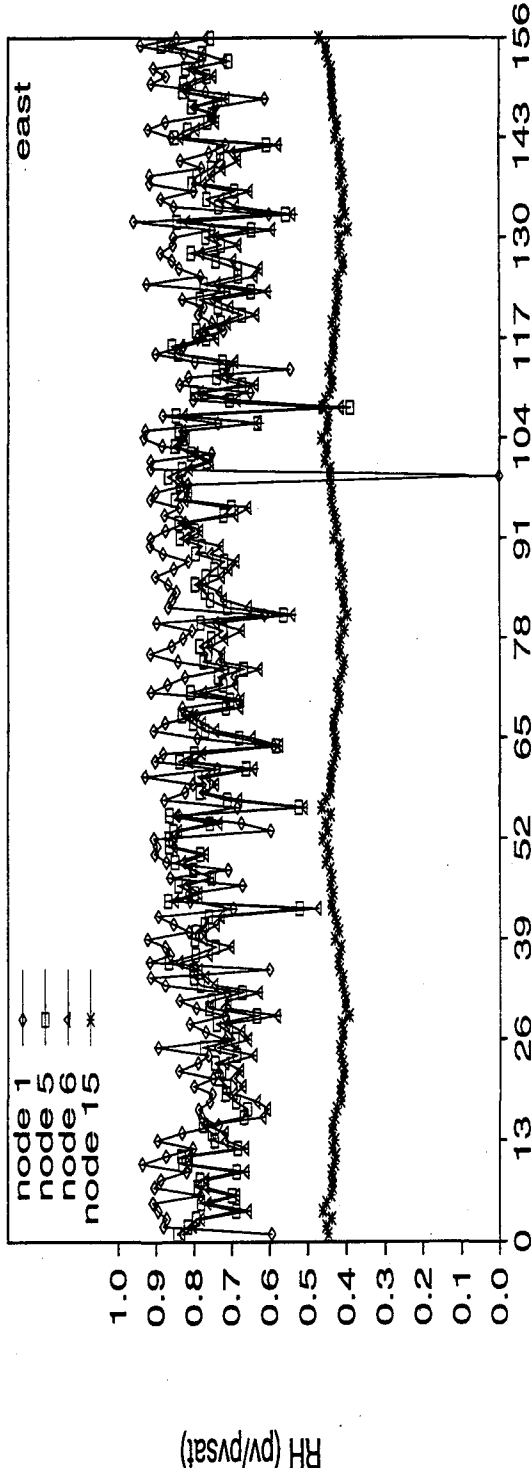
Figure 6.34 Vancouver RH versus
            Time in Weeks (WALL3
            Base Case)

moisture accumulation was considerably less. The brick was kept dry throughout the year. The insulation layer showed results similar to those of the base case wall-type behavior.

GENERAL REMARKS

For WALL2 the base, left and right retrofits performed without any net moisture accumulation for all locations except Resolute (see Appendix C). WALL2 base case for Resolute also performed without a net moisture accumulation, however both left and right retrofit strategies developed moisture accumulation within the concrete block. Overall this wall system was found to be more accommodating with respect to retrofitting than WALL1.

6.7   Moisture Spatial Performance for WALL3

The results of the spatial relative humidity distributions for WALL3 (base case, left- and right-retrofit are presented like those for WALL1 for various node points as a function time for the three cases of WALL3. Results will be shown only for the city of Vancouver, all other locations can be found in Appendix C. See Figures 6.31 to 6.33 which are the three WALL3 systems with their respective node-numbering.

Figure 6.31: Node grid layout for WALL3 base case
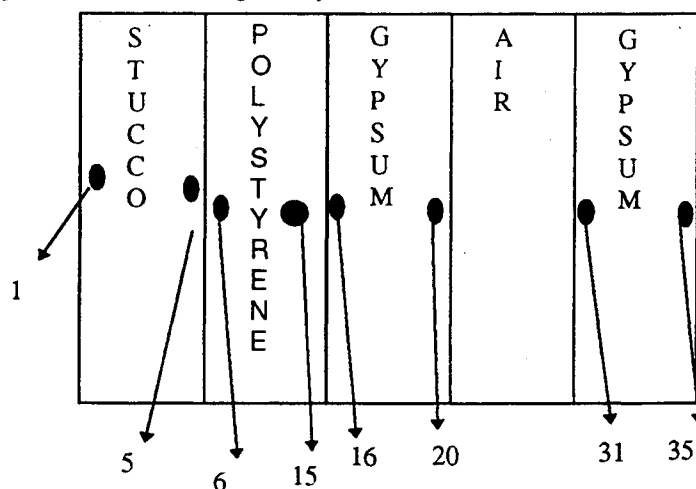
Figure 6.32: Node grid layout for WALL3 right-retrofit case
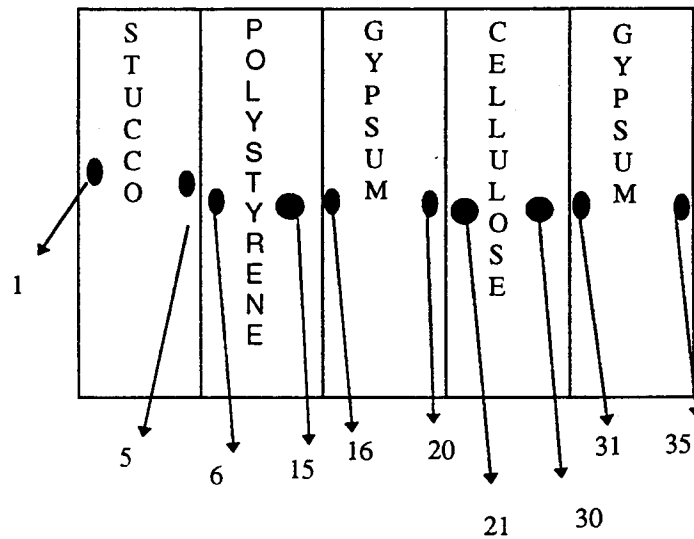
Figure 6.33: Node grid layout for WALL3 left-retrofit case
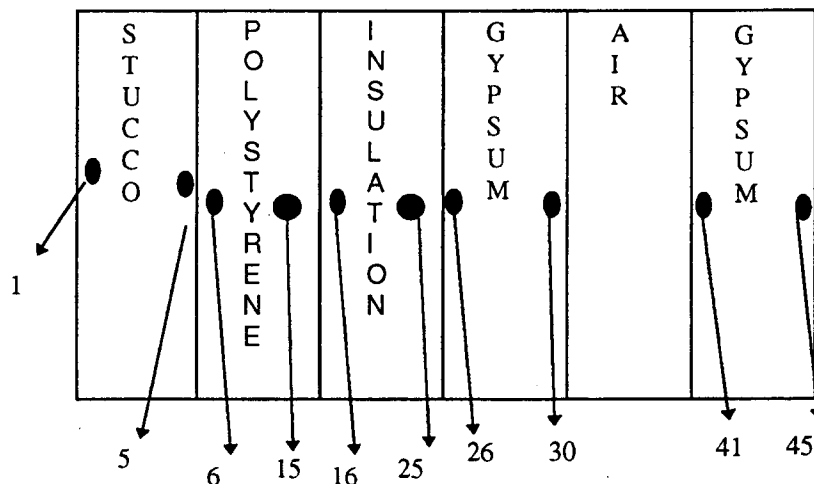
BASE CASE

Results for the base case are shown in Figures 6.34 and 6.35. For WALL3 the exterior stucco maintains high fluctuating relative humidities throughout the year. The interior-most node of the polystyrene board maintains a relative humidity level similar to that of the interior conditions. This particular wall has no vapor retarder, and, from the results presented in Figure 6.34 and 6.35, is the driest assembly among the three walls studied so far. The exterior and interior gypsum also show dry interior conditions.

RIGHT RETROFIT

Figures 6.36 and 6.37 show the spatial RH's for WALL3 (right-retrofit) for the City of Vancouver. For this retrofit, the air layer of the WALL3 (base case) was filled with

cellulose insulation. This reduces the fluctuations of the RH's and decreases the spatial RH's for the stucco and polystyrene layer. The right retrofit allows WALL3 to reduce the moisture induced stresses due to moisture gradients present in the outer facade of the wall.

LEFT RETROFIT

WALL3 (left-retrofit) results are shown in Figures 6.38 and 6.39. For this wall, an additional layer of fibre insulation was added between the polystyrene and the exterior-grade gypsum board. This retrofit produces slightly higher relative humidities in the exterior layers (stucco and polystyrene) and at the exterior most node of the insulation.

GENERAL REMARKS

WALL3 (base case) performs well without the type of problems associated with colder climates for all climate locations. For the base case, the relative humidity of the material layers did not exceed 95 % relative humidity. When the right retrofit is performed using the cellulose insulation, the relative humidities within the wall reduce. The relative humidity present in the exterior layers display the moisture damping effect of the insulation. The left retrofit slightly increases the moisture level and actually allows the development of a condensation layer. The left retrofit essentially alters the moisture free flow to a barrier system that has a retarder on the outer side of the wall (exterior finish). The condensation occurs between the interface of the insulation and polystyrene layer for the colder climates such as Resolute.

6.8 TEMPORAL MOISTURE RESULTS

Results here are processed in terms of total wall moisture performances and presented as a function of time during the 3rd year of simulation. A month here is defined as consisting of a 4-week period. Results are shown for all three wall systems, for each of the two retrofit strategies, for each of the seven cities and four orientations. All wall sections were at an elevation corresponding to the 5th floor of a 10 storey high-rise building. On each page, six figures are shown, each row displays similar orientations and wall types but different wall cases, i.e., starting from the left of the page: the base case, the left-retrofit case and the right-retrofit case. The results are displayed as follows; WALL1, WALL2 and WALL3 for each of the four orientations. In each figure, three curves, representing the maximum, average (calculated from the hourly simulations) and minimum total moisture, are plotted for each month. The moisture results are presented in Appendix C, Figures C1 to C42 for all seven cities.
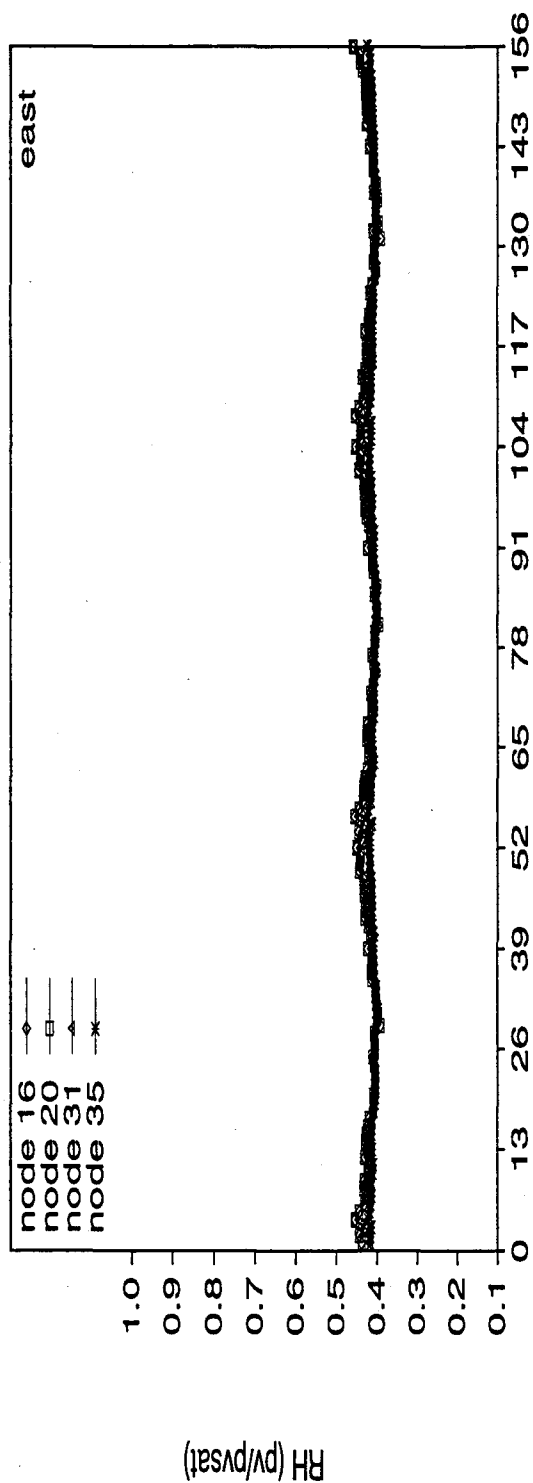
Figure 6.35Vancouver RH versus
          Time in Weeks (WALL3
          Base Case)
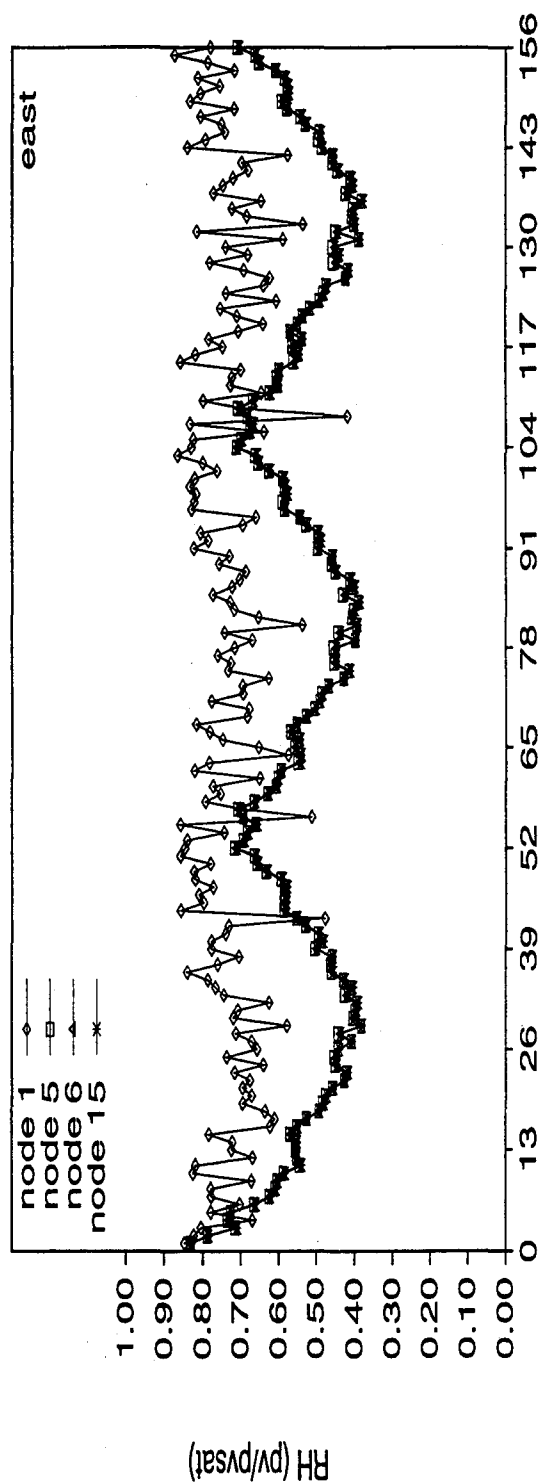
Figure 6.36 Vancouver RH versus
           Time in Weeks (WALL3
           Right Case)
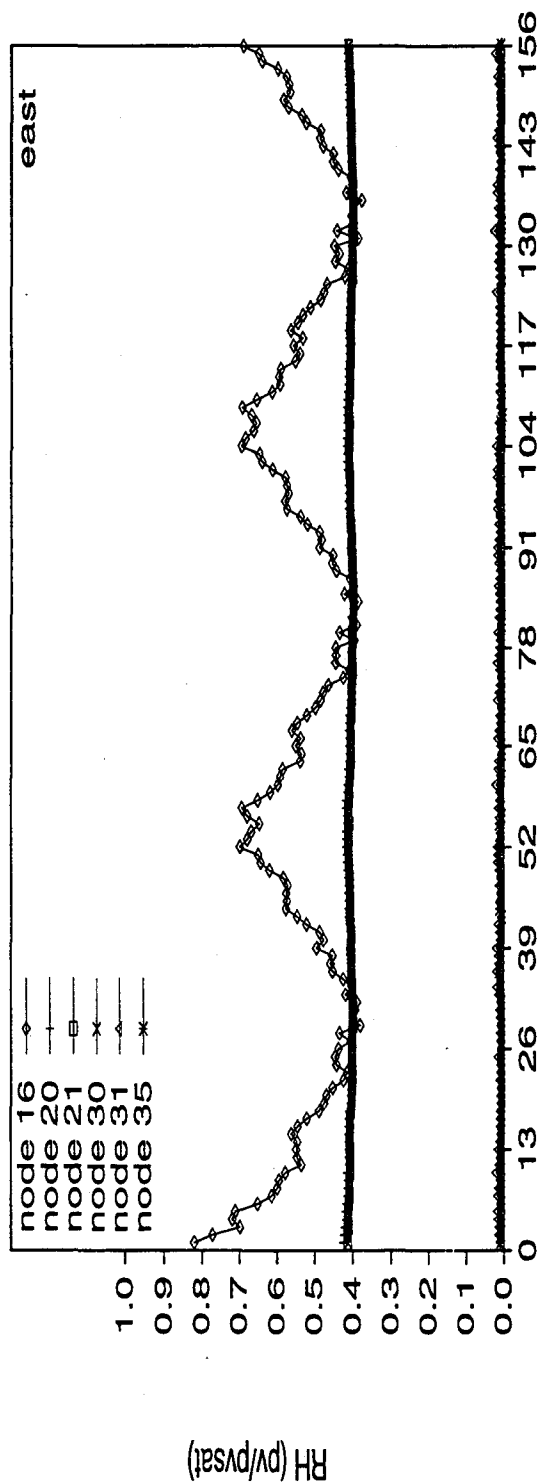
Figure 6.37 Vancouver RH versus
Time in Weeks (WALL3
Right Case)
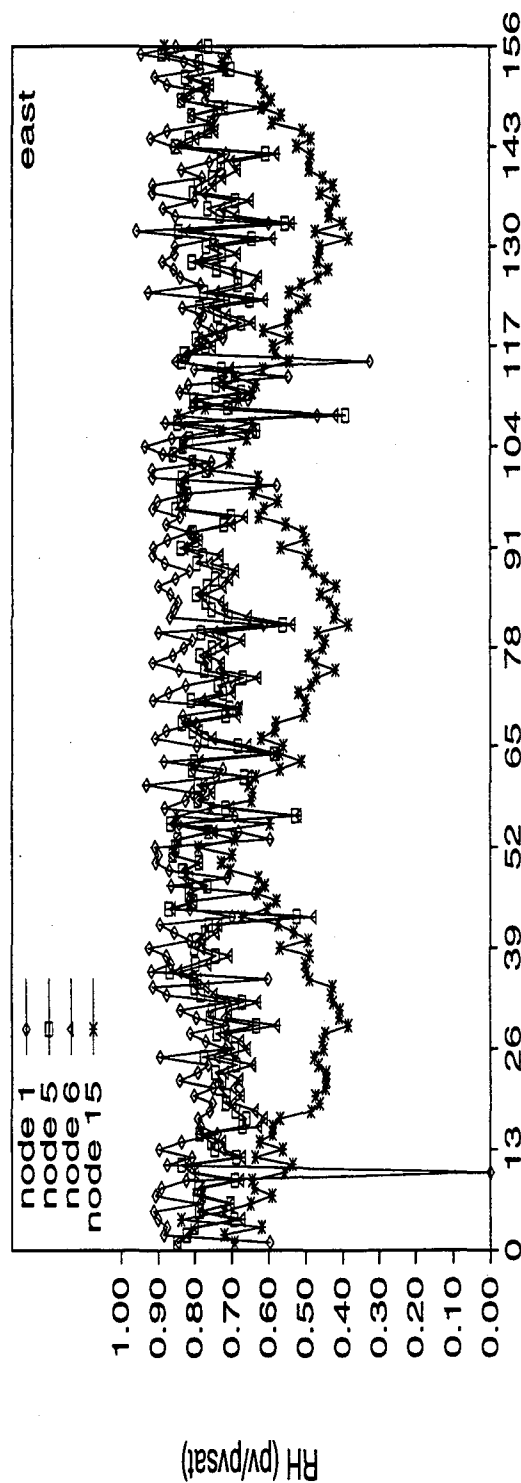
Figure 6.38 Vancouver RH versus
Time in Weeks (WALL3
Left Case)
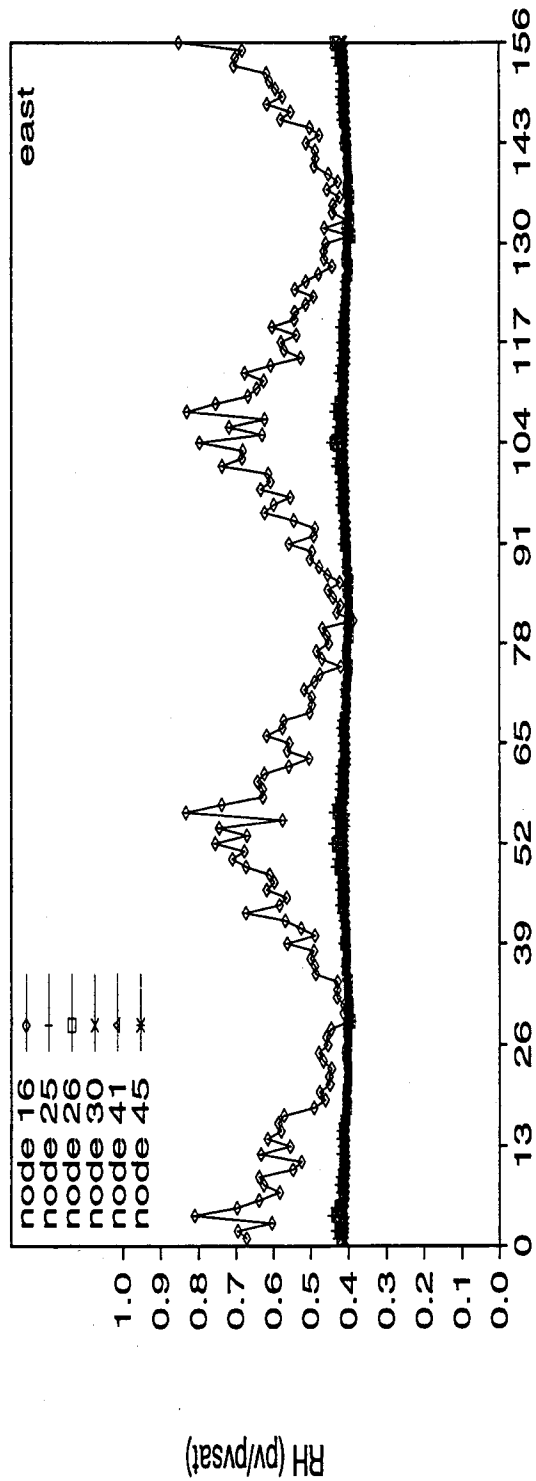
Figure 6.39 Vancouver RH versus
          Time in Weeks (WALL3
          Left Case)

WALL1 (VANCOUVER, OTTAWA, TORONTO and MONTREAL)

Figures C1 to C24 (see Appendix C) show results for WALL1, WALL2 and WALL3 for the cities of Vancouver, Ottawa, Toronto and Montreal. From the transient total moisture (kg/m^2), it is evident that the walls are subjected to large moisture loads that vary considerably throughout the year. This variation is a function not only of time of year but also of orientation of the wall as shown when comparing the south and west faces for a wall in Vancouver. For the base case and right-retrofit cases, maximum moisture changes of 25 kg/m^2 occurred during a year.

WALL1 results of the base case and right-retrofit follow each other fairly closely. In most instances, the values for the right-retrofit case for WALL1 are slightly larger. This is partly due to the lower temperatures at the exterior portion of the wall due to the use of thicker insulation. For WALL1, the effect of orientation was found to be very important. Depending on the orientation, wind speed and orientation, incident of solar radiation, and precipitation, maximum total moisture of 7.2 and 25 kg/m^2 respectively can be found when comparing west and east walls.

For the WALL1 (left-retrofit) case, wind-driven rain shows no influence, since the stucco layer was quite impermeable to liquid flow. This allowed the walls to remain very dry and moisture transport was minimal as long as the near-perfect impermeable conditions were maintained on both side of the wall (stucco and polyethylene sheet).

WALL2 (VANCOUVER, OTTAWA, TORONTO and MONTREAL)

Figures C1 to C24 (see AppendixC) show results for WALL1, WALL2 and WALL3. A strong dependency on wall orientation for the base and right-retrofit cases was found.

WALL3 (VANCOUVER, OTTAWA, TORONTO and MONTREAL)

WALL3 was composed of an EIFS-like system. WALL3 walls performed like the WALL1 (left-retrofit) wall. The annual transient moisture accumulation and drying cycle is also repeated for this wall system but the amplitude is substantially reduced.

WALL1, WALL2 and WALL3 (WINNIPEG, RESOLUTE, and FREDERICTON)

For these locations no hourly precipitation data were available and only ambient vapor transport mechanisms occurred at the surface boundary. Figures C25 to C42 show

results for the three cities namely Winnipeg, Resolute and Fredericton. Here only a mild effect of orientation was observed, primarily due to solar radiation. Results show the normal moisture accumulation and drying behavior, but the maximum total moisture was considerably less, up to 15 times the amount if precipitation was accounted for (comparing Ottawa and Fredericton). For the City of Resolute, WALL1 (base and right-retrofit case) can lead to serious problems. A yearly net accumulation occurred even when no rain was included in the analysis. For the City of Resolute, WALL3 (left-retrofit) increased the total moisture from 0.55 to 8 kg/m^2. Similar problems, but more serious, were found in WALL2. The impact of construction type and retrofit can have serious consequence to the service-life and durability concerns for climatic conditions similar to those in Resolute. However, all three walls perform satisfactorily with climatic conditions similar to those in Fredericton.

COMPARISON OF MOISTURE PERFORMANCE AS A FUNCTION OF CITY LOCATION

The effect of climatic condition is shown in Figures C41 to C46 for those cities that include wind-driven rain and in Figures C47 to C52 for those cases not including wind-driven rain.

(VANCOUVER, OTTAWA, TORONTO and MONTREAL)

Figures C43 to C48 show the strong effect of climatic conditions on the moisture performance for each wall system. Depending on the wall system, (base case, left-retrofit or right-retrofit), the climatic conditions strongly influence the moisture behavior. The appearance of moisture peaks occurs at different times for the north, south, east and west orientations. This means that the performance of high-rise systems can be completely different, depending on the particular orientation, climatic location, and height of the building. These effects can be closely related to the amount of rain precipitation available.

(WINNIPEG, RESOLUTE, and FREDERICTON)

Figures C49 to C52 show thermal performance results for Winnipeg, Resolute and Fredericton. The most prominent accumulation and drying occurred for the city of Resolute. Orientation effects were noted for the city of Resolute, but they were relatively small.

TEMPORAL HEAT FLUX RESULTS

Results are processed in terms of heat fluxes (W/m^2) experienced at the interior surface. These are shown in Figures C55 to C96. The thermal performance for the various orientations, retrofits cases, and the seven climatic locations are presented in these figures. A month here is defined as consisting of a 4-week period. On each page, six figures are shown, each row displays similar orientations and wall types but different wall cases, i.e., starting from the left of the page: the base case, the left-retrofit case and the right-retrofit case. The presentation sequence followed is, results for WALL1, WALL2 and WALL3 for each orientation. For each figure, three curves representing the maximum, average (calculated from the hourly simulations) and minimum heat flux are plotted for each month.

THERMAL PERFORMANCE OF WALL1, WALL2 and WALL3 (VANCOUVER, OTTAWA, TORONTO, MONTREAL, WINNIPEG, RESOLUTE and FREDERICTON)

Differences in yearly heat losses due to the presence of moisture range between 0 and 7% for WALL1, 0 and 5% for WALL2, and 0 and 2% for WALL3. The influence of rain on the thermal performance depends not only on the wall types, climatic conditions but also on orientation. The differences between the minimum, average, and maximum monthly heat fluxes depend on the type of retrofit. All wall systems have demonstrated both thermal and moisture interactions.

ROOF HYGROTHERMAL PERFORMANCE

The thermal and moisture behavior for the three flat roof systems for the seven selected cities were simulated for three years. In Appendix C, Figure C97 shows the typical monthly moisture performance of these roof structures. For all weather locations, the roof systems performed satisfactorily, no yearly net accumulation cases were observed. In Figures C97 (a to f), gravel and concrete are plotted against the y-axis on the right of the figure. For the ROOF1 and ROOF2 cases, the gravel was fully saturated at the beginning of the simulation, while all other layers varied from 80 to 50%. The results from all seven cities show that, without the addition of un-intentional moisture sources, these roof structures will perform satisfactorily independent of climatic location.

Figures C98 (a to f), C99 (a to f) and C100 (a to f) show the monthly thermal performance (minimum, average and maximum) for each of the seven cities for ROOF1, ROOF2 and ROOF3 respectively. The local effect of climatic location is more apparent in the thermal performance than in the moisture performance analysis. Essentially, these roofs are protected on both sides, and this allows them to perform well even under the harsh conditions of Resolute.

6.9 2-D SIMULATION RESULTS

Figure 6.40 depicts the wall used in the 2-D simulations. The simulations were performed using Ottawa as the climatic location for a 2 year period starting in the beginning of January. The wall used two paths, each 3 mm thick at the interior plane and only one path at the exterior bottom part of the wall.
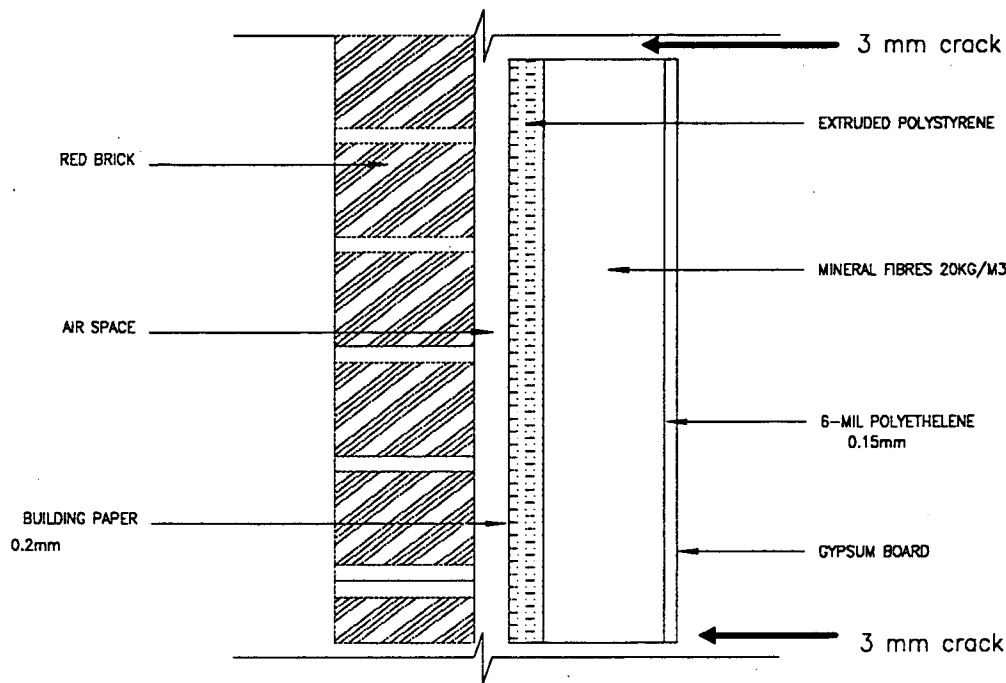
NOTE:ALL DIMENSIONS IN mm

Figure 6.40: 2-D wall

Five simulation cases were developed. (They are defined in Table 6.5)   The interior of the building was assumed to be positively pressurized by 10 Pa. Depending on the weather conditions, i.e., summer or winter (stack effect), the wind speed and orientation, and the interior overpressurization, the wall produced hourly no-flow, exfiltration or infiltration scenarios. Furthermore, the wall also received rain; but for comparison, all wall cases were given equal amounts of rain (no height effects). This was also necessary to limit the number of simulations required, and to determine for the first time the influence of stack effect (height) on the hygrothermal performance of a high-rise wall.

TABLE 6.5 Definition of 2-D Simulation Cases

Case Name	Definition
No-Opening	In this simulation case, the wall structure is made airtight and the openings were sealed. The effect of natural convection in the insulation and air cavities is present.
Stack-1m	Here the bottom of the wall is located 1 m above the neutral plane level (NPL). This wall is located in the middle region of the high-rise building. A 10-Pa overpressurization in the interior is used. The wind speed and orientation from the weather file are used, producing infiltration and exfiltration of air and moisture through the wall system.
Stack1m	Here the bottom of the wall is located 1 m below the NPL. This wall is located in the middle region of a high-rise building. A 10-Pa positive pressure in the interior is also used. The wind speed and orientation from the weather file are used, producing infiltration and exfiltration of air and moisture through the wall system.
Stack-20m	Here the bottom of the wall is located 20 m above the NPL. This wall is located at the top of the high-rise building. A 10-Pa overpressurization in the interior is also used. The wind speed and orientation from the weather file are used, producing infiltration and exfiltration of air and moisture through the wall system.
Stack20m	Here the bottom of the wall is located 20 m below the NPL. This wall is located at the bottom of the high-rise building. A 10-Pa overpressurization in the interior is used. The wind speed and orientation from the weather file are used, producing infiltration and exfiltration of air and moisture through the wall system.

In Figure 6.41, the total moisture in the wall is plotted out against time. The x-axis in this figure shows a section of the 2-year results starting from 7,000 hours (i.e. approaching the second year). These results show the effect of exfiltration, infiltration, and no-flow scenarios. All these conditions can exist on the same face of a tall high-rise building. During late fall and winter seasons, the effect of exfiltration can be important; however, even here during a rain spell, liquid diffusion (by leakage and capillarity) becomes the dominant transport mechanism.

Figure 6.41 gives an estimate (actual magnitude can only be calculated for a wall system if measured material properties and weather data are used) of the differences found in high-rise wall systems. Several interesting observations were found, one is that the wall system at the bottom floor (Stack20m) of this high-rise building was the driest wall (of all 5 cases) during late fall and winter seasons. This wall system (Stack20m) accumulates less water during these seasons when compared to the case where these openings were sealed (air-tight assembly). Investigating the spatial velocity distributions, it is evident that infiltration flow occurs during the late fall and winter season at the bottom floor. As cold, dry exterior air carries very small amounts of vapor, this forced convection flow actually dries the wall system. However, once the cold season is over, the Stack20m wall behaves in the same fashion as all the other four wall cases, under wind-driven rain conditions. Indeed during the late summer periods (11,000 h) the large spikes in moisture content that occur in Figure 6.41 are solely due to precipitation and are present for all five wall systems.

Figure 6.42 shows the accumulation within the insulation layer for the full 2-year period starting in January. This figure reveals the combined heat air and moisture transport performance of the wall system. The moisture accumulation during the winter period in the insulation layer was much less for Stack-20m than for Stack-1m. Even though more air was exfiltrating through the wall system in the Stack-20m case, the accumulation was less. This was primarily due to the fact that as more air flows through the insulation, it warms up the insulation layer and thus the potential for moisture accumulation via condensation is substantially reduced. However, the time for moisture accumulation for Stack-20m was greater than for Stack-1m due to the higher air flows when the potential for accumulation is lower. A maximum of 1.2 kg of moisture accumulated within the insulation layer during winter season for Stack-1m wall. For wall Stack20m (bottom), the insulation layer was found to be the driest.

Figure 6.43 shows that Stack-20m (top wall) had the highest moisture accumulation in the extruded polystyrene, as expected, followed by walls Stack-1m, Stack1m, No-opening and finally Stack20m. Similar moisture behaviour was observed in the building paper layer (see Figure 6.44) . This building paper layer can act as buffer zone to the wall system. Figure 6.45 shows the moisture accumulation in the air layer. As expected, high moisture contents (humidity ratios) are found only in the cases where substantial exfiltration occurs and this was so for cases Stack-20m and Stack-1m, and existed during late fall and winter.
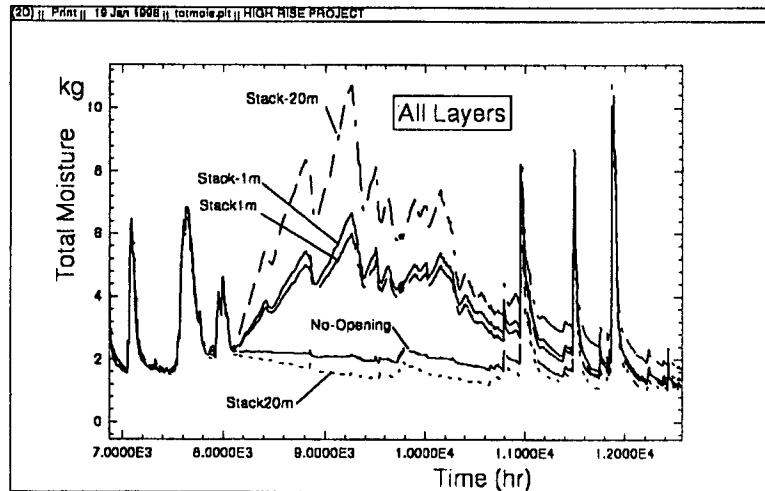
Figure 6.41: Total Moisture Performance
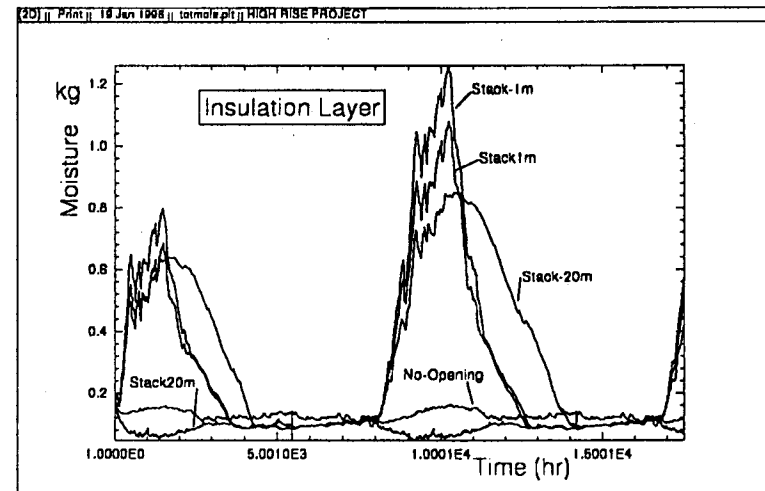
Figure 6.42 Insulation Moisture Performance
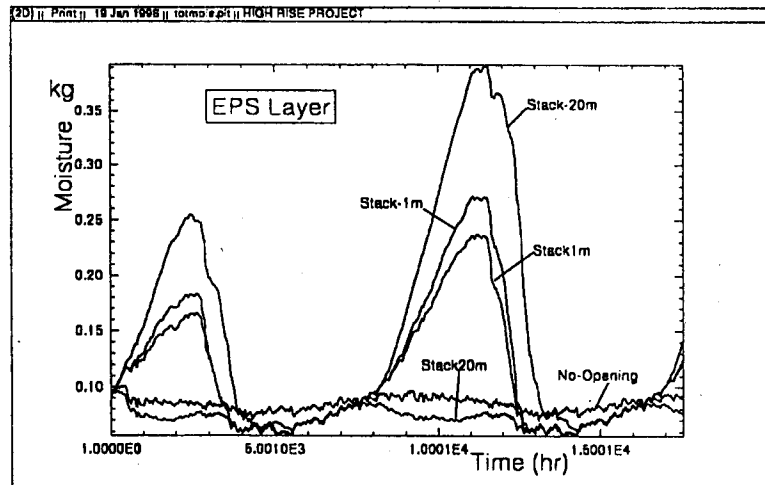
Figure 6.43: EPS Moisture Performance
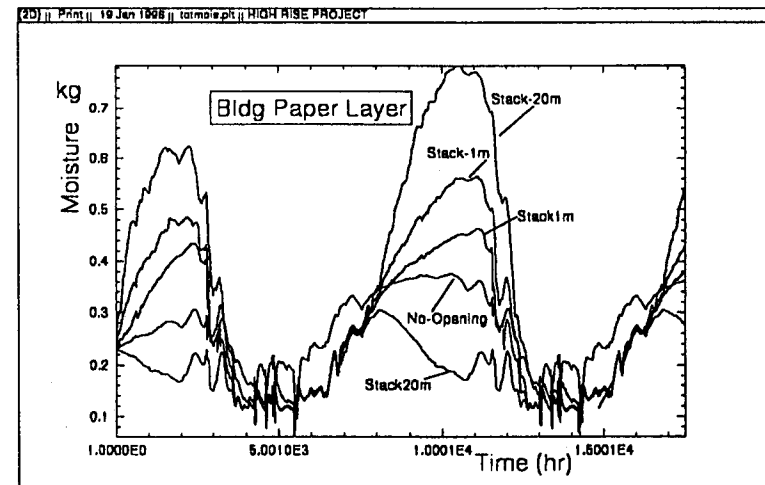
Figure 6.44: Building Paper Moisture Performance
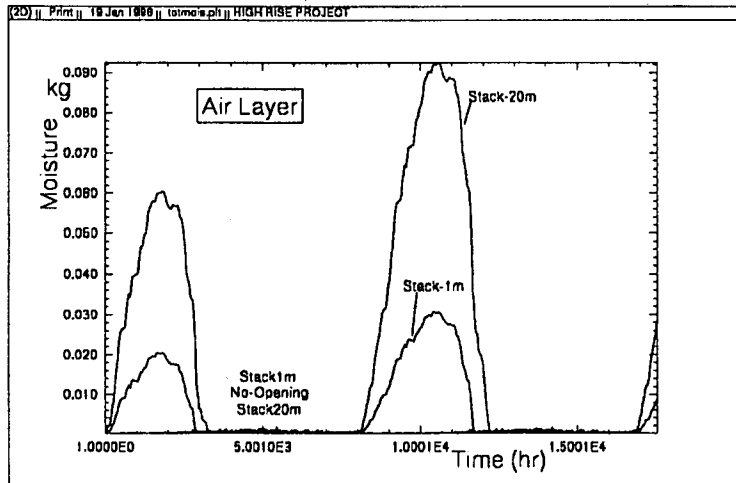
Figure 6.45: Air Layer Moisture Performance
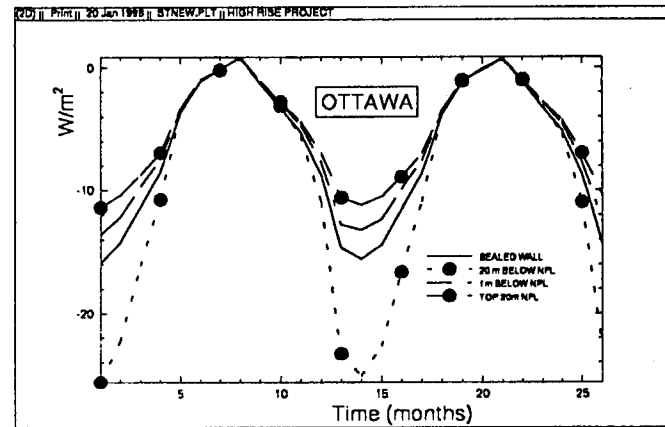
Figure 6.47: Monthly Averaged Heat Flux (Conductive)
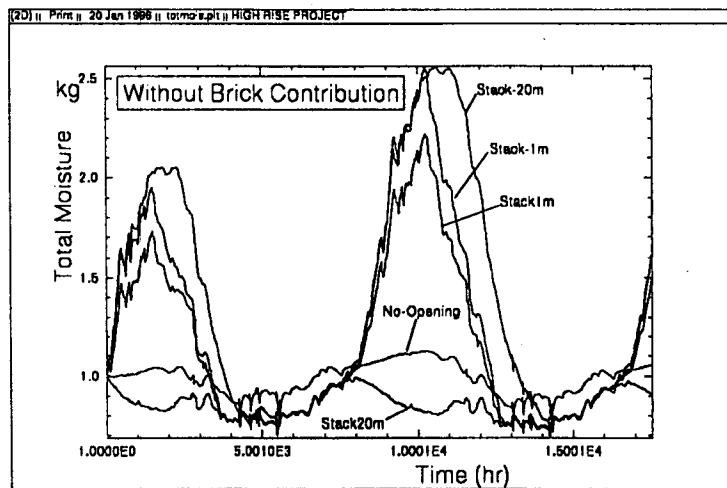
Figure 6.46: Without Brick Contribution

Figure 6.46 shows the moisture accumulation in the wall with all layers, except the brick layer. The brick layer was mostly affected by the rain accumulation; and was excluded for this comparison. By comparing Figures 6.41 and 6.46, one can see that 2.6 out of 13 kg means that approximately 75% of the moisture is concentrated on the outer leaf of the construction (brick veneer).

Finally, Figure 6.47 shows the conductive heat fluxes for the cases of No-Opening, Stack-20m, Stack20m and Stack-1m wall. The highest heat loss was found for Stack20m (20m Below NPL) followed by the No-Opening wall (sealed), then the exfiltration for walls Stack-1m and Stack-20m (1m above NPL and 20m above NPL). The walls (at the bottom of the building) act as dynamic walls and benefited by the warming of the ventilation air (inflitrating air) into the structure, but at a cost to the conductive heat losses (see Figure 6.47). However, as air exfiltrated into the structure for the upper walls, it warmed the wall layers and reduced the conductive component. As was observed in the simulations for the insulation layer, by warming this layer the amount of moisture accumulation was considerably reduced. But at the same time the amount of moisture accumulating in the outer leaf of the wall (brick veneer) increased considerably. An optimization of these behaviors in term of each materials durability thresholds should allow one to design building envelope systems that are more durable.

6.10 CONCLUDING REMARKS

This work investigated the hygrothermal performance of three wall and roof systems used in various locations within Canada. . Results from this work have demonstrated that state-of-the-art hygrothermal modeling, which accounts for the effects of air flow, surface rain, vapor and liquid transport, can provide a useful design assessment. A parametric study was developed that investigated the influence of location and orientation of the wall system. It also examined the effect of two types of retrofits: one on the outside of the structure and the other on the inside side. High-rise building envelope modeling has identified quantitatively for the first time, some of the more important hygrothermal processes, such as the influence of rain, and air exfiltration. The results from this study provide representative analysis of the interactions of moisture and thermal fields for a given set of material properties. As with any modeling endeavors, material properties directly influence the moisture behavior of the system. Material properties that have been used in this study are not necessarily the most representative ones found in Canada. However, results from this parametric study show the relative influences of climatic location, orientation, and retrofit strategy that are needed to develop general guidelines for wall design. For the 1-D analysis the wall systems were assumed ideal, just as a building envelope designer would develop. A perfect air-tightness plane was modeled for the 1-D results as no air flow was assumed. The development of the guidelines must be complemented with a set of field or laboratory data. This information on the system must be incorporated in the modeling activities, which in return allows one to predict the long-term performance of the system in a conclusive manner. To-date, a complete set of hygrothermal moisture data for any wall and roof systems is very difficult to find.

The following conclusions can be drawn from this work:

- Modeling hygrothermal transport in building envelope systems, as found in high-rise buildings, requires a sophisticated model that includes both vapor and liquid transport. Air-flow mechanisms must also be included in the model to determine the effects of infiltration/exfiltration on the thermal and moisture performances. ·

- Material properties being the transport coefficients for the complex porous- medium phenomena must be known accurately. Differences of the order of $\pm$ 25% can be acceptable for some hygrothermal properties but the correct material properties functional form and dependencies must be incorporated in the model. These

properties must also address the transport phenomena that occurs in both vapor and liquid regions.

- Boundary conditions similar to those experienced by high-rise buildings must be used in the modeling activities. These boundary conditions must include the effect of orientation, the ambient conditions, cavity venting, airtightness and localized rain precipitation.

- Building envelope system design and details must be translated from the architectural to the computational domain correctly. This work focused on evaluating the performances of various ideal systems (no defects). However, not surprisingly even under these conditions some wall systems were found to be prone to premature deterioration. All wall systems did not perform satisfactorily throughout, even under ideal conditions (i.e. no-air leakage).

- The idealized (no-air leakage and cracks) roof assemblies performed satisfactorily with respect to heat and moisture transport.

- Wind-driven rain was found to be a major source of moisture. Brick veneer assemblies were found prone to deterioration due to the high levels of moisture in the exterior facade due to rainwater. Wind-driven rain can increase the moisture content of walls by up to 40 times the nominal no-rain cases. Still today, nearly all design methods do not accommodate the effects of wind-driven rain.

- The thermal degradation due to the interaction of moisture in wall systems examined in this study ranged between 0 and 9%. Latent heat effect was found to be important contributor to the thermal degradation only when a net yearly accumulation or drying occurs.

- Defects in the wall system can produce either positive or negative roles with respect to the durability of a wall system: depending whether a wall section is subjected to a net infiltration or exfiltration mechanism, the wall may either dry out or accumulate large amounts of water. However, this study has confirms both lab and field hygrothermal results suggesting that no-air movement through the walls is preferable in all cases.

- Air leakages within the wall sections are complex 2-D and 3-D dimensional flow conditions: nevertheless, these produce localized thermal bridging and moisture accumulation and must be considered in some form or another.

- Results have demonstrated the significant effect of height on the hygrothermal performance of the wall systems for high-rise building. Height should be a serious design parameter for service-life and durability considerations.

- The effect of orientation of high-rise building envelope walls on the hygrothermal performance was found to be particularly important. Each climatic location was found to have wall orientations with high and low moisture accumulations. Special care and detailing must be taken depending on the climatic location of the building. The choice of material hygrothermal properties must be dependent on the orientation (climate) and height of the high-rise. Alternatively, water shedding, air cavity ventilation and capillary breaks must be incorporated in wall designs.

- The effect of wind-driven rain and air-exfiltration on the moisture accumulation of high-rise walls was found to be of the same magnitude for the cases examined in this report. This implies that steps must be made to provide both air-tightness of high-rise walls and the rain penetration control to avoid net moisture accumulation.

- Retrofit strategies must be evaluated for each climatic location based on the combined heat, air and moisture transport performance. Retrofitting high-rise buildings still remain a challenge to the building envelope designer. Each wall system with material properties that dependent on the thermal, vapor and liquid transport processes must be considered. How they interact within the complete wall system must also be understood. Modeling can provide insight into all such interactions, which, in turn will aid in the development of design and retrofit guidelines.

RECOMMENDATIONS FOR FURTHER RESEARCH
Major advancements in moisture engineering modeling have taken place during the past 5 years. Moisture models with internal validation checks will become available in the near future for qualified building envelope designers and specialists. These tools will able to assist in the design or retrofit and optimization of high-rise building envelope systems. Additional studies required to allow these future developments are:

1. Development of accurate experimental protocols and measurement probes to provide field measurements of moisture content. This is important for modeling verification and field assessments.

2. Develop through modeling additional infiltration-exfiltration research for various high-rise wall air-tightness characteristics. These could potentially lead to simplified correlation's for accessing the hygrothermal performance of different wall systems.

3. Develop validation field data to calibrate and refine modeling for various high-rise building envelopes. Wind-driven rain data and air leakage characteristics should be collected for a variety of high-rise buildings.

4. Develop a comprehensive material property database of Canadian construction materials by measuring the most important hygrothermal transport properties (vapor and liquid components). This is an activity that is needed as any progress in the area of modeling requires representative values of material properties.

5. Develop and characterize sub-system and system performances of high-rise wall systems. A particular sub-system performance that can be of particular interest is the effect of waterproofing of various masonry high-rise facades. An experimental and modeling activity in this area can determine the appropriateness of various new and old sealers available in the market as a function of weather location and building height.

6. Work should be carried out to determine retrofit strategies that minimize the extent of wind-driven rain damage such as waterproofing, water shedding details and others.

A general user friendly tool to perform moisture engineering analysis must be developed so that building practitioners can examine design and retrofit alternatives. An extensive catalogue with suggested retrofit strategies as a function of wall design and climatic locations within Canada could be developed in this context.

REFERENCES

SECTION 1

BIA, Brick Institute of America, 1985-87 Brick Veneer Steel Stud Panel Walls. Technical Notes on Brick Construction, 28B, Reston, Virginia

Canadian Roofing Contractors Association (CRCA), 1990. Roofing Specifications. Canadian Roofing Contractors Association, Ottawa, Ontario.

Canadian Standards Association (CSA), 1990. Windows: A National Standard of Canada. Canadian Standards Association, Toronto, Ontario.

Canada Mortgage and Housing Corporation (CMHC), 1991. Exterior Wall Construction in High-Rise Buildings prepared by R.G. Drysdale and G.T. Suter, Ottawa, Ontario.

Canada Mortgage and Housing Corporation (CMHC), 1991. Construction Problems in Multi-family Residential Buildings. prepared by R.G. Drysdale, Ontario.

Chambers, D.A., 1993. Letter dated 1993 08 12. City of Halifax Development and Planning Department, Halifax, Nova Scotia.

CERCA, Roofing Specifications, Canadian Roofing Contractors Association, Ottawa, Ontario

Edgar, J.R.S., 1992. Exterior Insulated Finish Systems: Detailing Avoids Problems. BECOR Annual Seminar, Ottawa, Ontario, May 28, 1992.

Goff, Kristin, 1992. Do your condo homework; Many owners run into problems when they fail to check before buying. The Ottawa Citizen, April 11, 1992, pp G1.

Geneen, Florence, 1992. The Conservation of the High-Rise Residential Stock . The 6th Conference on Building Science & Technology, Toronto, Ontario, March 5, 1992

G.K. Yuill & Associates (Manitoba) Ltd., 1992. Personal Communication, Sept., 1992.

Hemson Consulting Limited, 1992. City of Toronto High-Rise Apartment Conservation Study.Hemson Consulting Limited, Toronto, Ontario.

Hutcheon, N.B. and G.O.P. Handegord, 1983. Building Science for a Cold Climate. John Wiley & Sons, Toronto, Ontario.

Keller, H., 1989. Field Investigation of Brick Veneer/Steel Stud Wall Systems. Canada Mortgage and Housing Corporation Report, Ottawa, Ontario.

National Research Council of Canada (NRCC1), 1990. National Building Code of Canada 1990. National Research Council of Canada, Ottawa, Ontario.

National Research Council of Canada (NRCC2), 1990. The Supplement to the National Building Code of Canada 1990. National Research Council of Canada, Ottawa, Ontario.

ONHWP, Ontario New Home Warranty Program, 1991, Condominium Construction Guide Ontario Ministry of Housing and Ontario New Home Warranty Program, North York, Ontario

Pederson, C.R., 1990. Combined Heat and Moisture Transfer in Building Constructions. Ph.D. Thesis, Thermal Insulation Laboratory, Technical University of Denmark, Lyngby,Denmark.

SPB Strategic Planning Branch, 1991. Assessment Branch Reports: 1988, 1989, 1990, and 1991 Taxable Assessments by Mill Class and Land Use Code. City of Edmonton Forecasting and Policy Development Group, Planning and Development Department, Edmonton, Alberta.

City of Toronto Housing Department, (#92-003), 1992. High-Rise Apartment Conservation Study. Policy and Reserach Section, Toronto, Ontario.

Lawton,M. Morrison Hershfield Limited, 1993 Personal Communication. (Andrew Boyd)

Hemson Consulting Limited, 1992. City of Toronto High-Rise Apartment Conservation Study. Hemson Consulting Limited, Toronto, Ontario.

Cheung, M. 1993, Cladding Study A Literature Search, Technology Sector,

SECTION 2

Burch, D. and Thomas, "Controlling Moisture in Roof Cavities of Manufactured Housing", 1992, NISTIR 4916, Gaithersburg.

Hens, H. and Janssens A., "Enquiry on HAMCAT CODES", International Energy Agency, Heat, Air and Moisture Transfer in Insulated Envelope Parts, Report Annex 24, Task 1, Modeling, 1993.

Salonvaara M., Ojanen, T. IEA, Annex 24, HAMTIE, Calculation models, Classification of models TCCC2D and TRATMO2, Report numbers T1-SF-91/01,02,03.

BIBLIOGRAPHY

Fleming, W. and Lions P.L., Stochastic Differential Systems, Stochastic Control Theory and Applications, 1988, IMA Volume 10, Springer-Verlag

ASC (1993) *Theory Documentation for TASCflow*, Version 2.2, Advanced ScientificComputing Ltd., Waterloo, Canada.

Beam, R. and Warming, R. "An implicit factored scheme for the compressible Navier-Stokes Equations. AIAA Journal, Vol. 16, No. 4, April 1978, pp. 393-402.

Chorin, A.J. "A numerical method for solving incompressible viscous flow problem",Journal of Computational Physics, Vol.2, No.1 1966.

Douglas Burch "Controlling Moisture in Roof Cavities of Manufactured Housing", 1992, NISTIR 4916, NIST, Gaithersburg.

Hens, H. IEA, Annex 24, HAMTIE, First Common Exercise, Report number T1-B-91/05. Karagiozis, A. "Overview of the 2-D Hygrothermal Heat-Moisture Transport Model

LATENITE", Internal BPL/IRC Report, 1993.

Karagiozis, A. and Kumaran, K. Computer Model for Hygrothermal modeling of Building Envelopes, CFD Society of Canada, Montreal, June 1993.

Karagiozis A. and Salonvaara M., IEA Annex 24, First Common Exercise, Saskatoon, April 1992.

Karagiozis A. and Salonvaara M., IEA Annex 24, Third Common Exercise Holzikirchen, October 1994.

Karagiozis A. and Salonvaara M., IEA Annex 24, Fifth Common Exercise, Trondheim, April 1992.

Karagiozis A. and Salonvaara M., IEA Annex 24, Sixth Common Exercise, Rome, April 1992.

Karagiozis, A. von Karman Institute for Fluid Dynamics, The Development of Finite Element, Finite Volume and Finite Difference Method for the Navier StokesEquations, 1987.

Kiessel, H. IEA, Annex 24, HAMTIE, Third Common Exercise, Hozkirchen 1993.

Kumaran, M.K. "Heat, Air and Moisture Transport Through Building Materials and Components: Can We Calculate and Predict ?", Proceedings of the Sixth Conference on Building Science and Technology, Toronto, March 1992, pp. 129-144

Peaceman, D.W. and Rachford, H.H. "The numerical solution of parabolic andelliptical differential equation", J. Soc. Indust. Appl. Math., Vol. 3. 1955.

SECTION 3

Howell, J. R., Application of the Monte Carlo to Heat Transfer Problems, Advances in Heat Transfer, eds T.F. Irvine, Jr., and J.P. Harnett, vol. 5, pp 1-54, 1968

Hens, H. and Janssens A., "Inquiry on HAMCAT CODES", International Energy Agency, Heat, Air and Moisture Transfer in Insulated Envelope Parts, Report Annex 24, Task 1, Modeling, 1993.

Karagiozis, A. and Salonvaara, M, Influence of Material Properties on the Hygrothermal Performance of a High Rise Residential Wall, Accepted for ASHRAE 95 Symposium, Chicago, 1995

Karagiozis, A. "Overview of the 2-D Hygrothermal Heat-Moisture Transport Model LATENITE", Internal IRC/BPL Report, 1993.

Karagiozis, A. and Kumaran, K. Computer Models for Hygrothermal modeling of Building Envelopes, CFD Society of Canada, Montreal, June 1993.

Salonvaara M. and Karagiozis A., "Moisture Transport in Building Envelopes using an approximate Factorization Solution Method", CFD Society of Canada, Toronto, June 1-3 ,1994.

Hens, H. IEA, Annex 24, HAMTIE, First Common Exercise, Report number T1-B-91/05. Kiessel, H. IEA, Annex 24, HAMTIE, Third Common Exercise, Holzkirchen 1993.

Beam, R. and Warming, R.: "An implicit factored scheme for the compressible Navier-Stokes Equations."AIAA Journal, Vol. 16, No. 4, April 1978, pp. 393-402.

Karagiozis A. and Salonvaara M., IEA Annex 24, First Common Exercise, Saskatoon, April 1992

Salonvaara M. and Karagiozis A., "Moisture Transport in Building Envelopes using an approximate `Factorization Solution Method", CFD Society of Canada, Toronto, June 1-3 1994.

Karagiozis A. , Salonvaara M., and Kumar Kumaran, IEA Annex 24, Latenite Material Property Database, Trondheim, April 1994

de Wit, M. and van Schijndel, J., The Estimation of the moisture diffusivity. IEA Annex 24, Report T1-NL-93/04, 1993

SECTION 4

Karagiozis, A. "Overview of the 2-D Hygrothermal Heat-Moisture Transport Model LATENITE", Internal IRC/BPL Report, 1993.

Salonvaara, H.M., "TRAMTO2" VTT Finland, 1994

Pedersen, C.R., Combined Heat and Moisture Transport in Building Constructions, Phd Thesis, Thermal Insulation Laboratory, Technical University of Denmark, Report 214, 1990.

Kießl, H. IEA, Annex 24, Classification of WUFIZ, IEA Annex 24 , 1991

Salonvaara, M.H., and Karagiozis A.N., "Hygrothermal Performance of a High-rise Wall Structure Subjected to Rain", paper submitted to BETTEC95.

Lacy, R.E., "Driving -Rain Maps on the Onslaught of Rain on Buildings", Current Paper No. 54, Building Research Station, Garston, UK, 1965

Lacy, R.E., "Distribution of Rainfall Round a House", Meteorol. Magazine, 80 (1951) pp. 184-189

Schwarz, B., and Frank, W., Schlagregen, Berichte aus der Bauforschung, Heft 86, Berlin 1973

Hens, H. and Ali Mohamed, F., Preliminary Results on Driving Rain Estimation, Int. Energy Agency, Annex 24, T2-B-94/02

Choi, E. C. C.(1992) "Simulation of wind-driven-rain around a building", Journal of Wind Engineering, 52, pp.60-65.

Choi, E. C. C.(1991) "Numerical simulation of wind-driven rain falling onto a 2-D building", in Computational Mechanics, ed. by Cheung, Lee and Leung (Balkema Rotterdam), pp.1721-1727.

Wisse, J.A.(1994) "Driving Rain, A Numerical Study", 9th Symposium for Building Physics and Building Climatology, 14-16 Sept. 1994 Dresden.

British Standard Code of Practice for Assessing the Exposure of Walls to Wind-driven Rain. BS 8104: 1992, British Standards Institution, 1992

Surry, D., Inculet, D.R., Skerlj, P.F., Lin, J.X. and Davenport, A.G. "Wind, Rain and the Building Envelope",Wind, Rain and the Building Envelope Seminar, University of Western Ontario, May 16-17, 1994

ASC (1993) Theory Documentation for TASCflow, Version 2.2, Advanced Scientific Computing Ltd., Waterloo, Canada

Best, A.C., "The size distribution of raindrops", *Quarterly Journal of Royal Meteorology Society*, 76, 1950, pp.16-36"

Baskaran, A.(1992) "Review of design guidelines for pressure equalized rainscreen walls", NRC Internal Report No. 629.
Rodi, W.(1981) "Examples of turbulence models for incompressible flows, AIAA J., 20, pp. 267

Launder B.E. and Spalding D.B., (1974) "The numerical computation of turbulent flows", Comput. Meth. Apll. Mech. Eng., 3, pp. 269.

Murakami S. (1992) "Comparison of various turbulence models applied to a bluff body", First International Symposium on Computational Wind Engineering, Journal of Wind Engineering, No. 52 August

Pedersen C. (1990) "Combined Heat and Moisture Transfer in Building Constructions", PhD Thesis, Technical University of Denmark

Robinson G. and M.C. Baker (1975) "Wind-Driven Rain and Buildings", Technical Paper No. 445, National Research Council of Canada, Ottawa.

APPENDIX A1

Table of Contents

APPENDIX A1: MATERIAL PROPERTIES

Table A1-1 Density and heat capacity as well as air permeability of 41 materials compiled in the LATENITE Material Property Database (Karagiozis et al, 1994).

Table A1-1: Material properties.

#	MATERIAL	DENSITY, kg/m^3	HEAT CAPACITY, J/kgK	AIR PERMEABILITY, m^2
1	WOOD CHIP BOARD	700.0	2100.0	1.e-13
2	POROUS WOOD FIBRE BOARD	310.0	2100.0	1.e-13
3	GYPSUM1 BOARD	620.0	840.0	1.e-13
4	PINE WOOD	425.0	2390.0	6.e-14
5	MINERAL FIBRE	20.0	670.0	1.1-2.1e-9
6	AERATED CONCRETE	550.0	840.0	1.e-15
7	MORTAR	1800.0	840.0	1.e-16
8	CONCRETE	2200.0	840.0	1.e-16
9	EXPANDED CLAY AGGREGATE	1000.0	840.0	1.e-13
10	PLYWOOD	450.0	1880.0	1.e-16
11	EXTRUDED POLYSTYRENE	35.0	1470.0	1.e-16
12	EXPANDED POLYSTYRENE	30.0	1470.0	7.7e-8
13	WHITE BRICK	1730.0	840.0	1.e-14
14	RED BRICK	1670.0	840.0	3.e-13
15	SAND LIME STONE	1800.0	850.0	1.e-16
16	CELLULOSE1	30.0	1400.0	5.5e-7
17	POLYETHELENE SHEET 6-MIL	840.0	1256.0	1.e-20
18	AIR BARRIER	840.0	1256.0	1.e-20
19	ALUMINUM SIDING	840.0	1256.0	1.e-20
20	BRICK (REHEATED)	1800.0	800.0	3.e-13
21	BUILDING PAPER	840.0	1250.0	1.e-20
22	BUILT UP ROOFING	1120.0	1466.0	1.e-20
23	CELLULOSE2	80.0	1382.0	5.5e-7
24	CEMENT PARGE COATING	1920.0	838.0	1.e-20
25	CONCRETE BLOCK	2240.0	921.0	1.e-20
26	EXPANDED POLYSTYRENE	16.0	1214.0	7.7e-8
27	EXTERIOR GRADE PLYWOOD	510.0	1214.0	1.e-16
28	EXTRUDED PLOYSTRENE	42.0	1214.0	1.e-16
29	FIBER BOARD SHEATHING	266.0	1298.0	3.e-13
30	FOAM CORE SHEATHING	97.0	1298.0	1.e-16
31	GLASS FIBRE	11.0	712.0	1.1-2.1e-9
32	GRAVEL	1442.0	839.0	1.e-16
33	GYPSUM2 BOARD	670.0	1089.0	2.8e-11
34	KRAFT PAPER	840.0	1256.0	1.e-16
35	MICRO FINE PARTICLE	762.0	1298.0	4.8e-11
36	ORIENTED STRAND BOARD	641.0	1298.0	1.e-13
37	PERMEABLE BOARD	266.0	1298.0	3.e-13
38	ROOF SHINGLES	1121.0	1256.0	1.e-16
39	STUCCO FINISH	670.0	1089.0	2.8e-11
40	SUGAR PINE	365.0	1633.0	1.e-14
41	WAFERBOARD	706.0	1214.0	1.e-14

APPENDIX A1-1 (TASK A): Relative Influence of Heat, Air and Moisture Transport Properties Subjected to ± 25 % Uniform Variations in Properties of Individual Materials

Wall Structure

The high-rise wall structure selected for the numerical analysis is shown in Figure A1-1. The wall is composed of the following layers starting from the exterior to interior:

- a 102-mm red brick (or sandlime stone),
- a 25-mm air layer,
- a 25-mm semi-rigid glass fibre board,
- a 89 mm glass fibre batt,
- a 6-mil polyethylene film, and
- a 12.5-mm gypsum board.

BOUNDARY AND INITIAL CONDITIONS

The wall was exposed to outside air temperature and relative humidity that varied according to the weather data for the selected location. The weather data for Ottawa were selected for the numerical analysis. The simulations were carried out for a one-year exposure and started from the 1st of July. The solar radiation and long-wave radiation on the outer surfaces of the wall were included in the analysis. The wall was facing south. The additional moisture source, due to wind-driven rain, was also modeled using a 3-D commercial particle-tracking code (details are given in section 4). In this part of the study, no air infiltrating or exfiltrating was considered, thereby the primary mode of water transmission by diffusion. The interior surface of the walls were exposed to 40% relative humidity at 20 °C. The initial conditions of the wall were 20 °C and at equilibrium of 30% relative humidity.

MATERIAL PROPERTIES

Table A1-1 summarizes the variations of the different types of material properties used in the sensitivity analysis. Material properties were obtained from the LATENITE material property database of the model (Karagiozis et al. 1994). For each case, the liquid diffusivity and vapor permeability were varied by the same percentage for all materials in the construction. Each simulation is labeled first by the letter F, followed by either 75, 100 or 125 and then by another set of numbers of 75, 100 or 125. The first number set of 75 signifies a reduction in both the vapor permeability and liquid diffusivity by 25%, 100 signifies no reduction and 125 signifies a 25% increase in these

properties. The next set of number designates the choice of the value of the sorption isotherm properties in a similar fashion. For example, the designation F75100 means that the vapor and liquid diffusivity were reduced to 75% of their true value, while the sorption isotherm was maintained at 100% of its true value. To determine the sensitivity to the moisture transport properties on heat and moisture transport of a high-rise wall structure 19 simulations were performed.
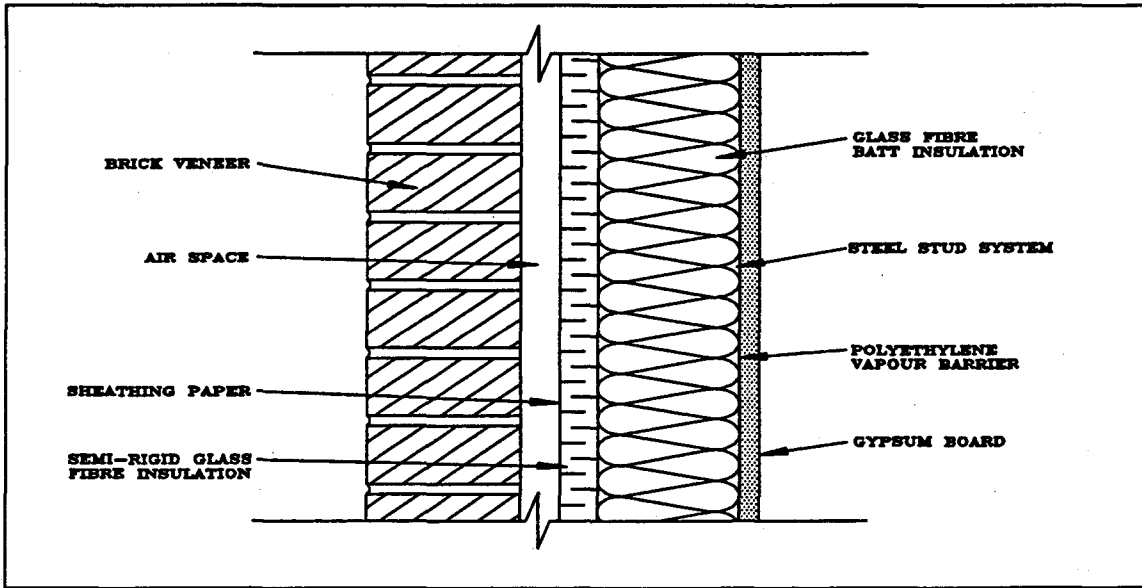
Figure A1-1: High-rise wall configuration.

The functional relationship used to prescribe the sorption variation was pinned so that the maximum moisture content was not exceeded. The following expressions were used given that a 100% moisture content is u^* [=sorption(rh), where rh is the relative humidity (0<rh<1)], then the implemented moisture content can be expressed as

$$u = f \cdot u^*$$ (1)

The functional expression for 75% case is given by

$$f = \left(1 - rh + rh^2\right)$$ (2)

and for 100% case $\qquad\qquad f = 1.0$ (3)

while for 125 % case is given by $\qquad f = \left(1 + rh - rh^2\right).$ (4)

Table A1-2 : Parametric study of Moisture Transport Properties

SORPTION-ISOTHERM	VAPOR PERMEABILITY	LIQUID MOISTURE DIFFUSIVITY
75 % ISOTHERM	75 % (δ_P)	75 % (D_w)
100 % ISOTHERM	100 % (δ_P)	100 % (D_w)
125 % ISOTHERM	125 % (δ_P)	125 % (D_w)

RESULTS

High water permeance of Brick Veneer (δ_P(rh=30%) = 31.2 $\cdot 10^{-10}$ kg/msPa)

Figures A1-2 to A1-3 show results for the high water vapor permeance brick facade. In Figure A1-2, the results illustrate the strong effect of the variation of the sorption curve. These Figures show the total amount of moisture in the wall assuming 1m depth. The starting date for the simulations (time equal to 0) is July 1. Here the wetting and drying seasons are clearly distinguished. The results show that in September the wall starts accumulating moisture, peaks in November, and dries out during the spring and summer season. This cyclic pattern resumes again in the following year, if further simulations are carried out. For this type of exterior brick veneer, the total moisture in the structure shows little influence of the 25% increase or decrease in the vapor and liquid moisture transport permeabilities and diffusivities, as shown in Figure A1-3. Figure A1-4 depicts the thermal performance of the wall. Here it is evident that for this particular wall system, the convective heat flow from inside and outside surfaces and the latent heat flows, show negligible influence even for variation of the sorption isotherm. The wall structure displays no particular moisture problems and the moisture contents in the layers of the wall are low. The increased vapor permeabilities and liquid diffusivities cause larger and more rapid changes in the moisture contents but because of the low moisture capacity of the wall, the heat flows are only minimally affected by the moisture movements. The thermal resistance offered by the brick layer is only a small part of the total thermal resistance of the wall. Moisture accumulation occurs mainly in the brick layer and there are no major moisture flows through the insulation layer that would reduce the effective thermal resistance of the wall.
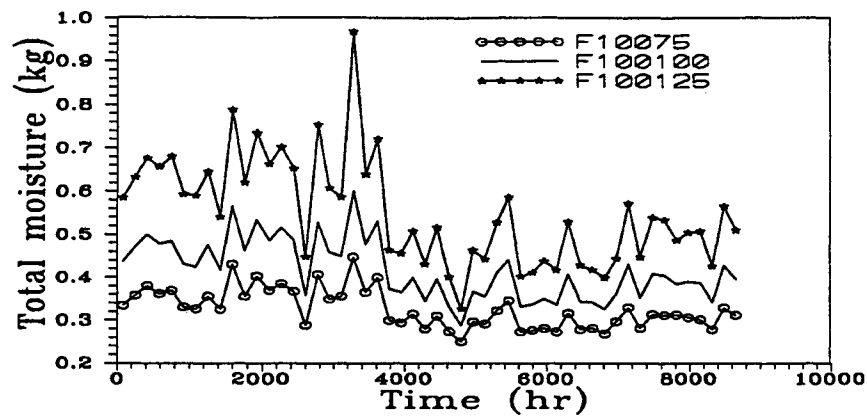
Figure A1-2 : Effect of sorption isotherm variation on moisture accumulation in the wall
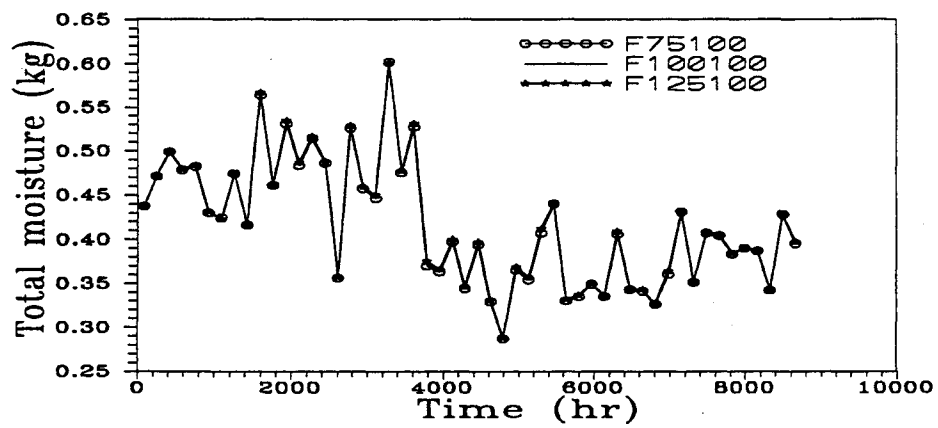
Figure A1-3 : Effect of variations in vapor permeability and liquid diffusivity on moisture accumulation in the wall (bricks).
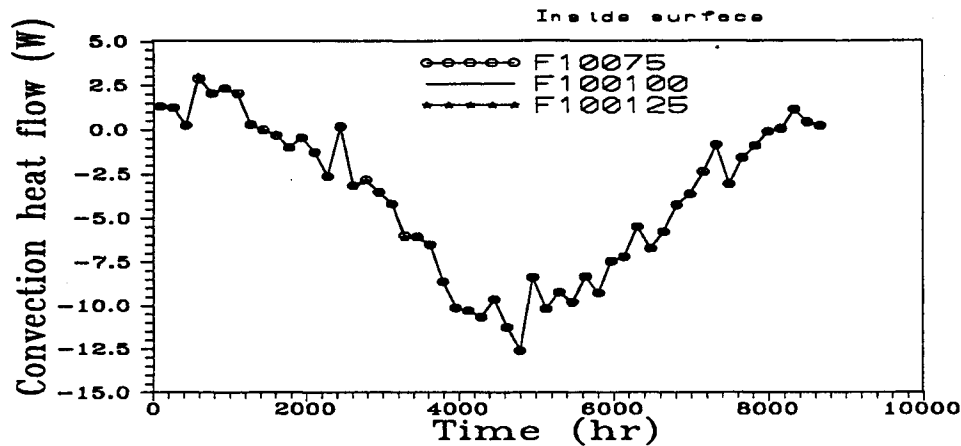
Figure A1-4: Effect of sorption isotherm variation on interior convective heat flow at the wall inside surface

Moisture Time Constant

The effect of moisture capacity on the hygrothermal performance of the wall section was studied by replacing the brick layer with sandlime stone. A comparison of the moisture capacity for three different materials is shown in Figure A1-5. Samples with a thickness of 10 cm were initially set at a temperature of +20°C and 90% relative humidity. One side of the layer is maintained at +20 °C and 50% RH and the other side at a temperature of 0°C and 0% RH. The changes in the moisture content were calculated. The differences in the time constants for moisture transfer can be seen in the slopes of the curves in Figure A1-5. Red brick responds fast to external changes, whereas pine and especially sandlime stone respond much slower. The red brick with its high permeances would respond even faster than the brick (see Figure A1-3).

Sandlime-stone wall

The walls with high moisture capacity (see Figure A1-6) showed greater differences in the total moisture contents than walls with lower moisture capacity (see Figure A1-3), when vapor permeabilities and liquid diffusivities were varied. The moisture contents in the walls with sandlime stone are higher than in the red brick walls. The higher moisture contents, however, did not have much effect on the heat flows at the inside surface of the walls (see Figure A1-7).

As for the red brick, the thermal resistance of the sandlime stone layer was very small in comparison to the thermal resistance of the insulation layer. The heat flows were

mainly controlled by the insulation layer. The heat flows at the inside surfaces of the walls overlap each other and displayed no significant differences.
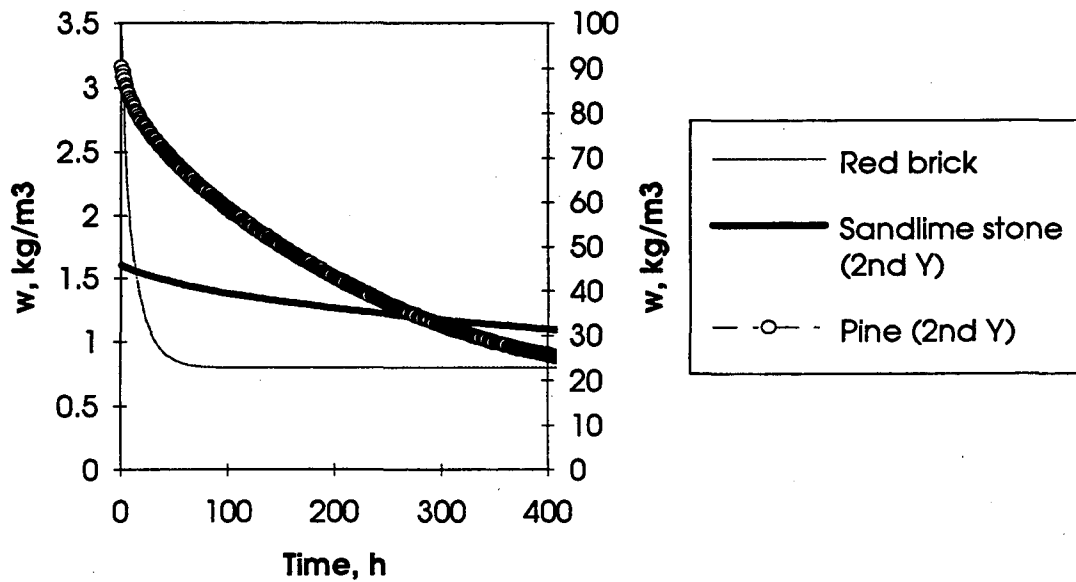
Figure A1-5: The effect of moisture capacity on the time constant of the walls. The y-axis for the red brick is on the left and the 2nd y-axis on the right is for pine and sandlime stone.
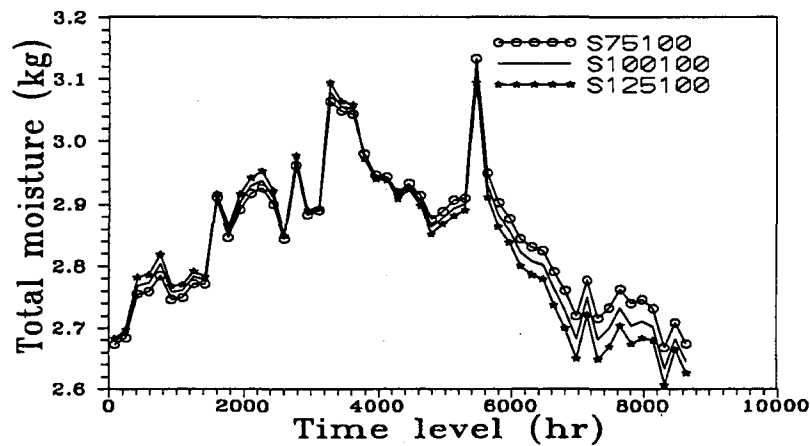
Figure A1-6: Effect of vapor permeability and liquid diffusivity variation on moisture accumulation in the high-rise wall sandlime stone.
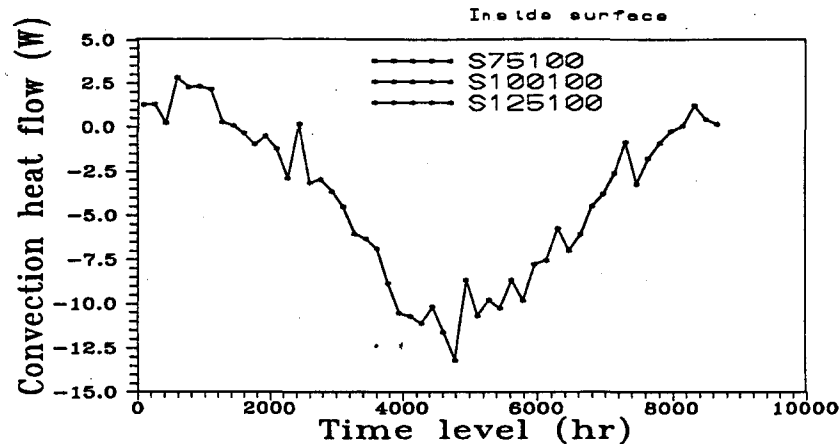
Figure A1-7: The effect of convection heat flow at the interior surface, as a function of vapor and liquid transport properties (sandlime stone)

2.4   TASK B: EFFECT OF SIMPLIFYING MATERIAL PROPERTY ON HYGROTHERMAL PERFORMANCE OF A WALL

Problem description

To determine the sensitivity of the moisture and heat transport properties functional dependency on the heat and moisture transport of a high-rise wall structure several simulations were performed. The high-rise wall structure selected for the numerical analysis is shown in Figure A1-8. The wall on the third floor of a 10-floor building is composed of the following layers, from the exterior to interior: a 90-mm facade brick (LATENITE database: material number 13), a 120-mm glass-fibre board (material number 5) and finally a 140-mm red brick (material number 14). The height of the wall is 1 m (1-dimensional simulations). The wall did not have a vapor barrier, which is normally required in cold climates like Canada.

The wall was exposed to outside air temperature and the relative humidity that varied according to the weather data for Ottawa. The simulations were carried out for a 1-year exposure and started from the 1st of January. The solar radiation and long-wave radiation on the outer surfaces of the wall were included in the analysis. The additional moisture source due to direct incident of rain was also modeled. In this study no air infiltrating or exfiltrating is considered, thereby the primary mode of water transmission is due to diffusion processes. Table A1-3 summarizes the different types of material property functions used in the sensitivity analysis.

BRICK VENEER —
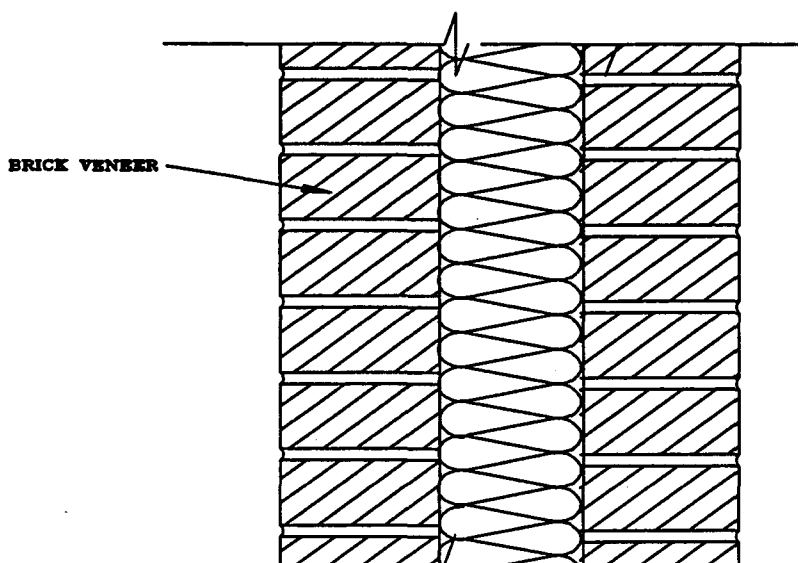
Figure A1-8: The analyzed wall structure in details. (from the exterior to interior: a 90-mm facade brick, a 120-mm glass-fibre board and finally a 140-mm red brick).

Designation/Definitions

For each case, the liquid diffusivity, vapor permeability, and thermal conductivity of the brick layers were varied. Each simulation is labeled by three letters: the first letter refers to the external brick layer, second letter refers to the internal brick layer and the last letter refers to the time-averaging of weather data. Designations for the simulated cases are displayed in Table A1-4.

Boundary and initial conditions

Internal conditions were kept constant: temperature 21°C and relative humidity at 40% (P_V = 997 Pa) throughout the year. The BMY Atmospheric Environment Service (AES) weather file of Ottawa was used in the simulations. The wall on the third floor of the building was facing North-West, i.e., the azimuth angle of the wall was 315 degrees.

Table A1-3: Keys to different cases.

Key	Material property function
F	full properties
E	exponential function for liquid moisture diffusivity D_W
	linear properties for thermal conductivity
C	constant properties
H	hourly time-averaging
D	daily time-averaging
W	weekly time-averaging

Table A1-4: Designations for the simulated cases. Material property function is either full, exponential/linear or   constant and time-averaging hourly, daily or weekly.

Key	Type of External brick's property function	Type of Internal brick's property function	Time-averaging
FFH	Full	Full	Hourly
FFD	Full	Full	Daily
FFW	Full	Full	Weekly
FEH	Full	Exponential/linear	Hourly
FED	Full	Exponential/linear	Daily
FEW	Full	Exponential/linear	Weekly
FCH	Full	Constant	Hourly
FCD	Full	Constant	Daily
FCW	Full	Constant	Weekly
EFH	Exponential/linear	Full	Hourly
EFD	Exponential/linear	Full	Daily
EFW	Exponential/linear	Full	Weekly
EEH	Exponential/linear	Exponential/linear	Hourly
EED	Exponential/linear	Exponential/linear	Daily
EEW	Exponential/linear	Exponential/linear	Weekly
ECH	Exponential/linear	Constant	Hourly
ECD	Exponential/linear	Constant	Daily
ECW	Exponential/linear	Constant	Weekly
CFH	Constant	Full	Hourly
CFD	Constant	Full	Daily
CFW	Constant	Full	Weekly
CEH	Constant	Exponential/linear	Hourly
CED	Constant	Exponential/linear	Daily
CEW	Constant	Exponential/linear	Weekly
CCH	Constant	Constant	Hourly
CCD	Constant	Constant	Daily
CCW	Constant	Constant	Weekly

The calculations started on the 1st of January. The initial conditions of the wall were 10, 15 and 17°C and 0.06-, 0.009-, 0.06-kg/kg moisture content for external brick, glass fibre and internal brick layer, respectively. The maximum capillary moisture content of the bricks is 0.111 kg/kg.

The heat and mass transfer coefficients for external and internal surfaces are presented in Table A1-5.

Methods of simplifying the properties of materials

The material properties used in the simplification analysis were: thermal conductivity, liquid moisture diffusivity, and vapour permeability. The simplified properties of the insulation layer (mineral fibre) were not considered, only the brick layers were used in the sensitivity analysis. Figures A1-9 through A1-12 show the material properties of red brick.

Table A1-5: Heat and moisture transfer coefficients for the external and internal surfaces.

Property	Surface	
	External	Internal
Heat transfer coefficients, W/ m^2K	20	8
Mass transfer coefficients, kg/m^2sPa	$1.5 \cdot 10^{-7}$	$5.0 \cdot 10^{-8}$
Short-wave absorptivity	0.6	-
Long-wave emissivity	0.9	-

The "full function" (Type F) and the "linear function" (Type E) of the thermal conductivity of the bricks is a linear function. The thermal conductivity of a dry brick was chosen as a constant function (Type C).

The liquid moisture diffusivity had three different function types: full, exponential and constant. The method to derive these functions arises from determinations of liquid moisture diffusivity, e.g., gamma-ray experiments, and from the sorptivity test or wetting experiment. The full function is derived from the analysis of transient moisture content distributions (gamma-ray experiments). The exponential function is de Wit's formula (de Wit 1993), in which sorptivity coefficient A is used to calculate liquid diffusivity. The constant function for liquid diffusivity is also derived from the sorptivity experiment. All these functions were tested by numerically simulating a wetting experiment to find out whether they all give the same total accumulation of moisture as a function time.

SORPTION-SUCTION CURVE
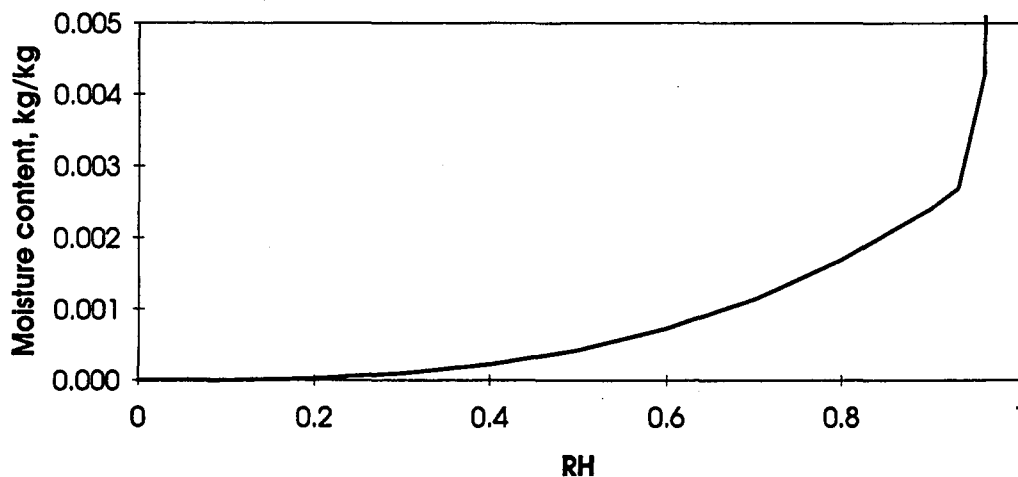
Figure A1-9: Sorption-suction curve of the red brick
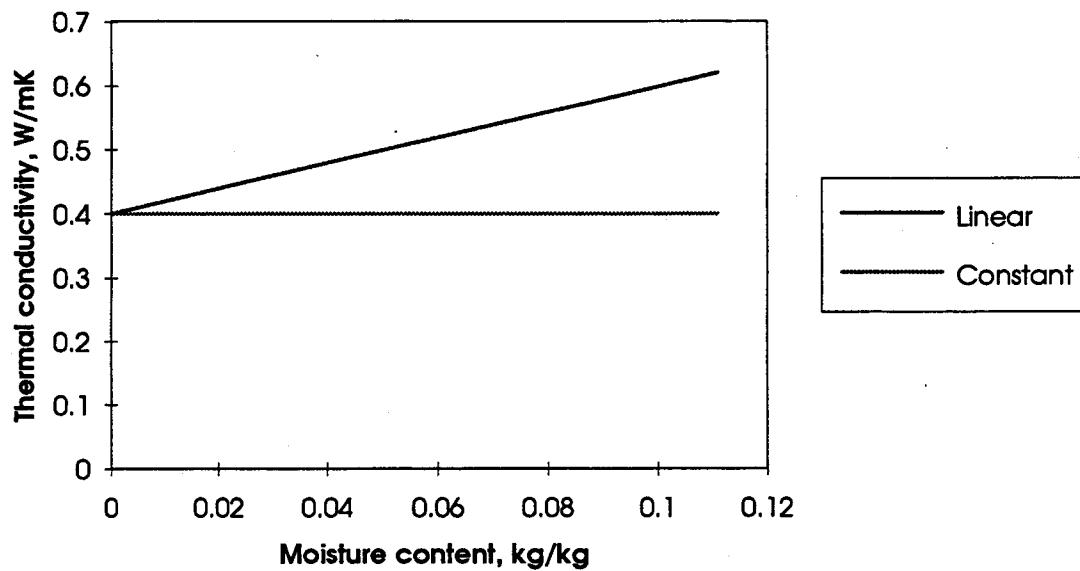
Figure A1-10: Thermal conductivity of the bricks

Total moisture diffusivity at +20°C
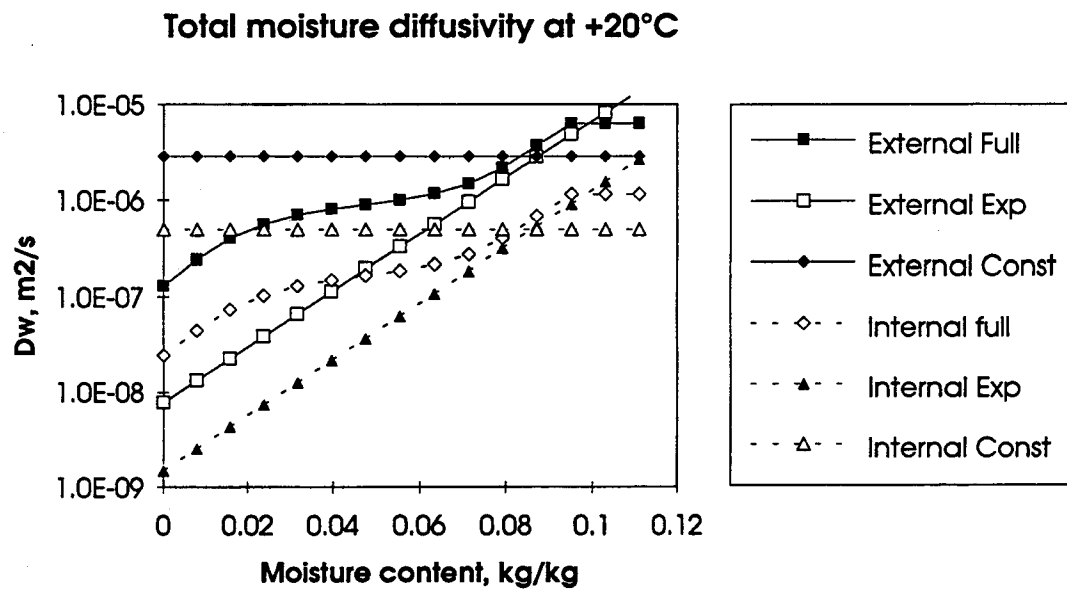
Figure A1-11: Total moisture diffusivity of the bricks
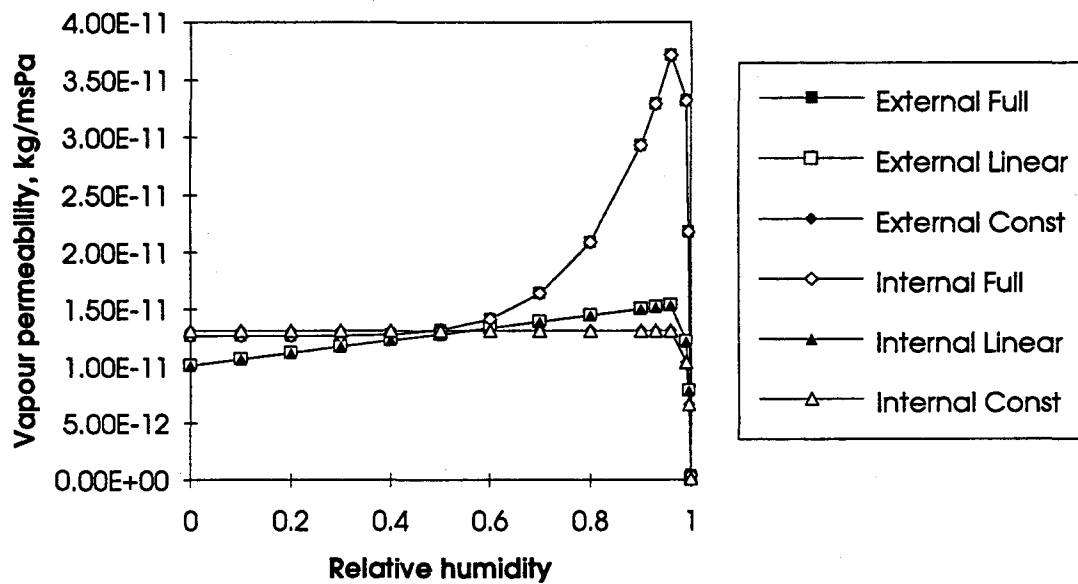
Figure A1-12: Vapor permeability of the bricks

The method of time-averaging the boundary conditions

The time step during the calculations was kept always at 1 hour. The external boundary conditions were time-averaged in some of the cases by using daily and weekly averaging. When time-averaging was used, a new weather file was created with constant values in sets of 24 hours (1 day) or 168 hours (1 week).

The time-averaging of the boundary conditions (weather file) was done in the following way:

- Solar radiation (direct, diffuse) to the wall was calculated using hourly weather data and the actual amount of radiation on the wall was averaged.

- Driving rain to the wall surface was calculated using hourly weather data and the actual amount of rainfall onto the wall was averaged.

The averaging method ensured that the same amount of solar energy and rain reached the external wall surface per year in each case.

Results

The following results have been plotted and they are presented for each set of simplification.

- **Heat fluxes: yearly heat loss, average daily heat fluxes full year, average daily heat fluxes drying period.**
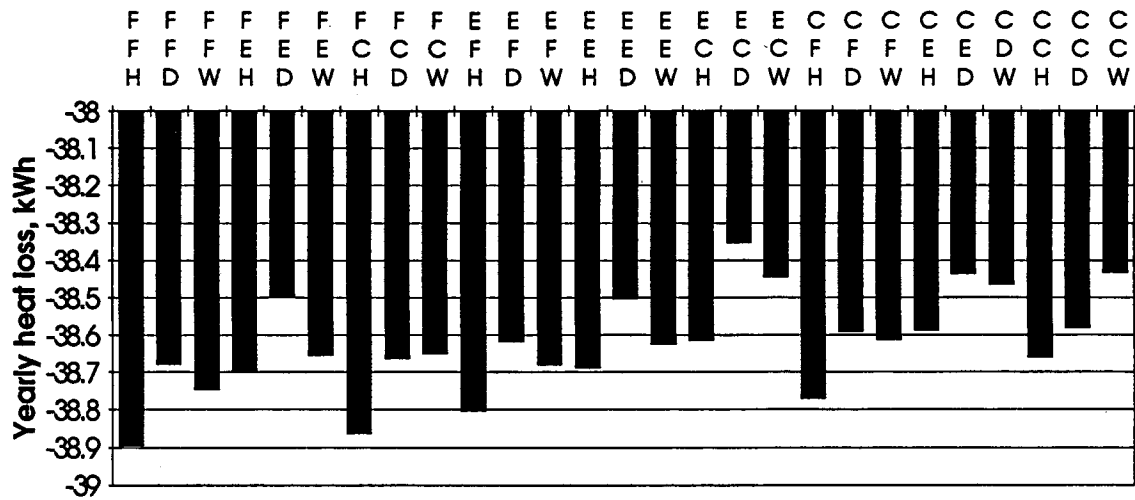
Figure A1-13: Total yearly heat loss. Heat flux is defined as sensible heat flux
(h·ΔT)
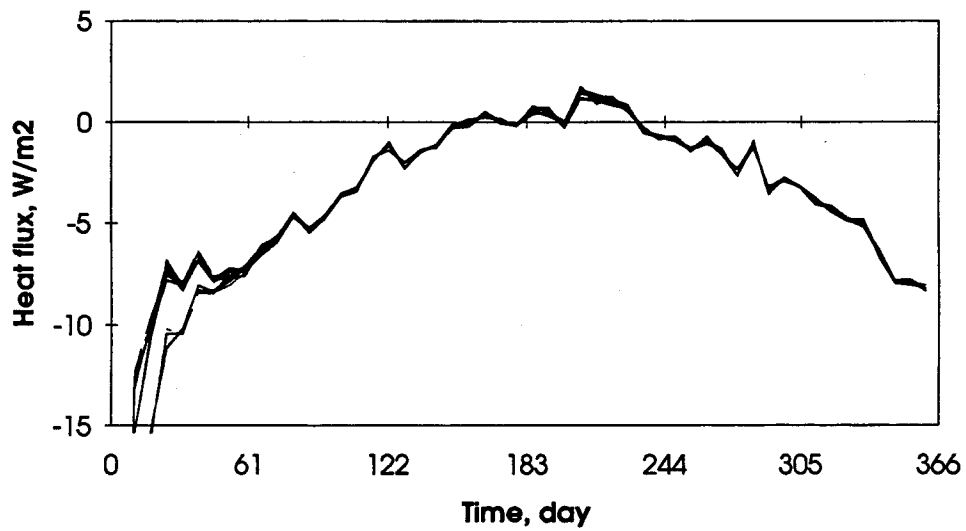
Figure A-14: Average daily heat fluxes at the inside surface
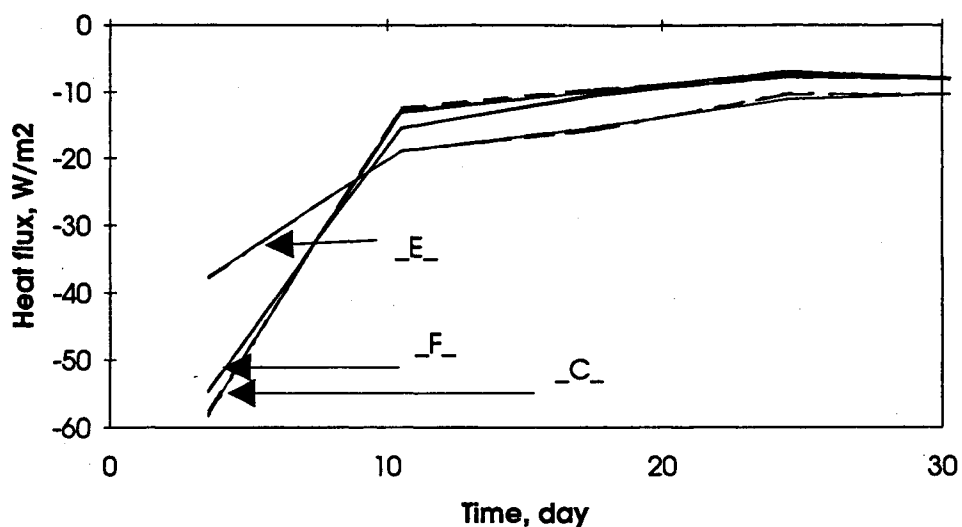
Figure A1-15: Daily average heat fluxes at the inside surface during the initial drying period (January). The different sets of curves are grouped together depending on the properties of the interior brick, e.g., all cases with full properties for interior brick (_F_) follow the same curve.

Total moisture content (kg/wall-m^2): hourly, daily and weekly cases in separate plots.
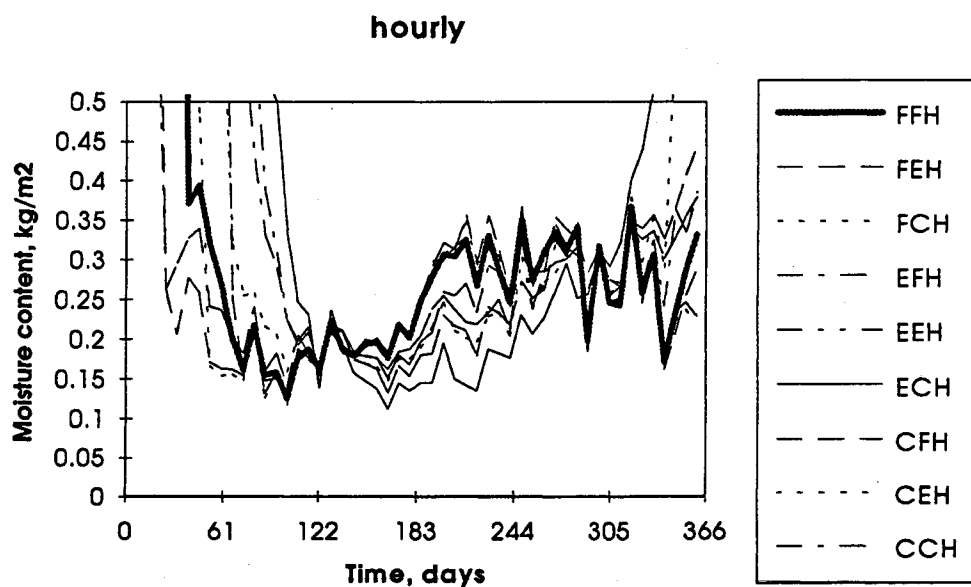
hourly

Figure A1-16: Total moisture: hourly time-averaging
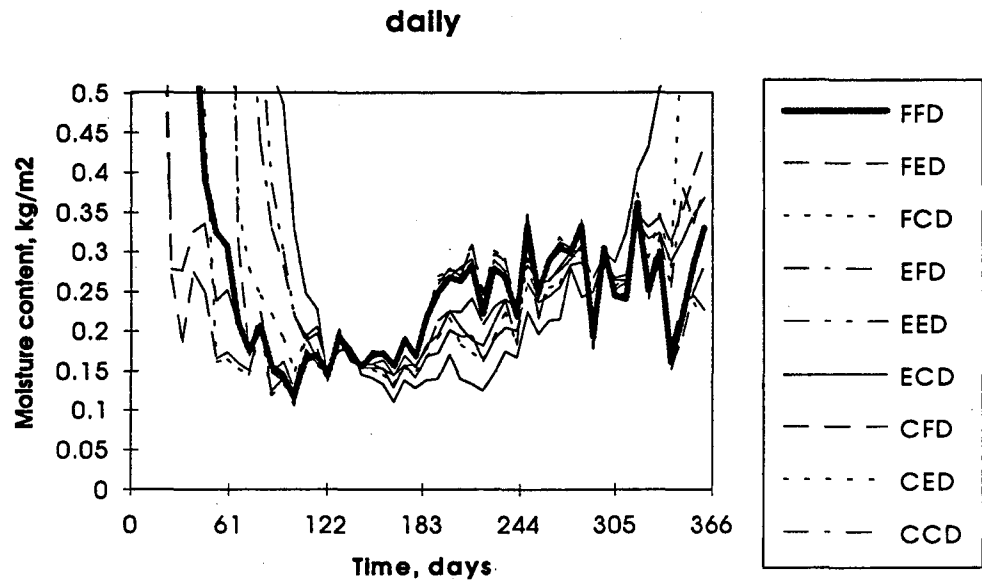
daily

Figure A1-17: Total moisture: daily time-averaging
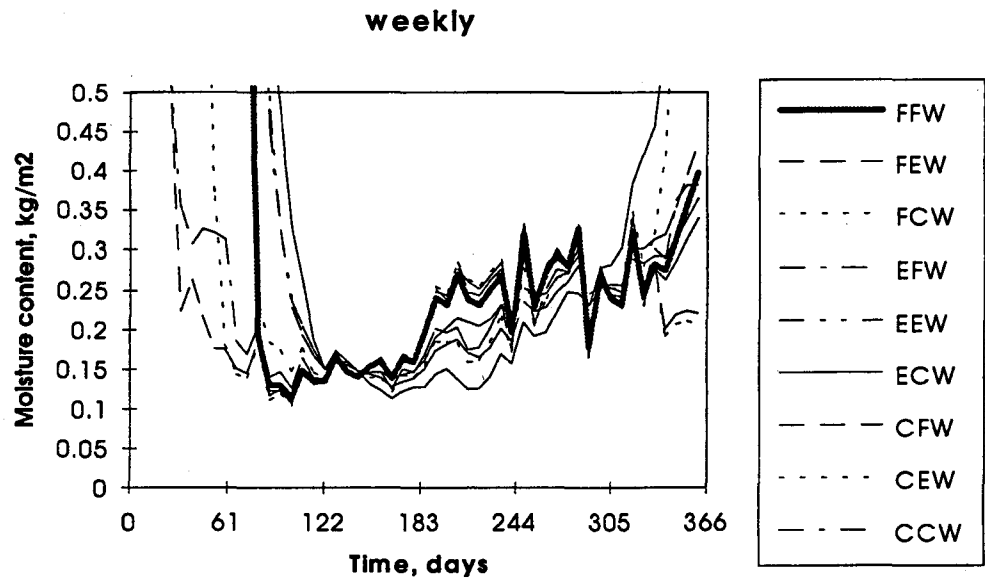
weekly

Figure A1-18: Total moisture: weekly time-averaging

Total moisture content (kg/wall-m^2): comparison of hourly, daily and weekly results with same material properties (Full-year and initial drying period)
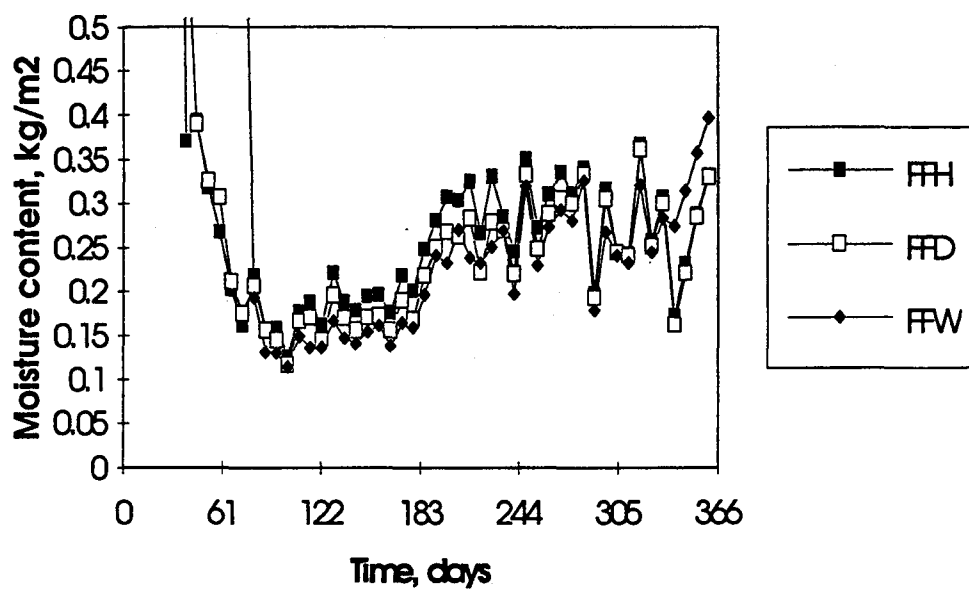
Figure A1-19: Total moisture: Case FF_, hourly, daily and weekly time-averaging
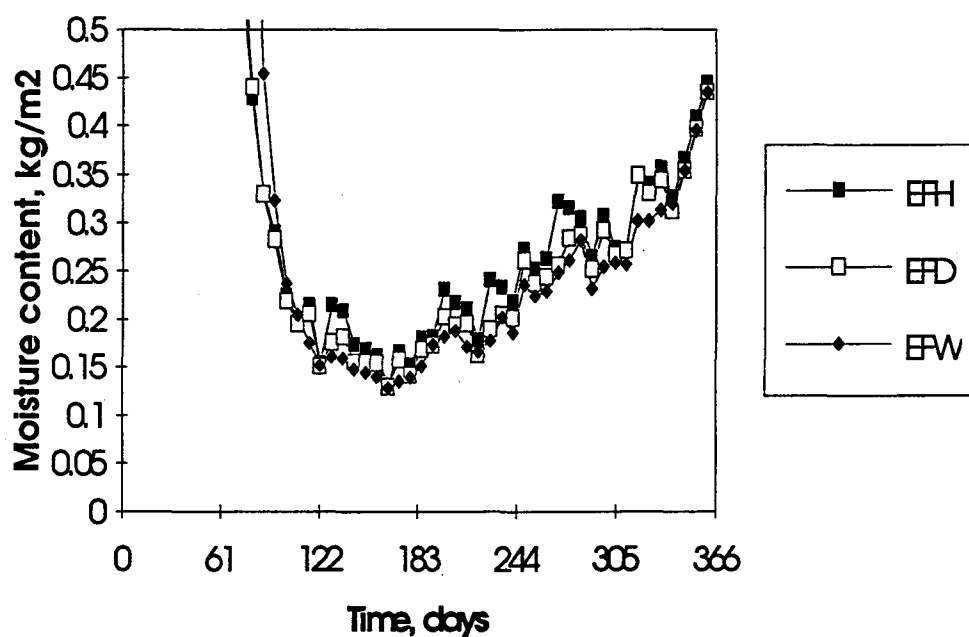
Figure A1-20: Total moisture: Case EF_, hourly, daily and weekly time-averaging
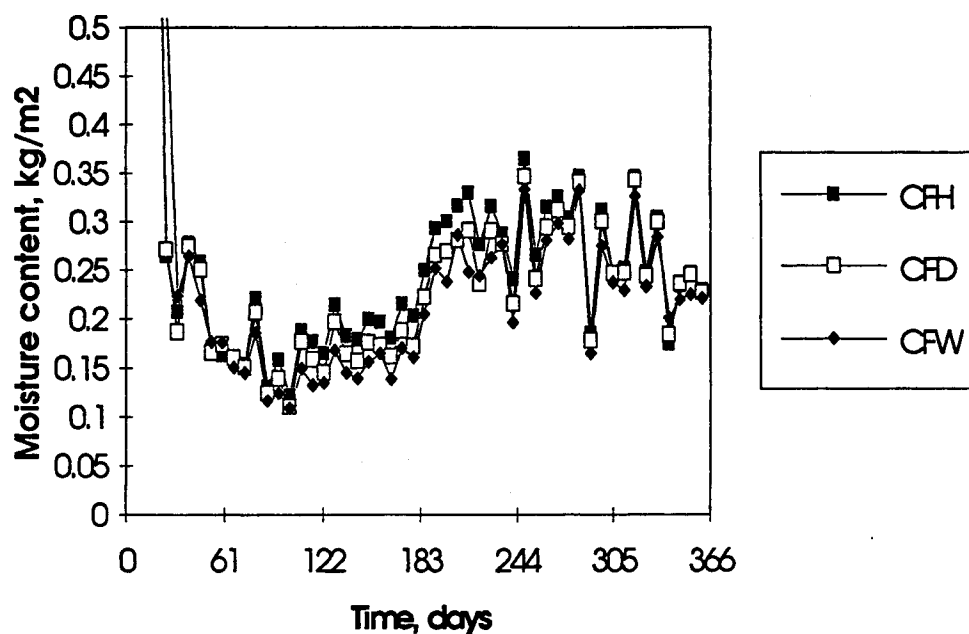
Figure A1-21: Total moisture: Case CF_, hourly, daily and weekly time-averaging
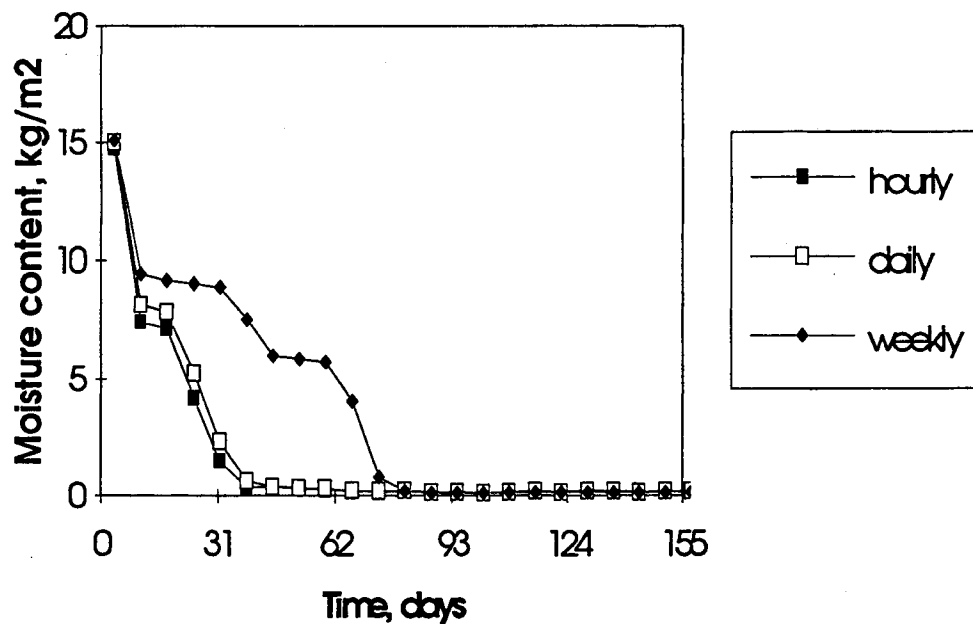
Figure A1-22: Total moisture: Case FF_, hourly, daily and weekly time-averaging
(Initial drying period)
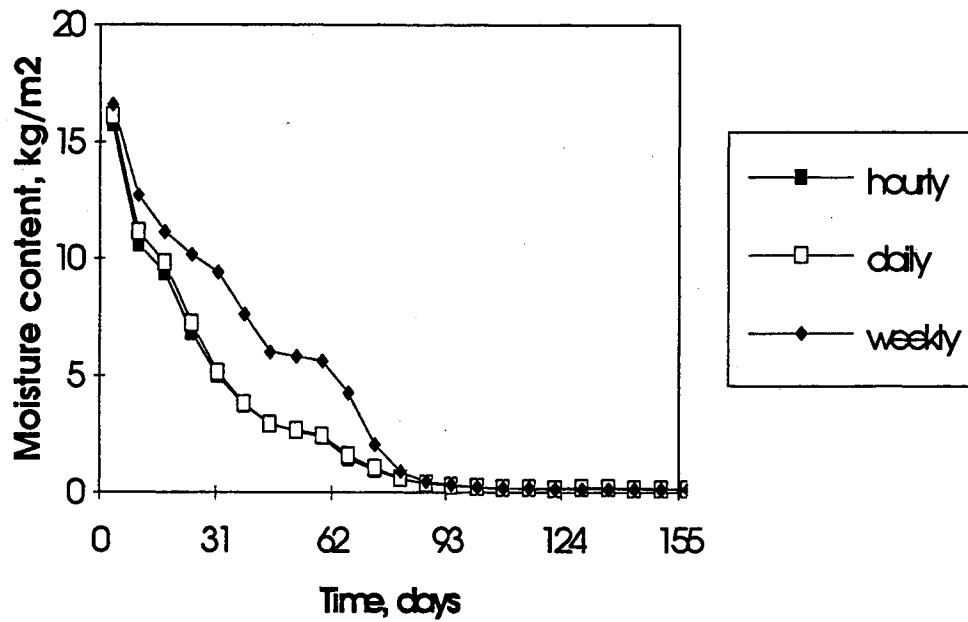
Figure A1-23: Total moisture: Case EE_, hourly, daily and weekly time-averaging
(Initial drying period)
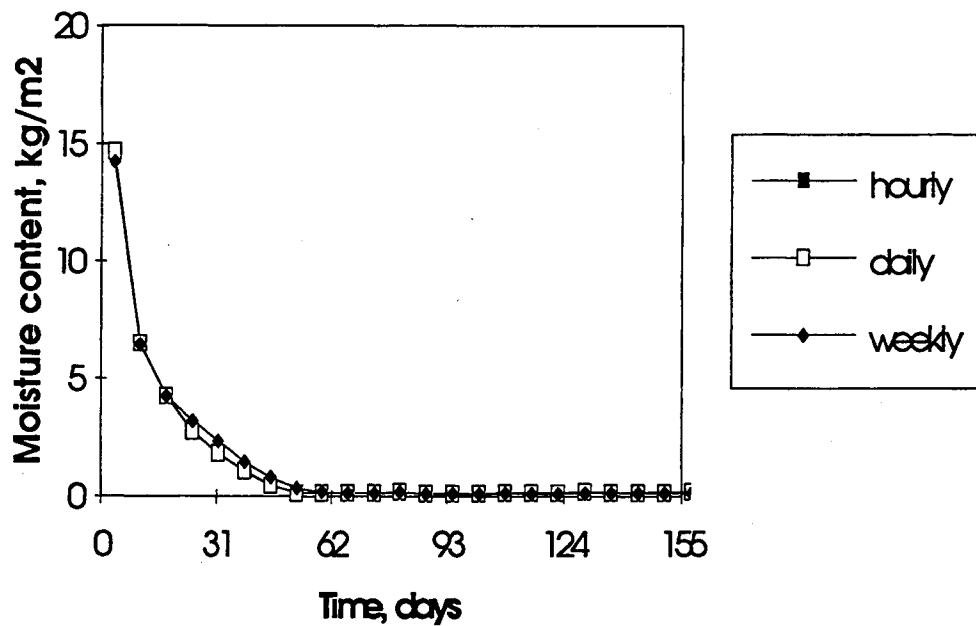
Figure A1-24: Total moisture: Case CE_, hourly, daily and weekly time-averaging
(Initial drying period)
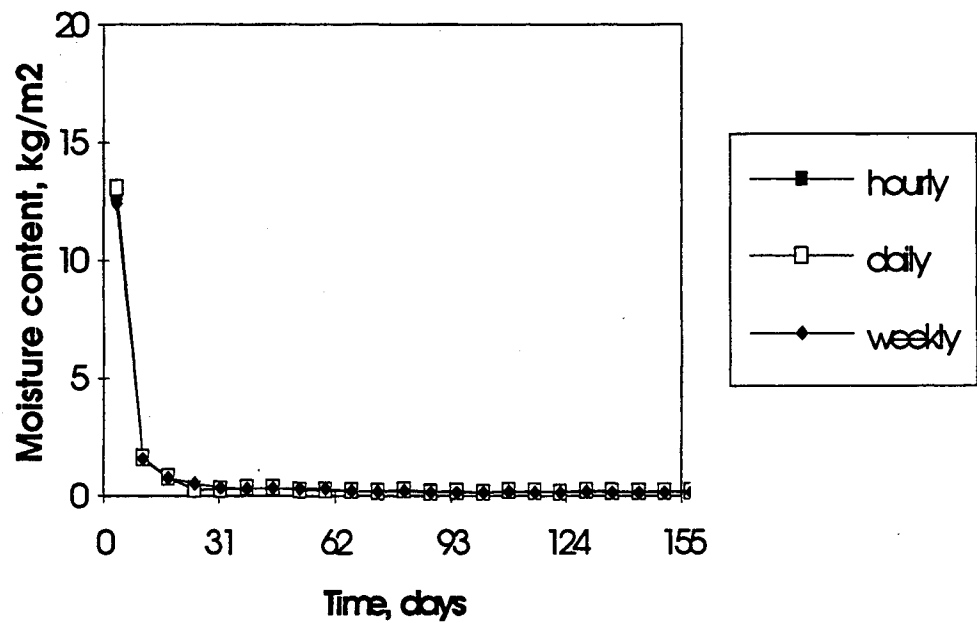
Figure A1-25: Total moisture: Case CC_, hourly, daily and weekly time-averaging (Initial drying period).

Relative humidity distribution 225 days (7.5 months) from the beginning of the year: comparison of hourly, daily and weekly results with same material properties
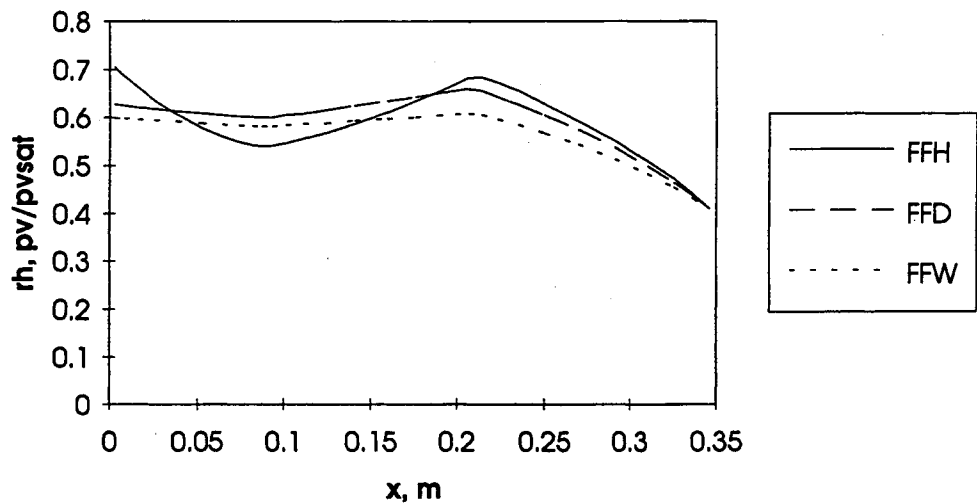
Figure A1-26:   Relative humidity distribution: Case FF_, hourly, daily and weekly time-averaging.
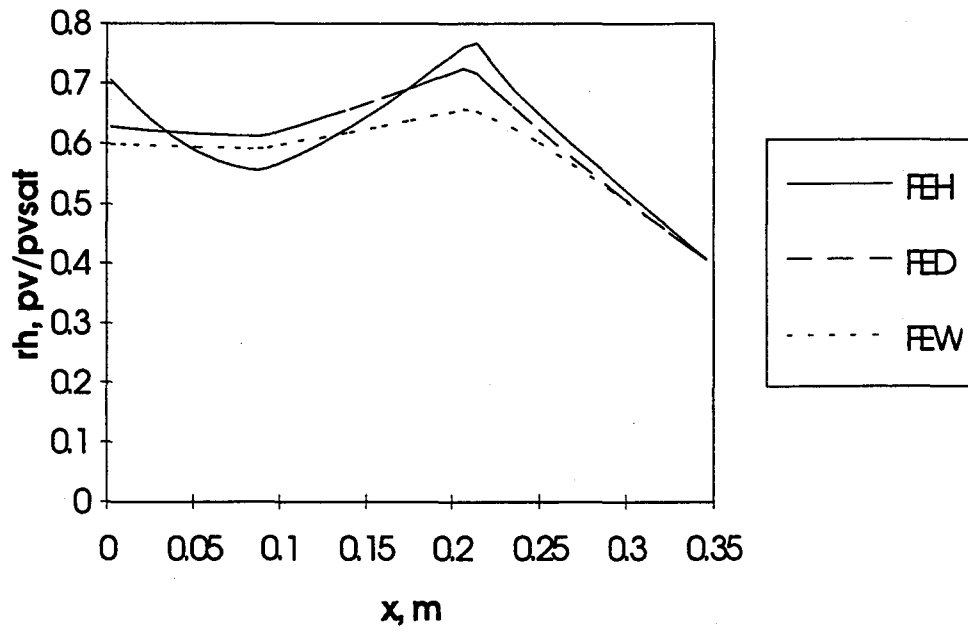
Figure A1-27: Relative humidity distribution: Case FE_, hourly, daily and weekly time-averaging
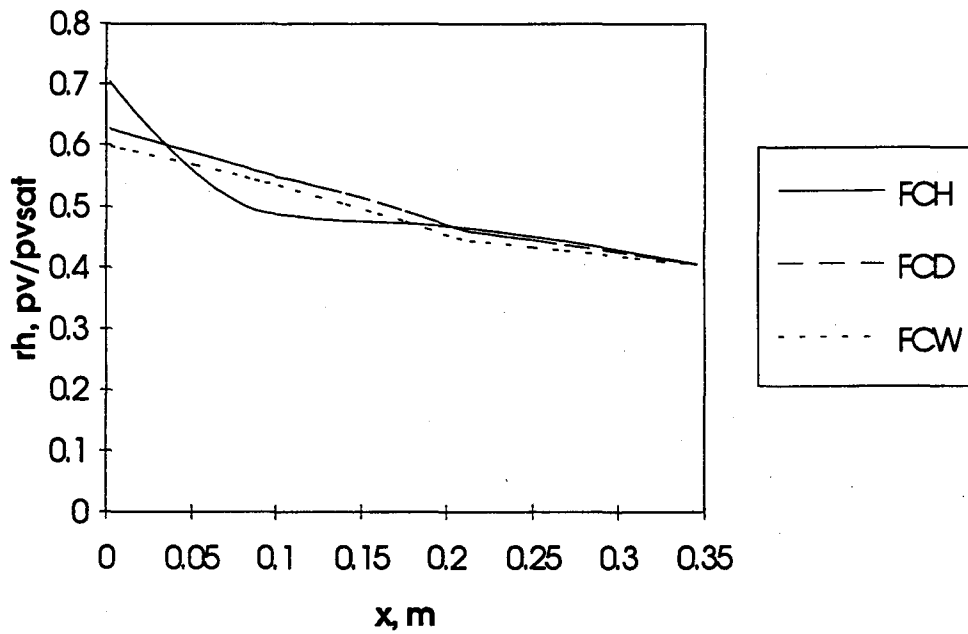
Figure A1-28: Relative humidity distribution: Case FC_, hourly, daily and weekly time-averaging
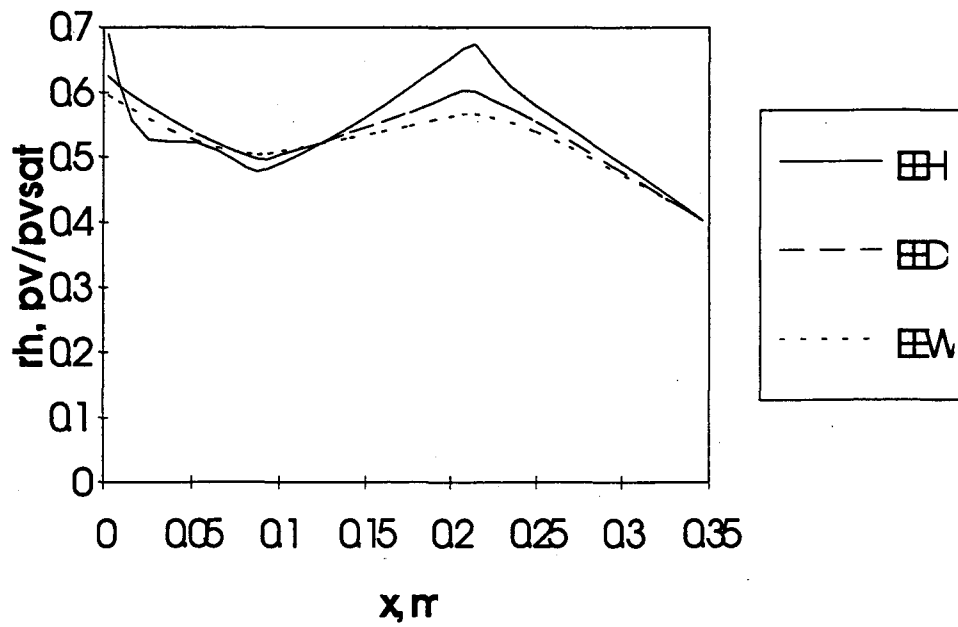
Figure A1-29: Relative humidity distribution: Case EE_, hourly, daily and weekly time-averaging
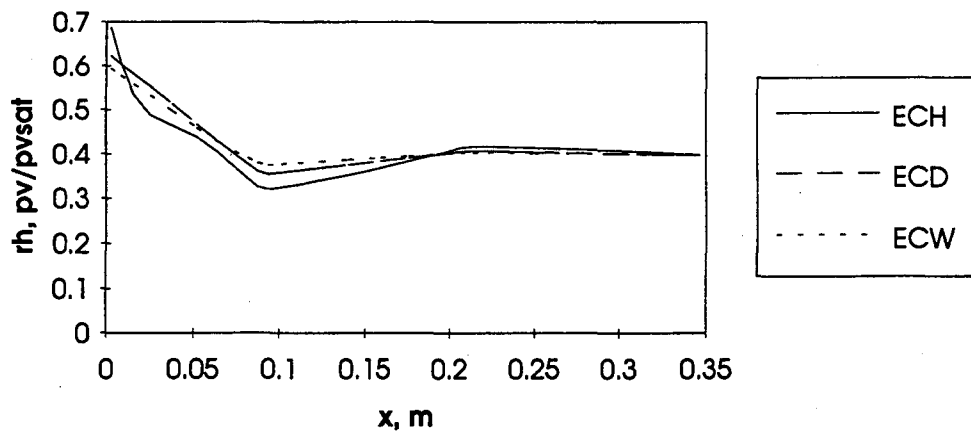
Figure A1-30: Relative humidity distribution: Case EC_, hourly, daily and weekly time-averaging
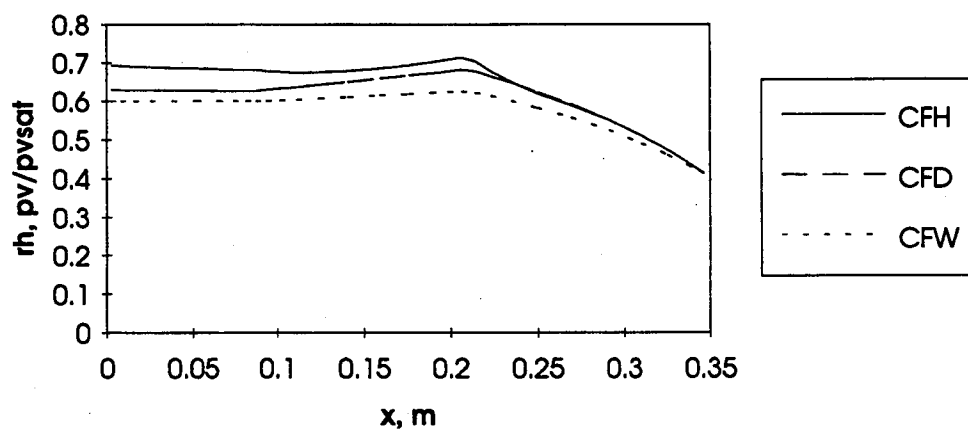
Figure A1-31: Relative humidity distribution: Case CF_, hourly, daily and weekly time-averaging
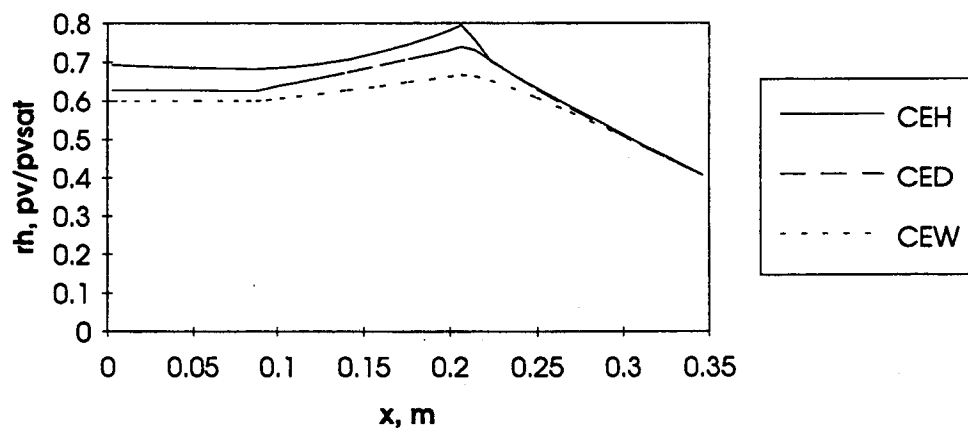
Figure A1-32 : Relative humidity distribution: Case CE_, hourly, daily and weekly time-averaging

Relative humidity of the inside surface of the external brick: cases with hourly weather data and minimum and maximum moisture contents of all the cases

NP 10, hourly weather

Legend:
- FFH
- FEH
- FCH
- EFH
- EEH
- ECH
- CFH
- CEH
- CCH
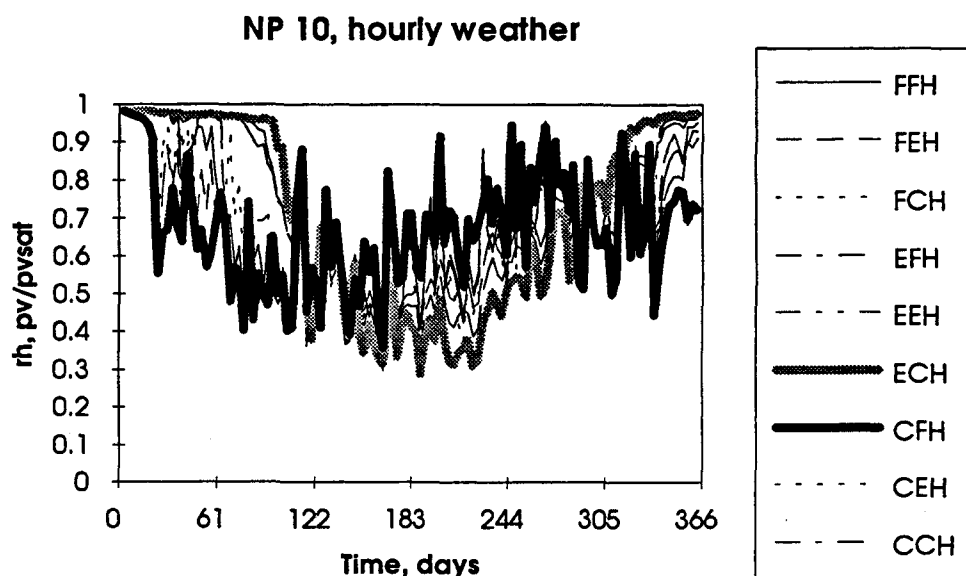
Figure A1-33: Relative humidity of the inside surface of the external brick for all the cases with hourly time-averaging

NP 10, all cases.

Legend:
- ■ Max
- □ Min
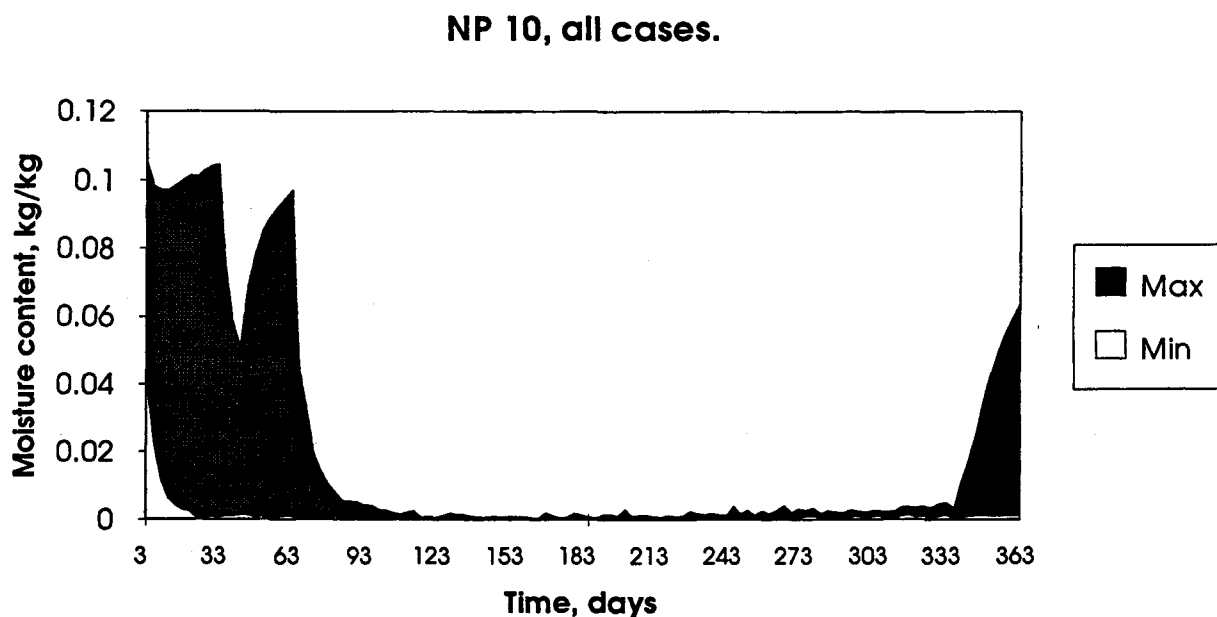
Figure A1-34:   Minimum and maximum moisture contents of the inside surface of the external brick for all the cases

NP 10, all cases.
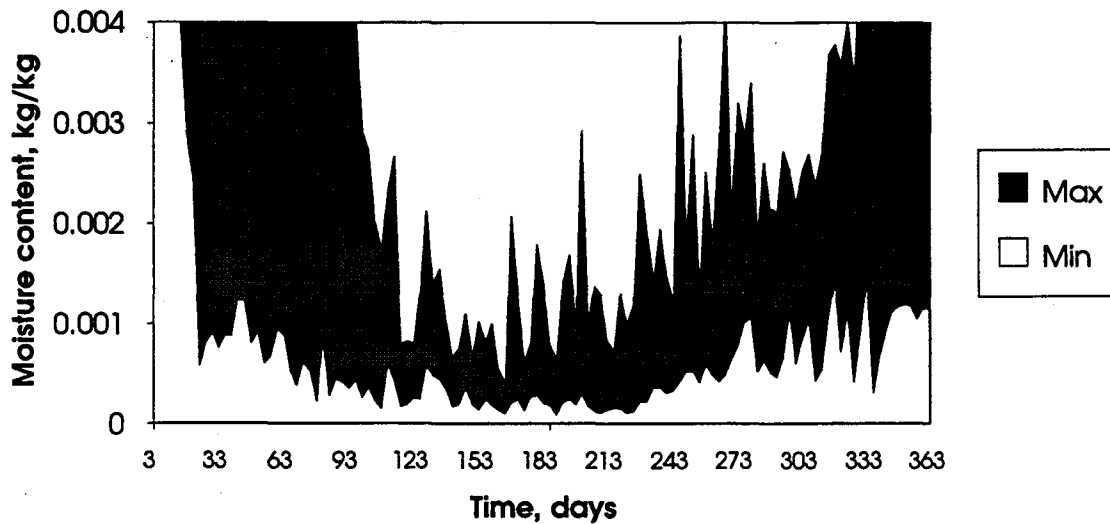
Figure A1-35: Minimum and maximum moisture contents of the inside surface of the external brick for all the cases

Relative humidity distribution 225 days (7.5 months) from the beginning of the year: comparison of cases where the properties of internal brick were simplified. Results with hourly weather data.
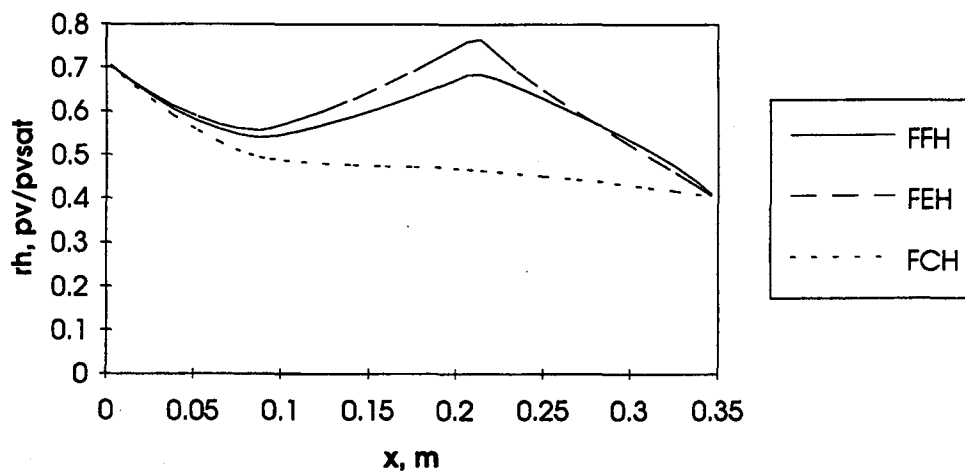
Figure A1-36: Relative-humidity distribution: Case F_H
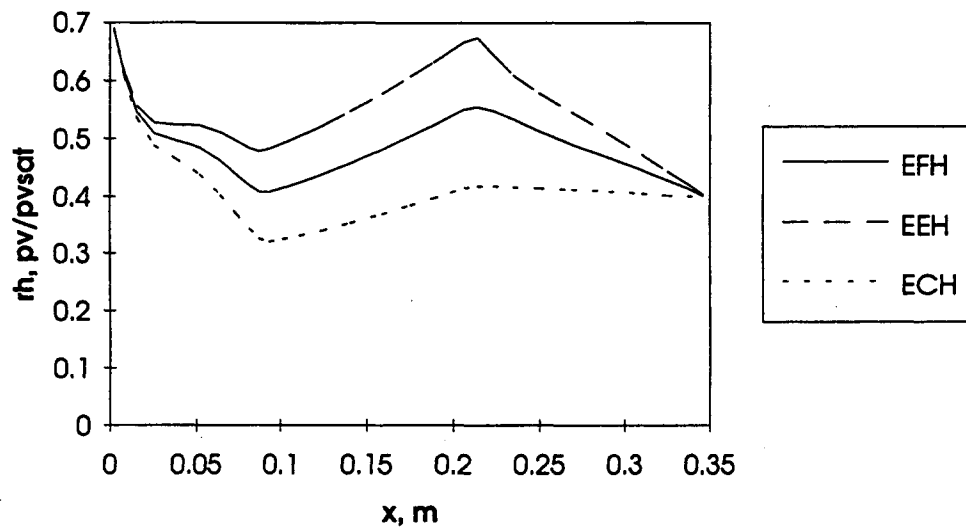
Figure A1-37: Relative-humidity distribution: Case E_H
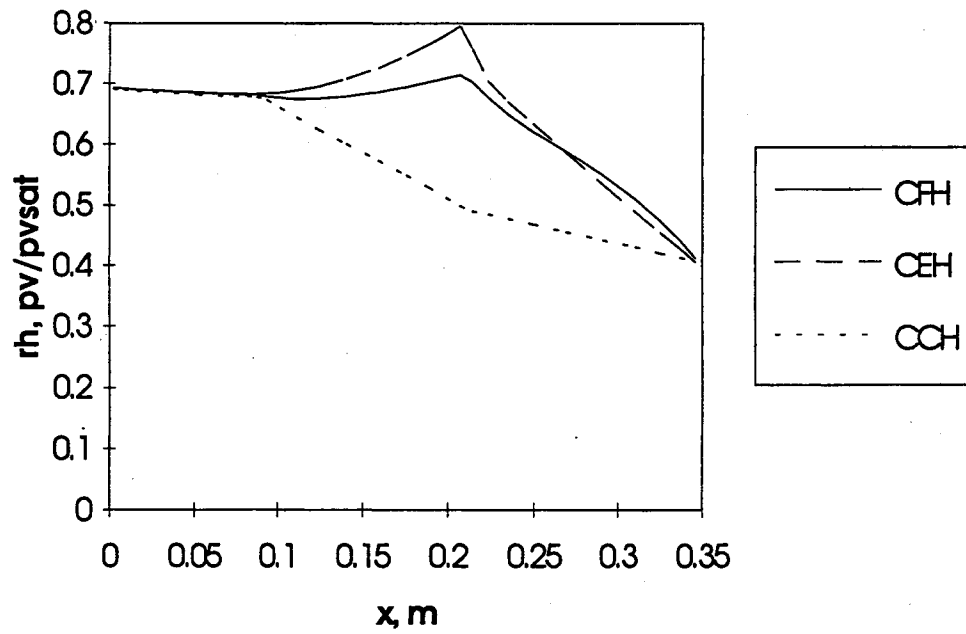
Figure A1-38: Relative-humidity distribution: Case C_H

Relative humidity distribution 225 days (7.5 months) from the beginning of the year: comparison of cases where the properties of external brick were simplified (results with hourly weather data)
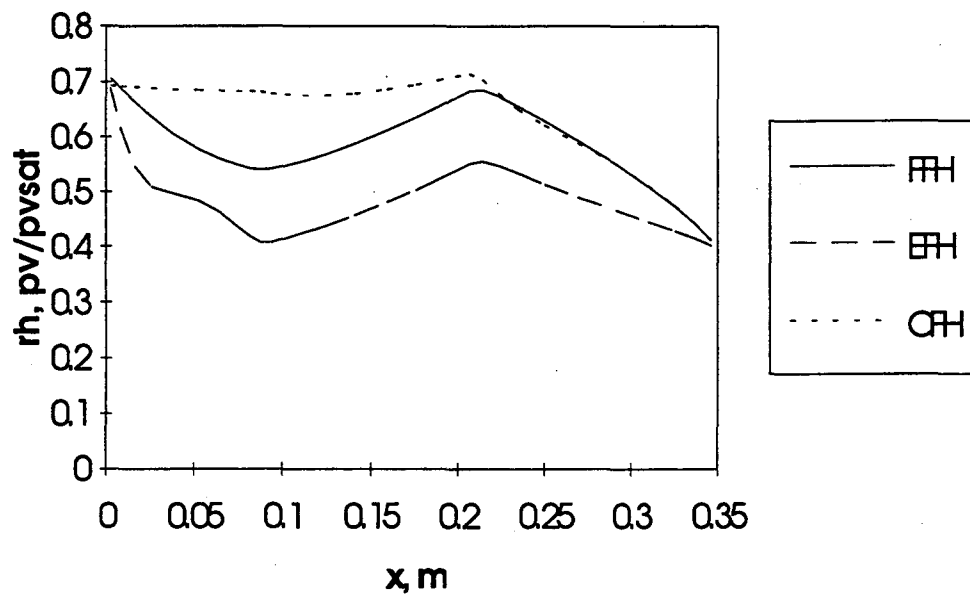
Figure A1-39: Relative humidity distribution: Case _FH
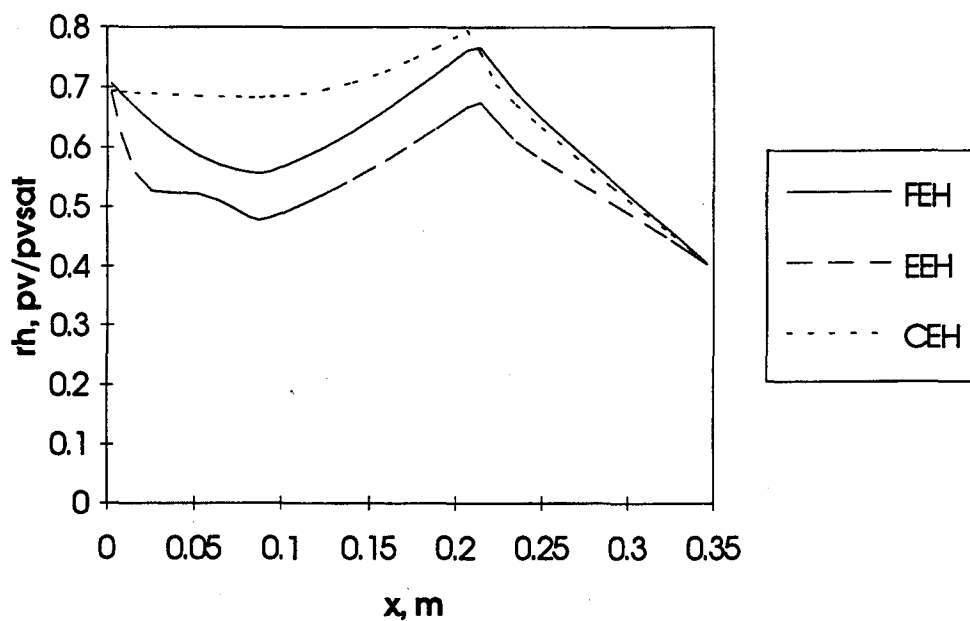
Figure A1-40: Relative humidity distribution: Case _EH
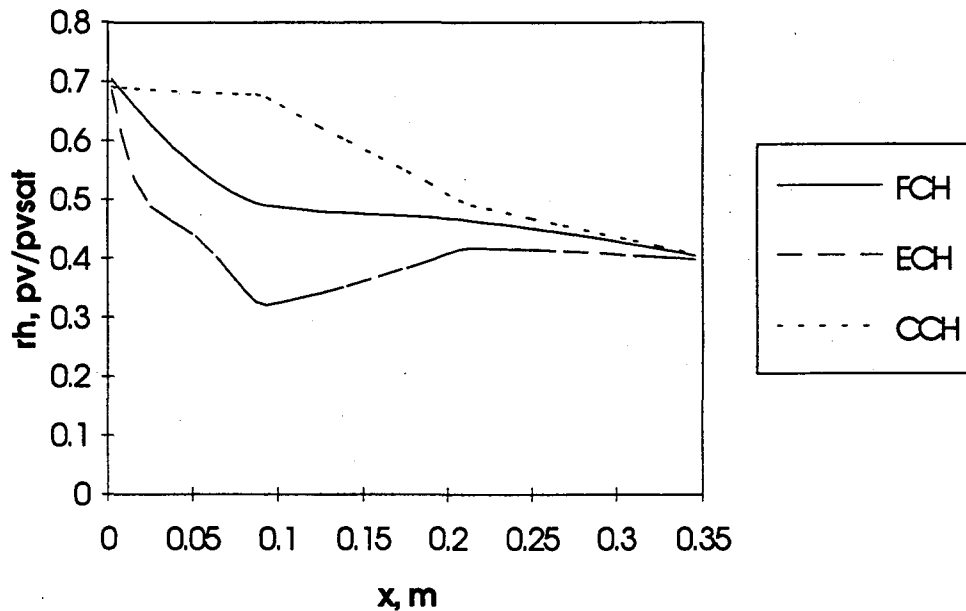
Figure A1-41: Relative humidity distribution: Case _CH

2.5 TASK C: Evaluation of the Impact of Variable Material Properties using Stochastic Modeling

Theory

Monte Carlo has been defined as a technique of solving a problem by using random numbers to realize random answers. The answer for the problem is then the average value of the random answers obtained. The basic concept of the Monte Carlo method is the random-walk process, also termed the Markov chain. A Markov chain is simply a chain of events. The probability of each successive event in the chain is uninfluenced by prior events. It is important to note the independence of each event in the sequence. To understand some of the very basic aspects of the method, we have chosen to describe here vapor transport by a simple diffusion process.

Let's assume that the vapor molecules are homogeneous (not necessary the media), meaning that the number density of the molecules per unit volume is uniform. Suppose that some

molecules are labeled somehow (e.g., Canadian) but are otherwise identical to all the other unlabelled (e.g., Finnish) molecules. In equilibrium, the number density $n(x,t)$ of the labeled molecules must also be uniform. If there is an excess concentration of the "Canadian" vapor

molecules at some position x, there must be a deficit of "Finnish" molecules at x in order to keep the total number density uniform. In such a situation, the "Canadian" molecules will move about so that the vapor concentration is made more uniform. If Γ denotes the flux of "Canadian" vapor molecules crossing point x; and D, the diffusion coefficient, then

$$\Gamma = -D\frac{\partial n}{\partial x} \qquad (3)$$

Since the number of Canadian vapor molecules must be conserved, the continuity equation is

$$\frac{\partial n}{\partial t} = -\frac{\partial \Gamma}{\partial x} \qquad (4)$$

and therefore

$$\frac{\partial n}{\partial t} = D\frac{\partial^2 n}{\partial x^2} \qquad (5)$$

The solution of these equation can be written as

$$n(x,t) = Np(x,t) \qquad (6)$$

where

$$p(x,t) = \frac{e^{-x^2/4Dt}}{(2\pi Dt)^{1/2}} \qquad (7)$$

N = defined as the total number of "Canadian" vapor molecules

p(x,t)= interpreted as the probability that a Canadian molecule found at x=0 at t=0 will be found between x and x+dx at time t. For example, a normal probability density function is depicted in Figure (A1-42).
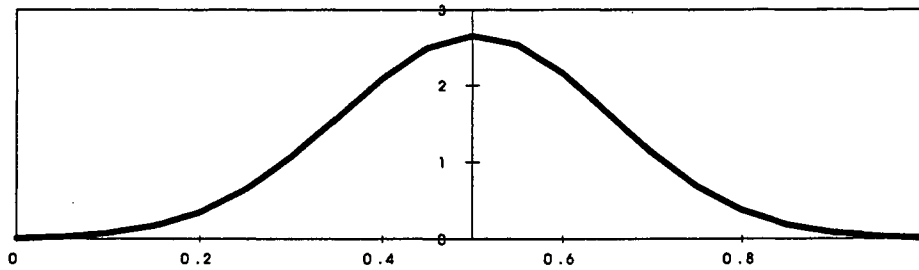
Figure A1-42 : Normal Probability Distribution

The mean square displacement at time t can be calculated as

$$\langle x^2 \rangle = \int_0^\infty x^2 p(x,t)dx = 2Dt$$

the diffusion coefficient can be written then as

$$D = \langle x^2 \rangle / 2t$$

The diffusion of the molecules may be considered as a random walk. Consider one Canadian vapor molecules initially at x=0. It has the same thermal velocity and travels straight line segments between collisions with the Finnish molecules. After each collision, it has an equal but random chance of moving to the right or left. The probability of being between x and x+dx after M steps of equal length b is

$$P(x, M)dx = \frac{e^{-x^2/2Mb}}{2\pi Mb^2} dx$$

Many other techniques concerning the Monte Carlo method are available in literature. The above merely shows basic principle and procedure of the method. It is important to note that the effective application of the Monte Carlo simulation technique depends on two important factors: the extent of knowledge of the process under study, qualitatively, and the amount of data available (quantitative). Knowledge of the process refers to the level of understanding of its behavior and characteristics.

IMPLEMENTATION

The relation of the differential equations describing the heat transfer and a simple stochastic model describing this phenomena has been known for some time [Howell, 1968]. The same governing differential equations imbedded in **LATENITE** were used, but allowing a probabilistic interpretation, i.e., if a random-walking factor is given at point (x,y) for each material property under investigation. The primary objective of this work was the parametric investigation of material property influences, a uniform probability density function was sought. However, due to the limited number of simulations employed some skewness existed, this will be discussed further. For the present investigation δ_P vapor permeability, D_w liquid diffusivity and thermal conductivity λ was randomized with ± 40 % of the full correlation of the property; i.e. the complete functional dependence on moisture content is taken into account.

Simulation Cases

Two independent tests were investigated, one (Case 1) where the stochastic processes requiring both the means and the variances of each investigated transport property varying

simultaneously every time step, and the other (Case 2) once in the beginning of each simulation. A Monte Carlo method was used to generate the probability factors for each investigated transport property in a controlled fashion allowing variations limited to ± 40 %. Ten yearly simulations were conducted for each test, twenty in total. Each test was allowed to be independent of each other.

Wall structure:

To determine the sensitivity to the moisture and heat transport properties on the heat and moisture transport of a high rise wall structure several simulations were performed. The high rise wall structure selected for the numerical analysis is shown in Figure A1-8. The wall is composed of the following layers starting from the exterior to interior, a 90 mm facade brick (LATENITE database: material number 13), a 120 mm glass fiber board (material number 5) and finally a 140 mm red brick (material number 14). The height of the wall is 1 m (1-dimensional simulations). This particular wall assembly has no vapor barrier. The wall was exposed to outside air temperature, and the relative humidity varied according to the weather data from the selected location (Ottawa). The simulations were carried out for a one-year exposure and started from the 1 st of January. For each case, the liquid diffusivity, vapor permeability and thermal conductivity of the layers were varied randomly with a variance of ± 40 %.

Boundary and initial conditions

Internal conditions were maintained constant at 21 °C and 40 % relative humidity (Pv= 997 Pa) throughout the 20 yearly simulations. The solar radiation and long wave radiation form the outer surfaces of the wall were included in the analysis. The BMY (Best Meteorological Year) weather file for the city of Ottawa was used. The daily, weekly and monthly averages of temperatures and relative humidities are plotted out in Figure A-43. Figure A-44 shows the daily, weekly and monthly averages of the solar fluxes on a south facing wall. The wall under consideration was centrally positioned on the third floor of a high rise building and was oriented facing North-West. All calculations started on the 1 st of January. Driving rain was used in the analysis as
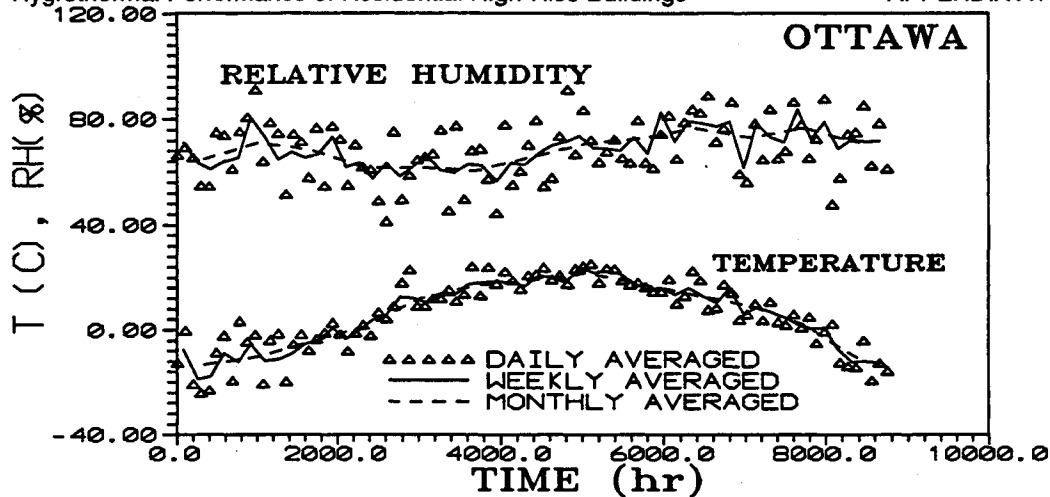
Figure A1-43 : Ottawa Weather Conditions for Daily, Weekly and Monthly Averaged Values

calculated by TASCflow. The additional moisture source due to direct incident of rain was also modeled. Inclusions of all these boundary conditions were considered in order to give the numerical analysis full credit in the sensitivity study. In this study no air infiltrating or exfiltrating is considered, thereby the primary mode of water transmission is due to diffusion processes.

The initial conditions of the wall were 10, 15 and 17 °C and 0.06, 0.009, 0.06 kg/kg moisture content for external brick, glass fiber and internal brick layer, respectively. The maximum capillary moisture content of the bricks is 0.111 kg/kg. Figure A1-45 plots out the moisture diffusivity employed for the internal brick. Here the ± 40 % maximum and minimum limits are shown for the Monte Carlo simulation.
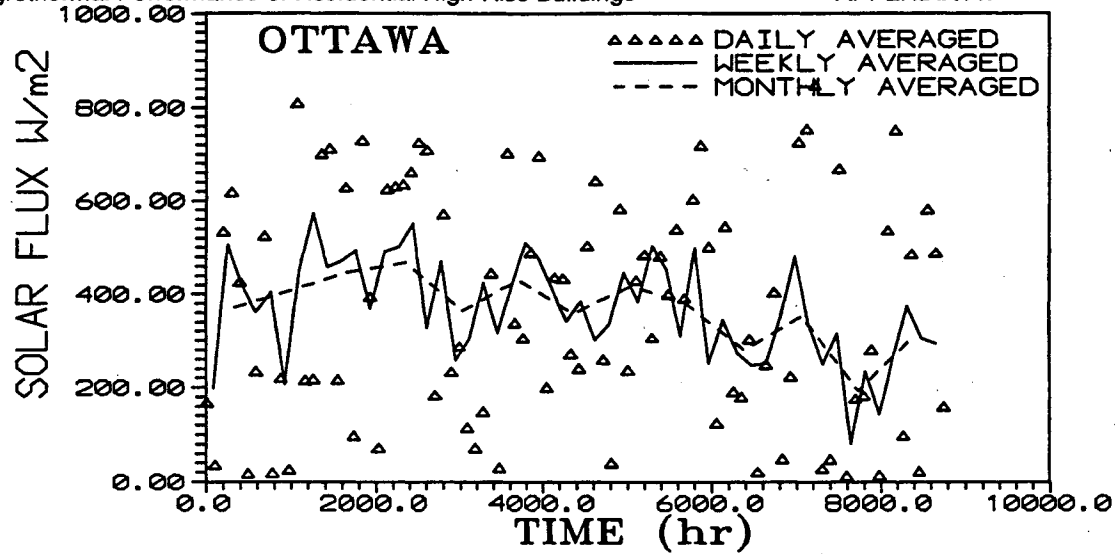
Figure A1-44: Ottawa Solar Fluxes for Daily, Weekly and Monthly Averaged Values

The heat and mass transfer coefficients for external and internal surfaces are presented in Table A1-6.
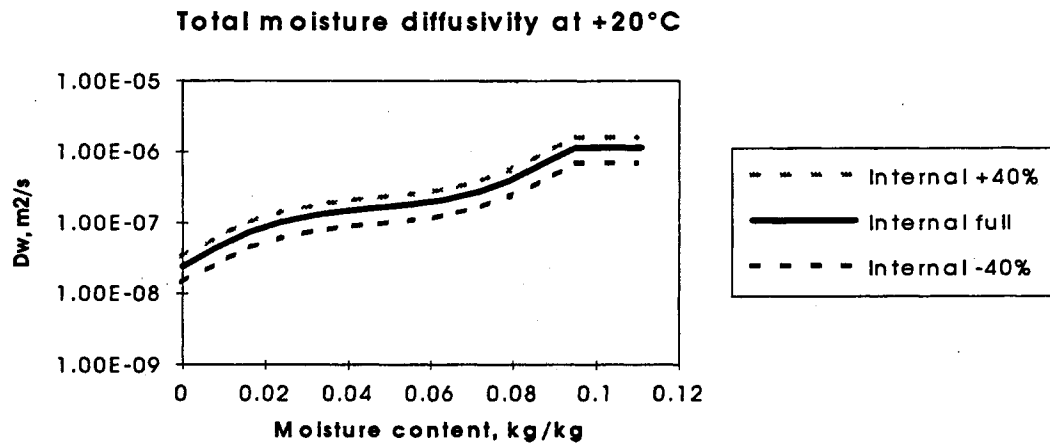
Figure A1-45 : Moisture Diffusivity Limits at ± 40 %

Table A1-6. Heat and moisture transfer coefficients for the external and internal surfaces.

Property	External surface	Internal surface
Heat transfer coefficients, W/ m^2K	20	8
Mass transfer coefficients, kg/m^2,s,Pa	$1.5 \cdot 10^{-7}$	$5.0 \cdot 10^{-8}$
Short wave absorptivity	0.6	-
Long wave emissivity	0.9	-

SIMULATIONS FOR CASE 2
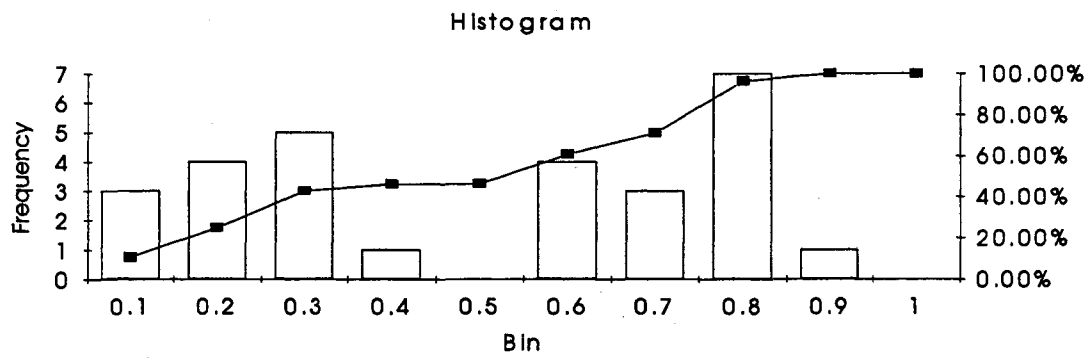
Figure A1-46. Frequency Histograms for Stochastic Simulation 1.
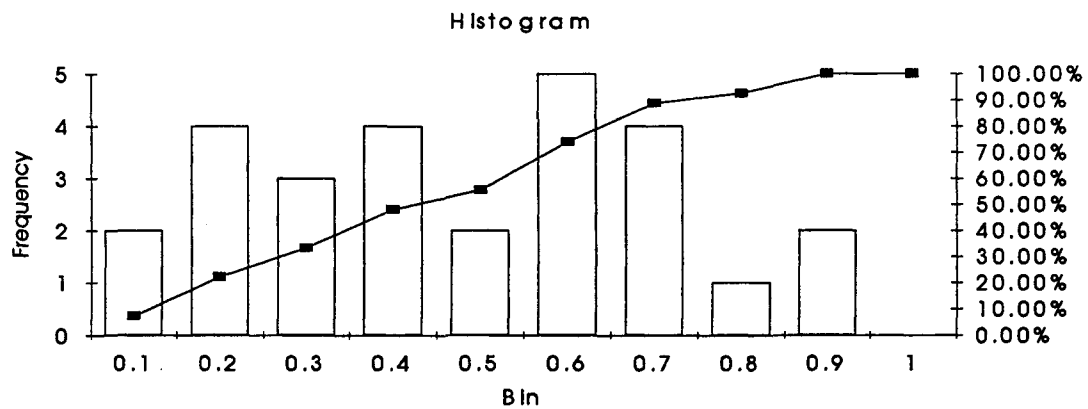
Figure A1-47. Frequency Histograms for Stochastic Simulation 2.

Histogram : Cases 11 to 20 combined
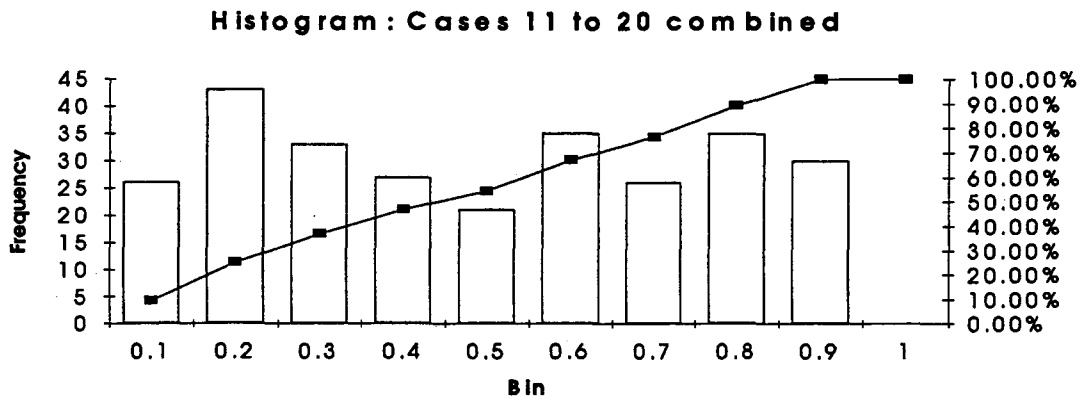
Figure A1-48. Combined Frequency Histograms for Stochastic Simulations 1-10

Stochastic runs: +/- 40%
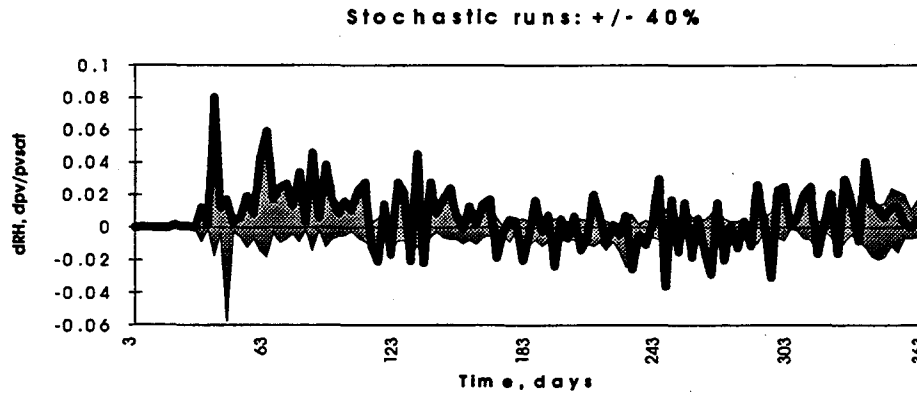
Figure A1-49. Relative humidity difference (daily averages) of the internal surface of external brick layer. Minimum and maximum variations and one of the 10 cases (solid line) are shown.

Stochastic runs: +/-40%
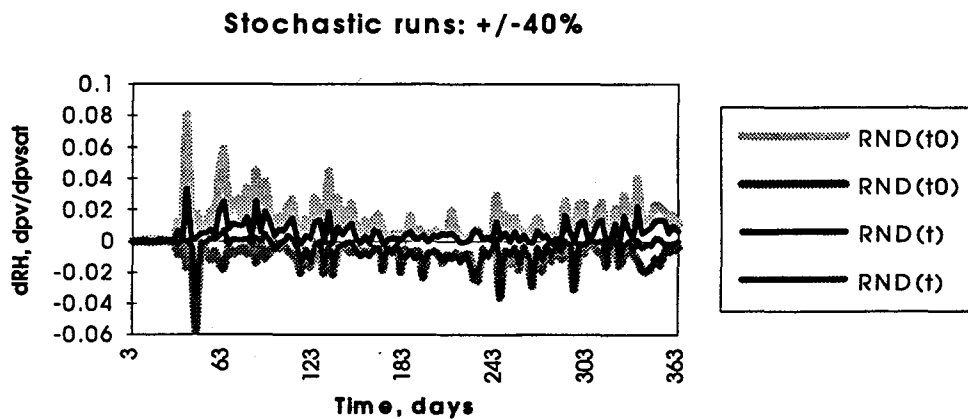
Figure A1-50. Relative humidity difference Comparing Case 1 (t) and Case 2 (t0) Simulations
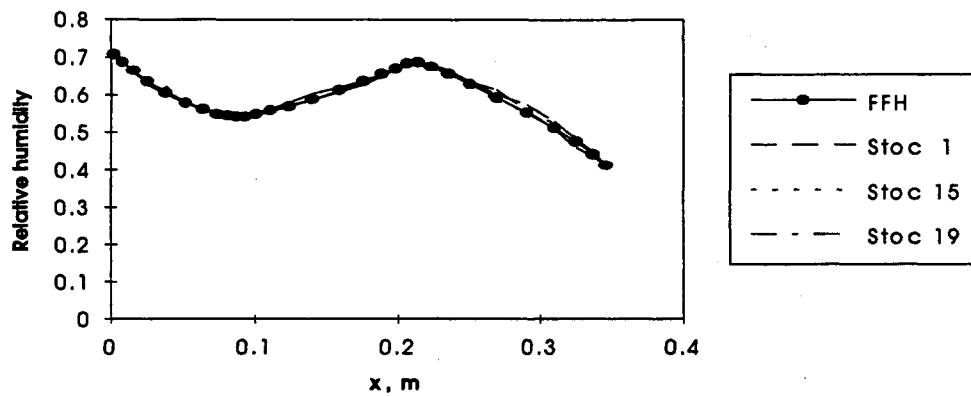
Figure A1-51. Comparison of Deterministic and Stochastic Simulations after 225 days≅ September
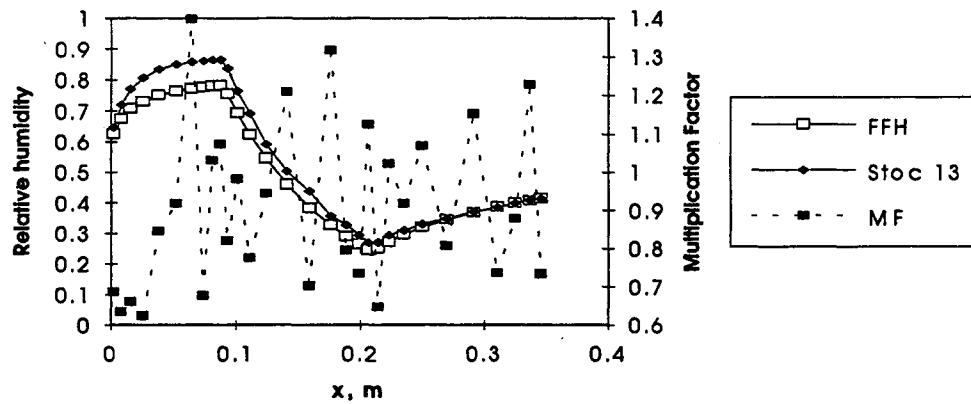
Figure A1-52. Comparison of Deterministic and Stochastic Simulations after 63 days≅ March
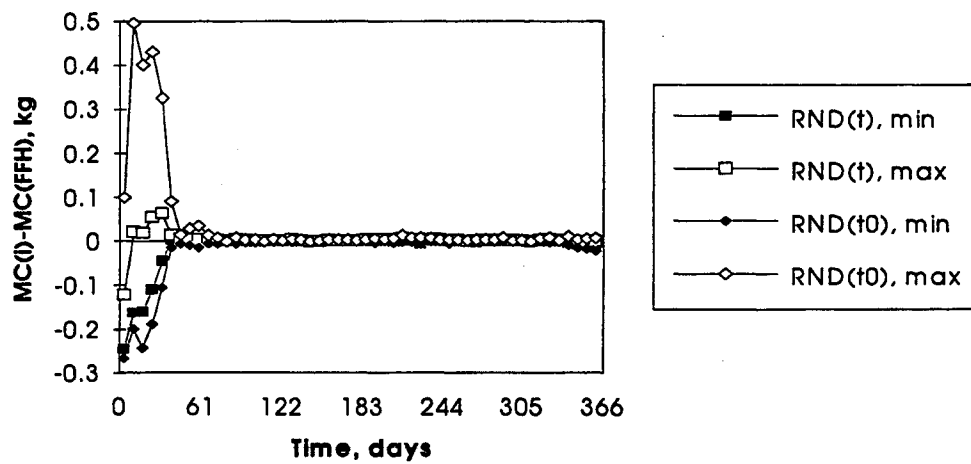
Figure A1-53. Total Moisture Differences between Stochastic Cases 1 and 2
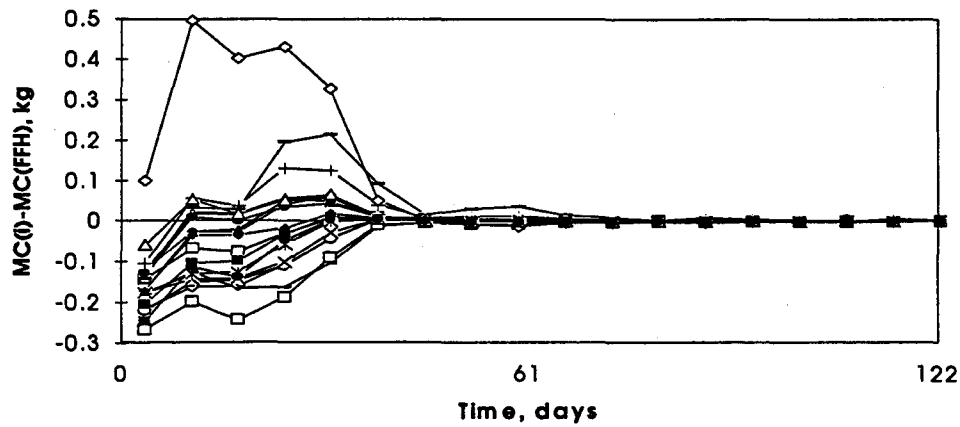
Figure A1-54. Total Moisture Differences between Stochastic Cases 1 and 2 during drying
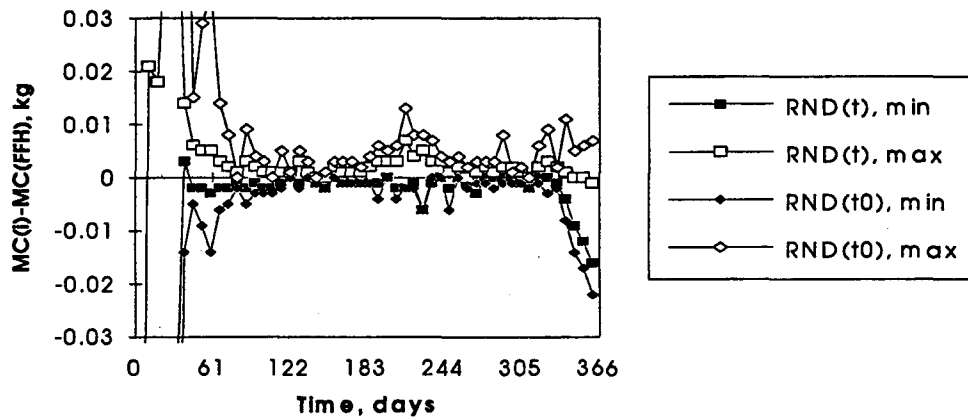
Figure A1-55. Total Moisture Differences between Stochastic Cases 1 and 2 after drying
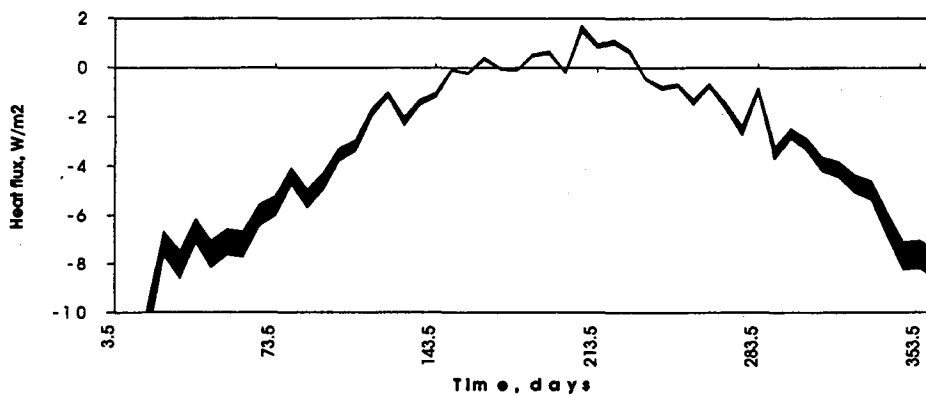
Figure A1-56. Minimum and maximum heat fluxes (daily averages) of all the stochastic runs
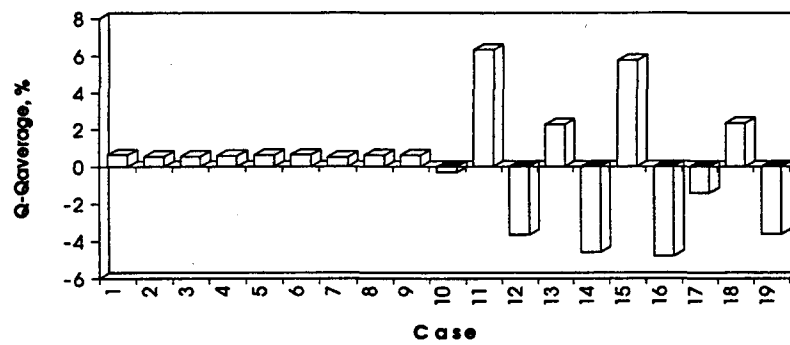
Figure A1-57. Differences in yearly average heat loss for stochastic runs. Material properties varied by ±40%.

APPENDIX B1

Table of Contents

APPENDIX B1　BOUNDARY CONDITIONS

Governing equations for turbulent flow

For incompressible turbulent flows, assuming that density fluctuations can be neglected, the mean form of the conservative equations of mass, and momentum, x_j, can be written as

Conservation of mass:

$$\frac{\partial}{\partial x_j}(\rho\, u_j) = 0 \text{ (1)} \tag{B1-1}$$

Conservation of momentum:

$$\frac{\partial}{\partial t}(\rho\, u_i) + \frac{\partial}{\partial x_j}(\rho\, u_j u_i) = -\frac{\partial P}{\partial x_j} - \frac{\partial}{\partial x_j}(\tau_{ij} + \rho\overline{u_i'u_j'}) + S_{u_i} \tag{B1-2}$$

where
u_j = velocities in the x_j-directions

ρ = density of the fluid

P = static pressure

τ_{ij} = viscous stress tensor

t = time

S_{u_i} = additional source terms.

All these variables are mean flow quantities (time-averaging) and u_i' represents the fluctuating part.

The term $\rho\overline{u_i'u_j'}$ which appears in the momentum equation [Equation (4-2)] is defined as the turbulent Reynolds stresses. These terms are not expressible in terms of the mean flow variables, therefore they must be related to known quantities via a turbulence model before solving the above equations. For k-ε model used in this study, local values of the turbulent kinetic energy k and its dissipation rate ε are obtained from the solution of the following semi-empirical equations:

$$\rho\frac{Dk}{Dt} = \frac{\partial}{\partial x_j}(\Gamma_k\frac{\partial k}{\partial x_j}) + P_k - \rho\varepsilon \tag{B1-3}$$

$$\rho\frac{D\varepsilon}{Dt} = \frac{\partial}{\partial x_j}(\Gamma_\varepsilon\frac{\partial \varepsilon}{\partial x_j}) + \frac{\varepsilon}{k}(c_{\varepsilon_1}P_k - c_{\varepsilon_2}\rho\varepsilon) \tag{B1-4}$$

where
　$k = \overline{u_i'u_i'}/2$ is turbulent kinetic energy
　Γ_k and Γ_ε = the diffusion coefficients ($\Gamma_k = \mu + \mu_t/\sigma_k$, $\Gamma_\varepsilon = \mu + \mu_t/\sigma_\varepsilon$)
　$P_k = -\rho\overline{u_i'u_j'}\,\partial u_i/\partial x_j$ is the production of k

$\varepsilon = \dfrac{\mu}{\rho}\overline{(\partial u_i' / \partial x_j)^2}$ is the dissipation of k

$\mu_{,} =$ the turbulent eddy viscosity

$\mu =$ the molecular viscosity

and the turbulence model constants are listed as:

$c_{\varepsilon_1} = 1.44$, $c_{\varepsilon_2} = 1.92$, $\sigma_k = 1.0$, $\sigma_\varepsilon = 1.3$, $c_\mu = 0.09$, $\Pr_t = 0.9$.

For this study the CFD code TASCflow (ASC 1993) was used.

Rain trajectories using the Lagrangian Particle Tracking Method

The governing equation of motion for rain droplets, employing the above assumptions, can be written as

$$\frac{\pi d^3}{6}\frac{du_p}{dt} = \frac{3\pi}{C_{cor}}\left(u_f - u_p\right) + F_e \qquad (B1\text{-}5)$$

where $d =$ the rain droplet diameter

$u =$ velocity

Fe = an external potential force

t refers to time (s)

p refers to particle

f refers to the fluid and

p refers to the rain droplet.

For a moderate rain droplet, the Reynolds number 0.01<Rep<260, the drag correction, introduced to account for experimental results on viscous drag of a solid sphere, is

$$C_{cor} = 1 + 0.1315(\text{Re}_P)^{0.82-0.05a}\ \text{Re}_P < 20 \qquad (B1\text{-}6)$$

$$= 1 + 0.1935(\text{Re}_P)^{0.6305}\ \text{Re}_P > 20 \qquad (B1\text{-}7)$$

where $\alpha = \log \text{Re}_P$ and the particle Reynolds number is calculated from:

$$\text{Re}_P = \rho_f\left|u_f - u_p\right|\frac{d}{\mu} \qquad (B1\text{-}8)$$

APPENDIX C

Table of Contents

Moisture Content Graphs
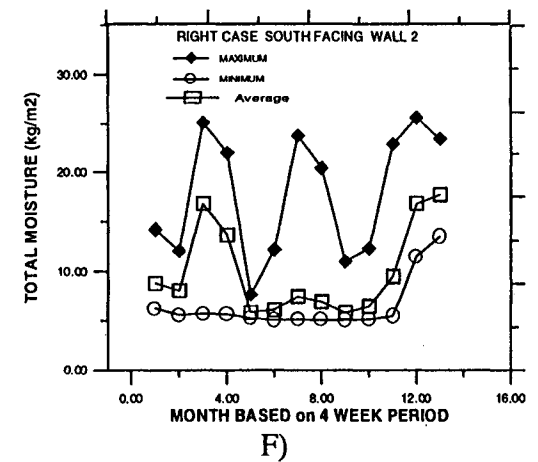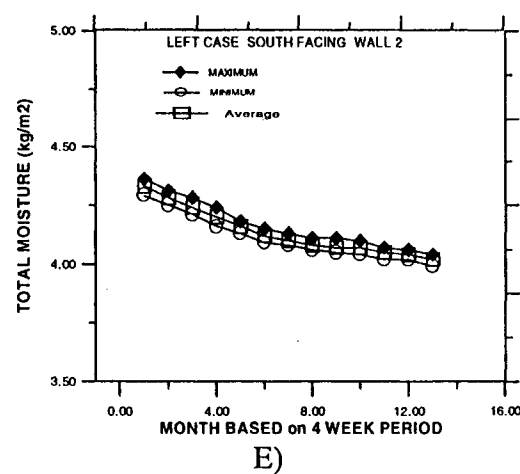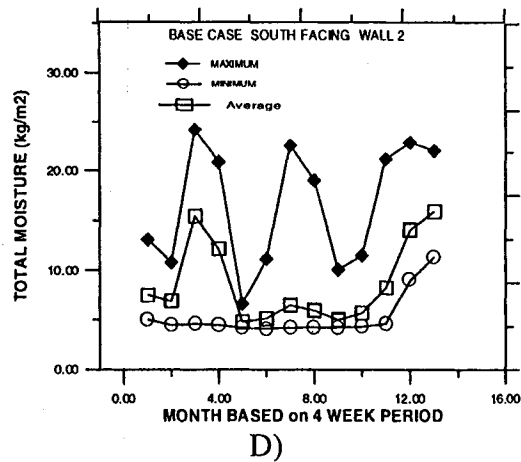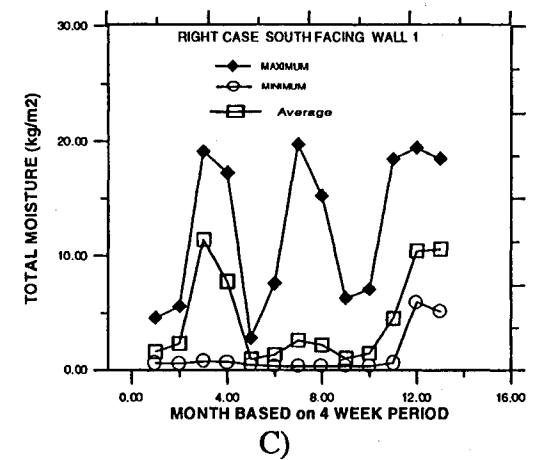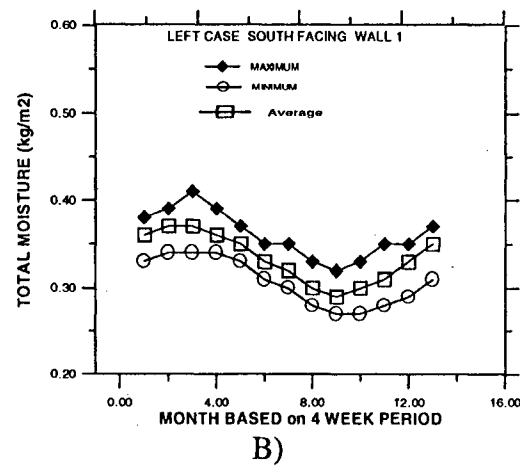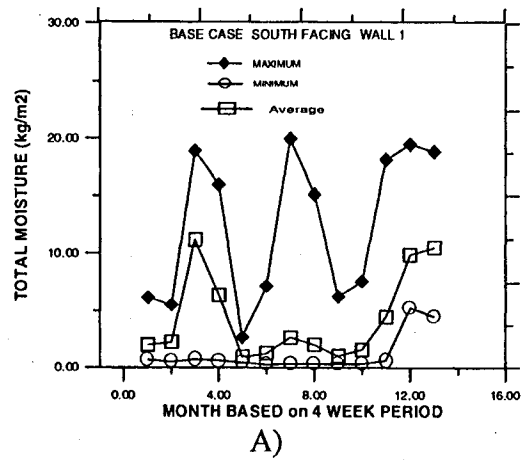
FIGURE C1
VANCOUVER

A)

B)

C)

D)

E)

F)
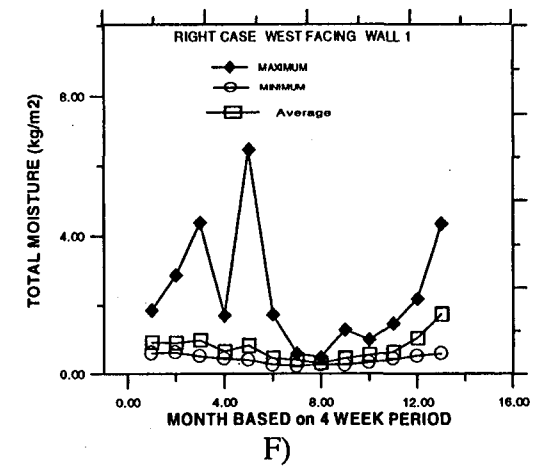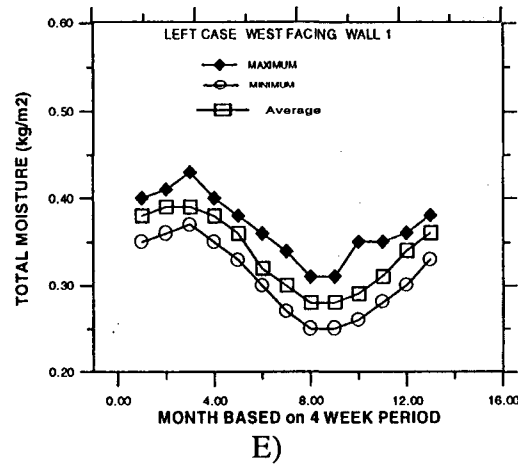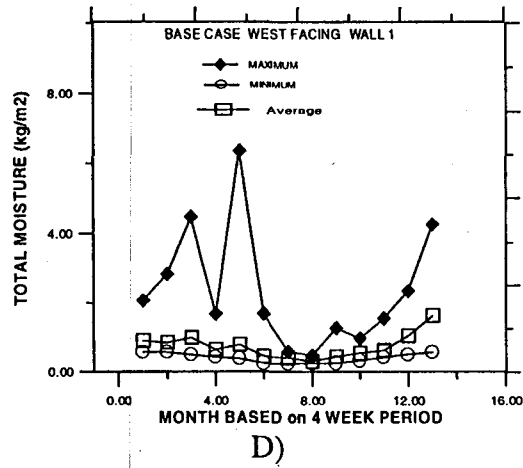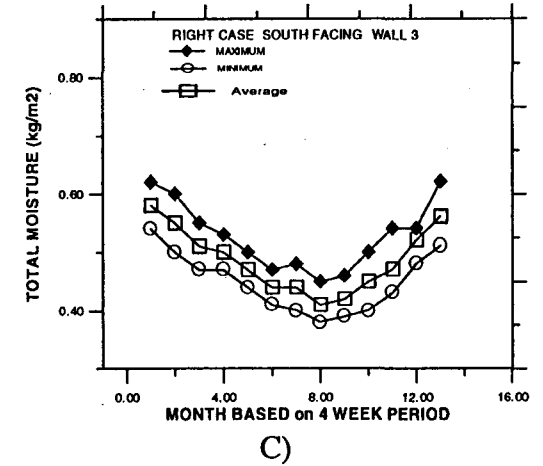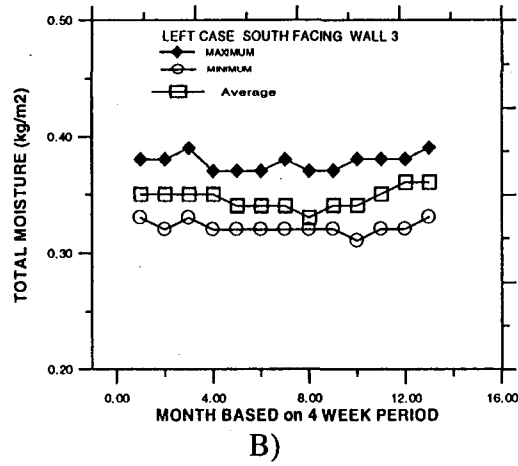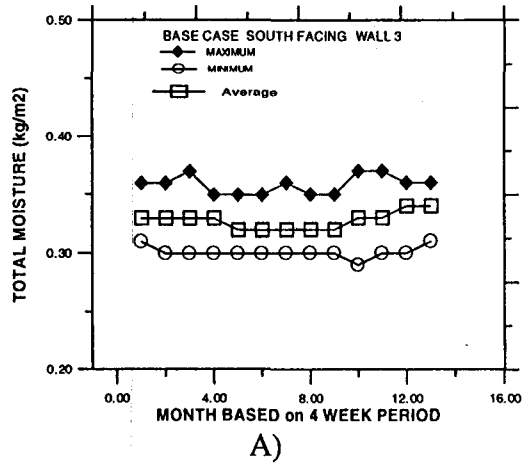
FIGURE C2
VANCOUVER
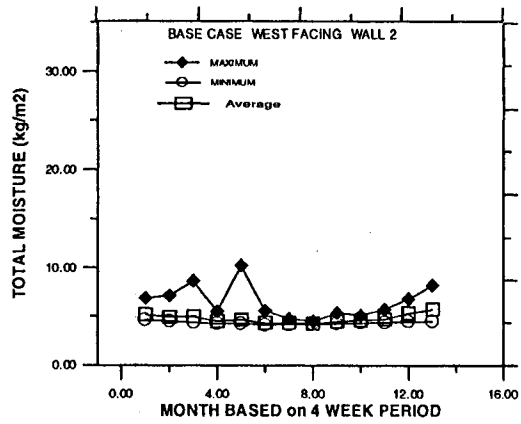
A)
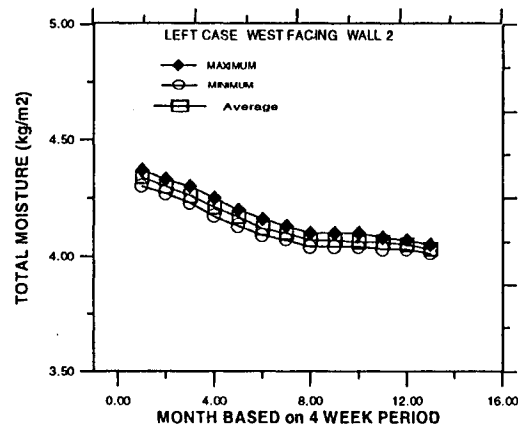
B)
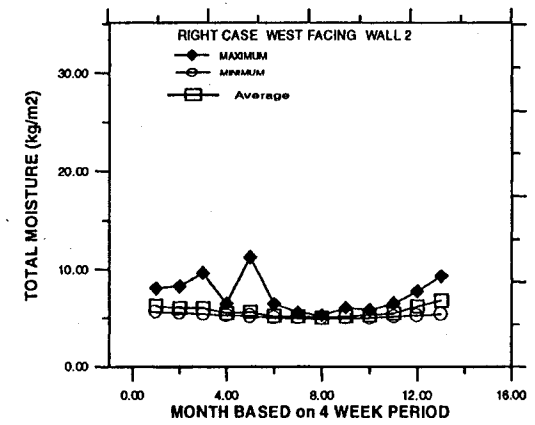
C)
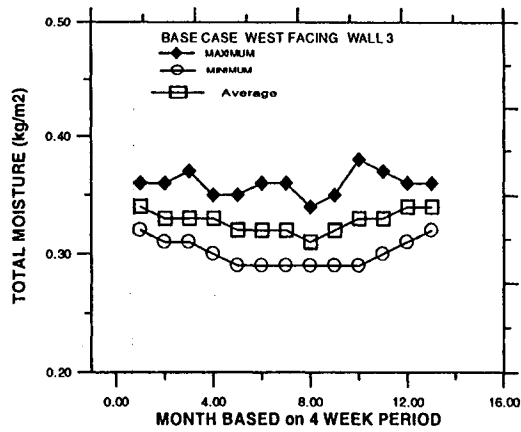
D)
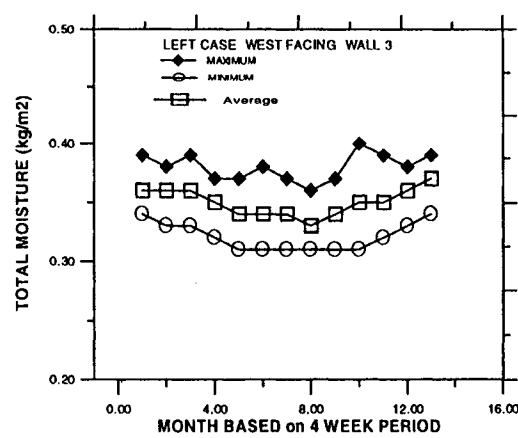
E)
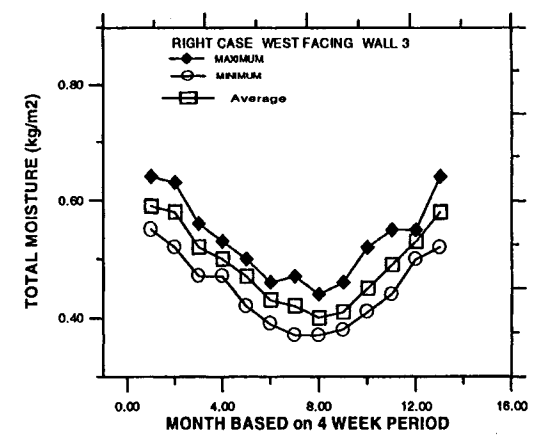
F)

FIGURE C3
VANCOUVER

A)

B)

C)

D)

E)

F)
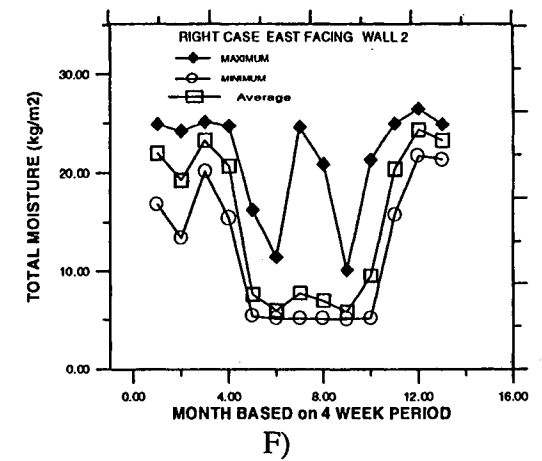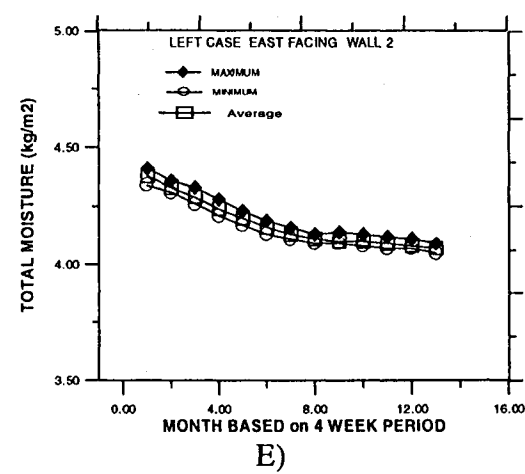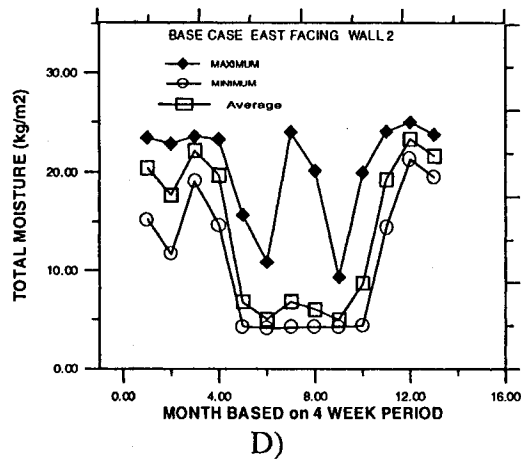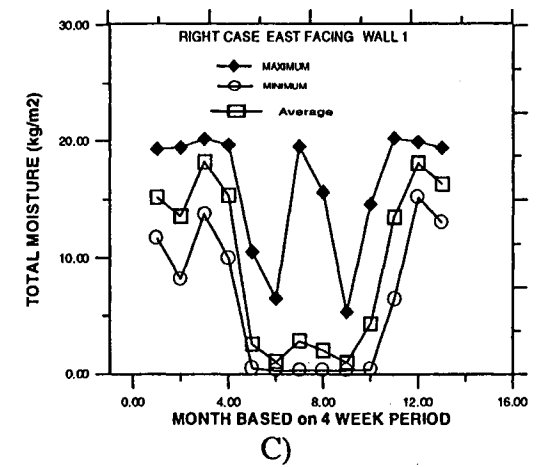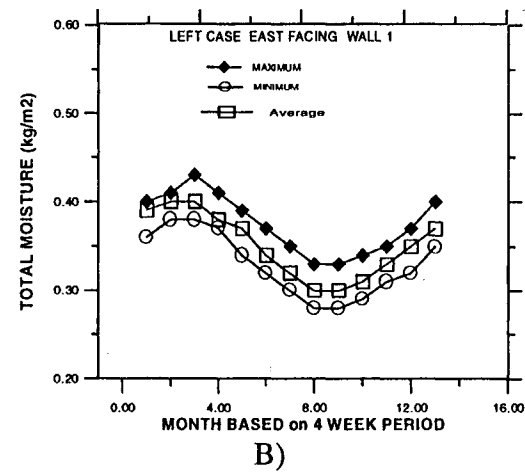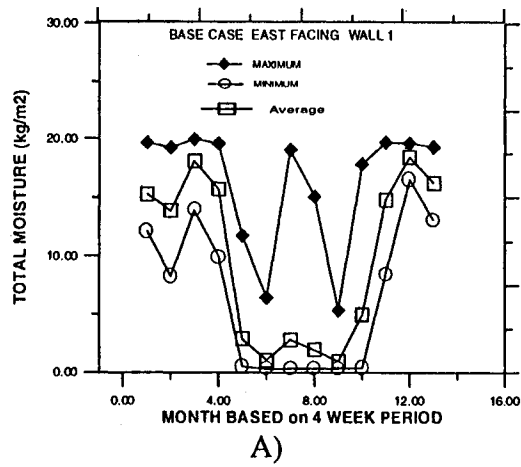
FIGURE C4
VANCOUVER
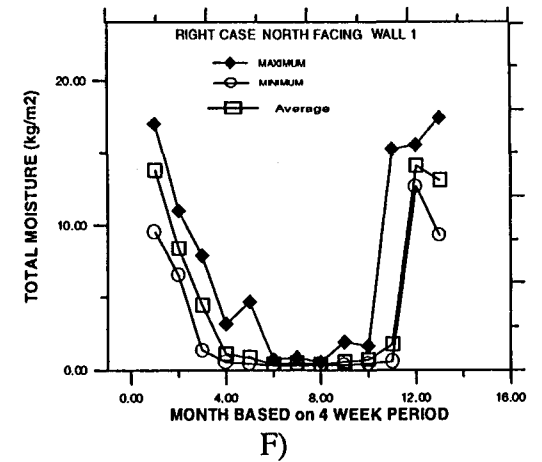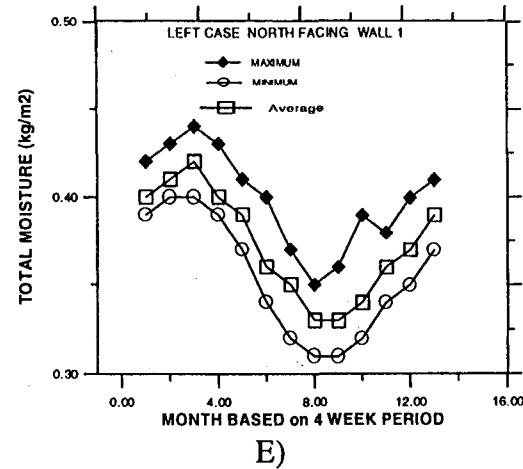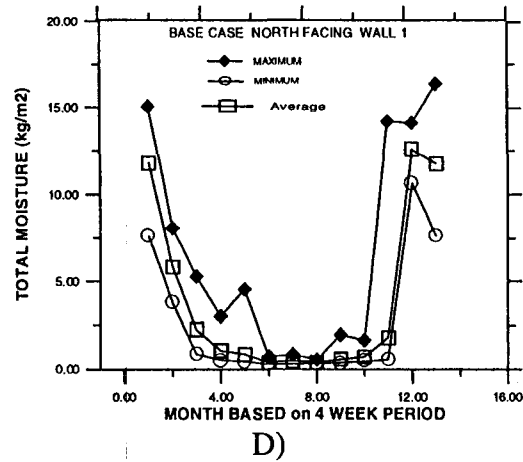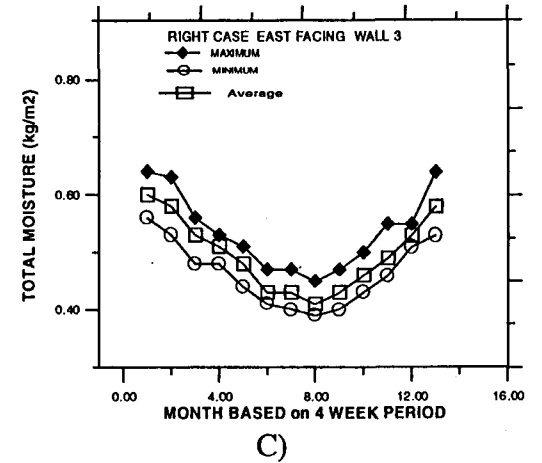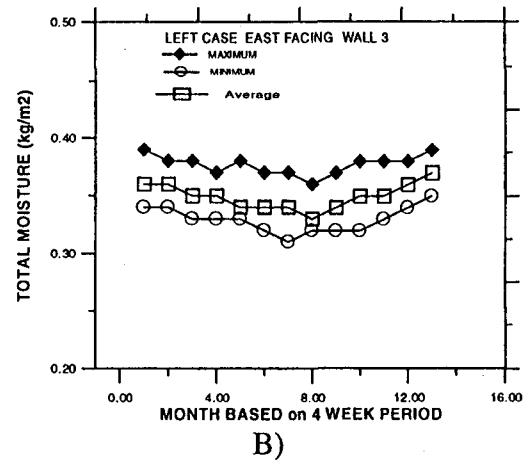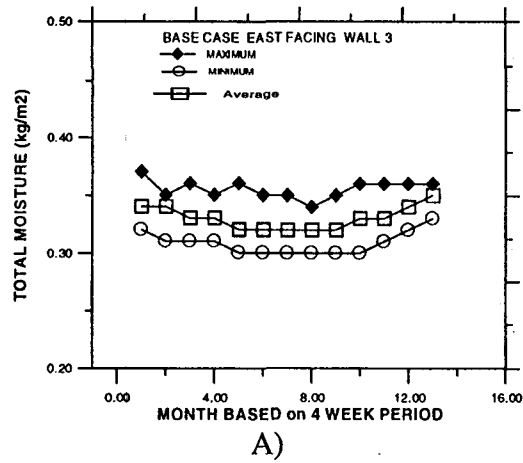
FIGURE C5
VANCOUVER

A)

B)

C)

D)

E)

F)
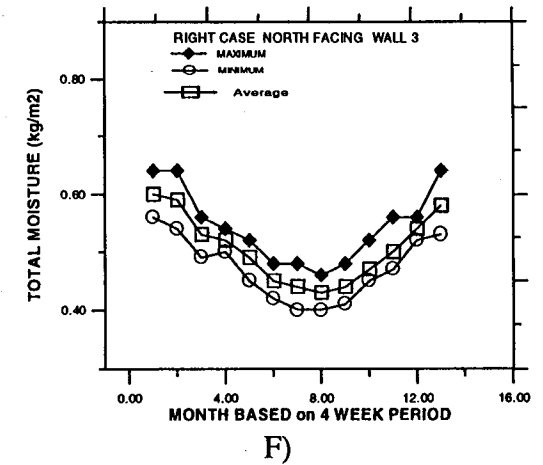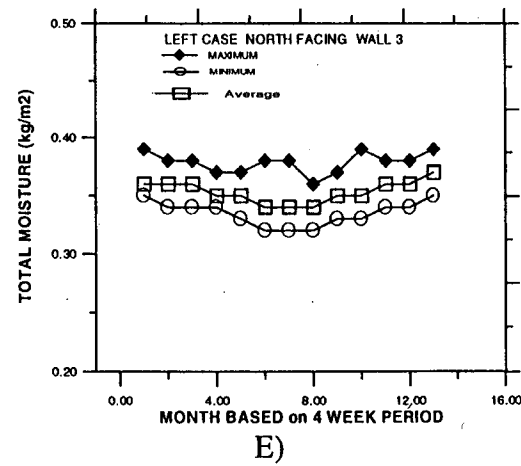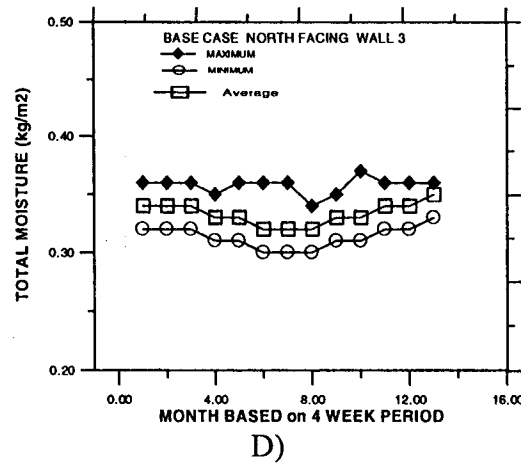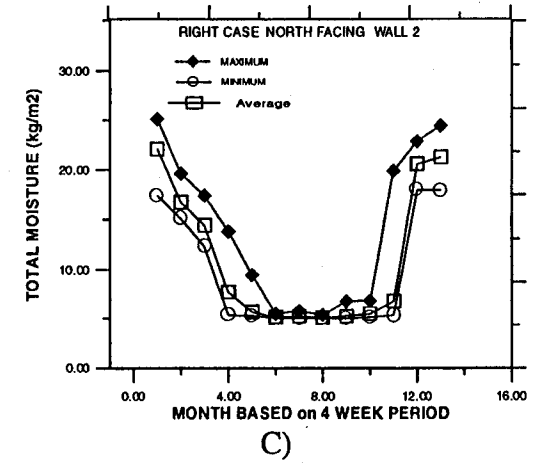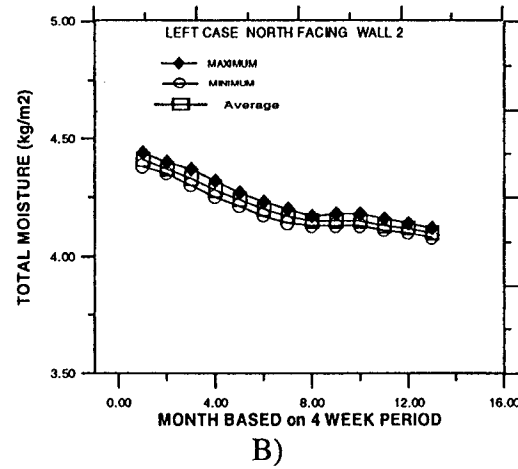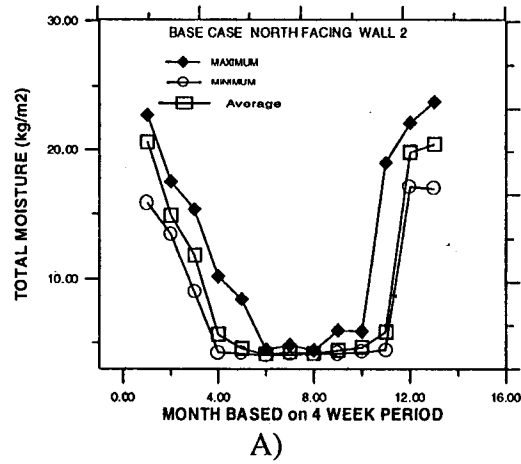
FIGURE C6
VANCOUVER

A)

B)

C)

D)

E)

F)
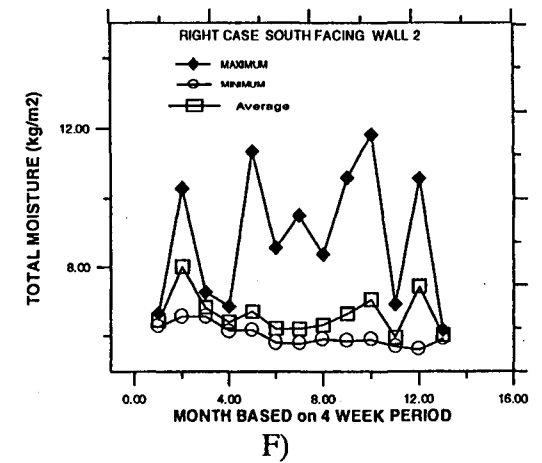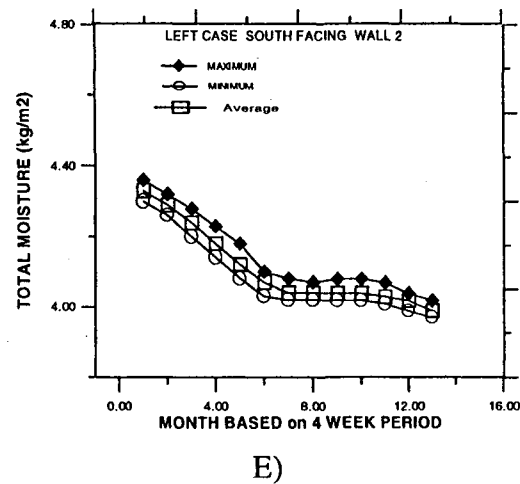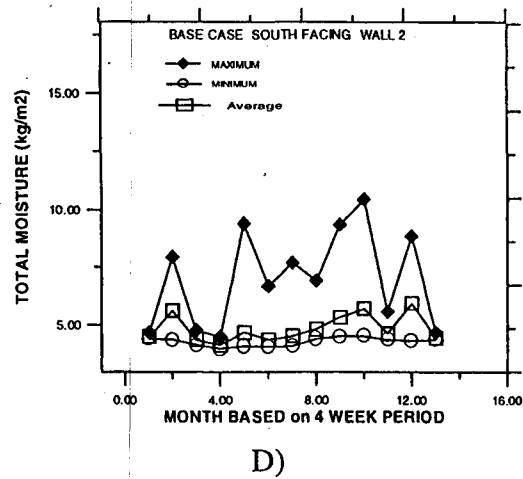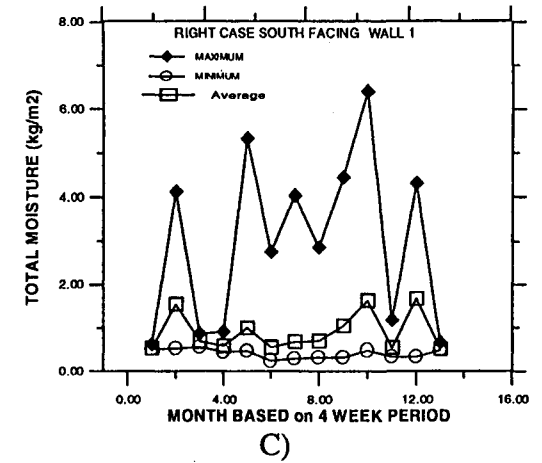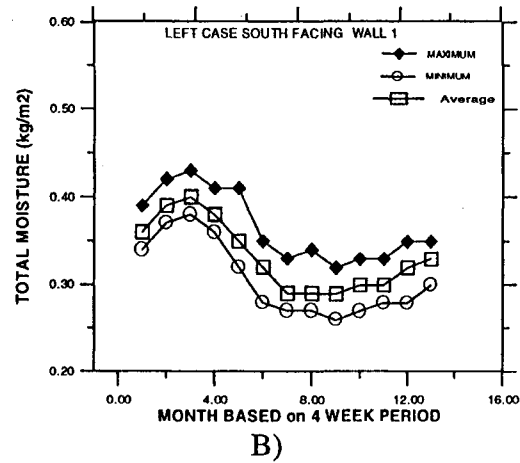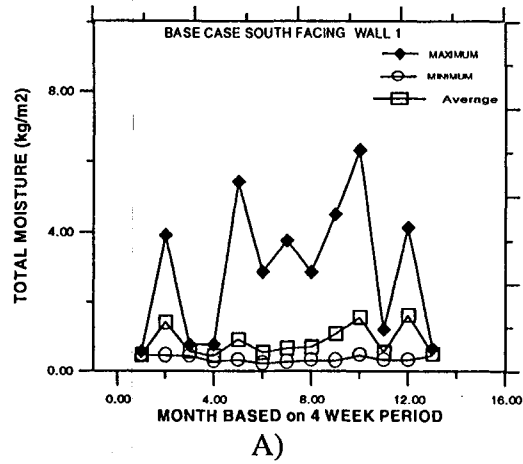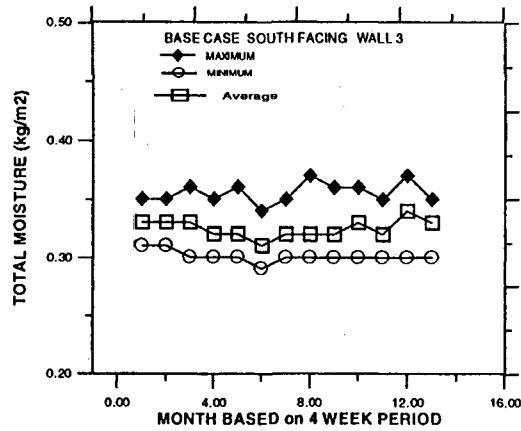
FIGURE C7
OTTAWA

A)
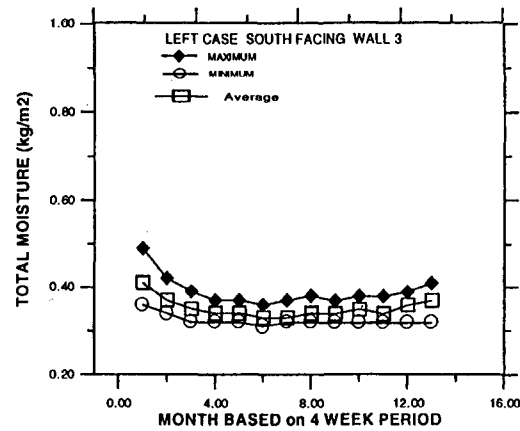
B)
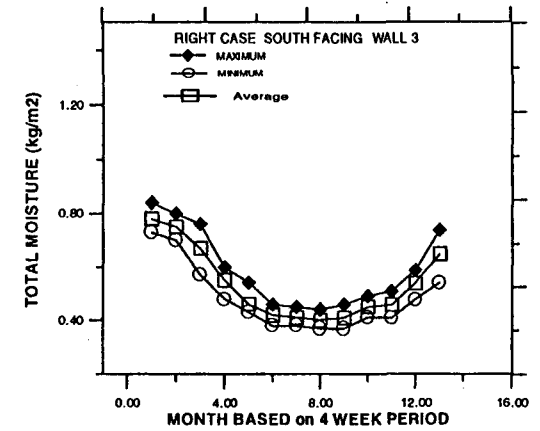
C)
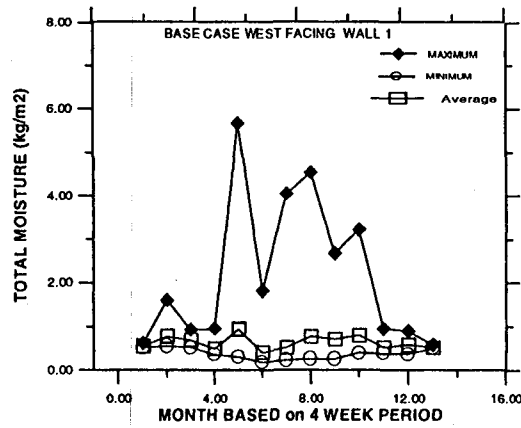
D)
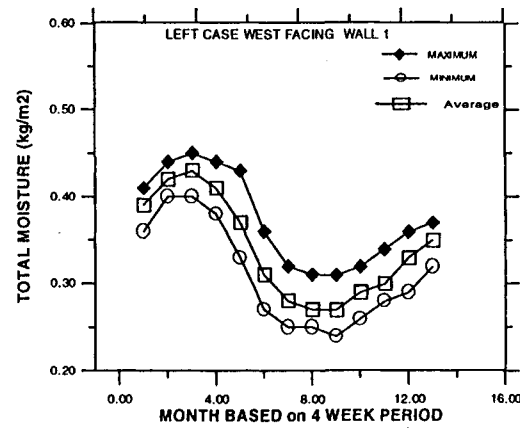
E)
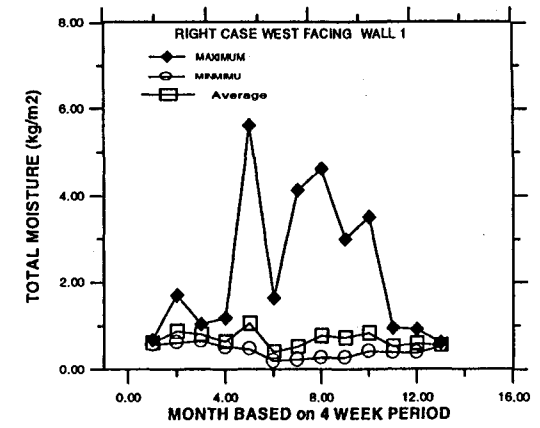
F)

FIGURE C8
OTTAWA
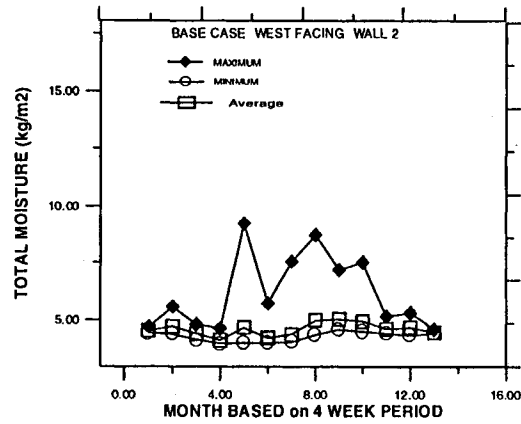
A)
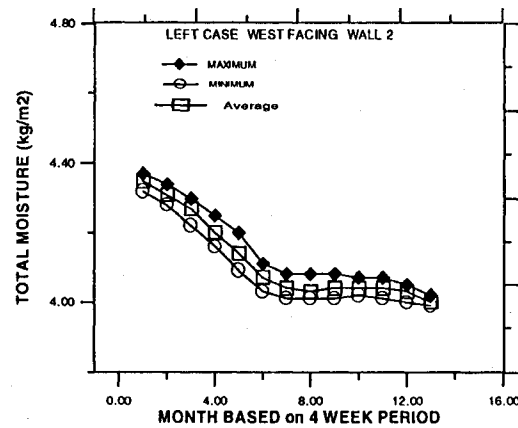
B)
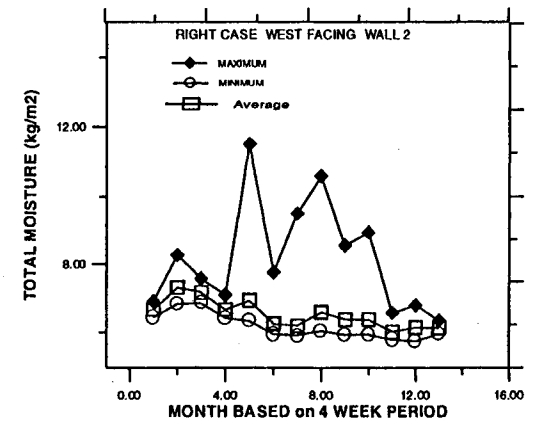
C)
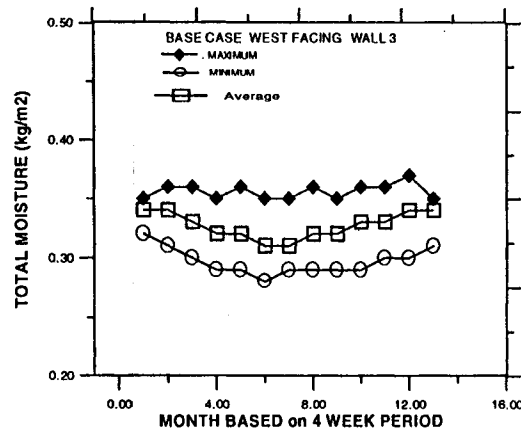
D)
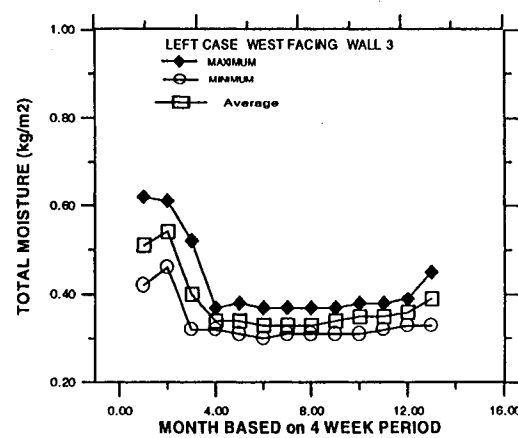
E)
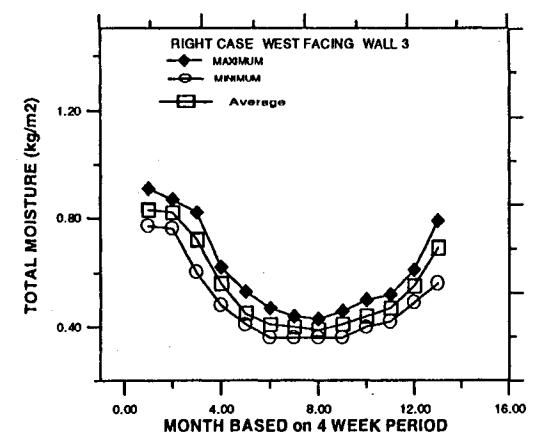
F)

FIGURE C9
OTTAWA
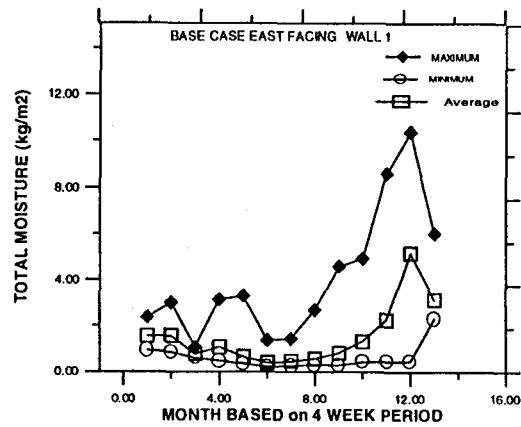
A)
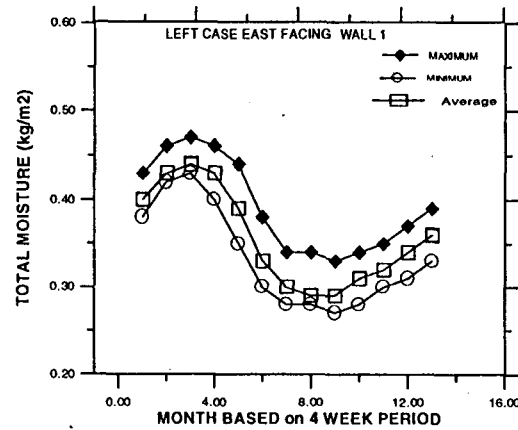
B)

C)

D)

E)

F)
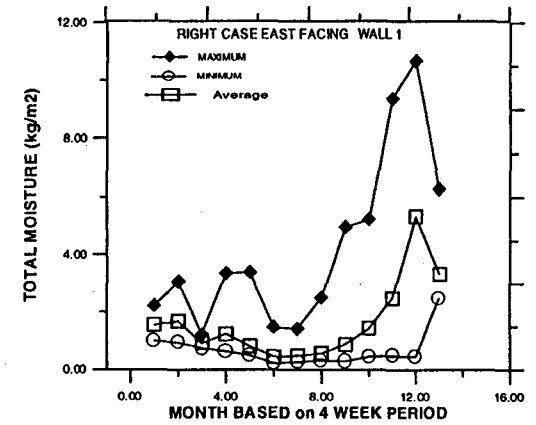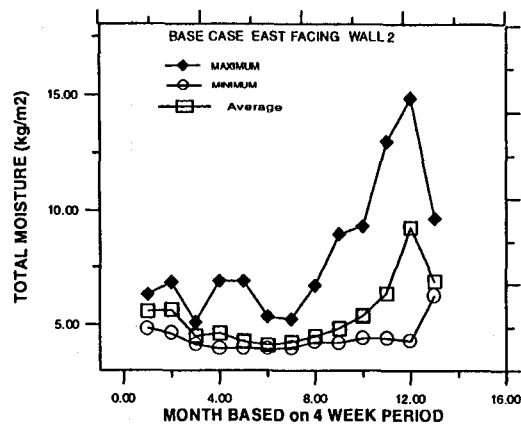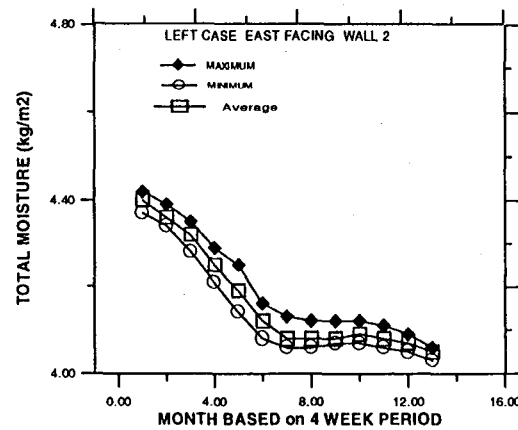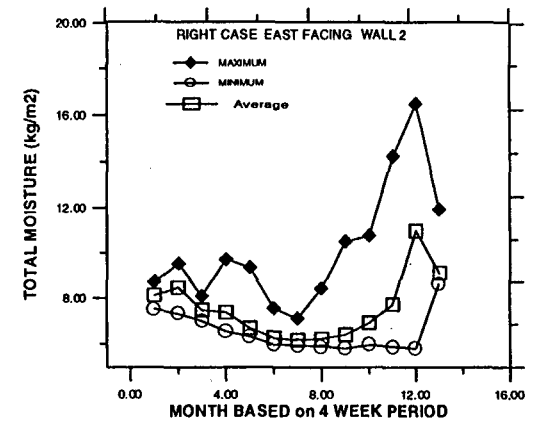
FIGURE C10
OTTAWA
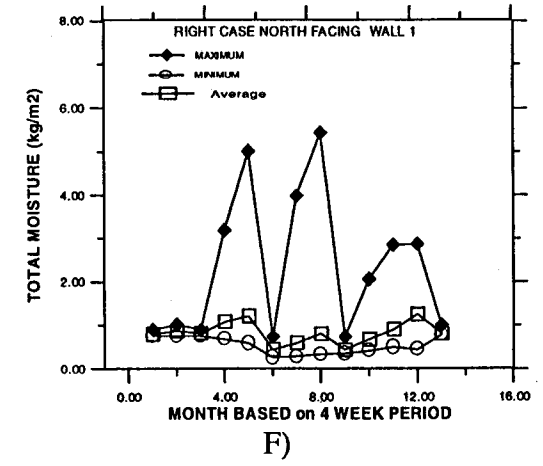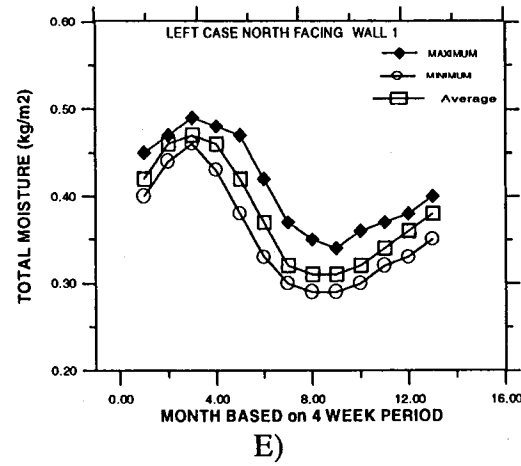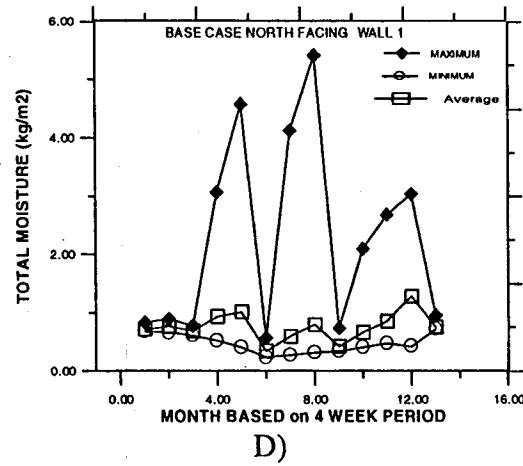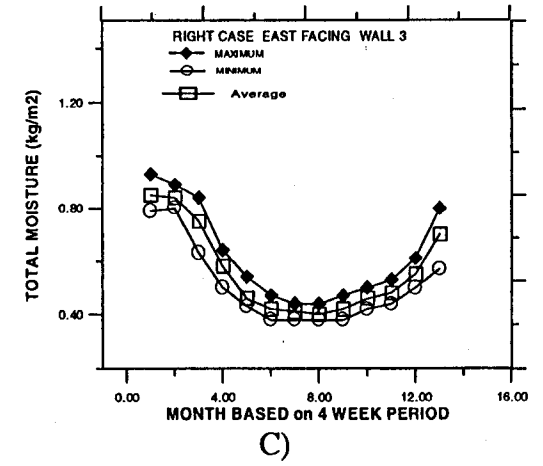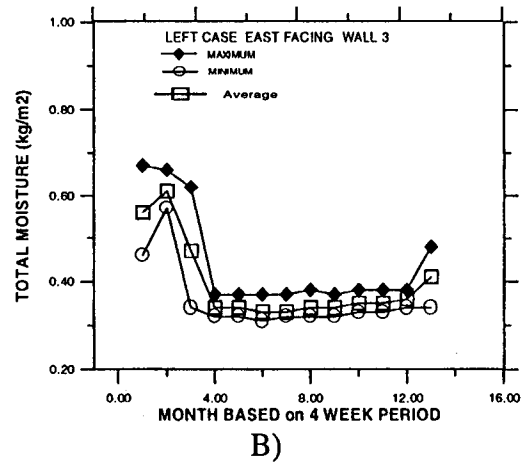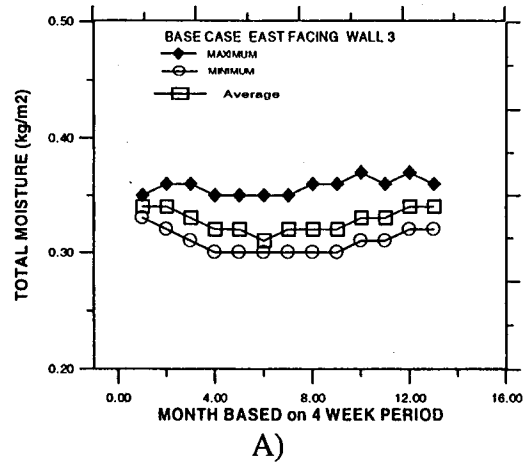
FIGURE C11
OTTAWA
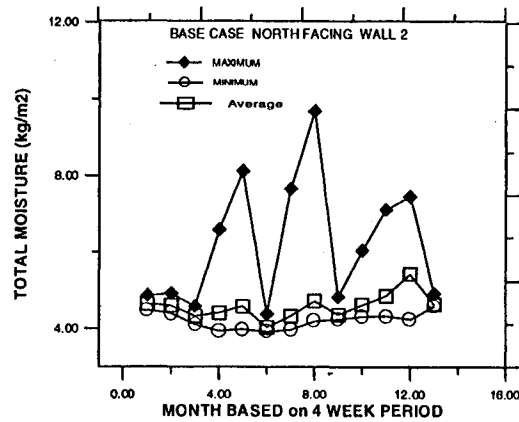
A)
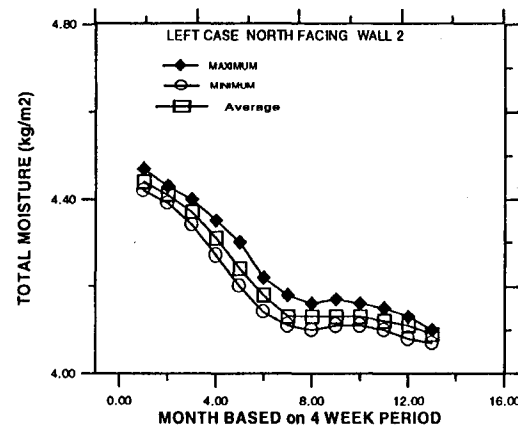
B)
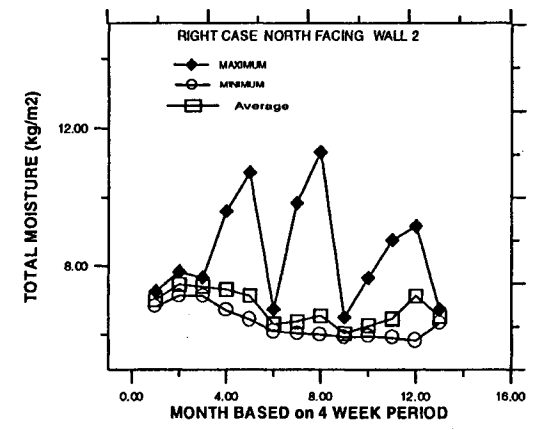
C)
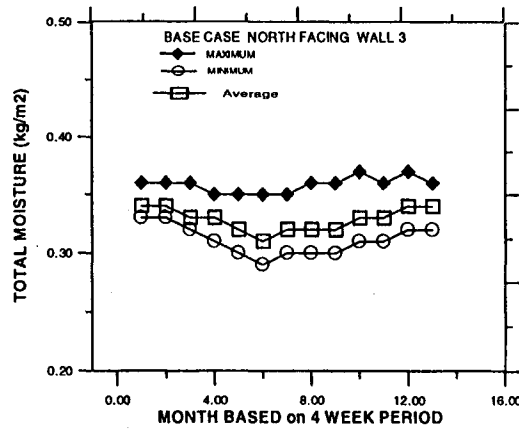
D)
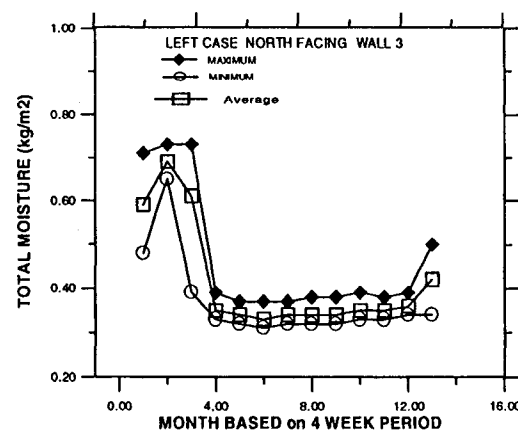
E)
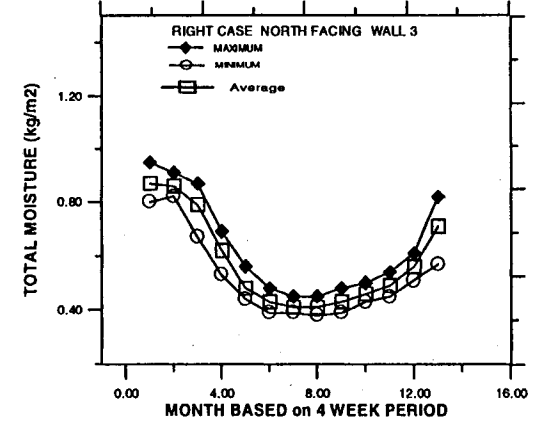
F)

FIGURE C12
OTTAWA

A)

B)

C)

D)

E)

F)
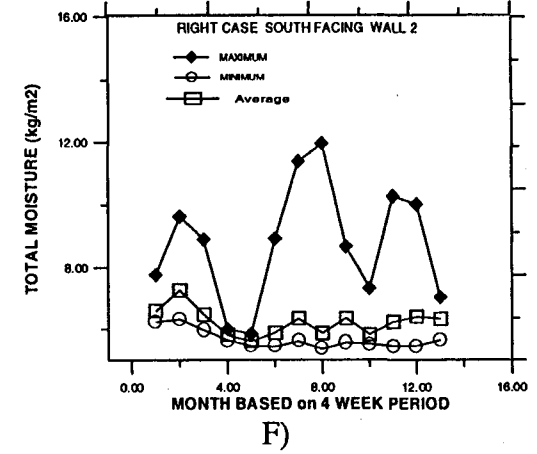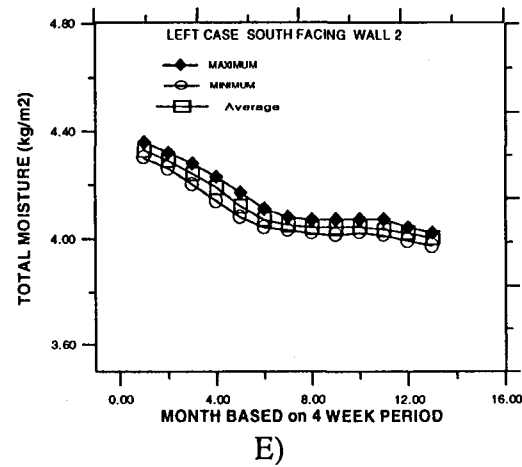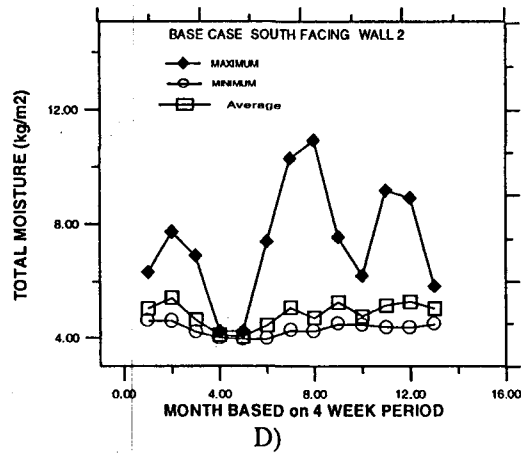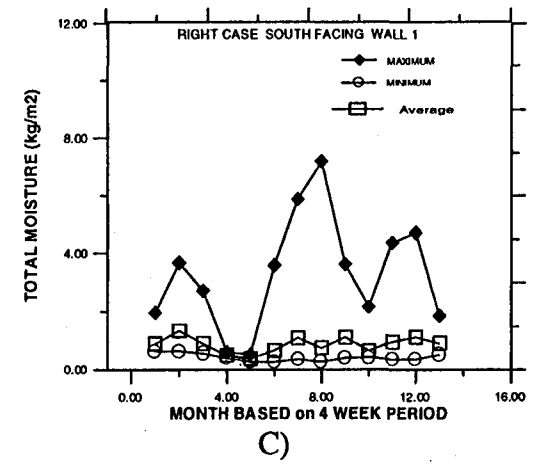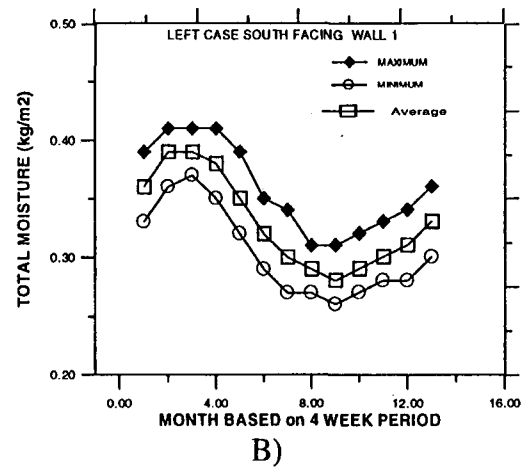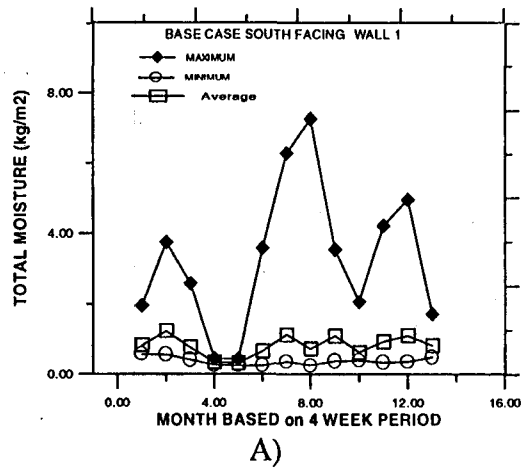
FIGURE C13
TORONTO

A)

B)

C)

D)

E)

F)
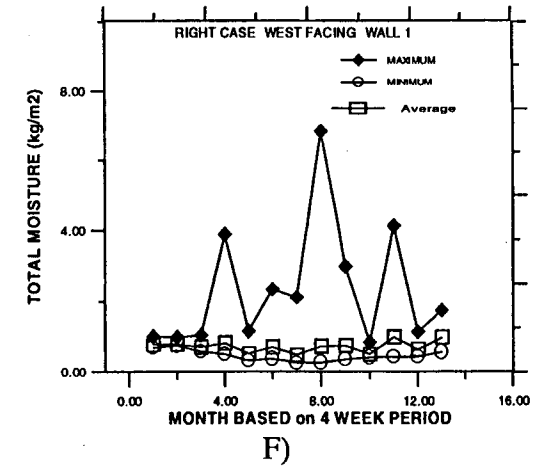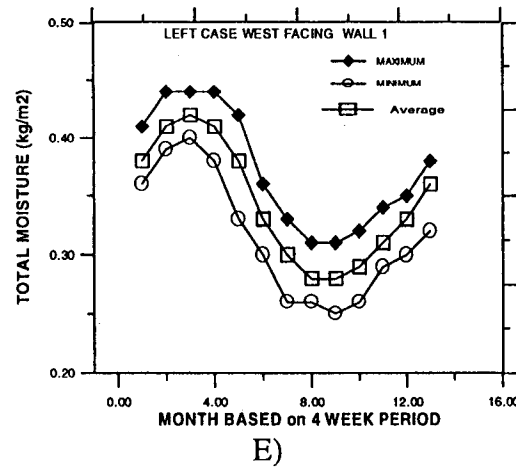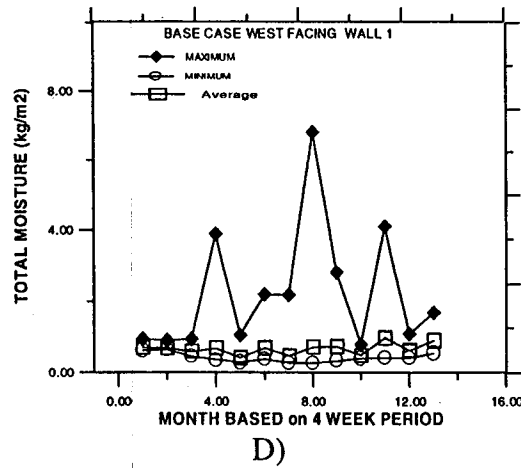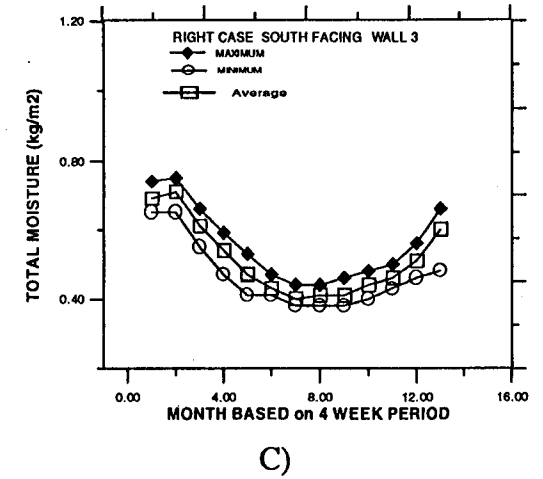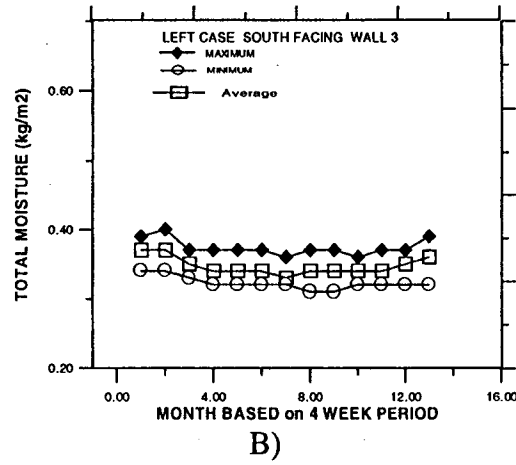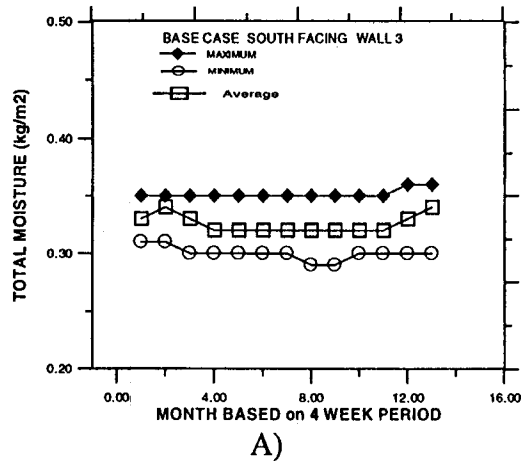
FIGURE C14
TORONTO

A)

B)

C)

D)

E)

F)
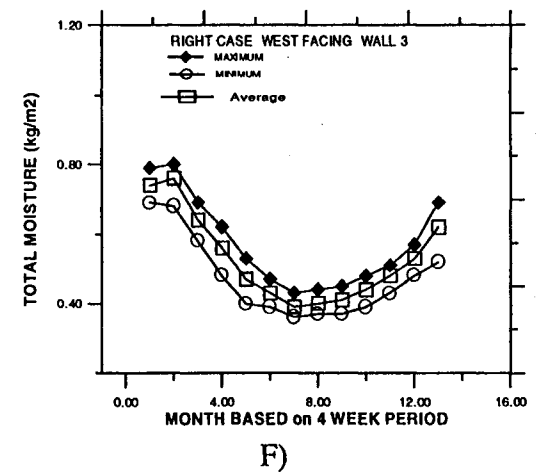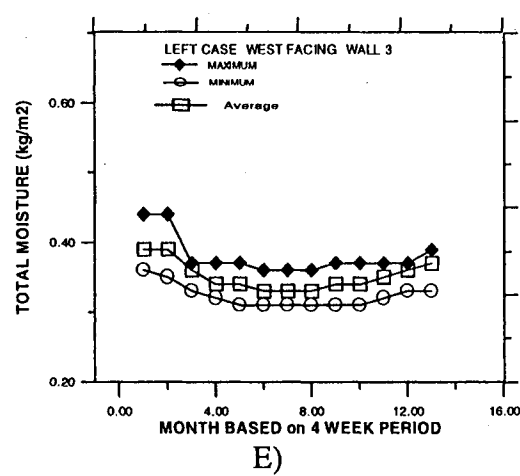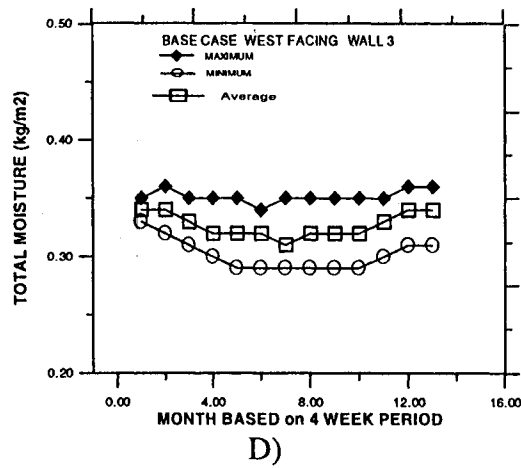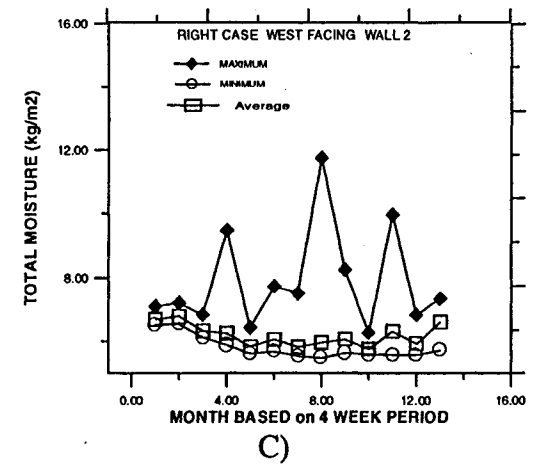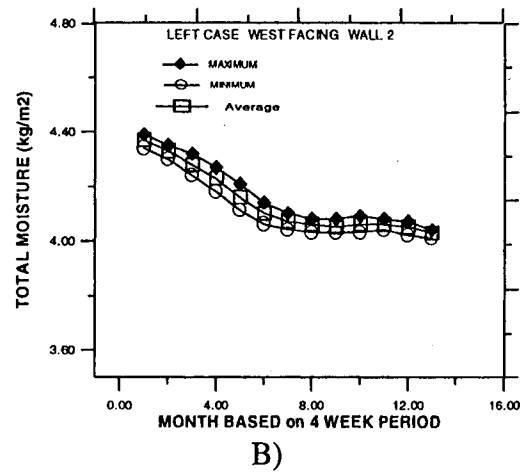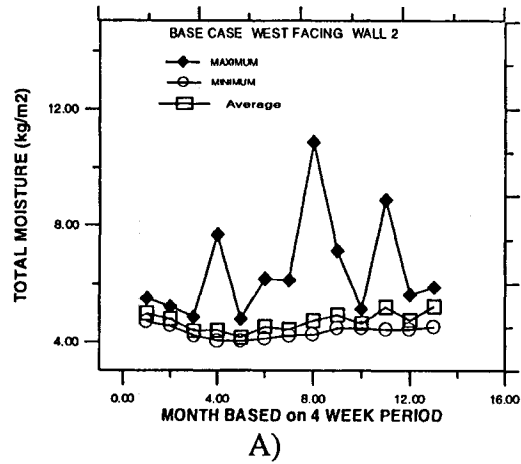
FIGURE C15
TORONTO

A)

B)

C)

D)

E)

F)
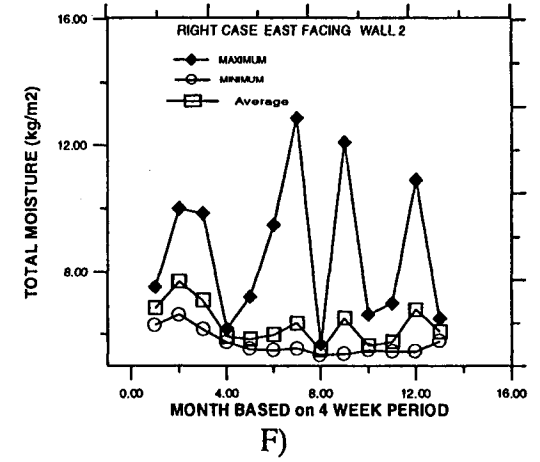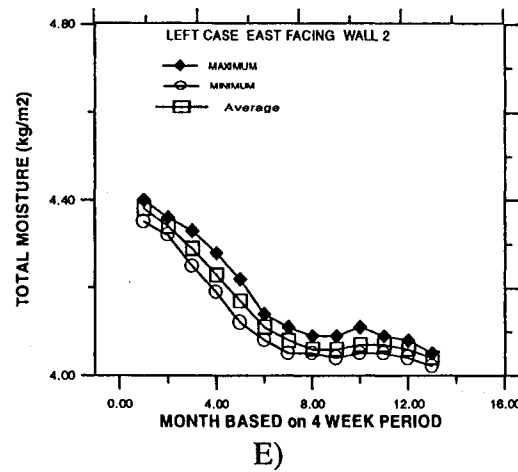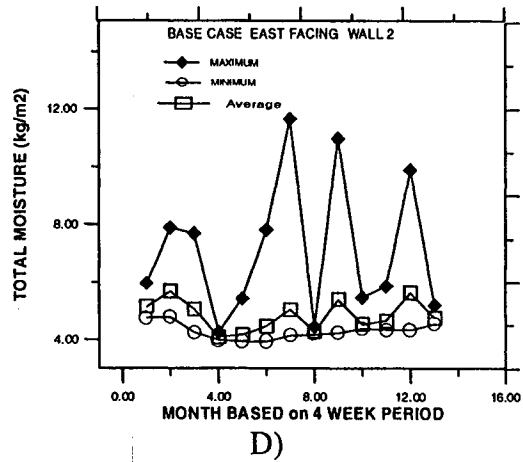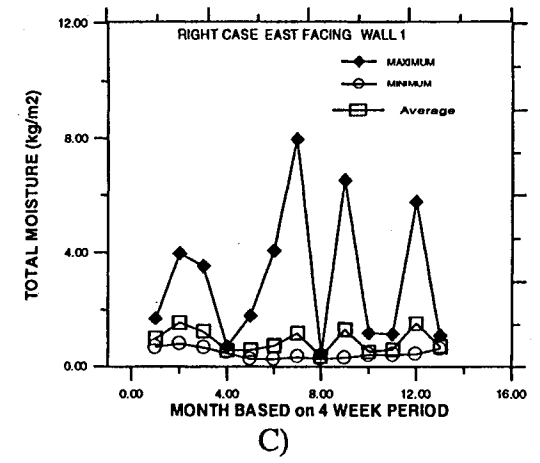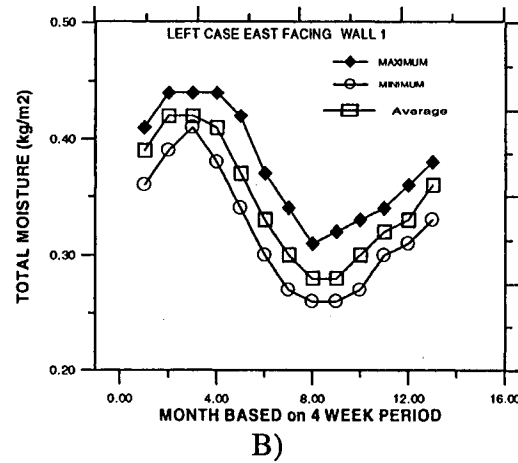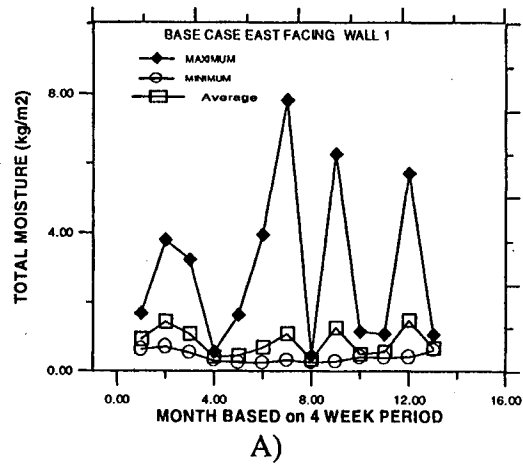
FIGURE C16
TORONTO
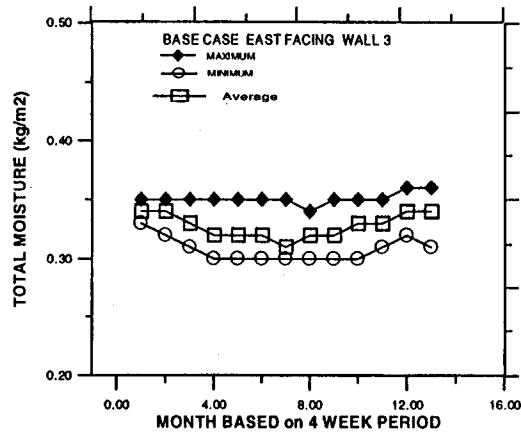
A)
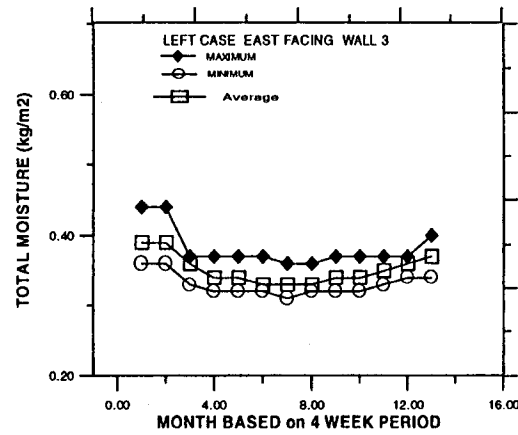
B)
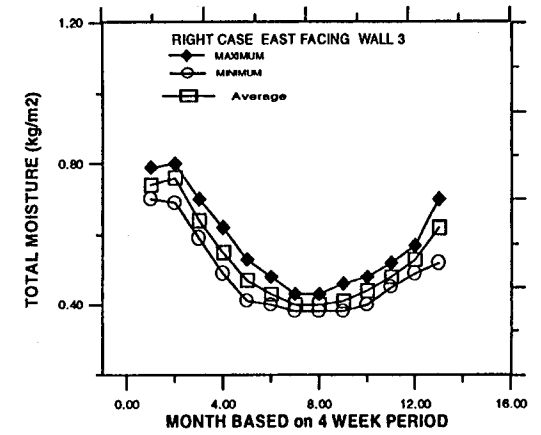
C)
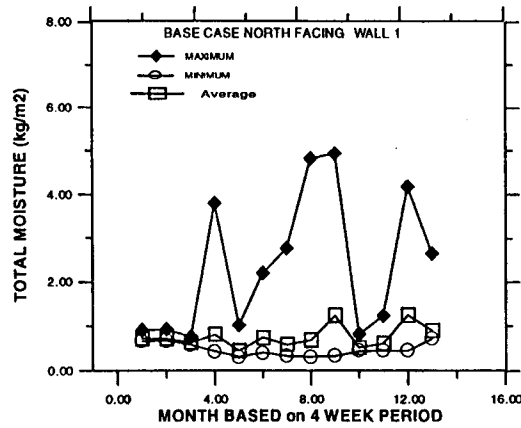
D)
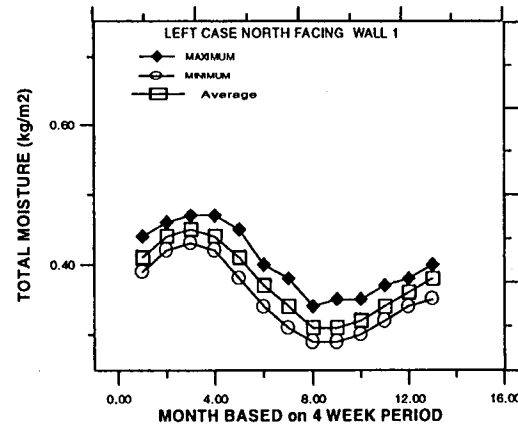
E)
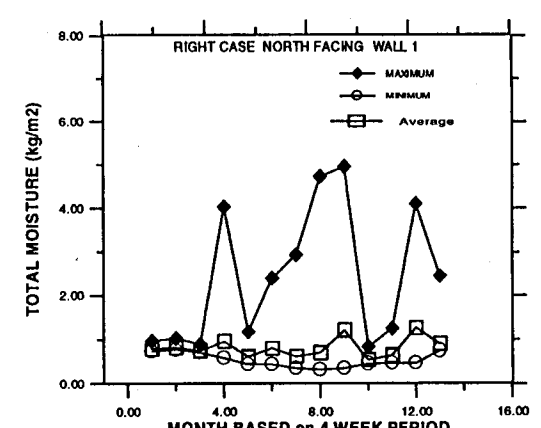
F)

FIGURE C17
TORONTO

A)

B)

C)

B)

E)

F)
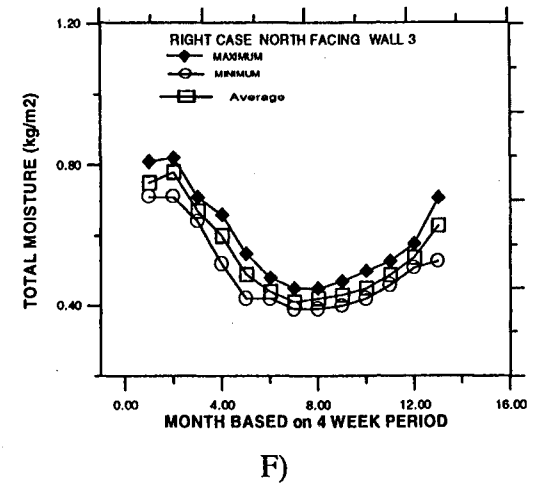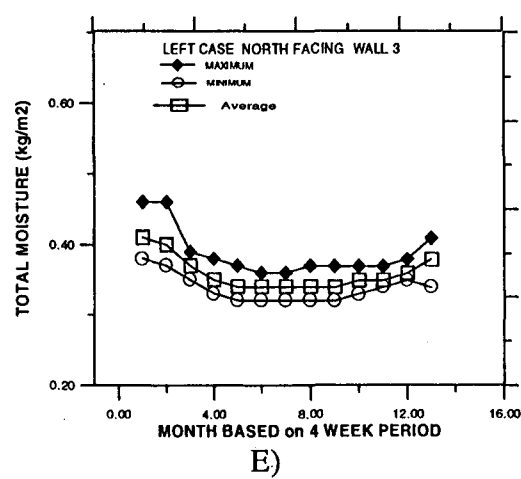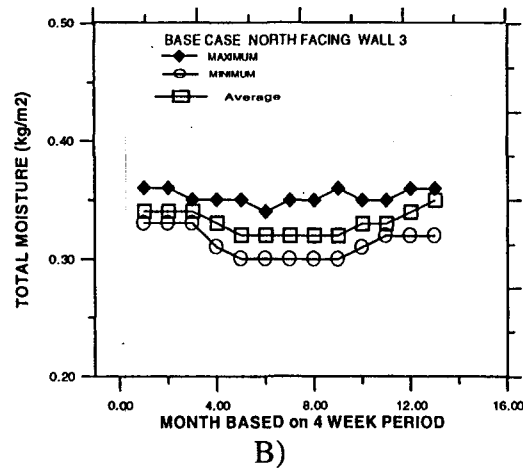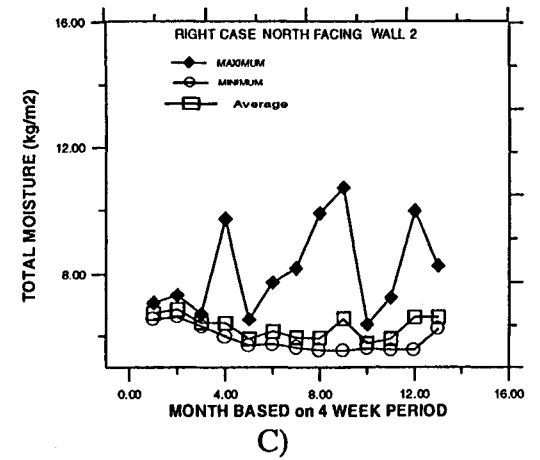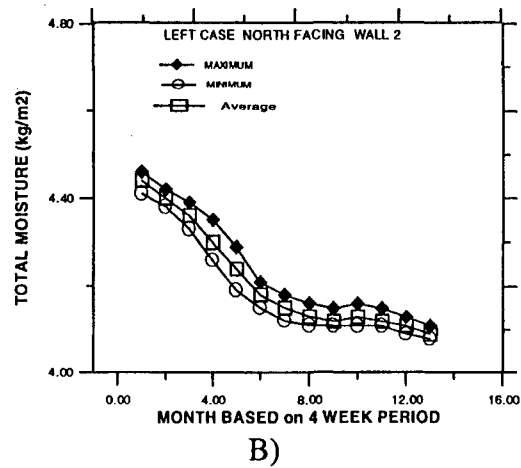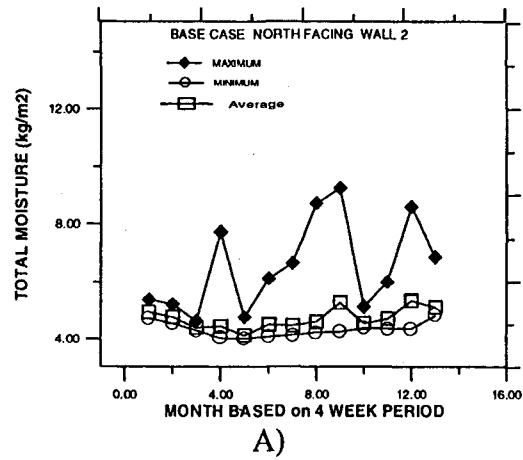
FIGURE C18
TORONTO

A)

B)

C)

D)

E)

F)
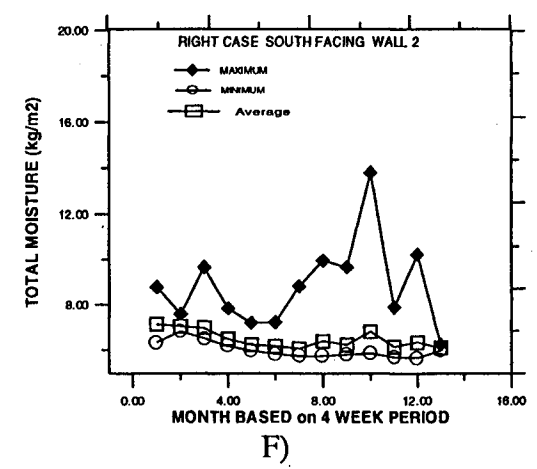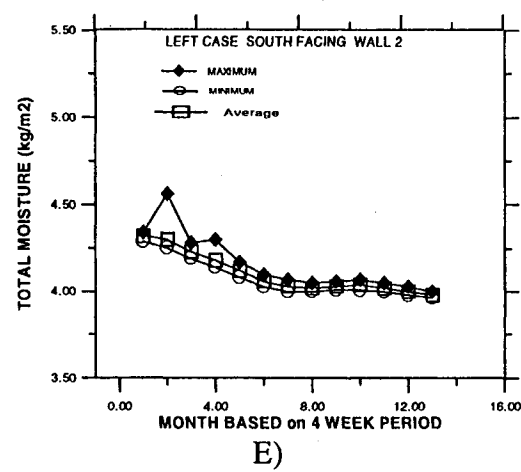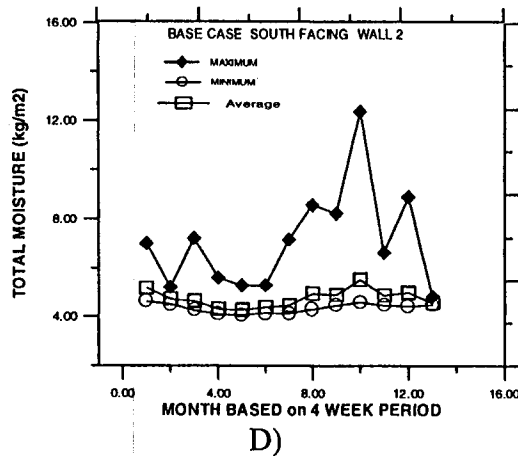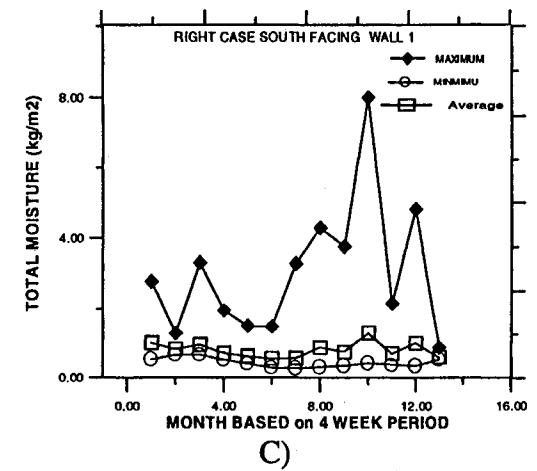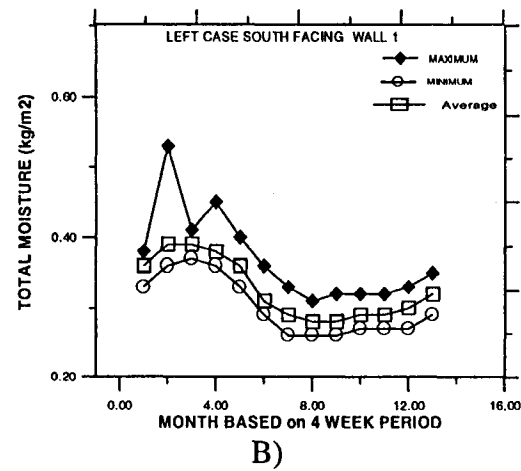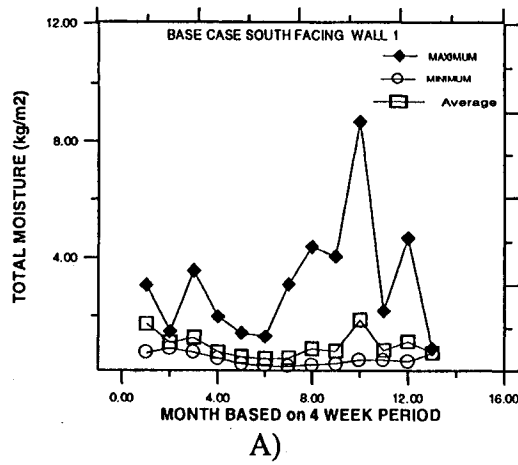
FIGURE C19
MONTREAL
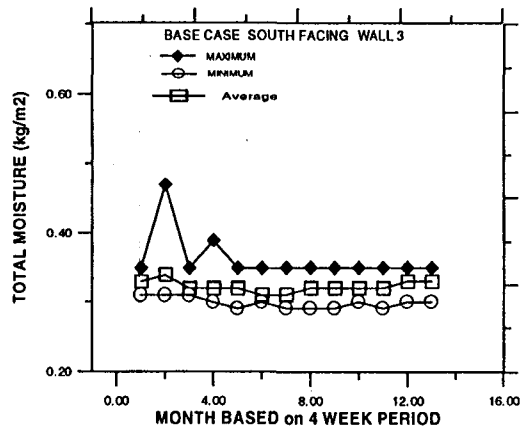
A)
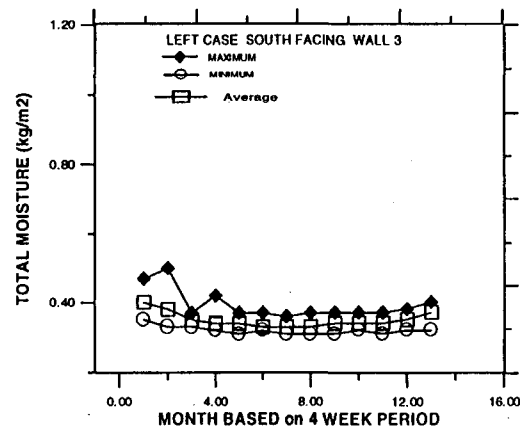
B)
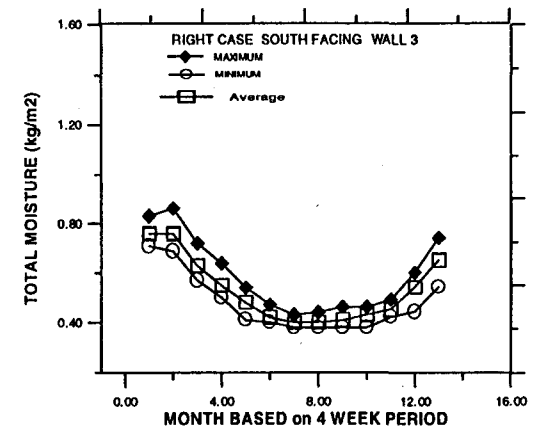
C)
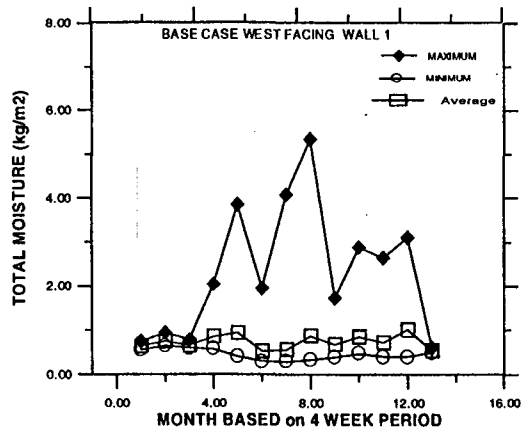
D)
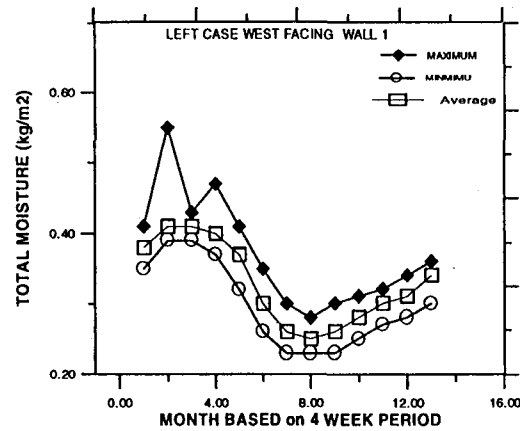
E)
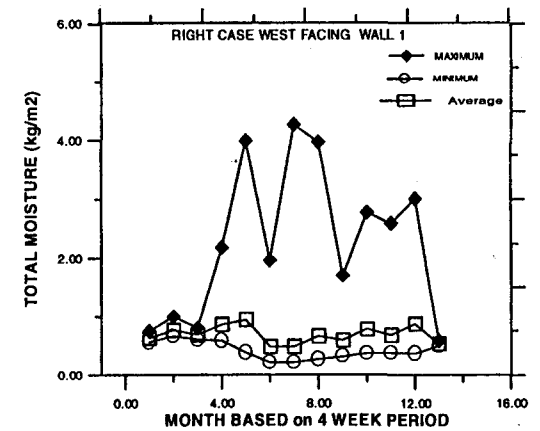
F)

FIGURE C20
MONTREAL
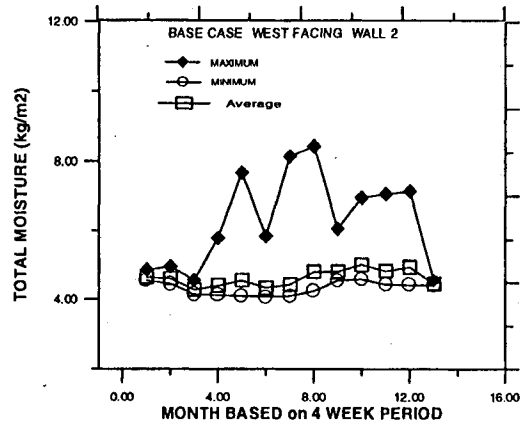
A)
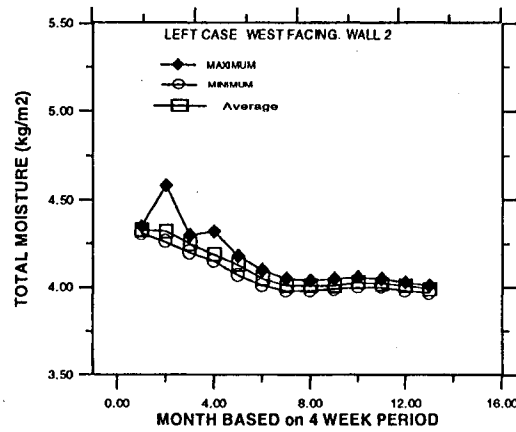
B)
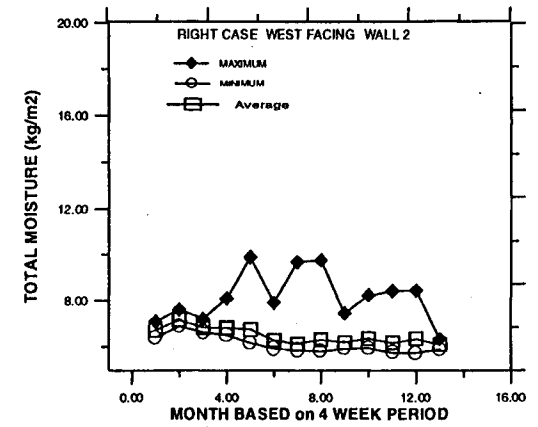
C)
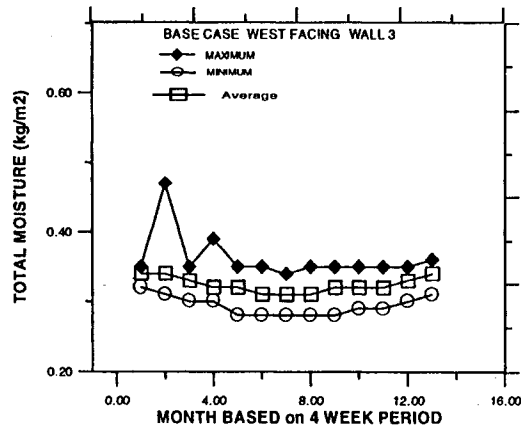
D)
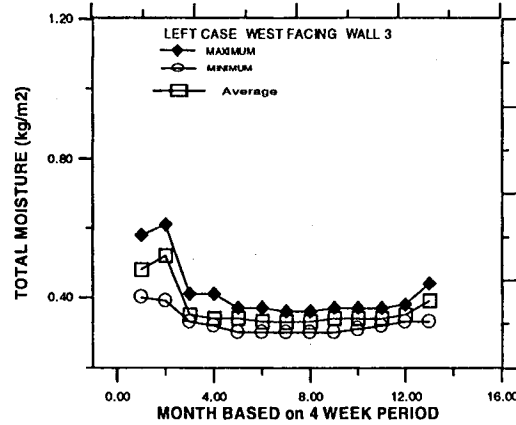
E)
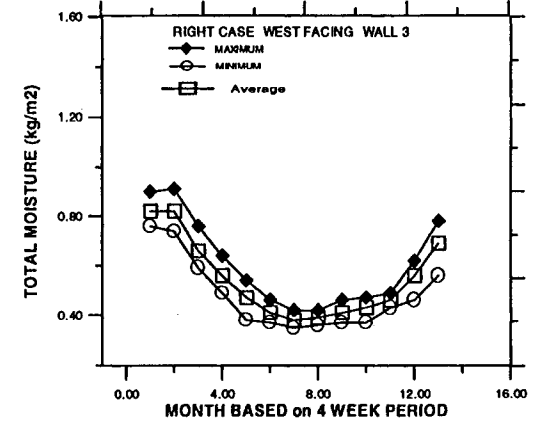
F)

FIGURE C21
MONTREAL

A)

B)

C)

D)

E)

F)
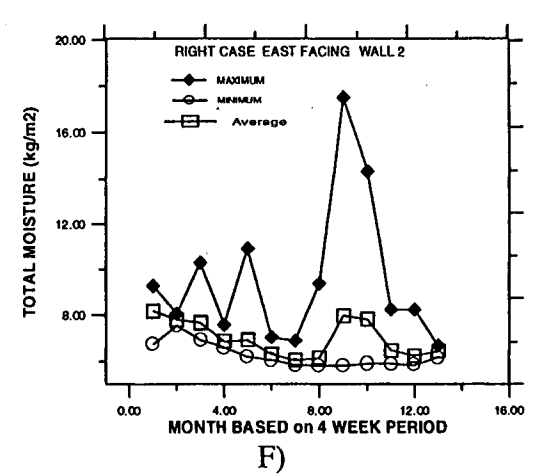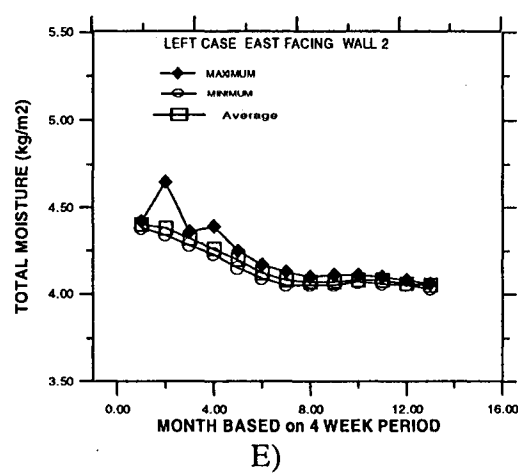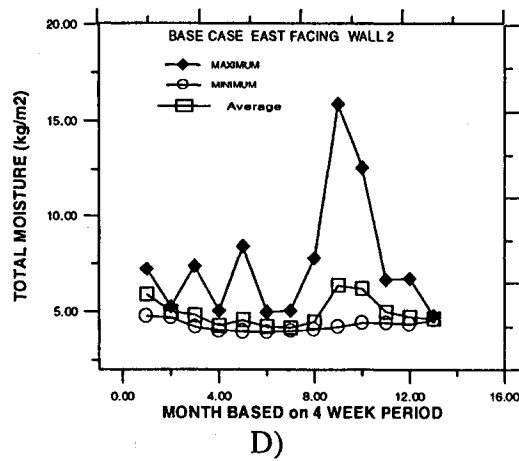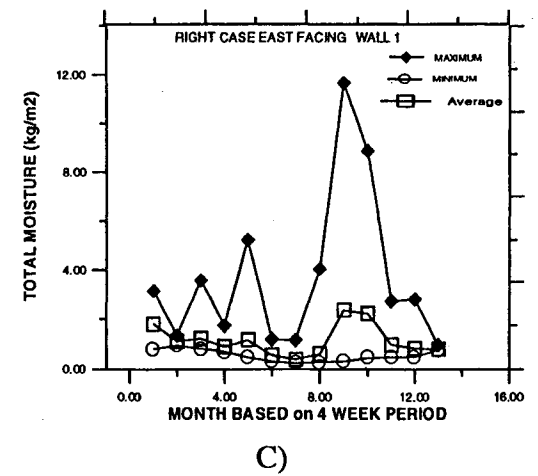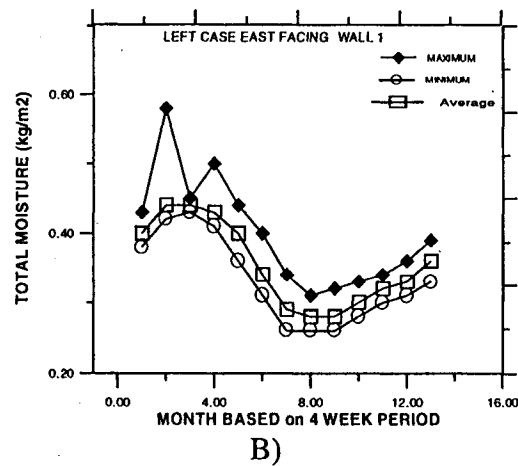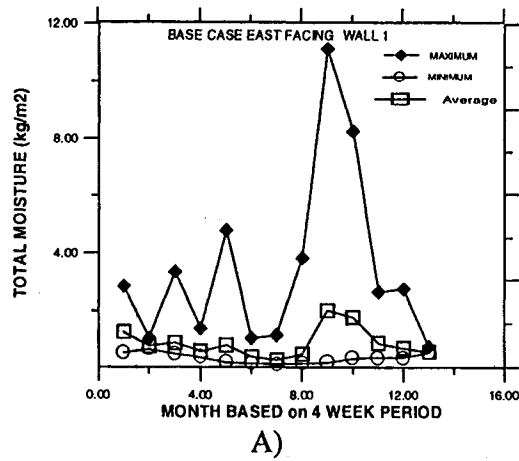
FIGURE C22
MONTREAL
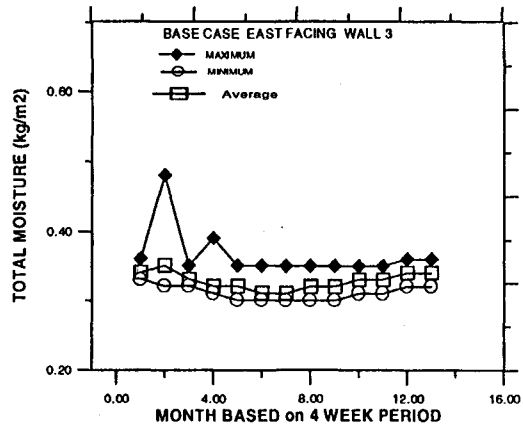
A)
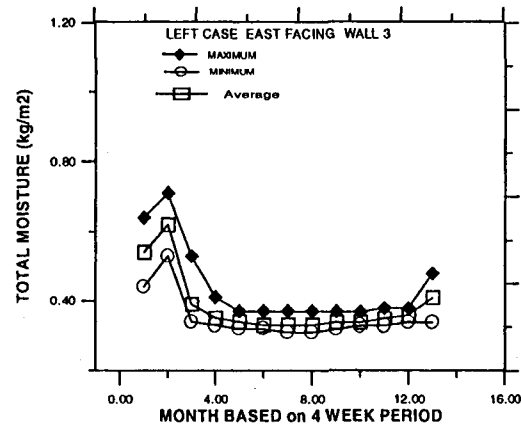
B)
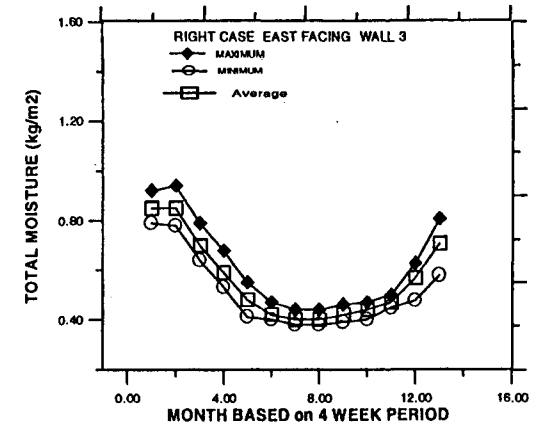
C)
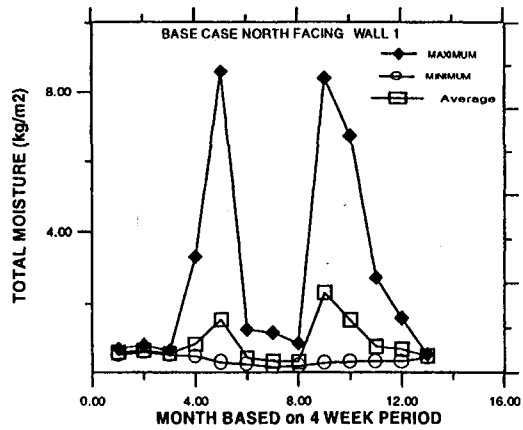
D)
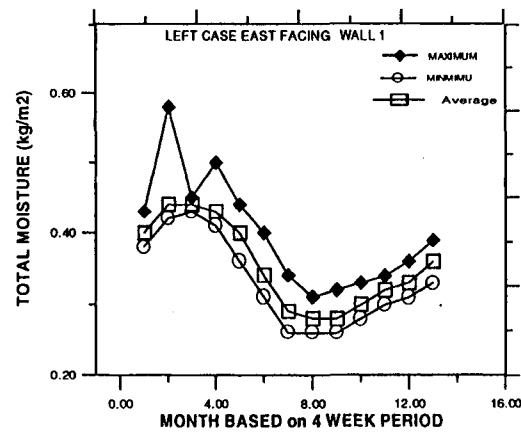
E)
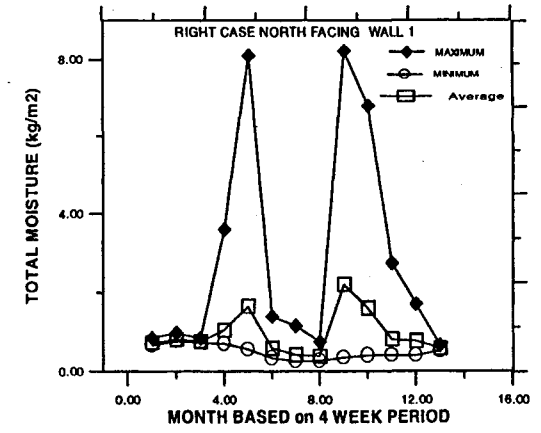
F)

FIGURE C23
MONTREAL

A)

B)

C)

D)

E)

F)
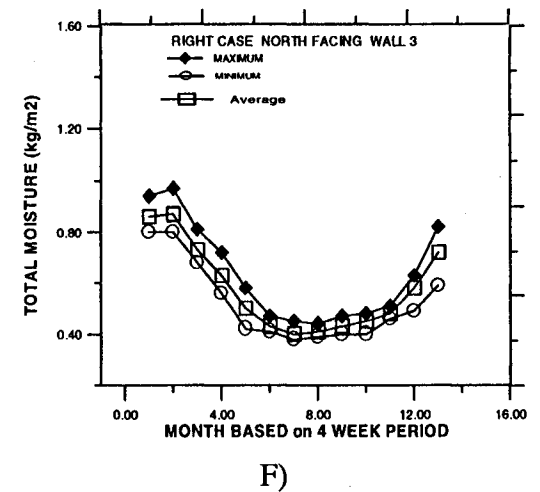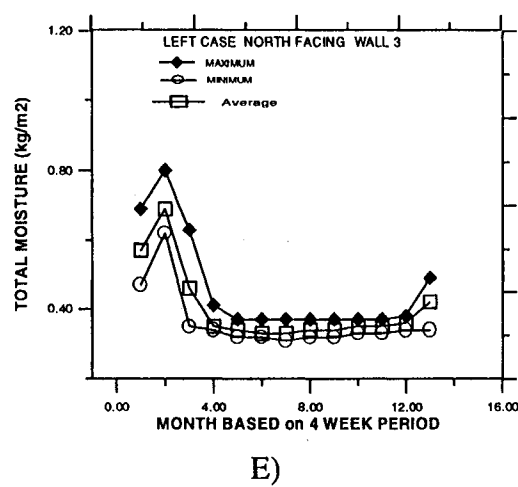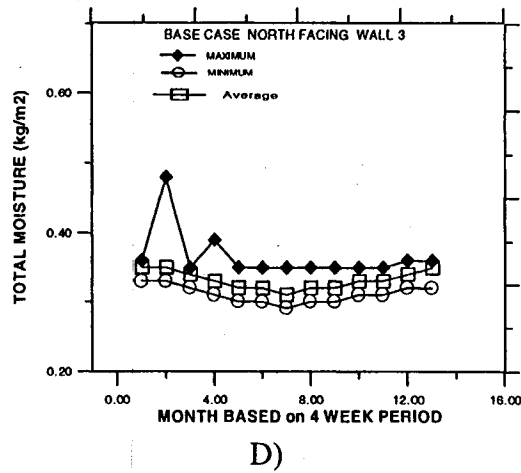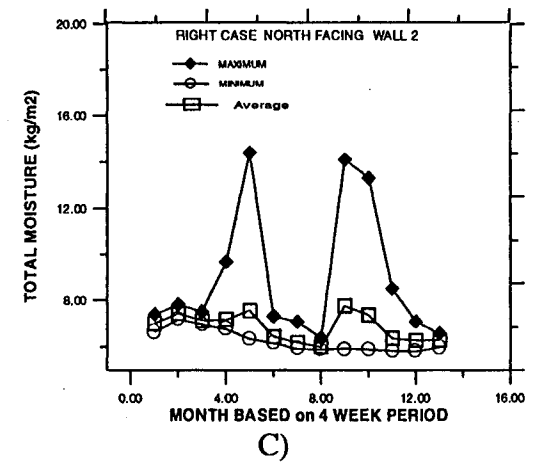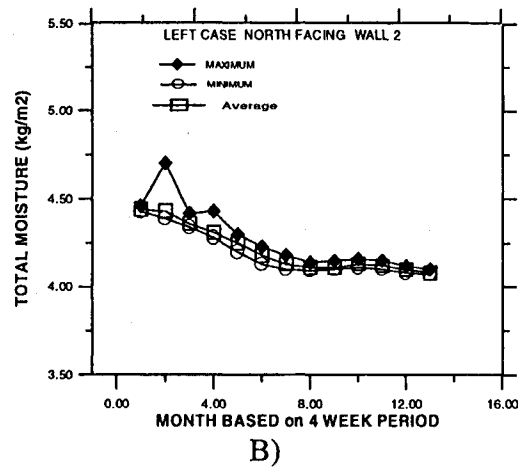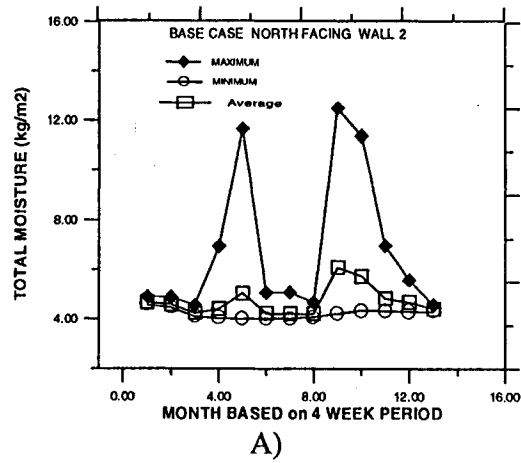
FIGURE C24
MONTREAL
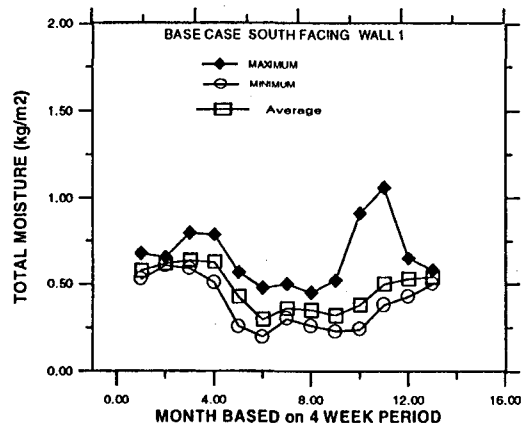
A)
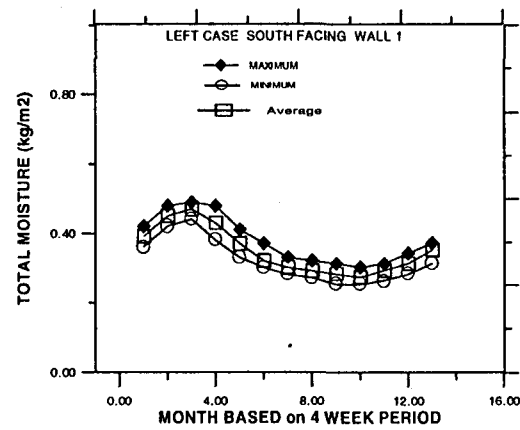
B)
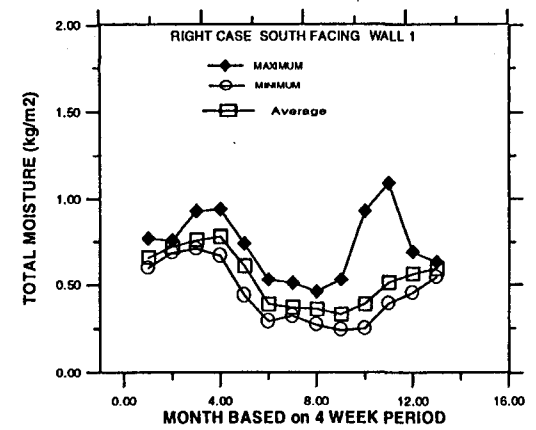
C)
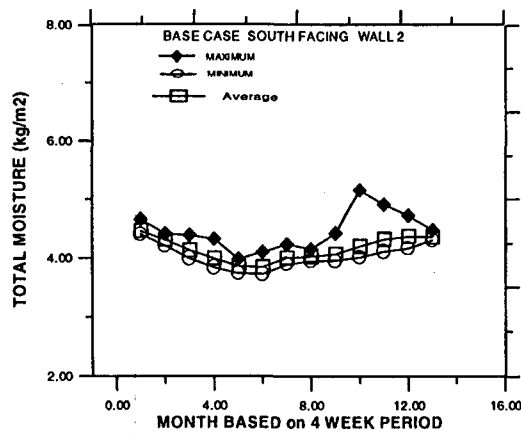
D)
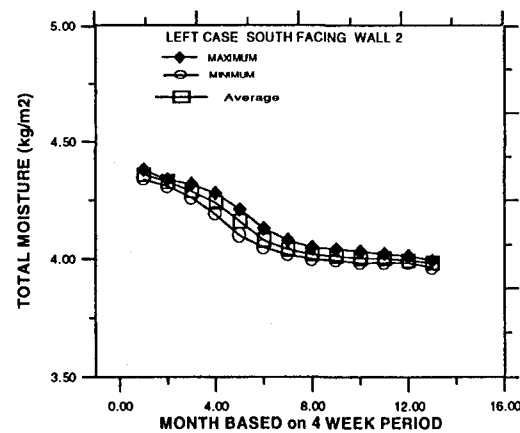
E)
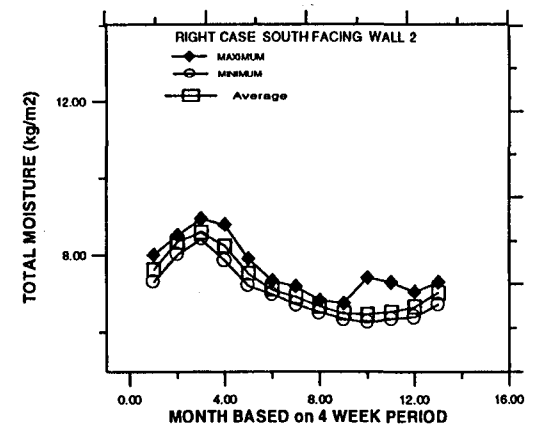
F)

FIGURE C25
WINNIPEG
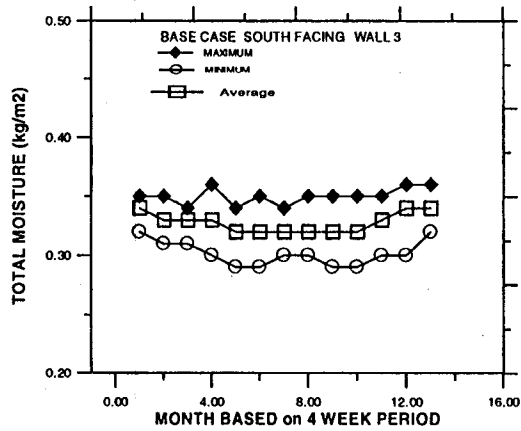
A)
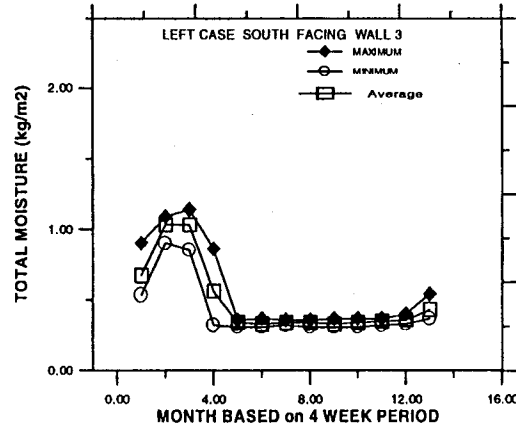
B)
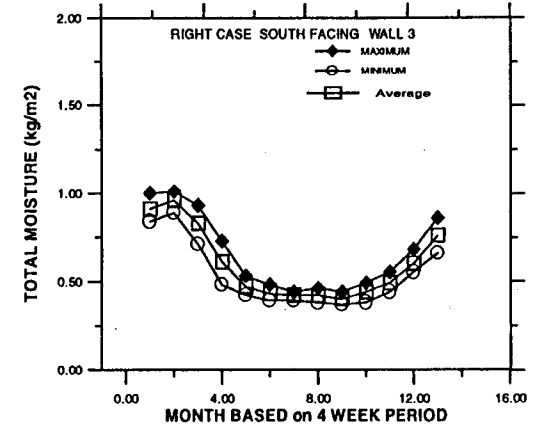
C)
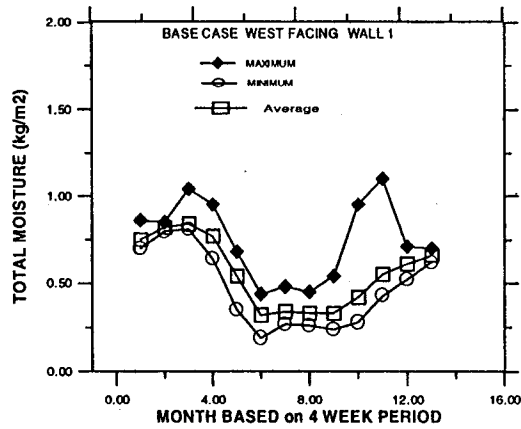
D)
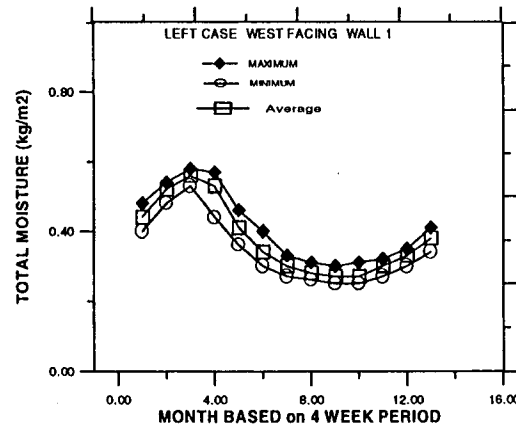
E)
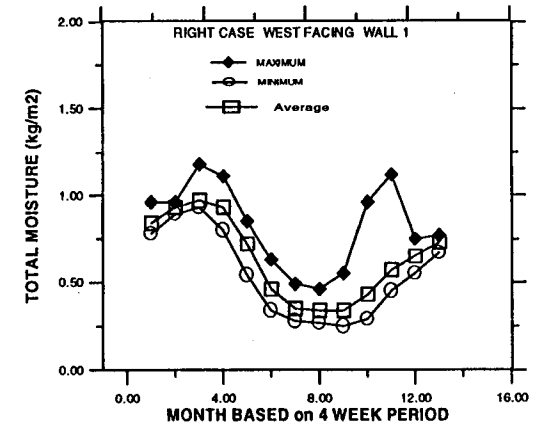
F)

FIGURE C26
WINNIPEG
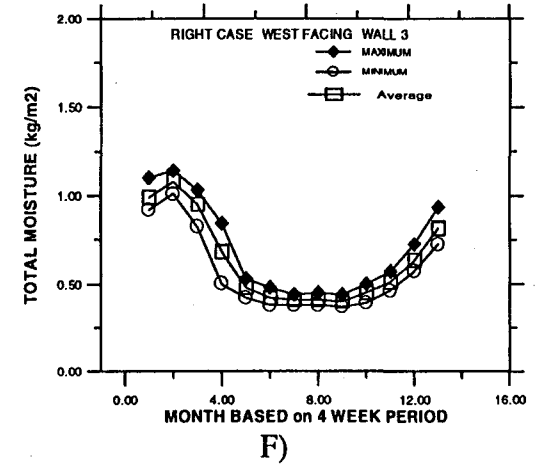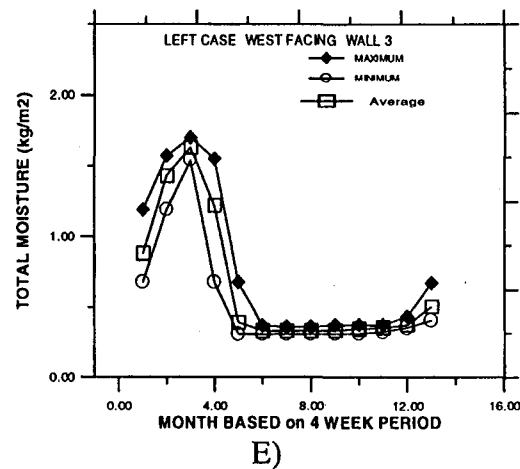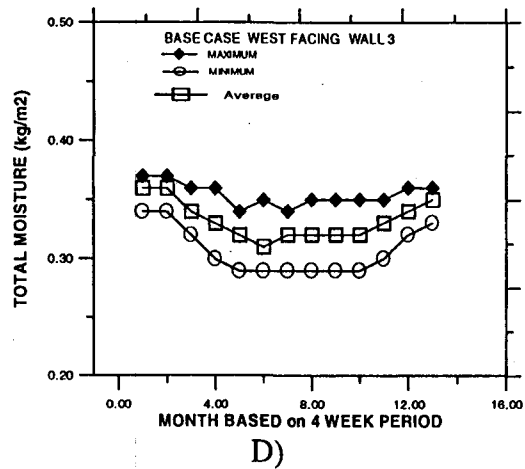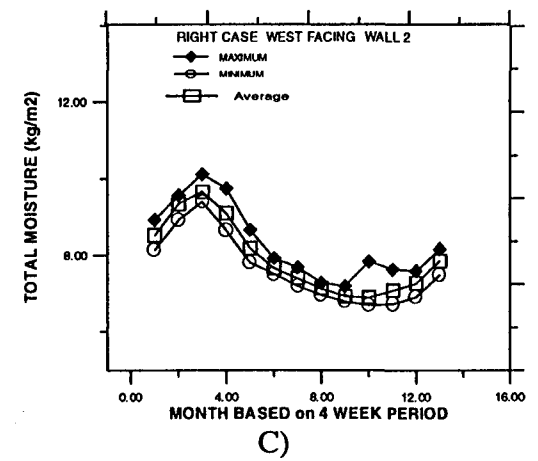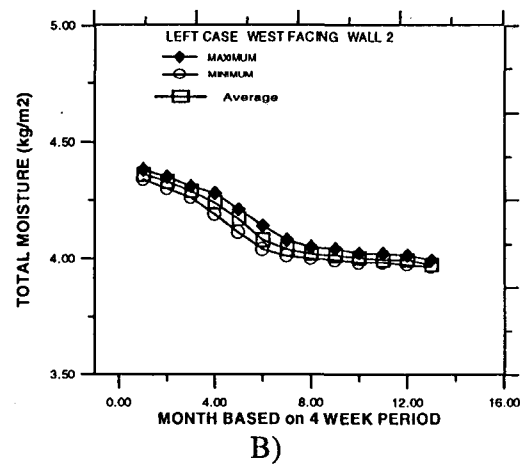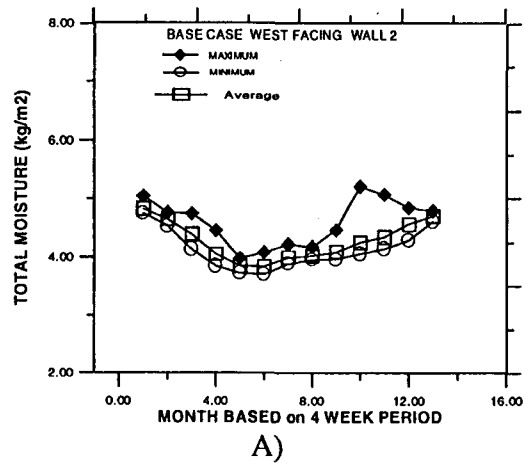
FIGURE C27
WINNIPEG

A)

B)

C)

D)

E)

F)
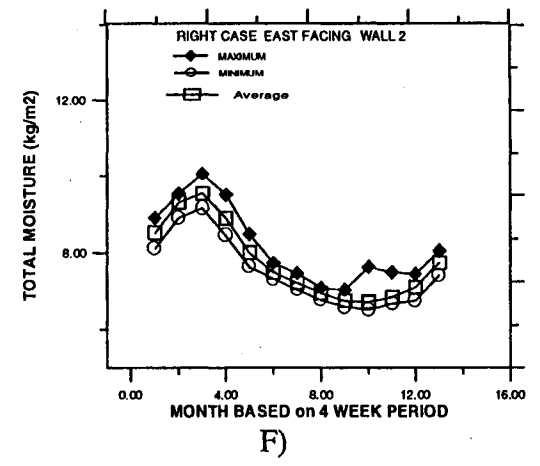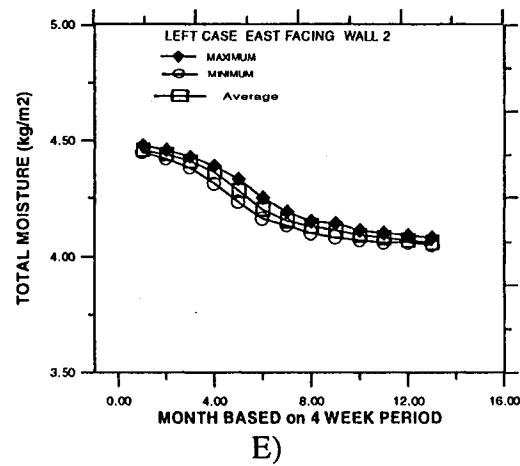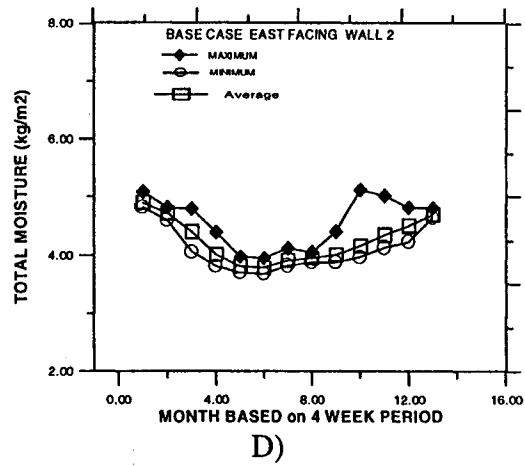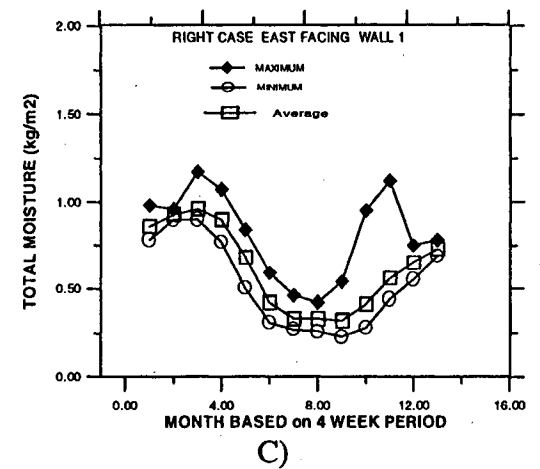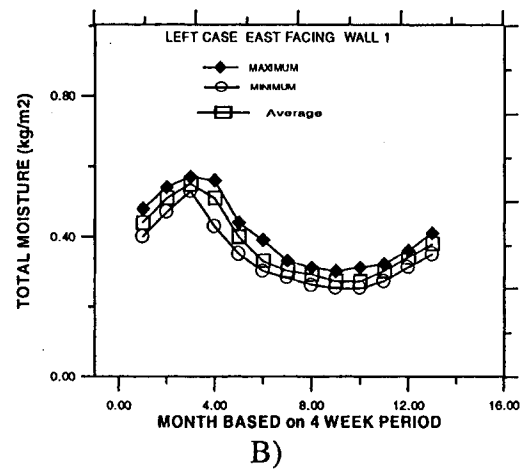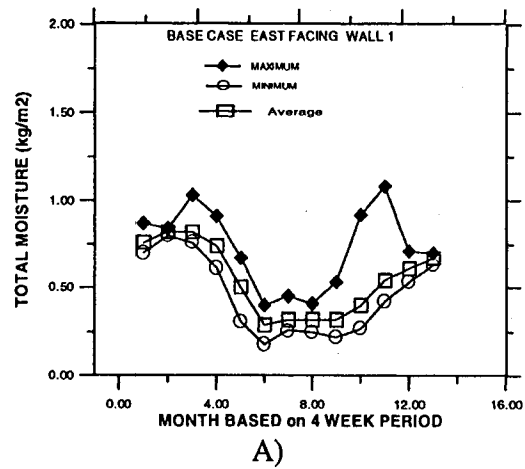
FIGURE C28
WINNIPEG

A)

B)

C)

D)

E)

F)

FIGURE C29
WINNIPEG

A)

B)

C)

D)

E)

F)
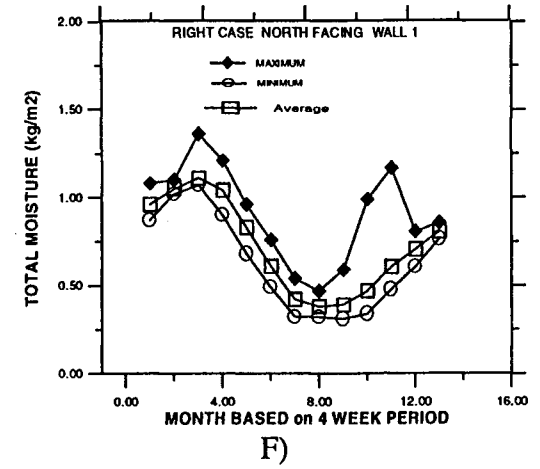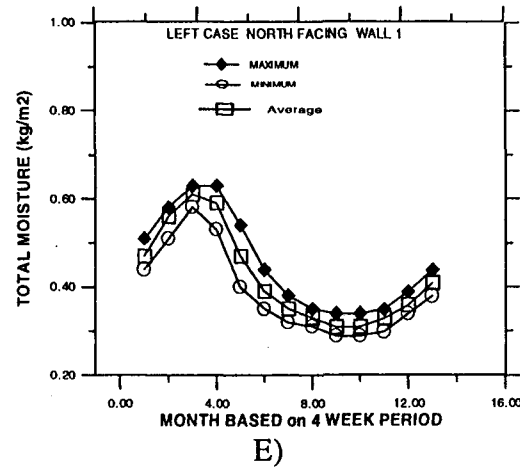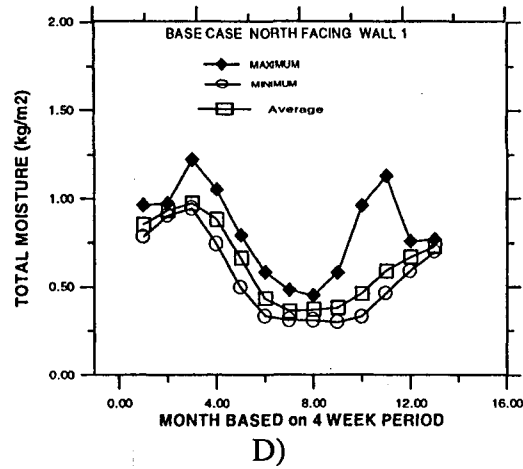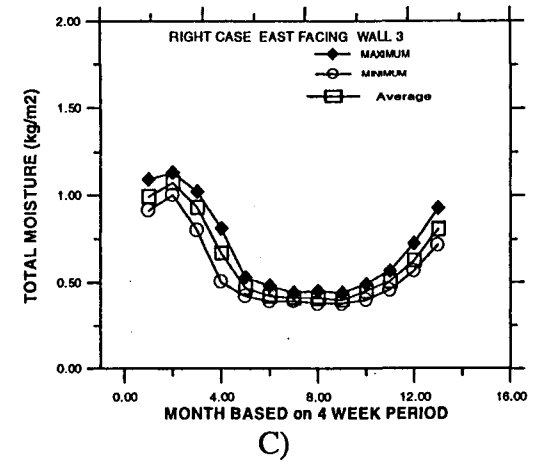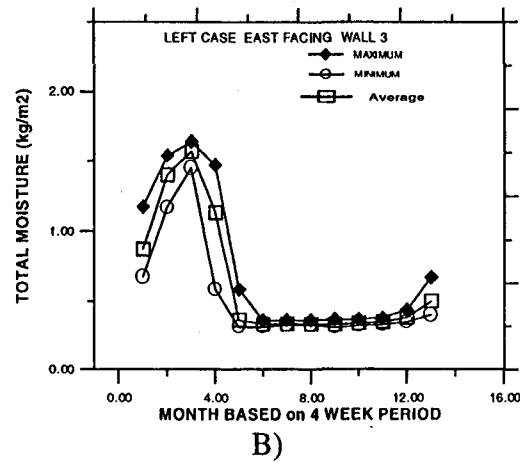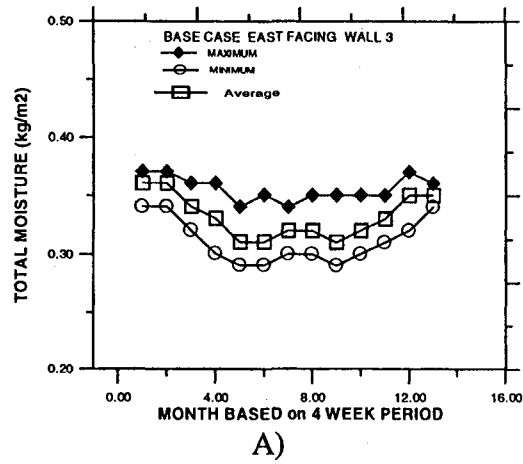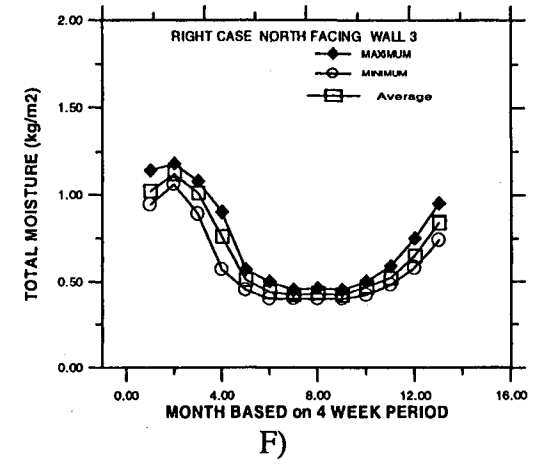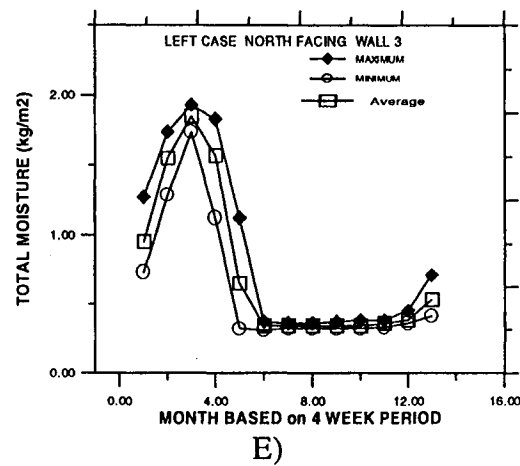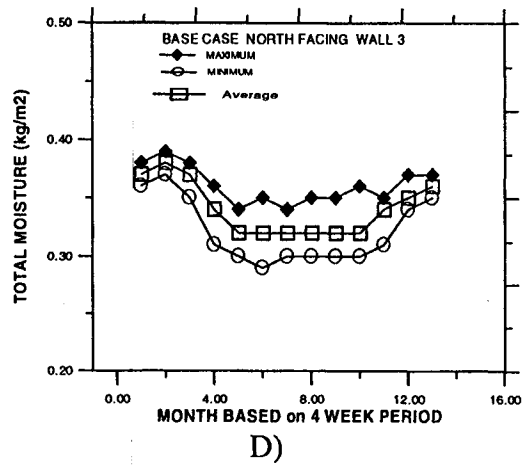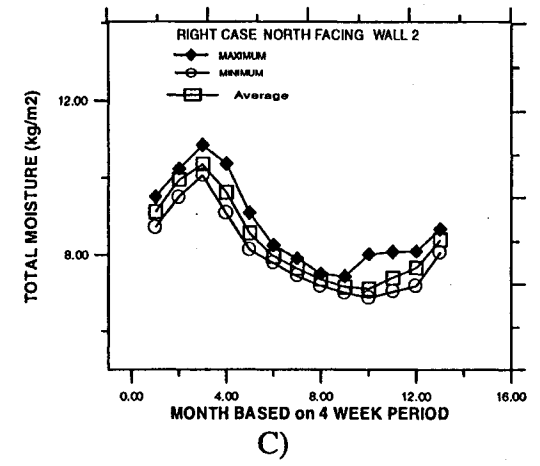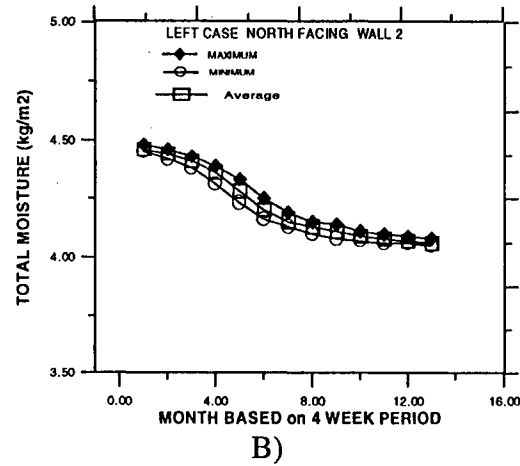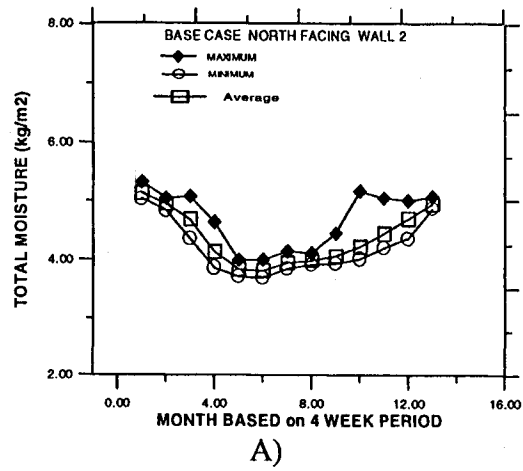
FIGURE C30
WINNIPEG
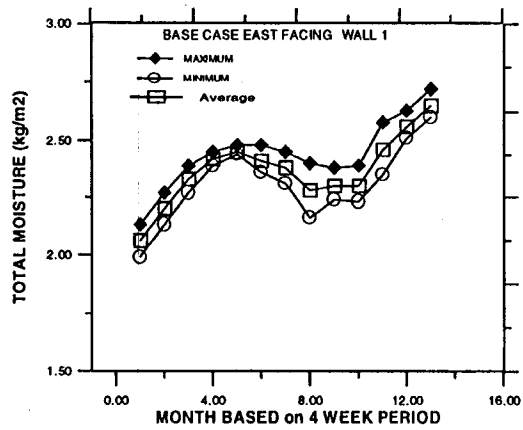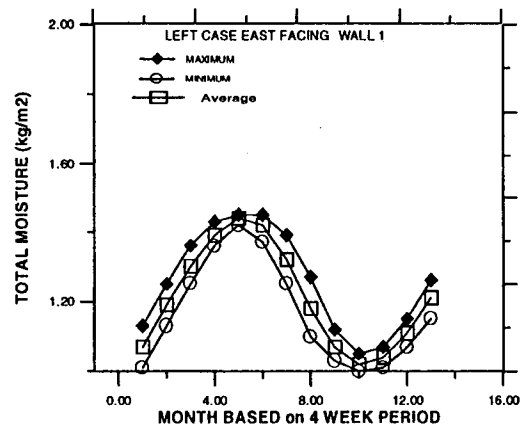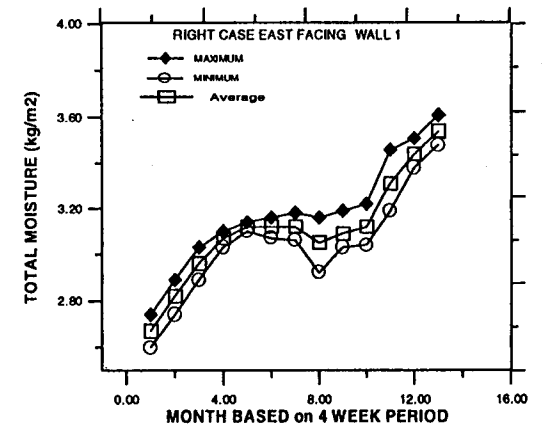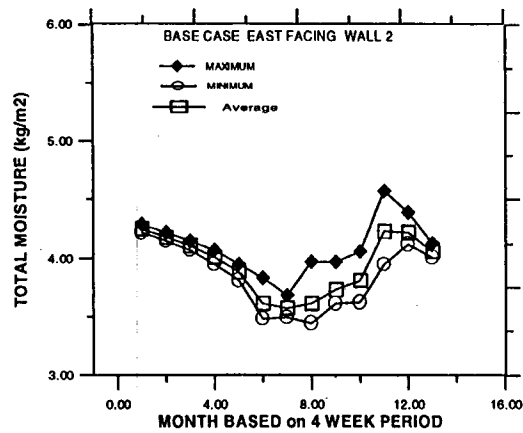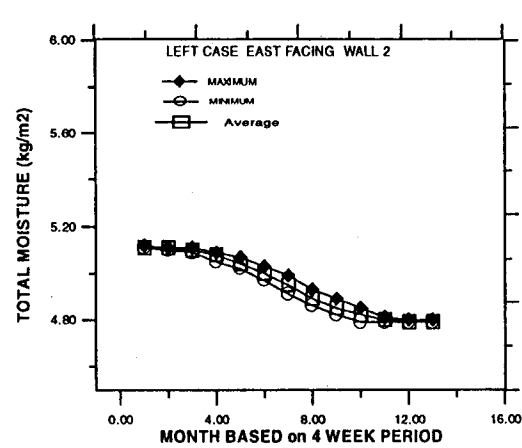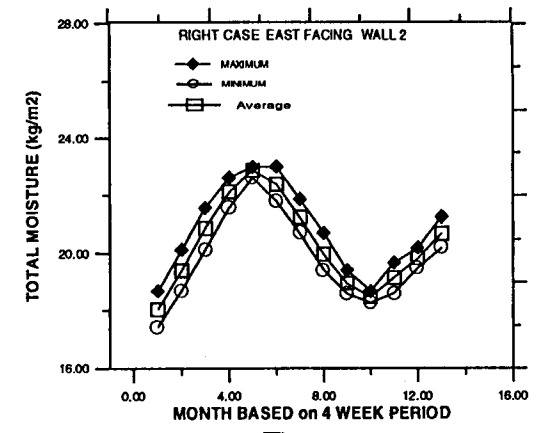
FIGURE C31
RESOLUTE

A)

B)

C)

D)

E)

F)
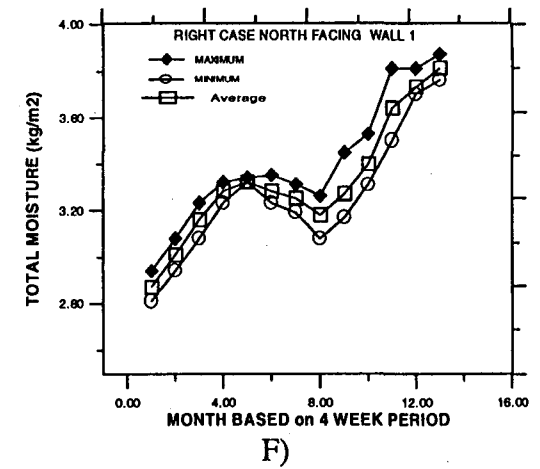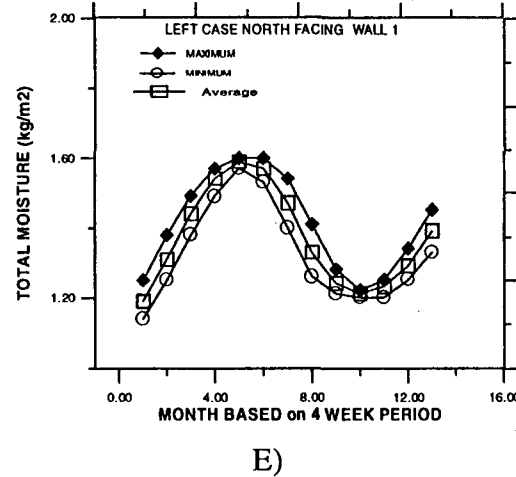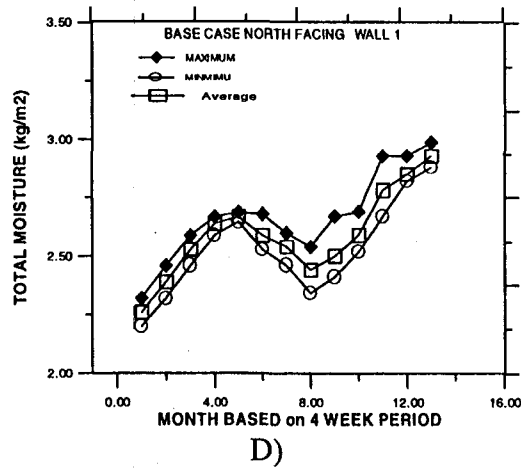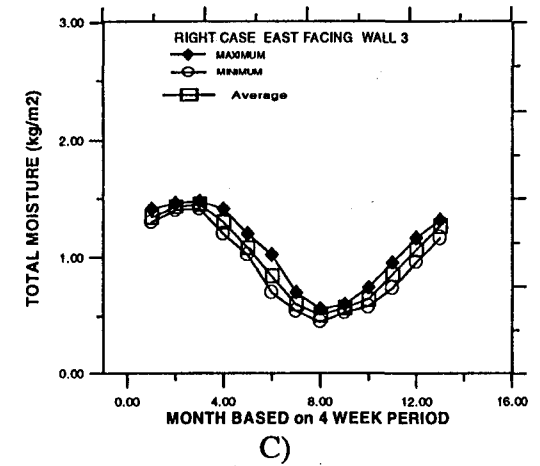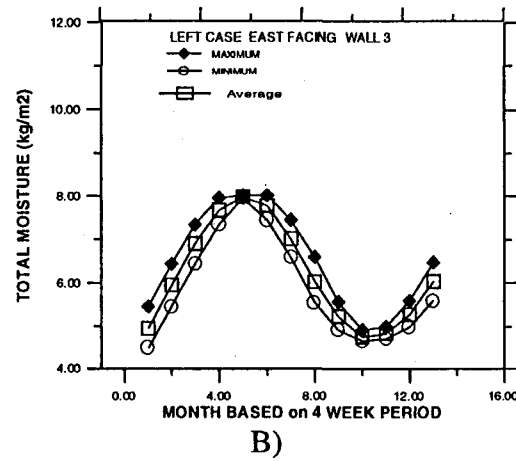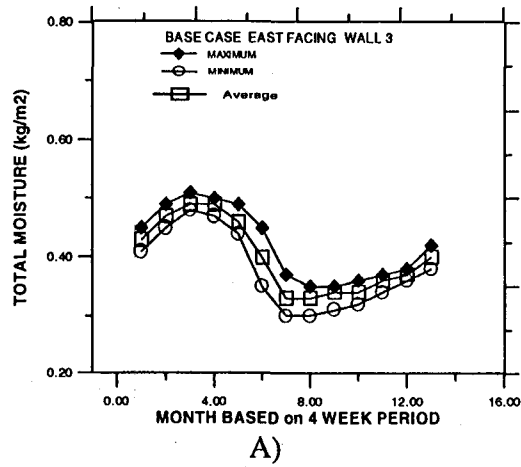
FIGURE C32
RESOLUTE

A)

B)

C)

D)

E)

F)
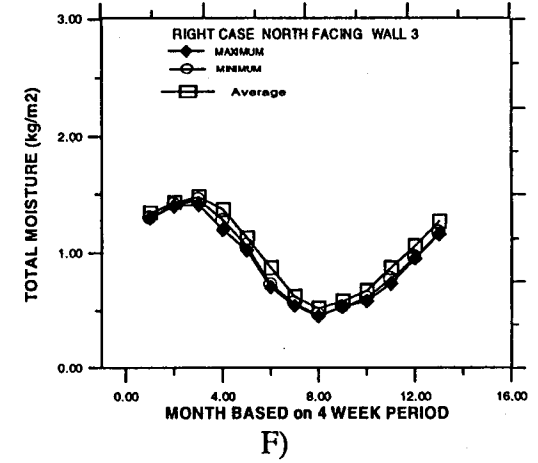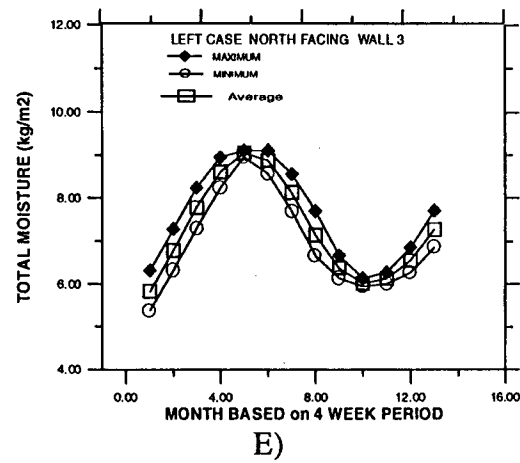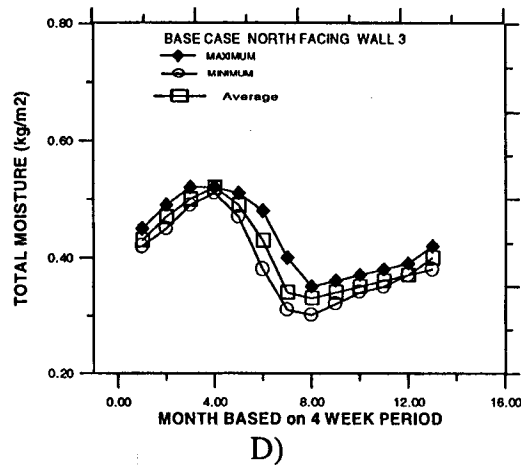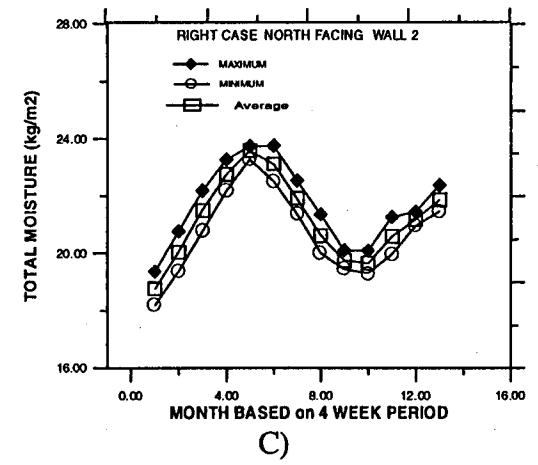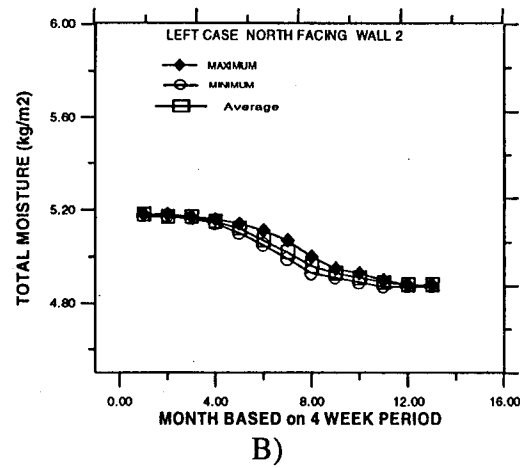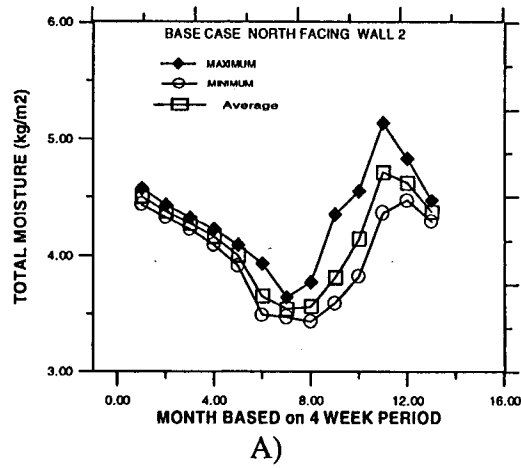
FIGURE C33
RESOLUTE
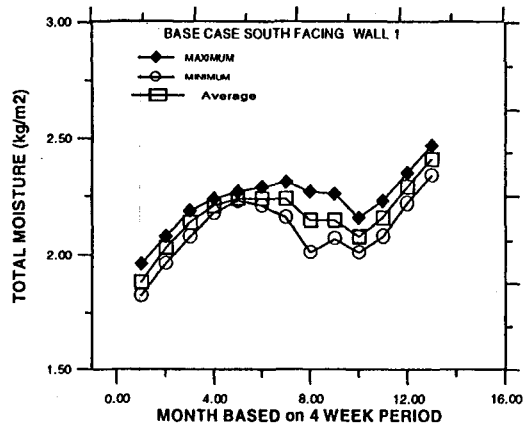
A)
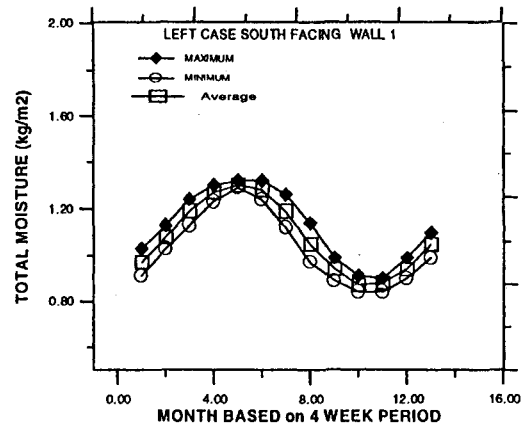
B)
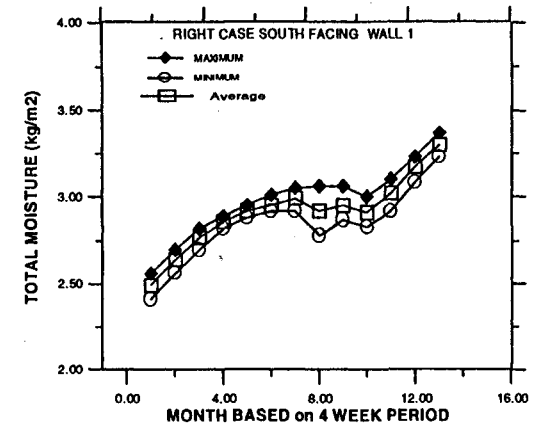
C)
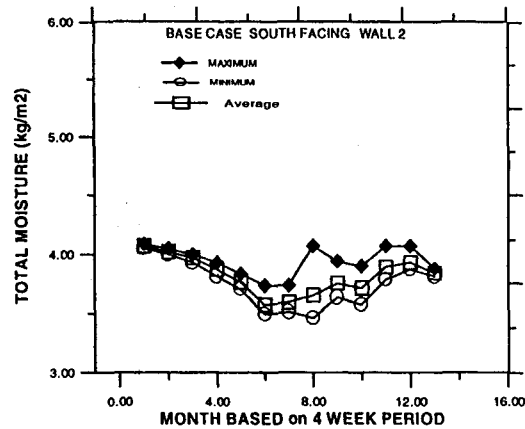
D)
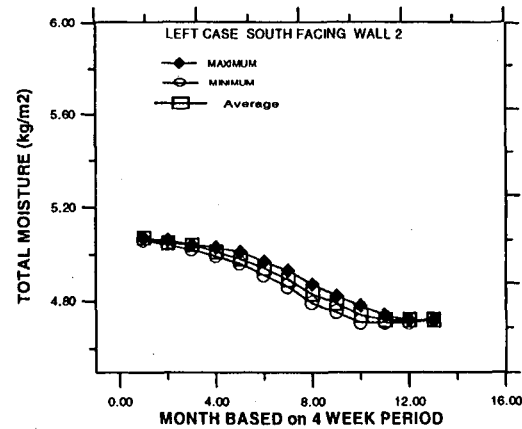
E)
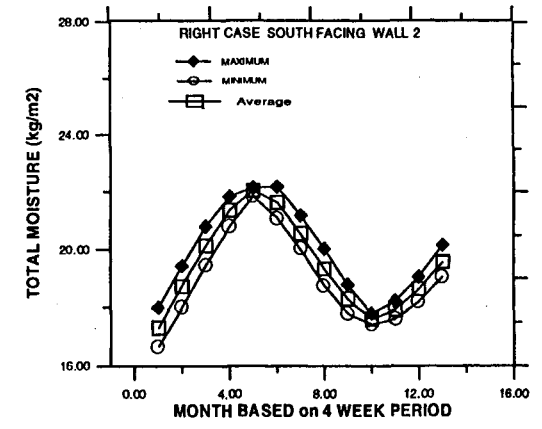
F)

FIGURE C34
RESOLUTE

A)

B)

C)

D)

E)

F)
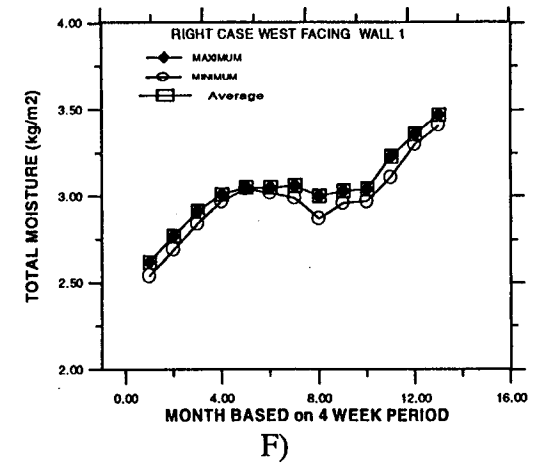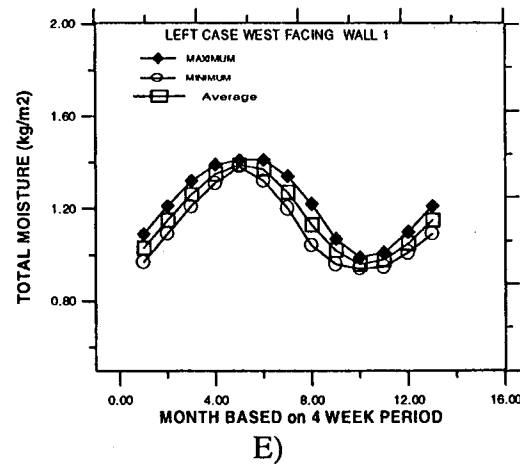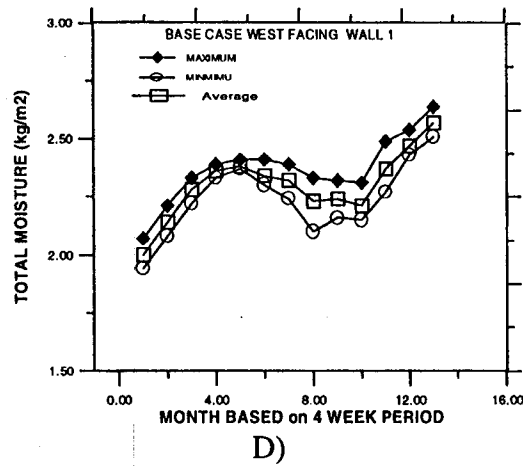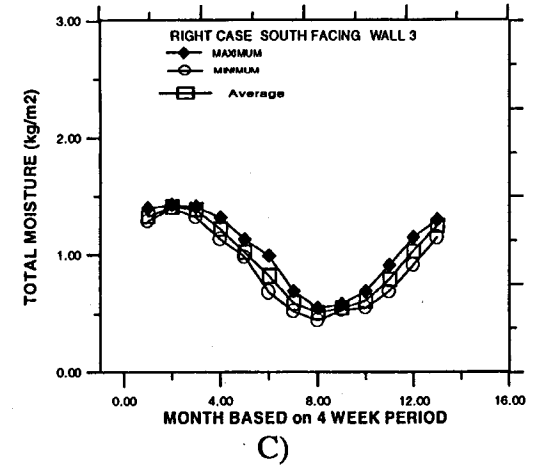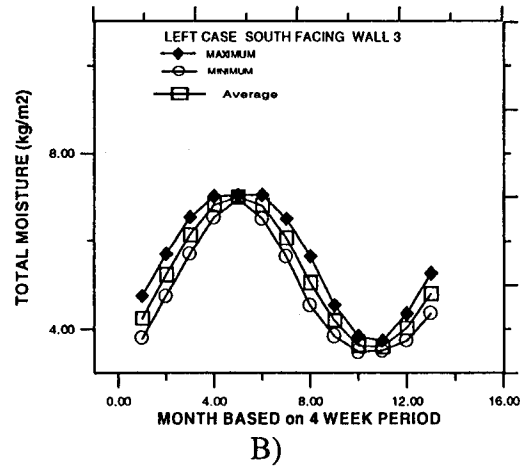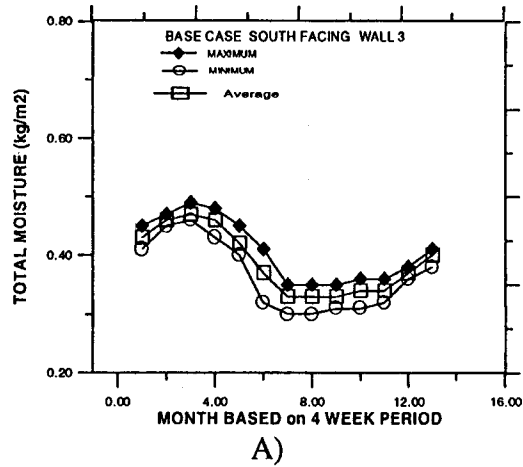
FIGURE C35
RESOLUTE

A)

B)

C)

D)

E)

F)
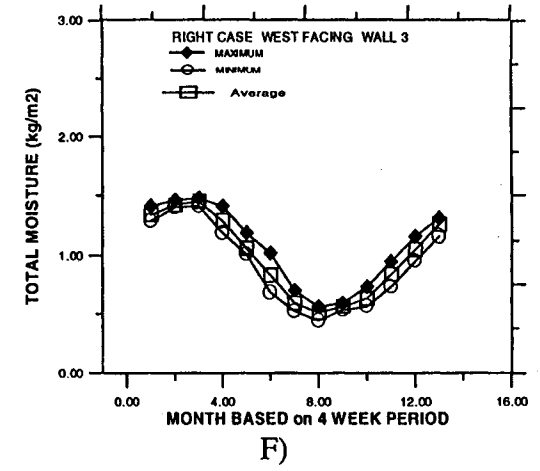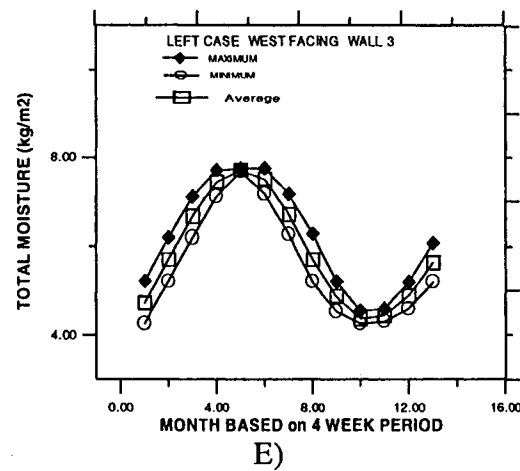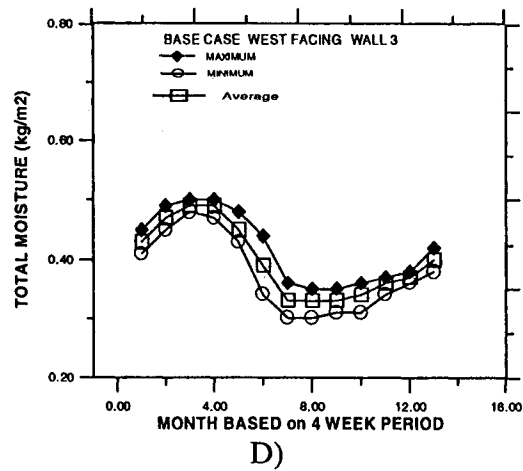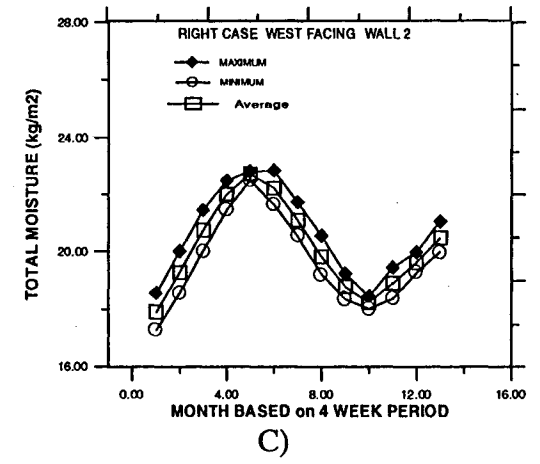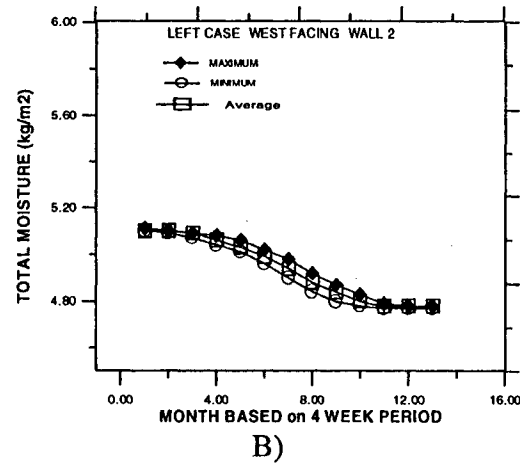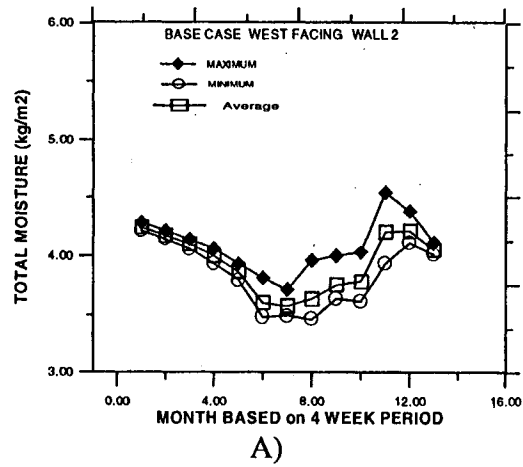
FIGURE C36
RESOLUTE

A)

B)

C)

D)

E)

F)
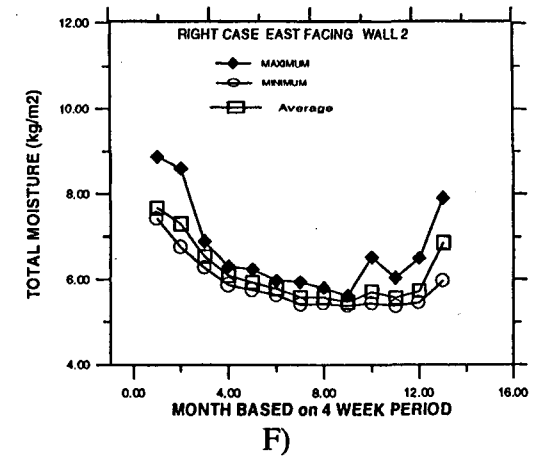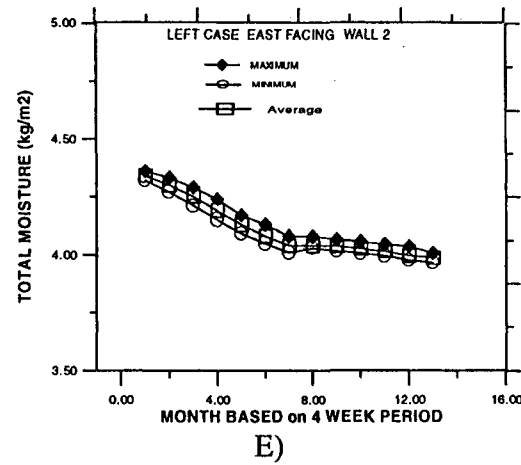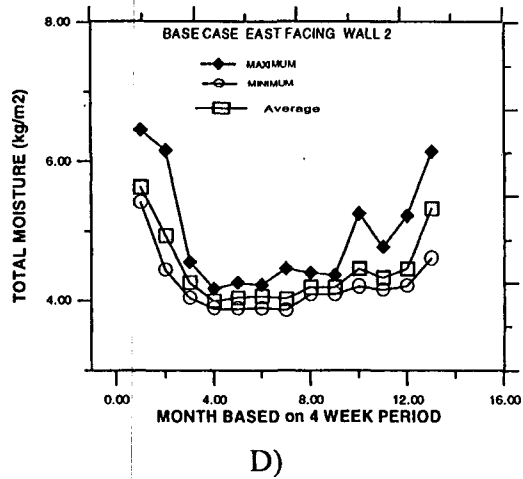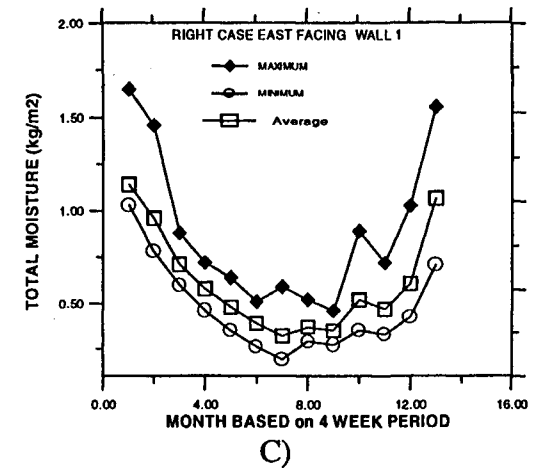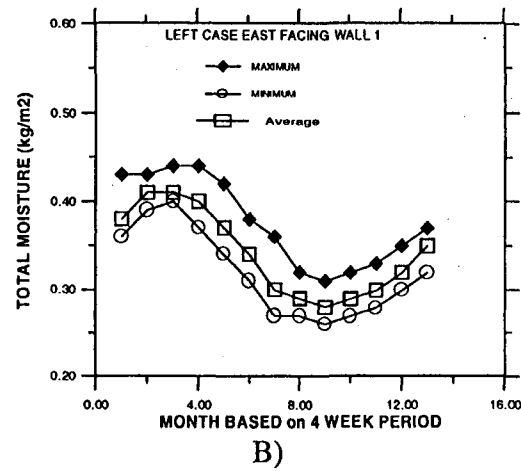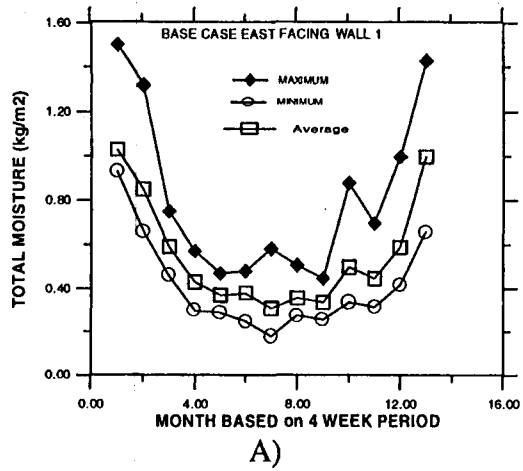
FIGURE C37
FREDERICTON
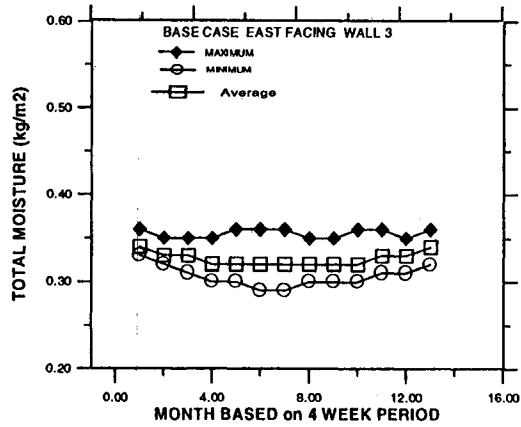
A)
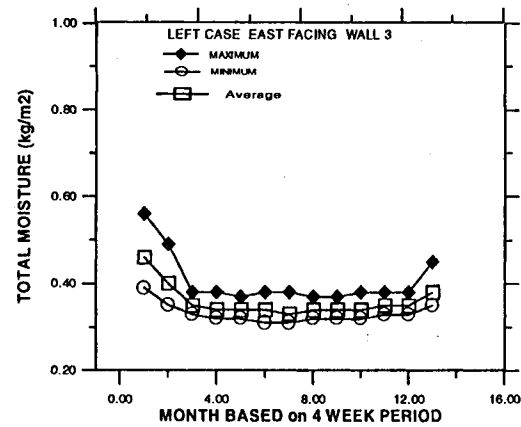
B)
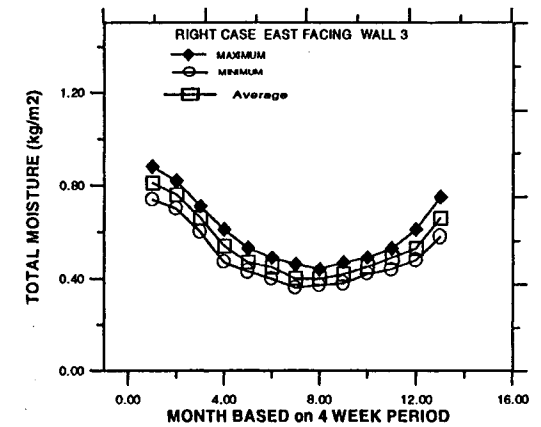
C)
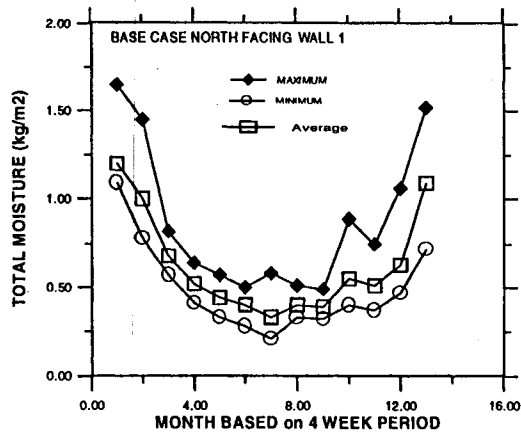
D)
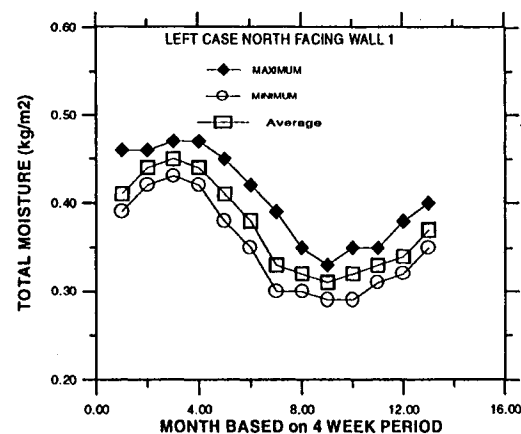
E)
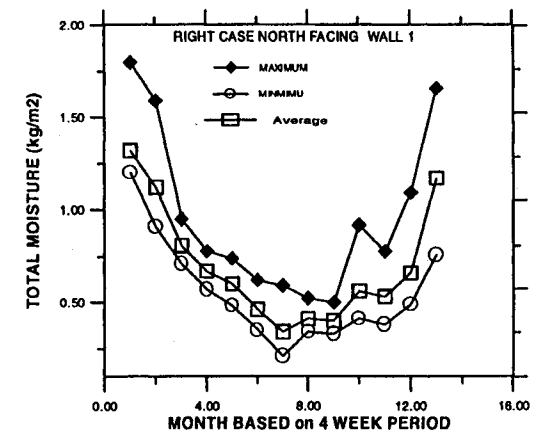
F)

FIGURE C38
FREDERICTON
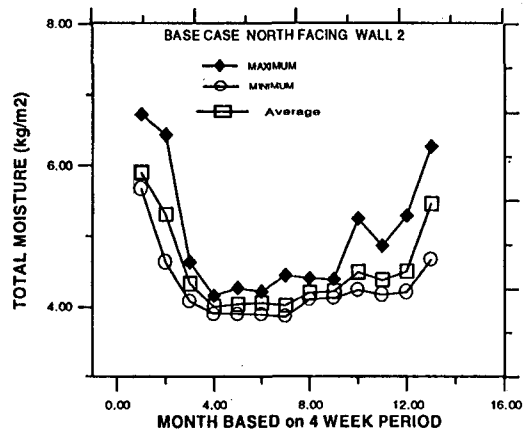
A)
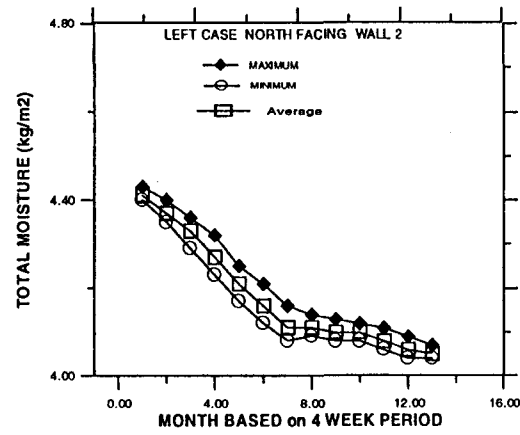
B)
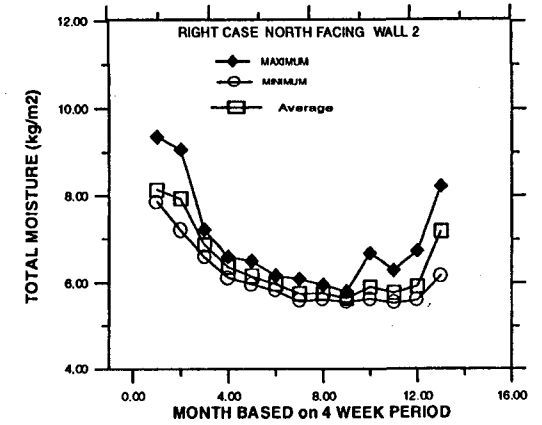
C)
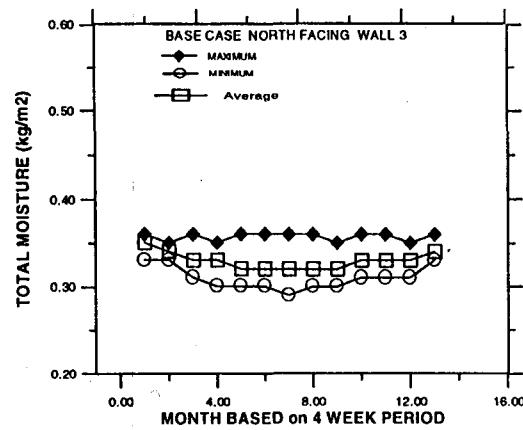
D)
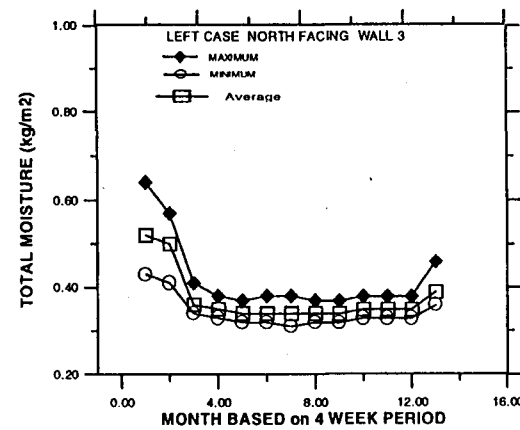
E)
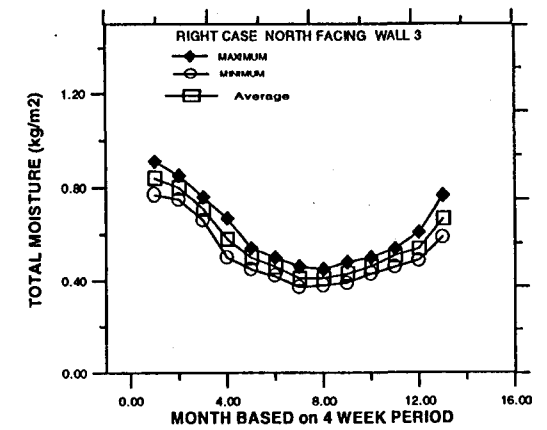
F)

FIGURE C39
FREDERICTON

A)

B)

C)

D)

E)

F)
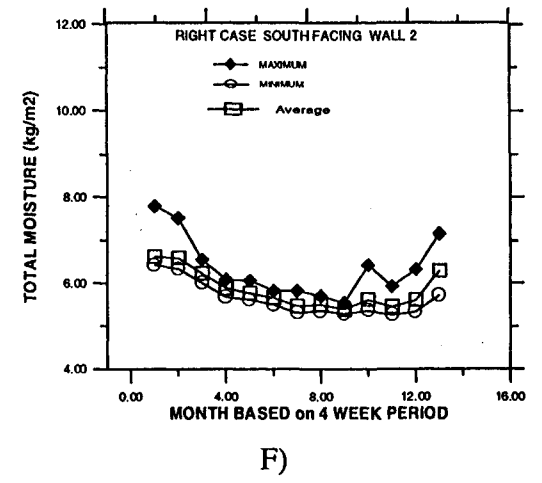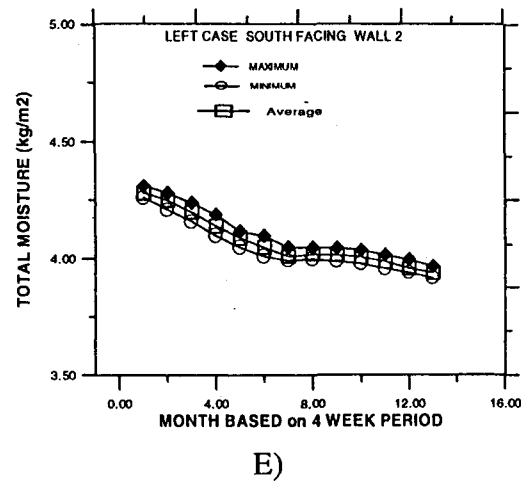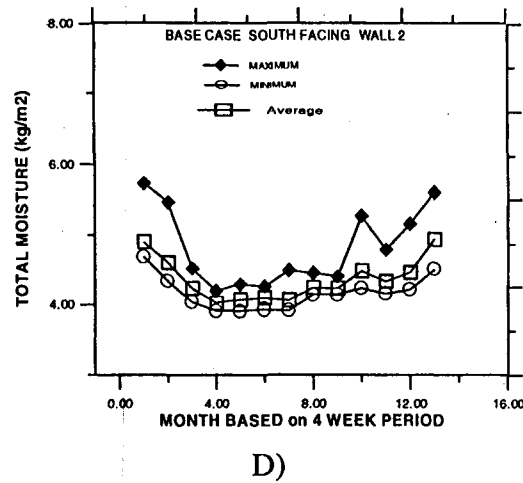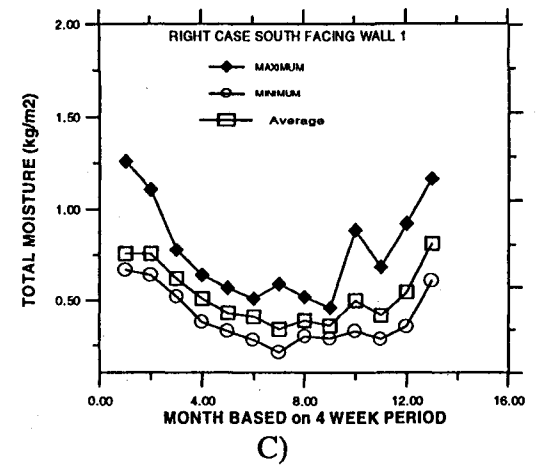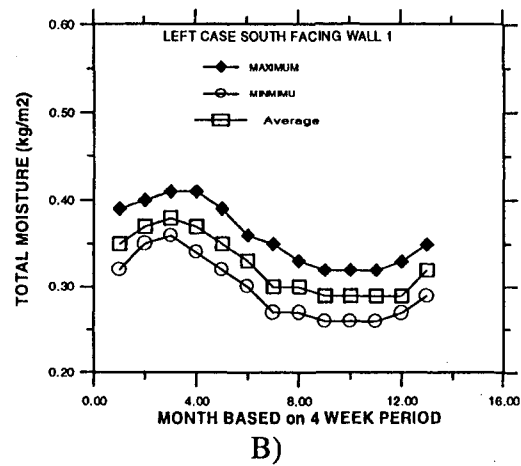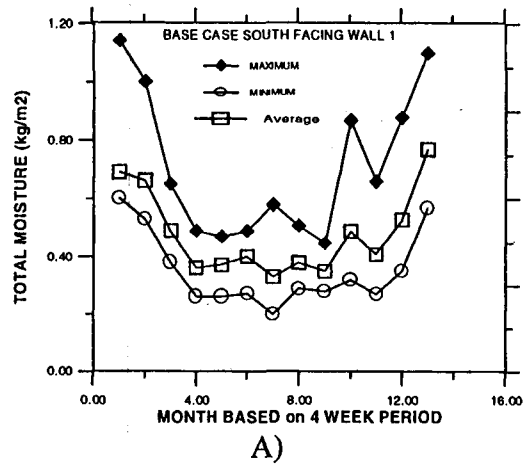
FIGURE C40
FREDERICTON
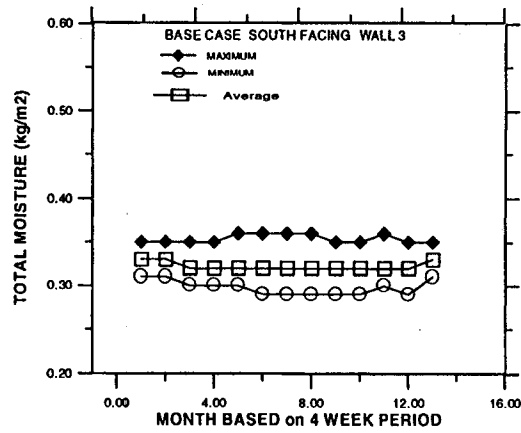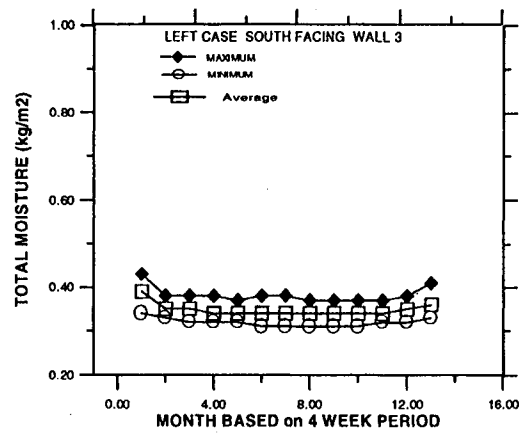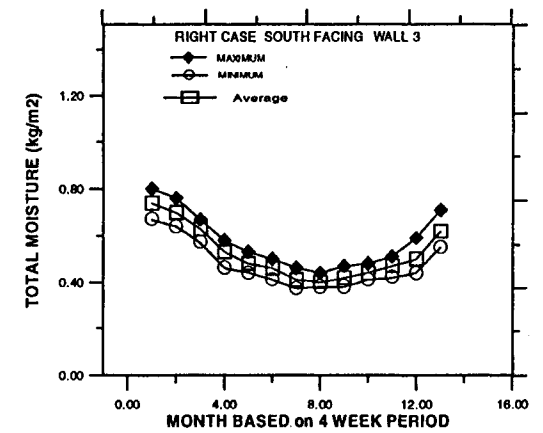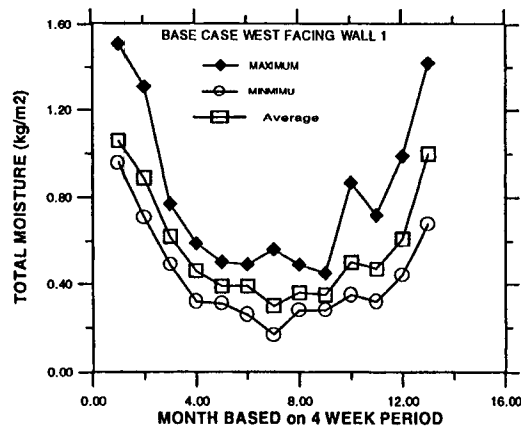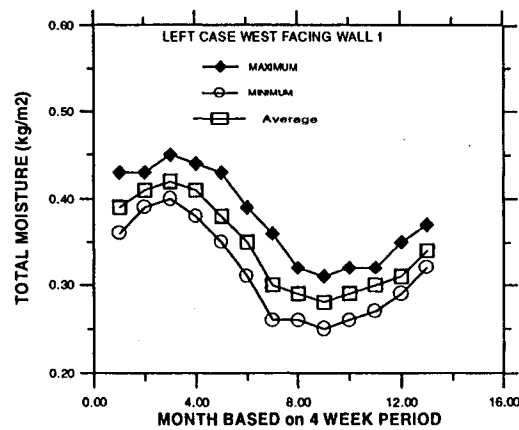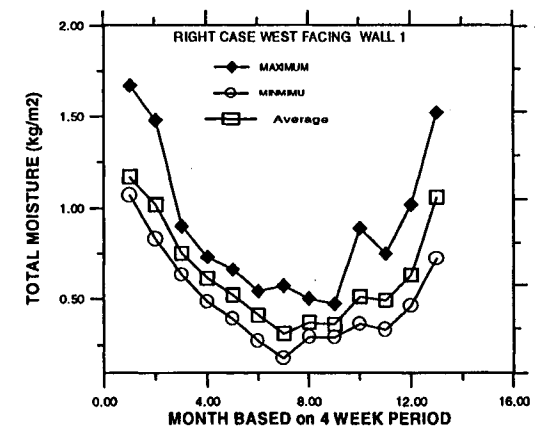
FIGURE C41
FREDERICTON
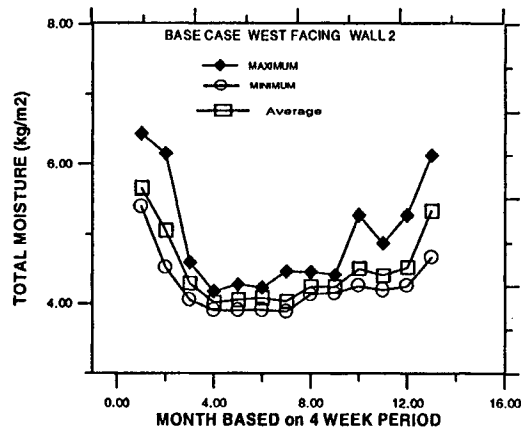
A)
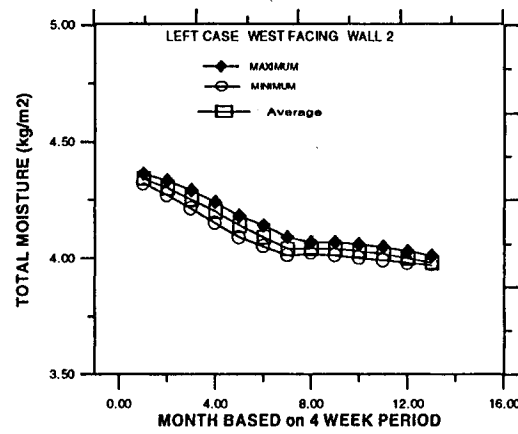
B)
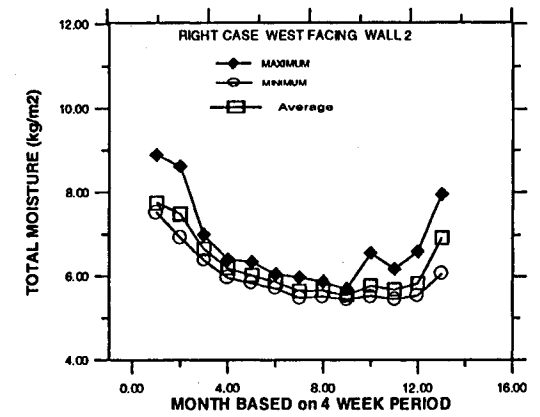
C)
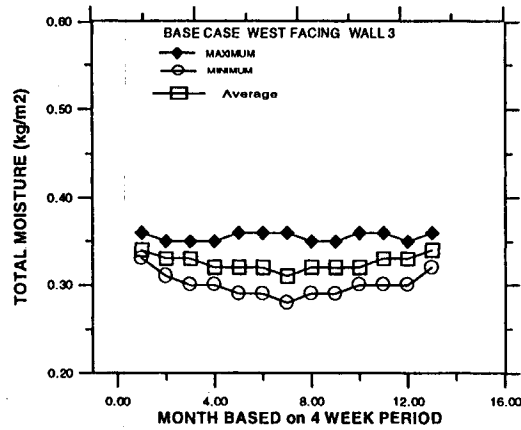
D)
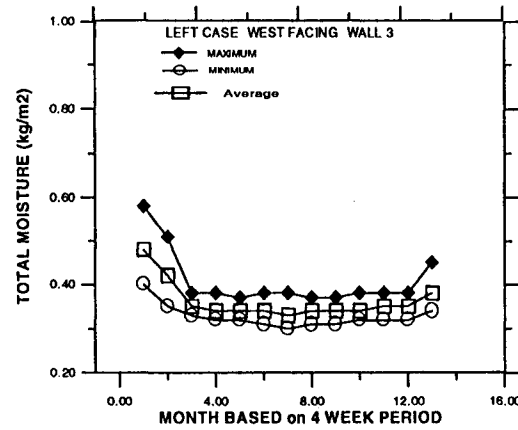
E)
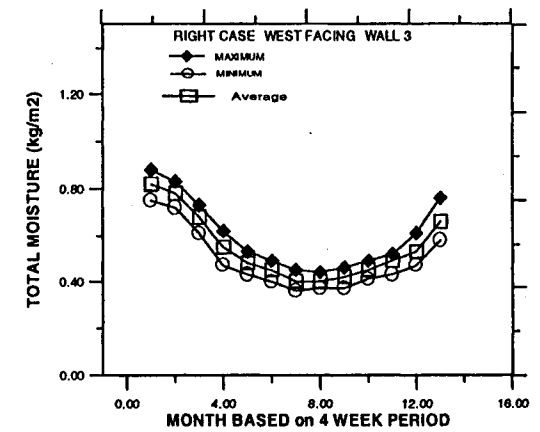
F)

FIGURE C42
FREDERICTON

A)

B)

C)

D)

E)

F)
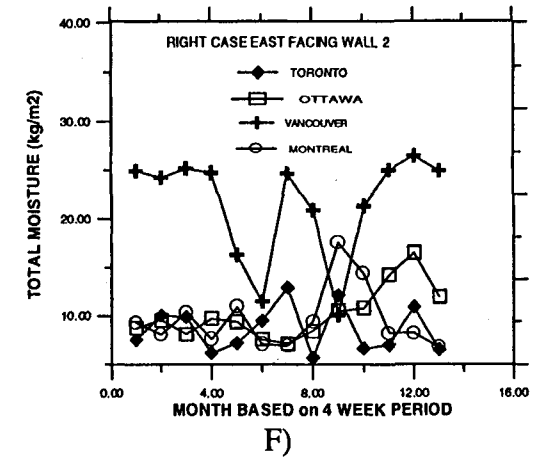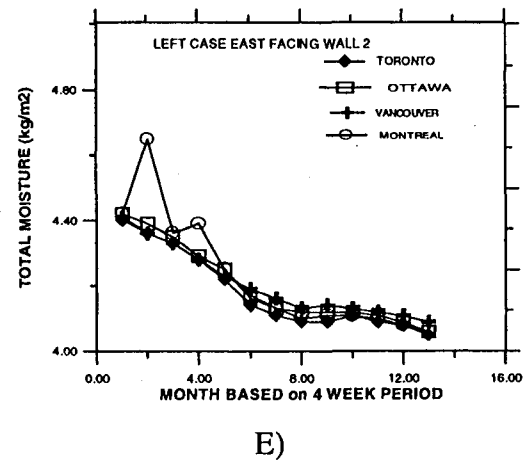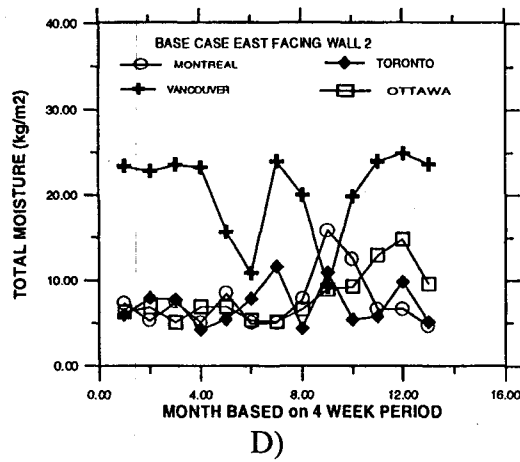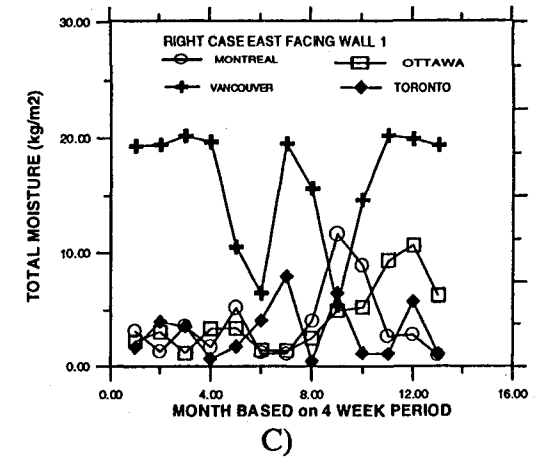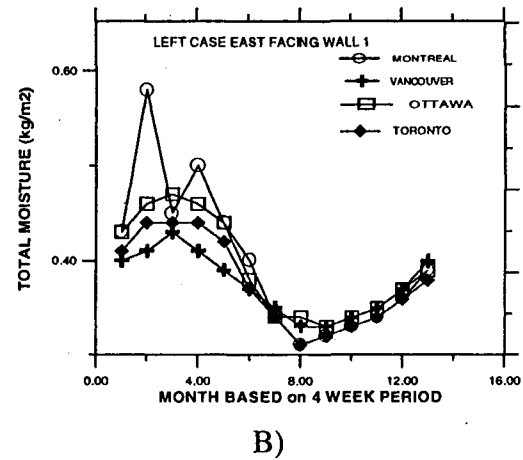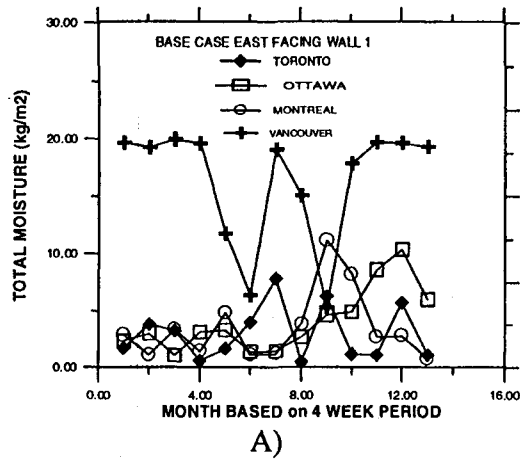
FIGURE C43
MAXIMUM MOISTURE CURVES
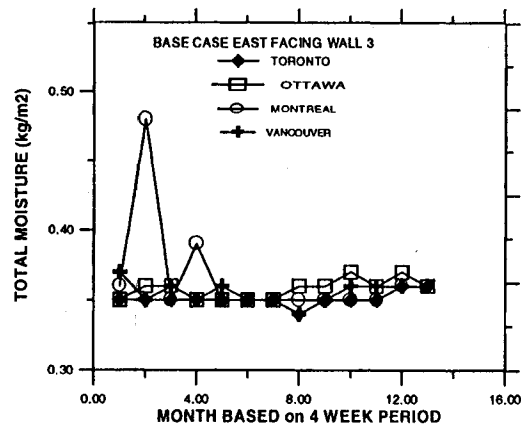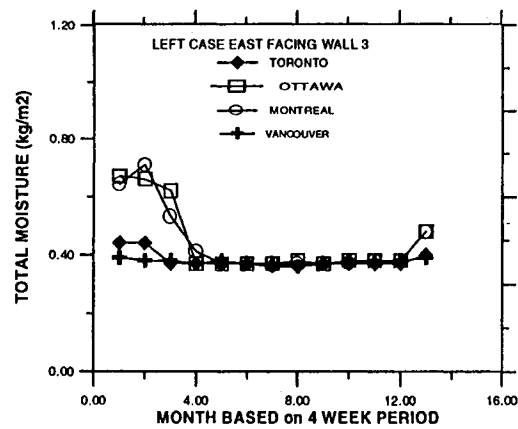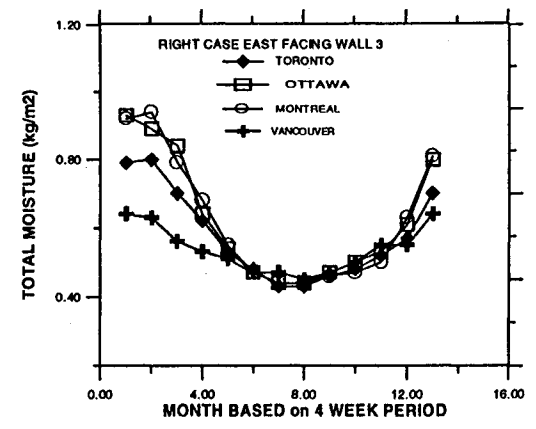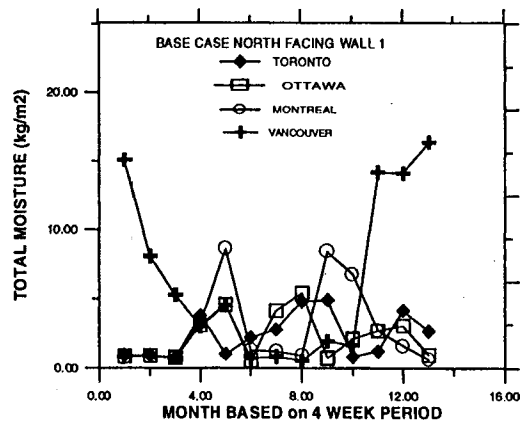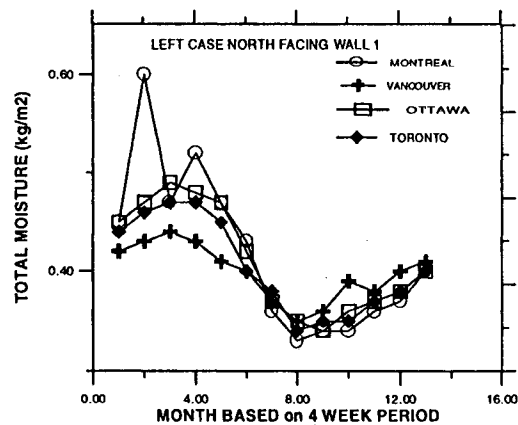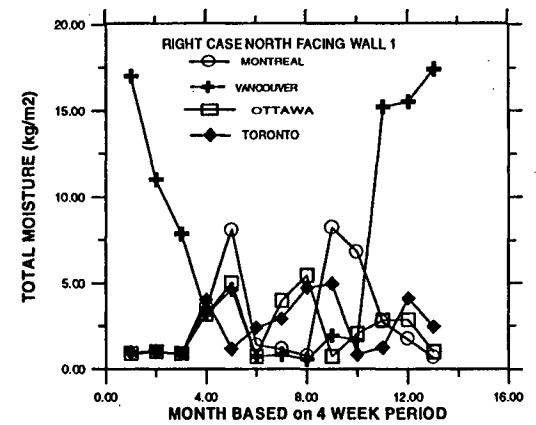
FIGURE C44
MAXIMUM MOISTURE CURVES

A)

B)

C)

D)

E)

F)
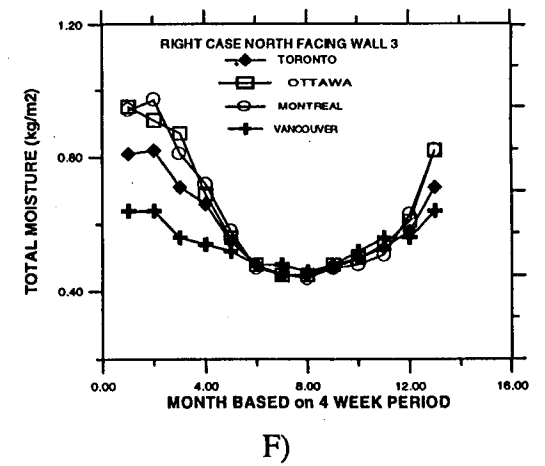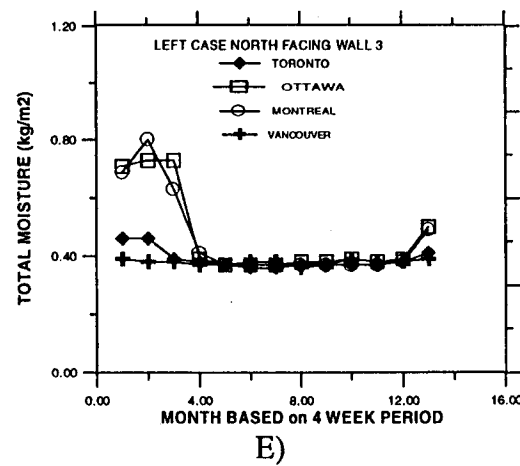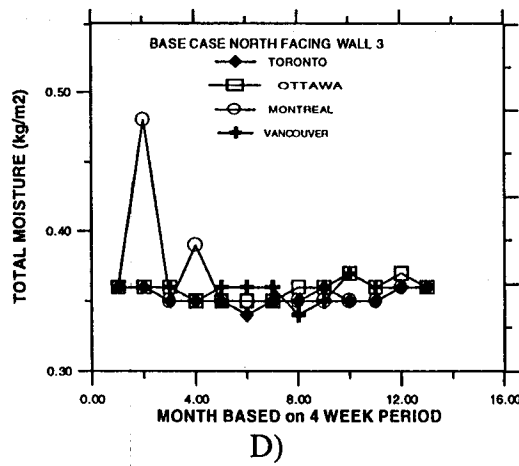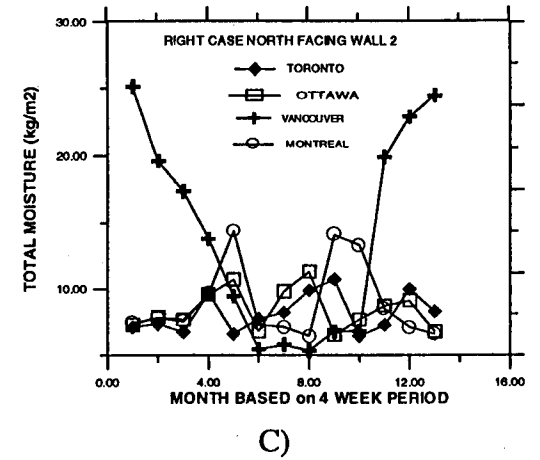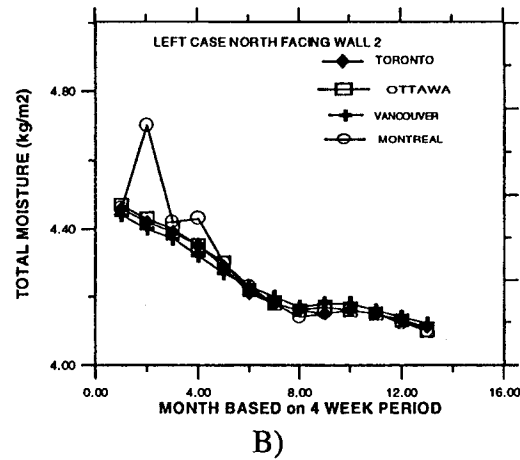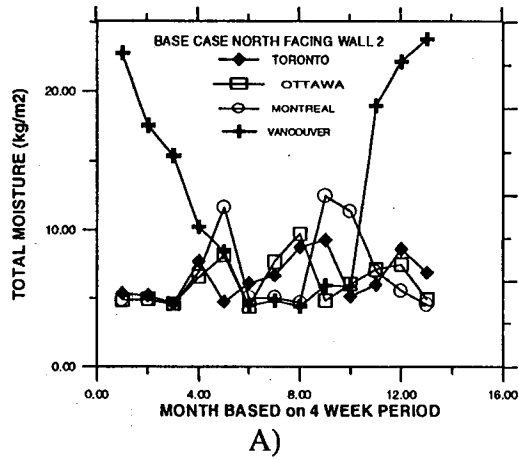
FIGURE C45
MAXIMUM MOISTURE CURVES
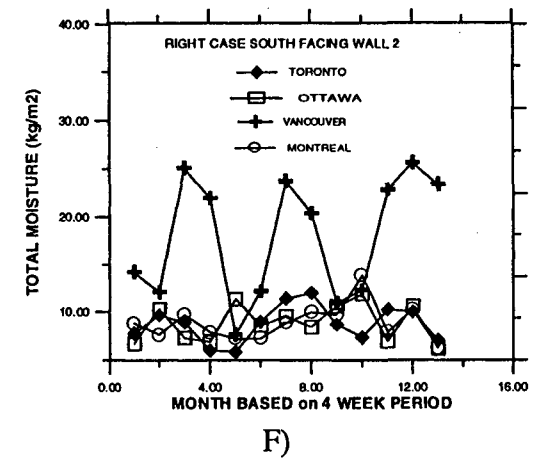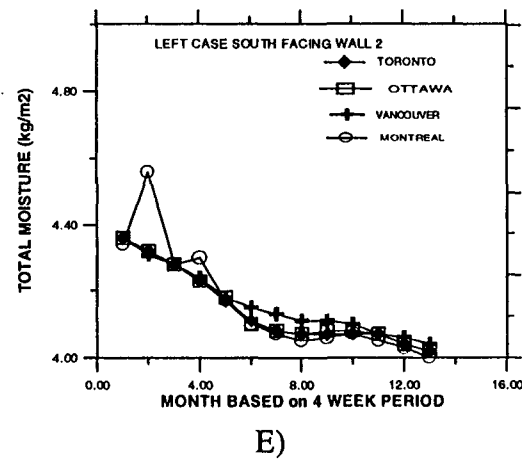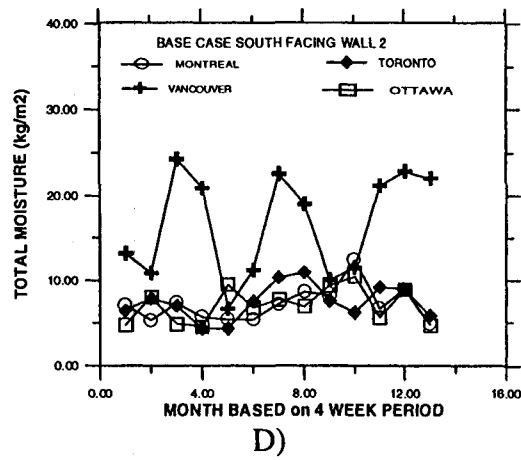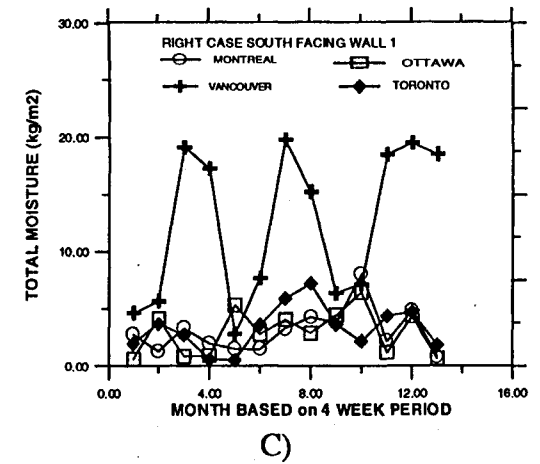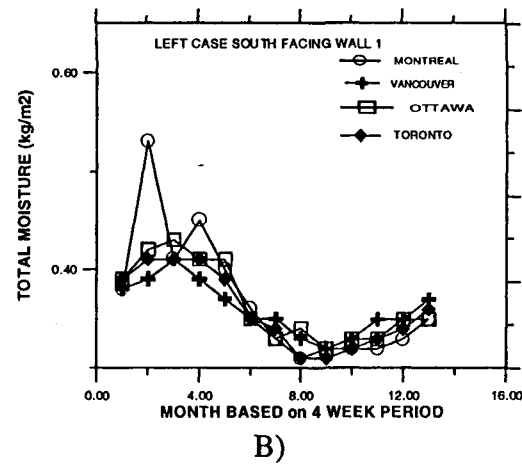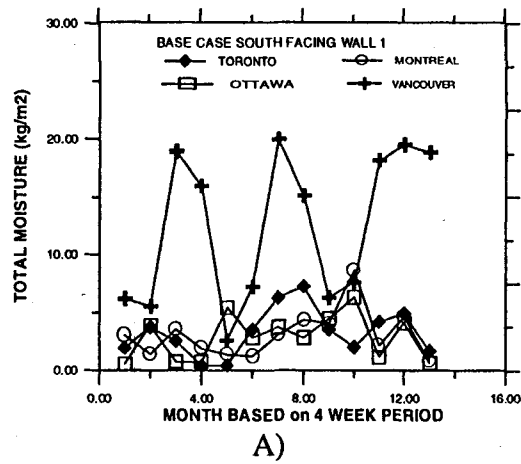
FIGURE C46
MAXIMUM MOISTURE CURVES

A)

B)

C)

D)

E)

F)
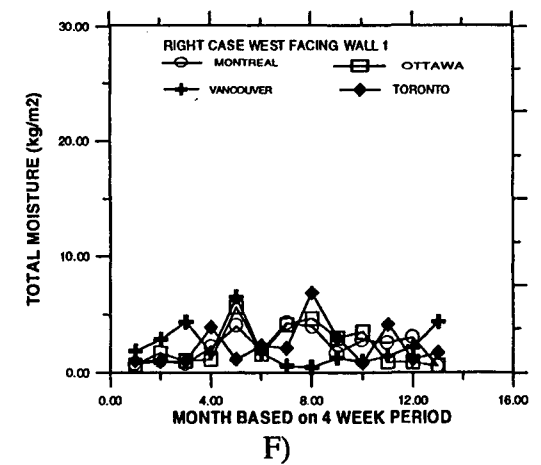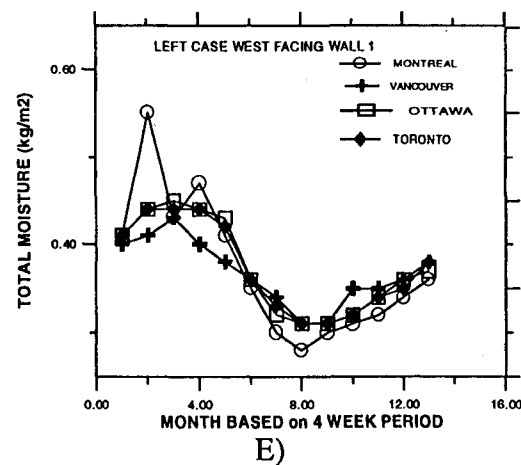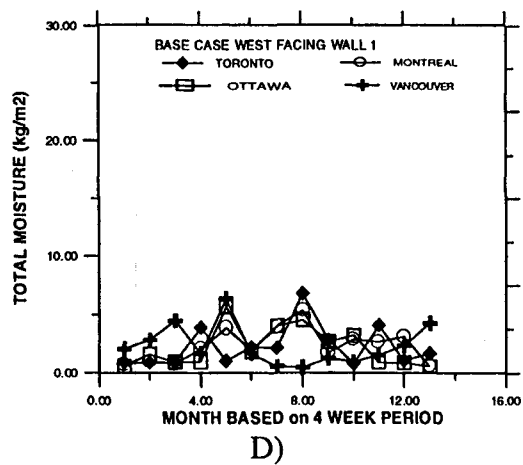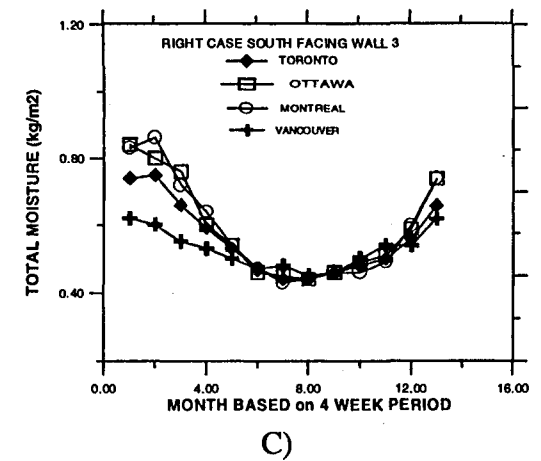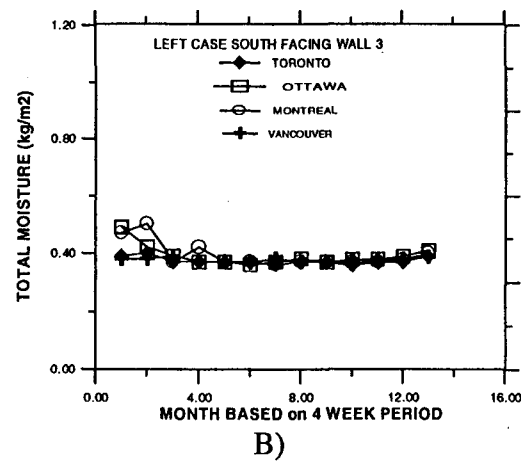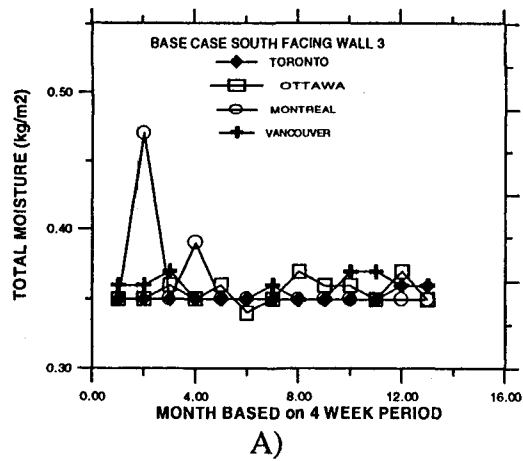
FIGURE C47
MAXIMUM MOISTURE CURVES
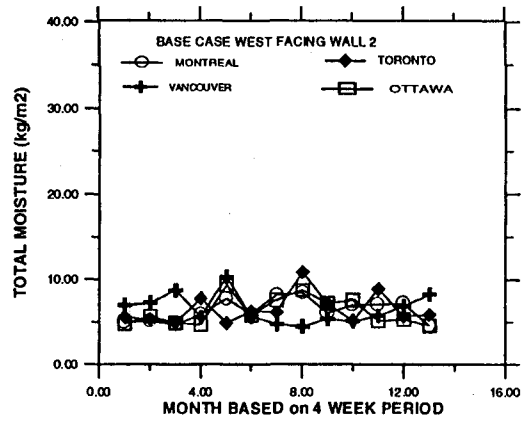
A)
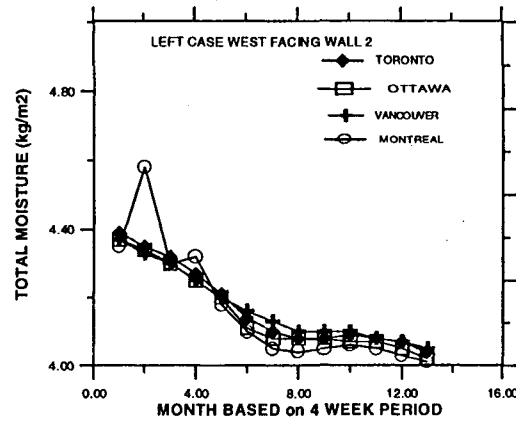
B)
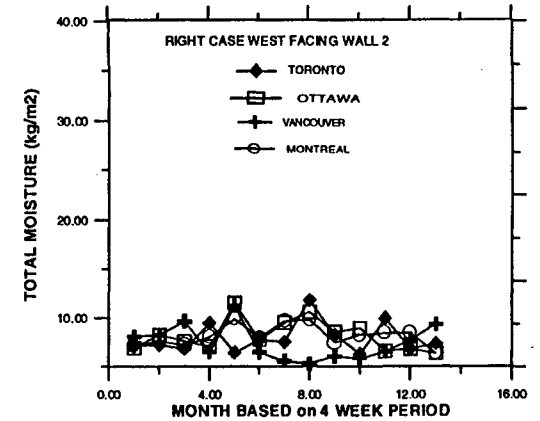
C)
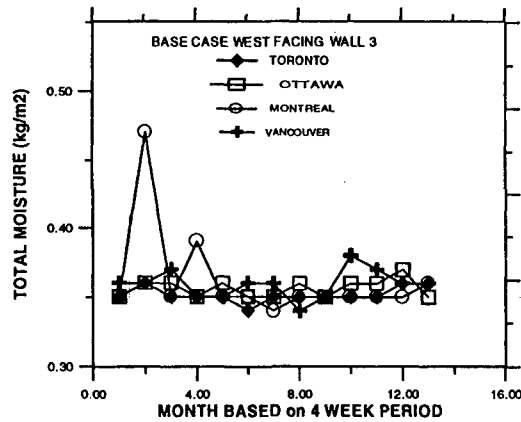
D)
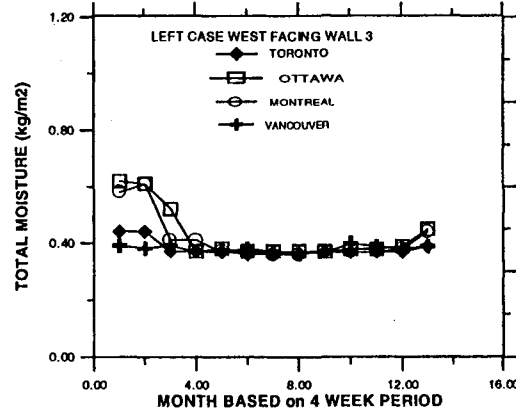
E)
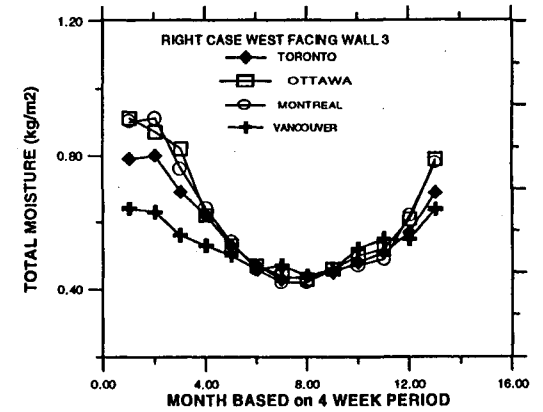
F)

FIGURE C48
MAXIMUM MOISTURE CURVES
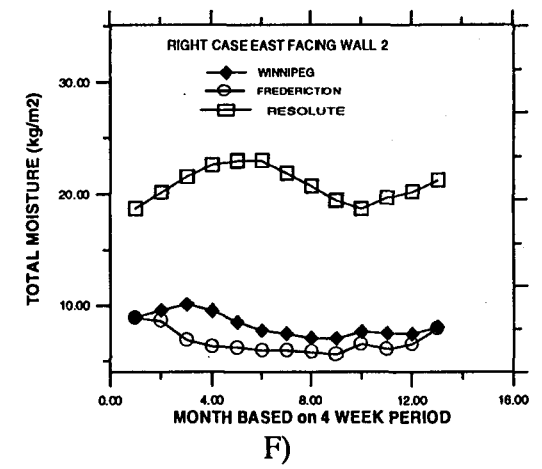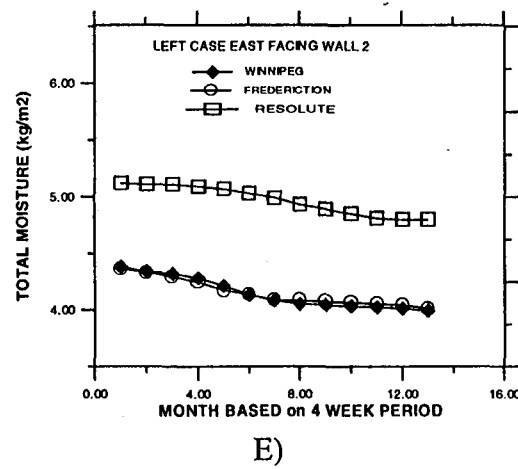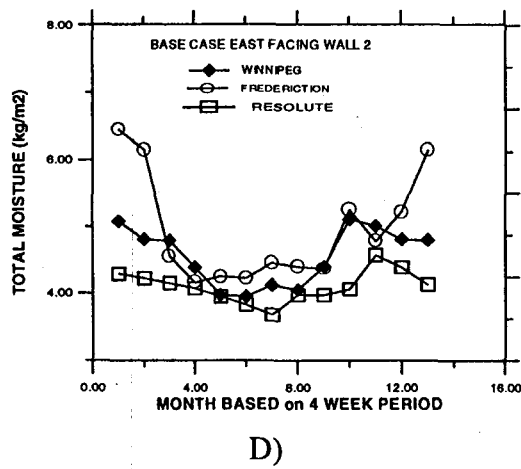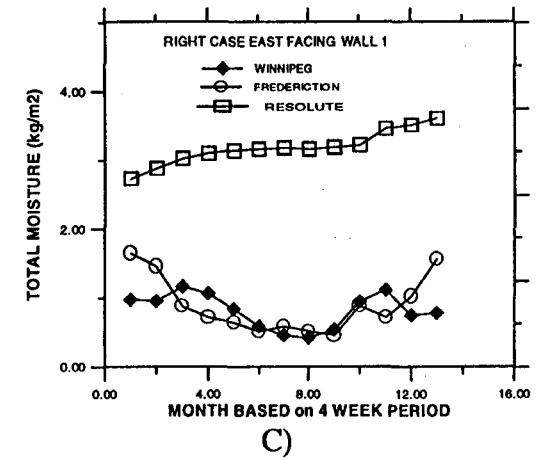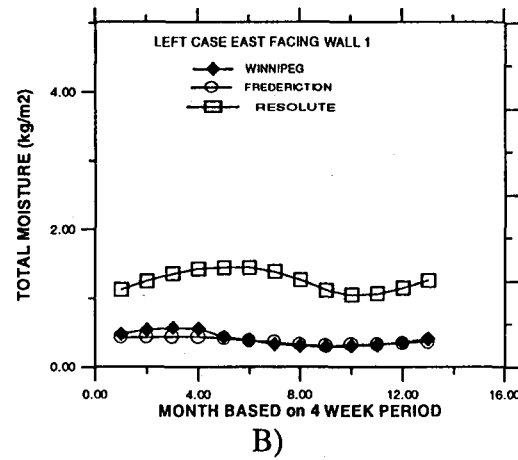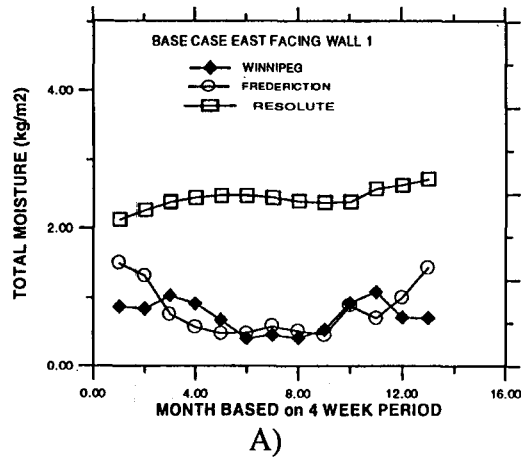
FIGURE C49
MAXIMUM MOISTURE CURVES
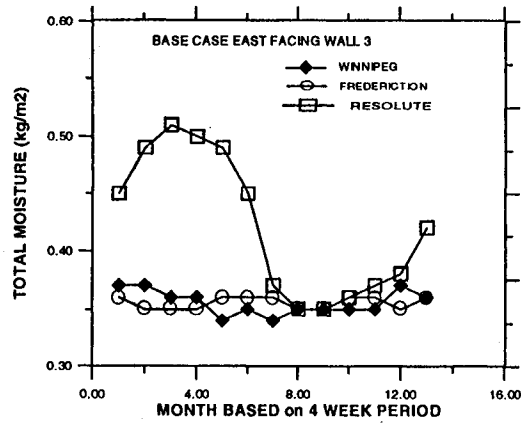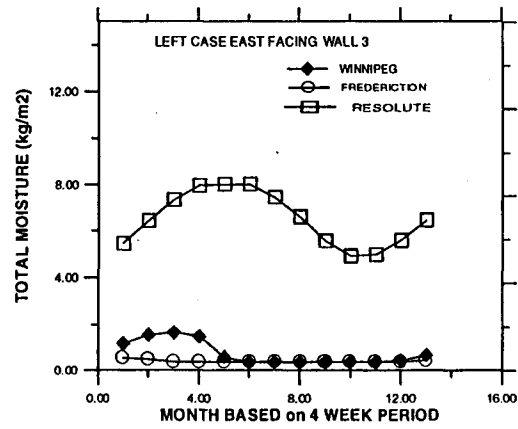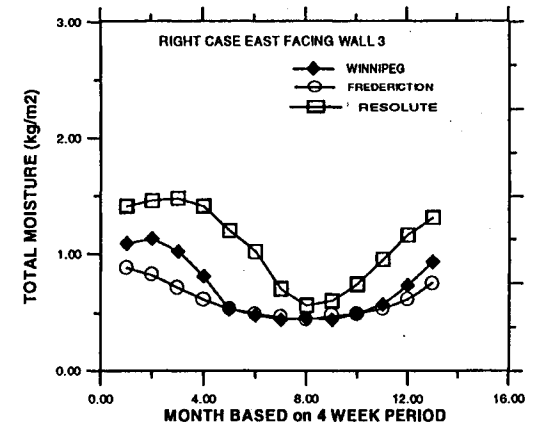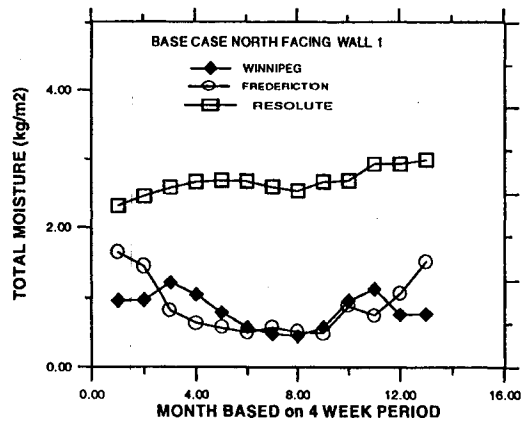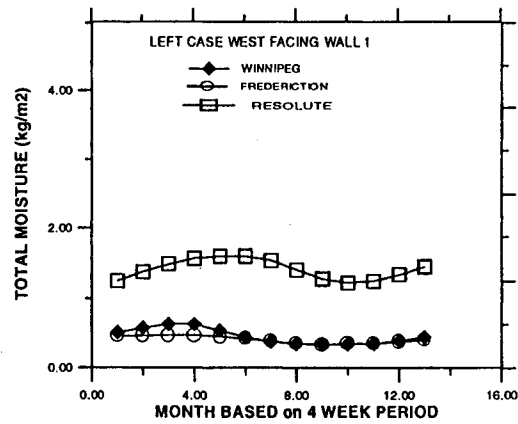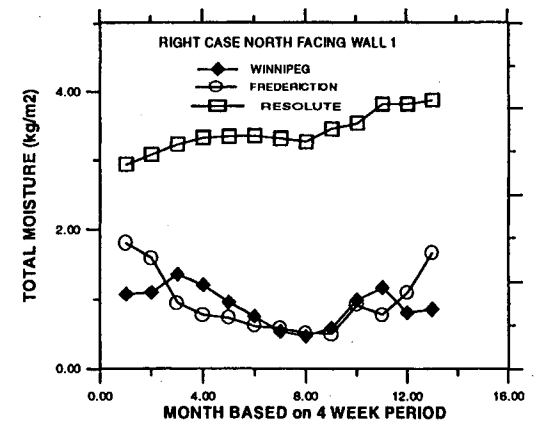
FIGURE C50
MAXIMUM MOISTURE CURVES
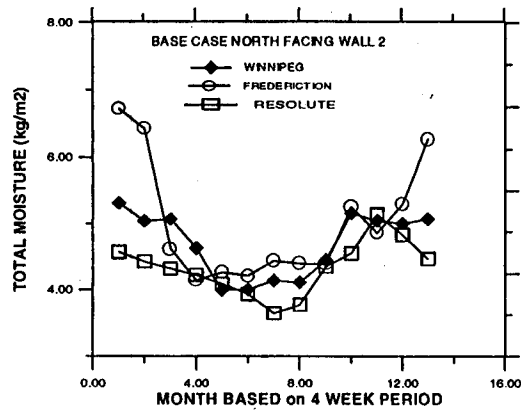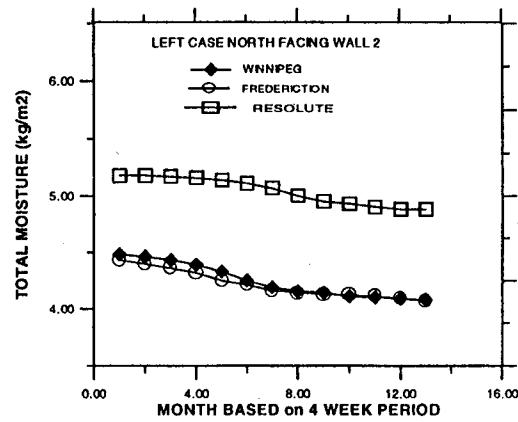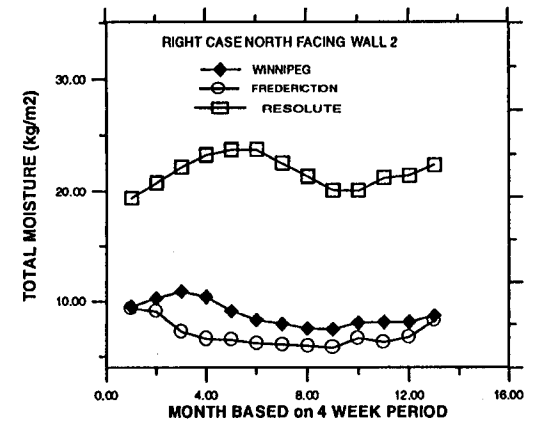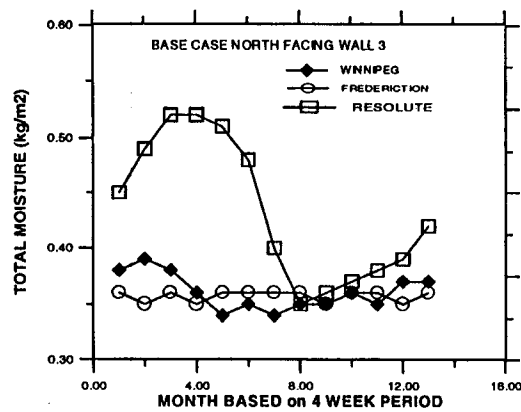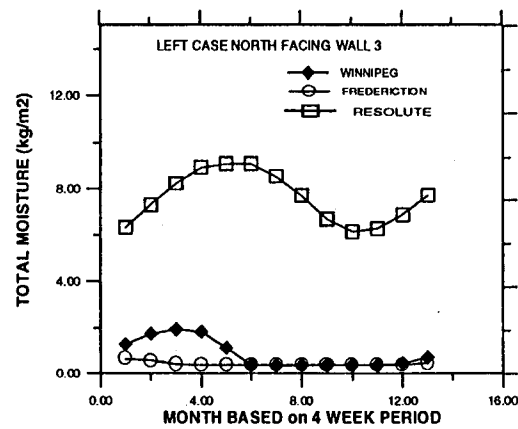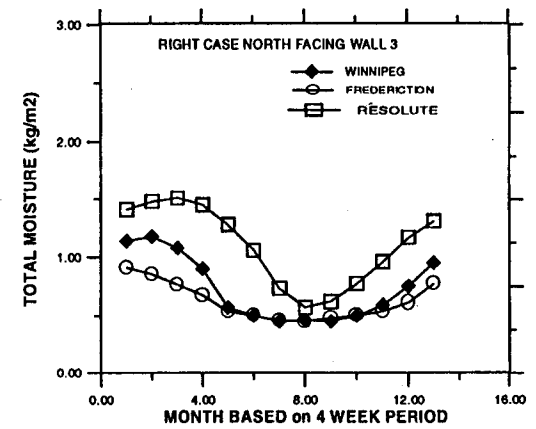
FIGURE C51
MAXIMUM MOISTURE CURVES
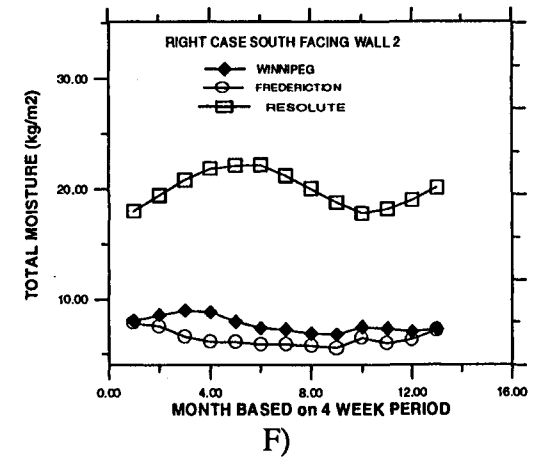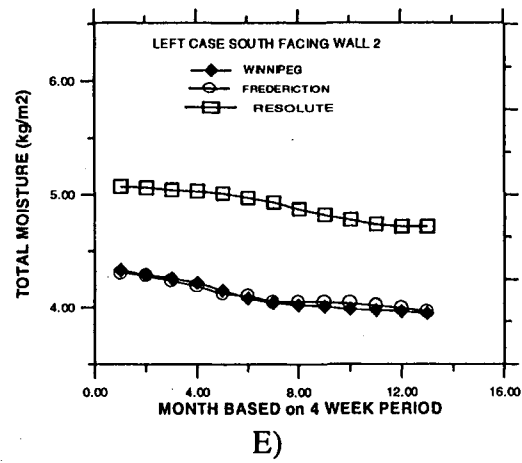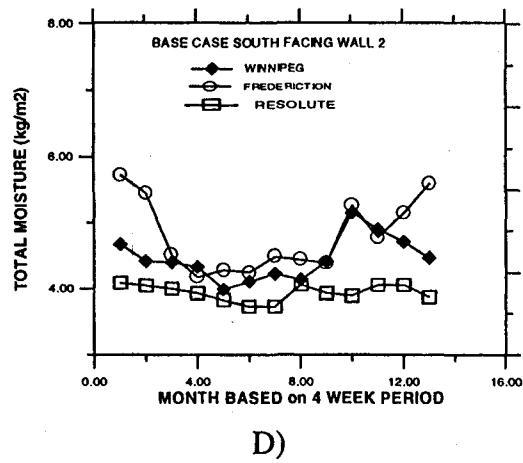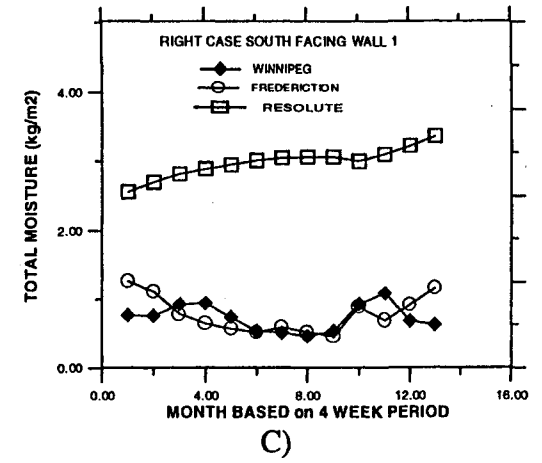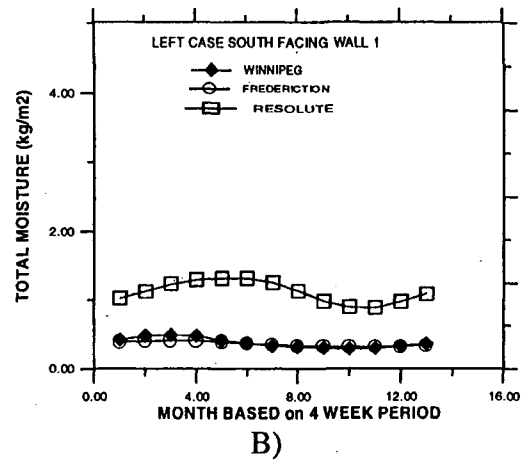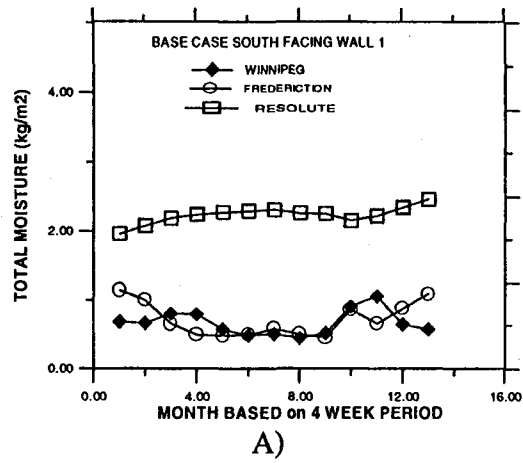
FIGURE C52
MAXIMUM MOISTURE CURVES
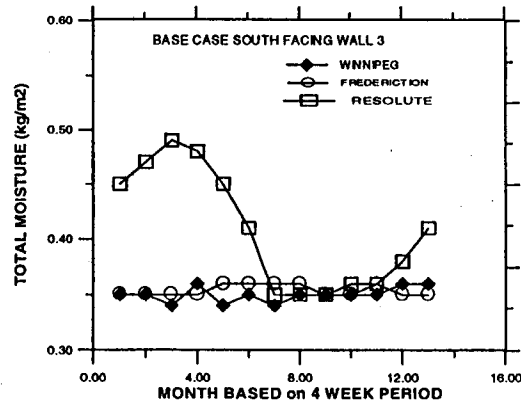
A)
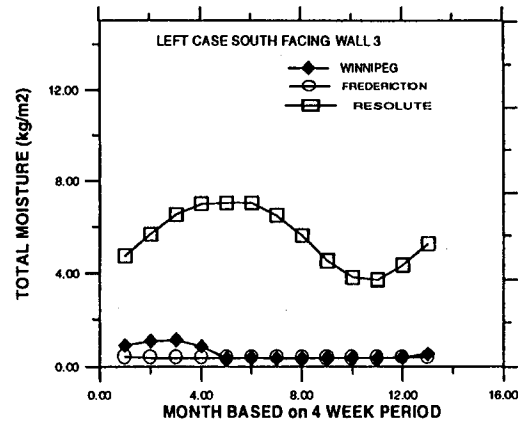
B)
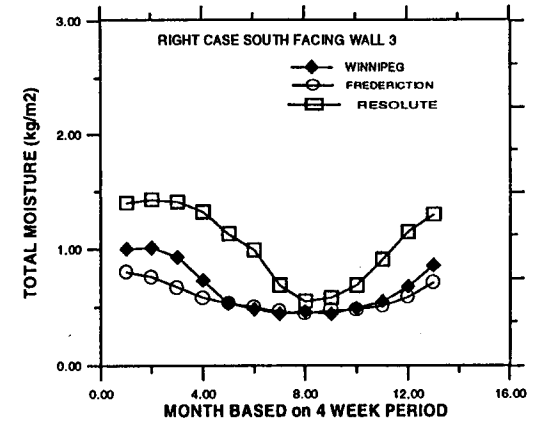
C)
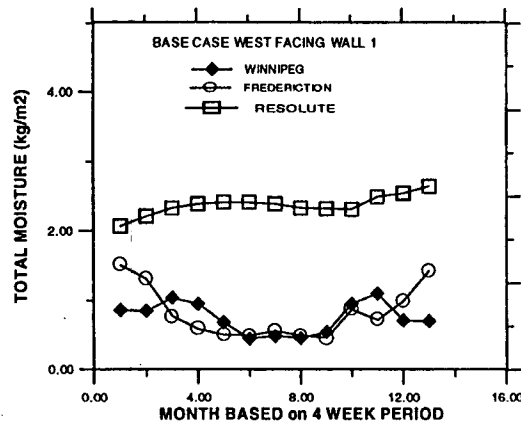
D)
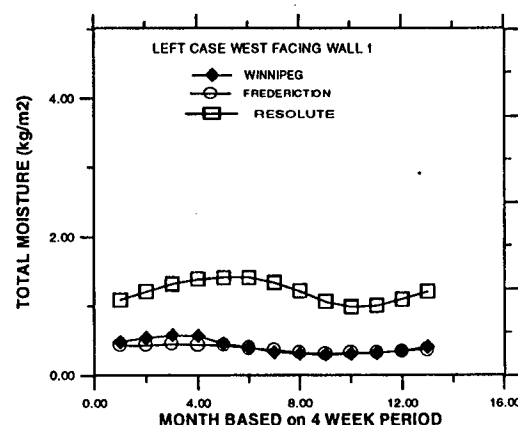
E)
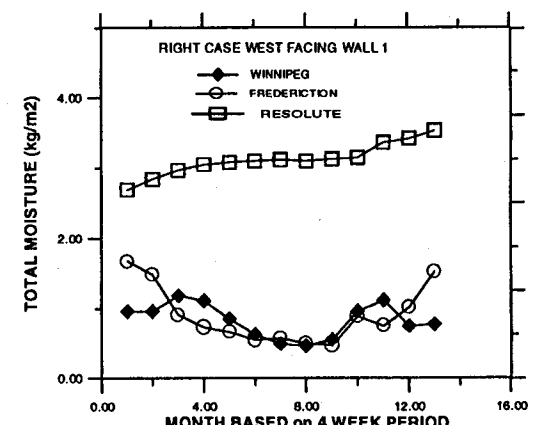
F)

FIGURE C53
MAXIMUM MOISTURE CURVES
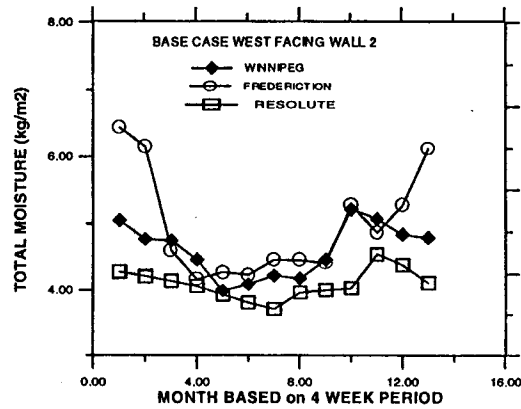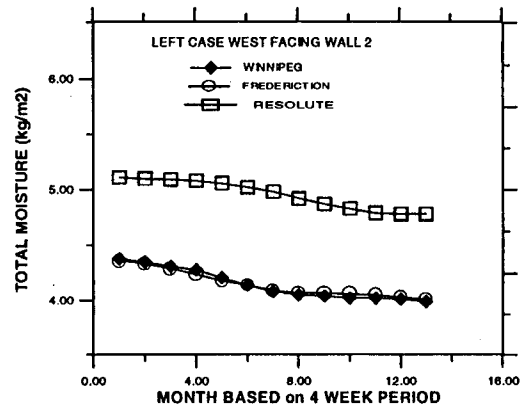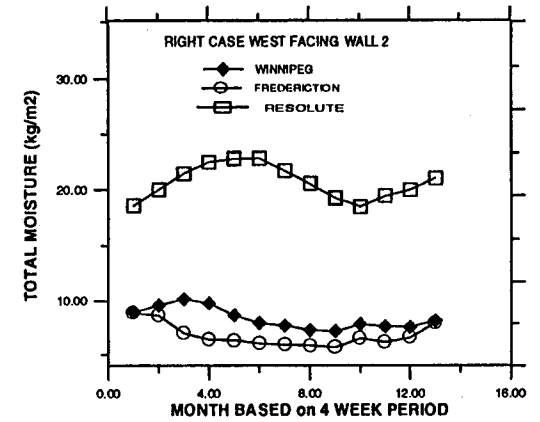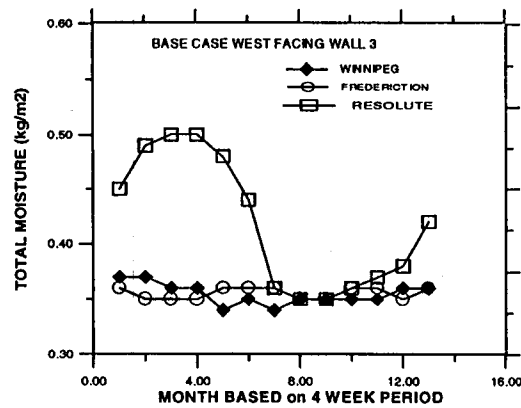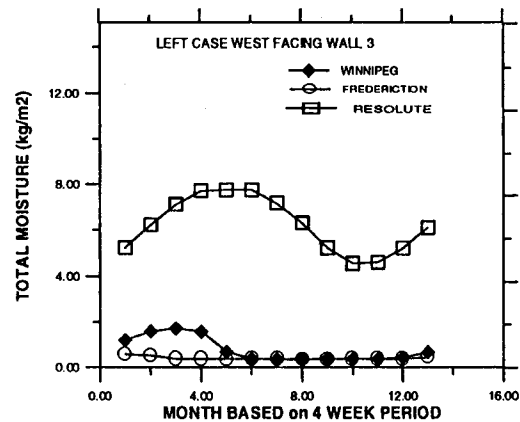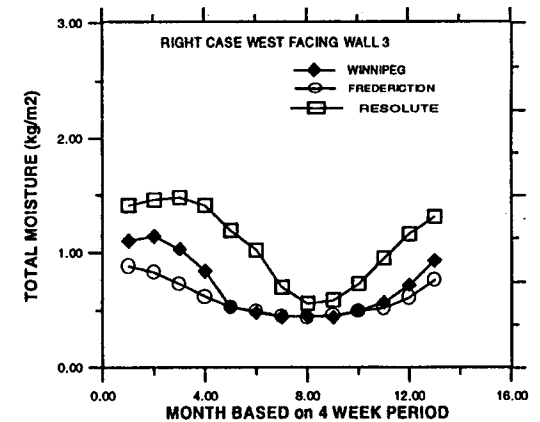
FIGURE C54
MAXIMUM MOISTURE CURVES

Heat Flux Graphs
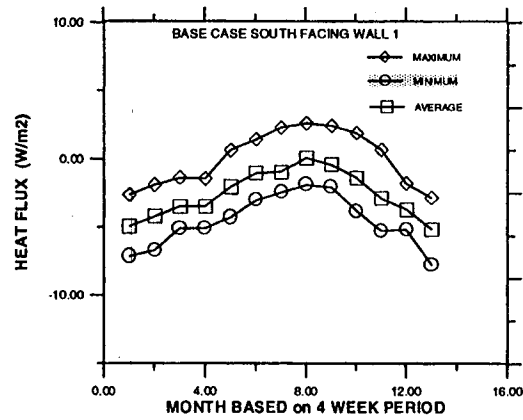
A)
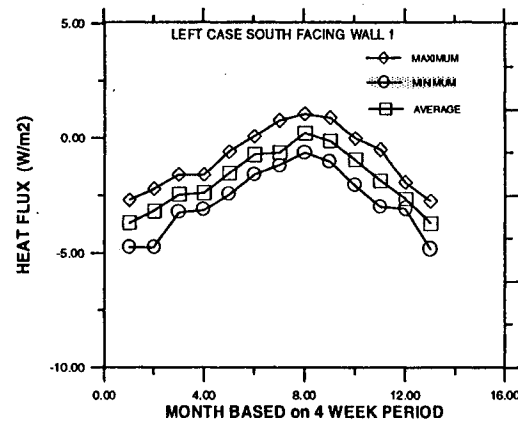
B)
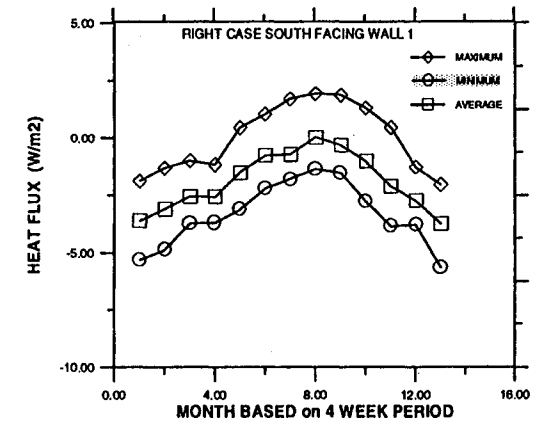
C)
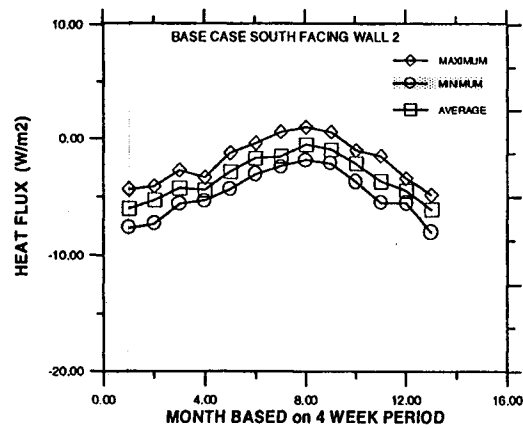
D)
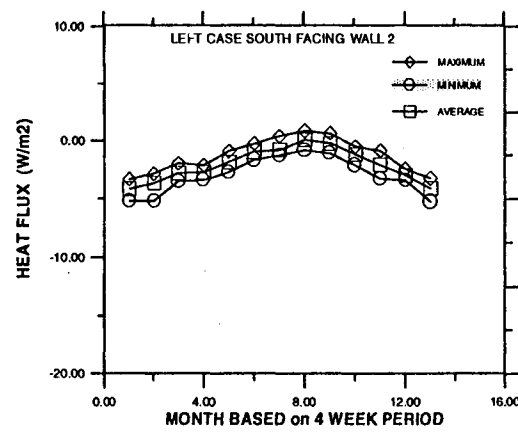
E)
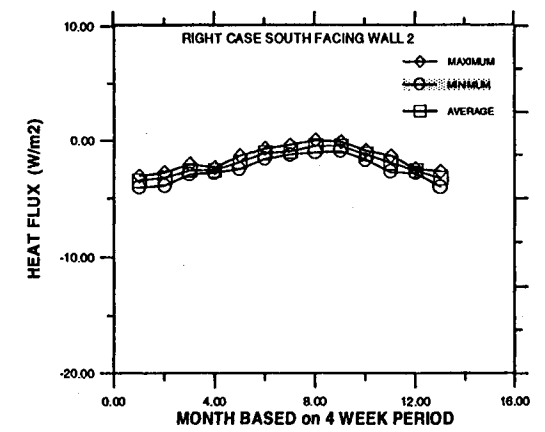
F)

FIGURE C55
VANCOUVER

A)

B)

C)

D)

E)

F)
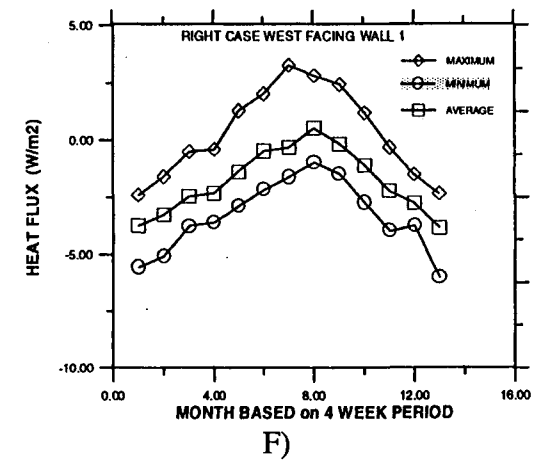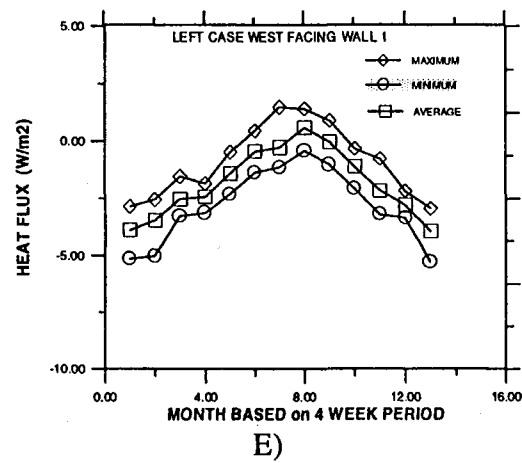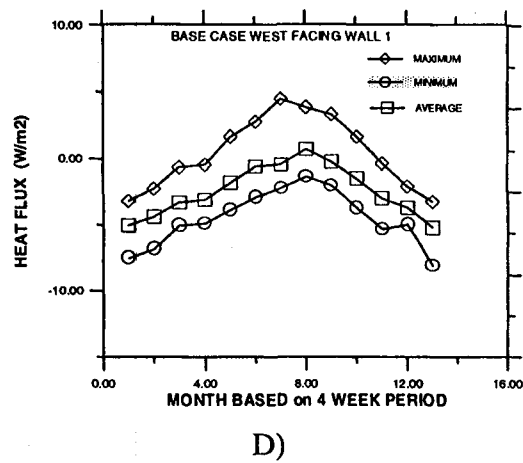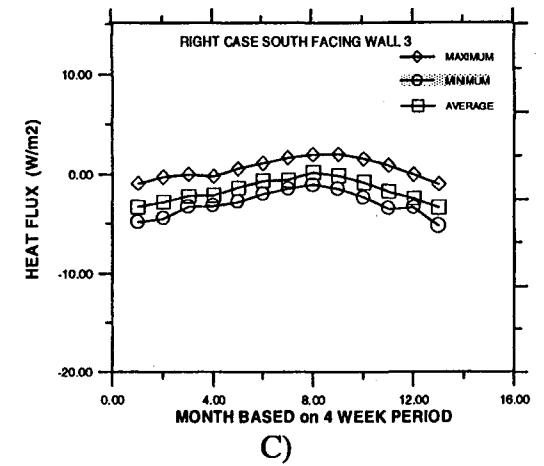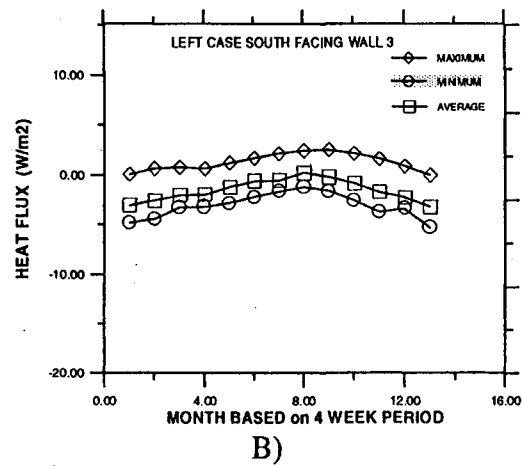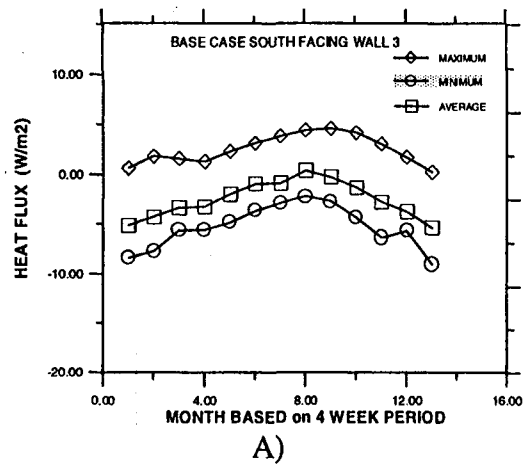
FIGURE C56
VANCOUVER
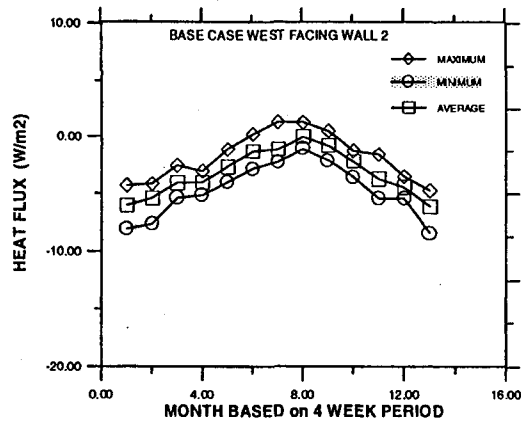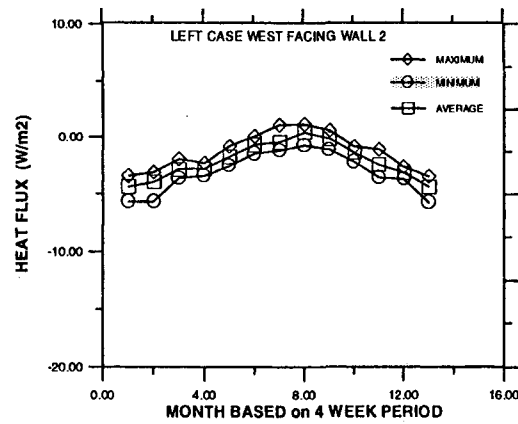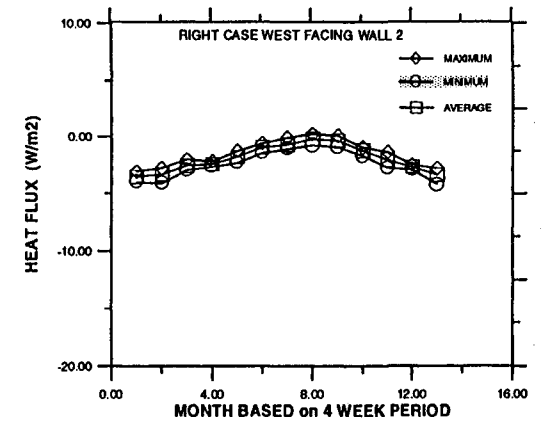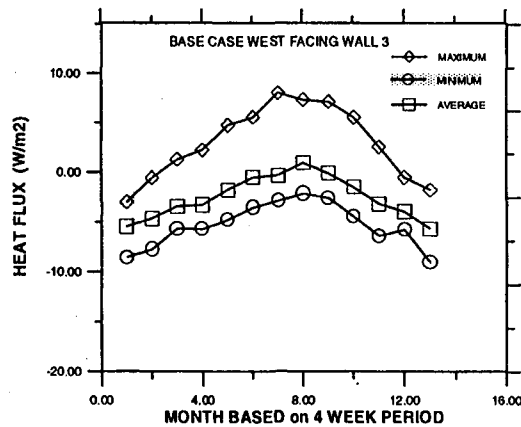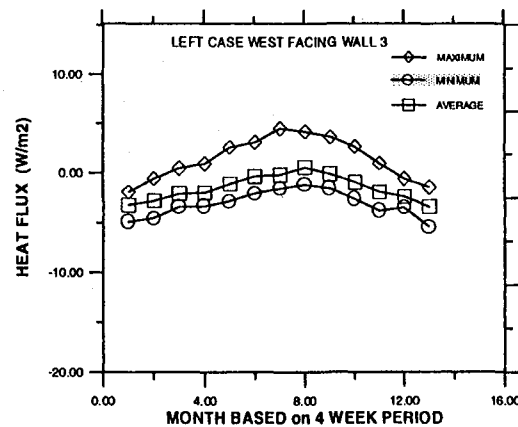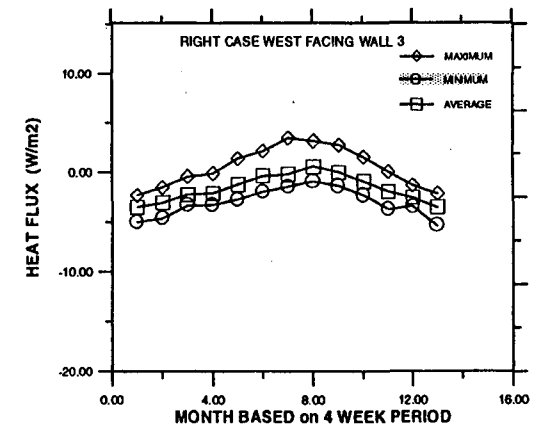
FIGURE C57
VANCOUVER
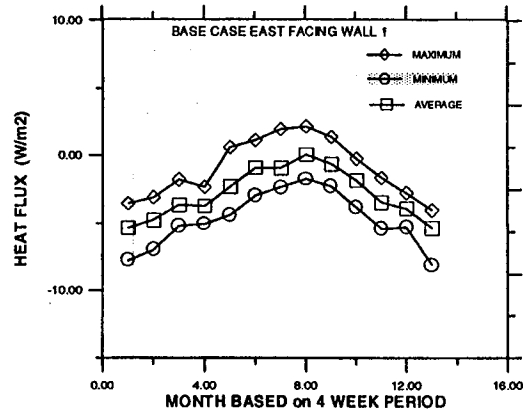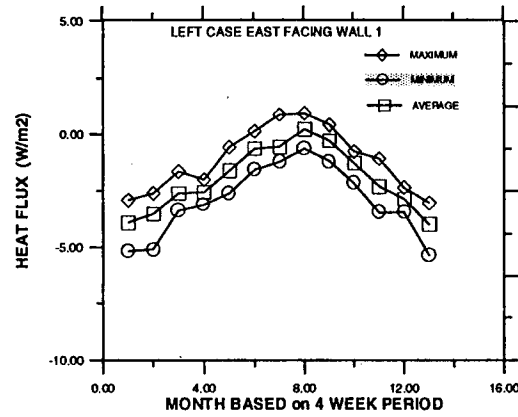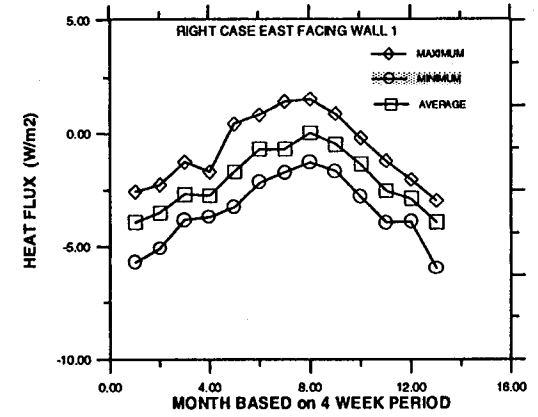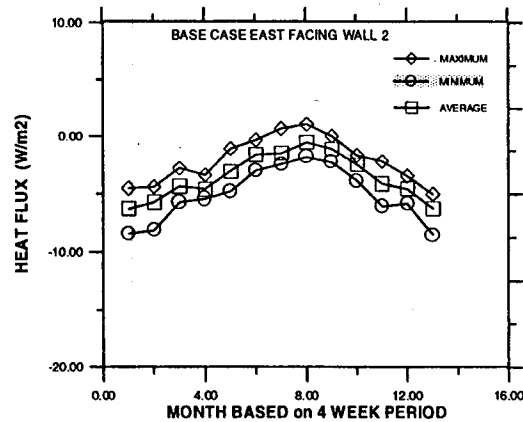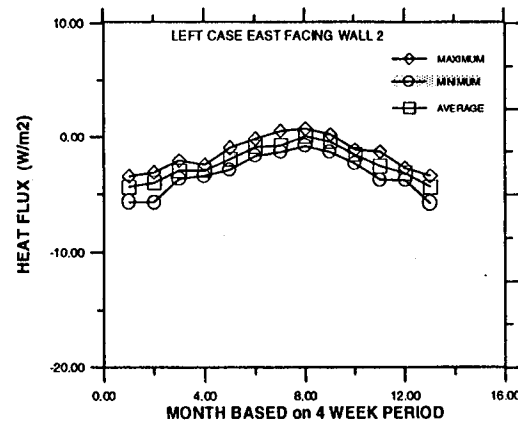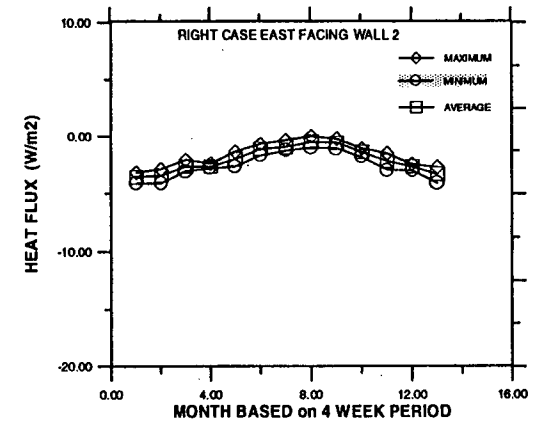
FIGURE C58
VANCOUVER

A)

B)

C)

D)

E)

F)
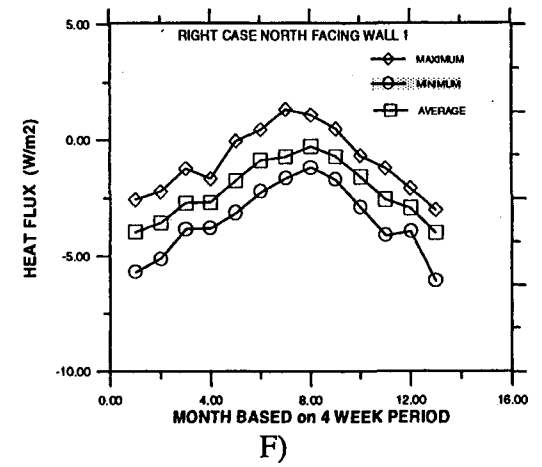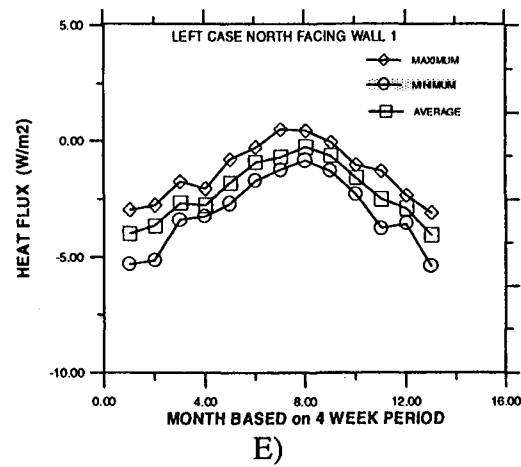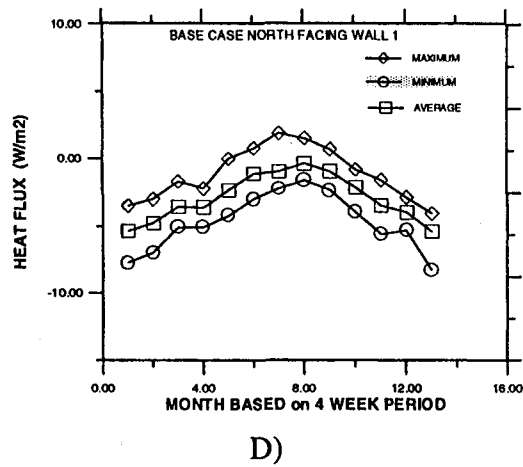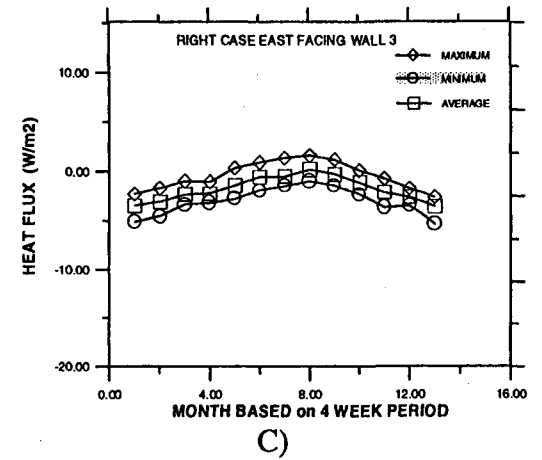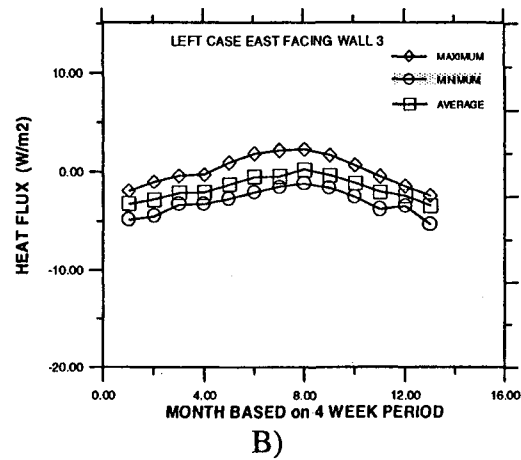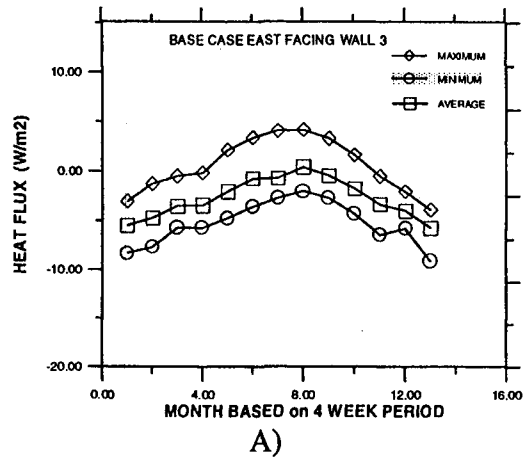
FIGURE C59
VANCOUVER

A)
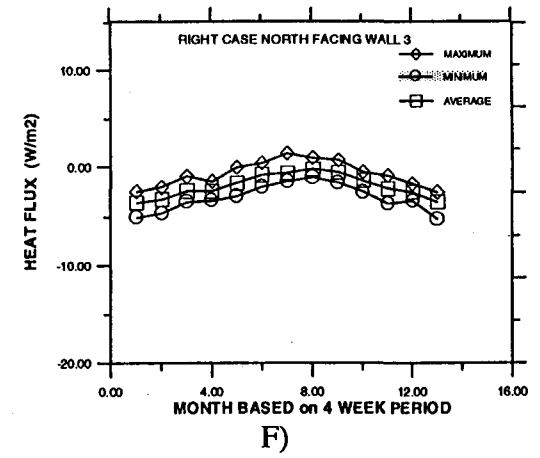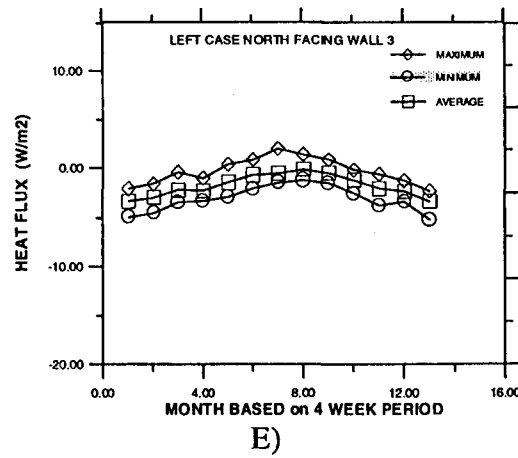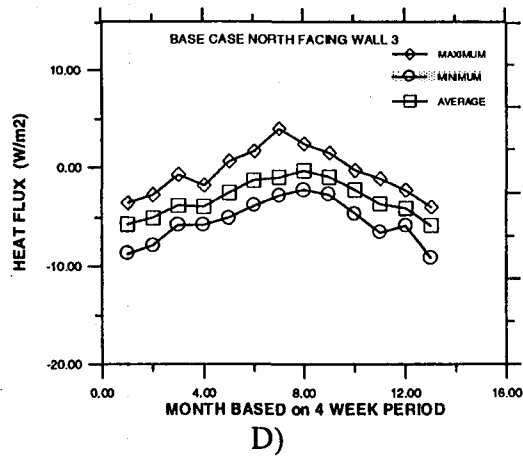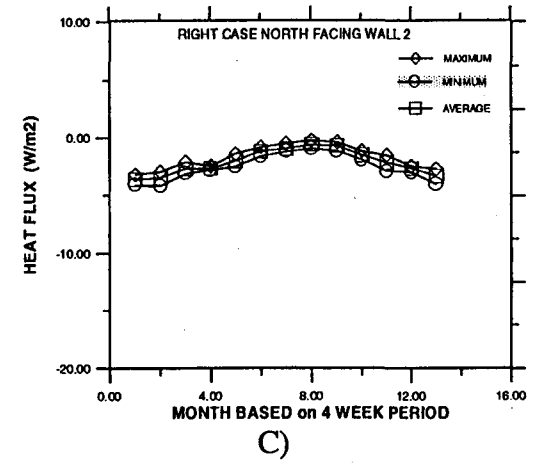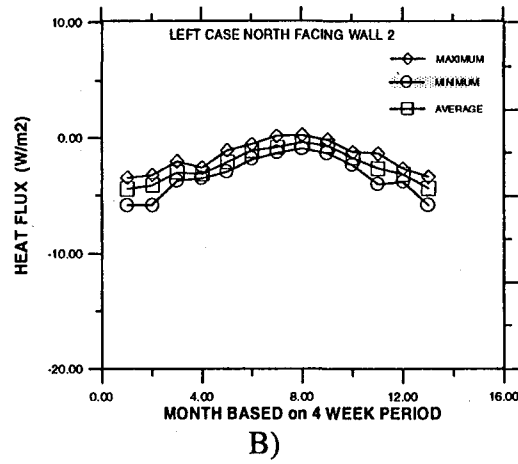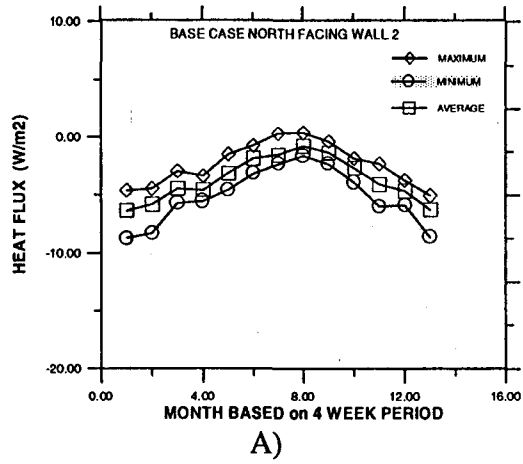
B)

C)

D)

E)

F)

FIGURE C60
VANCOUVER
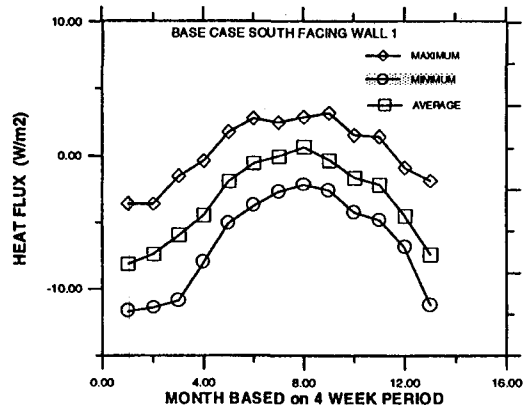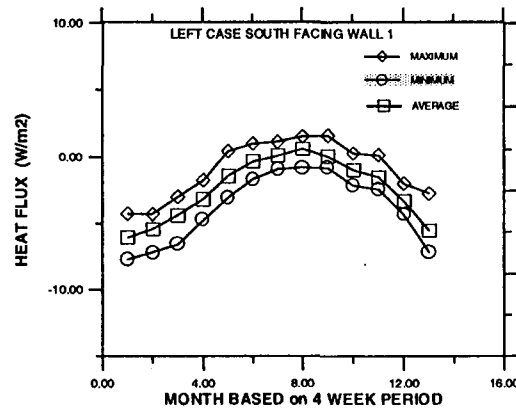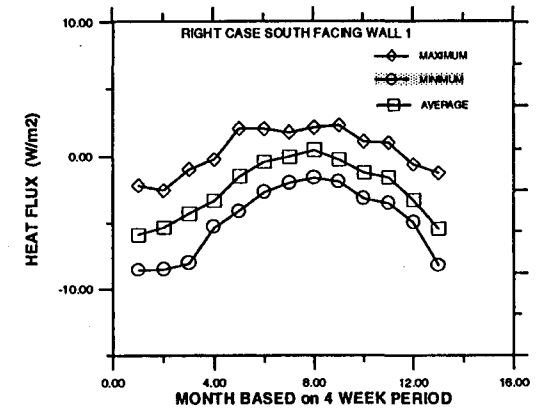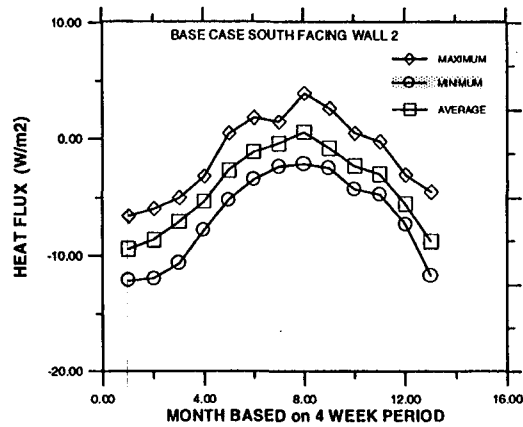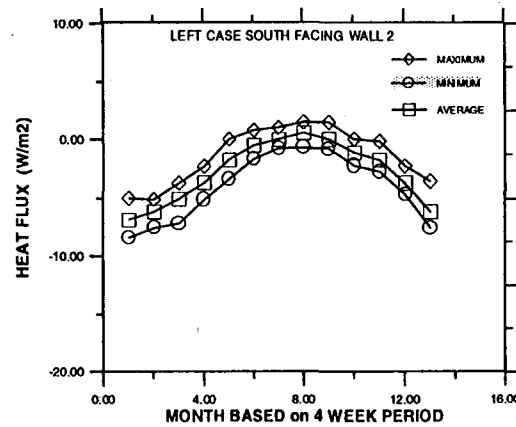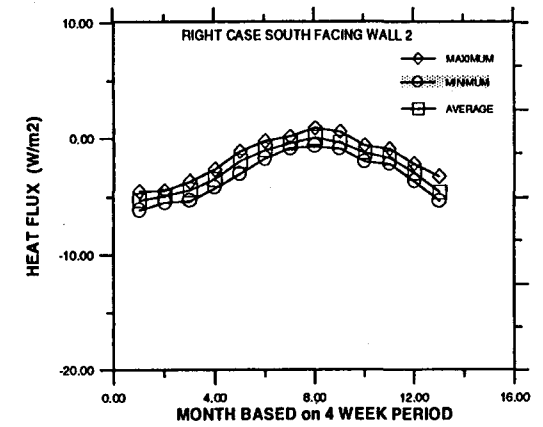
FIGURE C61
OTTAWA

A)

B)

C)

D)

E)

F)
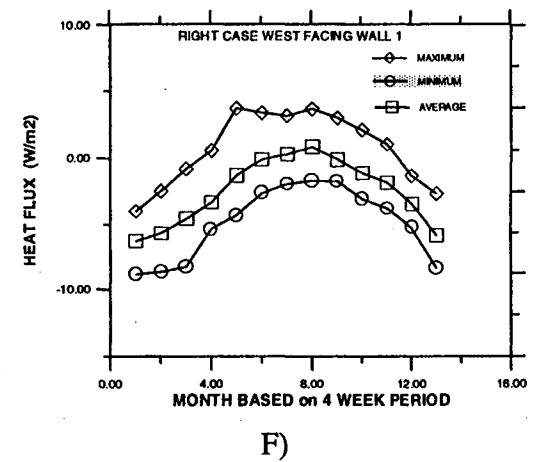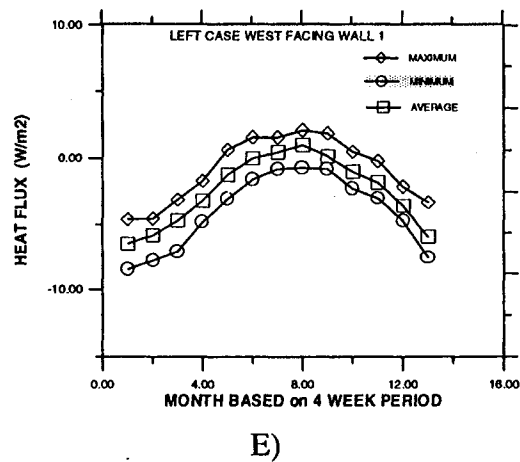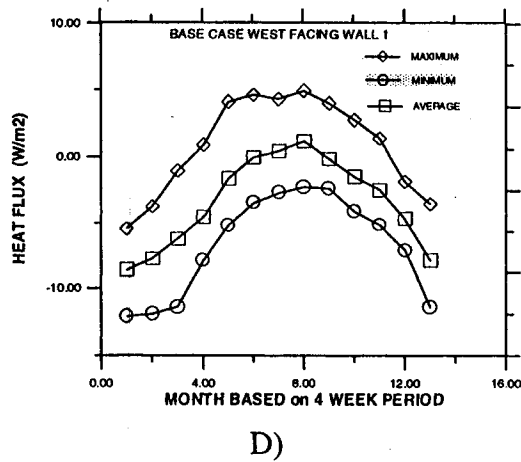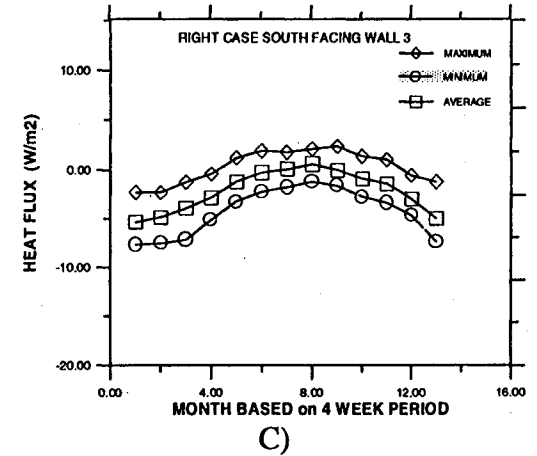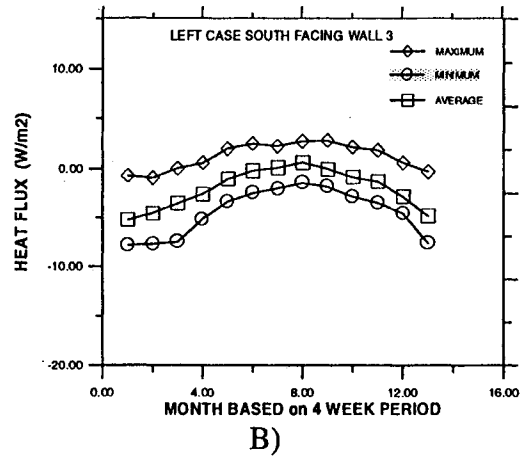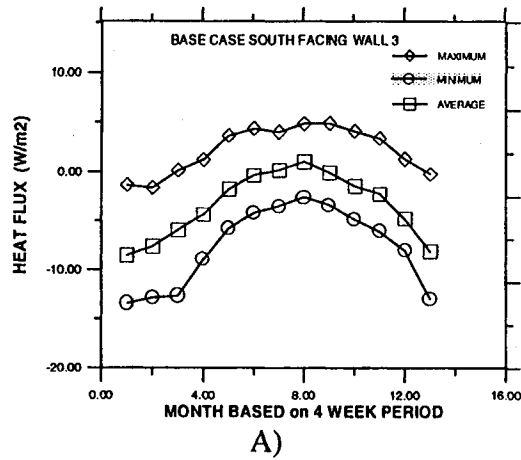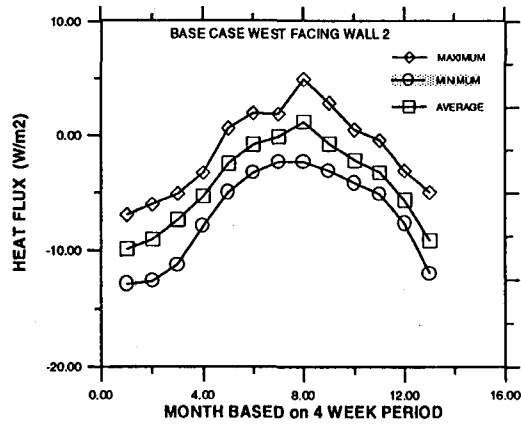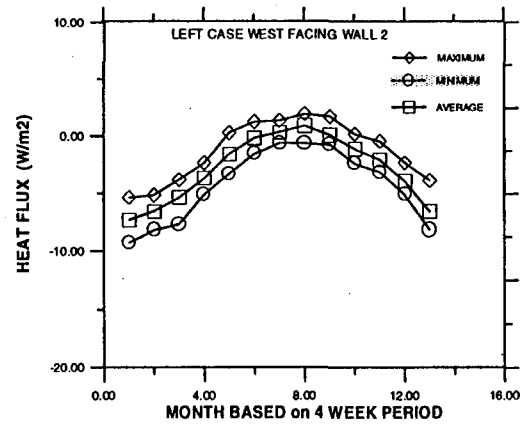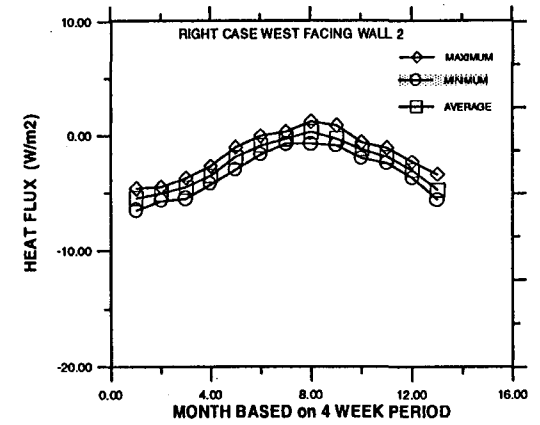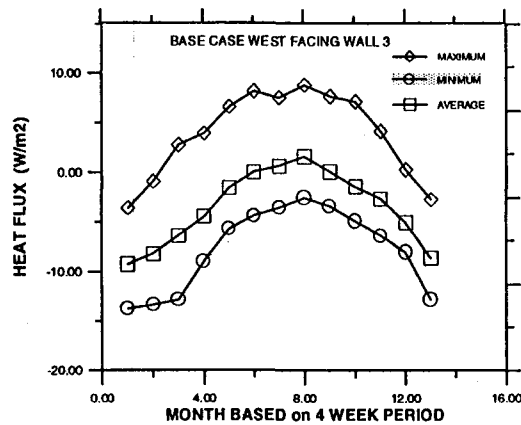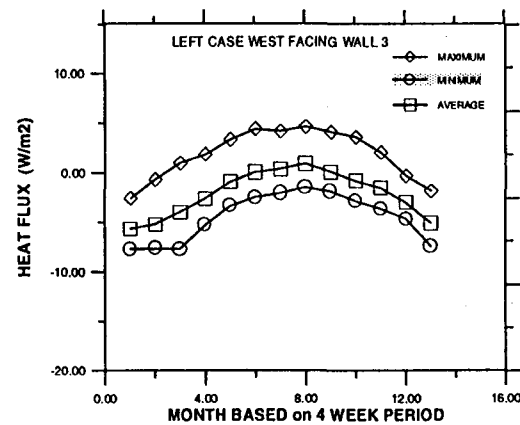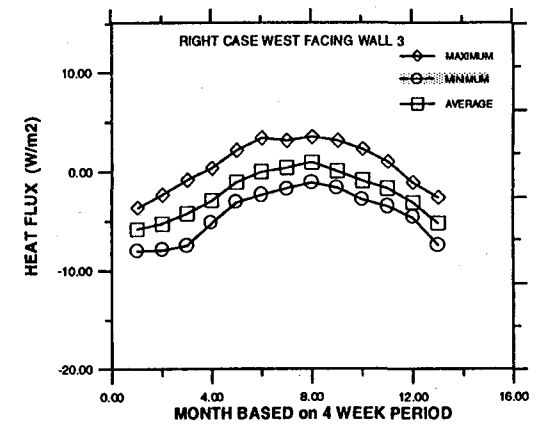
FIGURE C62
OTTAWA
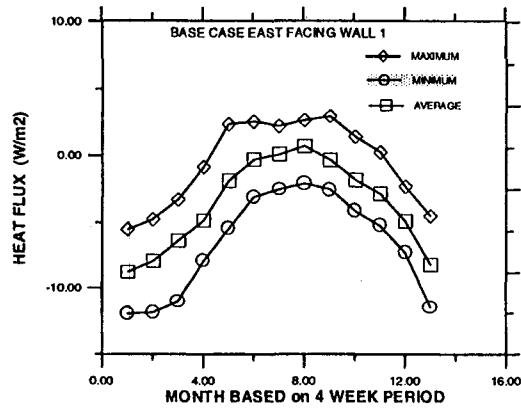
FIGURE C63
OTTAWA

A)
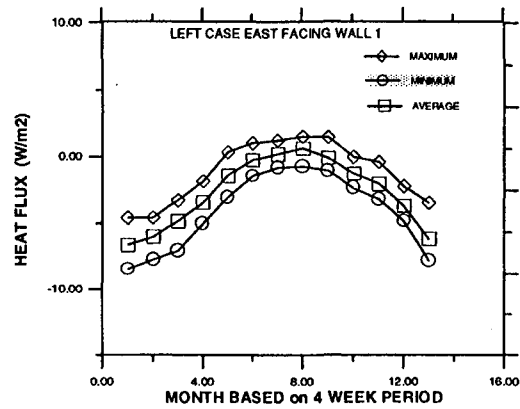
B)
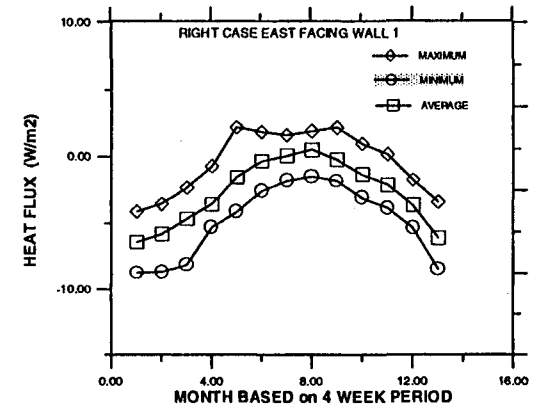
C)
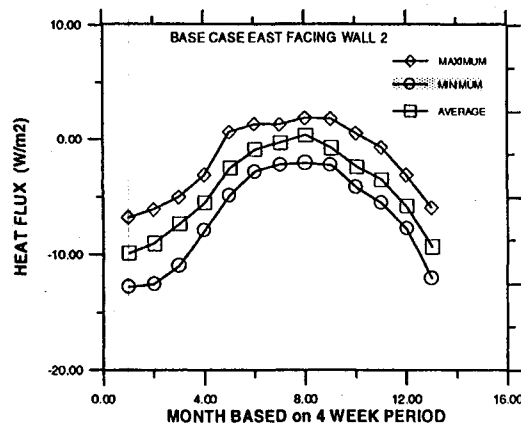
D)
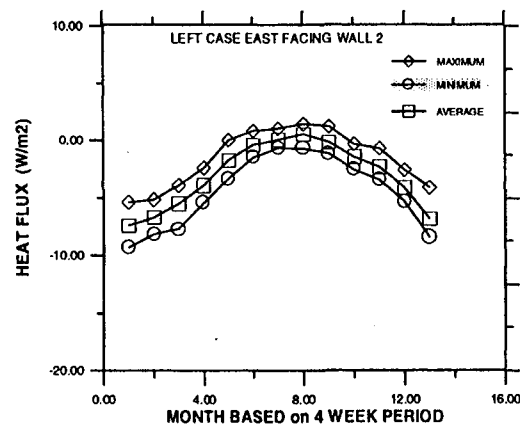
E)
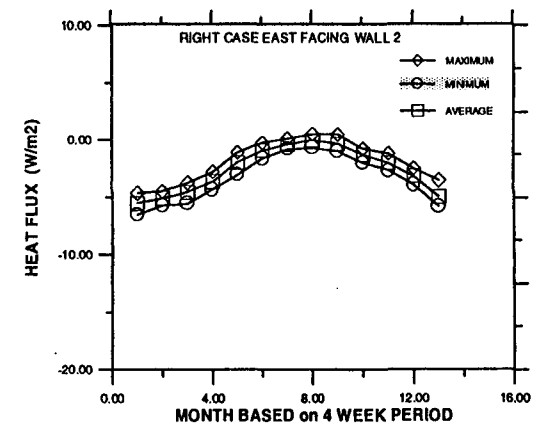
F)

FIGURE C64
OTTAWA
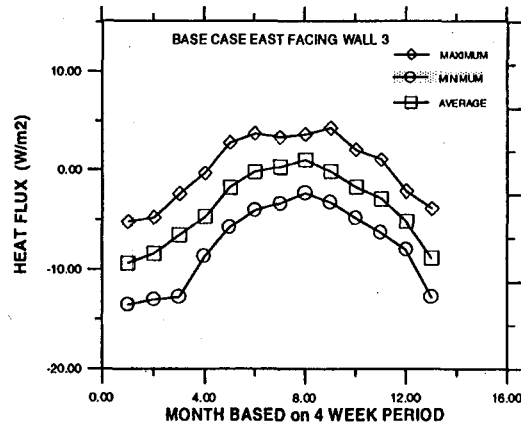
A)
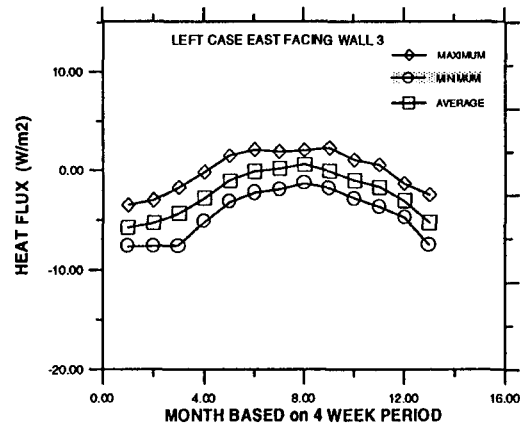
B)

C)

D)

E)

F)
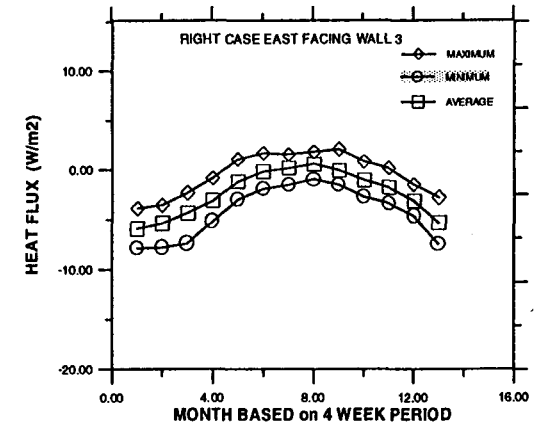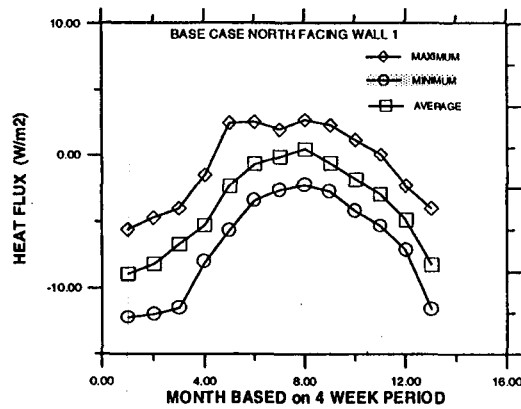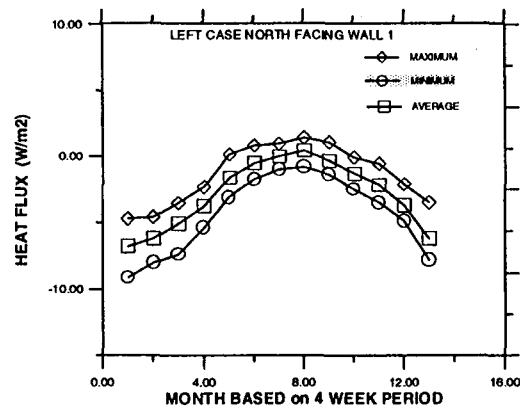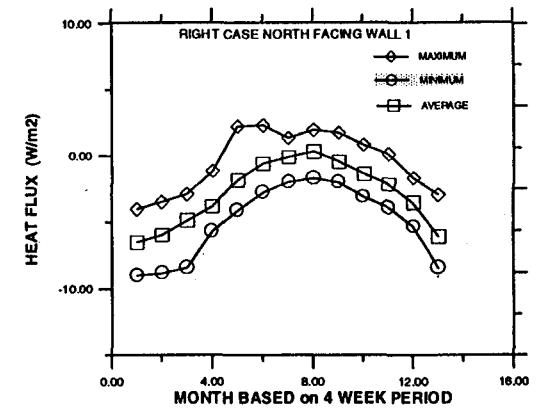
FIGURE C65
OTTAWA
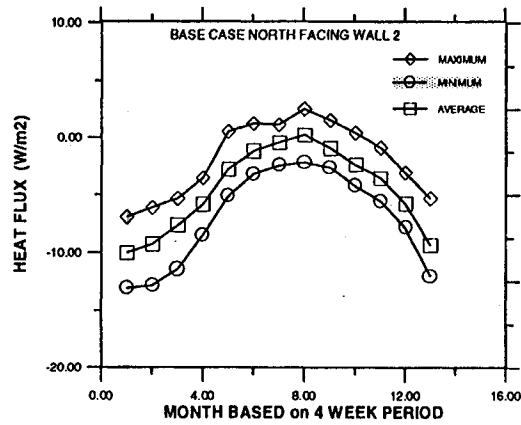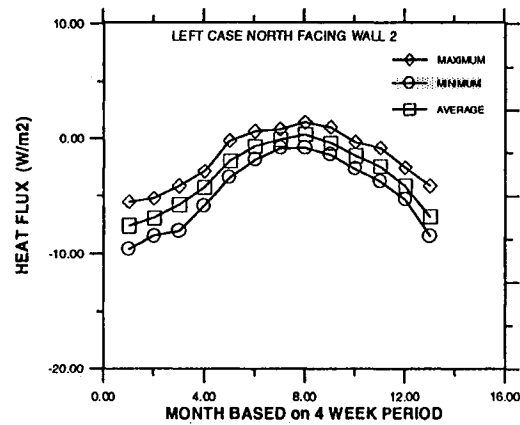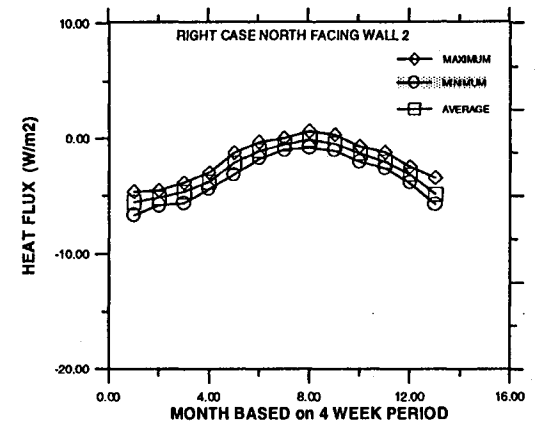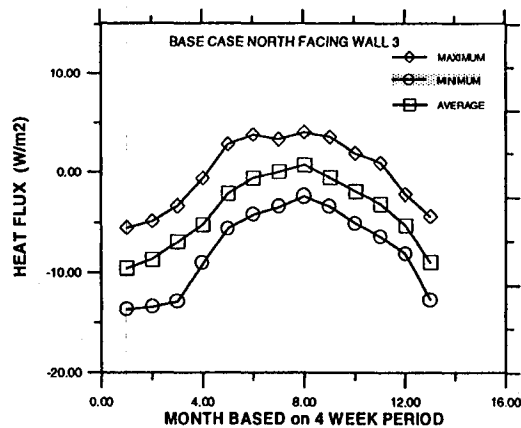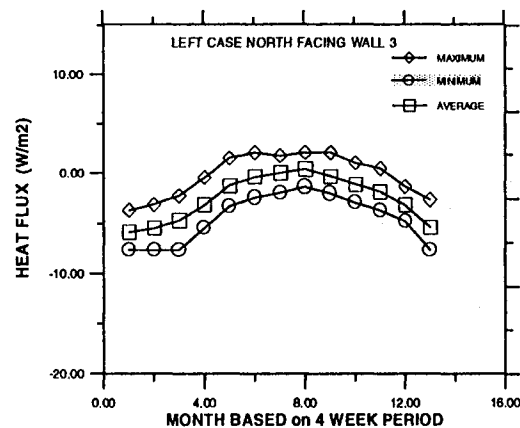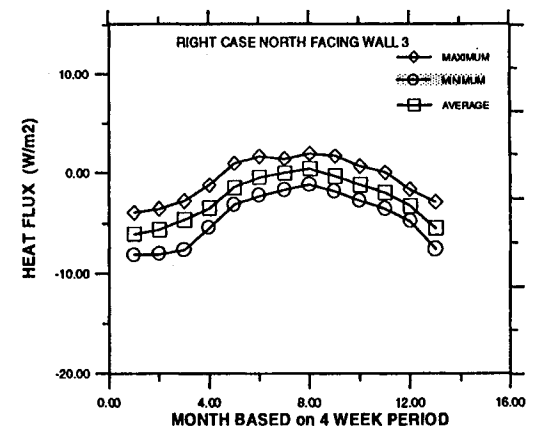
FIGURE C66
OTTAWA
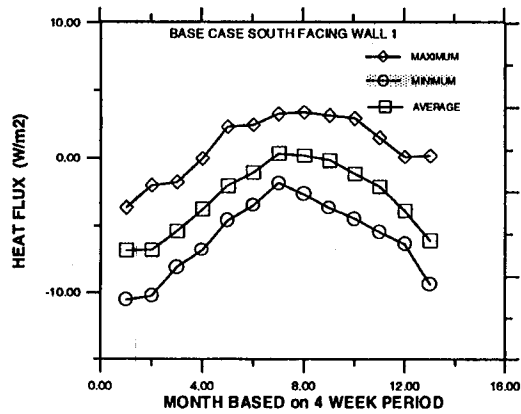
A)
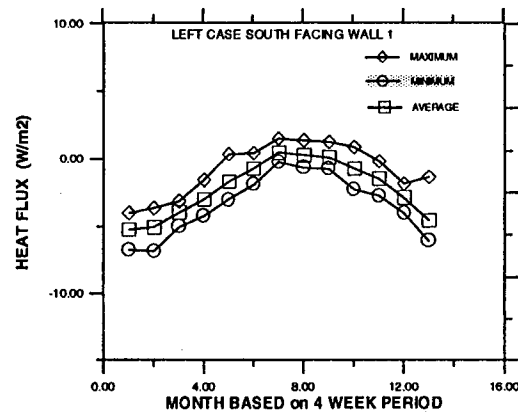
B)
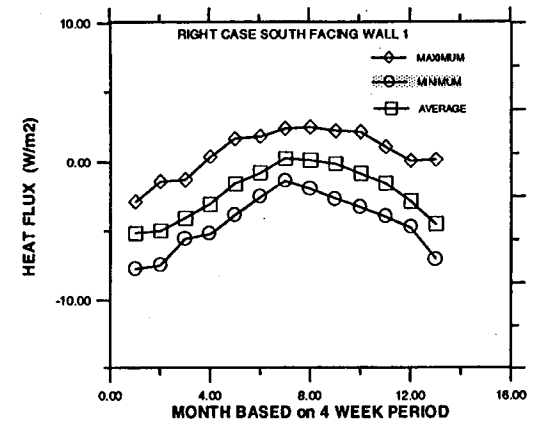
C)
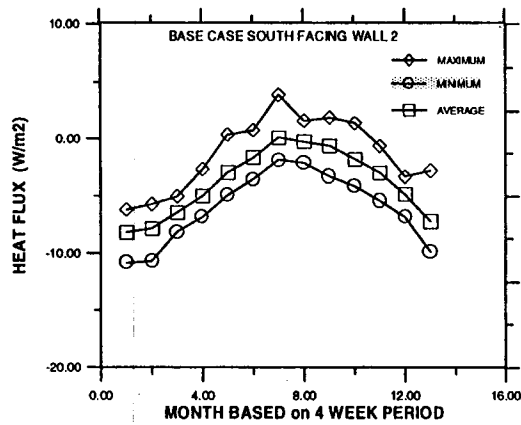
D)
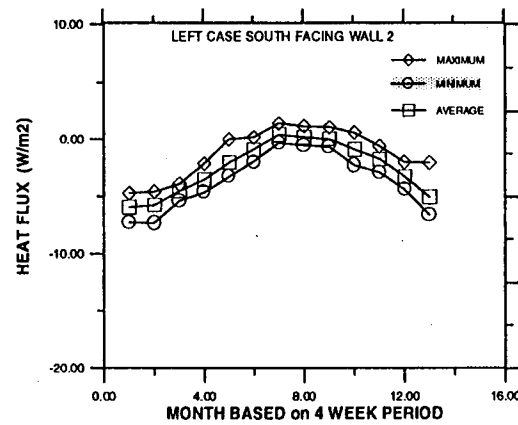
E)
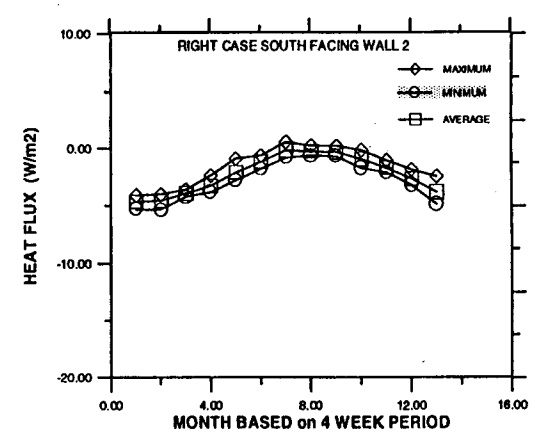
F)

FIGURE C67
TORONTO

A)

B)

C)

D)

E)

F)
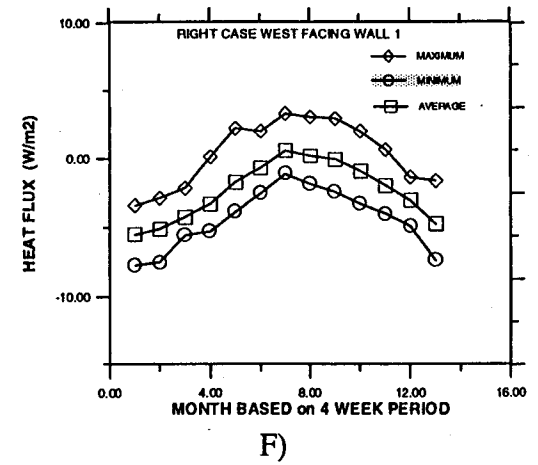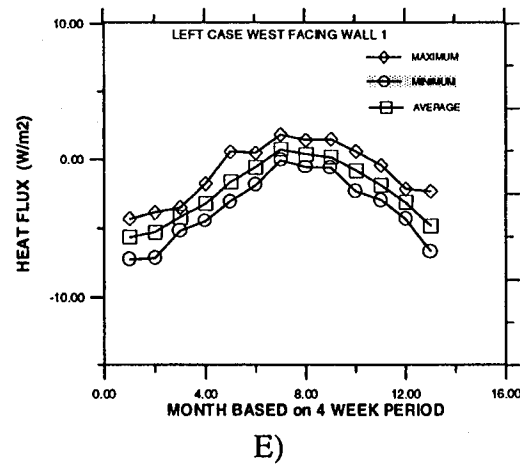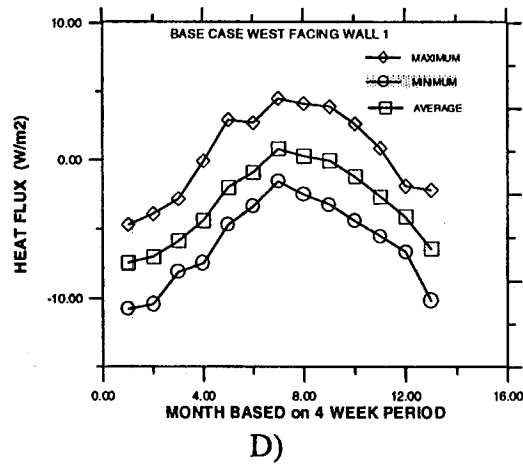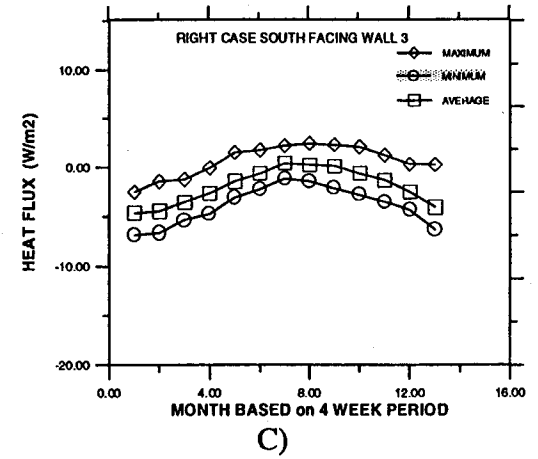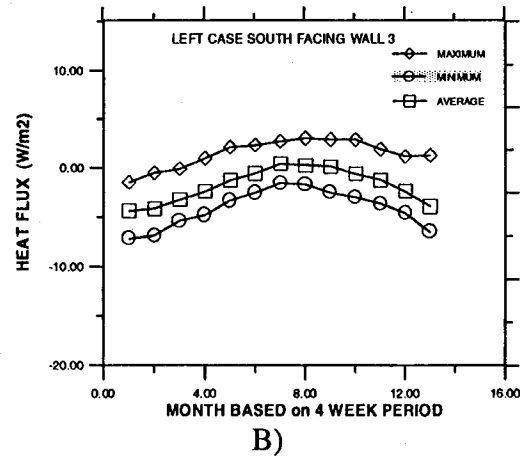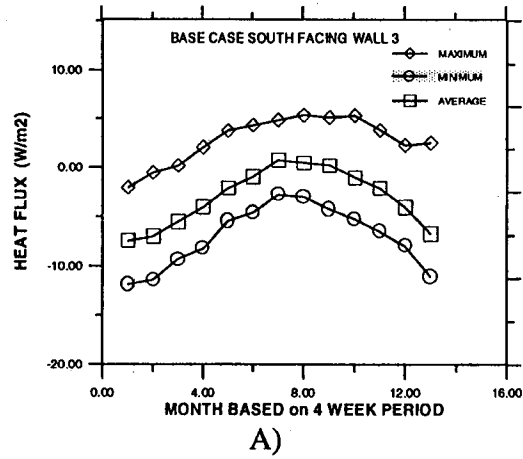
FIGURE C68
TORONTO
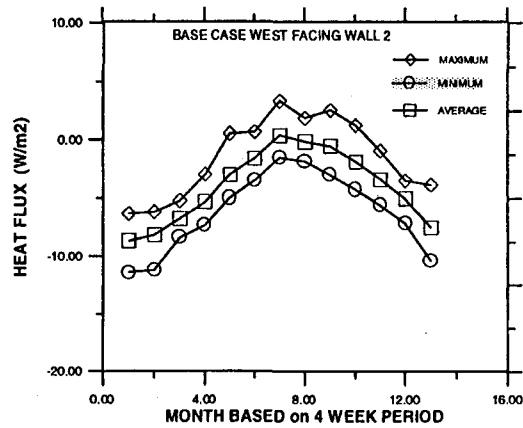
A)

DATA NOT AVAILABLE
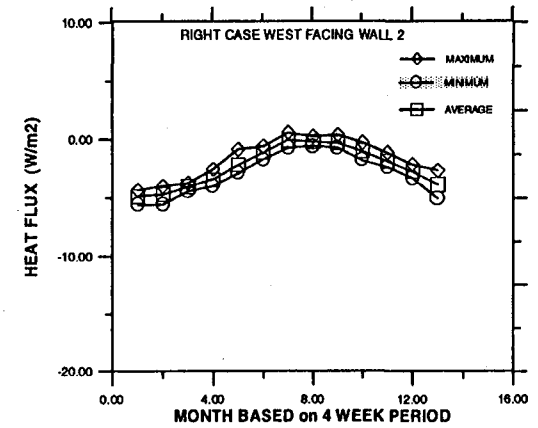
C)
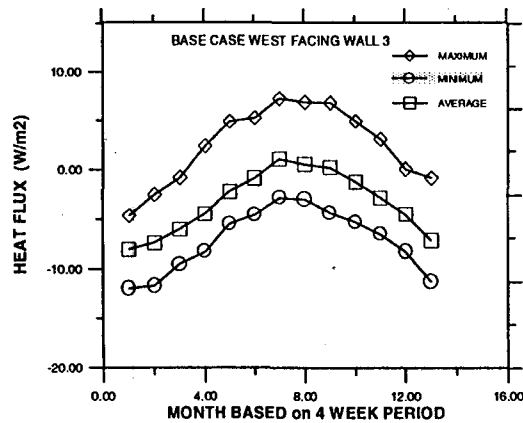
D)
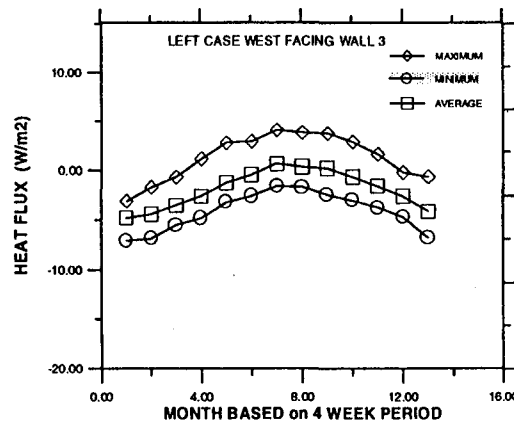
E)
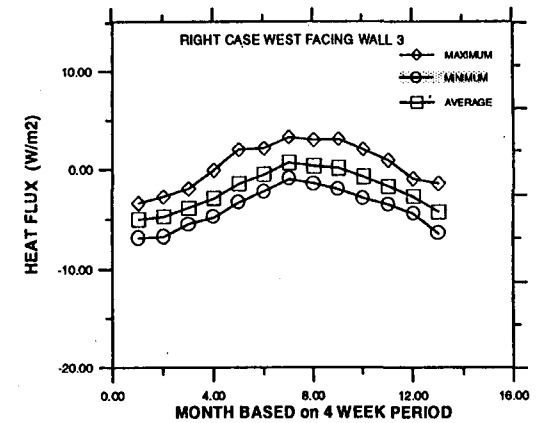
F)

FIGURE C69
TORONTO
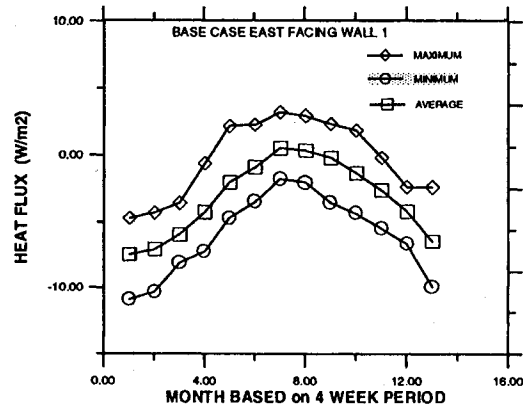
A)
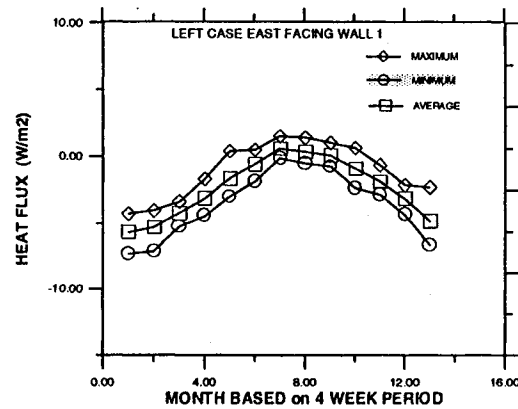
B)
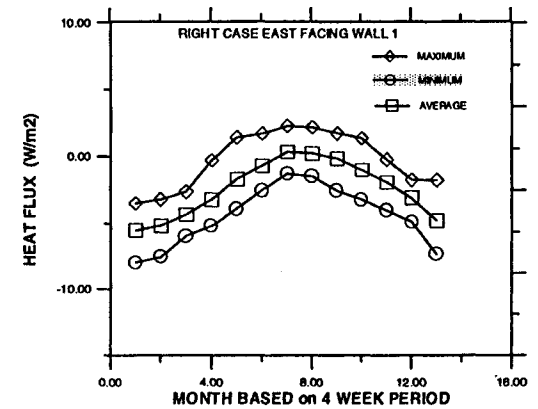
C)
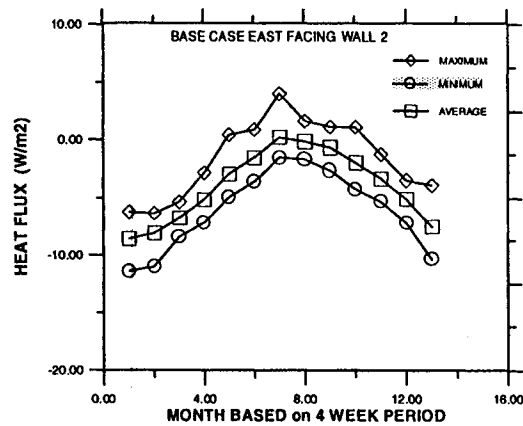
D)
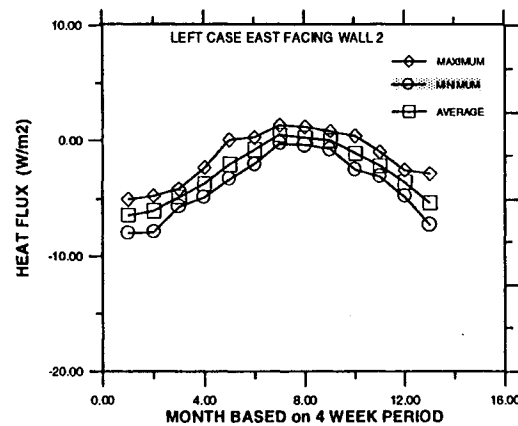
E)
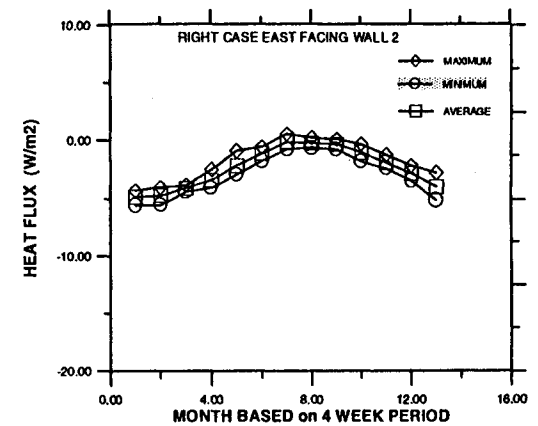
F)

FIGURE C70
TORONTO
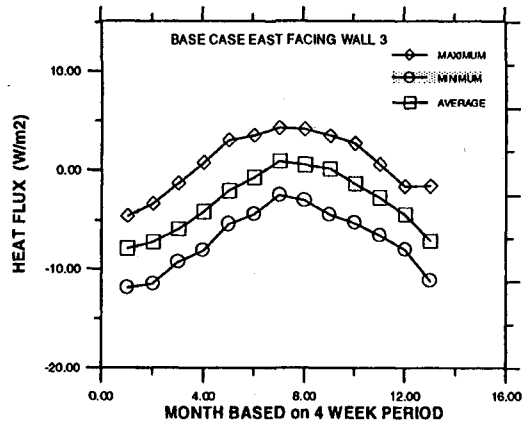
A)
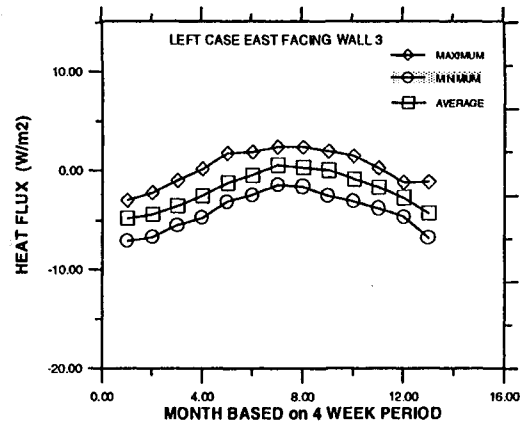
B)
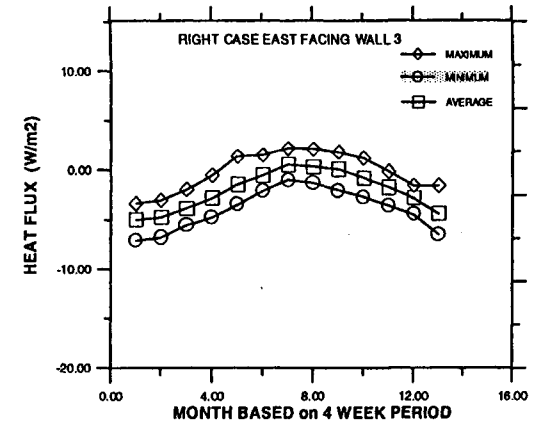
C)
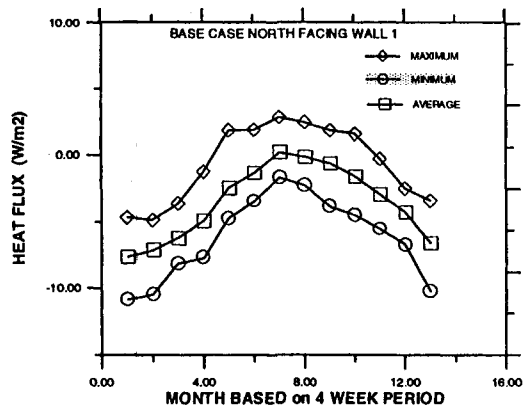
D)
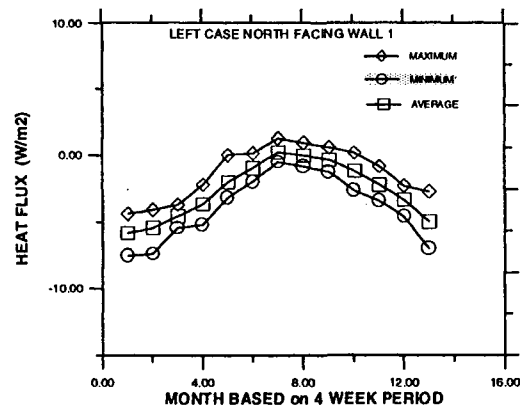
E)
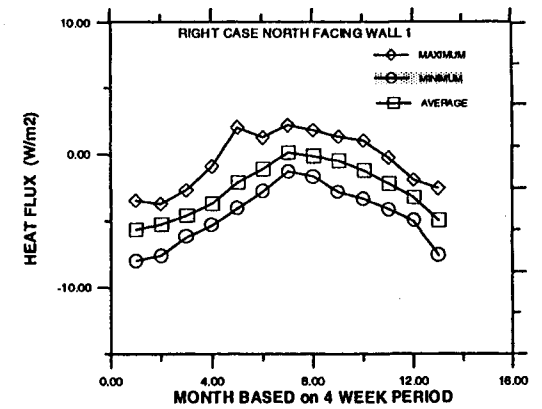
F)

FIGURE C71
TORONTO

A)

B)

C)

D)

E)

F)
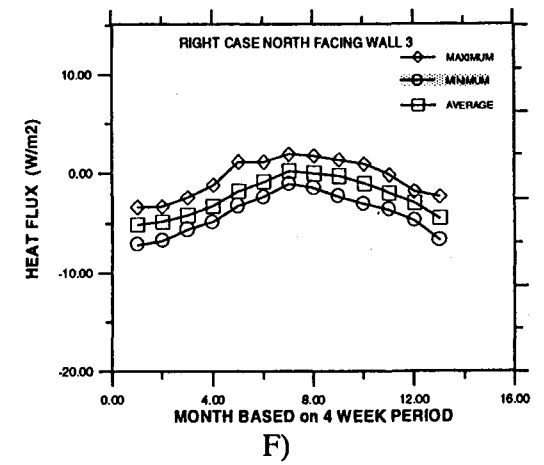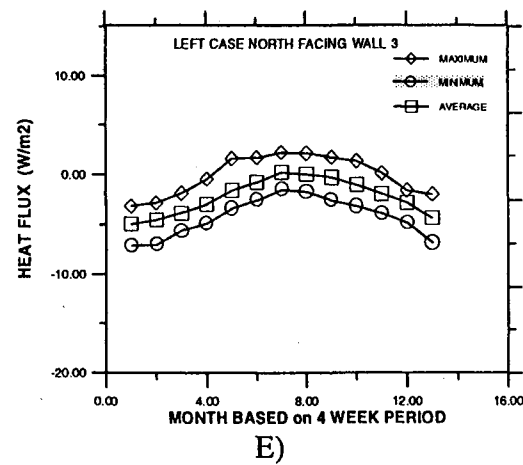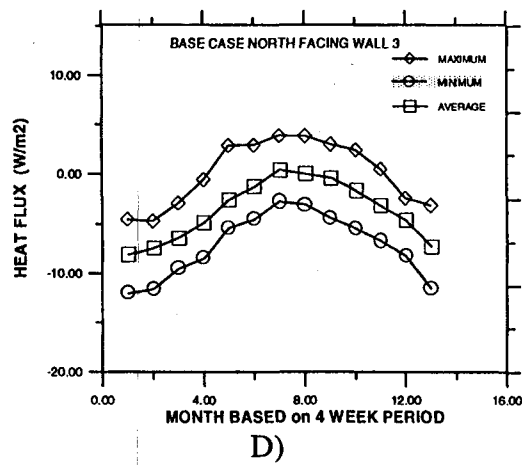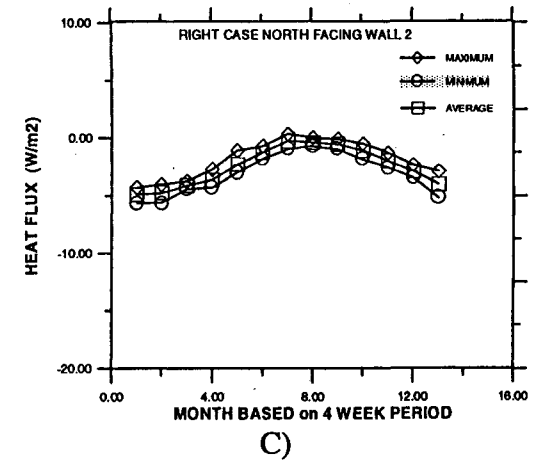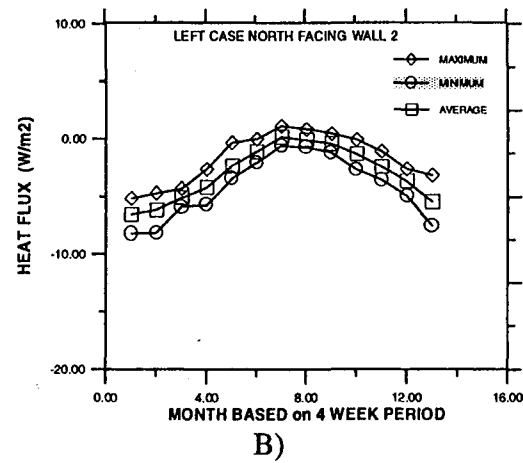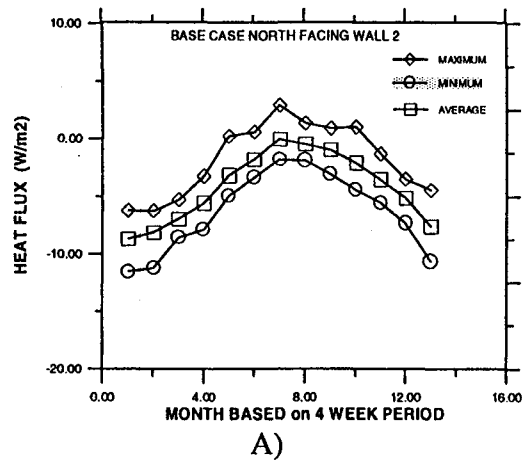
FIGURE C72
TORONTO
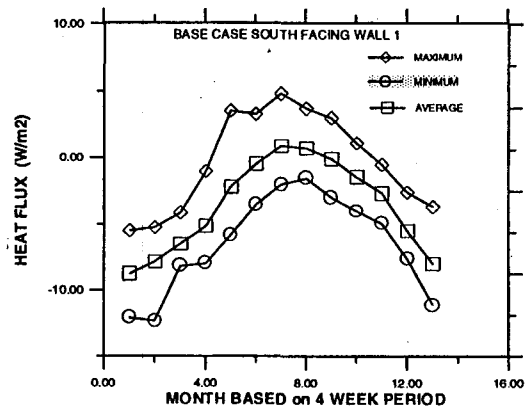
A)
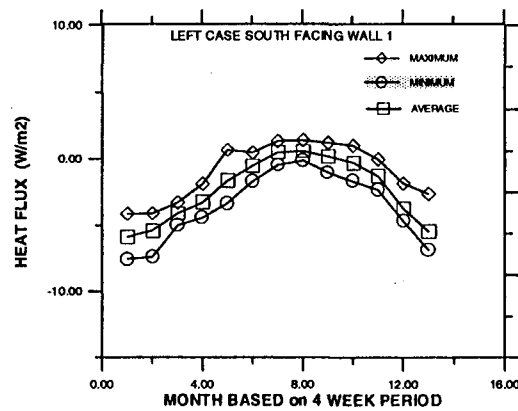
B)
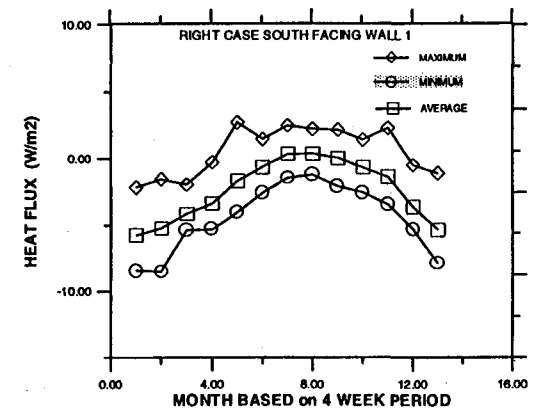
C)
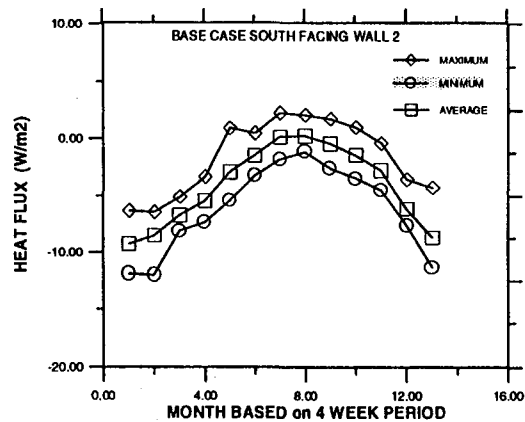
D)
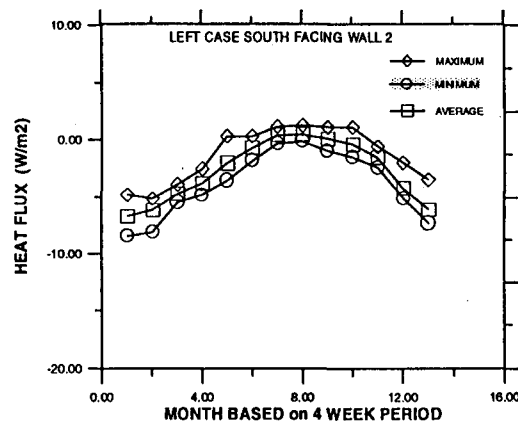
E)
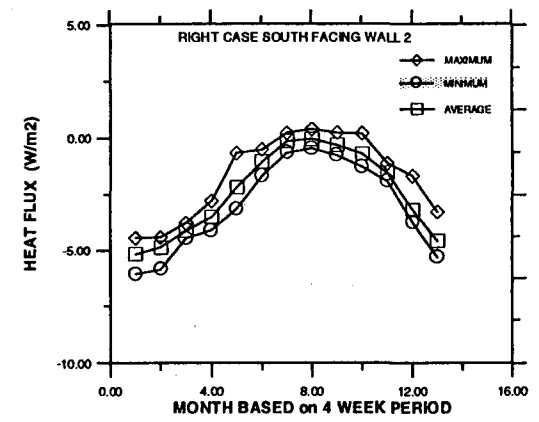
F)

FIGURE C73
MONTREAL

A)

B)

C)

D)

E)

F)
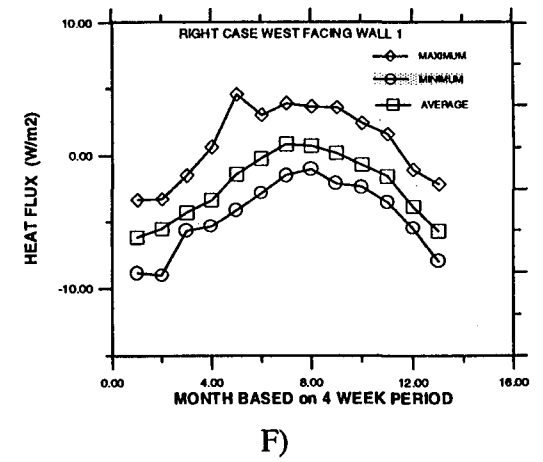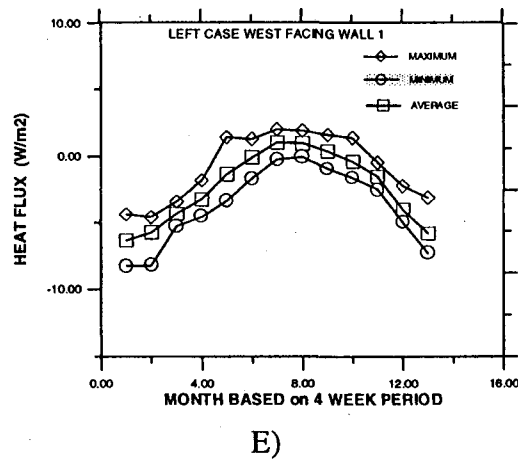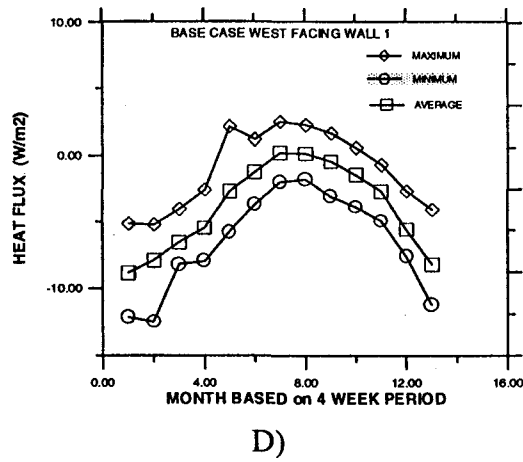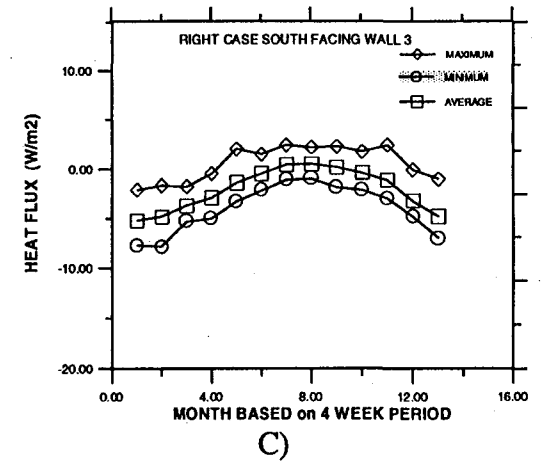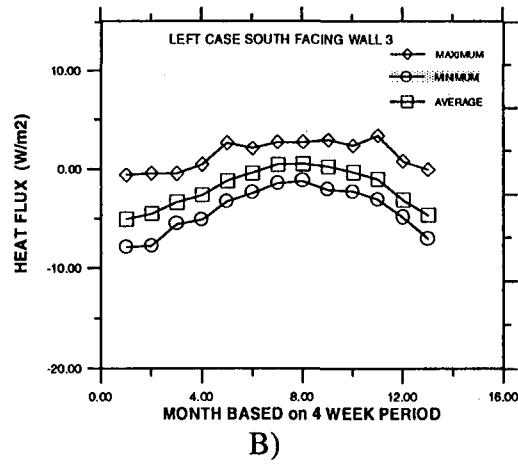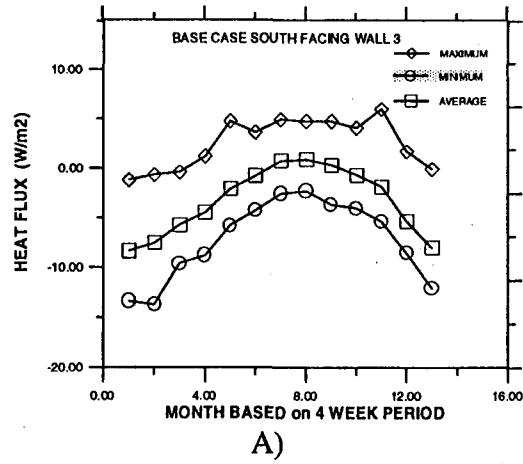
FIGURE C74
MONTREAL
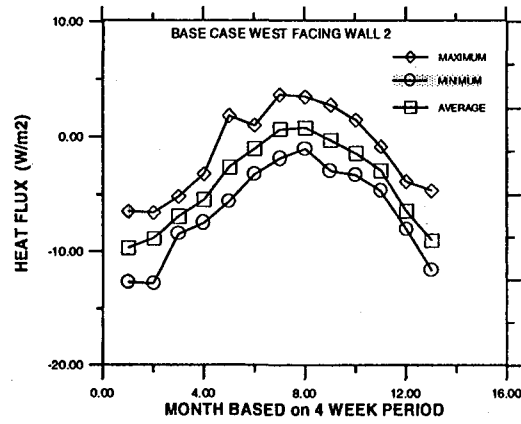
A)
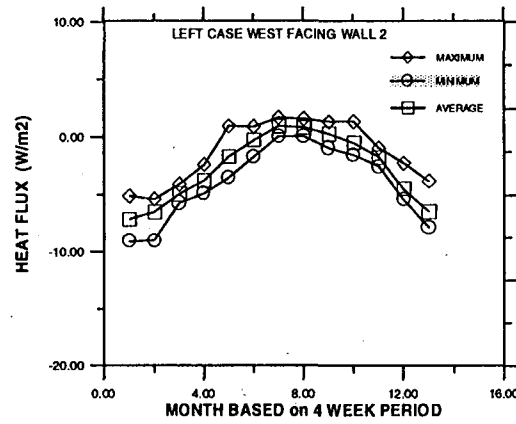
B)
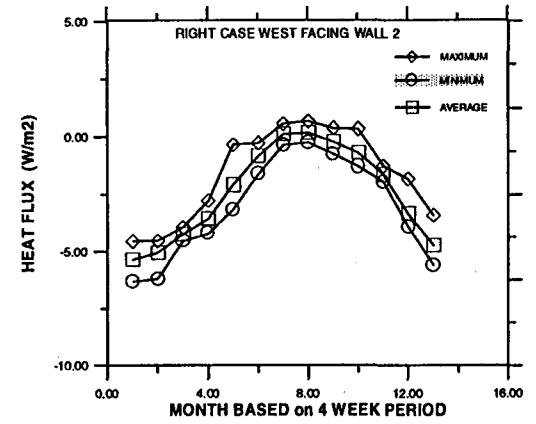
C)
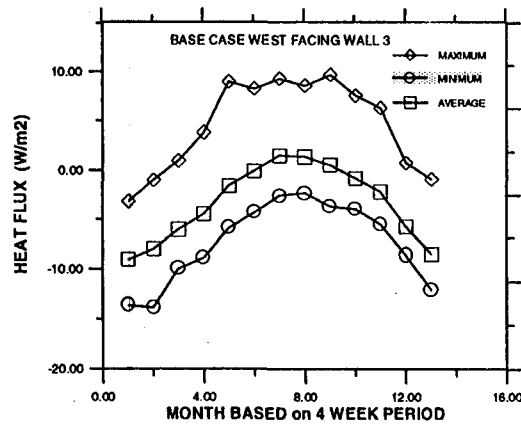
D)
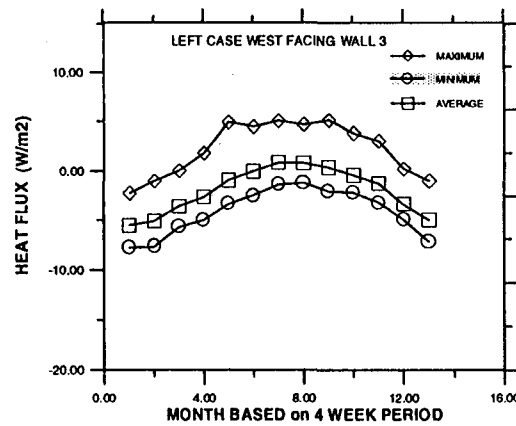
E)
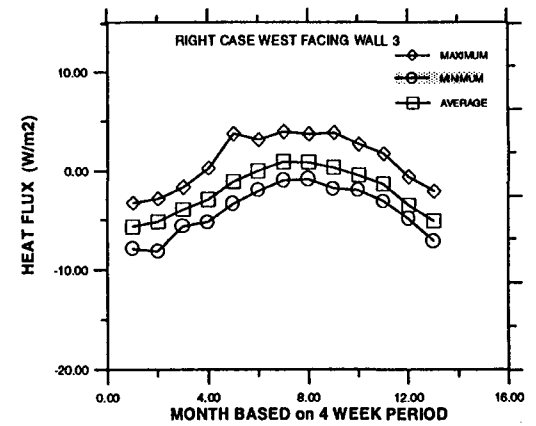
F)

FIGURE C75
MONTREAL
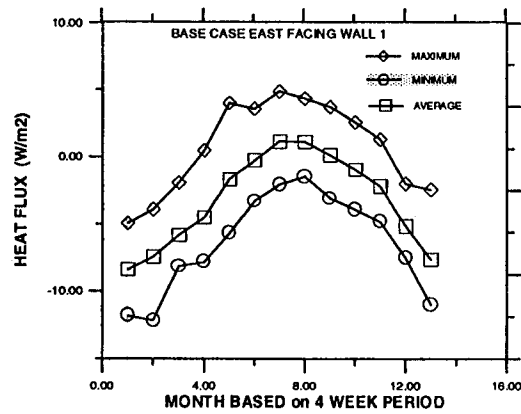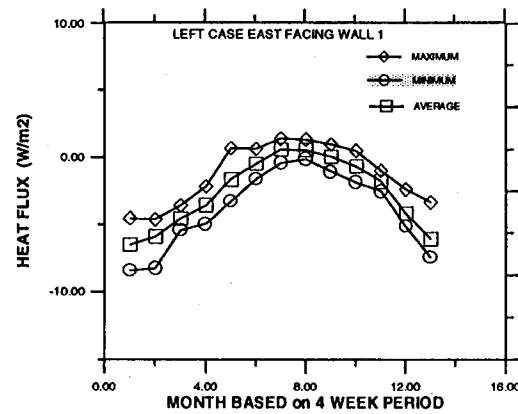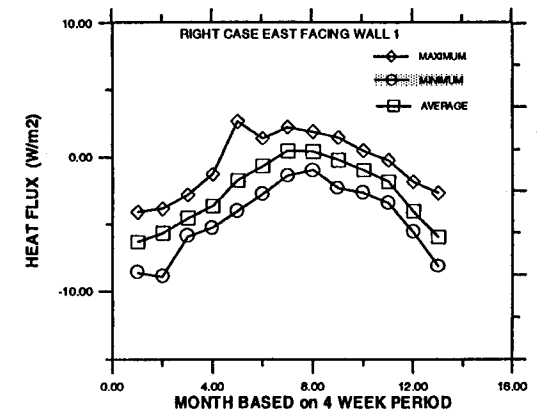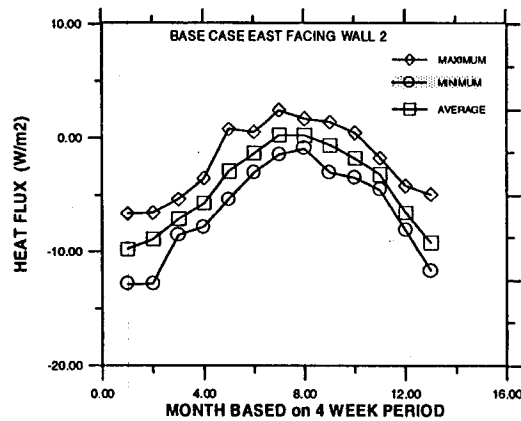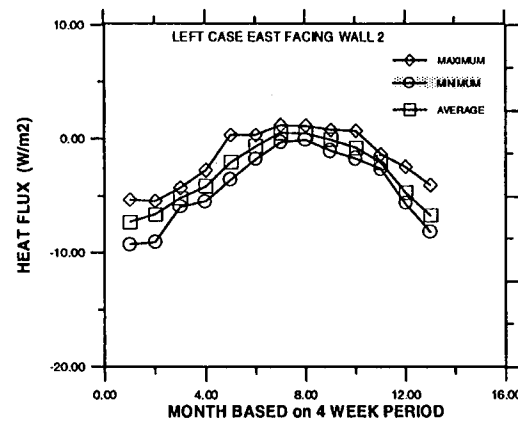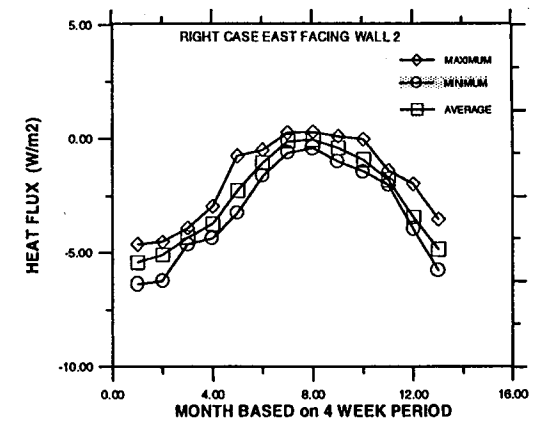
FIGURE C76
MONTREAL
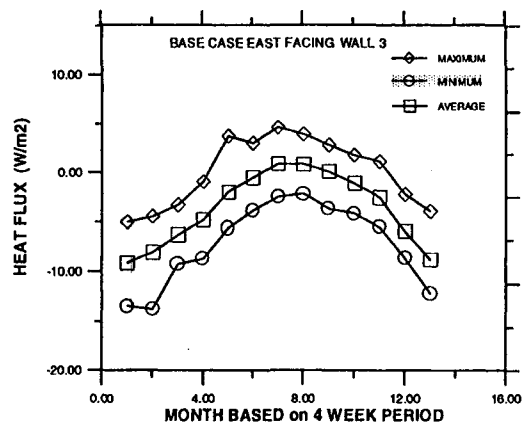
A)
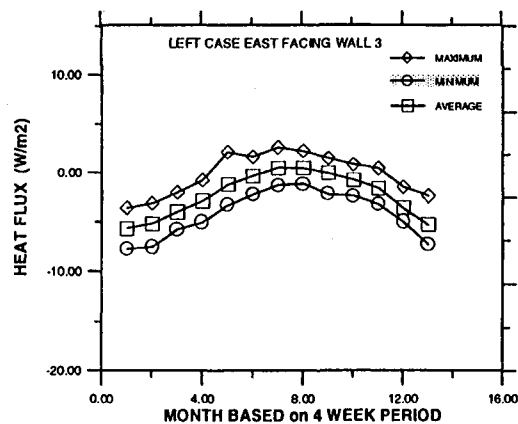
B)
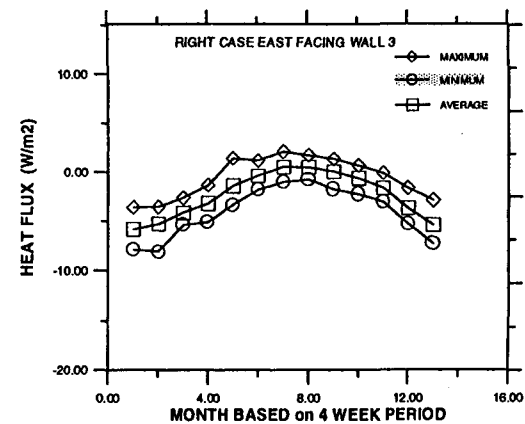
C)
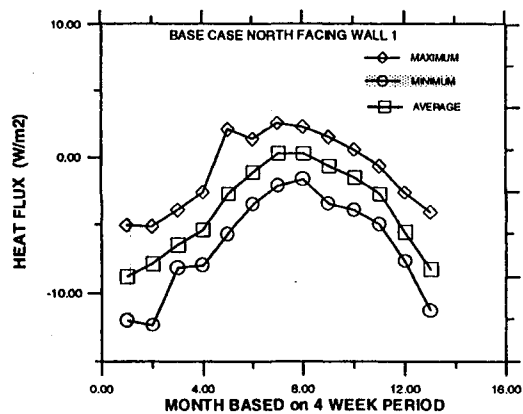
D)
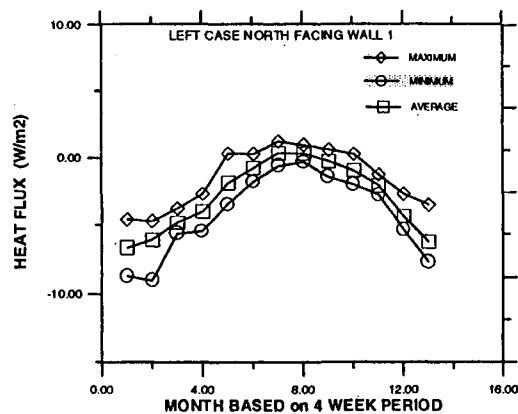
E)
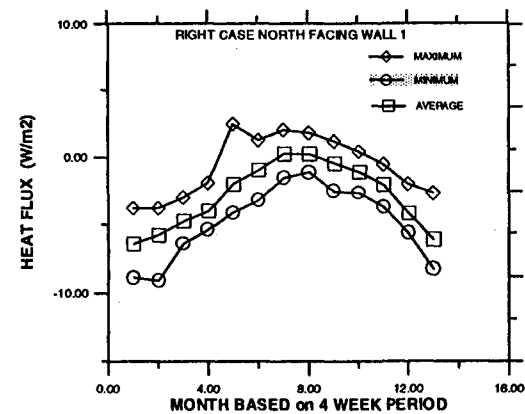
F)

FIGURE C77
MONTREAL

A)

B)

C)

D)

E)

F)
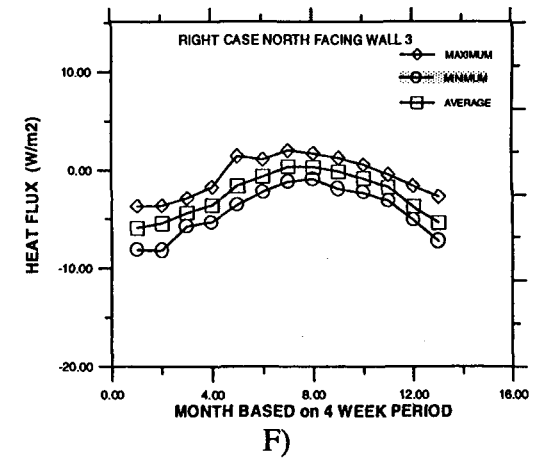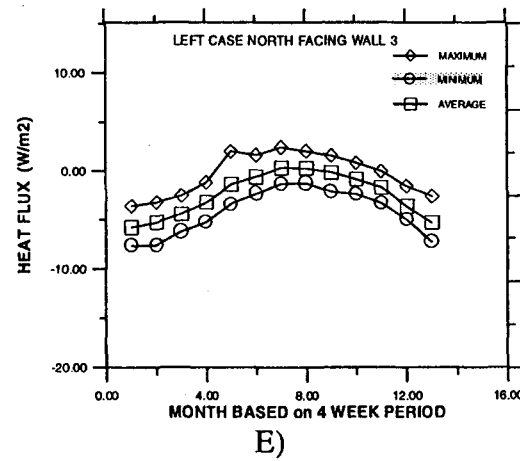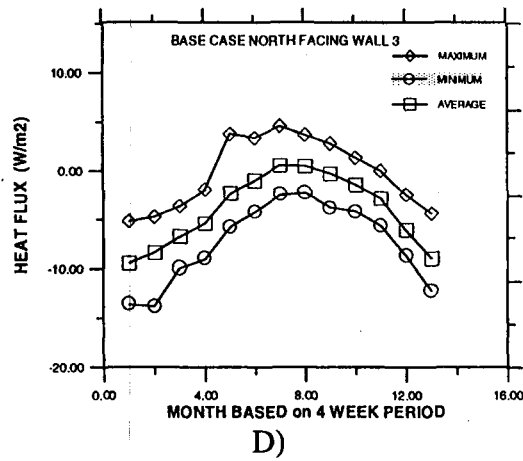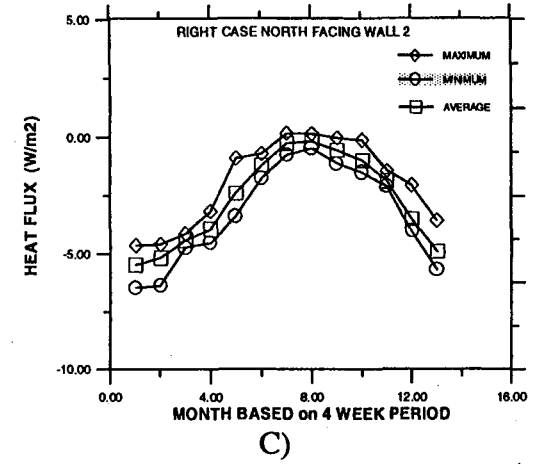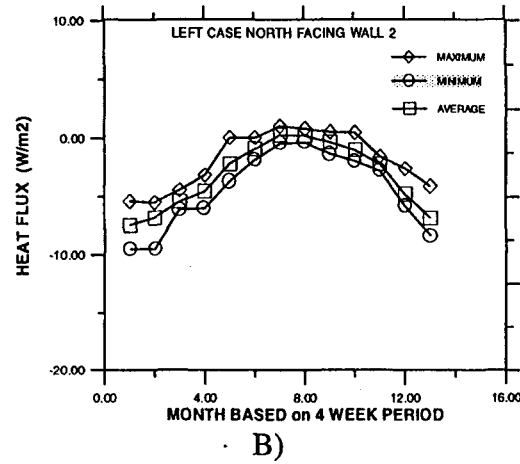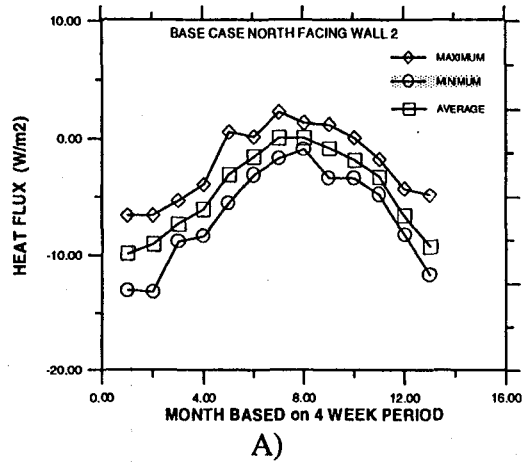
FIGURE C78
MONTREAL
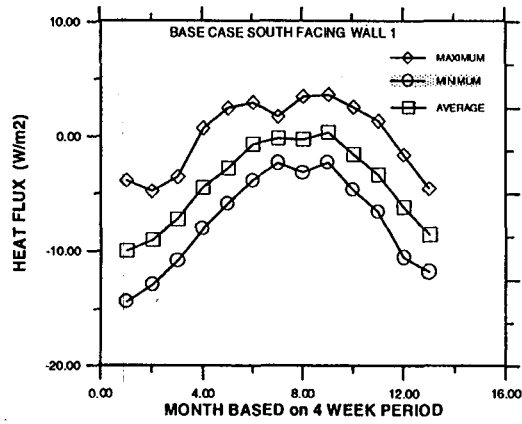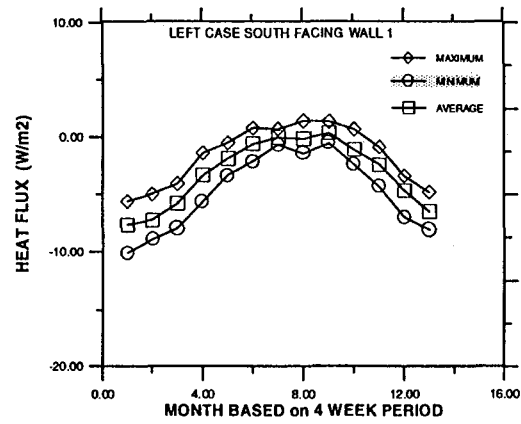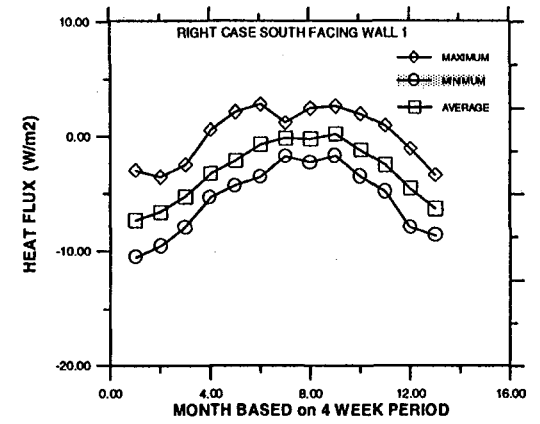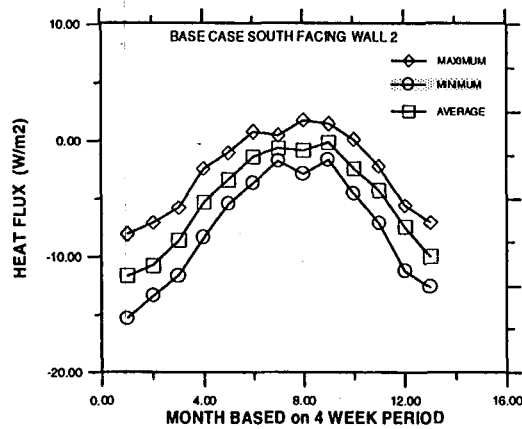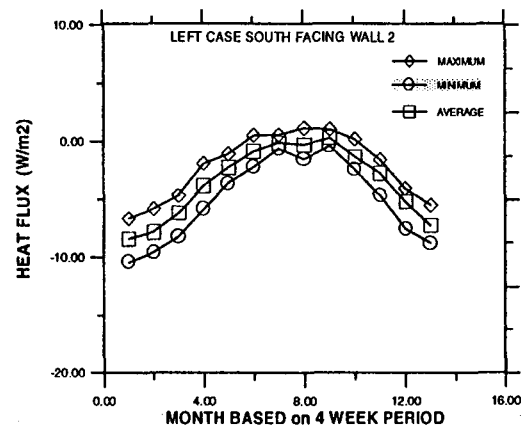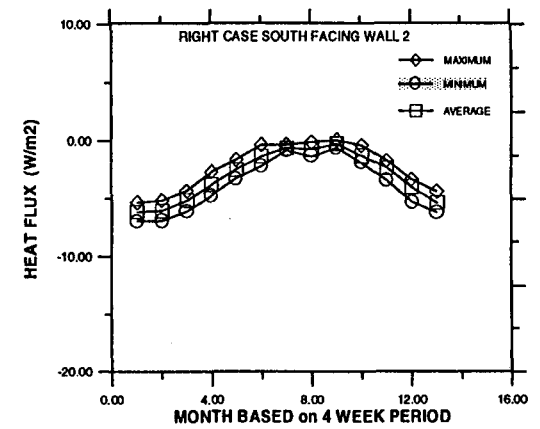
FIGURE C79
WINNIPEG

APPENDIX C

C83

FIGURE C80
WINNIPEG

FIGURE C81
WINNIPEG
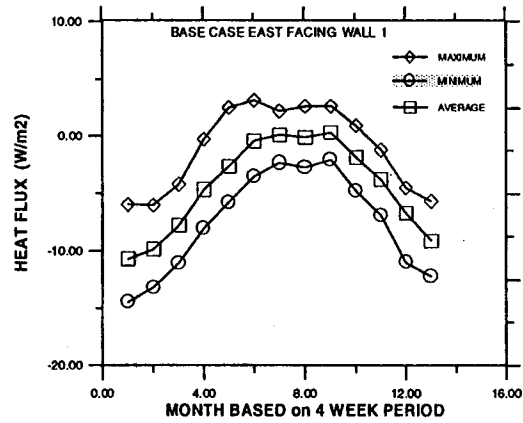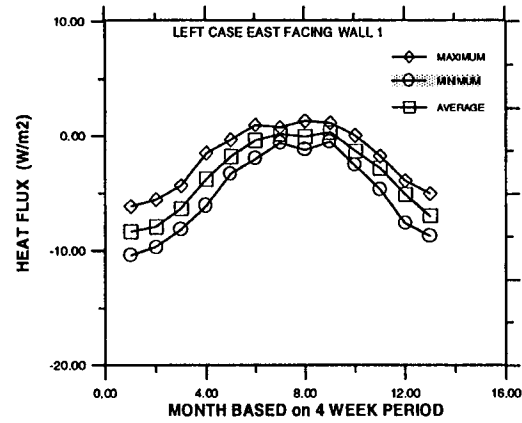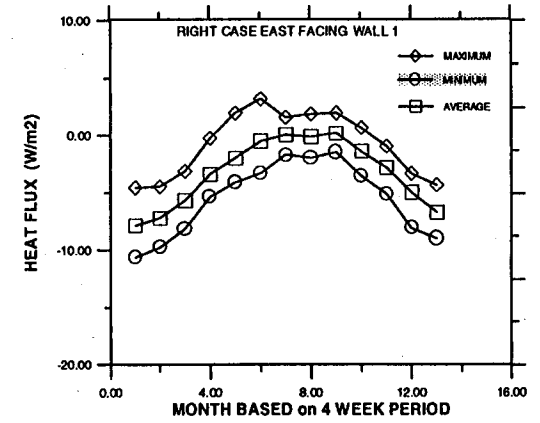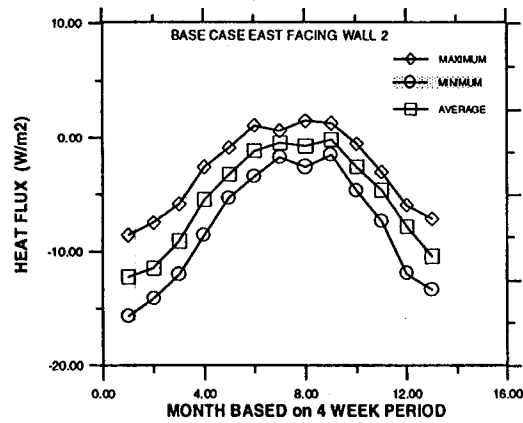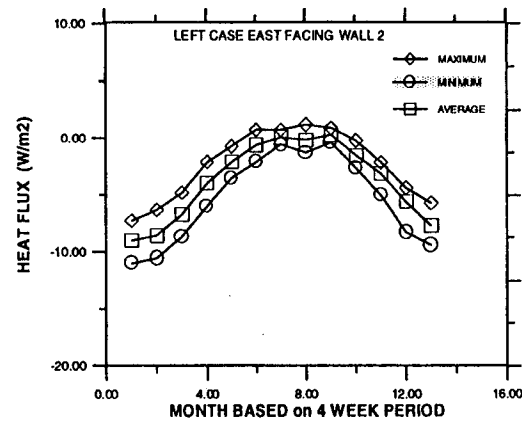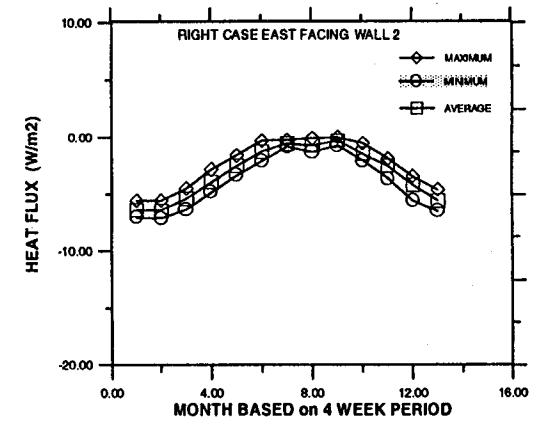
FIGURE C82
WINNIPEG

A)

B)

C)

D)

E)

F)
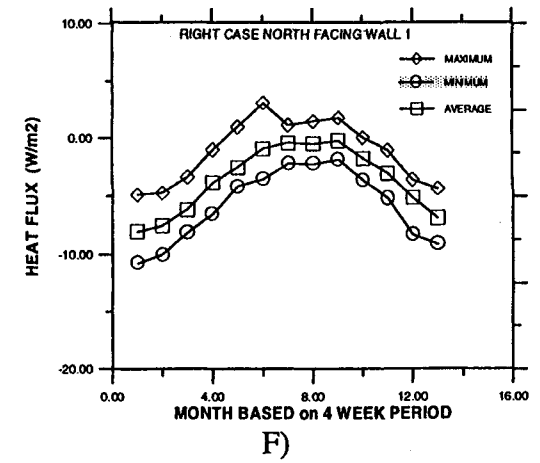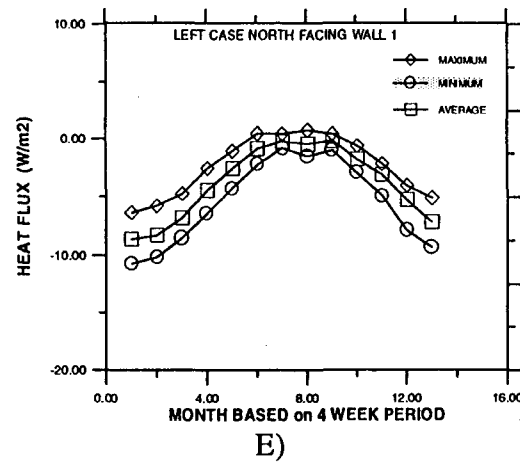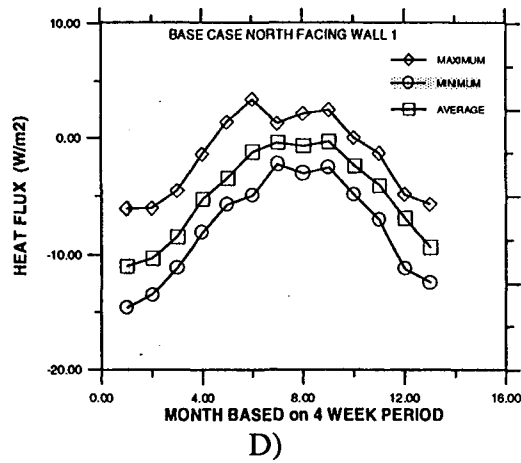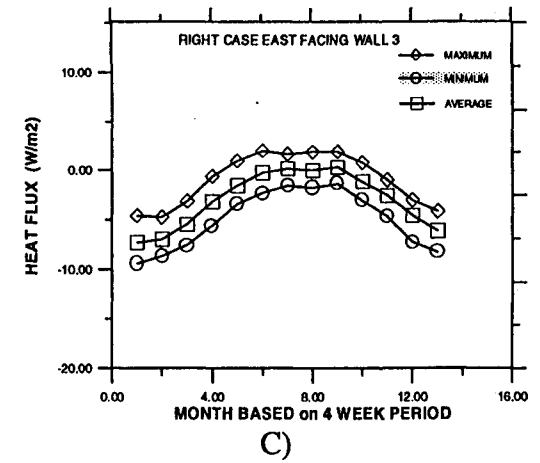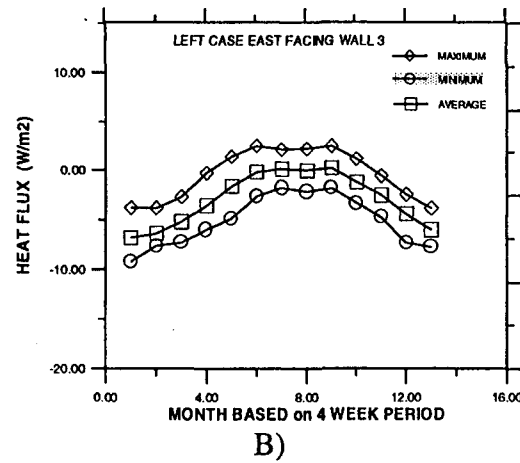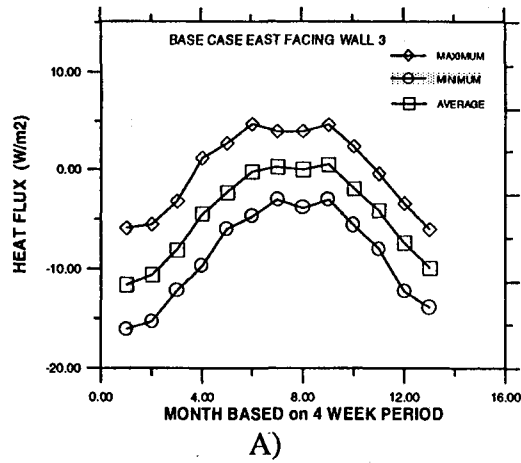
FIGURE C83
WINNIPEG
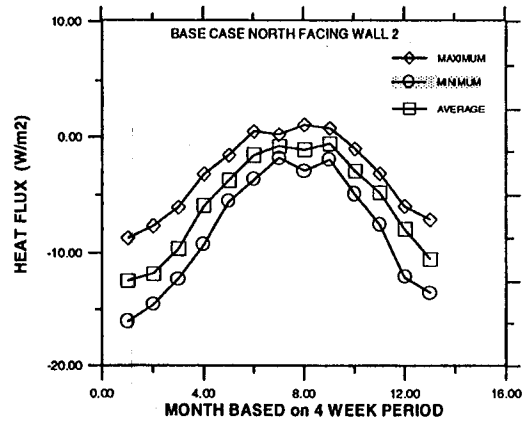
A)
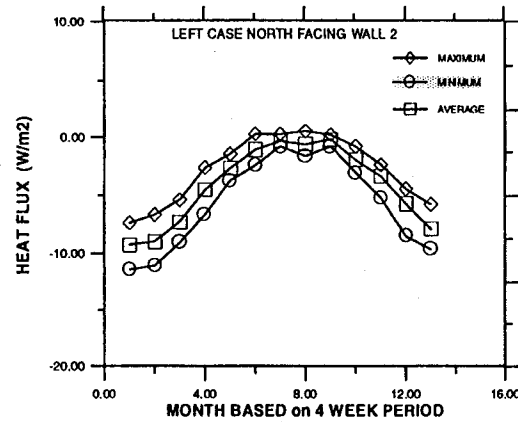
B)
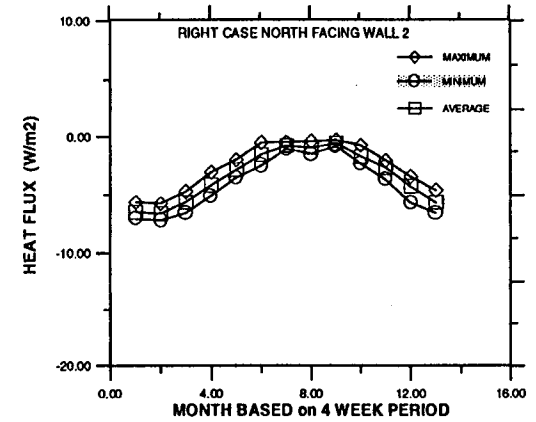
C)
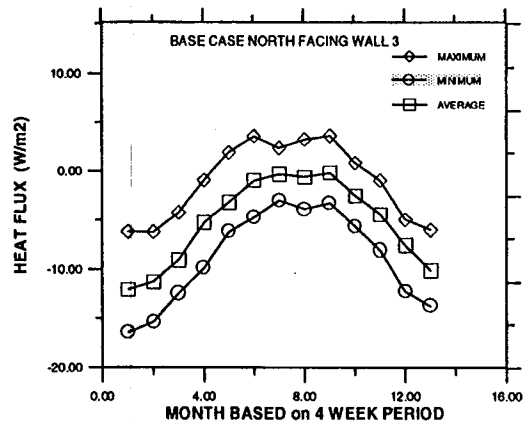
D)
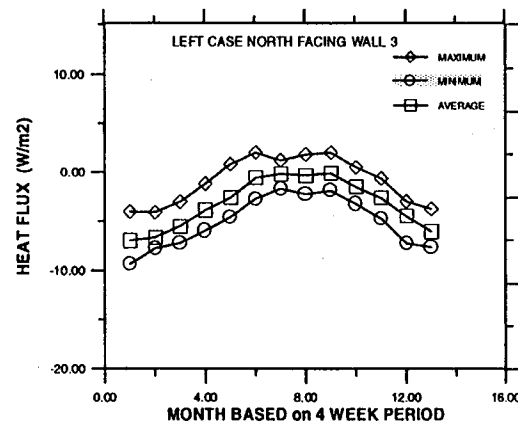
E)
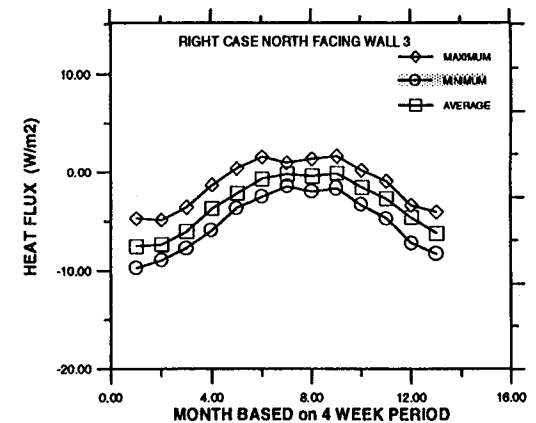
F)

FIGURE C84
WINNIPEG
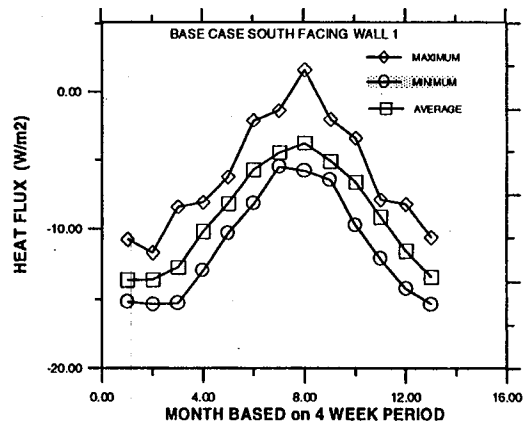
A)
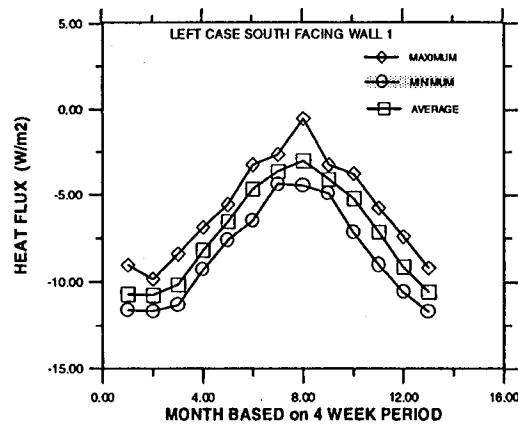
B)
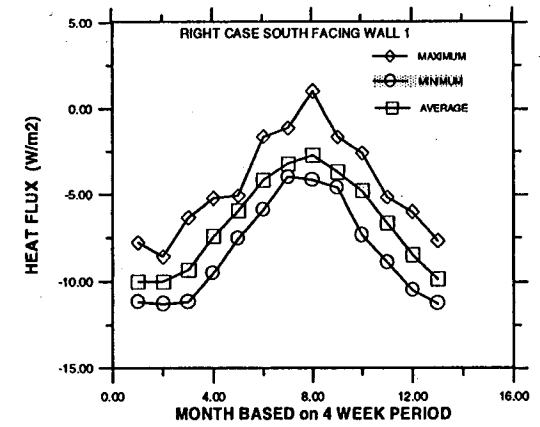
C)
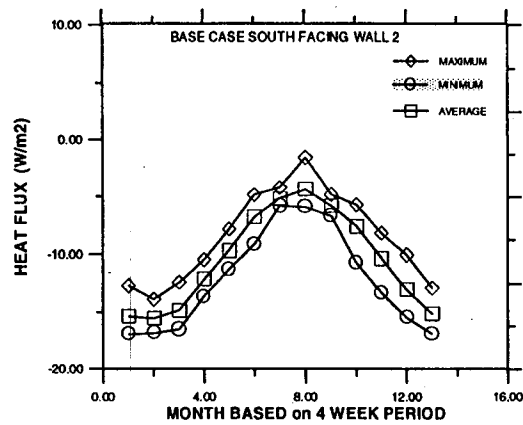
D)
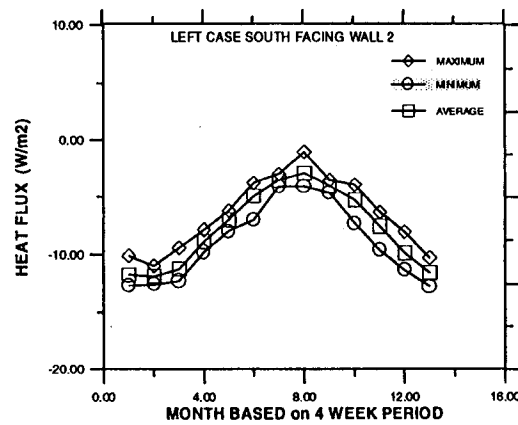
E)
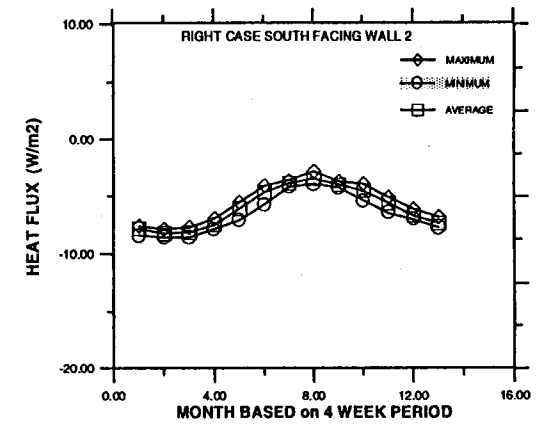
F)

FIGURE C85
RESOLUTE
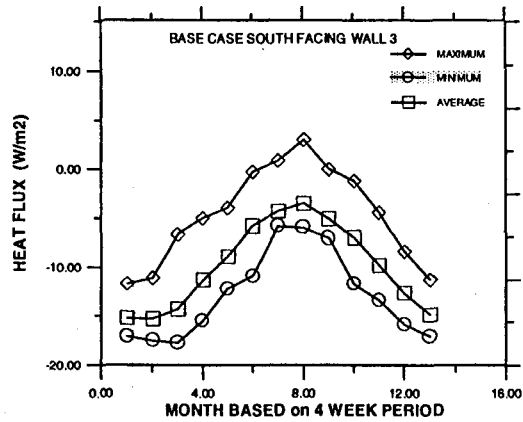
A)
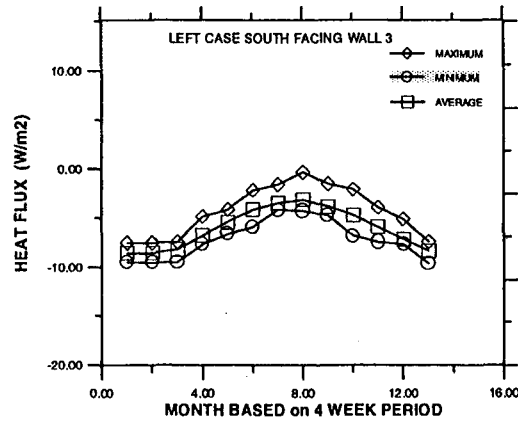
B)
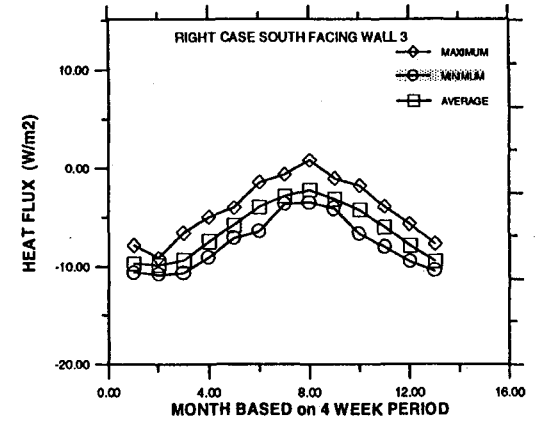
C)
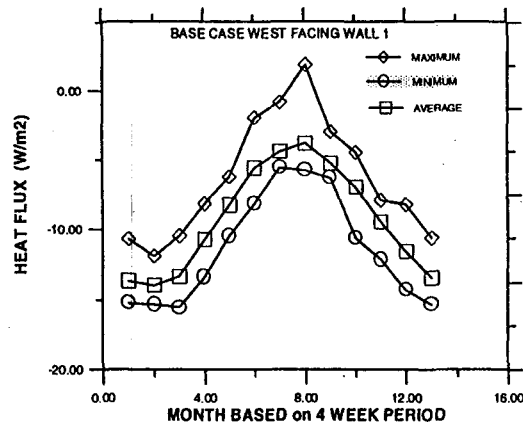
D)
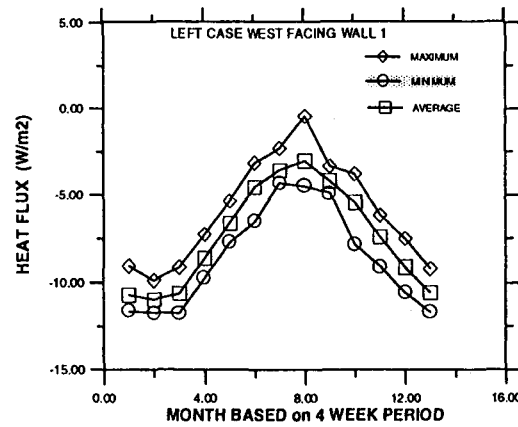
E)
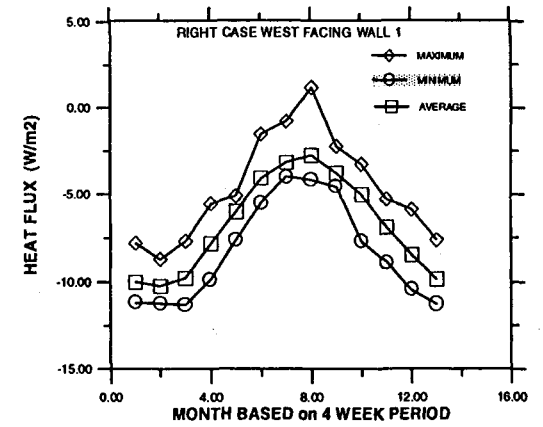
F)

FIGURE C86
RESOLUTE
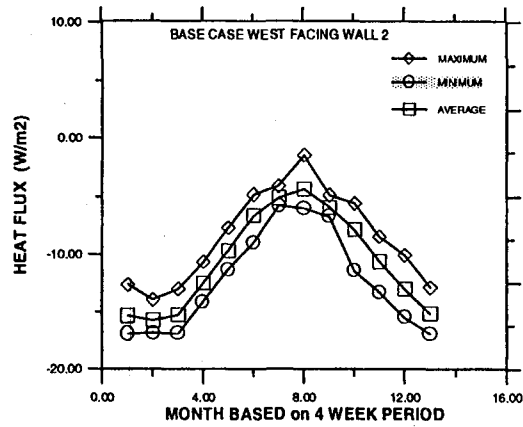
A)
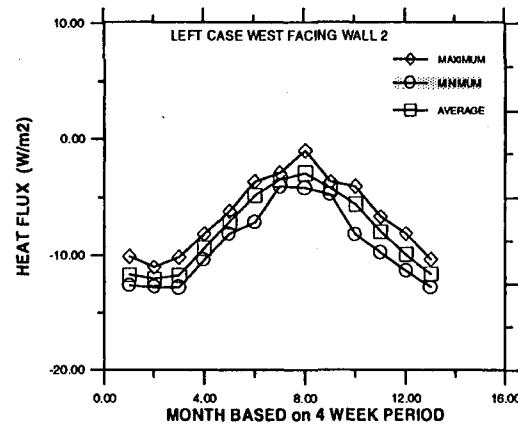
B)
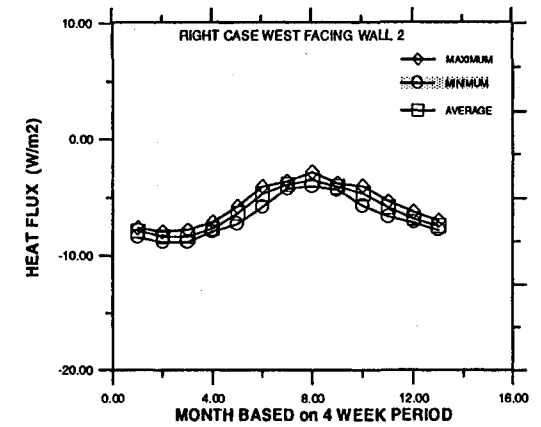
C)
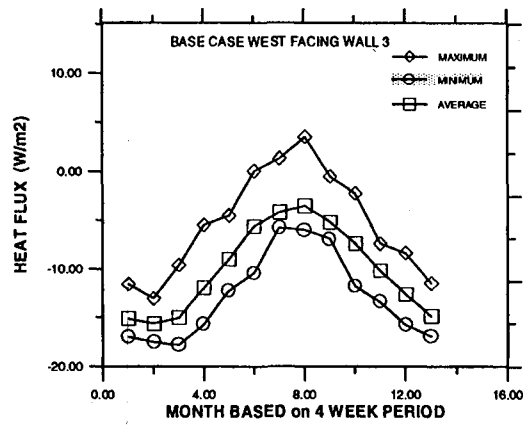
D)
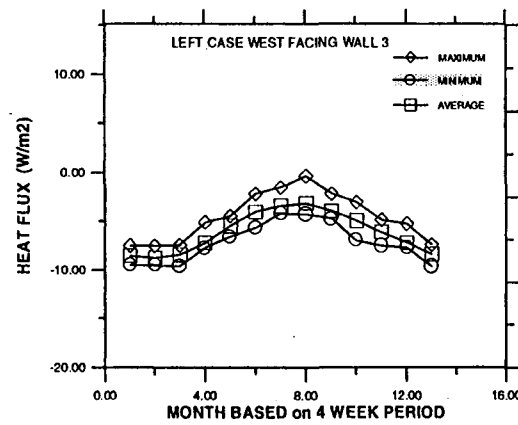
E)

F)
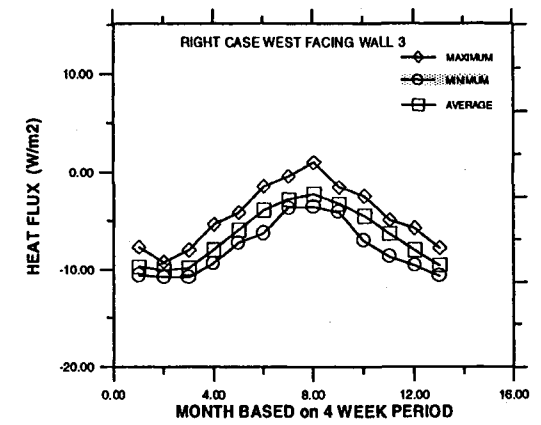
FIGURE C87
RESOLUTE
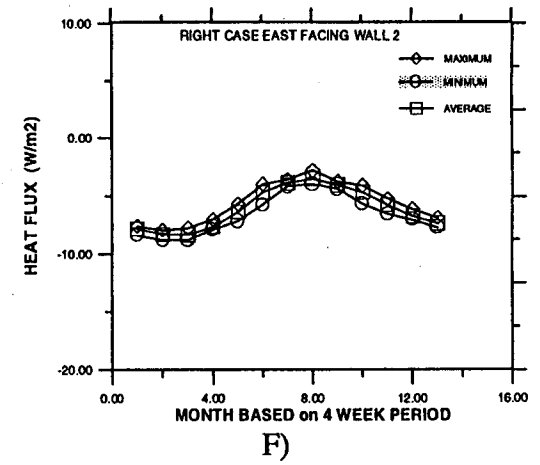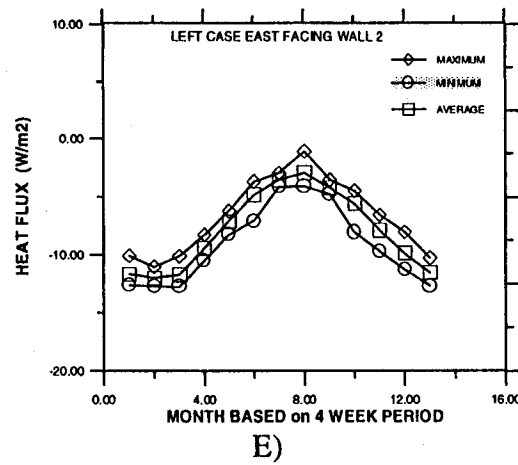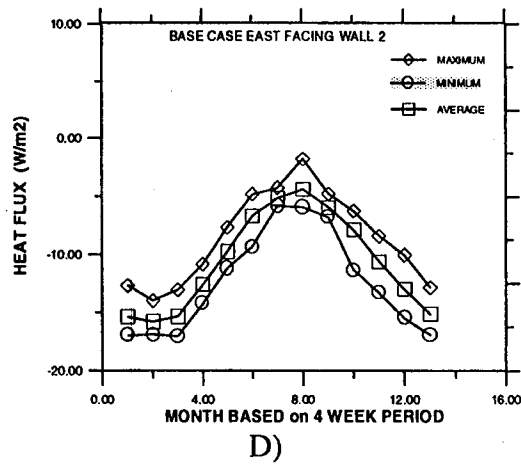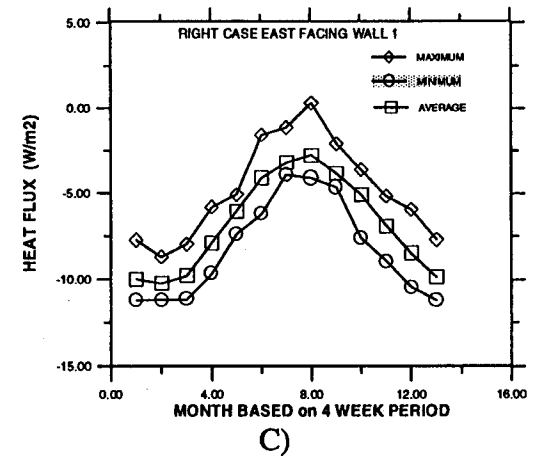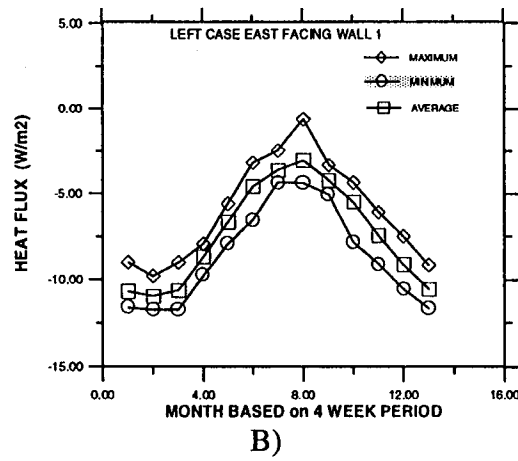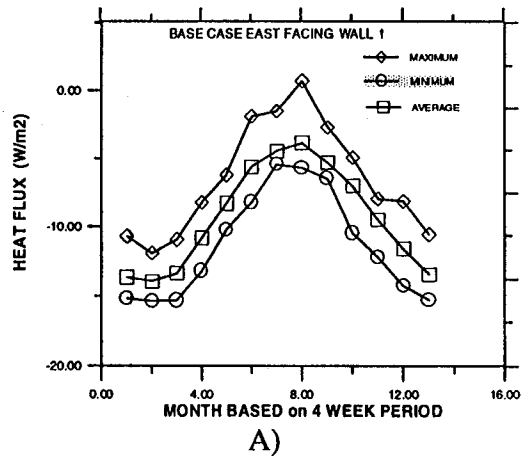
FIGURE C88
RESOLUTE
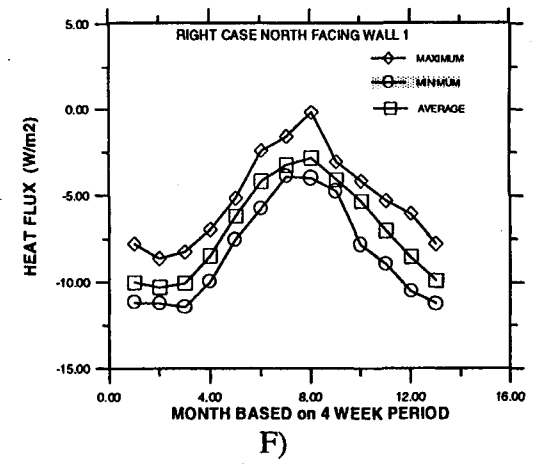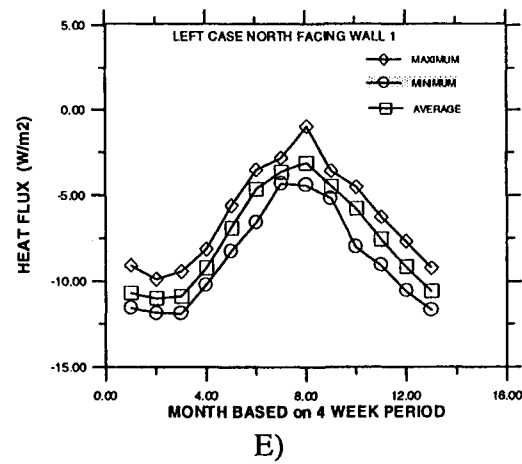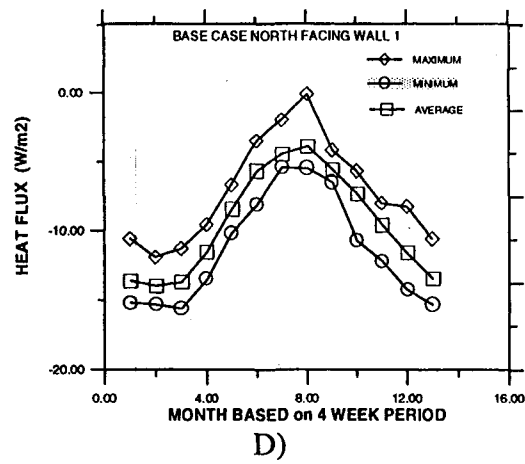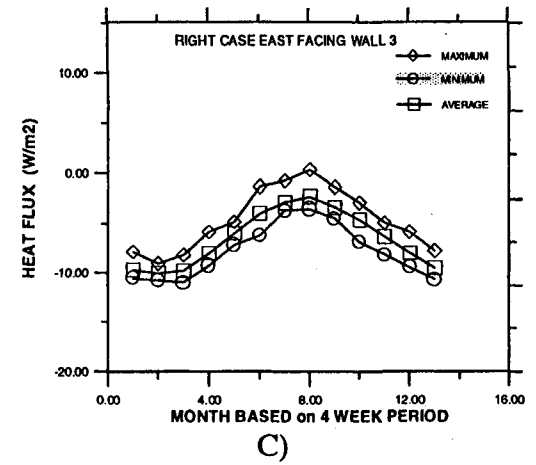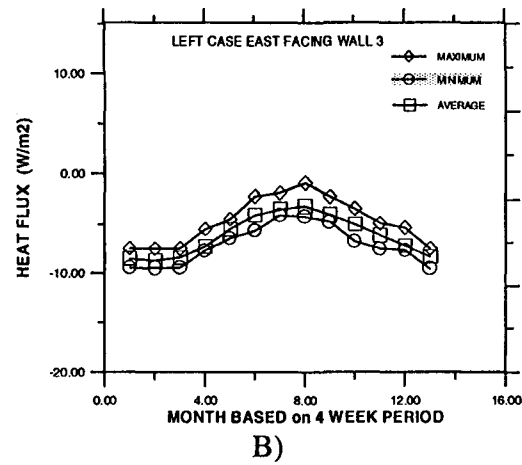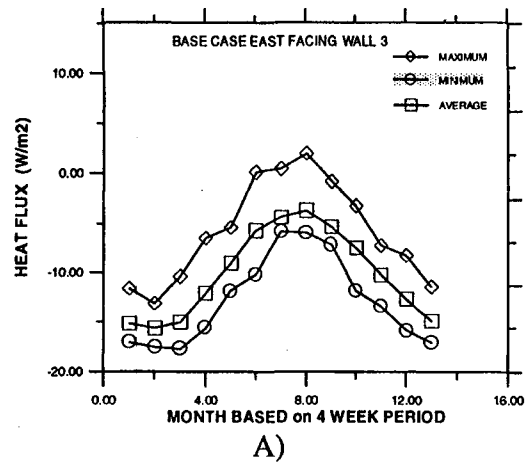
FIGURE C89
RESOLUTE
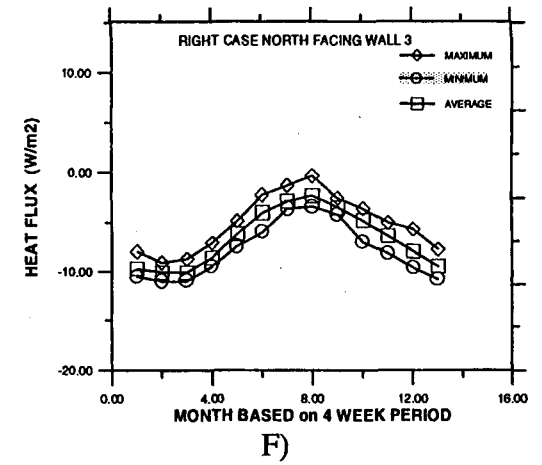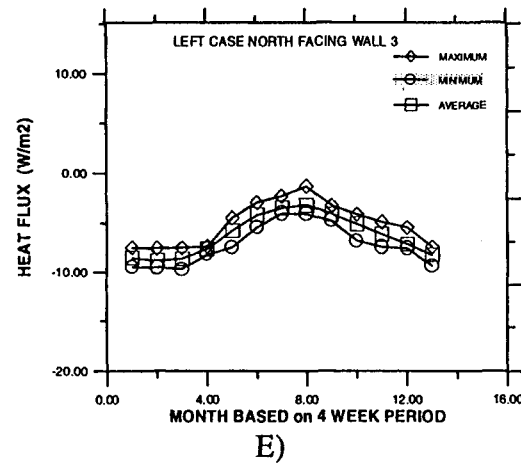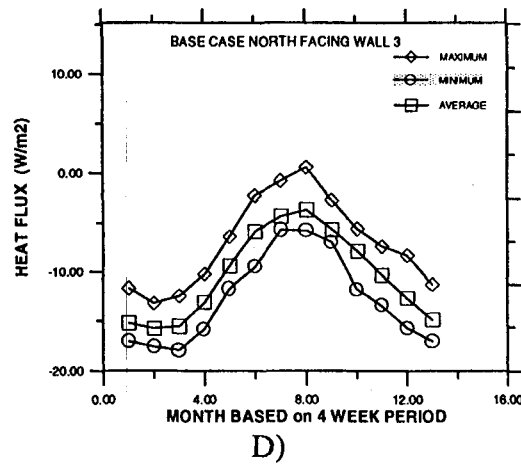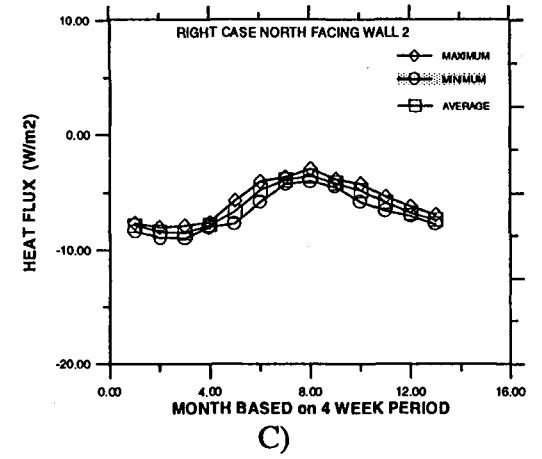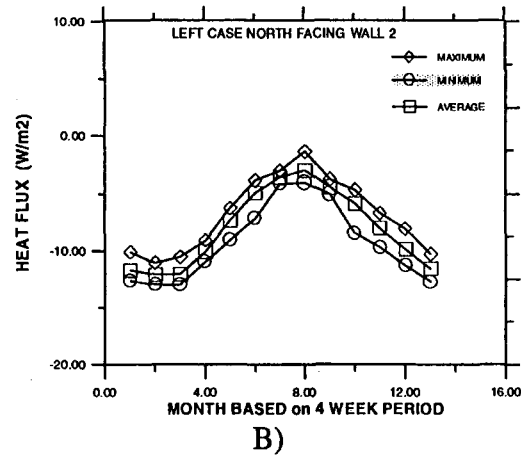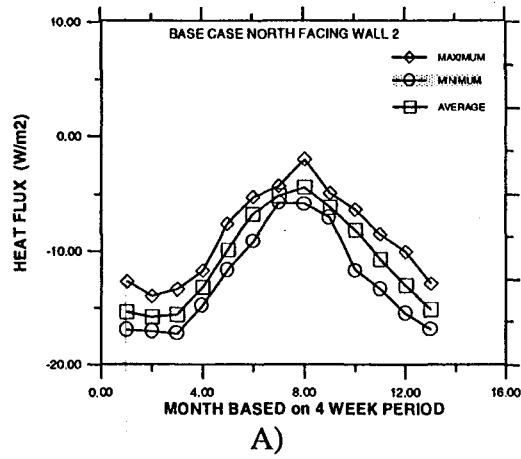
FIGURE C90
RESOLUTE
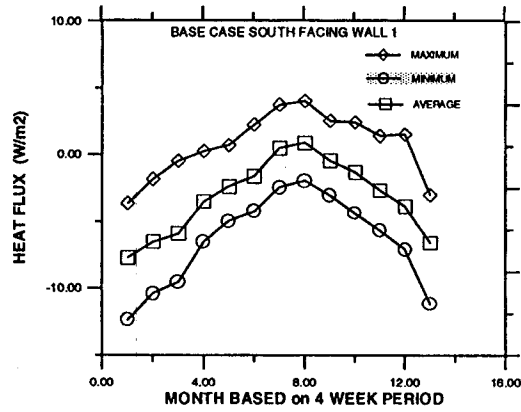
A)
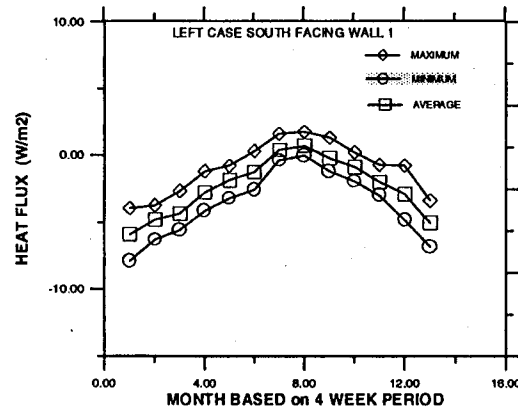
B)
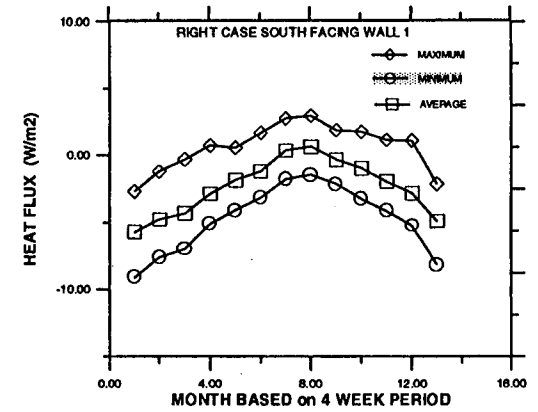
C)
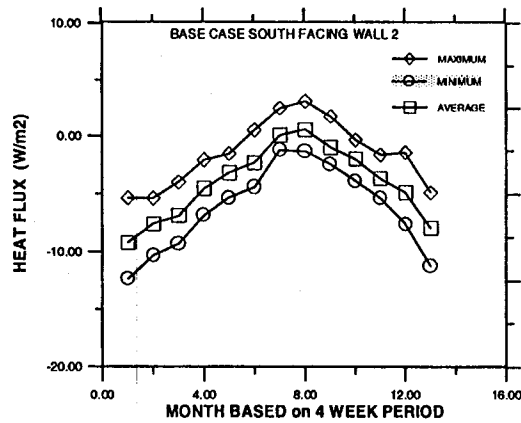
D)
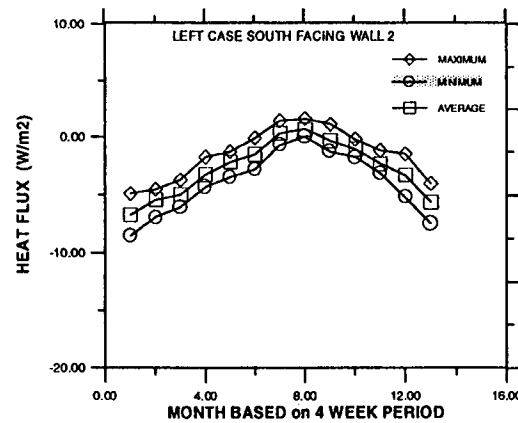
E)
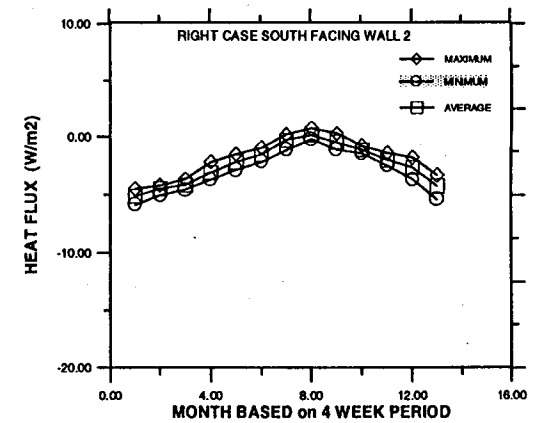
F)

FIGURE C91
FREDERICTON

A)

B)

C)

D)

E)

F)
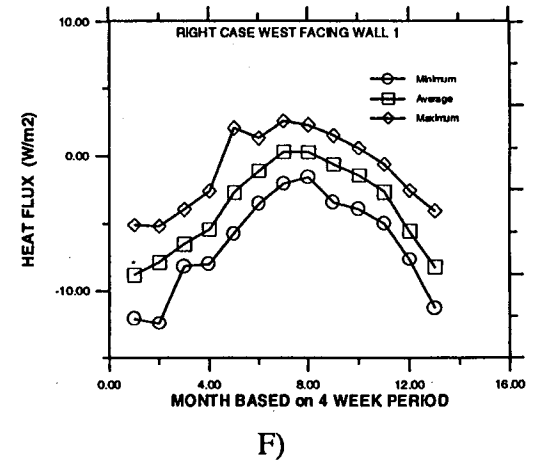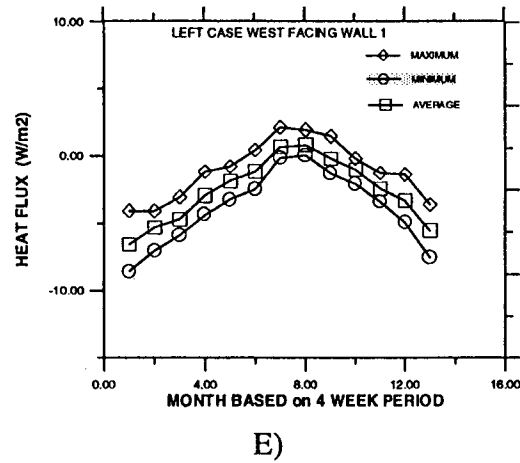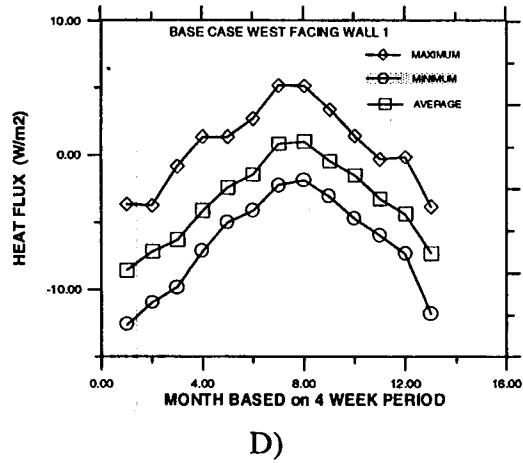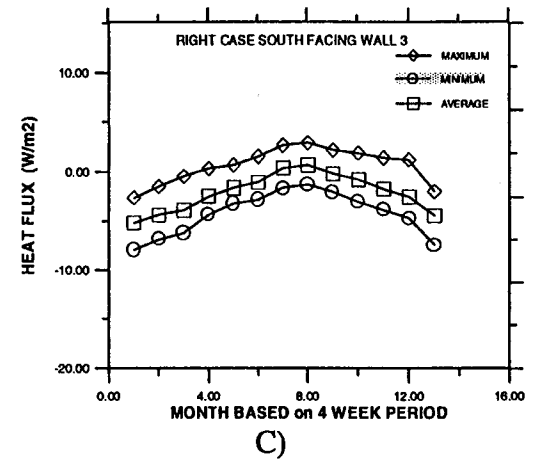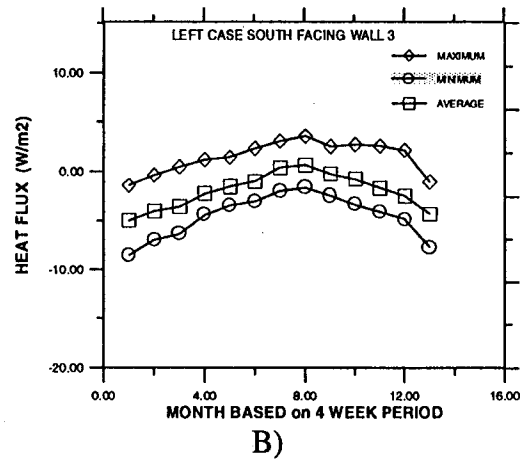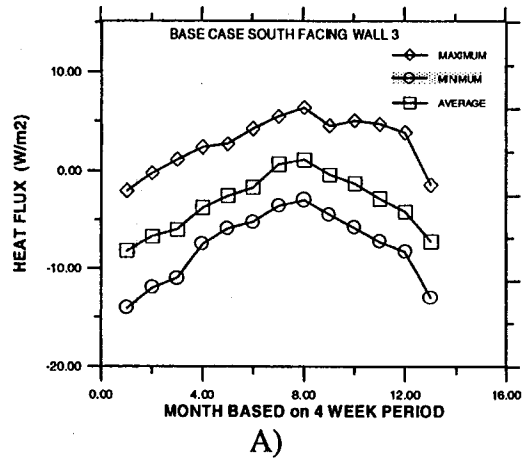
FIGURE C92
FREDERICTON
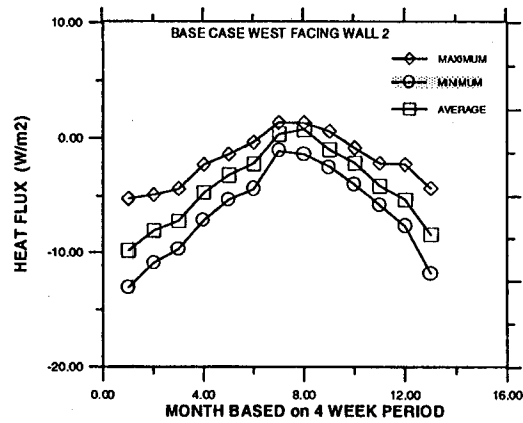
A)
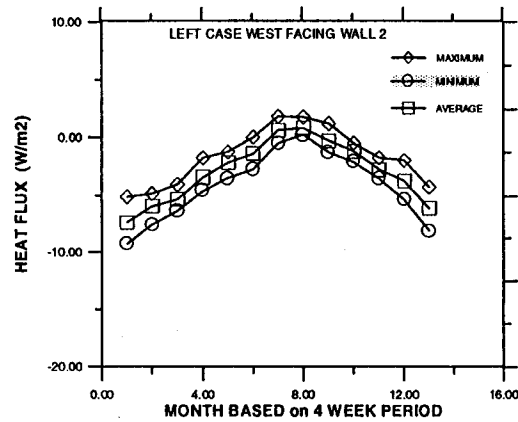
B)
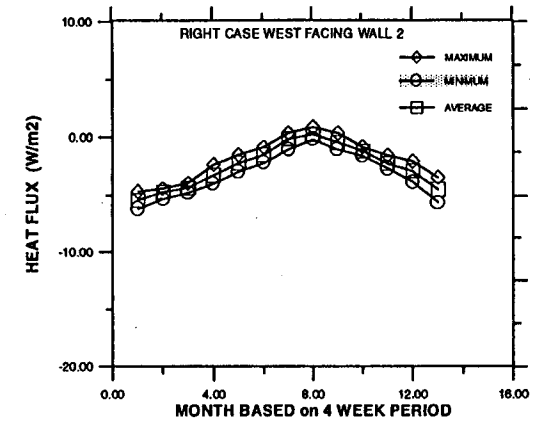
C)
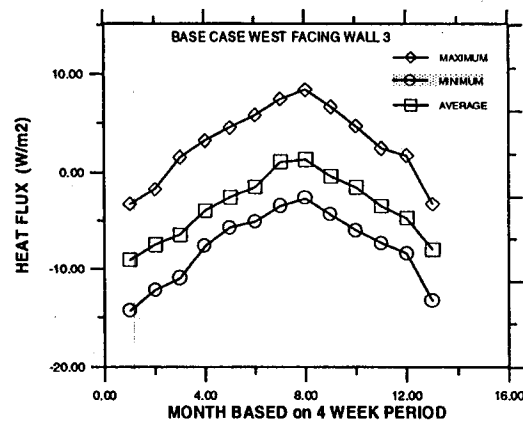
D)
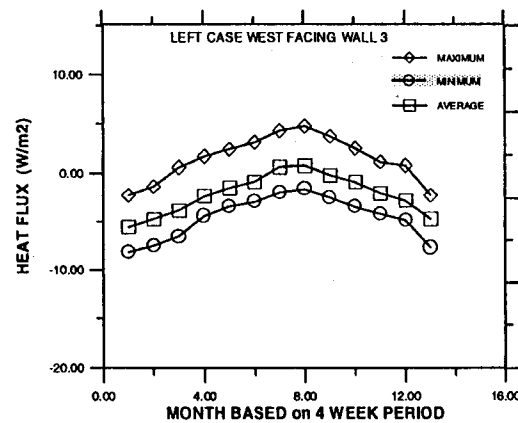
E)
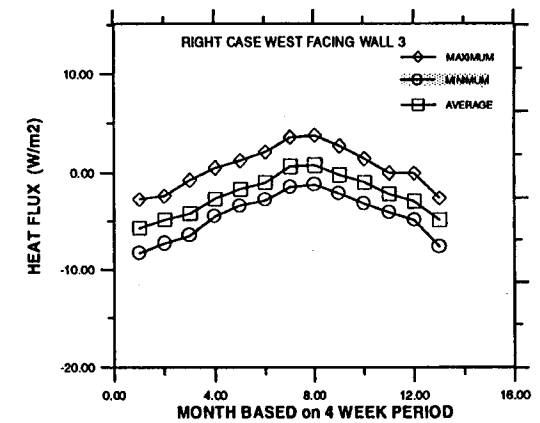
F)

FIGURE C93
FREDERICTON
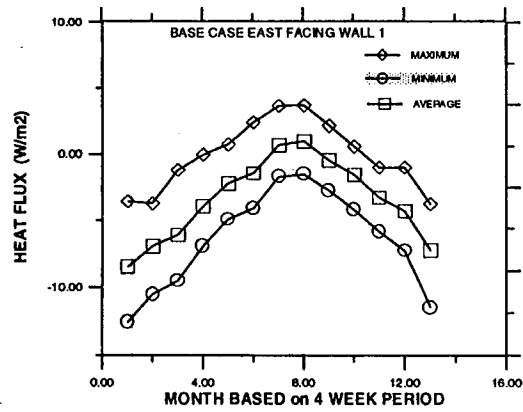
A)
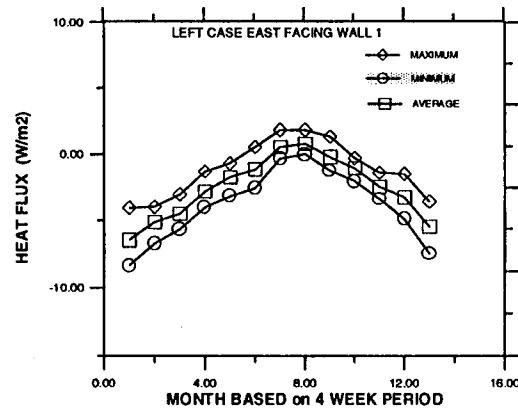
B)
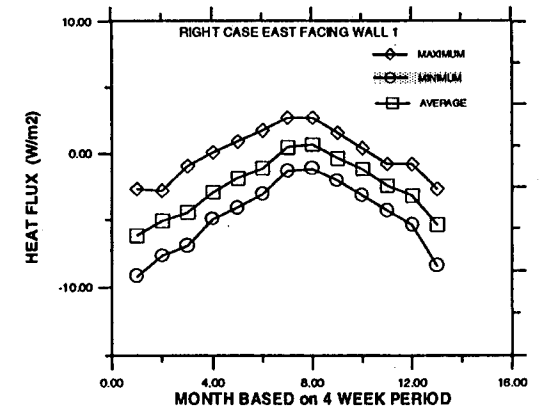
C)
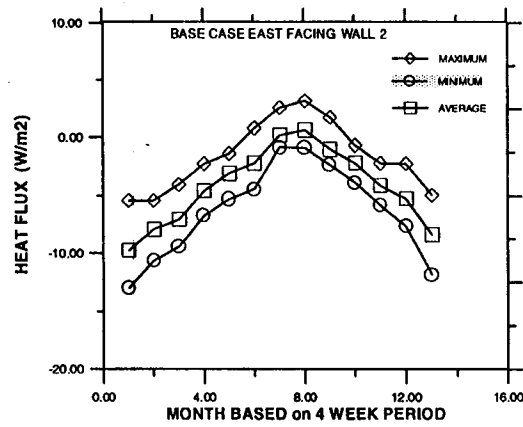
D)
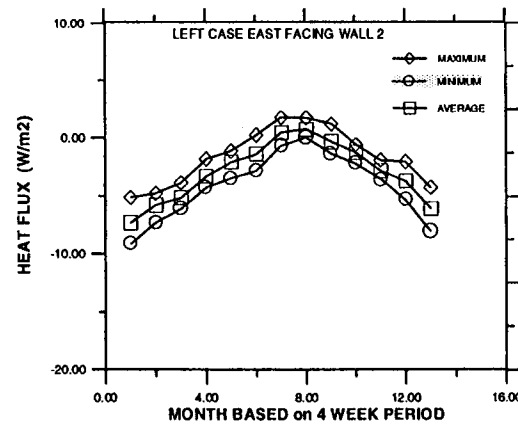
E)
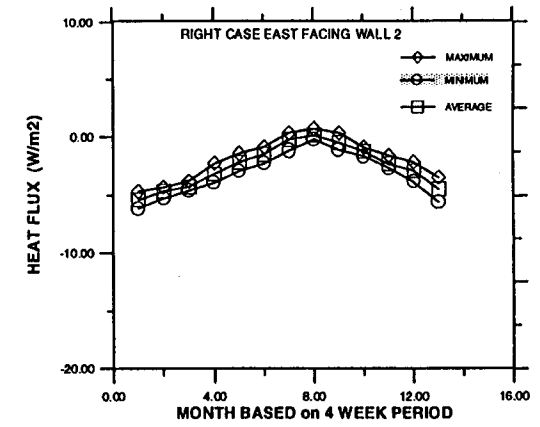
F)

FIGURE C94
FREDERICTON

A)

B)

C)

D)

E)

F)
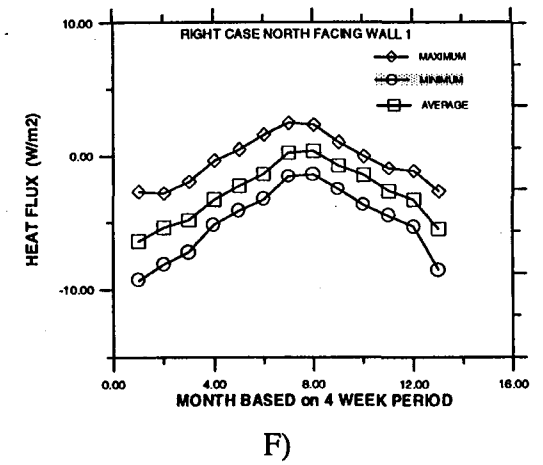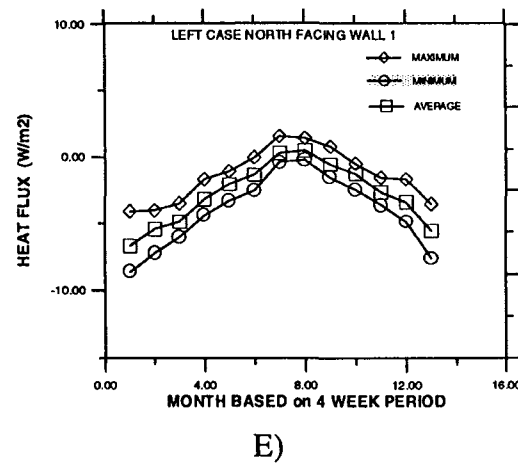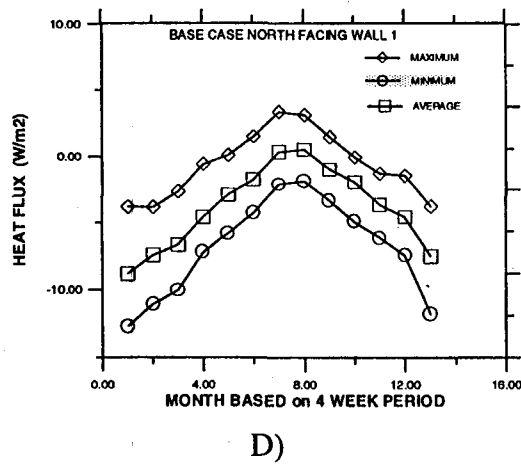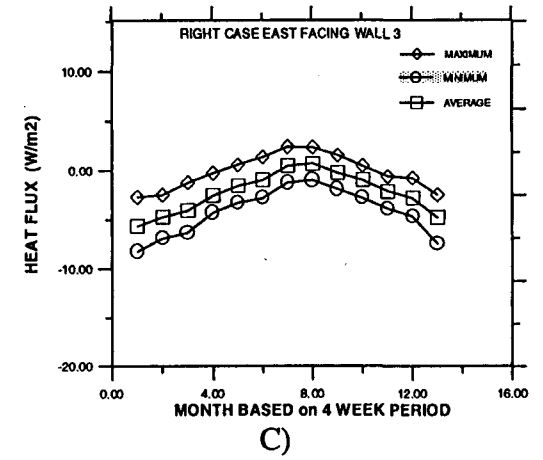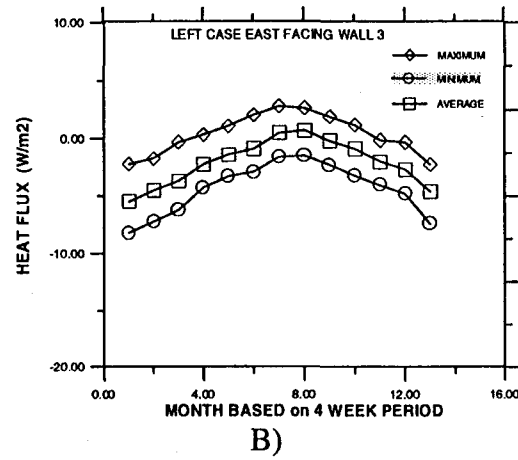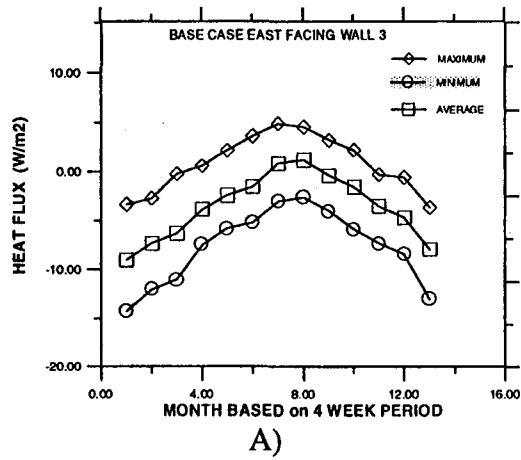
FIGURE C95
FREDERICTON
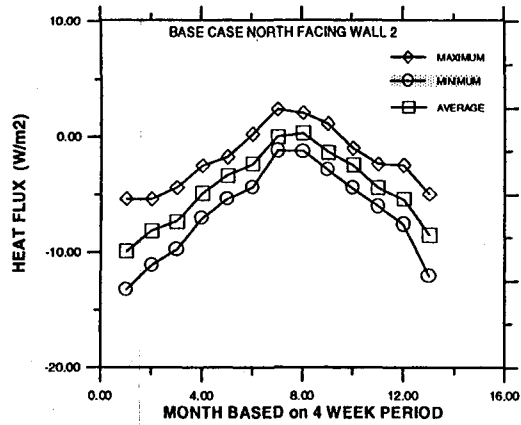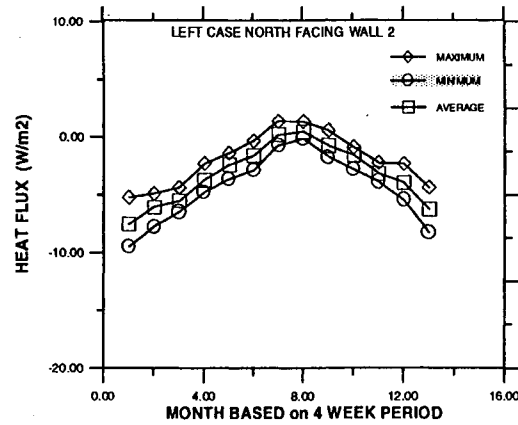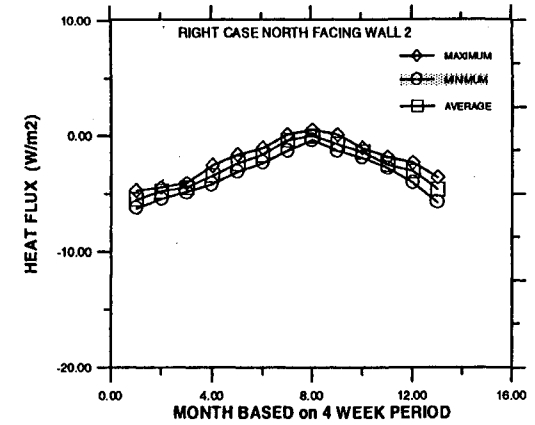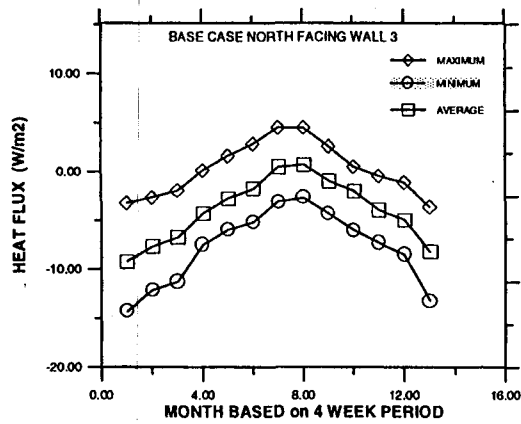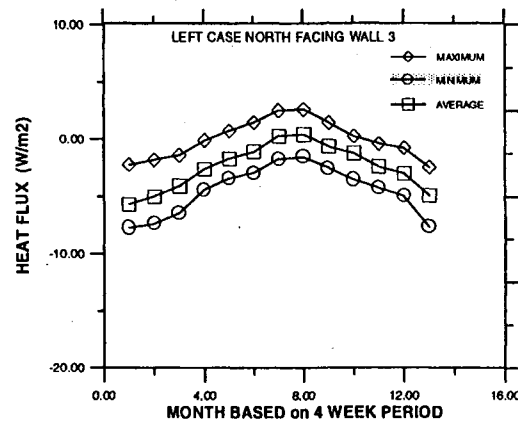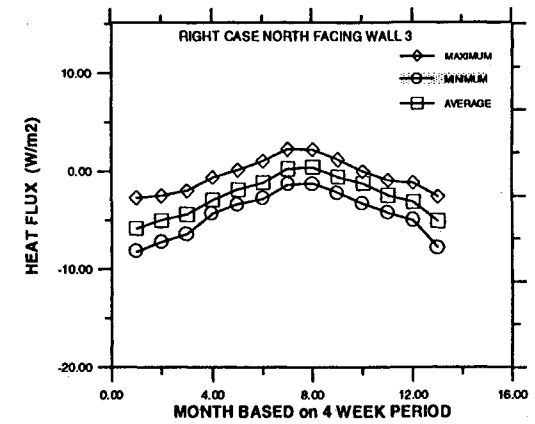
FIGURE C96
FREDERICTON

Total Moisture Content and Heat Flux for Roofs
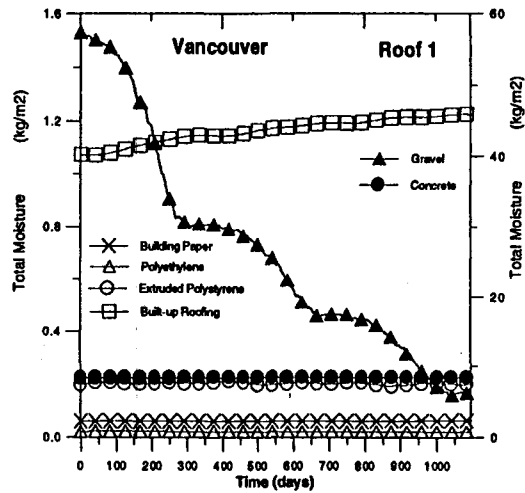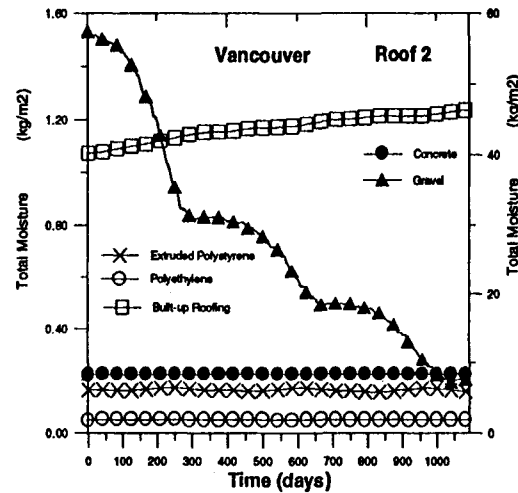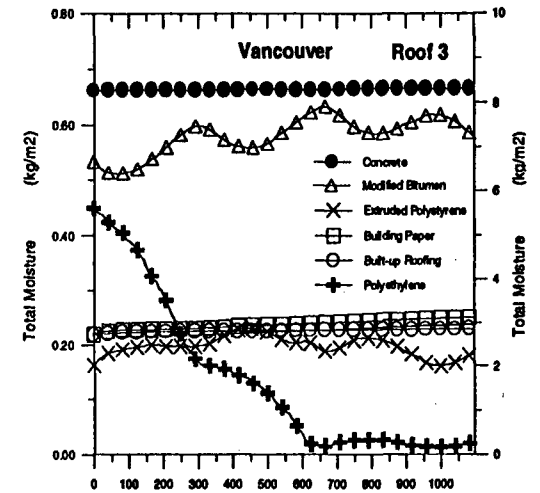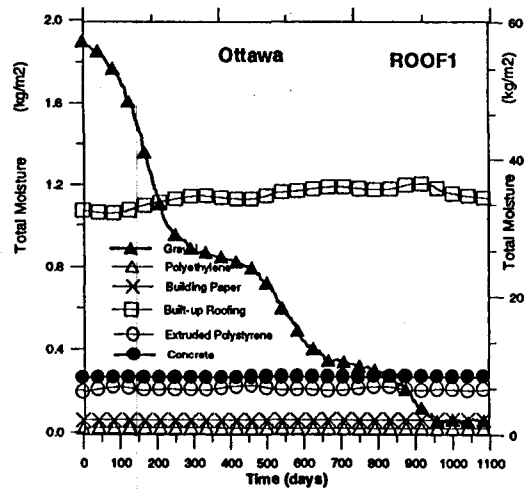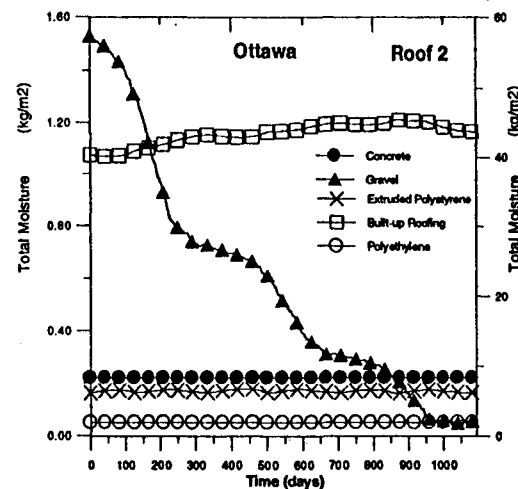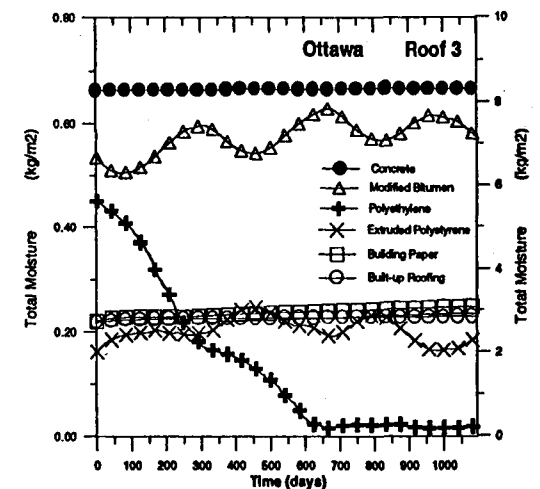
Figure C97 (ROOFS)

Figure C98 (ROOFS)
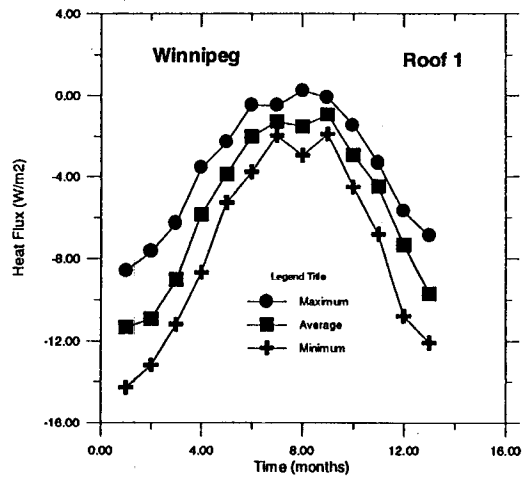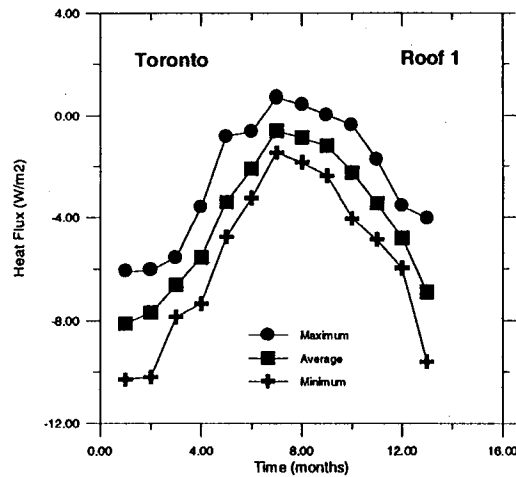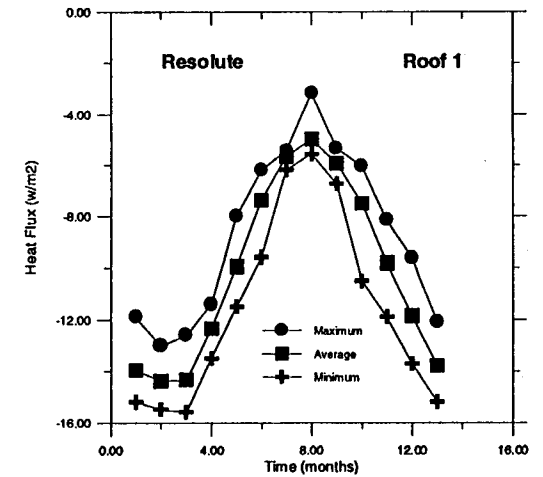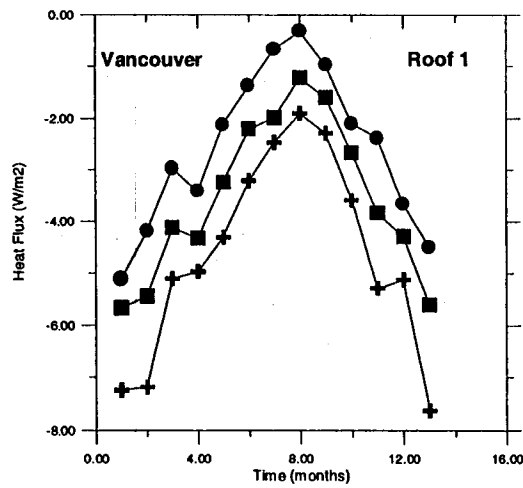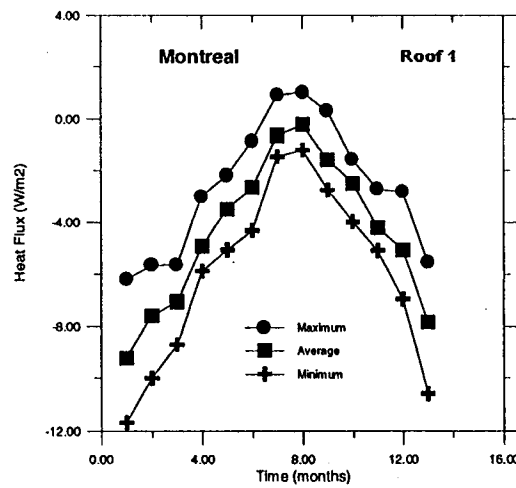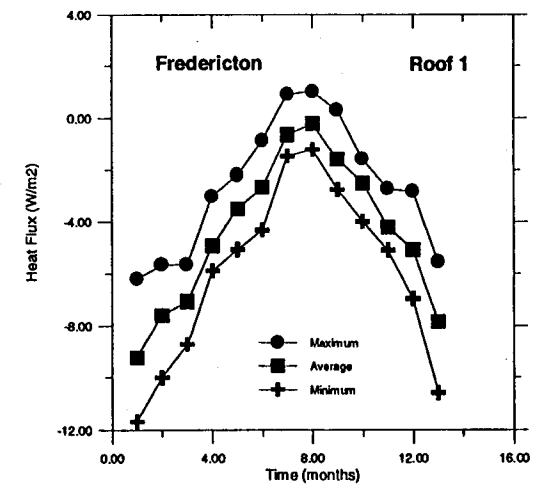
APPENDIX C

Figure C98 (ROOFS)

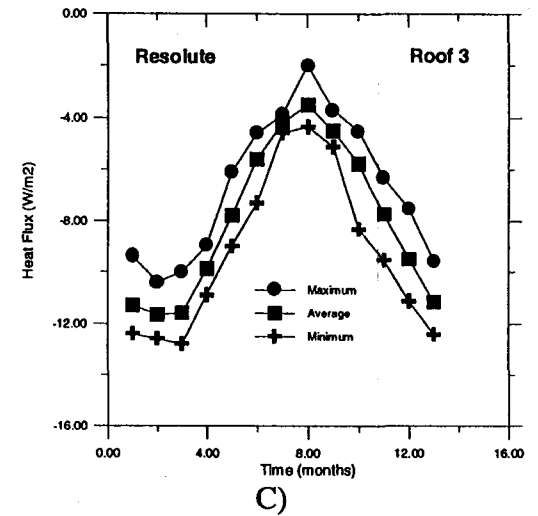Figure C99 (ROOFS)
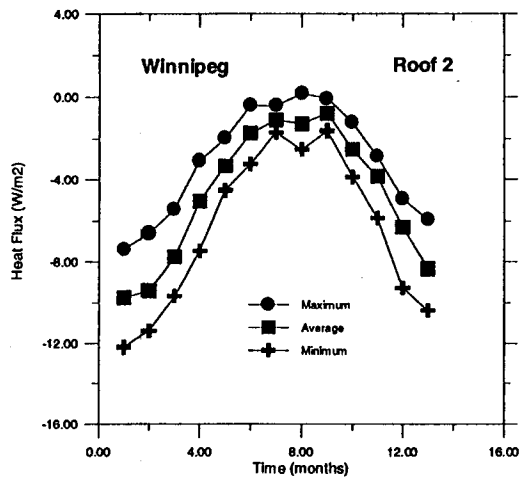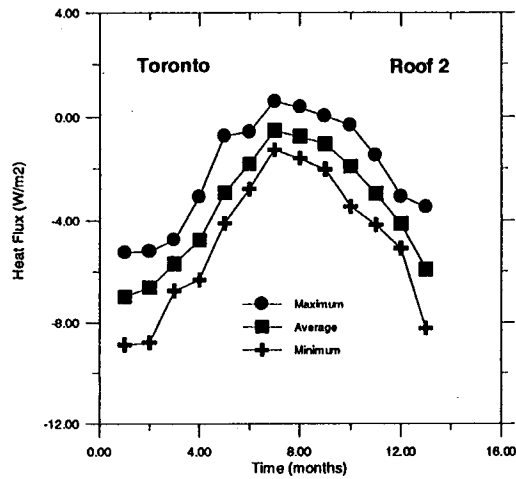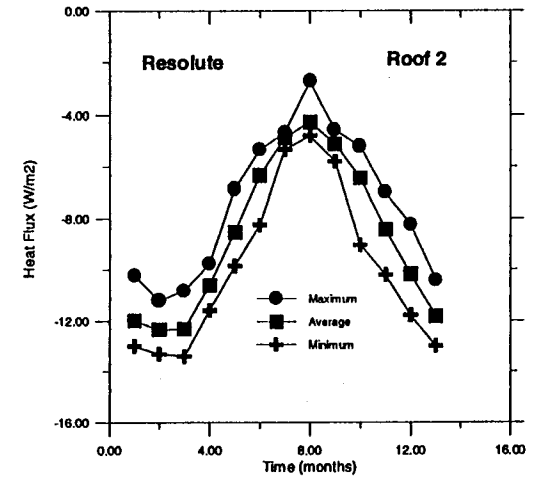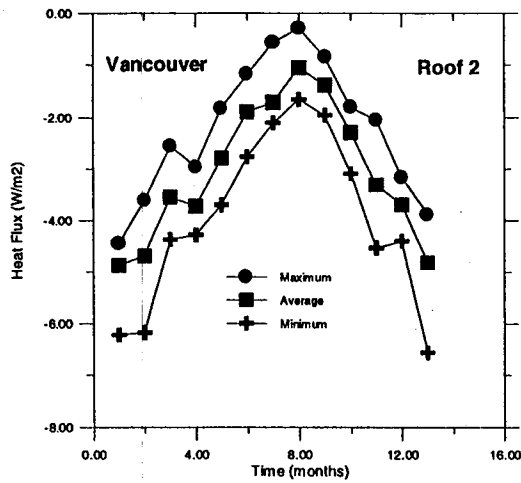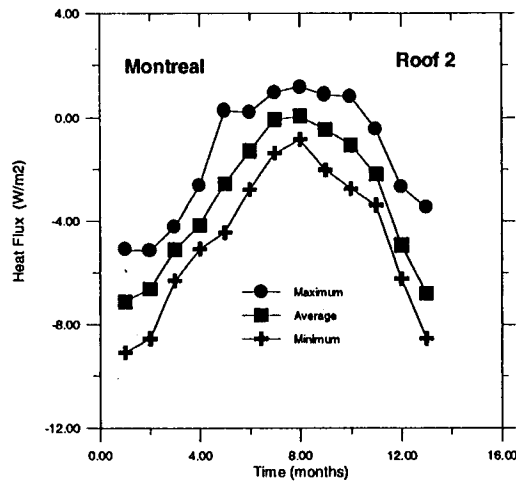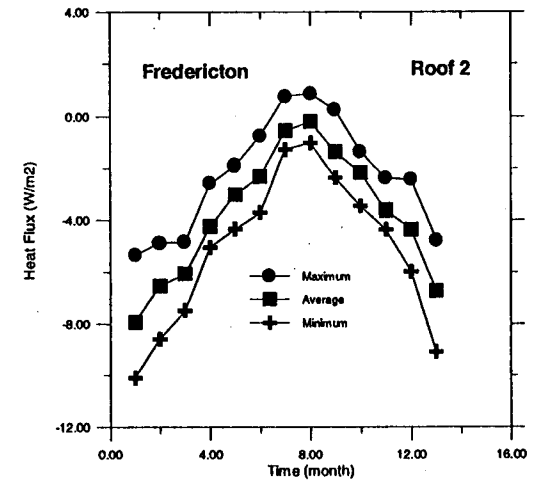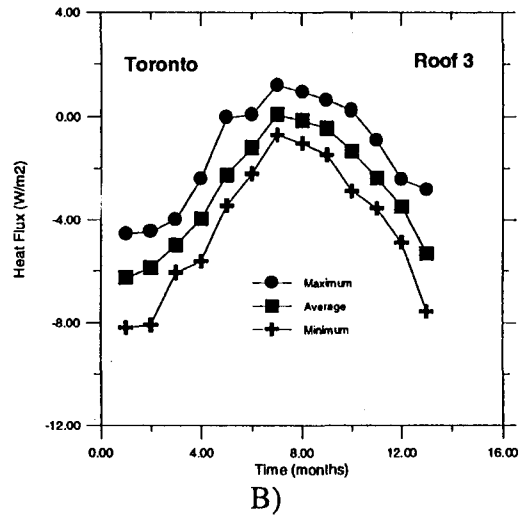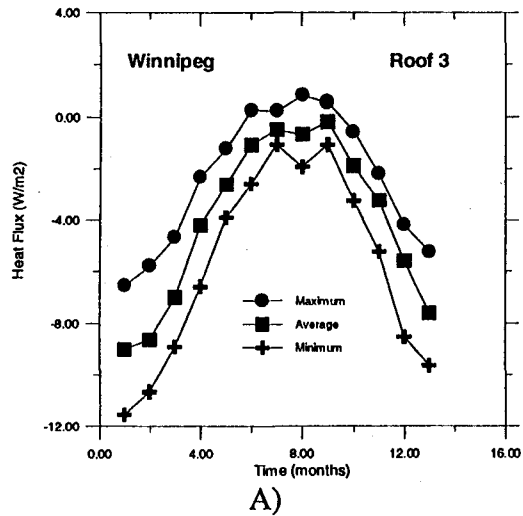
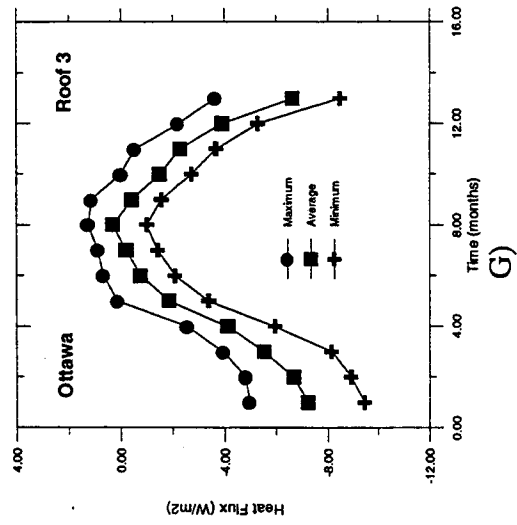# APPENDIX C

Figure C99 (ROOFS)

Figure C100 (ROOFS)

APPENDIX C
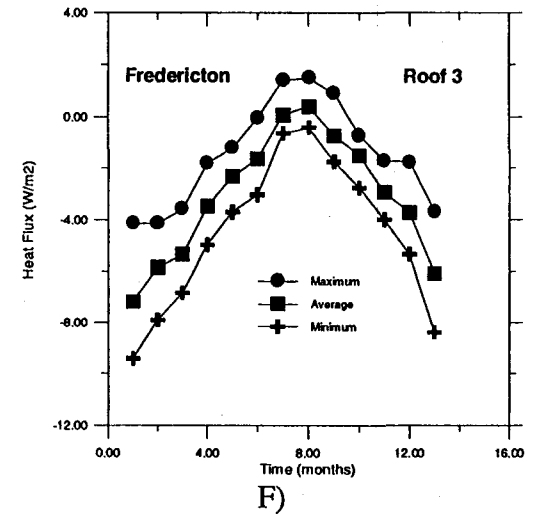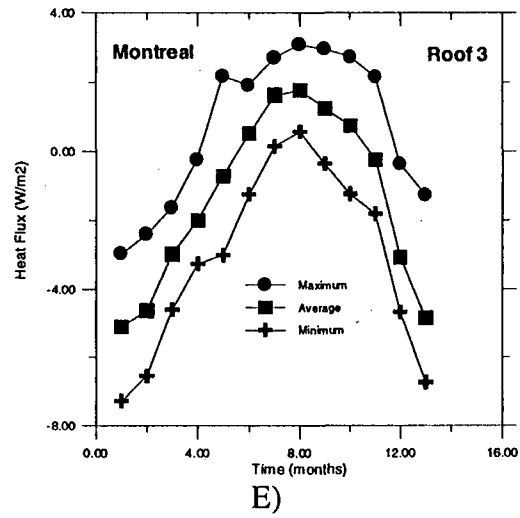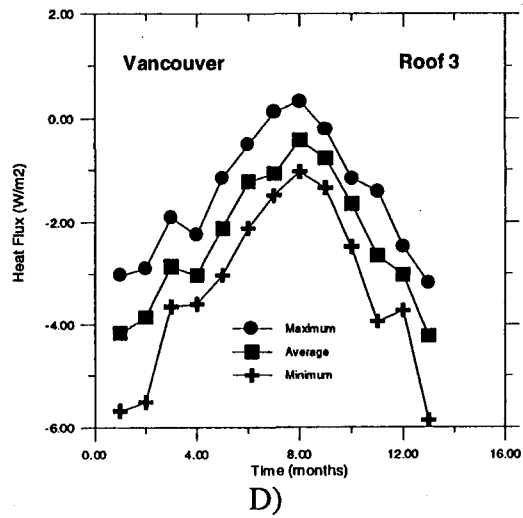
Figure C100 (ROOFS)

Visit our website at www.cmhc.ca